Rubber Technologist's Handbook

Volume 2

Edited by:
J. White, S.K. De
and K. Naskar

Smithers
iSmithers

Rubber Technologist's Handbook Volume 2

Edited by J. White, S.K. De and K. Naskar

***i*Smithers Rapra**

Shawbury, Shrewsbury, Shropshire, SY4 4NR, United Kingdom
Telephone: +44 (0)1939 250383 Fax: +44 (0)1939 251118
http://www.rapra.net

First Published in 2009 by

Smithers Rapra Technology Limited

Shawbury, Shrewsbury, Shropshire, SY4 4NR, UK

A catalogue record for this book is available from the British Library.

Softback ISBN: 978-1-84735-099-2
Hardback ISBN: 978-1-84735-100-5

Typeset by S A Hall Typesetting
Printed and bound by Lightning Source UK

This book is dedicated to the memory of

Giovanna Costa

20th January 1945 to 4th December 2007

Giovanna Costa, a Chemist highly esteemed for her activity in Macromolecular Research, left us suddenly on December 4, 2007. Her death came as a real shock to all those who knew Giovanna, as a scientist in the world community of polymer science.

Giovanna Costa was born in Fraconalto (AL), Italy on January 20th 1945. In 1970 she got her degree in Industrial Chemistry at the University of Genova. From 1970 to1972 she had a fellowship position at the Istituto di Chimica delle Macromolecole, ICM, CNR, Milano, founded by the Nobel Prize winner Giulio Natta. From 1972 to her death she was Researcher, Senior Researcher and finally Research Director at the present Istituto per lo Studio delle Macromolecole, ISMAC, of the Italian National Research Council in Genova. From 1981 to 1983 she was Visiting Researcher at Trinity College, University of Dublin (Ireland) in the Research Group of Professor D.C. Pepper. From 1996 to1997 she was director of Istituto di Studi Chimico-Fisici di Macromolecole Sintetiche e Naturali, CNR, Genova.

Giovanna Costa had many scientific interests ranging from synthesis and characterisation of polyolefins, aliphatic polyamides, liquid crystalline polymers and substituted polyacetylenes to structure-property relationships of multiphase polymer systems, such as composites based on liquid crystals, composite and nanocomposite thermoplastic- and rubber-based materials. To all these topics she made original and important contributions. Moreover, for many years she was lecturing of Macromolecular Chemistry in the frame of official courses at the University of Genova and Sassari, Italy.

Her high scientific activity brought her to hold first the office of Secretary (1995 – 2001) and then of President of Italian Association of Macromolecular Science and Technology, AIM, (2001 – 2003). She was Italian Representative at the European Polymer Federation 2001-2003 and on the Committee of the IUPAC Macromolecular Division 2002 - 2005. Moreover, she was Member of the Scientific Board of IMAG-CNR, Genova, and of ICTP-CNR, Naples, and President of the Scientific Board of CSMM-CNR, Pisa, Italy.

In all her working activity, Giovanna demonstrated her scientific aptitude and exactitude, her dignity and modesty, all this expressed with the great warmness and sweetness of her character. Giovanna was a very nice and gentle person, full of elegance and grace,

open-minded and soft in manner and speech. What was particularly attractive in her was the capability of creating a friendly and cheerful atmosphere anywhere and in any circumstance of her life. Giovanna did not know formal or competitive relationships in work. She was the most sincere and faithful friend for all her colleagues and a safe, maternal point of reference for young coworkers and students; they all will cherish the times they had talking with her. All those who knew her will deeply miss her.

Contents

Preface

The need for a second volume of Rubber Technologists Handbook has been in our mind since the publication in 2001 of the first volume wherein the preface states: 'It is obvious that several important topics could not be accommodated in the current volume and it is intended that a second volume of the handbook will be published by RAPRA Technology Ltd. in the near future to extend the coverage.' Publication of the current volume of the Rubber Technologists Handbook is the culmination of the last few year's efforts to keep the promise made in 2001.

This volume contains eleven chapters contributed by experts from the industry, research institutes and academic institutions. The first chapter by L. Conzatti, G. Costa, L. Falqui and A. Turturro deals with '*Microscopic Imaging of Rubber Compounds*'. The morphology of filler aggregates and agglomerates in rubber compounds can be followed by transmission electron microscopy. The number of filler aggregates in a definite volume, the radius, the aspect ratio, and their distribution, the volume of each particle and consequently, the total volume of filler can be calculated from three-dimensional transmission electron microscopy.

'*Intelligent Tyres*' is the subject matter of the second chapter by Brian Logan. An intelligent tyre is one that communicates useful information to the user. Some of the potential features of intelligent tyres are identification number, read and write memory, service history, temperature, cornering force, coefficient of friction, tyre mileage and tread wear. The challenge is to integrate them into tyres at a reasonable price. Cost is an important factor in successful market penetration, which in turn is linked to proper design choices and need for standards.

Jacques W.M. Noordermeer and Wilma K. Dierkes contributed the third chapter entitled '*Silica-filled Rubber Compounds*'. Application of technology of easy dispersion of precipitated silica in passenger tyre treads leads to reduced rolling resistance and corresponding fuel savings of cars. The challenges in the field include choice of coupling agents, mixing conditions and machinery.

In chapter four, W. Wennekes and R.N. Datta discusses '*Fibres in the Rubber Industry*'.

Starting from use of cotton, rayon, polyamides and polyesters, the authors discuss aramid, carbon fibre, and poly(ethylene naphthalate). Proper adhesion and bonding between fibres and the rubber matrix play an important role in the durability of a rubber product. The chapter discusses the characterisation of fibres and testing of bonded products.

Chapter five deals with '*Naval and Space Applications of Rubber*' contributed by C.M. Roland. Rubbers are found in a wide range of acoustic applications including sonar rubber domes, active sonar, and insulation, and are used in solid rocket propellant, blast mitigative coatings, aircraft tyres, airships, inflatable seacraft, combat rubber raiding craft, hovercraft, rubber sealants, rubber bullets, intrusion barriers, elastomeric torpedo launcher and mobile offshore base. Results of some of the projects are yet to be implemented in the fields.

M-J. Wang and Michael Morris contributed chapter six entitled, '*Advances in Fillers for the Rubber Industry*'. The chapter discusses chemically modified carbon blacks, inversion carbon blacks, carbon-silica dual phase filler, new precipitated silica, starch, organo-clays and powdered rubber.

Kinsuk Naskar in chapter seven entitled, '*Thermoplastic Elastomers by Dynamic Vulcanisation: The State of the Art*' describes recent findings on the effect of dynamic vulcanisation on different polymer blends in making of thermoplastic vulcanisates, their morphology and application areas.

Chapter eight entitled '*Polymers in Cable Applications*' by Dipak Khastgir deals with different materials in different types of cables and the polymer formulations to meet the service demands of the cables. The author also discusses the manufacturing processes of the cables.

N.M. Huntik and R.N. Datta contributed chapter nine entitled '*Durability of Rubber Components*'. The authors reviewed developments in long-term protection of rubber against aerobic ageing and the new approaches include: attachment of hydrocarbon chains to conventional antioxidants in order to increase the molecular weight and compatibility with rubber matrix, oligomeric or polymeric antioxidants, and polymer bound or covulcanisable antioxidants. The best approach to achieve non-staining ozone protection of rubber compounds is to use an inherently ozone-resistant, saturated backbone polymer in blends with a diene rubber.

In chapter ten entitled '*Radiochemical Ageing of Ethylene-Propylene-Diene Monomer Elastomers*', A. Rivaton and J-L. Gardette recommend incorporation of two types of stabilisers for achieving an effective stabilisation system. A synergistic effect is expected between an 'anti-rad' and antioxidant. Whilst antioxidants are active on the propagation of the chain oxidation reactions, 'anti-rad' stabilisers are effective in the initiation step.

Amalendu Sarkar in chapter eleven entitled '*Silicone Rubber*' discusses chemistry, manufacturing, properties, compounding, processing, vulcanisation and applications of silicone rubber.

We gratefully acknowledge the cooperation from all of the contributors and from Commissioning editor, Frances Gardiner. We would like thank all the staff of Smithers RAPRA Technology, who contributed to the excellent production of the handbook.

SKD is grateful to his grandchildren, Riju, Ritu and Ribhu for their patience and understanding during the course of editing of the manuscripts during his stay at San Jose, California.

JRW is grateful to his wife, Li Tong, for technical support as well as patience at home during the preparation of this volume.

KN is grateful to his little son, Kaustav and wife, Simontiny for their patience and support during the period of editing of the various chapters of this volume.

S.K. De
J.R. White
K. Naskar
March 2009

1 Microscopic Imaging of Rubber Compounds

L. Conzatti, G. Costa, L. Falqui and A. Turturro

1.1 Introduction

Rubber compounds are probably the most complex and most widely used class of materials. The ability of raw rubber to be compounded with various chemicals, with other polymers and with fillers like silica, carbon black, clay in fairly high concentrations, enables these compounds to achieve a wide range of properties. Tyres, shoe soles, belts, pulleys and gaskets are all examples of products requiring carefully optimised formulations, where precise amounts of many different components are present. Depending on the application field, different elastomers are used: polyurethanes when durability is required, thermoplastic rubber for moulding tools, polyamide-based elastomers endowed with extraordinary strength and toughness are used in top line sports gear and clothing; silicon and fluorine containing rubbers for high temperature applications.

However, as is well known, the most important rubber applications are tyres, representing approximately 70% of the worldwide natural and synthetic rubber consumption.

A tyre is a rather complicated composite object consisting of several synthetic rubbers (e.g., butadiene (BR), isoprene (IR), styrene-butadiene copolymers (SBR)) and natural rubbers (NR) along with numerous typical ingredients including antioxidants, reinforcing and crosslinking agents and process aids. The selection of the appropriate additives and fillers are critical to the performance of the ensuing rubber compounds. Indeed, elastomers give vulcanisates that can be hardly used without the addition of reinforcing fillers, mainly carbon black and silica.

Besides their use for changing colour, conductivity, absorption of radiation and so on, particulate fillers can also increase the strength of an amorphous rubber even more than 10 times, if the dispersed particles are sufficiently small to have a large surface area to interact with the matrix [1-8].

These active reinforcing additives must be able to give homogeneous and fine dispersions into the polymer matrix, strong interactions with the polymer, reduced tendency to flocculate and re-agglomerate during storage and vulcanisation of the compound.

Moreover, they should have negligible interactions with other ingredients, no deleterious effects on the curing process, no contribution to the oxidative degradation of the compound. Finally, they should be environmental friendly and have a low density in order to reduce the tyre weight, thus favouring a reduction of the fuel consumption.

Particle size, aggregate structure, morphology, surface characteristics and chemical composition of the filler are the most important parameters in determining its activity [3, 5, 6, 9, 10].

So far, the most widely used and effective fillers in the production of tyres are carbon black [1-10] and silica [3-7, 11, 12]. However, other additives, for example starch [13] and alumina [14], rice husk ash [15, 16] and, more recently, nanoclays [17-19] have been evaluated to meet future needs and performances. A new carbon-silica dual phase filler has been also proposed in recent years [7, 20, 21]. It is characterised by a high reinforcing potential because of its capability to establish higher filler-polymer and lower filler-filler interactions, as compared to the single components carbon black and silica. The effect of carbon black and silica mixtures on the interactions between fillers and matrix, and on the rheological behaviour of rubber compounds has been also investigated [22, 23].

1.2 Fillers and Elastomer Reinforcement

The reinforcement of rubber, which results in a pronounced increase of tensile strength, improved tear and abrasion resistance as compared to the neat elastomer, depends to a large extent on the molecular, chemical and rheological characteristics of the elastomer, on the filler properties and on the mixing process and technology [2, 10]. In particular, to cause a significant reinforcement the filler must have high specific surface area that, together with loading, determines the effective contact area between filler and polymer.

Two other important characteristics of the filler are structure and surface chemistry. Using transmission electron microscopy (TEM) techniques, carbon black primary particles appear to be of spherical shape, fused together to form aggregates. The latter connect through Van der Waals forces into agglomerates [5, 10, 24]. The structure of carbon black particles seems to be an intermediate between crystalline and amorphous materials, with quasi–crystalline domains built up by basal planes that are parallel but angularly distorted and the spacing between the layers different from that of pure graphite. The interaction energy between carbon black and the elastomer depends on the nature and number of active sites. Crystallite flat surface and amorphous carbon present on the surface are considered less energetic sites, while crystallite edges are usually considered as the most energetic sites. These sites determine the reinforcing properties of the carbon black in rubber.

The structure of the filler relates to the irregular shape of aggregates, which is determined by the extent and mechanism of the clustering of the primary particles. A schematic representation of carbon black particles is given in **Figure 1.1**.

The aggregates are generally classified into four shape categories [25]: 1 - spheroidal; 2 - ellipsoidal; 3 - linear; 4 - branched, as shown in **Figure 1.2**.

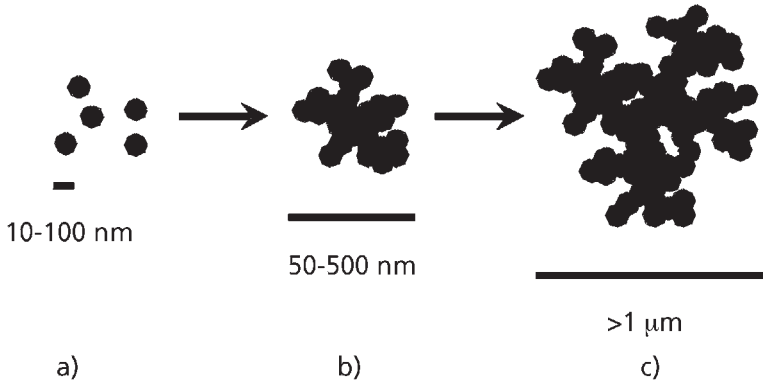

Figure 1.1 Carbon black: a) primary particles; b) aggregate (primary particles fused together); c) agglomerate

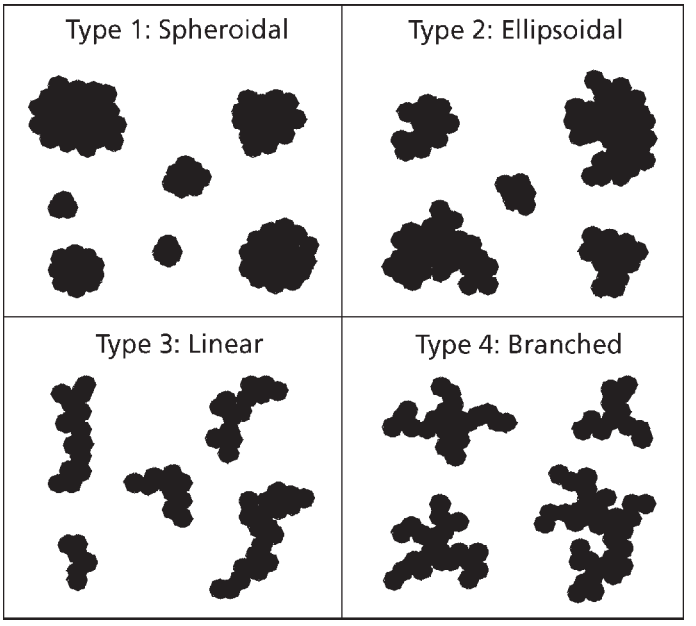

Figure 1.2 Shape categories of carbon black aggregates

Therefore, highly structured aggregates have a large void volume in which the elastomer chains can become entrapped, thus leading to an increased effective volume fraction of the filler [2, 7, 26-29].

Like carbon black, silicas and silicates form primary particles, aggregates and agglomerates during production. In fact, from electron microscopy observations, silicas are known to exist as quasi-spherical particles or aggregates both in the dry state and in rubber [30-34]. Typical dimensions in the case of silica are 5 to 40 nm for the diameter of the primary particle, 100 to 500 nm for the aggregates and >500 nm for the agglomerates. TEM micrographs of carbon black and silica aggregates are given in **Figure 1.3**.

Silicas can be produced by thermal and by wet chemical processes. The most important silicas for classical rubber grades are produced by precipitation from alkali silicate solutions (wet chemical route). Precipitated silicas are supplied as powders, granulates and micropearls for the rubber industry.

As previously mentioned, the surface activity plays a predominant role in the filler-elastomer interactions [27, 28]. The surface properties of synthetic silicas are related to the silanol groups of the silica surface and to the extent of hydration. On the surface of synthetic silicas there are three types of hydroxyl groups: isolated, vicinal (on adjacent silicon atoms) and geminal (two silanols on the same silicon atom). Some water molecules are strongly hydrogen-bonded to silanol groups, while in the outermost layer free water is physically adsorbed. Upon heating at 105 °C this free water is released; hydrogen-bonded water is released between 105 and 200 °C. At temperatures above 200 °C, the surface silanol groups condense to form siloxane bridges.

Precipitated silicas have a fully hydroxylated surface with 4 to 10 silanol groups per nm^2; the fumed silica surface is partially hydroxylated with about one-fourth of silanol groups compared to precipitated silicas. Therefore, silane coupling agents are often used both to reduce the silica surface polarity and to chemically bond silica particles to the

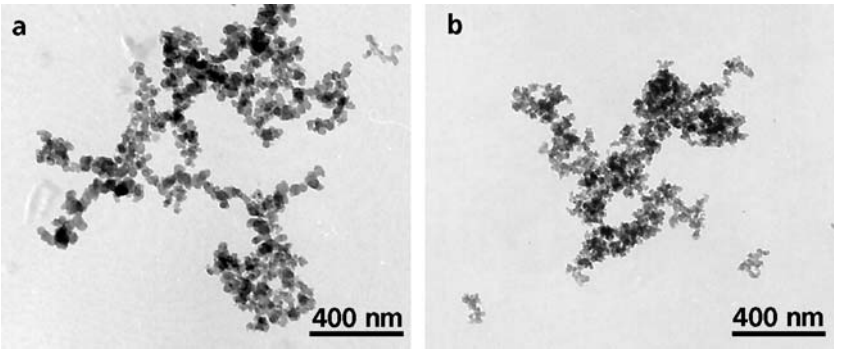

Figure 1.3 TEM micrographs of: a) carbon black CRX 2006; and b) silica Zeosil 1165

rubber during the vulcanisation step [27, 28, 35-41]. The surface modifier mainly used in the tyre industry is *bis*-triethoxysilylpropyl tetrasulfane (TESPT).

Also in the case of carbon black, some macromolecular chains of the matrix are chemically linked with the filler, due to high shear stress during mixing, and others are physically adsorbed at the filler surface, thus giving interactions of different strength [2, 3, 5, 27, 28]. From the discussion so far, it is evident that the performances of a compound is strictly connected with the interaction surface between the filler and macromolecular chains, and then with the dispersion of the filler into the polymer matrix, which determines the morphology of the system.

1.3 Characterisation of the Filler Dispersion

An indirect and qualitative evaluation of the filler distribution into the elastomer matrix can be deduced through bound rubber [2, 27-29] and green strength [28, 42, 43] measurements on uncured rubber compounds and from dynamic mechanical properties of the crosslinked materials [1, 2, 6, 7, 26, 28, 44-46]. However, a direct knowledge of the filler dispersion is of fundamental importance not only for understanding the reinforcing mechanism but also for achieving information on the quality of rubber processing. In fact, in dispersive mixing the main goal is to breakdown agglomerates and aggregates of the original filler into small particles, which must be evenly distributed within the matrix, to ensure uniform properties of the final compound and to achieve the highest reinforcing effect.

1.3.1 Techniques

Many methods can be followed to achieve direct information on the morphology of a polymer-based composite material. Microscopic, spectroscopic and scattering techniques have been used to characterise structure and morphological organisation of carbon black and silica, both in the dry state [5, 24, 25, 47-70] and in compounds [21, 24, 26, 44, 69-97]. Several papers report on the use of small angle x-ray scattering (SAXS) [33, 34, 65-68, 71-76], small angle neutron scattering (SANS) [33, 34, 65-68, 74, 75], and Raman imaging [76-77]. However, to have a complete assessment of the particle size and shape as well as of the distribution of the filler within the matrix, only the characterisation at a sub-micron scale is relevant, thus making the use of microscopy unavoidable.

1.3.2 Microscopy

Several types of equipment are used, depending on the information required: scanning electron microscopy (SEM) [24, 69, 78], TEM [24-26, 48-61, 69, 79-94], atomic force

microscopy (AFM) [21, 24, 44, 64, 69, 70, 95-97], scanning tunnelling microscopy (STM) [62, 63, 69, 70]. Indeed, morphological characterisation is usually performed at different scales: at the macroscopic level to obtain information on the incorporation of the filler into the rubber and, consequently, on the effectiveness of the mixing process; at the microscopic level to achieve details on the distribution and size of aggregates and then on the elastomer-filler interactions.

Most of the literature on the morphological characterisation of rubber compounds deals with the use of TEM [26, 69, 79, 94] and AFM [21, 44, 69, 70, 95-97]; both techniques give important and useful information, but each of them has some drawbacks.

Since about 1940 the electron microscope has been indispensable in determining the particle size of pigments. The classification of the various grades of carbon black used in the rubber industry has been possible only through TEM examination. Characterisation by TEM reaches a nanometric resolution and, in combination with image analytical procedures, allows a two-dimensional statistical analysis. Furthermore, if the loading is not too high, it enables recognition of different fillers present simultaneously in the compound, as for example carbon black and silica or particulates and layered nanofillers, and to achieve information on their dispersion.

There are two critical points in using this technique: the first one is the preparation of the specimen, this requires ultrathin cryosections to be obtained at very low temperature by ultramicrotomy; the second is its limitation to bi-dimensional analysis.

AFM seems to represent an alternative method to examine surface topography, adhesion, mechanical and other properties on a scale from a few hundred micrometers to nanometers. This technique does not require any particular preparation of the specimens if only their surface must be observed. Moreover, the use of tapping mode AFM (TMAFM), recently used for the study of soft polymers, minimises surface sample damage during scanning [95]. However, this technique has a significant limitation. In fact, to achieve information on the morphology in depth one must prepare sections, generally about 4 μm thick. The temperature for successful microtoming depends on the glass transition temperature (T_g) of the material: cured and filled rubbers are generally microtomed at about –120 °C, the same as for TEM specimen preparation. Finally, it must be underlined that the resolution of AFM is lower than that of TEM, as shown also in the literature [64, 95].

1.3.3 Automated Image Analysis

The major limitations to the morphological analysis of fillers are related to the low speed of operation and to the complexity of aggregates under investigation. Therefore, many attempts have been made to speed up the data processing from the morphological images.

Nowadays the potential of TEM and AFM has been greatly implemented by the possibility of using automated image analysis (AIA), which allows acquisition of structural details and quantitative information on the dispersion of the filler through the use of descriptors based on geometrical (area, perimeter, diameter, and so on), morphometric (shape ratio, roundness, and so on), compositional (area and/or volume fraction occupied from each class of objects, and so on) and structural parameters (state of aggregation, densitometric factors). Some morphometric descriptors are sketched in **Figure 1.4**.

Endter and Gebauer in 1956 [98] developed the first semi-automatic device for measurements of pigment particle size. Their instrument utilised a manually controlled light spot, which was adjusted to match the size of the particle. Its diameter was then recorded automatically. However, relatively poor results were produced because of differences in operator interpretation, as a consequence of poorly defined particle boundaries.

The first attempt to fully automate the analysis of carbon black particle and aggregate size in dry state or in rubber compounds, was made in 1969 by Hess and co-workers [49]. Analyses were carried out using a Quantimet (QTM) Image Analyzing Computer, based on a television scanning device able to directly analyse a microscope image [25, 49]. Limits and problems of this equipment were associated with image contrast and intensity when dealing with very fine particle size blacks. The most useful QTM measurements on the black aggregates were found to be mean aggregate area and mean length. Results from QTM determination showed a good correlation with results from DBPA, at least at a given particle size level.

Hess and McDonald, in 1974, reported a more practical automated size analysis method for carbon black [99], which is part of the ASTM procedure D3849 [100]. A Quantimet 720 system with the television camera linked directly to a TEM by a fibre optic coupling was used. This system was based on picture point (individual picture elements (pixels) of a digital image) rather than on a simple scan line-measuring concept. The measuring frame contained a total of about 500,000 pixels, each one having a specific x and y coordinate.

Figure 1.4 Morphometric descriptors: a) perimeter, P; b) area, A; c) aspect ratio, $F = L_1/L_2$

The techniques of image analysis have been rapidly evolved thanks to progress in image acquisition and to the development of algorithms and software, either for general or specific application. For these reasons more reliable and quantitative results on the morphology of fillers and on their dispersion into a polymer can be obtained. For example, by using fractal geometry [54, 55, 60], skeletonisation [55, 60], microdensitometry [60] and three-dimensional modelling techniques [57-59, 61], information on two-dimensional and three-dimensional structures can be achieved.

To assess the fractal dimension of carbon black, different techniques, such as SAXS, SANS and TEM/AIA, have been used [54, 55, 60]. From digitalised images obtained from TEM micrographs, perimeter and area values of aggregates are obtained and from these data the fractal dimension of the aggregate boundary is calculated. In particular, it has been found that the fractal dimension of the particle surface is independent of the carbon black grade, whereas the fractal value for the aggregate boundary is different for different grades. Fractal dimensions may be helpful to predict the reinforcing potential of carbon black and can be used to elucidate the reinforcement mechanism.

The skeletonisation is a specialised image analysis erosion technique that defines the mid-line of an object and provides quantitative and direct measurements on the degree of branching in carbon black aggregates [56, 60, 101]. The main findings indicate that the weight-average number of aggregate branches provides good distinction between grades of varying DBPA and the distribution of branches per aggregate becomes broader and flatter with increasing DBPA values. This technique has been used to evaluate the magnitude of aggregate breakdown when mixed with highly viscous systems, such as SBR and NR. The high mechanical modulus of compounds loaded with coarser carbon black appears to depend on the surface activity of the carbon black, probably because of the formation of new reactive sites at the surface during aggregate breakdown in the rubber [56].

However, the aforementioned analytical procedures are based on two-dimensional projected images, which provide only an approximation of spatial aggregate shape and size. Insight into spatial aggregate structure can be gained by viewing the aggregates at different tilting angles. It has been shown that aggregates can exhibit significant anisometry, with dimensional characteristics strongly dependent on the direction of measurements [57-59, 61]. Highly structured carbon blacks display bigger changes in two-dimensional projected size and shape than low structure grades, i.e., they are statistically more anisometric.

1.4 Analytical Procedure by TEM/AIA

Quantitative information on the filler dispersion can be attained by using TEM associated with image analysis techniques. In this respect, an accurate procedure for the analysis of TEM micrographs by automated image analysis has been set up within our research

facility. This is an effective method to obtain a quantitative description of the filler dispersion in rubber compounds, which is representative of the investigated systems. Specifically, NR, BR, SBR based compounds loaded with various amounts of silicas were investigated and results are discussed in Section 1.6.2. Details on the procedure are given in Sections 1.4.1-1.4.4.

1.4.1 Preparation of the Samples and TEM Images

The preliminary step is the sample preparation, which plays an essential role on the accuracy of the morphological analysis. In the experimental conditions adopted in our laboratory, the rubber specimens, cooled at least 40 °C below the T_g, are microtomed to obtain ultrathin sections of nominal thickness equal to 50 nm, with a diamond knife cooled to –60 °C. To obtain meaningful results a large number of cryosections (several hundreds) of 1 mm^2 of surface area, obtained from different zones of each sample, must be investigated.

Different magnifications are used to characterise each sample: low magnifications (3000-12000x) give indications of the overall dispersion and they are useful to control the overall homogeneity of the filler dispersion into the rubber matrix. Medium magnifications (20000-50000x) provide an accurate morphometric characterisation of the system through the application of selected morphological descriptors used to identify, count and measure the aggregates. High magnifications (>50000x) are helpful in the investigation of morphological details at the nanometer level.

1.4.2 Image Digitalisation

By using image analysis techniques it is possible to recognise, select, measure and compare morphometric parameters of complex structures dispersed into polymer matrices. The analysis of the micrographs of our samples is performed by the Image Pro® Plus software.

The image acquisition is one of the most important steps of micrograph analysis. In fact, the resolution that must be used to visualise and read the micrographs into a computer, in order to interpret and elaborate them, strongly influences the successive statistical analyses. Many instruments nowadays available for morphological investigations, such as optical and electron microscopes, are interfaced with Charge-Coupled-Devices (CCD) cameras or plane scanners at high resolution, which convert the image into a numeric form through a process known as image digitalisation.

The digitalisation process divides an image into a grid, or array of very small regions called picture elements, or pixels (**Figure 1.5**). In the computer the image is represented by this digital grid, or bitmap. Each pixel in the bitmap is identified by its position in

the grid, i.e., by its row (x) and column (y) number, and by an integer, which represents the grey tone of the image at that point [102].

Bit depth is the number of bits used to store information about each pixel. The higher the depth, the more colours are stored in an image. For example, 1 bit graphics are only capable of showing two colours, black and white. This is because there are only two combinations of numbers in one bit, 0 and 1. Images in grey scale have usually 8-bits of information - as a consequence there are 256 levels of grey, including absolute black, absolute white and 254 shades of grey in between (**Figure 1.6**).

When an image is digitalised, the width and height of the array are chosen and fixed. The total number of pixels in the image identifies the spatial resolution, which is measured in pixels per inch (ppi). The higher is the resolution the more pixels are in the image.

1.4.3 Image Analysis

When the digitalised image is saved, each successive step must be referred to the magnification of the original image. Choosing an appropriate calibration scale, each

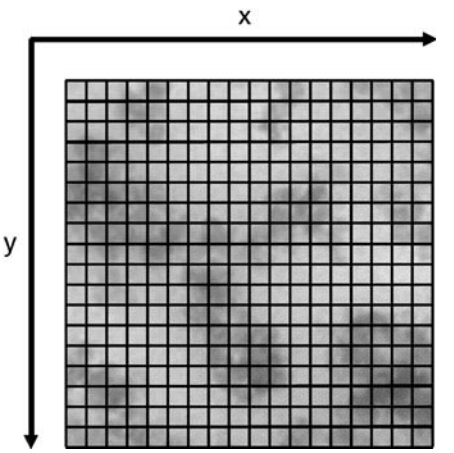

Figure 1.5. Spatial sampling of the image

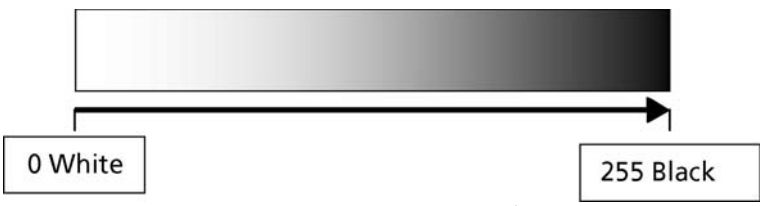

Figure 1.6 Grey tone scale

mathematical operation performed in terms of image pixel position, e.g., distances between objects, area, perimeter and shape of the objects, is converted into appropriate measure units (nanometres, microns, and so on).

To perform a correct analysis it is necessary to define within each micrograph a subset of pixels, called 'area of interest' (AOI), which does not contain the dark margins of the original image. It is important to note that original image and AOI will have exactly the same calibration scale.

Figure 1.7 shows a typical TEM micrograph of the system silica-SBR taken at 20000x. Due to the different electron density, the matrix appears lighter in colour than the silica and it is possible to distinguish the filler aggregates without applying particular selective contrasts. However, if the thickness of the cryosection is not perfectly uniform or if impurities are present, the matrix may not have a uniform shade, which makes the analysis more difficult and might introduce errors during the particle identification. Thus, for each system a careful choice of an appropriate filtering procedure is fundamental to identify exactly all the silica aggregates with their irregular and complex perimeters and to make sure that any single particle is selected. In fact, in the case of the single particle, the grey tone is only slightly deeper than that attributed to the polymer matrix.

In particular, for the SBR compound filled with silica a sequence of different image filters was selected and optimised to discriminate exactly the filler particles from the elastomer matrix. Each of them has its own function: i) to soften the image by eliminating high-frequency information using a Gaussian function. This has the effect of smoothing all the grey tones; ii) to enhance fine details, e.g., the filler aggregates; iii) to reduce the

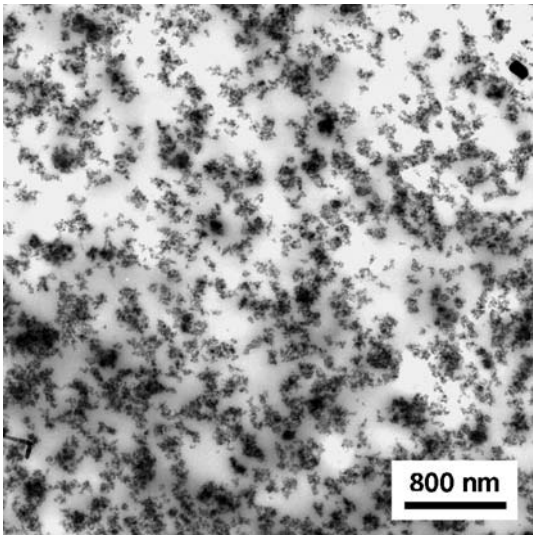

Figure 1.7 TEM micrograph of SBR loaded with 35 phr of TESPT-modified silica

intensity variations in the background pixels (attenuation of the differences in the grey tones both in the matrix and in the filler).

After this procedure the lighter homogeneous grey tone is assigned to the elastomer matrix, as shown in **Figure 1.8**. Once the image has been optimised, the subtraction of the polymer matrix, given by the lowest intensity grey, from the image makes it possible to apply the measuring procedures to all silica aggregates.

1.4.4 Statistical Analysis

Statistical and quantitative results of the filler dispersion into the matrix are attained through the analysis of 10-15 images taken in different positions of the sample. For a correct comparison between two different systems, exactly the same total area is analysed. In this way several thousands of objects are identified and the results can be considered representative of the system under investigation.

Afterwards, on the digital bi-dimensional images the morphometric descriptors (e.g., area, perimeter, aspect ratio, roundness, and so on) are applied.

Finally, after the selection of all the grey tones associated with the filler, the program automatically identifies and counts the silica particles (**Figure 1.9**) and collects the data in a file where the object number and the corresponding values of all the selected parameters are registered.

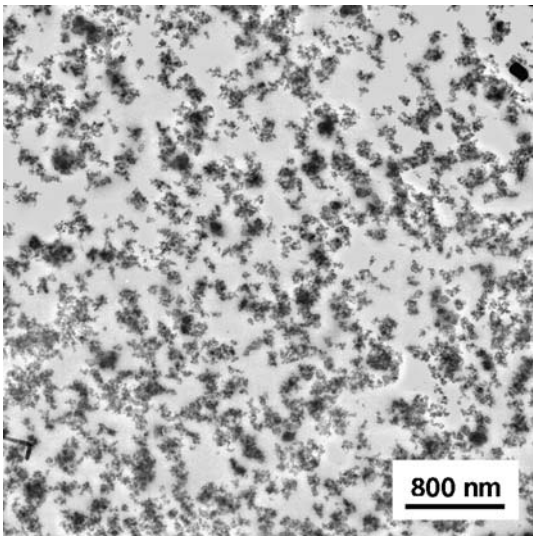

Figure 1.8 TEM micrograph of SBR loaded with 35 phr of TESPT-modified silica after the application of the filter sequence

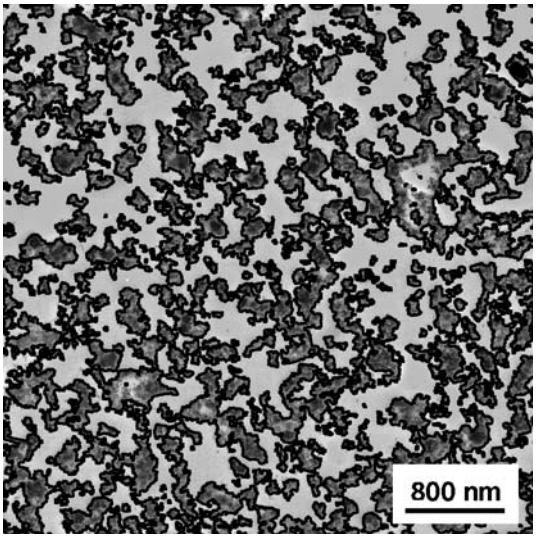

Figure 1.9 TEM micrograph from which all the aggregates are identified for the analysis

1.5 Morphology of Carbon Black Dispersions

1.5.1 Dry state

Even if considerable breakdown of the larger and more irregular aggregates occurs when carbon black and silica are mixed with rubber or other high viscosity vehicle systems, the original size of particles and aggregates and their distribution are probably the most important physical properties in terms of end use application.

Many papers have been devoted to the study of carbon black and silica used in preparing reinforced rubber compounds [5, 24, 25, 47-70].

In recent years, the most relevant results on carbon black aggregates were reported by Donnet and co-workers [64]. They have shown that AFM can be used to image carbon black aggregate dispersions. By depositing droplets of a suspension of carbon black in acetone onto a gold coated glass support, they made a very homogeneous dispersion of aggregates. Moreover, they never observed dendritic aggregates as usually imaged by TEM. This difference was ascribed to an agglomeration phenomenon occurring during the sample preparation. However, the resolution achieved by AFM is not as high as with TEM, therefore they observed aggregates with particles bigger (about 50 nm) than those generally obtained (about 20 nm) in the case of carbon black N115.

1.5.2 Compounds

A few papers deal with the characterisation of filled rubber compounds by microscopic investigations associated with image analysis and, to our knowledge, unlike the literature related to filler dispersions in the dry state, most of the scientific papers are devoted to composite systems loaded with silica. The increasing interest in this filler is that, when compared to carbon black, it improves tyre performance in terms of wet traction, rolling and wear resistance, together with the recent development of automated image analysis methods can account for this.

The automated measurements of aggregate size and shape of carbon black either in the dry state or dispersed into SBR/BR vulcanisates, was firstly made by Hess and co-workers [49]. They showed that a considerable breakdown of the pristine aggregates occurs when they are mixed with rubber, with significant reduction of their size. More recently, the microdispersion of carbon black in unvulcanised and vulcanised ethylene-propylene-diene rubber (EPDM) has been investigated by AFM [96]. Phase imaging was found to be the most useful mode to distinguish filler particles and to obtain their size distribution, as they have a bright shade in the dark rubber matrix. However, the grainy morphology at the rubber surface can interfere with the imaging of fillers, thus making the selection of the dispersed phase more difficult.

The use of different types of microscopic and automated image analyses, aimed to define the particle size, the aggregate morphology and structure of many grades of carbon blacks, as well as their distribution in elastomer-based composites, has been widely reviewed in [69].

1.6 Morphometric Analysis on Silica Filled Compounds

1.6.1 Atomic Force Microscopy/Automated Image Analysis

Atomic force microscopy has been used to investigate different filled elastomers [44, 95, 96]. Statistical analyses for SBR-based compounds, loaded with different amounts of precipitated silica (5-15 vol.%), was performed on AFM images to determine the distribution of the aggregate areas of the filler and to evaluate the bound-rubber layer [44]. Morphology, size distribution of filler particles have been determined for EPDM compounds loaded with up to 50 phr of silica by using tapping mode phase imaging [96]. The beneficial effect given by the addition of TESPT as a coupling agent was shown. In fact, when compared to untreated silica, a significant amount of much smaller particles was detected.

TMAFM was used to study silicone elastomers filled with silica [95]. A good contrast between the matrix and the filler structures can be achieved thus allowing determination of

the average particle size. Nevertheless, as several parameters can affect the phase contrast, a careful choice of the experimental conditions is necessary, in order to obtain quantitative and reliable results. A comparison between the average particle size, determined on AFM and TEM images, is given by the same authors. Even if a good agreement between the results obtained with the two techniques was found, the TEM values were always slightly lower, due to the higher resolution of TEM as compared to AFM.

1.6.2 Transmission Electron Microscopy/Automated Image Analysis

In a series of papers aimed at investigating the effect of the secondary structure of the filler on the mechanical properties of SBR and NBR/silica composites [85-87], transmission electron microscopy and image analysis, performed on digital binary images converted from TEM micrographs, were successfully used to determine the average size of filler aggregates, to detect the breakdown of the filler secondary network, and to support the existence of an entrapped rubber phase within the agglomerates. The following conclusions were drawn: the higher the hydrophilic character of the silica surface (number of silanol groups per unit surface area of silica), the larger is the size of the agglomerates; the larger the aggregates the higher is the content of bound rubber entrapped. Furthermore, the stress-strain behaviour of silica-filled SBR vulcanisates is significantly affected by the particle size.

Following the procedure described in Section 1.4, technical compounds based on different rubber matrices (BR, NR, SBR) and loaded with various kinds and amounts of silica have been analysed by TEM associated with automated image analysis [88-91].

As can be seen from **Figure 1.10**, by increasing the amount of filler it becomes more difficult to recognise morphometric differences in the filler particles by simple visual observations of the TEM micrographs. Thus, to attain quantitative and significant results on filler dispersion and, consequently, on the polymer/filler interactions, the analysis of TEM micrographs by automated image analysis was performed.

By applying this procedure a significant difference in terms of size and shape of the dispersed particles was found for the three compounds based on SBR, BR, NR rubbers and loaded with the same amount of silica, 35 phr [88, 89]. In fact, in NR and BR the number of filler particles is smaller than that counted in SBR, as can be seen in **Figure 1.11** where the difference is clearly evident in the range of lower surface area. Furthermore, by using as a morphological descriptor, the area to perimeter ratio (A/P), it was found that aggregates with similar surface area have quite different perimeters, i.e., different shape (**Figure 1.12**). In particular, the results indicate that interactions of silica are favoured with the SBR matrix.

In the case of SBR filled with 35 phr of silica untreated or surface modified by TESPT, it is not possible to identify any difference in size, shape and distribution of silica

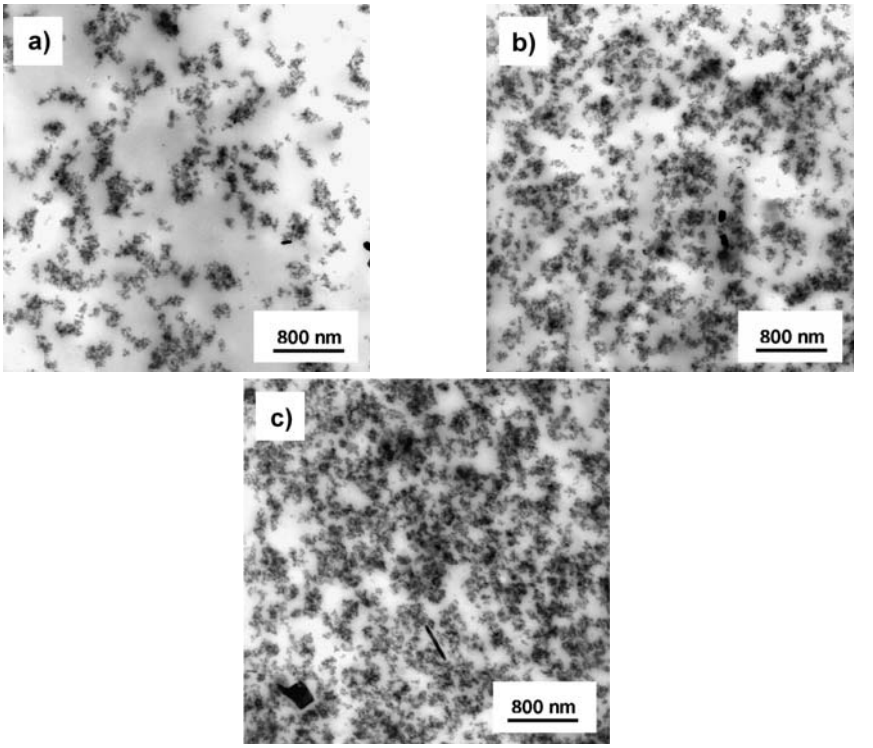

Figure 1.10 TEM micrographs of SBR compound loaded with unmodified silica: a) 20 phr; b) 35 phr; c) 50 phr

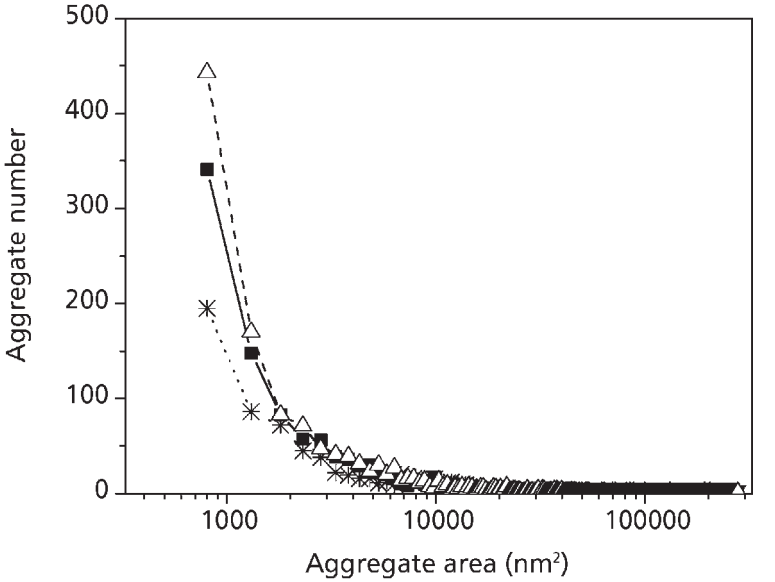

Figure 1.11 Aggregate number of silica against their area in compounds based on: △ SBR; ■ NR; ✳ BR

particles from TEM images (**Figure 1.13**). The selection and application of morphometric descriptors such as A/P, roundness ($P^2/4\pi A$) and shape factor ($\Phi = L_1/L_2$) from the AIA procedure allowed us to show that the two morphologies are different.

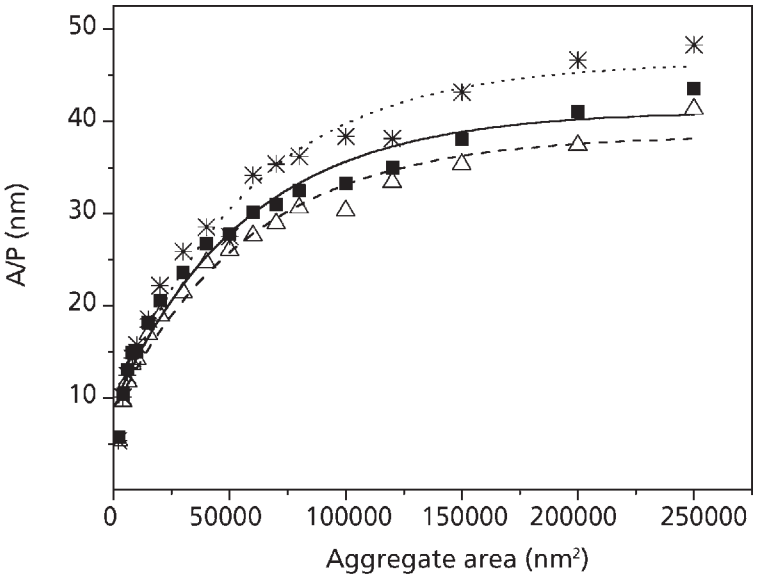

Figure 1.12 Area/Perimeter ratio of aggregates against their area in compounds based on: △ SBR; ■ NR; ✳ BR

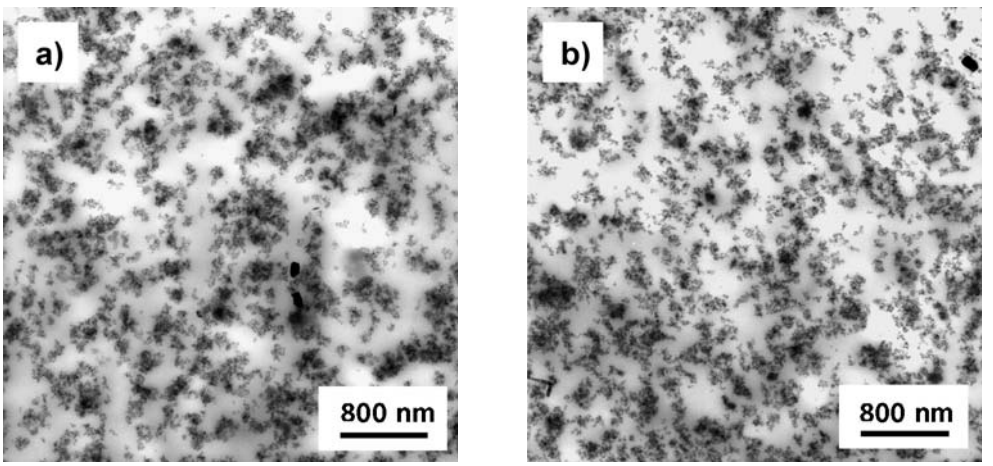

Figure 1.13 TEM micrographs of ultrathin sections of SBR-compounds loaded with 35 phr of silica: a) unmodified; b) TESPT-modified

In fact, the A/P ratio and the roundness give information on the irregularity of the perimeter and describe the degree of branching; the shape factor Φ, defined as the ratio between major (L_1) and minor (L_2) axes of the ellipse equivalent to the selected aggregate (**Figure 1.4c**), indicates a more or less elongated shape. Aggregates with regular and spherical shapes are characterised by values of $P^2/4\pi A$ and Φ near to unity, while values higher than one indicate more linear and considerably elongated structures.

All the silica particles were selected on the basis of proper ranges of area, i.e., only objects with very similar surface area (differences < 10%) were included in the same group. For each range, perimeter, A/P ratio, roundness and aspect ratio were evaluated. The behaviour of A/P as a function of consecutive ranges of area is given, as an example in **Figure 1.14**, where the beneficial effect of the surface modification is evident. Indeed, the A/P values of SBR-compounds loaded with 35 phr of modified silica are generally lower than those obtained for samples filled with the same amount of unmodified silica. This indicates that, in spite of having the similar area, aggregates of modified silica are characterised by higher perimeter, which means higher contact surface between filler and elastomer. Furthermore, it must be pointed out that, as a consequence of the increased filler-elastomer interactions, the maximum area of the filler particles is lower when TESPT is present.

On increasing silica loading (50 phr), a morphometric analysis based on the same procedure becomes more difficult, as can be deduced from **Figure 1.10c**.

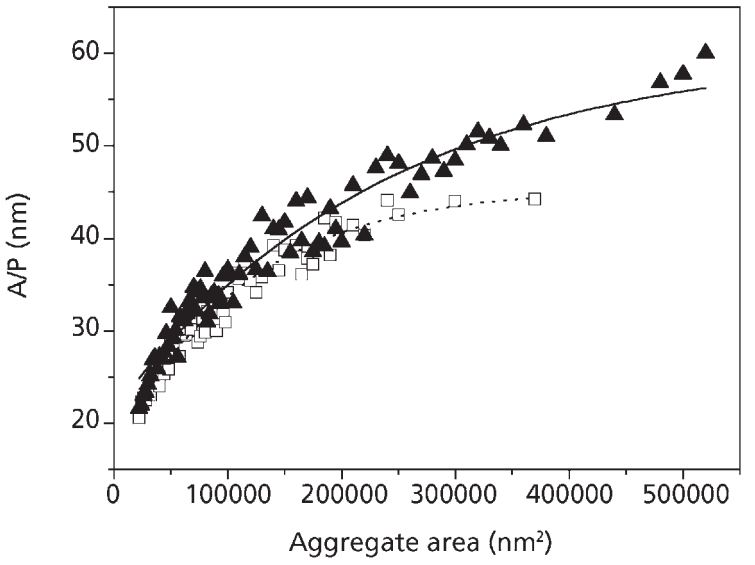

Figure 1.14 A/P ratio of aggregates in SBR-compounds loaded with 35 phr of filler as a function of their area: ▲ SiO_2; □ TESPT-SiO_2

Indeed, some of the results we have obtained by two-dimensional image analysis on this system are apparently contradictory (**Figure 1.15**): on one hand, as expected, the overall number of aggregates and the surface area covered by them is higher when silica is modified with TESPT; on the other hand, the size of the biggest aggregates is higher than that of unmodified silica particles. Superimposition of the aggregates, which can easily occur due to the high amount of filler, and can be favoured if the filler is better dispersed, together with the difficulty of identifying exactly the contact surface area between the filler and the matrix, might be responsible for these findings. A further contribution to the surface area covered by the filler might be given by the bound rubber, according to the results reported by Yatsuyanagi and co-workers [85].

Also the behaviour of A/P as a function of consecutive ranges of area reported in **Figure 1.15** does not supply any useful information. In fact, no significant differences can be seen between the two composites systems. Thus, to characterise compounds containing high amounts of filler, different methods must be exploited.

1.6.3 Microdensitometry and 3D-TEM/Electron Tomography

To achieve information on the dispersion of highly loaded compounds, where the three-dimensional superposition of the filler aggregates can easily occur, different methods, based on densitometric evaluations, were developed [94, 103].

In TEM images filler particles appear as dark objects because of their density, which is higher than that of the rubbery matrix. Since these images are the projection of thin sections (about 50 nm thick), some filler particles may overlap along the thickness

	SBR + SiO_2	SBR + TESPT-SiO_2
Total number of aggregates	3896	6033
Surface covered (%)	39	48
Minimum area (nm^2)	140	140
Maximum area (nm^2)	1280000	1450000

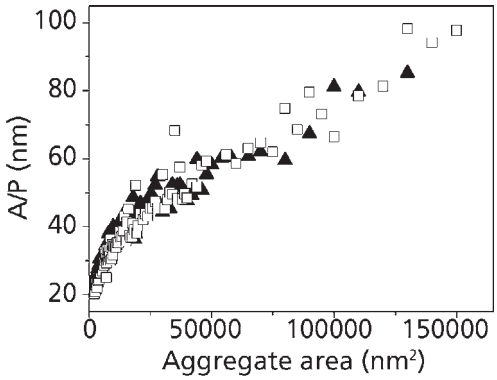

Figure 1.15 Results from TEM/AIA for SBR loaded with 50 phr of silica: ▲ SiO_2; □ TESPT-SiO_2

of the section. The more filler particles overlap, the darker is the TEM image at the specific position. A bitmap analysis of the grey value intensity of all pixels constituting the digitalised TEM image can be applied to investigate the distribution of the filler for highly loaded systems.

An interesting paper has been published recently [94], where the random field method has been applied. This method exploits the fluctuations in the grey-values without using a threshold grey-value, not always easy to define. Two random field parameters are determined, which describe the dispersion grade of the filler: variance, σ^2, which describes the level of fluctuation of the local filler loadings; median range, $h_{0.5}$, which is a measure of the size of objects such as clusters of filler particles or unfilled areas.

The Authors are currently progressing in the application of a procedure based on an appropriate calibration of the grey value intensity combined with the selection of fundamental morphological descriptors (shape and minimum size). This combination is aimed to discriminate the matrix and to separate it from single particles, aggregates and agglomerates of the filler. Darker pixels or linked pixel groups correspond to specific domains in which particle overlapping is more frequent and as a consequence agglomeration is stronger [103].

Although the densitometric approach for the investigation of TEM images does not provide many details about the dimension and shape of agglomerates, it appears to be a useful method to evaluate the distribution of the filler in highly loaded compounds.

A new approach to visualise and evaluate structural characteristics in a three-dimensional space (3D) of particulate silicas in natural rubber has been proposed very recently [92, 93]. The observations were carried out on compounds containing silica dispersed in NR either by conventional methods or by *in situ* preparation through the sol-gel process. A TEM combined with electron tomography, 3D-TEM, a powerful tool to evaluate the morphology in the three dimensions space both in bio and material science, was used. For three-dimensional structural observations, a series of TEM images at various angles were obtained, by tilting a very thin sample from –65° to +65°. The number of silica aggregates in a definite volume, the radius, the aspect ratio and their distribution, the volume of each particle and, consequently, the total volume of silica were calculated from 3D-TEM.

Acknowledgements

The authors like to thank Mr. G. Dondero for helpful collaboration in performing TEM analysis and Pirelli Pneumatici SpA for supplying rubber compounds.

References

1. A.R. Payne, *Journal of Applied Polymer Science*, 1962, **6**, 19, 57.

2. S. Wolff and M-J. Wang in *Carbon Black: Science and Technology*, 2nd Edition, Eds., J-B. Donnet, R.C. Bansal and M-J. Wang, Marcel Dekker, New York, NY, USA, 1993, Chapter 9, p.289.

3. E.M. Dannenberg, *Rubber Chemistry and Technology*, 1975, **48**, 3, 410.

4. W.H. Waddell and L.R. Evans, *Rubber Chemistry and Technology,* 1996, **69**, 3, 377.

5. J-B. Donnet, *Rubber Chemistry and Technology,* 1998, **71**, 3, 323.

6. M-J. Wang, *Rubber Chemistry and Technology,* 1998, **71**, 3, 520.

7. M-J. Wang, *Rubber Chemistry and Technology,* 1999, **72**, 2, 430.

8. K.A. Grosch, *Rubber Chemistry and Technology,* 1996, **69**, 3, 495.

9. G. Kraus in *Science and Technology of Rubber*, Eds., F.R. Eirich and J.R. Beatty, Academic Press, New York, NY, USA, 1978, Chapter 8.

10. J. Frölich, W. Niedermeier and H.D. Luginsland, *Composites Part A: Applied Science and Manufacturing*, 2005, **36**, 4, 449.

11. R. Rauline, inventor; Michelin & Cie, assignee; US 5,227, 425, 1993.

12. Y. Bomal, P. Cochet, B. Dejean, I. Gelling and R. Newell, *Kautschuk und Gummi Kunststoffe*, 1998, **51**, 4, 259.

13. F.G. Corvasce, T.D. Linster and G. Thielen, inventors; Goodyear Tyre & Rubber Co, assignee; EP 0,795,581B1, 2001.

14. E. Custodéro and J-C. Tardivat, inventors; Michelin & Cie, assignee; EP 0810258 B1, 2001.

15. H.M. Da Costa, L.L.Y. Visconte, R.C.R. Nunes and C.R.G. Furtado, *Journal of Applied Polymer Science*, 2002, **83,** 11, 2331.

16. P. Sae-Oui, C. Rakdee and P. Thanmathorn, *Journal of Applied Polymer Science*, 2002, **83,** 11, 2485.

17. E.N. Kresge and D.J. Lohse, inventors; Exxon Chemical Patents Inc., assignee; US 5,576,372, 1996.

18. F. Schön and W. Gronski, *Kautschuk und Gummi Kunststoffe*, 2003, **56**, 4, 166.

19. S. Varghese and J. Karger-Kocsis, *Journal of Applied Polymer Science*, 2004, **91**, 2, 813.

20. M-J. Wang, K. Mahmud, L.J. Murphy and W.J. Patterson, *Kautschuk und Gummi Kunststoffe*, 1998, **51**, 5, 348.

21. A.M. Shanmugharaj, S. Ray, S. Bandyopadhyay and A.K. Bhowmick, *Journal of Adhesion Science and Technology*, 2003, **17**, 9, 1167.

22. A. Croce, *Studio delle interazioni tra matrici elastomeriche e cariche rinforzanti a base di nero di carbonio e silice sia tal quale che modificata*, University of Genova, Italy, 2002.

23. S-S. Choi, C. Nah, S.G. Lee and C.W. Joo, *Polymer International*, 2003, **52**, 23.

24. W.M. Hess and C.R. Herd in *Carbon Black: Science and Technology*, 2nd Edition, Eds., J-B. Donnet, R.C. Bansal and M-J. Wang, Marcel Dekker, New York, NY, USA, 1993, Chapter 3, p.289.

25. W.M. Hess, G.C. McDonald and E. Urban, *Rubber Chemistry and Technology*, 1973, **46**, 1, 204.

26. A.I. Medalia, *Rubber Chemistry and Technology*, 1974, **47**, 2, 411.

27. S. Wolff, *Rubber Chemistry and Technology,* 1996, **69**, 3, 325.

28. S. Wolff, M-J. Wang and E.H. Tan, *Kautschuk und Gummi Kunststoffe*, 1994, **47**, 12, 873.

29. J.L. Leblanc, *Progress in Polymer Science*, 2002, **27**, 4, 627.

30. S.K. Watson in *Handbook of Fillers for Plastics*, Eds., H.S. Kats and J.V. Milewski, Van Nostrand Reinhold Company Inc., New York, NY, USA, 1987, Chapter 9, p.165.

31. H.W. Engels, H.J. Weidenhaupt, M. Abele and M. Pieroth in *Ullmann's Encyclopedia of Industrial Chemistry*, Volume A23, Refractory Ceramics to Silica-Carbide, 5th Edition, Eds., B. Elvers and S. Hawkins, Wiley-VCH Publishers, 1993, p.365.

32. S.K. Mowdood, J.L. Locatelli, Y. De Puydt and A. Serra in *Proceedings of Intertech Functional Tire Fillers 2001 Conference*, Fort Lauderdale, FL, USA, 2001.

33. D.W. Schaefer and C. Chen, *Rubber Chemistry and Technology*, 2002, **75**, 5, 773.

34. D.W. Schaefer, C. Suryawanshi, P. Pakdel, J. Ilavsky and P.R. Jemian, *Physica A: Statistical Mechanics and its Applications*, 2002, **314**, 1-4, 686.

35. A. Hunsche, U. Görl, A. Müller, M. Knaack and T. Göbel, *Kautschuk und Gummi Kunststoffe*, 1997, **50**, 12, 881.

36. A. Hunsche, U. Görl, H.G. Koban and T. Lehmann, *Kautschuk und Gummi Kunststoffe*, 1998, **51**, 7-8, 525.

37. U. Görl and A. Parkhouse, *Kautschuk und Gummi Kunststoffe*, 1999, **52**, 7-8, 493.

38. U. Görl, J. Münzenberg, D. Luginsland and A. Müller, *Kautschuk und Gummi Kunststoffe*, 1999, **52**, 9, 588.

39. J.W. ten Brinke, P.J. van Swaaij, L.A.E.M. Reuvekamp and J.W.M. Noordermeer, *Kautschuk und Gummi Kunststoffe*, 2002, **55**, 5, 244.

40. L.A.E.M. Reuvekamp, J.W. ten Brinke, P.J. van Swaaij and J.W.M. Noordermeer, *Rubber Chemistry and Technology*, 2002, **75**, 2, 187.

41. J.W. ten Brinke, S.C. Debnath, L.A.E.M. Reuvekamp and J.W.M. Noordermeer, *Composites Science and Technology*, 2003, **63**, 8, 1165.

42. G.R. Hamed, *Rubber Chemistry and Technology,* 1981, **54**, 2, 403.

43. P.L. Cho and G.R. Hamed, *Rubber Chemistry and Technology,* 1992, **65**, 2, 475.

44. P. Mélé, S. Marceau, D. Brown, Y. de Puydt and N.D. Albérola, *Polymer*, 2002, **43**, 20, 5577.

45. L. Flandin, D. Labarre, Y. Bomal and L. Ladouce-Stelandre, *Rubber Chemistry and Technology,* 2003, **76**, 1, 145.

46. C. Gauthier, E. Reynaud, R. Vassoille and L. Ladouce-Stelandre, *Polymer*, 2004, **45**, 8, 2761.

47. A.I. Medalia, *Journal of Colloid and Interface Science*, 1967, **24**, 393.

48. A.I. Medalia, *Journal of Colloid and Interface Science*, 1970, **32**, 1, 115.

49. W.M. Hess, L.L. Ban and G.C. McDonald, *Rubber Chemistry and Technology*, 1969, **42**, 4, 1209.

50. K.A. Burgess, C.E. Scott and W.M. Hess, *Rubber Chemistry and Technology*, 1971, **44**, 1, 230.

51. H.N. Mercer, A.H. Boyer, P.L. Brusky and M.L. Deviney, *Rubber Chemistry and Technology*, 1976, **49**, 4, 1068.

52. G.C. McDonald and W.M. Hess, *Rubber Chemistry and Technology*, 1977, **50**, 4, 842.

53. W.M. Hess and G.C. McDonald, *Rubber Chemistry and Technology*, 1983, **56**, 5, 892.

54. M. Gerspacher and C.P. O'Farrell, *Elastometrics*, 1991, **123**, 4, 35.

55. C.R. Herd, G.C. McDonald and W.M. Hess, *Rubber Chemistry and Technology*, 1992, **65**, 1, 107.

56. C.R. Herd, G.C. McDonald, R.E. Smith and W.M. Hess, *Rubber Chemistry and Technology*, 1993, **66**, 4, 491.

57. T.C. Gruber, T.W. Zerda and M. Gerspacher, *Rubber Chemistry and Technology*, 1994, **67**, 2, 280.

58. T.C. Gruber and C.R. Herd, *Rubber Chemistry and Technology*, 1997, **70**, 5, 727.

59. T.C. Gruber, *Kautschuk und Gummi Kunststoffe*, 1998, **51**, 3, 194.

60. S. Maas and W. Gronski, *Kautschuk und Gummi Kunststoffe*, 1999, **52**, 1, 26.

61. E.M. Hunt, C.R. Herd, D. Tandon and T.C. Gruber in *Proceedings of the Third International Conference on Carbon Black*, Mulhouse, France, 2000, p.129.

62. M-J. Wang, S. Wolff and B. Freund, *Rubber Chemistry and Technology*, 1994, **67**, 1, 27.

63. J-B. Donnet and T.K. Wang, *Macromolecular Symposia*, 1996, **108**, 97.

64. J-B. Donnet, E. Custodero and T.K. Wang, *Kautschuk und Gummi Kunststoffe*, 1996, **49**, 4, 274.

65. A.J. Hurd, D.W. Schaefer and J.E. Martin, *Physical Review A*, 1987, **35**, 5, 2361.

66. G. Beaucage and D.W. Schaefer, *Journal of Non-Crystalline Solids*, 1994, **172-174**, 2, 797.

67. D.W. Schaefer, T. Rieker, M. Agamalian, J.S. Lin, D. Fischer, S. Sukumaran, C.Y. Chen, G. Beaucage, C. Herd and J. Ivie, *Journal of Applied Crystallography*, 2000, **33,** 1, 587.

68. T.W. Zerda, J. Qian, C. Pantea and T. Ungar, *Materials Research Society Symposia*, 2001, **661**, 6.4.1.

69. W.M. Hess, C.R. Herd and E.B. Sebok, *Kautschuk und Gummi Kunststoffe*, 1994, **47**, 5, 328.

70. W. Niedermeier, J. Stierstorfer, S. Kreitmeier, O. Metz and D. Goritz, *Rubber Chemistry and Technology*, 1994, **67**, 1, 148.

71. G. Beaucage, S. Rane, D.W. Schaefer, G. Long and D. Fischer, *Journal of Polymer Science Part B: Polymer Physics*, 1999, **37**, 11, 1105.

72. F. Ehrburger-Dolle, M. Hindermann-Bischoff, E. Geissler, C. Rochas, F. Bley and F. Livet, *Materials Research Society Symposia*, 2001, **661**, 7.4.1.

73. F. Ehrburger-Dolle, F. Bley, E. Geissler, F. Livet, I. Morfin and C. Rochas, *Macromolecular Symposia*, 2003, **200**, 157.

74. S. Westermann, M. Kreitschmann, W. Pyckhout-Hintzen, D. Richter and E. Straube, *Physica B: Condensed Matter*, 1997, **234-236**, 306.

75. A. Botti, W. Pyckhout-Hintzen, D. Richter, V. Urban, E. Straube and J. Kohlbrecher, *Polymer*, 2003, **44**, 24, 7505.

76. R. Appel, T.W. Zerda and W.H. Waddell, *Applied Spectroscopy*, 2000, **54**, 11, 1559.

77. T.W. Zerda, G. Song and W.H. Waddell, *Rubber Chemistry and Technology*, 2003, **76**, 4, 769.

78. H. Ismail and P.K. Freakley, *Polymer-Plastics Technology and Engineering*, 1997, **36**, 6, 873.

79. W.M. Hess, C.E. Scott and J.E. Callan, *Rubber Chemistry and Technology*, 1967, **40**, 2, 371.

80. V.E. Hanchett and R.H. Geiss, *IBM Journal of Research and Development*, 1983, **27**, 4, 348.

81. J.M. Massie, R.C. Hirst and A.F. Halasa, *Rubber Chemistry and Technology*, 1993, **66**, 2, 276.

82. Y. Li, M-J. Wang, T. Zhang, F. Zhang and X. Fu, *Rubber Chemistry and Technology*, 1994, **67**, 4, 693.

83. L.R. Evans and W.H. Waddell, *Kautschuk und Gummi Kunststoffe*, 1995, **48**, 10, 718.

84. C.D. Eisenbach, A. Ribbe, A. Göldel, *Kautschuk und Gummi Kunststoffe*, 1996, **49**, 6, 406.

85. F. Yatsuyanagi, N. Suzuki, M. Ito and H. Kaidou, *Polymer*, 2001, **42**, 23, 9523.

86. N. Suzuki, F. Yatsuyanagi, M. Ito and H. Kaidou, *Journal of Applied Polymer Science*, 2002, **86**, 7, 1622.

87. N. Suzuki, M. Ito and S. Ono, *Journal of Applied Polymer Science*, 2005, **95**, 1, 74.

88. M. Castellano, L. Falqui, G. Costa, A. Turturro, B. Valenti and G. Castello, *Journal of Macromolecular Science B - Physics*, 2002, **41**, 3, 451.

89. L. Falqui, G. Costa, M. Castellano, A. Turturro and B. Valenti, *Rubber Chemistry and Technology*, 2003, **76**, 4, 899.

90. G. Costa, G. Dondero, L. Falqui, M. Castellano, A. Turturro and B. Valenti, *Macromolecular Symposia*, 2003, **193**, 195.

91. M. Castellano, L. Conzatti, A. Turturro, G. Costa and G. Busca, *Journal of Physical Chemistry B*, 2007, **111**, 17, 4495.

92. Y. Ikeda, A. Katoh, J. Shimanuki and S. Kohjiya, *Macromolecular Rapid Communications*, 2004, **25**, 12, 1186.

93. S. Kohjiya, A. Katoh, J. Shimanuki, T. Hasegawa and Y. Ikeda, *Polymer*, 2005, **46**, 12, 4440.

94. A. Tscheschel, J. Lacayo and D. Stoyan, *Journal of Microscopy*, 2005, **217**, 1, 75.

95. F. Clèment, A. Lapra, L. Bokobza, L. Monnerie and P. Mènez, *Polymer*, 2001, **42**, 14, 6259.

96. D. Trifonova-Van Haeringen, H. Shonherr, G.J. Vancso, L. van der Does, J.W.M. Noordermeer and P.J.P. Janssen, *Rubber Chemistry and Technology*, 1999, **72**, 5, 862.

97. A. Lapra, F. Clèment, L. Bokobza and L. Monnerie, *Rubber Chemistry and Technology*, 2003, **76**, 1, 60.

98. F. Endter and H. Gebauer, *Optik*, 1956, **13,** 97.

99. W.M. Hess and G.C. McDonald, *Measuring Dynamic properties of Vulcanisates, Rubber and Related Products: New Methods for Testing and Analysing*, ASTM, STP 553, ASTM, West Conshohocken, USA, 1974.

100. ASTM D3849, *Standard Test Method for carbon Black – Morphological Characterisation of Carbon using Electron Microscopy*, 2004.

101. J.C. Russ in *Computer-Assisted Microscopy: the Measurement and Analysis of Images*, Plenum Press, New York, NY, USA, 1990.

102. T.M. Cover and J.A. Thomas in *Elements of Information Theory*, Ed., D.L. Schilling, Wiley-Interscience, New York, NY, USA, 2001, Chapter 3, p.50.

103. Our unpublished results.

2 Intelligent Tyres

Brian Logan

2.1 Introduction

Many areas of rubber technology are well established. In contrast, intelligent tyres are in their infancy. Intelligent tyres blend the fields of electronics and tyre technology to offer tyres with unique benefits, from logistics to safety to integration with vehicle control systems. Just as electronics revolutionised the modern automobile industry, intelligent tyres will revolutionise the tyre industry.

Initially, the concept was to give the tyre an electronic serial number, which could track the tyre through manufacturing, distribution, and ultimate disposal. Since then, it has expanded to include pressure, temperature, and other parameters. At one time or another almost every major tyre company has announced that they were developing an intelligent tyre. Most of these concepts include sensors, and communication at radio frequencies.

As of November 2007 , the largest implementation of electronics in tyres is the use of radio frequency identification (RFID) tags in NASCAR racing tyres, implemented at the start of the 2006 racing season.

This chapter will describe intelligent tyres, starting with potential features. A brief history is covered, to help the reader understand its growth and the current environment. The major part of the chapter will discuss design considerations for such a system.

2.2 Features of the Intelligent Tyre

An intelligent tyre is one that communicates useful information to the user. **Table 2.1** lists examples of information and the benefits of that information.

It is important to note that not all of these features are practical or feasible at this time. Some have been demonstrated in prototype tyres, or claimed in patents, but have not yet been shown to be reliable in normal tyre service.

Looking at current electronics technology, the most likely features are an ID number (along with some memory), pressure, and temperature. The challenge is to integrate them into tyres at a reasonable price.

Table 2.1. Some of the potential features and benefits of intelligent tyres	
Features	**Benefits**
Unique Identification number (ID)	• Anti-theft • Tyre and casing tracking • Inventory control
Read/Write memory	• General tyre information (DOT number, size, type) • Tyre history • Tyre performance characteristics • Customer can write data
Service history	• Maximum temperature • Miles run at low pressure • Repair and retread history
Temperature	• Overload/abuse warning • Brake/wheel overheat alert • Converts from 'hot' to 'cold' pressure
Pressure	• Driver safety • Correct pressure to optimise treadwear • Correct pressure to optimise rolling resistance and fuel economy • Maximise carcass life • Detect leaks • Reduce likelihood of failure
Cornering force	• Vehicle handling • Input to vehicle stability control
Coefficient of friction	• Traction • Input to vehicle stability control
Tyre mileage	• Determine when to replace • Estimate cost of operation (cost per mile)
Treadwear	• Wear projections • Detect worn-out tyre
DOT: US Department of Transportation *The DOT number is assigned by the tyre manufacturer to track month and year of manufacture, essentially denoting a specific production lot. The format is standard throughout the industry (see Section 2.2.1)*	

2.2.1 Identification and Memory

Every tyre made for use in the United States is stamped with a standard number – the DOT number – which identifies the tyre manufacturer and plant, size and type, some additional information, and the week and year of its manufacture. The DOT consists of 12 alphanumeric digits. This is helpful if one wanted to know general information about that tyre. It also identifies the tyre's production lot. However, the DOT cannot

identify a unique tyre. In commercial applications, such as trucks, buses, earthmovers, and aircraft, knowledge of a tyre's service history is important. Fleets can use this data to track the costs associated with their tyres, which, next to fuel, are their largest operating expense. A unique identifier would allow the fleets to track that tyre's history. Such a number could also identify the tyre in case of theft. Currently, tyres can be branded with a unique number after manufacturing, using a branding iron, however, few fleets are interested in the added expense of branding.

RFID technology can achieve this goal. Many RFID tags have enough memory, and offer the capability to write additional data to the tag during their life, so that service history and other information could be stored.

2.2.2 Temperature

There are two temperatures that are of interest – the temperature of the tyre itself, and the temperature of the contained air cavity. The temperature being 'sensed' depends on the location of the sensor.

High temperature is the enemy of rubber. If the tyre temperature starts to increase, this is an indication that tyres should be checked. Overloading, excessive speed and underinflation all contribute to high tyre temperatures. Oxidation increases as temperature increases, which contributes to greater tyre wear. Tyre temperature could also indicate a mechanical problem. For instance, heat from a failing bearing, or a dragging brake, could conduct to the wheel and be seen in the tyre.

Tyre pressures should be set at 'cold' or ambient, temperature. The ability to determine the contained air cavity temperature allows the system to 'calculate' the equivalent cold pressures at any time, even when a tyre is hot.

Temperature sensing technology is readily available. Many pressure sensors integrate temperature sensing thermisters into their circuitry.

2.2.3 Inflation Pressure

The inflation pressure is a major operating parameter for the tyre. The load that a tyre is able to carry is directly related to tyre pressure. In fact, once the proper tyre is selected for a vehicle (proper load carrying capacity, speed rating, and so on), the single biggest influence on tyre life is maintaining the correct inflation pressure. Proper maintenance for all vehicles involves measuring and correcting tyre pressure.

If the tyre operates 'under inflated' it will deflect more, generating heat. In addition, excessive deflection in an underinflated tyre increases tyre rolling resistance, giving

poorer fuel economy. Improper inflation also gives an uneven tread footprint, which leads to poorer treadwear. Experiments have shown that 10% underinflation reduces treadwear by 5%, and fuel economy by 0.5% [1]. Over an extended running period, under-inflation will weaken the tyre's structural integrity, reducing the ability to retread that carcass.

All these factors demonstrate the need to operate tyres at the proper inflation pressure. These reasons are particularly important to commercial trucking fleets, who often have hundreds of vehicles and thousands of tyres. Next to the cost of the vehicle, tyres and fuel are two of the biggest expense items for commercial trucks. Miniaturised pressure sensors, suitable for use in tyres, are available today.

2.2.4 Cornering Forces

Measuring forces at the tyre gives the vehicle control system the feedback it can use to improve vehicle handling and maximise stability control. There are no production solutions for this type of measurement at this time; several approaches have been discussed. Continental's 'Side Wall Torsion Sensorsystem' (SWT), takes a novel approach, putting magnetic strips in the sidewall and measuring deformation with sensors mounted on the suspension [2]. There are other patents in this area, including one that uses a combination of strain sensors in the tread area to determine tyre traction [3].

2.2.5 Tyre Mileage

Measurement of tyre mileage – an odometer for the tyre –would help the fleet owner determine accurate mileage on that specific tyre. There are several patents that claim methods to determine tyre mileage. These basically count and store the revolutions that the tyre makes. Mileage can be calculated from that value [4, 5].

2.2.6 Treadwear

Measuring treadwear would be valuable, particularly in commercial tyres. Detection of low tread would allow the fleet manager to plan to replace that tyre. A reliable method to measure treadwear would have to be developed.

2.3 Historical Perspective

2.3.1 Tyres

The modern intelligent tyre can trace its beginnings to integrated circuits (IC), which promised sensing technology that would be small enough to attach to the tyre. However, patents involving electronics in tyres were granted much earlier, such as a 1966 patent that embedded a conductive wire in the sidewall of a tyre, as shown in **Figure 2.1** [6]. Early failure of the conductor wires would allow the operator to replace the tyre before failure.

Through the 1970s, patents were filed on various methods of sensing pressure in tyres. These generally involved attaching a pressure sensing device to the wheel, or alternatively to the valve stem [6].

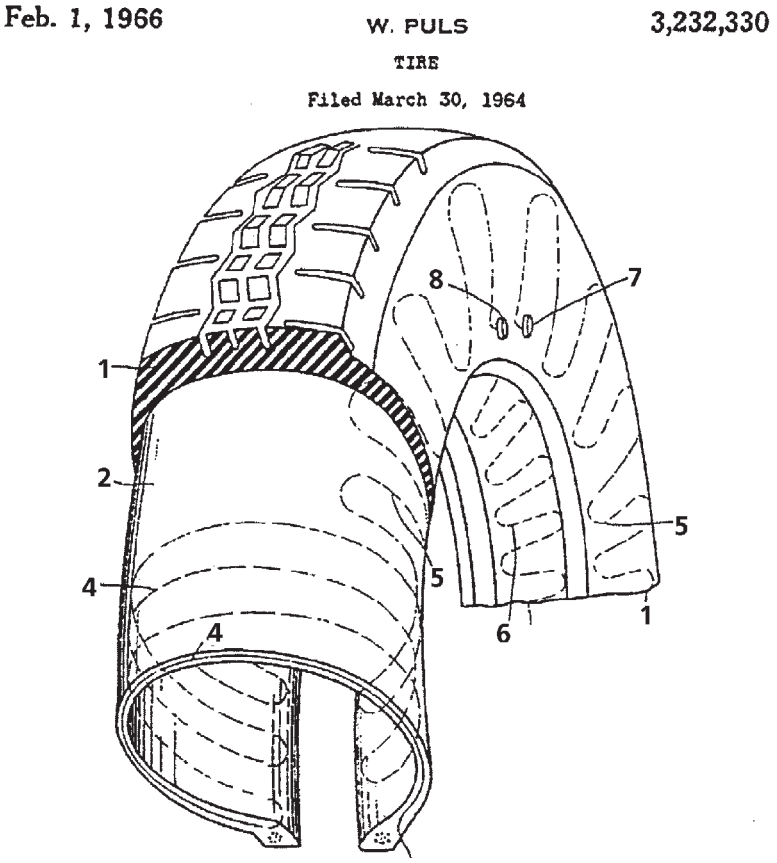

Figure 2.1 An early patent on tyre electronics (US Patent 3,232,330, 1966) [7]

In the late 1980s Goodyear announced they were working to put a 'chip' in a tyre, which led to a patent in 1990 [8]. Goodyear embedded an RFID chip in the tyre, enabling the tyre to have a unique identification number, which could be 'read' electronically. This process is depicted a Goodyear Press Release, shown in **Figure 2.2.**While RFID could be used in any tyre, truck tyres were the focus, because many customers added identification numbers to their truck tyres with a branding iron, as mentioned earlier.

By the mid 1990s there were intelligent tyre programmes at Goodyear, Bridgestone, and Michelin. In addition to ID numbers, these had added pressure and temperature sensing to the concept. Bridgestone announced they were developing a system that would read pressure and temperature for truck tyres. Michelin was working on a similar product for Earthmover tyres.

In 1995 Goodyear, along with Case Western Reserve University and Phase IV Engineering, received a research contract from the Defense Advanced Research Project Agency (DARPA), to develop an application of micro electrical mechanical system (MEMS) technology. The pressure sensor, in this case, was a MEMS device. Truck and aircraft tyres were produced for evaluation and testing.

In the late 1990s, Continental took a different approach. Rather than putting sensors in tyres, they built tyres with radial strips of magnetic rubber in the sidewall. Sensors were mounted on the suspension to detect deformation at different spots along the

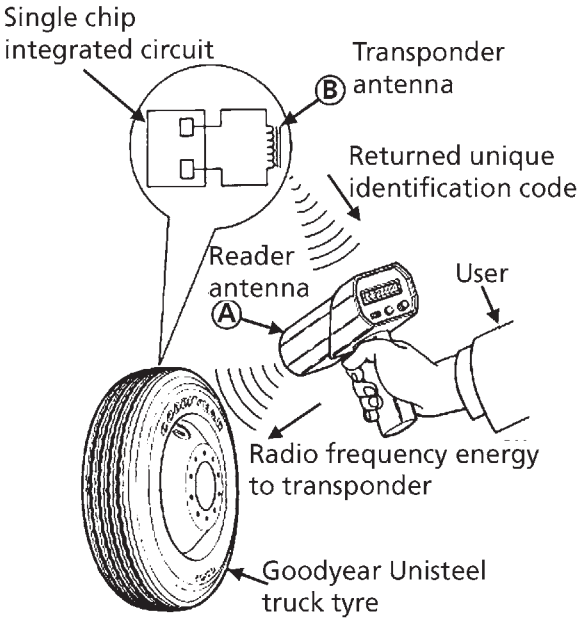

Figure 2.2 Goodyear Press Release, *Tire Talk*, 1992

sidewall, which was related to cornering force. Continental called this the Side Wall Torsion Sensor system or SWT [2]. Continental also evaluated several concepts that placed sensors in the tread, to measure tyre friction to the road [9, 10]. One of these concepts utilised surface acoustic wave (SAW) Technology.

Michelin introduced the first commercially available intelligent tyres in 1999, with their MEMS system for Earthmover tyres. They announced their eTyre, a product for the truck market, in 2002. Both measure pressure and temperature. Neither product seems to have very large use. In 2007 Michelin introduced eTire 2, which combined a separate SAW sensor and an RFID tag into a post-cure tyre patch. It is too early to tell if this product will have much penetration in the market.

In 2003, Goodyear and Siemens announced Tyre *IQ*™ [11]. This system was designed for passenger tyres and vehicles, to comply with the TREAD Act (see Section 2.3.3). Tyre *IQ*™ integrated tyre electronics have antennas placed at each wheel position. Data from the tyres are able to interact with the vehicle electronic control unit (ECU). This product was not adopted by the OEMs, who chose the less expensive wheel-based systems (see Sections 2.3.2 and 2.3.3), or "indirect" systems, that used antilock braking systems (ABS) to compare rotational speed of each wheel, and inferred inflation based on a differential in speeds at each wheel position.

In 2005, Bridgestone and Continental have announced a jointly developed tyre pressure monitoring system for commercial vehicles. It is not in production as of November 2007.

To date, the largest volume of tyres that use electonics are NASCAR racing tyres. NASCAR wanted to improve control of both new and used racing tyres, to give teams access to the same number of tyres, regardless of the team's budget. Goodyear developed a racing tyre with a unique RFID tag in every tyre. The RFID tag, cured into the tyre's sidewall, contains a unique tyre ID. Implemented at the start of the 2006 racing season, this involves production of more than 100,000 tyres per year.

2.3.2 Competing Products – Wheel-based Systems

Tyre companies were not the only ones looking to monitor tyre pressure automatically. Companies like EPIC, Schrader, and Unicomm Signal (now SmarTire) developed products that attached to the wheel, and transmitted tyre pressure at radio frequencies to an on-board reader. Most of these products were developed for passenger cars, rather than commercial vehicles. An example of a wheel-based tyre pressure monitoring system (TPMS), which attaches to the valve stem, is shown in **Figure 2.3**.

These products were relatively expensive and were sold as specialty items. However, the advent of the runflat tyre began to change that. Runflat tyres are designed to support the vehicle load, for a limited distance and speed (typically 50 miles at 50 mph), if the

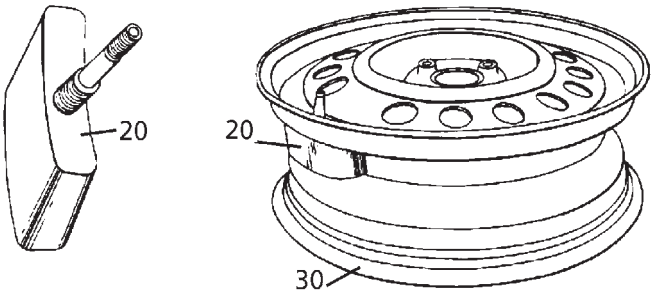

Figure 2.3 Wheel-based tyre pressure monitoring system [12]. Sensor and batteries are in device 20, at the base of the valve stem. The drawing on the right shows the device attached to wheel. (Schrader Bridgeport patent)

tyre has lost all its air. The runflat tyre requires a TPMS, because, even when the tyre was flat, the vehicle handled so well that the driver was unlikely to know it. When flat, a monitor was necessary to notify the driver that the tyre should be inspected and repaired, before exceeding its runflat range or speed. The earliest original equipment manufacturer (OEM) fitment of runflat tyres was on the Corvette in the mid 1990s. The Corvette used a wheel-based TPMS made by EPIC Technologies.

Runflat tyres, however, were still a small percentage of the total tyre market. There were few OEM fitments, and aftermarket sales of runflats tyres, which required the additional purchase of a monitoring system as well, were small. TPMS remained specialty products, with low volume and relatively large costs.

2.3.3 The TREAD Act of 2000

The environment for tyre pressure monitoring changed with the TREAD Act of 2000. This law requires a low pressure warning system on all passenger vehicles sold in the United States (full compliance is scheduled for September of 2007). The TREAD Act changed the business case for tyre pressure monitoring, essentially legislating a large market for the devices. More OEM suppliers have entered the market with wheel-based TPMS products, and electronic circuits and sensors are being developed on a larger scale, driving down their costs.

Since they are commercially available, wheel-based systems are currently being sourced to meet the requirements of the TREAD Act. However, a tyre-based 'intelligent tyre' offers several advantages over wheel-based systems. First, current wheel-based systems can be damaged during mounting and dismounting operations. Secondly, the ability to identify and track the tyre with an electronic ID number is not readily available with basic wheel-based systems.

2.3.4 Outlook for Intelligent Tyres

The large market for TPMS will drive down the cost of components, like pressure sensors. In addition, electronics firms will be more willing to develop components for intelligent tyres. This bodes well for the development of intelligent tyres – assuming that the costs can remain competitive with wheel-based systems.

2.4 Design of the Intelligent Tyre System

It is important to remember that the intelligent tyre is part of a system, and all parts must work together as a whole. The tyre design, the electronics, the readers, and other components combine to make up this system.

For the purpose of this chapter, we will use the term 'tag' to denote any electronics package added to the tyre. **Figure 2.4** depicts the system and the considerations at each component. Discussion of these considerations, beginning with the tyre, follows.

2.4.1 Tyre

Three factors must be considered when designing the tyre: the impact on the tyre's performance; the location of the electronic device; and the method of attaching it to the tyre. Each is considered in this section.

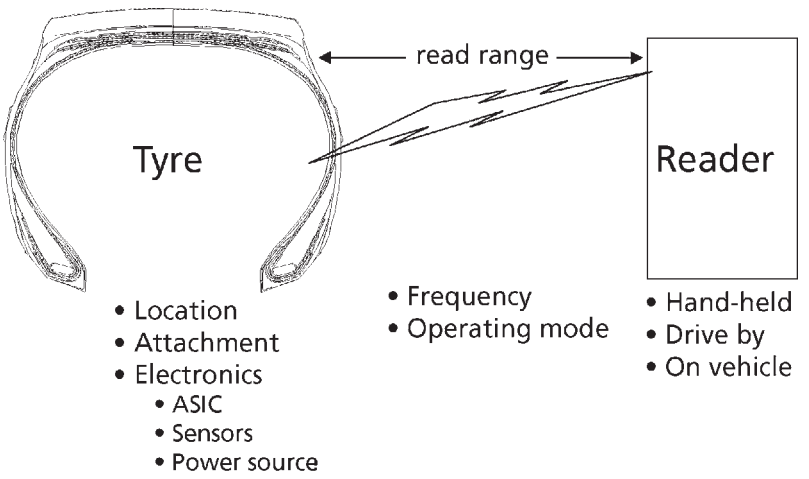

Figure 2.4 Intelligent tyre system: tyre, signal, reader

2.4.1.1 The Impact on Tyre Performance

The first consideration is the tyre itself. The art and science of tyre design balances many factors when developing a tyre for a specific application. A tyre is a compromise, balancing characteristics such as handling, rolling resistance, wear, or hydroplane resistance.

The intelligent tyre components must integrate with the other elements of tyre design without affecting the tyre's characteristics. The following are some design criteria that the tyre designer must take into account when integrating electronics into an 'intelligent tyre'.

Weight: The added weight of the electronic device will add extra mass to the tyre. This can affect tyre parameters such as balance, uniformity, ride quality (noise, vibration, and harshness), and possibly rolling resistance. Of course, the lighter and smaller the tyre tag, the less effect it will have on these parameters. The weight of the tyre tag, and its effects on uniformity and balance, is magnified at higher diameters. For instance, a transponder located in the centreline of the tread will have a much greater effect on balance than one of equal weight located in the bead area. If small enough, the imbalance could be offset during the mounting and balancing operation. It could also be countered by adding a balancing patch of appropriate weight and location to the tyre.

Durability: Durability is a key consideration of every tyre design. Added thickness at the location of the electronics can generate more heat at that location. Excessive heat detracts from durability. In addition, if the electronics are located within the tyre structure (for example, between two plies), one must be certain that its presence does not initiate a separation.

If the electronics are contained in a patch that is applied after the tyre is cured, care must be taken that the patch installation does not damage the tyre. Proper procedures must be followed for patch installation.

2.4.1.2 Location of the Device

Some alternative locations for a tyre tag are shown in **Figure 2.5**. Many factors influence this location.

The first is the sensor function. If one was interested in the temperature at the belt edge, for example, placing a tag there is the ideal location. Of course, this is an area of high stress, so it might not be satisfactory for durability reasons. On the other hand, if one wished to measure contained air pressure, burying the sensor within the tyre's structure would shield it from the actual pressure. To accurately read pressure, the transponder must have access to the tyre's air cavity.

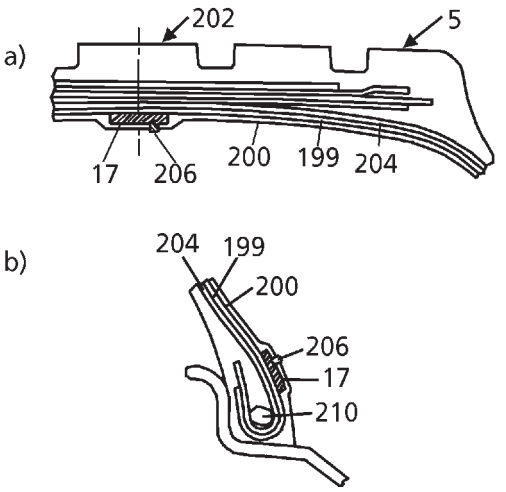

Figure 2.5 Alternative locations of transponder in crown and bead area (Bridgestone Patent)[13] 17 – monitoring device assembly, 199 – tie gum ply, 200 – inner liner ply, 202 – tyre crown, 204 – body, ply, 206 – removable dowel, 210 – tyre bead

If one was only interested in the tyre's ID number, locating the electronics on the outside of a tyre is also possible. In this case it would be susceptible to damage from cutting or curb scuffing. It would also be exposed to tampering. For example, if the unique ID number was used to identify the ownership of the tyre, it could be readily cut away by a tyre thief.

The stresses in the tyre also affect the choice of the location of the tyre electronics. Locating the transponder in the tread, which goes through the footprint, or the upper sidewall, which goes through high flexing, can make the challenge of attaching the transponder for the life of the tyre more difficult. Many patents show the transponder located in the lower sidewall near the bead, which is a more stable location, relatively.

Another factor in the location of the tag is the ability to transmit the signal through the tyre. As will be discussed later in this chapter, certain frequencies are better able to penetrate steel plies, and other tyre materials. A frequency that does not transmit through wire is likely to perform better with the tag in the sidewall of a tyre, rather than the tread area of a steel belted radial.

For truck tyres, where dual tyre application is common, locating the transponder in the sidewall may make it difficult or impossible to read while it is on the vehicle. If the system has short read range, it would be very difficult to read the inside tyre, or to read a tag in one of the facing sidewalls (see **Figure 2.6**).

Figure 2.6 Dual assembly for truck

Photograph© Brian Logan

A centreline location offers improved access. It is also satisfactory for inventory purposes, if tyres are in a rack. The tread is accessible but the sidewall is not. On the other hand, if the tyre is on the vehicle, it is possible that a centreline tag would be in the footprint. Depending on the read range, it may be difficult to read.

Low aspect ratio passenger tyres (some are as low as 25%) present a different challenge, because there is not much area to attach the tag in the sidewall. In this case, the tread may be the only feasible area.

Finally, the location of the reader/receiver and its antenna may dictate the location of the tag in the tyre. In the case of a tyre that sends a signal to a receiver on board a vehicle, the metal present in and around the wheel well can shield, deflect, or otherwise interfere with reception. The outside sidewall, which would have a clearer path to a reader, may be a better choice.

On the other hand, if the reader and tyre need to be in close proximity, the inside sidewall offers a short distance to the vehicle suspension or wheel well, where a reader can be located. This layout is one used in the Goodyear/Siemens Tyre *IQ*™ system (**Figure 2.7**).

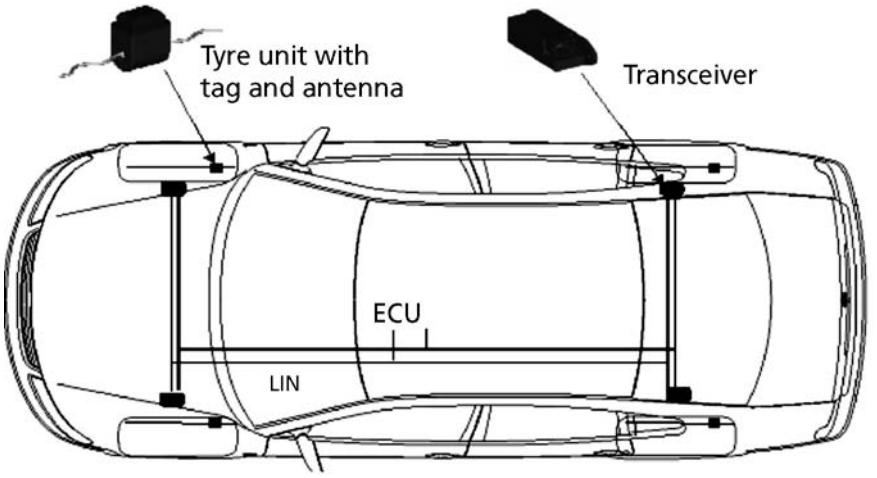

Figure 2.7 Location of electronics in tyre close to vehicle-mounted antenna (Goodyear-Siemens [11) ECU – Electronic Control Unit, LIN – Local Interconnect Network

Reproduced with permission from SAE International Paper # 2003-01-1279.
©2003, SAE International

2.4.1.3 Method of Attaching the Electronics to the Tyre

The electronics in a tyre must survive significant forces. Compared with a wheel-based system, the electronics in the tyre will always be at a larger diameter than the rim, which means that centrifugal forces are higher. Additional forces can be present, as the tyre goes through the footprint or from road shock.

Compounding this problem is the compliant nature of the tyre. The structure itself can deform, putting greater stresses on the bond between the tyre and electronic device.

There are several approaches to attaching the tag:

Vulcanisation: For the tyre engineer, a logical mechanism is the chemical bond developed during vulcanisation of the tyre. This requires the electronics to be built into, or otherwise attached to the tyre, prior to cure.

Success of this approach depends on several factors – size of the tag, location, and vulcanisation conditions. If the tag is small, it could conceivably be buried inside the tyre structure. A Goodyear patent in 1993 shows a small transponder – in this case an RFID tag – located within the apex of a large truck tyre (**Figure 2.8**) [14]. This configuration minimises the disturbance to the contour of the ply and other components, and is less likely to affect the properties of the tyre.

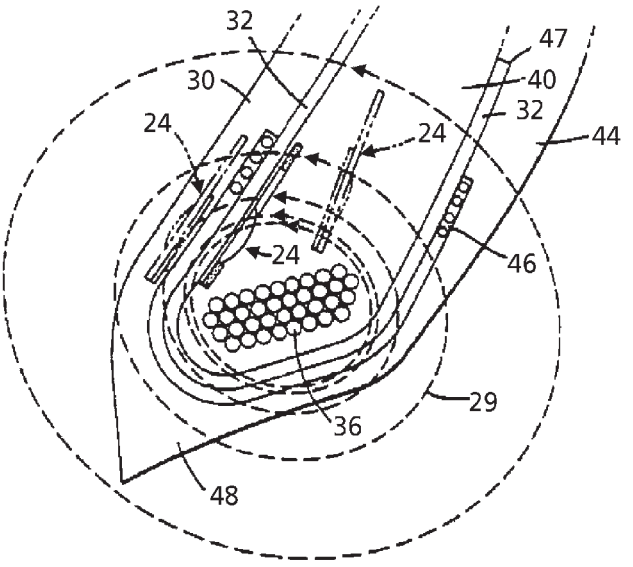

Figure 2.8 Small tag in bead area of tyre [14]. Item 24 shows several locations for an RFID transponder (Goodyear patent). 24 – transponder, 29 – magnetic flux lines, 30 – tyre inner liner, 32 – tyre ply, 36 – steel wire bead, 40 – tyre apex, 44 – tire sidewall, 46 – steel-reinforced chipper, 47 – ply ending, 48 – toe region of the tyre

If the location of the electronics is on the tyre's inner liner, as in **Figure 2.5**, care must be taken that the bladder is able to flow smoothly over the area. If the electronic device were large, this area would be a potential for trapped air or other bladder-related curing problems.

In either case, the electronics must be able to withstand the temperatures and pressures of curing.

Post-cure patch: A patching process is used in the industry to repair tyres that have been punctured or damaged during service. The electronic device can be located within that patch, or attached to its surface. Again, it is important that the electronics have good adhesion to the adjacent rubber.

Post cure application offers a number of advantages. One is production flexibility. Once the tyre is cured, a patch can be applied to a tyre at any time. It could be installed at the dealer's, warehouse, retread facility – or at a customer's location. This type of application is done on the surface of the tyre, on the liner or the outside.

Post cure application offers other advantages. The electronics, which might include a battery, do not have to survive the temperatures and pressures of curing. For a relatively

large transponder package, which might interfere with the bladder as mentioned previously, post cure application would be a solution.

There are a number of issues with post cure application, however.

First, the liner surface of the tyre is generally coated with a silicone-based release agent. This coating allows the curing bladder to release from the liner surface after cure. Release agent is also on the outside surface of the tyre, to prevent it from sticking to the mould. This silicone must be removed to insure a good bond. Surface preparation generally involves scraping the surface, grinding with a buffing wheel, and then buffing with a wire brush. In the case of the liner, care must be taken that the liner surface is not damaged during preparation. Because this is a manual operation, variability in cleaning could cause variation of adhesion from tyre-to-tyre.

Another issue is that the bond of a post-applied patch is generally not as strong as that developed during the initial vulcanisation.

In addition to these technical reasons, the extra steps of cleaning and applying the patch will add to the cost of the finished product.

Regardless of whether the electronics are cured in or patched in, they need to develop good adhesion with the adjacent rubber.

Mechanical Connection: There are a number of patents that combine the 'cured-in' or 'patched-in' approach, with a mechanical method to fasten the tag to the tyre. These cure or patch a 'docking station' to the liner of the tyre. The electronic device is then attached mechanically to the patch.

Adhesives: Another method of attachment is to use conventional adhesives, rather than rubber chemistry. At least one patent [15] suggests epoxy or other conventional adhesives could be used to apply the transponder. Again, surface preparation of the tyre is important for a strong bond.

2.4.2 Electronics

This section is not meant to discuss details of electronics design, or to replace a physics or electronics text. Its purpose is to familiarise the reader with different components, design issues, and trade-offs in the electronic components used with intelligent tyres.

2.4.2.1 Electronic Circuitry

There are two ways to approach the circuitry for intelligent tyre tags. One approach is with discrete components. However, assembling discrete components is not suited for

high volume production. This technique also leads to a larger and more costly product. A better approach is with integrated circuits. In addition to being smaller and more suitable for volume production, the integrated circuit eliminates many of the connections of discrete components. These connections would be susceptible to failure through the thermal or mechanical stresses seen in a tyre's life.

For a tyre with electronic components, the integrated circuit is the 'brains' of the tyre. Because of the specific processing required in the case of the intelligent tyre, it is specifically developed for that application. Such a circuit is called Application Specific Integrated Circuit, or ASIC. It is helpful to discuss some of the challenges of ASIC design.

The development of an ASIC begins with the design of the electronic circuit, consisting of discrete components – transistors, diodes, and other circuit elements. This design is then transformed into the physical layout of numerous semiconductor layers that will result in the equivalent circuit.

These layers and circuit elements are very small, and arranged so that identical ASIC, as small as a few square millimeters, are placed side-by-side on a high purity silicon wafer. The wafer is 10, 15, or 20 cm in diameter.

More complicated circuits, and those with larger memory requirements, are physically larger. IC designers work to minimise the area that an integrated circuit covers on the wafer. With a smaller ASIC, more chips can be produced from the wafer. This results

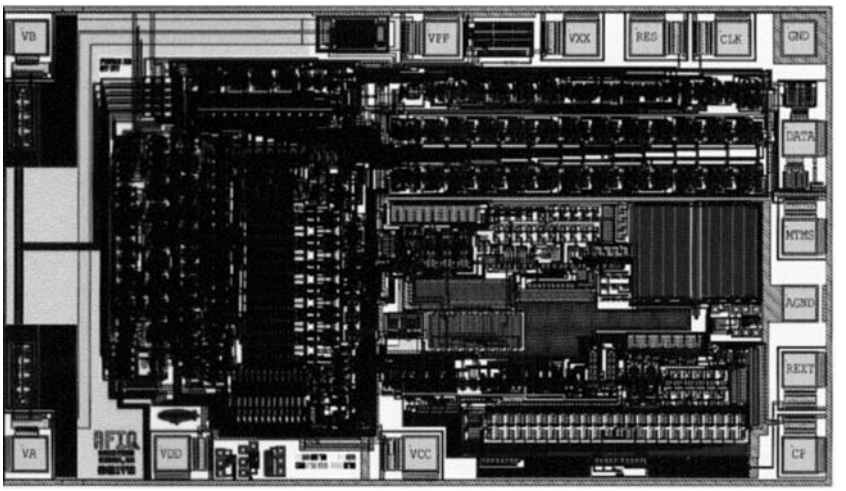

Figure 2.9 This layout of an ASIC measures 4.5 mm^2 area (The Goodyear Tire & Rubber Co.)

in lower costs, which is why many ASIC are designed with a minimum amount of memory.

2.4.2.2 Sensors and Sensing Devices

Sensor technology is constantly advancing. As new sensors evolve, many will have application in tyres, measuring forces, pressures, temperatures and other parameters.

Today's pressure sensors are micromachined MEMS devices. They basically consist of a diaphragm over a cavity (**Figure 2.10**). As pressure over the surface of the diaphragm increases, the diaphragm deflects. The pressure is related to this deflection.

One type of sensor, a piezoresistive sensor, has a Wheatstone bridge circuit on the diaphragm. As pressure changes, the strain on the diaphragm changes, and the Wheatstone bridge measures that strain.

Another type of sensor works like a capacitor. The diaphragm is one electrode, and the bottom of the cavity is the other. As the diaphragm deflects, the gap between the diaphragm and the bottom of the cavity changes. This changes the capacitance of the device.

These devices generate electrical outputs, depending on the pressure. They require sophisticated circuitry (ASIC) to interpret the values and send them to the reader.

A different sensing technology uses SAW. SAW devices are piezoelectric crystal substrates with metallic traces on their surface. When interrogated by a certain radio frequency, they respond with a reflected signal. Strains on the crystal – related to pressure or temperature – change this response. An advantage of the SAW device is that it is not dependent on a complex integrated circuit (ASIC) or internal power source. That would make the electronics that are in the tyre less expensive. The trade-off is that the reader must be more sophisticated (and costly), and be able to detect the change in response.

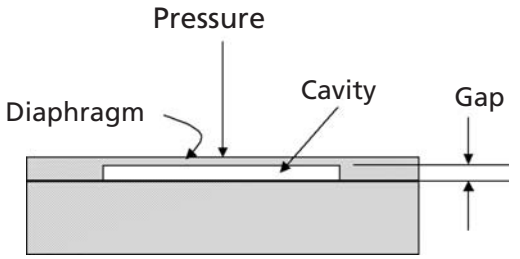

Figure 2.10 Pressure sensor. Pressure on the diaphragm causes the gap distance to change

2.4.2.3 Powering the Electronics

A major design consideration with intelligent tyre electronics is the energy, or power, needed to run them. The first commercial TPMS system for the Corvette – a wheel-mounted unit – generated its own power. It had a piezoelectric material, set on a small cantilevered beam, which would vibrate as the car drove down the road, generating electrical power.

This power source is not used in today's TPMS systems. Battery power proved more reliable and less costly. Today, every direct, wheel-based TPMS system for passenger vehicles is battery powered.

Tags powered by batteries are called 'active' systems. These contrast with 'passive' systems, which use power from the reader to supply energy to their circuits. Because of the limitations of powering both active and passive systems, designers need to manage the power requirements for each type.

2.4.2.3.1 Active Systems

The advantage of batteries is that they have an ample supply of power to run the electronics – at least, until the battery runs down. However, batteries also have disadvantages – their life, added cost, weight, ability to withstand tyre manufacturing temperatures, and disposal issues.

The first area to consider is battery life. Obviously, if the system were 'on' all the time, battery life would be short. Electronics engineers develop and analyse a 'battery life budget'. They determine the power requirements of each component of their system. Then, they will assume a duty cycle – the number of miles driven, average trip distance, and so on, to estimate the power draw of their transponder. This is used to predict the system's battery life.

Current, wheel-based TPMS have developed a number of strategies that extend battery life, and these techniques could be applied to active, tyre-based systems. These range from motion detectors, to built-in timers, to systems that only broadcast when the pressure changes. Of course, all these strategies increase the complexity of the electronics, and the cost of the system.

In addition to battery life, batteries present several other technical challenges. One is the weight of the battery. Centrifugal forces on the device, at high speeds, can be quite large. The extra battery mass would increase these forces. Another challenge for an active device is the tyre manufacturing process itself. Low cost batteries are unable to withstand curing conditions. This limitation can also be an issue with the retreading process. One solution could be to remove the device prior to retreading.

Finally, having a battery present in the tyre can add to disposal issues. This may become more of an issue in the future, and may require that the battery or transponder be removed at the end of the tyre's life.

2.4.3.2.2 Passive Systems

Many current RFID systems are passive. Passive technology works when a signal from the reader creates power in the circuit of the transponder itself. This voltage 'powers-up' the transponder, and sends a signal back to the reader, which interprets the data. **Figure 2.11** represents this technology at low frequencies, which is in the magnetic inductance area of the spectrum. The idea is the same, although the physics is slightly different, at higher frequencies.

The biggest challenge to using passive technology is to get enough power to the transponder. The Federal Communications Commission (FCC) limits the power and frequencies that can be used. The radio frequency signal must pass through the sidewall, tread, and, in the case of a radial truck tyre, multiple layers of wire cord making up the carcass and belts. The energy reaching the transponder can be significantly reduced.

Generally, the read range of a passive system is less than that of an active system, whose battery can power it to a higher level. By having to 'power-up' the transponder from outside the tyre, there is less energy available for sensors.

One approach to powering a passive system is to design it with an energy storage device built as part of the transponder. The reader sends a signal to the transponder. Rather

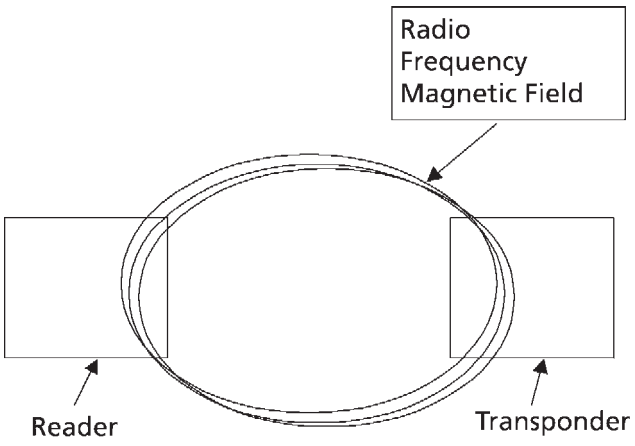

Figure 2.11 Passive technology - low frequency

than immediately responding to the signal, the power is stored in a capacitor or 'energy accumulator'. When the power in the accumulator is large enough, it is used to power the circuit, read the sensors, and send the message back to the reader [16]. This makes the transponder, and the whole system, more complicated and costly than a simple passive device. In addition, the time that is used to charge the capacitor makes the response slower than it would normally be.

A comparison of active and passive technologies is listed in **Table 2.2**. The strengths of one generally correspond to the weaknesses of the other.

Table 2.2. Comparison of active and passive RF technologies

Active	Passive
Advantages • Has power to read at greater distances • Has power to use off-the-shelf sensor technology • Battery gives options for future features (i.e., memory, new sensors)	**Advantages** • Unit is smaller and lighter • No complications of a battery • Simpler, lower cost unit
Disadvantages • Size and weight of unit • Battery costs • Battery cannot take high temperatures	**Disadvantages** • Challenge of antenna design • Power availability • Reader range • Requires sensor technology that draws low power

2.4.2.3.3 Power Generation

As mentioned previously, the first wheel-based versions of the low-pressure warning device on the Corvette were powered by a piezoelectric source. For tyres, their deflection and deformation offer the potential for a piezoelectric material to generate power. Practical design questions remain as to the amount of power such a system could generate, and the rate at which it is generated. There are several patents citing energy generation, using piezoelectric energy [17], or static electricity built up during tyre rotation [18]. They have not yet been commercialised.

2.4.3 Signal from Tyre

Nearly all of the intelligent tyre concepts use radio frequency to communicate with the tyre. Two important questions in selecting a frequency (in addition to the government regulations) are:

1. How far will the frequency transmit? and
2. How well does it work with the materials in the tyre?

2.4.3.1 Radio Frequencies

The range of radio frequencies – the *radio frequency spectrum* – is regulated by the governments around the world. This is to prevent all the competing radio signals – commercial radio, television, military, cellular phones, and so on – from interfering with one another. In the United States, the regulatory body is the FCC. **Table 2.3** compares the frequency and wavelength of various parts of the radio frequency spectrum.

If one wanted to operate a TV station, for instance, one must obtain a license from the FCC to broadcast at that frequency. That would prevent someone else from interfering with those signals.

Certain bands of frequencies – which vary between countries or regions – are 'unlicensed'. In unlicensed frequencies, competing signals are regulated by the allowed power and other transmission aspects. This reduces the likelihood of interference, by reducing the range and duration of the transmission. It does not totally eliminate interference - any competing signal, within range of the receiver, could interfere with it. For practical purposes, the intelligent tyres should be designed to operate in these 'unlicensed' frequency bands.

There are several implications of these regulations. The first is that the restrictions on frequency and power levels limit the read range of the system, i.e., how far away from the tyre you can read the data. Read range is also affected by the ability of different frequencies to transmit through materials like steel and carbon, which are present in tyres.

Table 2.3. Frequency chart [19]

	Frequency	Classification	Wavelength
Radio waves	30 GHz – 300 GHz	extra high frequency (EHF)	1 cm
	3 GHz – 30 GHz	super high frequency (SHF)	10 cm
	300 MHz – 3 GHz	ultra high frequency (UHF)	1 m
	30 MHz – 300 MHz	very high frequency (VHF)	10 m
	3 MHz – 30 MHz	high frequency (HF)	100 m
	300 kHz – 3 MHz	medium frequency (MF)	1 km
	30 kHz – 300 kHz	low frequency (LF)	10 km
	3 kHz – 30 kHz	very low frequency (VLF)	100 km
Sound	0 – 20 kHz		

A second implication of these regulations is that they vary from country to country, in both specific frequencies and power levels. This means that different electronic components of an intelligent tyre may be required for different regions of the world. In these days, with tyres being shipped between countries, this can be an especially important consideration.

These unlicensed bands are discussed next. For the purpose of discussion, these ranges are the standards for the United States. Since regulations are subject to change, one should check the latest rules.

Low frequency (LF), are really magnetic waves rather than radio waves. The unlicensed band of LF waves are typically between 125 kHz and 134 kHz. LF signals transmit through most materials. This is helpful in tyres, because tyres have steel wire and carbon black in the rubber, which can block or weaken the strength of the signal. Another advantage of LF is that the physics is fairly well known. Many companies have been making LF transponders and readers for many years. The downside of LF is that transmission does not travel very far. While it can get out of a tyre, it can't go very far beyond its surface.

Another disadvantage of LF is that data transmission rate, a function of the frequency, is fairly low. This may not be an issue when reading a single tyre in a warehouse or parked at a truck stop, but it could prohibit reading on a fast-moving conveyor, a drive-by reader, or a tyre rotating at high speed on the vehicle.

High frequency (HF), is at 13.56 MHz. Transmission range is a little longer than LF. However, there are fewer applications of HF technology, with fewer manufacturers. This limits the availability, and cost, of HF.

Ultra high frequency (UHF) 315 MHz and 433 MHz are standard frequencies for the automobile industry [20]. In the US, 315 MHz has become the standard for active, wheel-based TPMS devices. Generally, these systems share their receiver with remote keyless entry (RKE) systems. While able to transmit through passenger tyres, reception of the signal is very sensitive to the location of the receiver antenna. This frequency also has difficulty transmitting through a steel ply tyre, like truck or earthmover.

In the United States, the unlicensed band between 902 and 928 MHz is becoming more common in RFID applications. This frequency band can have a long read range, in the order of 3 – 9 m in air. However, it is attenuated by numerous materials, including metal, carbon, and water. Transmission through a tyre varies, depending on tag design and the location of the transponder inside the tyre. The US also requires that the signal is broadcast for no more than 400 milliseconds on any one of 124 channels in that frequency range, in any 20 second interval. This concept of transmitting at different frequencies across a frequency range, is called *frequency hopping*, and is meant to reduce interference between users.

Microwave Frequency. Two additional unlicensed frequencies, 2.45 GHz and 5.8 GHz, are of interest. They offer the potential for smaller antennas (antenna length is a function of their wavelength), which may allow smaller transponders to be installed in tyres. The small volume of commercial products at these frequencies means that their current cost is relatively high.

The advantages and disadvantages of various frequencies are summarised in **Table 2.4**.

2.4.3.2 Operating Mode

Intelligent tyre operation can be characterised by the manner in which the signal is initiated and responds. Passive tags will only respond when they receive a signal from the reader, which is often called an 'interrogator'. When the signal is received, they transmit the data in response. These tags are called *transponder*s. This mode is particularly flexible. The tyre can be interrogated during manufacturing, distribution, inventory, and mounting operation. It can also be interrogated during vehicle operation, assuming the read range and physics of the system allow it.

Another operating mode is a system that transmits data autonomously, without a signal from the reader. This is the common operational mode of wheel-based tyre pressure monitoring systems. These devices are classified as *transmitters*. Due to the nature of these transmitters, the reader or receiver must wait and listen for the signal from the tyre. This is satisfactory when driving down the highway, but not satisfactory if the mechanic wants to read the tyre ID number or pressure when the vehicle is parked in a garage. Identifying the location of the signal is another issue. This becomes a problem when the system signals that a tyre is low and requires more inflation. The operator must determine the low tyre by checking each tyre manually. There are several ways to identify the tyre's location. If the read range is short, one can locate a reader/antenna at each wheel position. When that specific reader receives the signal, the wheel position

Table 2.4 Frequency summary

Frequency	Advantages	Disadvantages
125 kHz 13.54 MHz	• Good tyre transmission • Worldwide use (different power levels)	• Short range • Low data rate
900 MHz	• Long range • High data rate	• Regional rules • Low tyre penetration
2.45 GHz	• Worldwide use (different power levels) • High data rate	• Moderate range • Low tyre penetration

is known. This works well with passive devices, and is the mode of operation of the Goodyear/Siemens Tyre *IQ*™ system. Systems with autonomous transmitters can identify the specific tyre if the system is 'taught' which tyre ID number is mounted at which wheel position. Various procedures can be used to perform this. Of course, this complicates tyre installation, and, if tyres are rotated, or a tyre is replaced, the system must learn the 'new' position of the tyres.

A hybrid design is also possible. For instance, Siemen's wheel-mounted system, TyreGuard 1™ offers the capability of low frequency *initiators* located at each wheel position. These initiators have fairly low range. The initiator for a specific wheel transmits a signal at low frequency, which 'wakes up' the active circuit of that tyre. The tyre responds with a signal at its normal frequency. The reader then knows that the signal came from that specific tyre.

2.4.4 Readers

The reader is a critical part of the intelligent tyre system. In most cases, this is the primary user interface to the tyre data. Readers must be designed for the operating mode of the tyre tag. For example, for 'autonomous' tags, which transmit on their own, the reader must be on and 'listening' or the transmission will be lost. In contrast, passive tags transmit 'on-demand'. They only react to a signal from the reader/interrogator. Readers can be classified as three general types – hand-held, drive-by, and on-board. This designates the location and function of the reader.

2.4.4.1 Hand-Held

A hand-held reader is the most flexible. The operator can 'read' the tyre during manufacturing, shipping, inventory, or after mounting the tyre on the vehicle. Another advantage to a hand-held reader is that a visual and/or audible signal can be given when the tyre is successfully read. This allows the operator to verify that the tyre has been read, and make sure that the reader did not miss it. The hand-held reader will not work very well with an intelligent tyre that transmits autonomously. In such a case, the operator may have to wait to read until the next transmission. This problem can be overcome if the system is designed so the reader initiates the read, as discussed earlier.

2.4.4.2 Drive-by

The drive-by reader offers several advantages over the hand-held. First, it is automated. If placed at the fuel island or entrance gate at a truck terminal, every tyre could be checked for proper inflation without requiring someone to check them. A drive-by

reader also might allow easier access to read the tyre. For example, if the transponder was located on the inside dual tyre of a truck or bus, it would be difficult to reach with a hand-held reader, but a drive-by reader might be developed to do this. In the case where the transponder was located in the tread area, the reader could be located in the road surface, as a plate or a pad over which the vehicle is driven.

There are several design challenges to a drive-by reader. One of them is the read range. If the read range is fairly short, the tyre must be close to the reader. This may require the vehicle to be driven through a narrow path or opening. The tyre must also remain in the 'read zone' long enough to be read. This may require that the vehicle be driven very slowly.

Like the hand-held reader, if the tyre tag is autonomous, you cannot be certain that the tags will broadcast when the tyre is within read range. For that purpose, an initiator would be critical to the design.

Another challenge is making certain that all tyres were successfully read. If an 18 wheel truck and trailer go through the drive-by reader, and only 17 tyres are read, the truck must either be driven through again, or a hand-held reader would be used on the 'missing' tyre.

As much as one would hope for 100% read rate, this may not always be the case. A read could be missed because of radio interference, damaged electronics in the tyre, or a 'wrong' tyre – one without the proper electronics. In contrast, with a hand-held reader, the operator can interrogate each tyre until there is a successful read, and then move on to the next.

2.4.4.3 On-board

A third configuration is to mount the reader on board the vehicle. With a reader on the vehicle, tyre information could be read during vehicle operation. This is most appropriate when the system includes data about the tyre's state, i.e., its temperature, pressure, or some other parameter. These data could then be used for tyre pressure monitoring, as required by the TREAD Act, or it could be used as input to the vehicle's stability control system. As with the other readers, the system's operating mode depends on the design of the electronic tag. An autonomous system would notify the user if tyre pressures were low. However, if one wished to know *which tyre* was low, it would take additional design features. Solutions to identifying tyre location have been discussed in the section on operating mode. For example, the system could be taught to relate ID to the wheel position, or could be designed with an initiator.

2.5 Standards

Starting in the mid 1990s, there was a great deal of interest in intelligent tyre technology, particularly by the trucking industry. Fleet operators understood the value of proper tyre maintenance, as tyres represented a large amount of their operating costs. Proper inflation resulted in improved fuel economy and tyre mileage. As development and testing by the tyre companies progressed, the fleet customers asked that they develop common standards. These fleets, with hundreds or even thousands of vehicles, generally used tyres from more than one manufacturer. The fleets did not want different readers for different brands of tyres. Industry groups were formed to discuss standards, with representatives from vehicle manufacturers, electronics firms, and tyre companies. Each tyre company was working on its unique design, which offered its own advantages, and agreement could not be reached. The lack of standards will be one obstacle in the adoption of intelligent tyres. This is an issue the tyre companies will have to address.

AIAG Standard for Tyre RFID. For the purpose of tyre identification, the industry has reached agreement. The 902-928 MHz band was also chosen as the frequency in the Automotive Industry Action Group (AIAG) B11 standard for identifying tyres. This standard was developed to meet the automotive OEM needs to read a tyre's DOT serial number on an auto assembly line. UHF was selected because it was the best at meeting performance requirements, including read range. However, as of November 2007, no manufacturer was using the RFID B-11 tags in tyres for Original Equipment Manufacturers. To date, most OEM continue to use two-dimensional bar codes.

Table 2.5 lists the worldwide standards relating to RFID.

2.6 Summary

This chapter has discussed many aspects of intelligent tyres. Like all products, successful market penetration will depend on proper design choices, and whether their features offer value to tyre customers. Cost is one factor in successful implementation. As the costs of sensors come down, and new technologies evolve, the value of intelligent tyres will be more evident. At the current time, an intelligent tyre featuring an electronic ID (RFID) may be the closest to large-scale implementation, but the benefits must still justify the costs, which would be large for a major fleet. The tyre companies must also address standards before intelligent tyres become widespread. With few systems being sold, there is no pressing need for a standard. When designs evolve with lower costs, it is more likely that customers will demand a standard.

Table 2.5. Standards relating to RFID	
125 kHz	ISO 11784/5 [21] Animal Standard Read Only ISO 14223/1 [22] Animal Standard Read/Write ISO 18000-2 [23] Mode 1 Air Interface
13.56 MHz	ISO 15693 [24] Air Interface ISO 18000-3 [25] Air Interface
860-956 MHz (UHF)	ISO 18000-6 [26] Type A & B Air Interface AIAG B-11 [27] Tyre & Wheel RFID/2D Barcode Identification ANSI MH 10.8.2 [28] Data Application Identifier ANSI MH 10.8.4 [29] RFID for Returnable Containers ISO 15434 [30] Syntax ISO 15418 [31] Data & Application Identifiers EAN.UCC GTAG - EAN.UCC EPC EAN.UCC EPC UHF gen2
EAN: European article number *UCC: Uniform Code Council* *GTAG: Global standard for RFID tags* *EPC: Electronic Products Code* *UHF: Ultrahigh frequency* *Gen2: Second generation standard*	

Acknowledgement

The author would like to thank Dr Robert Benedict, Richard Crano, Stephen Roth, and Peter Shepler for their feedback on this chapter. He would like to acknowledge his colleagues at Goodyear and other firms for insight gained while working on these concepts, especially Gary Belski, Robert Brown, William Dunn, Dr George Giakos, Steve Lederer, Richard Pollack, and Gary Tubb.

References

1. F.S. Charles and T.L. Ford, *Heavy Truck Tire Engineering, The L Ray Buckendale Lecture*, Society of Automotive Engineers, Detroit, MI, USA, 1988.

2. *Rubber and Plastics News*, 1999, **28**, 18, 37.

3. D.M. Adderton and S.C. Minne, inventors; Michelin Recherche et Technique SA, assignee; US 6,637,276, 2003.

4. W.H. Ko and H. Xi, inventors; no assignee; US 6,438,193, 2002.

5. J.E. Lee, Jr., H.J. Kulka and J.H. Schramm, inventors; Computer Methods Corporation, assignee; US 5,731,754, 1998.

6. H. Cohn in *Proceedings of the 159th ACS Rubber Division Meeting*, Akron , OH, USA, Spring 2001, Paper No.47.

7. W. Puls, inventor; no assignee; US 3232 330, 1966.

8. W.F. Dunn and R.W. Brown, inventors; Goodyear Tire and Rubber Company, assignee; US 4,911,217, 1990.

9. A. Pohl, R. Steindl and L. Reindl, *IEEE Transactions on Instrumentation and Measurement*, 1999, **48**, 6, 1041.

10. M. Fach, V. Bachmann, B Breuer in *Proceedings of the International Tire Exhibition and Conference*, Akron, OH, USA, 1998, Paper No.23A.

11. R.L. Benedict, P.R. Shepler, M. Fischer and D. Wagner, *Proceedings of SAE 2003 World Congress*, Detroit, MI, USA, Paper No.1279.

12. J.H. Robinson, III, inventor; Schrader-Bridgeport International, Inc., assignee, US 5,838,229, 1998.

13. R.W. Koch, J.L. Turner, G.J. Walenga, H. Takigawa and K. Okamoto, inventors; Bridgestone/Firestone, assignee; US 5,573,610, 1996.

14. R.S. Pollack, J.R. Phelan, R.M. Ames, G.R. Starkey, R.W. Brown, G.T. Belski and W.F. Dunn inventors; The Goodyear Tire and Rubber Company, assignee; US 5,181,975, 1993.

15. R.W. Koch and P.B. Wilson, inventors; Bridgestone/Firestone Research, assignee; US 6,309,494, 2001.

16. J.H. Schuermann, G. Heinecke and R. Kremer, inventors; Texas Instruments Deutschland GmbH, assignee; US 5,053,774, 1991.

17. J.D. Adamson and G.P. O'Brien, inventors; Michelin Recherche et Technique SA, assignee; US 6,725713, 2004.

18. J.D. Adamson and G.P. O'Brien, inventors; Michelin Recherche et Technique SA, assignee; US 6,847,126, 2005.

19. N. Calder, *Nigel Calder's Cruising Handbook*, International Marine Publishing, Camden, ME, USA, 2001, p.556.

20. M. Fischer, *Tire Pressure Monitoring*, Die Bibliothek der Technik Series, No.243, Verlag Moderne Industrie/Siemens VDO, Landsberg, Germany, 2003.

21. ISO 11784, *Radio-Frequency Identification of Animals - Code Structure*, 2004.

22. ISO 14223-1, *Radiofrequency Identification of Animals - Advanced Transponders - Part 1: Air Interface*, 2003.

23. ISO/IEC 18000-2, *Information technology - Radio frequency identification for item management - Part 2: Parameters for air interface communications below 135 kHz*, 2004.

24. ISO/IEC15693, *Identification cards - Contactless integrated circuit(s) cards - Vicinity cards*, 2000.

25. ISO/IEC 18000-3, *Information technology - Radio frequency identification for item management - Part 3: Parameters for air interface communications at 13,56 MHz*, 2004.

26. ISO 18000-6, *Information technology - Radio frequency identification for item management - Part 6: Parameters for air interface communications at 860 MHz to 960 MHz*, 2004.

27. AIAG B-11, *Tire and Wheel Label and Radio Frequency Identification (RFID) Standard*, 2004.

28. ANSI MH 10.8.2, *Data Identifier and Application Identifier Standard*, 2002.

29. ANSI MH 10.8.4, *Unit Loads and Transport Packages RFID Tags for Returnable Containers*, 2002.

30. ISO/IEC15434, *Information technology - Automatic identification and data capture techniques - Syntax for high-capacity ADC media*, 2006.

31. ISO/IEC 15418, *Information technology - EAN/UCC Application Identifiers and Fact Data Identifiers and Maintenance*, 1999.

3 Silica-Filled Rubber Compounds

Jacques W.M. Noordermeer and Wilma K. Dierkes

3.1 Introduction

Rubbers (or elastomers) are in general not used in their purest form, but are reinforced with fillers as unfilled rubbers are generally not very strong. The addition of fillers fundamentally changes the properties of rubber. The modulus of unfilled rubbers rises with increasing temperature, as predicted by the kinetic theory of rubber elasticity. The addition of fillers significantly changes the temperature coefficient of the modulus, it can even alter the sign of the coefficient, resulting in a decrease of the modulus with increasing temperature. Another effect of blending rubbers with fillers is the transition to non-linear behaviour. The use of reinforcing fillers gives the material unique properties: a combination of high elasticity and high strength.

Since the early 1900s carbon black has been the preferred reinforcing filler for rubber. It is available in a great variety of types [1, 2] and is used in virtually all sorts of rubbers. Usage of precipitated silicas and silicates emerged in the early 1950s, firstly because of the white colour imparted to rubber compounds, for shoe-soles and heels. Later these fillers gained significance in use in quality components of tyres and mechanical goods. For soles of athletic footwear, these white reinforcing fillers provide an improved resistance to wear and tear with the option of using all possible colours. In technical rubber goods, precipitated silicas are often used to increase tear resistance or to decrease self-heating.

Silicas have quickly gained commercial importance in the 1970s in heavy-service tyres for earth moving and mining equipment [3]. It has become common practice in the meantime to improve the cutting and chipping resistance of heavy truck tyres by adding 10-25 phr of silica to the conventional carbon-black loaded tread compounds. The carbon black level is then adjusted to maintain appropriate compound hardness. The addition of silica also results in reduced abrasion resistance and improved (wet) traction of the truck tyres, however at the expense of some increased heat build-up. The latter can be kept to an acceptable level by use of an appropriate coupling agent. Further, silica enhances the adhesion between the steel cord reinforcement and the rubber in radial tyres.

The largest breakthrough of precipitated silica, particularly in passenger tyres has happened over the last decade. On account of the development of a new generation of

'easy dispersion' silicas, it has been possible to break out of the conventional 'magic triangle of tyre technology', the compromise between low rolling resistance of a tyre, improved wet grip and maintained longevity. The replacement of carbon black by easy dispersion silica fillers, combined with special rubber types and the selection of a proper coupling agent, allows for a significantly reduced rolling resistance of tyres, and as a consequence reduced fuel consumption of the vehicle, while keeping the wet traction and abrasion resistance on the same level [4]. The importance of this development is emphasised by the contemporary situation of limited reserves of non-regenerative energy and environmental problems. The fuel savings capacity of such a tyre is 3 to 4% compared to a tyre with treads made from compounds with carbon black, corresponding to a reduction of rolling resistance of 20%. This environmental and economic incentive of silica technology is enough to overcome the higher production costs due to the difficult processing behaviour and the higher raw material costs of these tyres.

3.2 Characteristics of High-Dispersion Silicas

3.2.1 Various Classes of Silicas: Pyrogenic versus Precipitated, and their Production

There are two main classes of silicas in use in the polymer industry, differing in their way of production and resultant properties. 'Fumed silicas' are manufactured by the flame hydrolysis of silicon tetrachloride:

$$SiCl_4 + 2\ H_2O \rightarrow SiO_2 + 4\ HCl \qquad (3.1)$$

As nearly all water formed is used for the hydrolysis, these silicas are relatively low in bound water. They have generally less than 1.5 wt% of adsorbed water. Within the rubber industry, fumed silicas are nearly exclusively employed in silicone rubber compounds, and are therefore of little interest in the present context.

Hydrated amorphous silicas are prepared by precipitation from water-soluble sodium silicate ('water-glass') with an acid. Various acids may be used, including mineral acids such as sulfuric acid and hydrochloric acid. Carbonic acid, e.g., carbon dioxide charged to the aqueous solution of the metal silicate, may also be used. A by-product of the reaction is a sodium salt, which must be washed out [5, 6]. It has to be taken into account that the formation of precipitated silica is a reversible equilibrium process. Under special process conditions of pH and temperature, the reaction may be temporarily stopped or even reversed. The chemical reaction is carried out in precipitation tanks, equipped with stirrers to achieve excellent mixing of the components. Typical reaction times are between one and four hours at temperatures between 50 and 90 °C.

In the very beginning of the precipitation process small isolated particles, primary particles, are formed. Their particle size is in the order of a few nanometers. With time, the amount and size of these particles increases. Subsequently, the primary particles start to form aggregates with a particle size of a few hundred nanometers, characterised by Si-O-Si bonds between the primary particles (**Figure 3.1**). These bonds are irreversible. The ongoing process results in continuous growth of the number and size of these aggregates, until the aggregates start to condense in even larger units: agglomerates. These agglomerates are held together by reversible Van der Waals forces and hydrogen bonds. Agglomerates can be broken down to the size of aggregates by mechanical treatment.

For the development of highly dispersible silicas as commonly used in modern low rolling resistance tyres, it is important to find the best combination of aggregate and agglomerate size. The silica must be well prepared to be sufficiently porous for the aggregates to be able to be easily penetrated by the rubber. This increases the contact area between silica and rubber [7]. One way to achieve this is to interrupt the addition of acid halfway and let the precipitate ripen for some time before precipitation is restarted [8]. Most commonly the precipitation is started at a pH around 8–10, and completed at a pH of around 4-5. By stepwise precipitations at various pH values, inhomogeneous or bi-modal size distributions with various size ratios can be achieved, which are claimed to provide even lower rolling resistance tyre compounds [9-15]. Bi-modality of the filler can also be achieved during the mixing of the tyre rubber compound later on, by blending two fillers with different particle size distribution [16, 17].

Of particular importance is the drying operation of the highly dispersible silicas. The conditions used for drying determine the residual water content of the silica, its specific surface area, the structure and particle size distribution. One conventional way of recovery is filtration of the silica, washing and subsequent drying of the filter residue in tunnel driers for several hours. It leads to strong agglomeration of the silica aggregates and results in poor dispersibility in rubber. The most preferred drying technique for highly

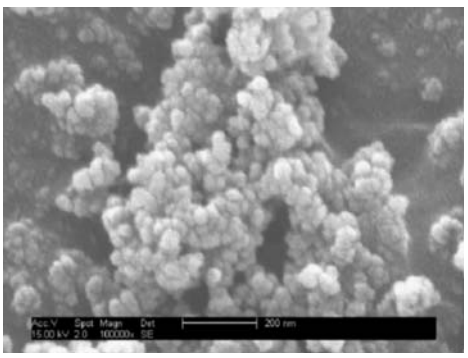

Figure 3.1 Silica aggregates - scale 1 cm = 200 nm

dispersible silicas is spray-drying for a short period of only a few seconds [5, 6, 18]. With the combination of stepwise precipitation and spray-drying, the best performing, highly dispersible silicas are obtained.

3.2.2 Properties of Highly Dispersible Silicas

Due to the large variety of production processes and process variations, there is an enormous diversity in types of silica. Attempts were made in the past to come to a classification like the one used for carbon blacks in ISO and ASTM, but these never came into effect, because of the complicated nature of the various silicas. For the reinforcing properties of silicas their particle dimensions, surface morphology, surface activity and their bonding ability for coupling agents are of particular importance. The most commonly accepted methods of characterisation of highly dispersible silicas are given here [19, 20].

Highly dispersible precipitated amorphous silicas have primary particle dimensions in the range of 10-50 nm in diameter, as determined by N_2-adsorption using the Brunauer-Emmett-Teller (BET) method [21, 22]. This method measures the overall surface area of the particles, including the micropores. The BET-surface may vary between 50 and 350 m^2/g, more specifically between 50 and 200 m^2/g. The micropores are generally small in size: < 2 nm, into which only low molecular weight chemical compounds like coupling agents and vulcanisation agents may penetrate, but no polymer molecules. This results in a loss of active components. Both *N*-cetyl-*N*,*N*,*N*-trimethylammonium-bromide (CTAB) or mercury are larger molecules that cannot penetrate into the pores and therefore measure the external surface area of the ultimate primary particles [23]. Typical CTAB-surface levels range between 100-200 m^2/g. In order to keep the microporosity to a minimum, the ratio between BET- and CTAB-surface is recommended to be close to unity for optimal reinforcement properties [12].

During silica particle growth many primary particles condense into aggregates of typical dimensions of 100-200 nm, which are in effect the reinforcing species in the rubber compound. The degree of condensation in the aggregates, commonly designated by 'structure', determines the interparticle void volume and pore diameter within the aggregates. The classical test method for 'structure' is the adsorption of dibutylphthalate (DBP value). The higher the DBP value, the higher the structure. A conventional silica has a typical DBP value of 175 g/100 g, *versus* a highly structured silica with a DBP value above 200 g/100 g. Another method is the DBP measurement while increasing the pressure on the silica from 0 to 30 MPa: the so-called crushed-DBP. It demonstrates that the structure of the highly-dispersible silica is higher and less fragile than the structure of conventional silicas. The improved dispersion characteristics of highly dispersible silicas can be explained by the high aggregate porosity, surviving for a longer time than that of conventional silica. The polymer has more room and time to penetrate into

the voids, while conventional silicas are initially strongly compacted and difficult to disperse [5, 6, 24].

Silica particles are formed from the polymerisation of silicic acid into complex amorphous polycyclic ring structures. Internal defects in these ring structures result in the occurrence of silanol groups (≡ Si – O – H) on the surface of the silica particles. These silanol groups are classified as:

- Isolated - A single silanol group on a silicon atom;
- Geminal - Two silanol groups on the same silicon atom;
- Vicinal - Two silanol groups on neighbouring silicon atoms.

These silanol-groups show a strong affinity for water molecules, bound by hydrogen bridges. Multiple layers of water may be absorbed onto the silica surface, depending on the drying conditions. The temperature for dehydration, at which all physisorbed water is removed from the silica surface, cannot be determined unambiguously, because the porosity largely influences water desorption. It is generally agreed that prolonged heating at 100 °C, or drying at 120 °C removes all physisorbed water. The number of silanol groups remaining on the surface amounts then to 4.6 ± 0.5 OH/nm^2 [19]. These silanol groups constitute sites for reaction with alkoxysilane coupling agents. Complete dehydration before mixing with rubber and coupling agents is not wanted, because the presence of significant quantities of physisorbed water promotes the chemisorption of these silane coupling agents.

3.2.3 Compatibility Aspects

A condition for filler reinforcement is the interaction between the filler particles and the polymer [25]. One of the models for the adsorption of polymers onto the surface of reinforcing fillers is based on the uncoiling of the polymeric chains and multiple adsorption of these chains onto the filler surface. The released adsorption enthalpy is partly compensating the loss in chain conformation entropy, enabling the chains to abandon their coiled conformation and to take the form of a train. With multiple contacts per polymer chain, the bonding strength of a polymer molecule is in the range of a chemisorptive interaction.

The degree of wetting of the filler by a polymer depends on the difference of the solubility parameters [26]. The surface concentration of adsorbed chains is inversely proportional to the difference in the solubility parameters between the polymer and the filler [27]. For the silica-polymer system the difference in the solubility parameters is large, with the effect that the two materials are not easily compatible. When a coupling agent is used, a hydrophobic shell is formed around the filler particle and the compatibility of the two materials increases.

3.3 Coupling Agents

Carbon black is considered to be more reinforcing for rubber tyre treads than silica, if the silica is used without a coupling agent. Silica is characterised by weaker filler-polymer interactions and correspondingly higher filler-filler interactions than carbon black. This results in a higher compound viscosity, a higher modulus at low strain amplitudes, a lower modulus at high strain amplitudes and a lower bound rubber content [28].

While various treatments and procedures have been devised to overcome such deficiencies, compounds capable of reacting with both the silica surface and the rubber elastomer molecules are used. Such coupling agents may be premixed, or pre-reacted with the silica particles or added to the rubber mix during the rubber/silica mixing stage. If the coupling agent and silica are added separately to the rubber mix during mixing, it is considered that the coupling agent then combines *in situ* with the silica.

3.3.1 Types of Commonly used Coupling Agents

Most coupling agents are composed of a silane moiety, which is capable of reacting with the silica surface, and also a part capable of reacting with the rubber, particularly with a sulfur vulcanisable rubber containing carbon-to-carbon double bonds. In this manner, the coupler acts as a connecting bridge between the silica and the rubber and thereby enhances the rubber reinforcement aspect of the silica. Usually the rubber reactive component of the coupling agent is temperature sensitive in order to combine with the rubber during the final, and high temperature, sulfur vulcanisation stage. However, some degree of bonding may occur between the rubber-reactive component of the coupling agent and the rubber during the initial mixing stages: resulting in an unwanted increase in compound viscosity and consequent premature scorch and poor processability.

3-Mercaptopropyl(trimethoxy)silane, $[(CH_3O)_3\,Si - (CH_2)_3 - SH]$, was proposed as one of the first coupling agents for rubber applications. Addition of this coupler to silica-styrene-butadiene rubber (SBR) and silica-natural rubber (NR) formulations increased tensile strength, tear resistance and modulus, and decreased hysteresis and lowered the permanent set [29, 30]. However, several properties of this coupling agent turned out to be disadvantageous. As a mercaptan it produced a unpleasant odour during mixing, especially at elevated temperatures. The reactivity of the methoxy-silyl bond towards silica was considered to be too high to allow for sufficient mixing prior to the reaction. The silylation reaction results in the evolution of methanol, a highly toxic substance. The reactivity of the mercapto-functionality towards the vinyl pendant groups in 1,2-vinyl-butadiene monomer moieties in SBR or BR is so high, that premature scorch problems occur during mixing [31, 32], particularly, where high vinyl-containing solution polymerised SBR (S-SBR) is used for green tyre purposes [4]. Therefore, its use has remained limited.

More than one hundred different organosilanes were synthesised by Wolff and co-workers for use in silica-rubber compounds [33, 34]. Two silanes were found to be suitable as coupling agents at that time:

$$(C_2H_5O)_3\ Si - (CH_2)_3 - S_x - (CH_2)_3 - Si\ (OC_2H_5)_3 \qquad x \sim 4$$

Bis(triethoxysilylpropyl)tetrasufide (TESPT) (3.2)

and

$$(C_2H_5O)_3\ Si - (CH_2)_3 - SCN$$

3-Thiocyanatopropyl-triethoxysilane (TCPTS) (3.3)

TESPT has most commonly been in use since then. The ethoxy-silyl groups are less reactive towards silica than methoxy-silyl groups. TESPT represents a mixture of silanes with different sulfur ranks, ranging from S_1 to approximately S_6, with even some free sulfur present. The average sulfur rank corresponds to 3.83. TESPT was supposed to provide a sort of shielding of the very reactive mercapto-functionality during rubber mixing conditions, and so to prevent the unpleasant smell, but to release the mercapto-functionality during vulcanisation conditions and vigorously adds to the rubber matrix. However, poly-sulfur containing compounds, similar to sulfur donor accelerators, are known to release reactive sulfur moieties of probably radical nature in rubber compounds under vulcanisation conditions. Results of recent studies show that TESPT reacts in a similar manner during vulcanisation and so couples to the rubber molecules [35-38].

3.3.2 Reactions Between Silica, Silane Coupling Agent and Rubber Polymer

The formation of a hydrophobic shell around the silica particle by the silica-silane reaction prevents the formation of a filler-filler network due to the reduction of the specific surface energy [39]. Prior to the chemical reaction of the silane with the silanol groups on the silica surface, the silane molecule has to make contact with the silica surface by adsorption [40, 41]. Then the chemical reaction of silica with an alkoxy-silyl moiety of the coupling agent takes place in a two-step, endothermic reaction. The primary step is the reaction of alkoxy-groups with silanol groups on the silica filler surface [42]. Two possible mechanisms are reported:

1. Direct reaction of the silanol groups with the alkoxy groups of the coupling-agent, and,

2. Hydrolysis of the alkoxy-groups followed by a condensation reaction with the silanol-groups [43, 44].

The fact that the rate of silanisation is influenced by the moisture content of the silica, supports the mechanism wherein a hydrolysis step is involved. The reaction follows

a pseudo first-order kinetic law. **Figure 3.2** shows the mechanism of the primary reaction.

The secondary reaction, shown in **Figure 3.3**, is a condensation reaction between adjacent molecules of the coupling agent on the filler surface or between alkoxy groups of the coupling agent and silanol groups of the silica [45-48]. It is generally accepted that, again, a hydrolysis step is involved in the reaction. In comparison to the primary reaction this step is slower by a factor of approximately 10. The energy of activation for both reactions, the primary and the secondary, is within the range of 30 to 50 kJ/mol. This value is rather low, indicating that the temperature dependence of the reaction rate is not very strong. The rates of both reactions are influenced by the acidity of the matrix, and the reaction is acid- as well as alkaline-catalysed. The reaction rate is reduced by steric hindrance and an electron donating effect of the leaving group [49]. Not all ethoxy groups react during the silanisation reaction: the reaction results in two silane-silica bonds per silyl group, with one hydrolysed ethoxy group remaining [50]. The secondary reaction has only slight influence on the properties of the compound, so

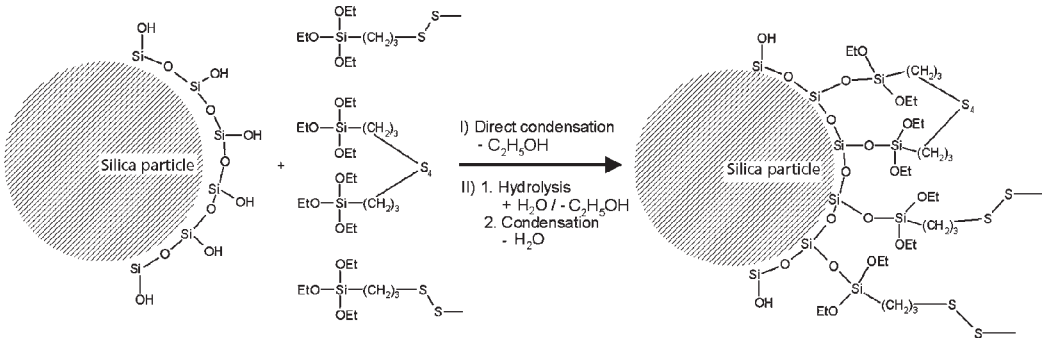

Figure 3.2. The primary reaction of silica with a silane [45]

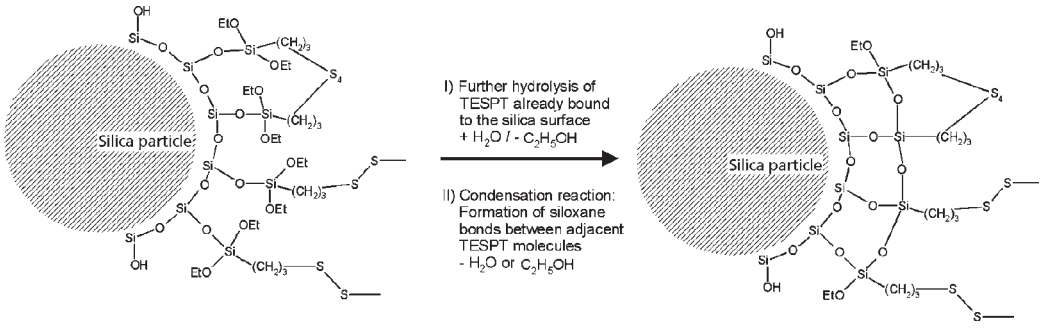

Figure 3.3 The secondary reaction of silica with a silane [45]

the incomplete reaction does not negatively influence the final quality of the material. On the contrary, in the case of bis-(dimethylethoxysilylpropyl) tetrasulfide (DMESPT), the primary reaction potentially takes place, but the secondary reaction is not possible. A reaction of the sulfur moiety with the rubber can also take place and coupling of the silica to the rubber can be achieved. Surprisingly, a better dispersion of the silica is reached even then with TESPT. The tensile strength of the DMESPT-containing compound is lower when compared to TESPT, but all other mechanical properties are similar to TESPT [51-54].

The coupling agents need a moiety enabling them to react with the polymer during vulcanisation in order to be reinforcing. This is shown in experiments with coupling agents, which can react with the filler but not with the polymer: the reinforcing effect is reduced, as the formation of bound rubber is impossible [55]. In general, the moiety reacting with the polymer is a sulfur-group, either a poly- or disulfidic group or a blocked sulfur-group. Other functional groups, used to link the coupling agents to the polymer, are double bonds which need to be activated by the addition of an active sulfur-compound or by the generation of a radical species, in order to obtain simultaneous crosslinking of the polymer and the coupling agent with comparable reaction rates during curing. **Figure 3.4** shows a general reaction scheme for the formation of the filler-polymer bond.

The polysulfidic moieties of the silanes are unstable, and cleavage of the sulfur groups results in active sulfur moieties. A notorious problem with TESPT is the balance between its reactivity towards the silica, requiring a temperature of at least 130 °C to obtain an acceptable speed, and its reactivity towards the rubber, which becomes noticeable at temperatures above 145 °C. It leaves the rubber processor a very narrow window in the mixing operation, so as to limit the duration of the mixing cycle by quickly reaching a high temperature in the mix, without the risk of creating premature scorch in the mixer.

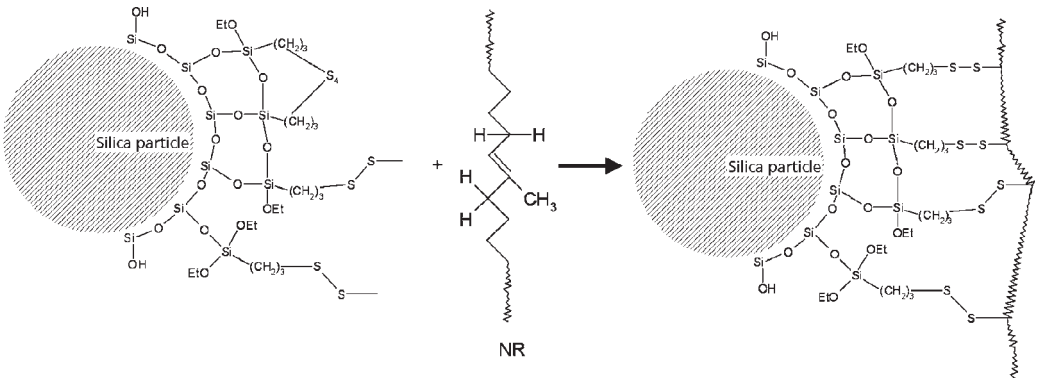

Figure 3.4 General scheme of the reaction of a polysulfidic silane with an unsaturated polymer

This danger does not exist if TCPTS is used for the silanisation. Silica modified with TCPTS forms only monosulfidic rubber-to-filler bonds in accelerator/sulfur cure systems, and is therefore mainly restricted to the use in mechanical goods and the preparation of modified silica. With TESPT, on the other hand, the reaction time increases if the optimum temperature is not attained [56].

3.3.3 Kinetics

The silanisation reaction is not a simple single-step reaction, but consists of several steps:

- Diffusion of the silane coupling agent molecules to the active sites on the filler surface;
- Adsorption of the silane molecules onto the filler surface;
- Hydrolysis of ethoxy groups of the coupling agent;
- Reaction of the first hydrolysed ethoxy group with the silanol groups of the silica filler (primary reaction);
- Reaction of the hydrolysed ethoxy groups with silanol groups of the silica or adjacent silane molecules (secondary reaction).

In a rubber compound these reactions are preceded by dispersion and distribution of the filler and blending with the coupling agent. Further side-reactions may occur such as homocondensation of the silane without being bound to the filler surface and adsorption of ethanol onto the filler surface.

With all these reactions taken into consideration, the kinetics of the silanisation reaction depend on numerous factors. The diffusion of the silane depends on the temperature of the matrix and the type of silane, the compatibility of the silane with the polymer matrix and steric properties of the silane. The adsorption of the coupling agent is influenced by the surface concentration and accessibility of the silanol groups on the silica surface. The equilibrium concentration of the silane-molecules adsorbed on the silica surface also depends on the temperature and the presence of other polar molecules that can be adsorbed. The ethoxy groups of the silane molecules react with water in a stepwise process of hydrolysis, but at the same time condensation of the reactive silanol groups occurs, resulting in an equilibrium concentration of more than 10 different reaction products [57]. The kinetics of these reactions are rather complicated, but under certain conditions they can be represented as combined in a pseudo first-order reaction [58].

3.3.3.1 The Silane

Polarity, geometry and type of functional groups determine the reaction kinetics of a silane. The silanes used as coupling agents on an industrial scale for the present application

differ in general in terms of the functional group bound to the propyl group.

The influence of the hydrolysable group on the silane coupling activity was determined by the comparison of methoxy, ethoxy and propoxy derivatives. The rate of the silanisation reaction decreases in the order:

$$CH_3O- > C_2H_5O- > C_3H_7O- > C_4H_9O-$$

With the propoxy and butoxy groups the reaction rate is generally too slow. The methoxy group reacts very rapidly, but for toxicological reasons it is not used as a silanisation agent – at least not for the *in situ* process – because it evolves methanol. This leaves the ethoxy group, which reacts quickly enough and which is toxicologically sufficiently harmless, if necessary precautions are taken.

The steric properties of the silane molecule affect the mobility of the silane in the matrix and limit the availability of silanol groups on the filler surface, once the silane is bound to the filler surface. The compatibility of the silane with the filler and the matrix is determined by the differences in polarity and solubility factors. A low compatibility results in a difficult homogenous distribution of the coupling agent in the matrix.

3.3.3.2 The Filler

Structure of the filler, acidity, moisture content as well as concentration and availability of the silanol groups on the surface are major influencing factors for understanding the kinetics of the reaction with the silane. The structure of the filler influences the silanisation kinetics as it is an important characteristic for the filler dispersibility and availability of the silanol groups. The concentration of silanol groups as one component in the silanisation reaction directly determines the rate of silanisation.

Acidity of the filler has an influence on the reaction rate of the silanisation, besides its influence on the curing characteristics. The silanisation reaction is catalysed by bases and by acids. Both, high as well as low acidity levels increase the reaction rate, mainly by increasing the rate of hydrolysis of the ethoxy-groups of the silane. Alkalis have a stronger effect compared to acids. The primary reaction is more sensitive to the acidity of the reaction medium than the secondary reaction [46, 48, 59].

Both reaction rates, the rate of the primary reaction as well as the rate of the secondary reaction, are influenced by the moisture content of the silica. The primary reaction is accelerated by increasing concentrations of water on the filler, but it is less sensitive to moisture than the secondary reaction. The rate of the primary reaction increases with increasing moisture content of the filler up to 6%. At 6% moisture content, a maximum reaction rate is achieved and no further improvement is achieved for higher moisture levels. However, the rate of the secondary reaction does not show the plateau value at 6% of moisture, but increases further with higher moisture levels [47, 48, 60].

3.3.3.3 Reaction Conditions

The reaction conditions, such as the presence of other compounding ingredients, reaction temperature, energy input and ethanol removal, influence the silanisation reaction. The competing reaction of other additives such as zinc oxide, stearic acid, alcohols and amines influence the kinetics of the silanisation reaction as they block active sites on the filler surface. Amines, either as a part of the silane molecule or added separately, have a high affinity to the silica surface and are easily adsorbed, but at the same time they have a catalytic effect on the hydrolysis reaction [58, 61, 62].

3.3.4 Alternative Coupling Agents

3.3.4.1 Silane-Based Coupling Agents

A large diversity of alternative coupling agents relative to TESPT has been developed since the upswing in silica use for passenger tyre purposes. All conceivable variants of TESPT have been claimed, with variations in alkoxy-groups attached to the silicon atom, and all sorts of sulfur moieties [63-66].

Mercapto-terminated alkylsilanes affect the cure kinetics more than the other alkylsilanes, with a considerably pronounced scorch shortening. Silanes with their mercapto groups in α-position increase the vulcanisation rate more than silanes with their sulfur-containing groups in γ-position. On the other hand, γ-derivatives resulted in a higher reinforcement, than those with the mercapto group in the α-position. Mercaptosilanes were found to be the most effective in coupling, but are not commonly used for reason of their scorch sensitivity [67].

The effects of silane coupling agents with structures similar to TESPT but with various sulfur ranks on the viscosity, curing characteristics and dynamic and mechanical properties of low rolling resistance silica filled SBR/polybutadiene tyre tread compounds were broadly investigated [55, 68-71]. TESPT, a tetrasulfide, is successively replaced by the disulfide, bis(triethoxysilylpropyl)disulfide (TESPD). TESPD is less prone to scorch and provides some extra processing latitude [72, 73]. However, the work by Hasse and co-workers [70, 71] and ten Brinke and co-workers [55] have shown, that the sulfur released from the coupling agent adds to the sulfur in the curative package, and so establishes a total pool of sulfur for vulcanisation. A change from TESPT to TESPD on an equimolar basis, without correction for the reduction in sulfur quantity leads to inferior cured properties. A nearly equal performance to TESPT is reached when a correction is made for the reduced sulfur level in the final mix by adding a corresponding amount of elemental sulfur to the curing package. The processing and property changes depend on whether the sulfur is added in the mixer or in the curative package.

A series of silane-based coupling agents with variations in sulfur rank, alkyl- and various alkoxy-groups attached to the silicon atoms, and also multiple alkyl-polysulfide blocks between the silicon atoms, were tested in comparison with TESPT [74, 75]. Increased moduli, hardness and elasticity were found and much lower values of tan δ at 60 °C, predictive of the rolling resistance of a tyre. Surprisingly, a higher tan δ at 0 °C was also observed, which can be considered as an indication of a better wet grip of a tyre.

Another type of coupling agent is represented by blocked silanes, where the mercapto-group of 3-mercaptopropyl(triethoxy)silane is blocked by esterification with an organic acid, e.g., creating an octane-thioester [76]:

$(EtO)_3Si - (CH_2)_3 - S - (CO) - (CH_2)_6 - CH_3$ (3.4)
(NXT Silane, GE Silicones, Wilton, CT, USA)

The blocked sulfur group prevents sulfur donation during the first mixing steps and is supposed to split during the addition of the curative package, thermally or with the aid of a deblocking agent such as an amine or alcohol. The coupling agent contains, on a molar basis, a higher number of alkyl groups compared to the commonly used silanes, resulting in a better hydrophobicity effect. The ratio of ethoxy groups to alkyl groups is lower, resulting in less ethanol generation for a similar hydrophobation effect [77].

Oligomeric silanes are also proposed as couplers for silica to rubber [78]. Bis(triethoxysilyl)-polybutadiene is one example of such an oligomer consisting of 27 butadiene units on average, with triethoxysilyl-groups as terminal groups:

$(EtO)_3Si-[CH_2-CH=CH-CH_2]_n-Si(EtO)_3$ (3.5)
(Rhenofit 1715, Rheinchemie, Mannheim, Germany)

The average molecular weight of the oligomer is 1800 g/mol. The filler-polymer network has to be established during the vulcanisation reaction, and a special activator for the reaction between the coupling agent and the polymer has to be added during the final mixing step. The high molecular weight of this silane results in a lower volatility compared to the commonly used silanes. The ratio of alkoxy groups to alkyl groups is low, resulting in a reduction of ethanol generation. The compound is sulfur free, therefore no scorch reaction can occur and the material can be processed at higher temperatures, up to 175 °C. As this coupling agent does not contain a sulfur-moiety for the reaction with the polymer, a sulfur-donor has to be added to the compound. This molecule donates sulfur during the curing step and enhances the reaction of the double bond of the coupling agent with the polymer.

3.3.4.2 Other Coupling Agents

A wide variety of non-silane based compounds have also been proposed as coupling agents for silica-rubber compounds. It should be noted, however, that in most cases the

reaction mechanisms of these coupling agents with silica, have not been elucidated. A brief selection of these alternative coupling agents will be covered next.

The interaction of bis(diisopropyl)thiophosphoryl disulfide (DIPDIS) with silica and hydrocarbon rubber was studied by Mandal and co-workers [79].

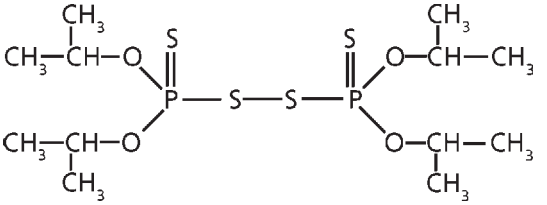

Bis(diisopropyl)thiophosphoryl disulfide (DIPDIS) (3.6)

It was shown that DIPDIS can simultaneously combine with natural rubber and silica during cure and is thus likely to influence the physical properties of the vulcanisates in a similar way as silane coupling agents like TESPT.

Organo-sulfonamides have been proposed as silica couplers:

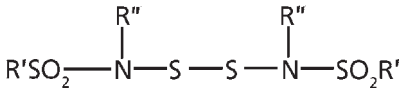

Organo-sulfonamides (3.7)

with R´ and R´´: alkyl groups. The properties (modulus, tan δ, hardness and abrasion resistance) of a natural rubber compound, containing benzene sulfonamide as coupling agent were comparable to a compound containing TESPT [80].

The properties of a silica-reinforced polyisoprene rubber containing a dialkyleneamide-polysulfide were determined and compared with a TESPT containing compound:

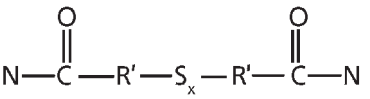

Dialkyleneamide-polysulfide, x = 2 to 7 (3.8)

The use of dialkylenamide-polysulfides resulted in higher modulus, higher hardness at room temperature and higher rebound values than the control with TESPT [81].

Because of the disadvantages of the silane coupling agents, aromatic bismaleimides were tested as silica couplers. A silica-reinforced natural rubber compound containing an aromatic bismaleimide was compared with a compound containing TESPT [82].

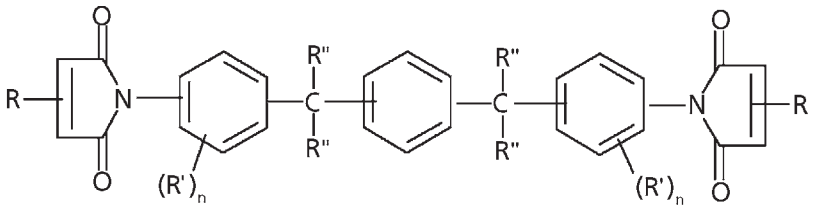

Aromatic bismaleimide (3.9)

No conclusions were drawn by the authors, but from the results it can be concluded that the properties of both compounds were comparable. Apparently, the aromatic bismaleimide is a good alternative, because it does not have scorch problems and does not hydrolyse upon storage, which a silane coupling agent does, and finally leads to a less reactive compound.

Since the introduction of silane coupling agents for silica filled rubber compounds, numerous other compounds have been proposed as cheaper and/or better coupling agents for silica. Metal and ammonium salts of salicylic acid [83]; metal and ammonium salts of phenoxyacetic acid [84]; mercaptopyridines [85]; nicotinamide [86]; phosphonates [87]; borate compounds [88]; asymmetric siloxy-compounds [89-92] and sodium, potassium or lithium salts thereof [93]; unsaturated siloxy compounds [94]; ether-containing siloxy compounds [95]; nitrogen containing siloxy compounds [96]; sulfanylsilanes [97]; sulfur functionalised polyorganosiloxanes [98]; silane/rubber accelerator combinations in one molecule [99, 100].

3.4 Characterisation Methods for Silica-Rubber Coupling

3.4.1 Rubber Reinforcement by Silica versus Carbon Black

It is generally accepted that the reinforcement mechanism of carbon black is essentially due to the formation of a co-continuous reinforcement network. The interparticle forces are based on, for example, London or van der Waals attractive forces and repulsive Lennard-Jones forces [101]. The filler particles also act as large polyfunctional crosslink sites, which cause non-affine deformation leading to strain amplification. Upon straining the carbon black reinforced rubber network, it stores energy, the carbon black network is disrupted, and furthermore the polymer molecules rearrange along the carbon black particles, because they are not chemically but rather physically adsorbed. These combined processes release energy in the form of heat. Upon removal of the strain, the stored energy in the polymeric matrix reforms the filler network. These exchanges of energy are possible because the filler network is mechanically 'trapped' in the net of the polymeric network, which is the deformation carrier. The hysteresis in carbon black reinforced rubbers is mainly due to the energy dissipation during repeated destruction and reconstruction of the filler network.

Silica is characterised by weaker filler-polymer interactions and stronger filler-filler interactions than carbon black. To enhance the filler-polymer interactions, a coupling agent is necessary; this also improves the distribution and dispersion of silica. Without coupling agent, the filler particles remain clustered in large agglomerates and aggregates, adversely affecting the tear strength and abrasion resistance of the silica compounds. The role of the coupling agent is twofold: firstly, the silica particle is hydrophobised, thus improving the dispersion. Secondly, it is turning the silica particle into a polyfunctional crosslink site, thereby chemically coupling the rubber polymers to the silica surface. Considerably less silica is required to obtain the same increase in modulus relative to the unfilled rubber, than with carbon black. This gives a compound with relatively more rubber, and therefore greater elasticity.

3.4.2 The Payne Effect

Above a critical filler concentration, the percolation threshold, the properties of the reinforced rubber material change adversely, because the filler-filler network is established. This results for example in a sharp inflection in increase of electrical conductivity of a carbon black filled compound. The continuous disruption and restoration of this filler network upon deformation is manifested in the so-called Payne-effect [102, 103], as represented in **Figure 3.5**. It illustrates the strain-dependence of the modulus and the strain-independent contributions to the complex shear or tensile moduli for carbon black filled compounds and silica filled compounds.

The main contributions to the complex modulus are:

- The strain independent hydrodynamic effect, due to the mechanical obstruction to deformation by the presence of (spherical) particles in the polymer matrix, as exemplified by Smallwood [104];
- The strain independent contribution of the polymer network, as commonly represented by polymer network theories, to be proportional to the network chain density or crosslink density;
- The strain independent filler-polymer interaction or 'in-rubber structure', where the filler particle acts as poly-functional crosslink site;
- The strain dependent filler-filler interaction: the Payne effect.

Silica filled compounds show a stronger Payne effect in general than carbon black filled compounds, because of their much stronger filler-filler interaction, at the cost of a lower filler-polymer interaction. The Payne-effect for carbon-black filled compounds is observed in strain ranges of 0.1 to 10%, whereas for silica filled compounds this range is shifted to about 10-fold higher strain ranges. With proper silica-rubber coupling, the filler-polymer interaction is strongly enhanced and the Payne effect may even practically vanish [105]. Correspondingly, the zero strain modulus is reduced, which may dictate

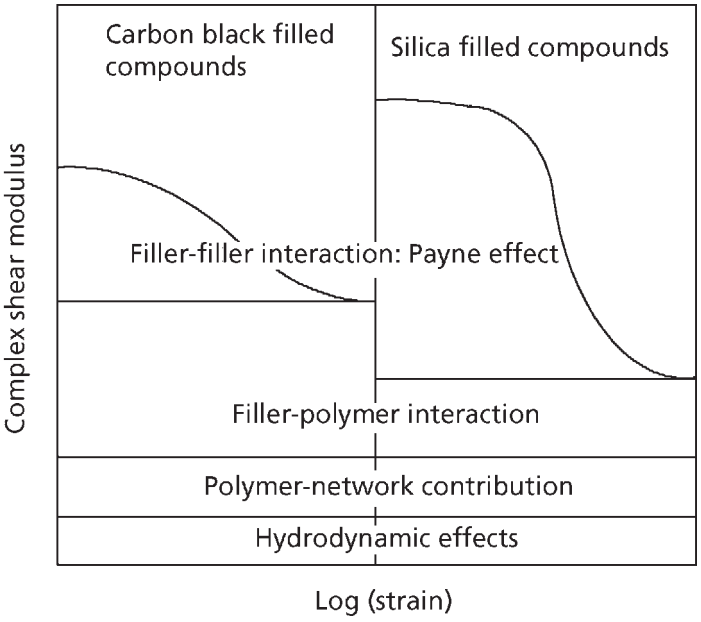

Figure 3.5 Effects contributing to the complex shear modulus

the addition of extra silica to restore the modulus and hardness. To find the optimum balance between the amount of silica, the degree of dispersion during mixing, the right amount of the appropriate coupling agent to aid the dispersion and to enhance silica-rubber coupling, is typically the task of the silica compounder. Measurement of the Payne effect of silica compounds, in the unvulcanised state as well as after vulcanisation by dynamic mechanical testing, is one of the most powerful tools to quantify silica filler-filler *versus* filler-polymer interaction.

3.4.3 Hysteresis Properties: tan δ at 60 °C

The incorporation of reinforcing fillers into rubber results in most cases in an increase of the storage and loss moduli, G´ and G´´, and an increase in hysteresis, as quantified by the loss angle δ, where tan δ = G´´/G´ [106]. When properly dispersed and coupled to the rubber matrix *via* a coupling agent, as represented by a low Payne effect, silica also shows less hysteretic loss at elevated temperatures, relative to carbon black. **Figure 3.6** depicts the typical dependence of the tan δ as a function of temperature for a typical 'Green Tyre' compound containing 75 parts per hundred rubber (phr) N234 carbon black *versus* 75 phr Zeosil 1165MP silica (Rhône Poulenc) and 12 phr X50S (a mixture of 50% TESPT and 50% carbon black N330) [39]. In tyre technology it is common to take the tan δ in the temperature range below 0 °C as indicative for winter use, from

around 0 to 30 °C as representative for the performance of a tyre with respect to (wet) traction or skid resistance.

The temperature range between 30 and 70 °C comprises the running temperature of a tyre. Under these temperature conditions the loss angle is essentially a measure for the degree of rolling resistance. **Figure 3.6** clearly shows the large gain in lower tan δ at 60 °C with silica relative to carbon black, responsible for the generally lower rolling resistance of silica, at the cost of some lower (dry) skid resistance. The skid resistance of silica-reinforced tyres on wet roads is compensated for by the more hydrophilic nature of silica *versus* carbon black. Tan δ at 60 °C is also often used as a measure of the reinforcing power of silica in rubber compounds, more closely related to its application in tyres.

3.4.4 Alternative Means to Quantify Filler-Filler and Filler-Polymer Interaction

There are various other methods used to quantify filler-filler and filler-polymer interactions in the context of silica-reinforcement of rubber. Quite a common one is based on measuring the compound Mooney viscosity, as indicative of the degree of silanisation of the silica [107]: a lower compound Mooney viscosity means that better silanisation will be obtained in the mixing process. Another method indicative of the reinforcing power of a well-dispersed and well coupled silica is the shape of the tensile stress-strain curve after vulcanisation. Silica compounds are characterised by a steep upswing of the tensile stress

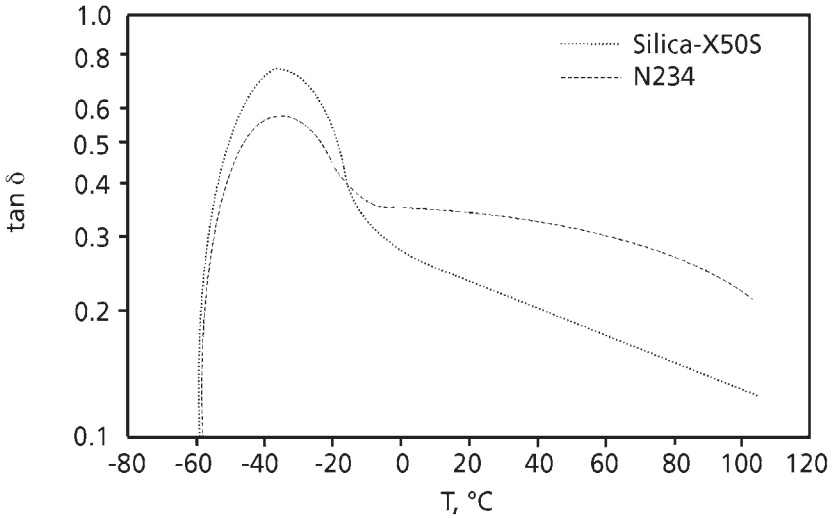

Figure 3.6 Temperature profile of the phase angle for a 75 phr N234 carbon black filled, *versus* a 75 phr silica/12 phr X50S reinforced green tyre compound [39]

after an initial slow beginning at the first 100% strain. The ratio of the moduli M_{300} at 300% strain and M_{100} at 100% strain: M_{300}/M_{100}, is also often used. It is surprising how well the M_{300}/M_{100}, although being of an entirely different nature, corresponds with tan δ-values: a higher M_{300}/M_{100} corresponding to a lower tan δ [55].

All sorts of common rubber tests such as resilience tests, fatigue tests, abrasion resistance, and so on are used as well for the purpose of quantification of the reinforcing power of silica in rubber compounds.

3.5 Mixing of Silica-Rubber Compounds

Because of the intricate interaction between silica and rubber *via* the coupling agent, and the *in situ* nature of the silanisation of the silica by the coupling agent during the mixing operation, it is of utmost importance to properly define and control the mixing conditions. Rubber mixing is commonly done on internal batch mixers, of the tangential or intermeshing type. These mixers are laid out for carbon black mixing, a pure physical dispersion effect. However, for silica mixing in the presence of silane coupling agents, the internal mixer is also considered to operate as a chemical reactor, which the equipment has not been designed for. Substantial amounts of ethanol are generated during the reaction of silica with silane, which need to be removed from the compound in this mixer, which in essence is a closed entity. Special adjustments of the equipment may be envisaged to enhance the removal of ethanol and so improve the silanisation efficiency [108, 109], however the practical implementation has remained limited. For the time being it is commonly acknowledged, that internal mixers of the 'intermeshing' rotor type perform better than those with 'tangential' rotors [110].

3.5.1 Effect of TESPT on the Properties of Uncured and Cured Compounds [62, 111]

In order to illustrate the need for a coupling agent like TESPT, compounds mixed according to a 'Green Tyre' recipe [4] and procedure in **Tables 3.1** and **3.2**, in the presence and absence of TESPT coupling agent, will be discussed next.

The compounds were mixed in three steps, the first two in a Brabender Plasticorder lab station tangential internal mixer with a mixing chamber of 390 ml, the third on a Schwabenthan Polymix 80T 300 ml two roll mill. Cooling water was kept at 50 °C. The dump temperature of the compound in the internal mixer was varied by adjusting the mixer rotor speed and the fill factor. After each mixing step the compound was sheeted out and cooled on the two-roll mill. The third step on the mill was to add the accelerators CBS and DPG and the sulfur to the compound. The complete mixing procedure is given in **Table 3.2**.

Table 3.1. 'Green Tyre' compound recipe		
Component	**Source**	**phr**
S-SBR (Buna®VSL 5025-1 HM)[a)]	Bayer AG	75
BR (Kosyn® KBR 01)	Korea Kumho Petrochemical Company	25
Silica (Zeosil® 1165 MP)	Rhodia Silices	80
TESPT (Silquest® A-1289)	Osi Specialties Crompton Corporation	0.7
Aromatic Oil (Enerflex® 75)	BP Oil Europe	32.5
ZnO	Merck	2.5
Stearic acid	Merck	2.5
Sulfur	JT Baker	1.4
CBS (Santocure®)	Flexsys BV	1.7
DPG (Perkacit®)	Flexsys BV	2
Total		**229.6**
[a)] vinyl content 50%, styrene content 25%, oil content 37.5 phr *CBS: N-Cyclohexyl benzthiazol sufenamide* *DPG: Diphenyl guanidine*		

Table 3.2. Mixing procedure	
Step 1:	
Time (min.sec)	
0.00	Open mixer; add rubber
0.20	Close mixer
1.20	Open mixer; add ½ silica, ½ silane, ½ oil, ZnO, stearic acid
1.50	Close mixer
2.50	Open mixer; add ½ silica, ½ silane, ½ oil
3.30	Close mixer
4.30	Open mixer; sweep
4.45	Close mixer
6.45	Dump
Step 2:	
Time (min.sec)	
0.00	Load compound for second time
5.00	Dump
Step 3:	
Add accelerators and sulfur on the two-roll mill at 40 °C	

The Mooney viscosities of the compounds after two mixing steps are listed in **Table 3.3**. Irrespective of dump temperature, the compounds without TESPT show very high Mooney viscosities. This is the first indication of a poor dispersion of the silica filler. With TESPT present in the compound much lower values are obtained.

The Payne effect was measured with a rubber process analyser (RPA) 2000 (Alpha Technologies). The storage modulus (G´) at a low strain of 0.56%, as a measure for the filler-filler interaction, is plotted *versus* the dump temperature for compounds in absence and presence of TESPT in **Figure 3.7**. G´ decreases with increasing dump temperature for the compound without TESPT. But relatively high values are obtained, a second indication that there is a large amount of filler-filler interaction due to poor dispersion of the silica. With TESPT present, significantly lower G´ values are obtained over the

Table 3.3. Influence of dump temperature and coupling agent on Mooney viscosity

Without TESPT		With TESPT	
Dump temperature, (°C)	Mooney viscosity, ML (1+4) 100 °C	Dump temperature, (°C)	Mooney viscosity, ML (1+4) 100 °C
112	158	115	-
132	171	133	77
151	173	149	86
169	163	169	90
185	164	183	116

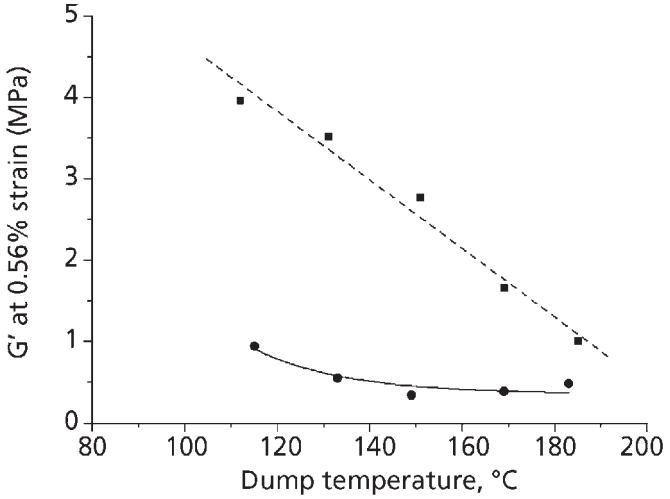

Figure 3.7 Storage modulus G´ at 0.56% strain as a function of mixer dump temperature: (■) without TESPT, (●) with TESPT

whole dump temperature range; especially at low dump temperatures, representing more common practical mixing conditions.

The presence of TESPT has a major influence on the tensile properties after curing for 12 minutes at 160 °C (**Figure 3.8**). In absence of TESPT a lower tensile strength and a larger elongation at break are obtained compared to a compound with TESPT.

Other vulcanised compound properties are shown in **Table 3.4**. The Shore A hardness remains more or less constant with increasing dump temperature. In the presence of TESPT, slightly lower Shore A hardness values are obtained, indicating a better dispersion of the silica and corresponding lower filler-filler interaction. The tan δ values at 60 °C, indicative of the rolling resistance of a tyre, differ significantly with dump temperature, irrespective of the presence of TESPT. Another way to look at the rolling resistance is M_{300}/M_{100}, as explained in Section 3.4.3 of this chapter. M_{300}/M_{100} is higher for the compound with TESPT. The effects of dump temperature are most conspicuous for compounds with TESPT present. An increase in dump temperature results in higher M_{300}/M_{100} values. For the compound without TESPT, there is no clear effect of the dump temperature on M_{300}/M_{100} visible. Compounds without TESPT are irreproducible and result in scatter of the data.

The results presented show that, when TESPT is omitted in the tyre tread compound, processing is much more difficult due to the high viscosity of the compound. Further, poor dynamic and mechanical properties are obtained without TESPT. A coupling agent such as TESPT is a prerequisite to overcome the processing problems and to obtain good dynamic and mechanical properties.

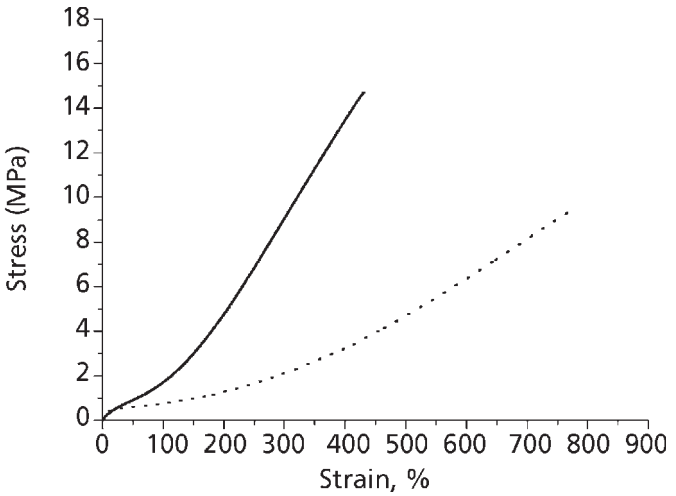

Figure 3.8 Stress-strain curve for a compound without TESPT (. . .) and with TESPT (——)

Table 3.4. Influence of dump temperature and presence of TESPT on cured mechanical properties

Without TESPT				With TESPT			
Dump temperature, (°C)	Hardness, (Shore A)	Tan δ at 60 °C	M_{300}/M_{300}	Dump temperature, (°C)	Hardness, (Shore A)	Tan δ at 60 °C	M_{300}/M_{300}
112	76	0.190	1.84	115	-	-	4.57
132	76	0.144	2.02	133	64	0.183	4.54
151	73	0.147	1.98	149	63	0.176	5.09
169	73	0.181	2.42	169	55	0.143	6.39
185	75	0.190	2.96	183	65	0.131	7.57

3.5.2 Properties of Uncured Compounds in Relation to the Dump Temperature in the Presence of TESPT Silane Coupling Agent

The most direct indication of a premature silica-silane-rubber reaction is a change in Mooney viscosity of the compounds, still without the curing additives present (see **Figure 3.9**). At dump temperatures above 150 °C, a gradual increase in compound Mooney viscosity is observed, indicative of the scorch problems provoked by TESPT at too high mixing temperatures. The premature reaction of the coupling agent towards silica and rubber should also raise the bound rubber content as given in **Figure 3.9b**. Although there is quite some scatter in the data, there is still a slight trend of bound rubber increasing with higher dump temperatures. The limited accuracy of bound rubber measurements, particularly for silica compounds, was observed by others as well [112, 113] and blamed on the complexity of the system. These measurements only have limited significance.

In order to study the reaction between TESPT and silica and with the rubber matrix in more detail, the Payne effect was measured with the RPA by subjecting uncured compounds to different strain amplitudes. **Figure 3.10a** shows the effect of the dump temperature on the dynamic storage modulus G´ at the low strain value of 0.56%, as a measure for filler-filler interaction. It decreases steadily up to a dump temperature of 150 °C after which it slightly increases again. At 100% strain, where filler-filler interaction basically does not play a role anymore, G´ remains constant up to 150 °C, after which it increases substantially, see **Figure 3.10b**.

The decrease in the G´ at low strain and the constant compound Mooney viscosity up to dump temperatures of 150 °C are obviously due to the primary and secondary reactions of the coupling agent with the silica surface. A higher degree of coupling leads to less filler-filler interaction, and therefore a decrease in G´ at low strain with increasing dump temperature. The

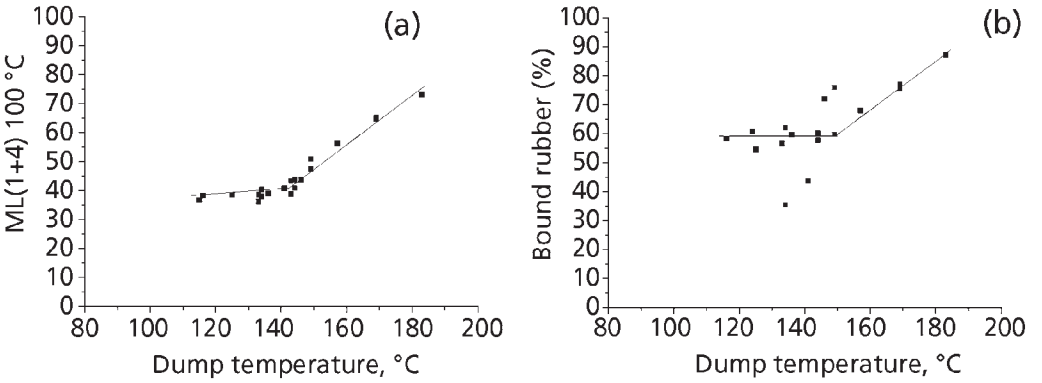

Figure 3.9 (a) Mooney viscosity and (b) bound rubber content as a function of dump temperature

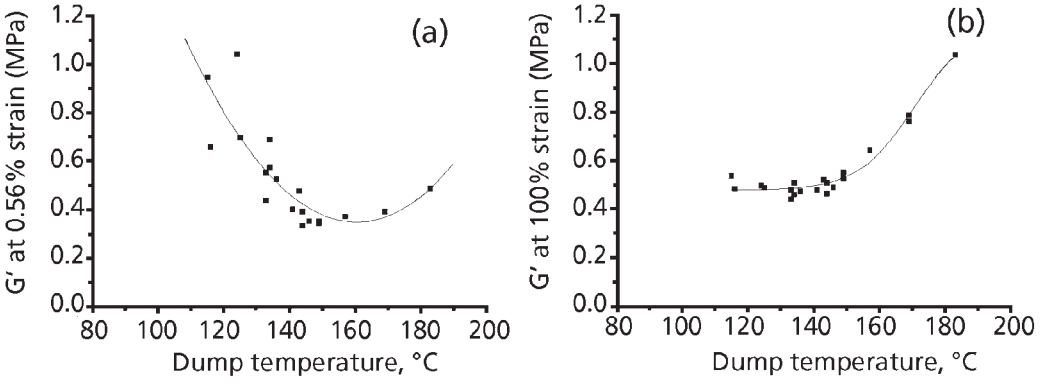

Figure 3.10 Influence of dump temperature on the Payne effect, (a) *versus* storage modulus at 0.56% strain; (b) *versus* storage modulus at 100% strain

increase in G˝ and Mooney viscosity observable at dump temperatures above 150 °C is indicative of scorch due to the reaction between the coupling agent and the rubber matrix, resulting in the premature filler ↔ coupling agent ↔ rubber network.

The relative increase in G˝ measured at 100% strain between dump temperatures of 150 and 180 °C is much larger than that observed at 0.56% strain. This difference is difficult to explain, but is related to performance characteristics of the system concerned. At low strain values, the silica-filler network is fully developed and has a strong influence on the G˝. At higher strain values, the filler-network is broken and hence its effect on G˝ disappears, irrespective of whether measured at 150 or 180 °C. The degree of scorch due to TESPT at 180 °C makes itself felt the same at low and high strain values. Hence,

the scorch is independent of strain and of the reinforcing effect of the filler. The larger relative increase in G´ observed at 100% strain, at which the reinforcing effect of the filler is much lower than at 0.56% strain, is indicative of an increase in the modulus of elasticity caused by the scorch occurring in the early curing stages.

3.5.3 Effect of the Dump Temperature on the Tensile Properties of Cured Samples

The tensile properties of cured compounds are shown in **Figure 3.11**, with the dump temperature as a variable. Above 130 °C dump temperature, the elastic Young's modulus

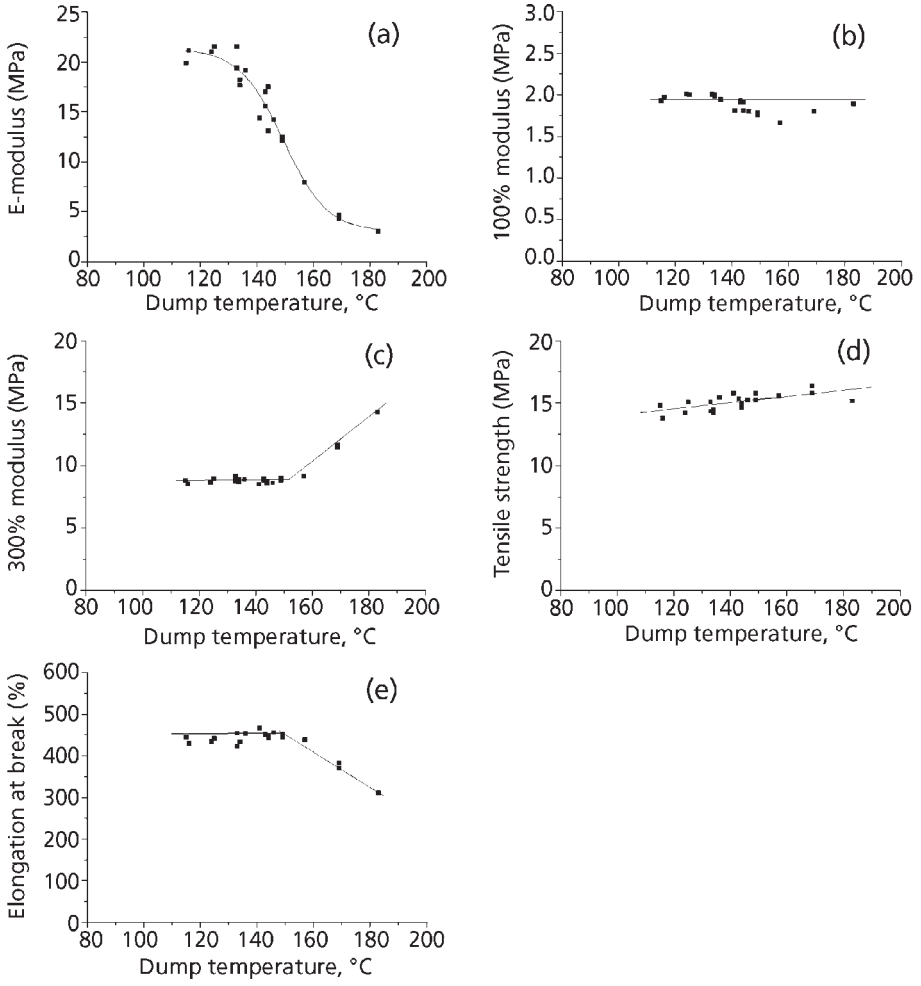

Figure 3.11 Tensile properties of cured compounds as a function of dump temperature. (a) Elastic Young's modulus, (b) 100% modulus, (c) 300% modulus, (d) Tensile strength, (e) Elongation at break

starts to decrease. This decrease can be attributed to a reaction between the silica and the coupling agent. As the elastic Young's modulus is by definition a low-strain property, it is also sensitive to filler–filler interaction between silica aggregates like the G´ at low strain amplitudes. The effects of filler-filler interaction make themselves felt all the way through the vulcanisation step.

The dump temperature does not have a significant influence on the 100% modulus. However, the 300% modulus remains practically constant up to a dump temperature of 150 °C and then increases, as shown in **Figure 3.11c**. The results of the dynamic measurements of unvulcanised compounds at low and high strain amplitudes (**Figures 3.10a** and **b**), bear a striking resemblance to those of the stress–strain measurements of vulcanised compounds at low and high strain amplitudes (**Figure 3.11a** and **c**). The tensile strength shows a slow, steady increase with increasing dump temperature (**Figure 3.11d**). At dump temperatures above 150 °C the elongation at break shows a substantial decrease (**Figure 3.11e**), as is commonly observed when crosslinking occurs.

Tan δ, as measured with the RPA 2000, and M_{300}/M_{100} values, as derived from the data in **Figure 3.11** are given in **Figure 3.12**, as a function of mixer dump temperature.

Both material properties show an improvement in the rolling resistance with increasing dump temperature. M_{300}/M_{100} increases with increasing dump temperature, and tan δ decreases. The increase of M_{300}/M_{100} is mainly due to an increase in the 300% modulus (**Figure 3.11b** and **c**). High dump temperatures correspond to lower rolling resistance, as shown by the two measurements. On the other hand, at too high dump temperatures many processing problems arise due to scorch of the compound in the mixer.

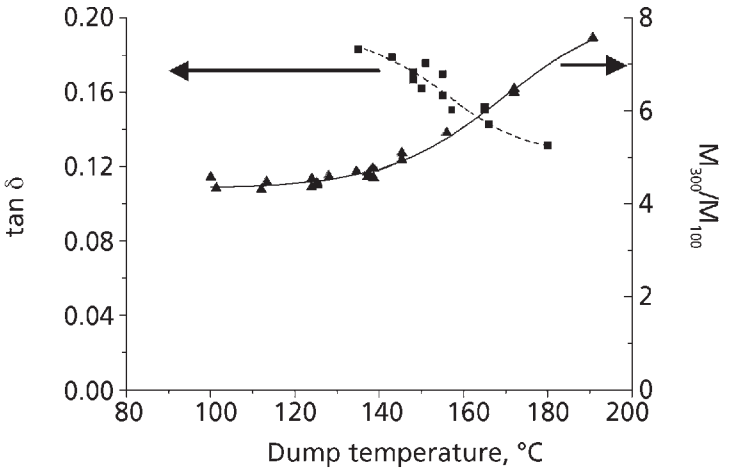

Figure 3.12 Tan δ (■) and M_{300}/M_{100} (▲) as a function of the dump temperature

3.5.4 Interactions Between Time and Temperature as an Indication of Reaction Kinetics of the Coupling Reaction

In order to quantify the effects of exposure temperature and time in some detail, experiments were performed using the Schwabenthan Polymix 80T two-roll mill at different milling temperatures. First, the compound as given in **Table 3.1** was mixed in the Brabender mixer using a fill factor of 70% and a rotor speed of 100 rpm. After completing the Brabender mixing cycle with a dump temperature of 150 °C, the compounds were milled for 10 minutes on the two-roll mill at different temperatures. **Figure 3.13a** shows the G´ at 0.56% strain as a function of the applied mill temperature. The same trend is visible as with the different dump temperatures after Brabender mixing (**Figure 3.10a**), G´ decreases with increase in temperature up to 150 °C and then increases at higher temperatures. **Figure 3.13b** shows the effect of the mill temperature on G´ at 100% strain. It remains more or less constant up to 140 °C, after which it shows only a slight, virtually insignificant, increase. This is more or less the same behaviour as that observed at different dump temperatures (**Figure 3.10b**), except that the effects are now much less discernible.

In spite of the fact that the compounds had reached a dump temperature of 150 °C once already during the first step in the Brabender mixer, extended milling at 150 °C led to a further decrease in G´ at 0.56% strain, even after 10 minutes milling. This implies that the reaction between the coupling agent and the silica was still not complete by the end of the first 6.45 minutes mixing in the Brabender mixer at a dump temperature of 150 °C. Therefore, the effect of different mixing times in the Brabender mixer was further investigated, keeping the temperature constant at 150 °C during the first mixing step, after the last addition of ingredients at 4.45 minutes. The results in **Figure 3.14a** show, that G´ at low strain does not reach a constant value, even after 15 minutes of mixing at 150 °C. However, in the second mixing cycle, as shown in **Table 3.2**, the G´ reaches a

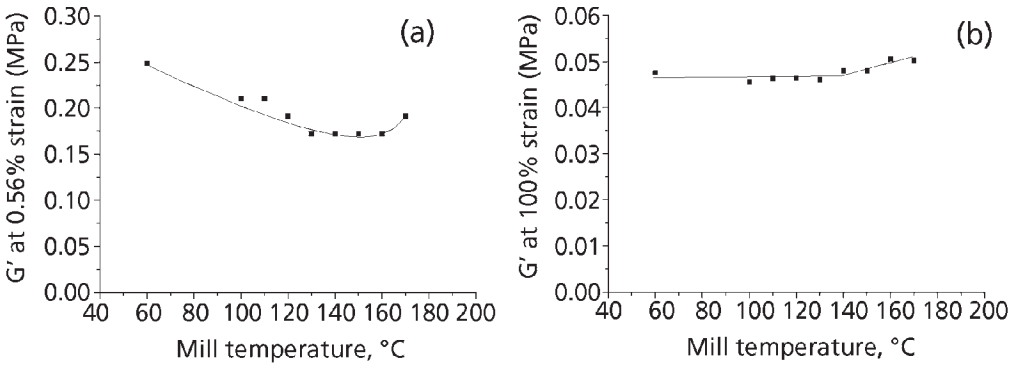

Figure 3.13 Influence of milling temperature on the storage modulus at (a) 0.56% strain, and (b) 100% strain

constant value after the compound has gone through mixing for more than 10 minutes in the first step (**Figure 3.14b**). To obtain a properly reproducible compound, it must be mixed for at least 10 minutes up to a maximum temperature of 150 °C during the first step, preferably followed by a second mixing step of about five minutes. The reactions between TESPT and silica are very slow indeed. The primary and secondary reactions between silane and silica proceed at a slower rate under the conditions used, as previously suggested by Hunsche and co-workers [47]. It should be born in mind though, that the removal of ethanol coming from the silane-silica reaction is one of the major driving forces for the reaction to proceed, which is strongly dependent on the mixer configuration, fill factor, instantaneous temperature and whether special precautions have been made to aid the removal of this ethanol [107].

3.5.5 Effect of Mixer Size and Rotor Type

To test the influence of mixer size and rotor type, compounds were mixed in a Shaw Intermix intermeshing five litre mixer. With this mixer, variation of the rotor speed influences the dump temperature more directly than with a tangential mixer like the Brabender. Several rotor speeds and fill factors were applied. Results of dynamic storage modulus G´ are presented in **Figure 3.15** for both types of mixers. The same trend is visible for the two mixers. Slightly lower G´ at 0.56% strain values were obtained for the five litre mixer, indicative of a somewhat better mixing performance of the intermeshing rotor mixer than the tangential one (**Figure 3.15a**). Similarly, the same trend in the G´ curve at 100% strain is observed as for the 390 ml mixer (**Figure 3.15b**). The temperature where the G´ starts to increase is slightly higher for the larger mixer. The reaction of the coupling agent with the rubber starts in the five litre mixer at 160 °C, whereas the reaction in the 390 ml mixer starts at approximately 150 °C. This may be due to a more homogeneous temperature profile in the intermeshing mixer relative to the tangential one, preventing overheated spots in the mixer chamber.

3.5.6 Considerations on Mixer Operation

The results of the experiments clearly illustrate the effects of time and temperature on the various reactions which may take place: the primary and secondary reactions between the coupling agent and the silica surface at temperatures up to 150 °C and the reaction of the sulfur moiety in the coupling agent with the rubber matrix at temperatures above 160 °C. The latter reaction may in principle be the result of two mechanisms. The first is a sort of bonding of the coupling agent to the rubber polymer, after the coupling agent has already reacted with the silica particle. The second may be the donation of sulfur to the rubber compound by the coupling agent, which hence triggers a sort of curing of the rubber by making use of its own released sulfur [38]. Which of these two mechanisms prevails under the test conditions used cannot be concluded from the results.

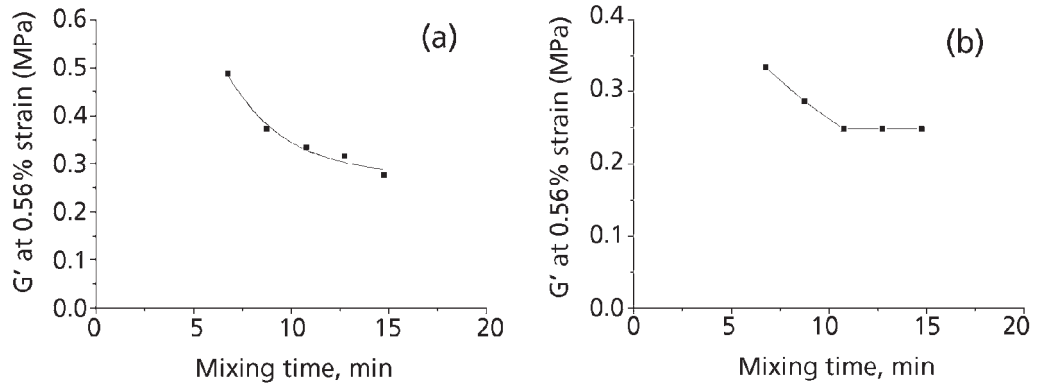

Figure 3.14. Influence of continued mixing time on the storage modulus at 0.56% strain (a) during the first mixing step and (b) after the second mixing step

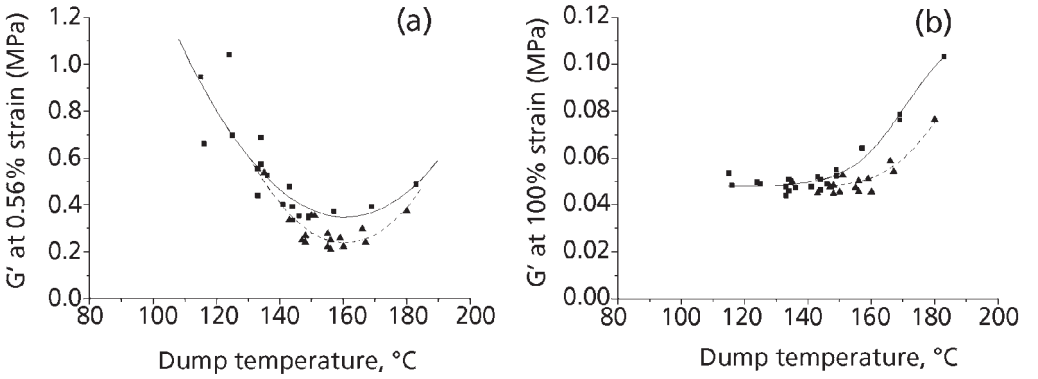

Figure 3.15 Influence of mixer size on the storage modulus at (a) 0.56% strain and at (b) 100% strain; (■) Brabender 390 ml mixer, (▲) Shaw 5 litre mixer

It is clearly shown, though, that a temperature of approximately 160 °C should not be exceeded during the mixing when TESPT is used as coupling agent. The Young's modulus of elasticity and G′ at low strain, which may both be regarded as indicative parameters for the coupling reaction between the filler particle and the coupling agent, show that a mixing dump temperature of at least 130 °C is required for proper reaction. Luginsland arrived at similar conclusions *via* different experiments [37, 42].

The results of the experiments also show that long mixing times and high temperatures are required to ensure that the TESPT coupling agent reacts with the silica surface to the desired extent, but that the temperatures must not become too high, because otherwise scorch/curing will occur. Different mixing times and batch temperatures and differences in other parameters such as the specific mixing energy evidently lead to substantial differences

in the properties of the cured compound. The mixing time and batch temperature become interdependent during the mixing, and are also influenced by the properties of the mixer used and the other mixing conditions. So mixing silica compounds with the aid of coupling agents can be regarded as 'reactive mixing'. Such mixing demands control principles that are a good deal more complex than those commonly used in carbon-black mixing, representing a new dimension in rubber technology.

3.6 Conclusions

A large breakthrough in the use of easy dispersion precipitated silica technology has occurred over the last decade by its application in passenger tyre treads, for reasons of reduced rolling resistance of the tyres and corresponding fuel savings of cars. It consists of an intricate mutual interplay of many factors: the particular highly dispersible silica, the application of a proper functioning coupling agent and selection of the appropriate raw rubber types. Furthermore, the intricate coupling of the coupling agent to the precipitated silica needs to happen at the same time as the rubber-silica compound is mixed in internal mixers, thereby using the internal mixer as a chemical reactor, for which purpose these machines have not been designed. The mixing/reaction conditions need to be carefully chosen and monitored in order to achieve proper coupling to the silica, without the risk of a premature reaction of the coupling agent with the rubber polymers, leading to premature scorch. The reaction of the coupling agent with the rubber polymers is required to take place only during the final vulcanisation stage. The dump temperature during mixing has been shown to be a parameter of paramount importance in mixing silica and rubber with the aid of TESPT as coupling agent. A minimum dump temperature of 130 °C is required to ensure that the silica and the coupling agent react to the desired extent, but at temperatures above 160 °C either the coupling agent starts to react with the rubber matrix or the TESPT starts to donate sulfur.

New challenges are facing the silica, rubber and tyre industry, and the rubber mixing machines manufacturers, to develop new and innovative concepts to optimise this technology further, whereupon it is expected to largely replace the use of carbon black in tyre tread compounds in due course.

References

1. R.K. Iler, *The Colloid Chemistry of Silica and Silicates*, Cornell University Press, Ithaca, NY, USA, 1955.

2. R.K. Iler, *The Chemistry of Silica: Solubility, Polymerisation*, Colloid and Surface Properties and Biochemistry, John Wiley & Sons, NY, USA, 1979.

3. M.P. Wagner, *Rubber Chemistry and Technology*, 1976, **49**, 3, 703.

4. R. Rauline, inventor; Compagnie Generale des Etablissements Michelin, assignee; EP 0501227A1, 1992.

5. A. Blume and S. Uhrlandt in *Proceedings of the 157th ACS, Rubber Division Meeting*, Dallas, TX, USA, Spring 2000, Paper No.32.

6. A. Blume and S. Uhrlandt, *Rubber World*, 2002, **226**, 1, 30.

7. Y. Bomal, S. Touzet, R. Barruel, P. Cochet and B. Dejean, *Kautschuk und Gummi Kunststoffe*, 1997, **50**, 6, 434.

8. Y. Chevallier and J-C. Morawski, inventors; Rhone-Poulenc Chimie, assignee; EP 0157703B1, 1989.

9. W. Hendrick and I.I.M. Tijburg, inventors; AKZO-PQ Silica VOF, assignee; EP1200346, 2002.

10. Y. Chevallier and R. Valero, inventors; Rhodia Chimie, assignee; WO 02051749A1, 2002.

11. S. Uhrlandt, R. Schmoll, A. Blume and D. Luginsland, inventors; Degussa AG, assignee; DE 10112652, 2002.

12. H-D. Luginsland, A. Wehmeier, O. Stenzel and S. Uhrlandt, inventors; Degussa AG, assignee; WO 2004/065443 A2, 2004.

13. H-D. Luginsland, A. Wehmeier, O. Stenzel and S. Uhrlandt, inventors; Degussa AG, assignee; DE 10358466A1, 2003.

14. D-H. Luginsland, A. Wehmeier, O. Stenzel, A. Blume and S. Uhrlandt, inventors; Degussa AG, assignee; WO 2004/065299 A1, 2004.

15. No inventors; Degussa AG, assignee; DE 10358449.8, 2004.

16. T.F.E. Materne and G. Agostini, inventors; The Goodyear Tire & Rubber Company, assignee; EP 0942029A2, 1999.

17. T.F.E. Materne, G. Agostini, F. Visel, U.W. Ernst and R.J. Zimmer, inventors; The Goodyear Tire & Rubber Company, assignee; EP 1078954 A2, 2001.

18. H. Ferch and H-E. Toussaint, *Kautschuk und Gummi Kunststoffe*, 1996, **49**, 9, 589.

19. E.F. Vansant, P. Van DerVoort and K.C. Vrancken in *Characterisation and Chemical Modification of the Silica Surface*, Eds., B. Delmon and J.T. Yates, Studies in Surface Science and Catalysis, Volume 93, Elsevier, Amsterdam, The Netherlands, 1995.

20. T.A. Okel in *Proceedings of the 167th ACS, Rubber Division Meeting*, San Antonio, TX, USA, Spring 2005, Paper No.C.

21. S. Brunauer, P.H. Emmet and E. Teller, *Journal of the American Chemical Society*, 1938, **60**, 2, 309.

22. ISO 5794-1, Annex D, *Rubber Compounding Ingredients - Silica, Precipitated, Hydrated - Part 1: Non-Rubber Tests*, 2005.

23. ASTM 3765, *Standard Test Method for Carbon Black – CTAB (Cetyltriethylammonium Bromide) Surface Area*, 2004.

24. L-Ph.A.E.M. Reuvekamp, *Reactive mixing of silica and rubber for tyres and engine mounts*, Twente University Press, Enschede, the Netherlands, 2003. [Thesis]

25. E.M. Dannenberg, *Rubber Chemistry and Technology*, 1975, **48**, 3, 410.

26. R.H. Schuster in *Proceedings of the 148th ACS, Rubber Division Meeting*, Cleveland, OH, USA, Fall 1995, Paper No.93.

27. R.H. Schuster, *International Polymer Science and Technology*, 1996, **23**, 11, T/9.

28. S. Wolff, M-J. Wang and E-H. Tan, *Kautschuk und Gummi Kunststoffe*, 1994, **47**, 2, 102.

29. D.M. Schwaber and F. Rodriguez, *Rubber and Plastics Age,* 1967, **48**, 1087.

30. E.M. Dannenberg, *Elastomerics*, 1981, **113**, 12, 30.

31. E. Klemm and U. Gorski, *Angewandte Makromolekulare Chemie*, 1993, **207**, 187.

32. U. Gorski and E. Klemm, *Angewandte Makromolekulare Chemie*, 1998, **254**, 11.

33. F. Thurn, K. Burmeister, J. Pochert and S. Wolff, inventors; Deutsch Gold- und Silber-Scheideanstadt Vormals Roessler, assignee; US 3,873,489, 1975.

34. F. Thurn and S. Wolff, *Kautschuk und Gummi Kunststoffe*, 1975, **28**, 12, 733.

35. U. Görl and J. Münzenberg in *Proceedings of the 151st ACS, Rubber Division Meeting*, Anaheim, CA, USA, Spring 1997, Paper No.38.

36. H-D. Luginsland, *Kautschuk und Gummi Kunststoffe,* 2000, **53**, 1, 10.

37. H-D. Luginsland and A. Hasse in *Proceedings of the 157th ACS, Rubber*

Division Meeting, Dallas, TX, USA, Spring 2000, Paper No.34.

38. S.C. Debnath, R.N. Datta and J.W.M. Noordermeer, *Rubber Chemistry and Technology*, 2003, **76**, 5, 1311.

39. M-J. Wang, *Rubber Chemistry and Technology*, 1998, **71**, 3, 520.

40. J.G. Matisons, A.E. Jokinen and J.B. Rosenholm, *Journal of Colloid and Interface Science*, 1997, **194**, 1, 263.

41. A. Burneau and J-P. Gallas in *The Surface Properties of Silicas*, Ed., A.P. Legrand, John Wiley & Sons, Chichester, UK, 1988.

42. H-D. Luginsland in *Proceedings of the Rubberchem 99 Conference*, Antwerp, Belgium, 1999, Paper No.22.

43. D.W. Sindorf and G.E. Maciel, *Journal of Physical Chemistry*, 1982, **86**, 26, 5208.

44. D.W. Sindorf and G.E. Maciel, *Journal of the American Chemical Society*, 1983, 105, 12, 3767.

45. U. Görl and A. Hunsche in *Proceedings of the 150th ACS, Rubber Division Meeting*, Louisville, KY, USA, Fall 1996, Paper No.76.

46. A. Hunsche, U. Görl, A. Müller, M. Knaack and T. Göbel, *Kautschuk und Gummi Kunststoffe*, 1997, **50**, 12, 881.

47. A. Hunsche, U. Görl, H. G. Koban and T. Lehmann, *Kautschuk und Gummi Kunststoffe*, 1998, **51**, 7-8, 525.

48. U. Görl, A. Hunsche, A. Müller and H. G. Koban, *Rubber Chemistry and Technology*, 1997, **70**, 4, 608.

49. E.R. Pohl, A. Chaves, C.T. Danehey, A. Sussman and V. Benett in *Silanes and Other Coupling Agents, Volume 2*, Ed., K.L. Mittal, VSP, Utrecht, The Netherlands, 2000.

50. M. Marrone, T. Montanari, G. Busca, L. Conzatti, G. Costa, M. Castellano and A. Tuturro, *Journal of Physical Chemistry B*, 2004, **108**, 11, 3563.

51. L.A.E.M. Reuvekamp, P.J. van Swaaij and J.W.M. Noordermeer, *Rubber Kautschuk Gummi Kunsstoffe*, in print.

52. H-D. Luginsland, inventor; Degussa Hüls AG assignee; DE 19915281A1, 2000.

53. P. Barruel and N. Guennouni, inventors; Rhodia Chimie, assignee; WO 2002/083719, 2002.

54. O. Durel, R. Rauline and N. Guennouni, inventors; Michelin Recherche et Technique SA, assignee; US 7,217,751, 2007.

55. J.W.M. Noordermeer, L.A.E.M. Reuvekamp, P.J. van Swaaij and J.W. ten Brinke, *Rubber Chemistry and Technology*, 2003, **76**, 1, 12.

56. S. Wolff, *Rubber Chemistry and Technology*, 1996, **69**, 3, 325.

57. B. Ankles, J.R. Steinmetz, J. Zazyczny and P. Metha in *Silanes and Other Coupling Agents*, Ed., K.L. Mittal, VSP, Utrecht, The Netherlands, 1992.

58. F.D. Blum, W. Meesiri, H-J. Kang and J.E. Gambogi in *Silanes and Other Coupling Agents*, Ed., K.L. Mittal, VSP, Utrecht, The Netherlands, 1992.

59. W. Posthumus, P.C.M.M. Magusin, J.C.M. Brokken-Zijp, A.H.A. Tinnemans and J. R. van der Linde, *Journal of Colloid and Interface Science*, 2004, **269**, 1, 109.

60. M. Zaborski, A. Vidal, G. Ligner, H. Balard, E. Papirer and A. Burneau, *Langmuir*, 1989, **5**, 2, 447.

61. L.A.E.M. Reuvekamp, S.C. Debnath, J.W. ten Brinke, P.J. van Swaaij and J.W.M. Noordermeer, *Rubber Chemistry and Technology*, 2004, **77**, 1, 34.

62. L.A.E.M. Reuvekamp, J.W. ten Brinke, P.J. van Swaaij and J.W.M. Noordermeer, *Rubber Chemistry and Technology*, 2002, **75**, 2, 187.

63. T. Scholl and H-J. Weidenhaupt, inventors; Bayer AG, assignee; EP 0680997A1, 1995.

64. T. Scholl, H-J. Weidenhaupt and U. Eisele, inventors; Bayer AG, assignee; EP 0670347B1, 1998.

65. T.F.E. Materne and F. Kayser, inventors; The Goodyear Tire & Rubber Company, assignee; US 6,403,693, 2002.

66. T.F.E. Materne, D.E. Bowen, III, F. Kayser and E.S. Castner, inventors; The Goodyear Tire & Rubber Company, assignee; US 6,313,220, 2000.

67. P. Vondrácek, M. Hradec, V. Chvalovsky and H.D. Khanh, *Rubber Chemistry and Technology*, 1984, **57**, 4, 675.

68. R.W. Cruse, M. H. Hofstetter, L.M. Panzer and R.J. Pickwell, *Proceedings of the 150th ACS, Rubber Division Meeting*, Louisville, KY, USA, Fall 1996, Paper No.75.

69. R.W. Cruse, M.H. Hofstetter, L.M. Panzer and R.J. Pickwell, *Rubber & Plastics News*, 1997, **26**, 18, 14.

70. A. Hasse, O. Klockmann, A. Wehmeier and H-D. Luginsland, *Proceedings of the 160th ACS, Rubber Division Meeting*, Cleveland, OH, USA, Fall 2001, Paper No.91.

71. A. Hasse, O. Klockmann, A. Wehmeier and H-D. Luginsland, *Kautschuk und Gummi Kunststoffe*, 2002, **55**, 5, 236.

72. H-D. Luginsland, *Proceedings of the 155th ACS, Rubber Division Meeting*, Chicago, Il., USA, Spring 1999, Paper No.74.

73. A. Hasse and H-D. Luginsland in *Proceedings of the Nordic Council of Rubber Technology, International Rubber Conference, IRC 2000*, Helsinki, Finland, 2000, Paper No.72.

74. T. Scholl and H-J. Weidenhaupt, inventors; Bayer AG, assignee; EP 0680997A1, 1995.

75. T. Scholl, H-J. Weidenhaupt and U. Eisele, inventors; Bayer AG, assignee; EP 0670347 B1, 1998.

76. R.W. Cruse, R.J. Pickwell, K.J. Weller and E.R. Pohl, inventors; OSi Specialties Inc., assignee; WO 9909036, 1999.

77. P.G. Joshi, R.W. Cruse, R.J. Pickwell, K.J. Weller, W.E. Sloan, M. Hofstetter, E.R. Pohl, M.F. Stout and F.D. Osterholtz, *Tire Technology International,* 2004, p.166.

78. T. Früh, L. Steger and L. Heiliger in *Proceedings of the DIK Kautschuk-Herbst-Kolloquium*, Hannover, Germany, 2002, p.175.

79. S.K. Mandal, R.N. Datta, P.K. Das and D.K. Basu, *Journal of Applied Polymer Science*, 1988, **35**, 4, 987.

80. P.H. Sandstrom, R.J. Hopper and J.A. Kuczkowski, inventors; The Goodyear Tire & Rubber Company, assignee; EP 0723991A1, 1996.

81. L.G. Wideman and P.H. Sandstrom, inventors; The Goodyear Tire & Rubber Company, assignee; US 5,641,820, 1997.

82. J. Muse, Jr., P.H. Sandstrom and L.G. Wideman, inventors; The Goodyear Tire & Rubber Company, assignee; EP 0536701B1, 1996.

83. L.G. Wideman and P.H. Sandstrom, inventors; The Goodyear Tire & Rubber Company, assignee; EP 0700956A1, 1996.

84. L.G. Wideman, P.H. Sandstrom and D.J. Keith, inventors; The Goodyear Tire & Rubber Company, assignee; EP 0682067A1, 1995.

85. G. Kraus, inventor; Philips Petroleum Company, assignee; US 4,482,663, 1984.

86. P.H. Sandstrom and L.G. Wideman, inventors; The Goodyear Tire & Rubber Company, assignee; US 5,504,137, 1996.

87. G.D. Macdonnell and C.J. Stacy, inventors; Philips Petroleum Company, assignee; US 4,386,185, 1983.

88. T.F.E. Materne, R.J. Zimmer, F. Visel and U.E. Frank, inventors; The Goodyear Tire & Rubber Company, assignee; EP 0941995A2, 1999.

89. G. Agostini, T.F.E. Materne, M.N. Junio, F. Visel and U.E. Frank, inventors; The Goodyear Tire & Rubber Company, assignee; EP 0794187A1, 1997.

90. T.F.E. Materne, R.J. Zimmer, F. Visel, U.E. Frank and G. Agostini, inventors; The Goodyear Tire & Rubber Company, assignee; EP 0945456A2, 1999.

91. T.F. Materne, G. Agostini, F. Visel and M.P. Cohen, inventors; The Goodyear Tire & Rubber Company, assignee; EP 0939081A1, 1999.

92. T.F.E. Materne, inventor; The Goodyear Tire & Rubber Company, assignee; EP 0939080A1, 1999.

93. R.J. Zimmer F. Visel, U.E. Frank and T.F.E. Materne, inventors; The Goodyear Tire & Rubber Company, assignee; EP 0794188A1, 1997.

94. F. Kayser, W. Lauer and T.F.E. Materne, inventors; The Goodyear Tire & Rubber Company, assignee; EP 1076060A1, 2001.

95. F. Kayser, W. Lauer and T.F.E. Materne, inventors; The Goodyear Tire & Rubber Company, assignee; EP 1076061A1, 2001.

96. . Kayser, W. Lauer and T.F.E. Materne, inventors; The Goodyear Tire & Rubber Company, assignee; EP 1076059A1, 2001.

97. C. Batz-Sohn and H-D. Luginsland, inventors; Degussa Hüls AG, assignee; DE 19844607A1, 2000.

98. H-D. Luginsland, R. Krafczyk and W. Lortz, inventors; Degussa Hüls AG, assignee; EP 0997489A2, 2000.

99. M.P. Cohen, D.K. Parker and L.G. Wideman, inventors; The Goodyear Tire & Rubber Company, assignee; US 5,675,014, 1996. [Ph.D thesis]

100. J.W. ten Brinke, *Silica Reinforced Tyre Rubbers: Mechanistic Aspects of the Role of Coupling Agents*, Twente University Press, Enschede, The Netherlands, 2002.

101. J.M. Funt, *Rubber Chemistry and Technology*, 1988, **61**, 5, 842.

102. A.R. Payne, *Rubber and Plastics Age*, 1961, **42**, 8, 8963.

103. A.R. Payne, *Rubber Chemistry and Technology*, 1966, **39**, 2, 365.

104. H.M. Smallwood, *Journal of Applied Physics*, 1944, **15**, 11, 758.

105. J. Fröhlich and H-D. Luginsland, *Rubber World*, 2001, **224**, 1, 28.

106. M-J. Wang and W.J. Patterson, *International Rubber Conference (IRC '96)*, Manchester, UK, 1996, Paper No.43.

107. W.K. Dierkes and J.W.M. Noordermeer, *Proceedings of the 167th ACS, Rubber Division Meeting*, San Antonio, TX, USA, Spring 2005, Paper No. 46.

108. W. Dierkes, J.W.M. Noordermeer, M. Rinker, K-U. Kelting and C. van der Pol, *Kautschuk und Gummi Kunststoffe*, 2003, **55**, 6, 338.

109. W. Dierkes, J.W.M. Noordermeer, K-U. Kelting and A. Limper *Rubber World*, 2004, **229**, 6, 33.

110. D. Berkemeier, W. Haeder, M. Rinker and G. Heiss, *Rubber World*, 2005, **224**, 4, 34.

111. L.A.E.M. Reuvekamp, J.W. ten Brinke, P.J. van Swaaij and J.W.M. Noordermeer, *Kautschuk und Gummi Kunststoffe*, 2002, **55**, 1-2, 41.

112. C.M. Blow, *Polymer*, 1973, **14**, 7, 309.

113. E. Sheng, I. Sutherland, R.H. Bradley and P.K. Freakley, *European Polymer Journal*, 1996, **32**, 1, 35.

4 Fibres in the Rubber Industry

W. Wennekes and R.N. Datta

4.1 Introduction

The modern world relies on fibre/rubber composites. Fibres have always been very important to mankind in the beginning as a material for clothing, but later on used for many other applications. Until about 1890 only natural fibres were available. Just before the end of the 19th century the first synthetic fibres based on cellulose were developed. Cellulose is insoluble in water and in order to make this soluble, several derivatisation methods were tried. The first attempt was nitration (cellulose nitrate), which proved to give better gun powder than fibres. Cooper Rayon and viscose Rayon followed, the latter becoming the first large-volume synthetic fibre material. The cellulose yarns, including cellulose acetate are considered to be half-synthetic because the raw material is still a natural polymer. The first, full synthetic fibre was developed by DuPont. Nylon or polyamide 6,6 was introduced in 1936 (Carothers). A few years later polyamide 6 (Schlack, 1941), and polyester (Whinfield and Dickson, 1942) were introduced. Polypropylene was added to the list around 1960 (Natta). The development of 'advanced fibres', took place around 1970. Most of these fibres were produced from fully aromatic polymer with high temperature stability. Eventually this led to the discovery of liquid-crystalline behaviour of poly(paraphenylene terephthalimide) (PPTA), (Aramid, DuPont, 1969), the first superstrong fibre. The second superstrong fibre was gelspun polyethylene (Dyneema, DSM, 1979) [1-12].

A survey of the developments is given in **Tables 4.1** and **4.2**.

It is to be remembered that within the last 75 years, there has been a great move away from natural materials (cotton) to synthetic products, both with regards to fibres and the polymers used, resulting in a wide variety of engineered composites, to meet many and varied performance requirements. In this chapter we will concentrate on fibres type, characteristics and their use in variety of rubber products, such as tyres, hose, belts, etc.

4.2 Fibre Types and General Properties

The use of fibres, twisted into yarns and used as fabrics is a technology that dates back over 10,000 years. The first spinning and weaving of cotton began in India. Trade

Table 4.1. Survey of the developments of synthetic fibres	
Year	**Fibres**
1845	Nitrocellulose, Schonbein
1885	Viscose Rayon, Cross, Bevan, Beadle
1891	Nitrate Rayon yarn production, Chardonnet
1899	Copper Rayon spinning process, Fremery (later Enka group)
1911	Viscose Rayon yarn production
1935	PA 6,6, yarn production in 1939, Carothers (DuPont)
1938	PA 6, yarn production in 1950, Schlack (IG Farben)
1941	PET, yarn pilot plant 1948, Whinfield, Dickson (ICI)
1969	Aromatic polyamides, Kwolek (DuPont)
1979	Gelspinning polyethylene, Lemstra, Smith (DSM)
PA: polyamide *PET: polyethylene terephthalate*	

Table 4.2.		
Type of fibre	**Year of invention**	**Introduction in tyre reinforcement [1]**
Cotton	approximately 7000 years ago	1900
Viscose Rayon [2]	1885	1938
Polyamide 6,6 [3]	1935	1947
Polyamide 6 [4]	1938	1947
Poly(ethylene terephthalate) [5]	1941	1962
Aromatic polyamide [6-10]	1969	1974
Gelspun polyethylene [11]	1979	-

Table 4.3. Annual world demand for several textile fibres in 1997 [12]	
Fibre type	**World demand (kt)**
Cotton	19453
Regenerated celluloses (e.g., Rayon)	505
PET	10810
Nylon	4843
Others	201

routes developed by Alexander the Great introduced the textiles of India to the rest of the Middle East and Europe. One of the first man made fibres was viscose Rayon, it was commercialised in 1905. A major invention was Nylon, it was commercial in 1938, polyester 10 years later. A second generation of high-performance fibres started with aramid (1970s). The annual world demand of these fibres is given in **Table 4.3**.

4.2.1 Cotton

Cotton is a natural fibre, consisting of the seed hairs of a range of plant species in Mallow family (Genus *Gossypium*). The plants are grown, mainly as an annual crop, in many countries around the world between latitudes 40° N and 40° S.

The production process starts with sowing the seed and proceeds through to picking, baling, carding etc. Cotton is seen to be of moderate strength. However, this is coupled with relatively high bulk, so that dense fabrics of lower strength can be produced. Cotton has largely been replaced by the stronger man-made fibres, but still finds application where the requirement is not primarily for high strength but also demands a reasonable bulk.

The other advantage possessed by cotton derives from its staple nature. This relates to its use as an adhesion contributor, particularly in polyvinylchloride applications, where cotton is widely used in combination with the synthetics. In these fabrics, the strength is primarily obtained from the synthetic and cotton contributes both bulk and the means whereby adhesion is obtained.

4.2.2 Rayon

The structure of Rayon is shown in **Figure 4.1**.

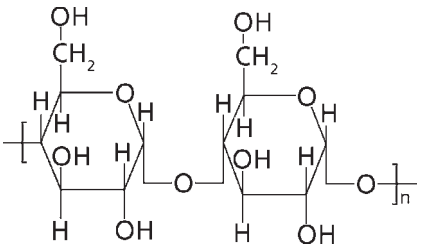

Figure 4.1 Chemical formula of Rayon

The production of Rayon is based on regenerated cellulose. The raw material is usually cotton or wood pulp [13]. This cotton or wood pulp is treated with carbon disulfide in a basic solution; cellulose xanthate is formed **Figure 4.2**.

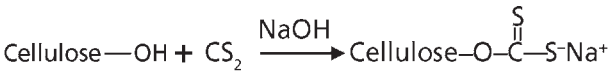

Figure 4.2 Formation of cellulose xanthate

The solution of cellulose xanthate is passed through a slit and is regenerated in an acidic solution **Figure 4.3**.

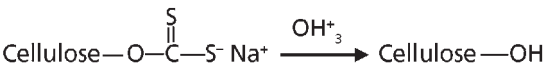

Figure 4.3 Regeneration of cellulose

The first Rayon tyre cord was used in 1923 [14]. From the 1930s the tenacity and durability were improved and Super I, Super II and Super III grades were developed. Up until the 1970s, the breaking strength was improving. The improvement was realised by making the Rayon denser and more uniform in structure. The degree of polymerisation was also higher for the high tenacity Rayon in comparison to the regular Rayon.

One disadvantage of the Rayons lies in their sensitivity to moisture; in moist conditions, they lose a significant proportion of their dry strength. For many applications, where the direct ingress of moisture is restricted, this does not pose a very significant problem (as for example in tyres, hose and moulded edge conveyer belting).

The main application of Rayon is as staple fibre. Spinning is carried out from clusters of spinnerets and bundles are collectively processed as a tow. Rayon staple fibre is applied unblended, but is also used in blends with cotton and/or polyester, in outerwear. Textile filament yarns have become a small product; one may still find them applied in lining fabrics.

Rayon tyre cord has survived the strong competition with polyester, at least in Europe. Rayon has an unproblematic adhesion to rubber, a high modulus and a perfect fatigue behaviour, and therefore remains the ideal reinforcement for high-speed radial tyres.

4.2.3 Polyamides

Polyamide is the generic name of linear aliphatic polyamides (**Figure 4.4**). Polyamides were the first synthetic fibres to be produced commercially [15]. In the literature, only polyamide 6 and polyamide 6,6 are named as being used for reinforcing rubber. Polyamide 6 is produced from caprolactam by ring-opening polymerisation.

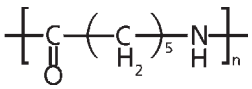

Figure 4.4 Chemical formula of polyamide 6, PA 6

Polyamide 6,6 is produced by polycondensation of hexamethylene diamine and adipic acid (**Figure 4.5**). A high molecular weight (MW) leads to a high tensile strength but the dimensional stability decreases at high temperature [14]. Therefore a balance in MW has to be obtained.

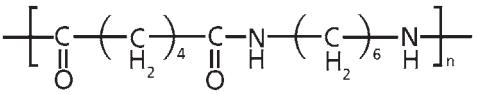

Figure 4.5 Chemical formula of polyamide 6,6, PA 6,6

The early difference between the USA (in which PA 6,6 was taken up preferentially) and Europe (PA 6) is still visible. PA6,6 seems to be the larger volume product but PA 6 is still large in South American countries, Eastern Europe and India. PA 4,6 has found limited application as an industrial yarn. Other polyamides (PA 11, PA 12) are not important as fibre materials.

Polyamide 6 has a melting point of 225 °C and is spun at 260-280 (290) °C. Polyamide 6,6 has a higher melting point of 265 °C and is spun at 290-300 (310) °C. The temperatures between brackets are for spinning of industrial yarns from higher MW polymers.

Thermal degradation is relatively unproblematic for polyamide 6, but is more severe for polyamide 6,6 because of the higher spinning temperature and the tendency of polyamide 6,6 to crosslink. Polyamides are prone to oxidative degradation, resulting in yellowing. The nitrogen gas in the chip's hoppers must therefore be completely free of oxygen. For industrial yarns the oxidative and heat resistance must be improved by the addition of a stabiliser. HR-systems (heat resistance) can be based on organic stabilisers, but inorganic systems based on copper and halogen (iodine) salts are more common.

For rubber reinforcement PA 6 has the disadvantage of its low melting point. Nevertheless it is still widely applied in India and South America, also in automobile tyres. PA 6,6 is used on large scale: in conveyor belts, rubber hoses and tyres. In radial tyres polyamides cannot be used in the walls because their modulus is too low. However, in old-fashioned bias-belted tyres, for bumpy roads (Third World), polyamide is the perfect choice for reinforcement. Aircraft tyres also have the 'diagonal' construction, and usually contain many layers of Nylon cords. One nevertheless finds polyamide, especially PA 6,6, in radial tyres, not in the sidewalls but as a capply above or around the steel belt. Capply or overlay layer is used mainly in high performance and ultra high performance tyres.

4.2.4 Polyester, Poly(ethylene terephthalate) (PET)

Polyester is the general name of fibres made from poly(ethylene terephthalate) (**Figure 4.6**). The two major methods for synthesising polyester is by ester interchange via dimethyl terephthalate (Europe) and by direct esterification of terephthalic acid by ethylene glycol (America) [13]. Polyester and PET are almost synonyms. Other polyesters have hardly any significance as fibre materials.

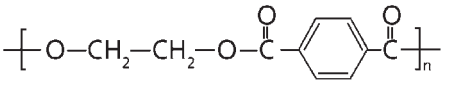

Figure 4.6 Chemical formula of poly(ethylene terephthalate)

Broadly polyester combines the strength and elongation characteristics of the Nylons with modulus characteristics of the Rayons. This combination of properties suits many applications, but there are two main areas where problems exist. The first concerns adhesion: being relatively inert chemically, it is somewhat more difficult to obtain adequate levels of adhesion with polyester than with Rayon or Nylon. However, as shown later, methods of treatment have been developed to overcome this. The second area relates to thermal shrinkage, which is even greater than with Nylon. Processes exist to modify the shrinkage characteristics of polyester and there are also various grades of fibres with differing shrinkage/modulus relationship, achieved by modification of the basic polymer. By judicious selection of the yarn type, the final properties of the cord or fabric can be tailored to the requirements of the specific applications.

Polyester is the most important reinforcing material for radial tyres. The cords run radially, from rim to rim, and their high modulus reduces the deformation of the rolling tyre, and thus fuel consumption. The properties of the reinforcement in the tyre depend on how well the modulus is retained during the dipping and curing processes. Therefore, tyre yarns are always spun at high speeds (>3000 m/min), which gives lower shrinkage and somewhat lower tenacity in the yarn. After dipping of the cords and curing of the rubber these yarns offer the best strength/modulus combination.

The most important applications of polyester industrial yarns have been mentioned in the above text: tyres, other rubber reinforcement, narrow and wide fabrics, nets, ropes and cables, sewing yarns. It is not unusual that a company would list 20 different types of polyester yarn, each type further divided into various yarn titers and twist levels.

4.2.5 Aramid

Aramid fibres are fibres made of poly-(*p*-phenylene terephthalamide) (PPTA) (**Figure 4.7**). It is synthesised from terephthalic acid chloride and *p*-phenylene diamine. The monomers are dissolved in typical amine solvents and polymerisation takes place. After polymerisation, the solution is coagulated by water.

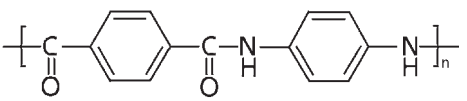

Figure 4.7 Chemical formula of aramid (Twaron, Kevlar)

The polymer is dissolved in concentrated sulfuric acid and spun into an aqueous bath. A schematic representation of this process is given in **Scheme 4.1** [13, 16].

The properties of aramid are more akin to those of inorganic materials than to the other textile fibres. The tensile strength, even assessed by engineering method as strength per unit cross-section area, is of the same order as those of steel and glass. The modulus is also very high, but this is coupled with a very low value for elongation at break, which introduces some difficulties in certain applications. The major disadvantage of this low elongation occurs when aramid is used in several layers. When flat, each layer of textile is able to contribute its own share of strength, but on bending, the low elongation of the outermost layer prevents it from accommodating to the curve, which places the other layers in compression. This directly reduces the contribution of the inner plies to the total strength but also, and more seriously, the performance of aramid in compression is not good. However, many applications have been developed which enable the excellent properties of aramid to be realised and solutions have been found to overcome the problem related to low elongation. The field of application of aramid is enormous, one of them is in the reinforcement of rubber (high-pressure hoses, conveyor and transmission belts; automobile tyres, bicycle tyres for puncture resistance). For rubber applications, the aramid is used as such (with high twist factor to obtain higher elongation) or cords are made in combination with Nylon (known as a hybrid).

It is to be mentioned here that, similar to polyester the adhesion of aramid yarn to rubber is weak and therefore various methods are used to develop optimum adhesion.

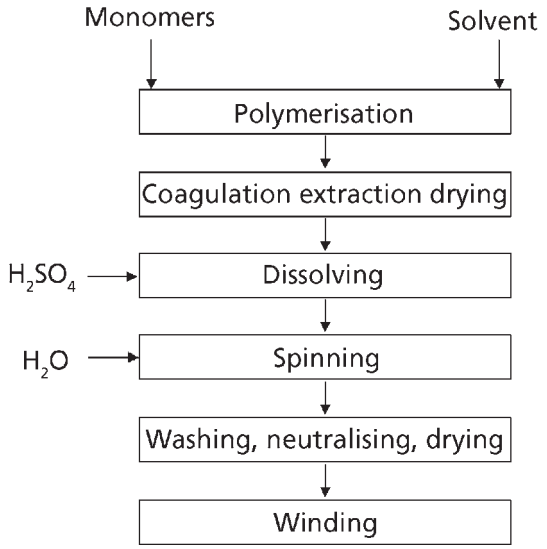

Scheme 4.1 Representation of the aramid fibre production process

4.2.6 Others

There are various fibres available starting from carbon fibre, poly(ethylene naphthalate) (PEN), acrylics, poly(vinyl alcohol) to polyurethane fibres. The important fibres for the rubber industry are carbon fibre and PEN and others are used in various diverse applications.

4.2.6.1 Carbon Fibre

Carbon fibres are not directly spun but are the product of a complicated after-treatment. Nowadays, most carbon fibres (90%) are produced from an acrylic precursor. An early choice, cellulose Rayon is no longer used as a precursor. Production from pitch has been developed, but is still a small-volume business.

Most textile acrylics are based on polyacrylonitrile (PAN) containing 10-15% comonomers. For carbon fibre precursors lower comonomer levels are used (approximately 5%); comonomers are selected that promote the reactions in the after-treatment (methyl acrylate, itaconic acid). Wet spinning is preferred because the cross section can be better controlled then. In dry spinning skin formation can hardly be prevented and eventually the cross section collapses into a 'dog bone' shape, which is not desirable in carbon fibre applications.

Precursor filaments are drawn to much higher draw ratios (≥ 10x) than textile yarns. Precursor filaments must be free of solid particles; sharp filtration of spinning solutions is therefore required. Textbooks even mention spinning under 'clean room' conditions.

The after treatment proceeds in three steps: cyclisation, oxidation and carbonisation/graphitisation. All steps are carried out under tension. In the cyclisation step (around 200 °C) N-containing rings are formed, in a ladder structure: PAN, 'Orlon', is transferred into 'Black Orlon' (**Figure 4.8**). This first step is still without loss of material. In the second step this structure is made unmeltable by careful oxidation and stabilisation, at temperatures between 200 and 300 °C. Some hydrogen is removed, carbonyl groups and double bonds are formed and the aromatic character is increased. The third step is a pyrolysis reaction carried out in an inert atmosphere, at temperatures which are gradually increased, from 400 to 1700 and further to 2800 °C. Below 1000 °C most volatile products are formed: H_2O, HCN, NH_3, CO, CO_2, N_2, etc. Note that the nitrogen content of PAN is about 28%, while the weight loss of PAN to carbon fibre is about 50%.

The term graphitisation is not really correct because a true graphite structure is not formed. The graphite layers, condensed ring systems, are indeed there, but the layers are not strictly coordinated. This 'misfit' in the coordination of layers is called turbostratic. Nevertheless, carbon fibres are often referred to as graphite fibres, especially in the USA.

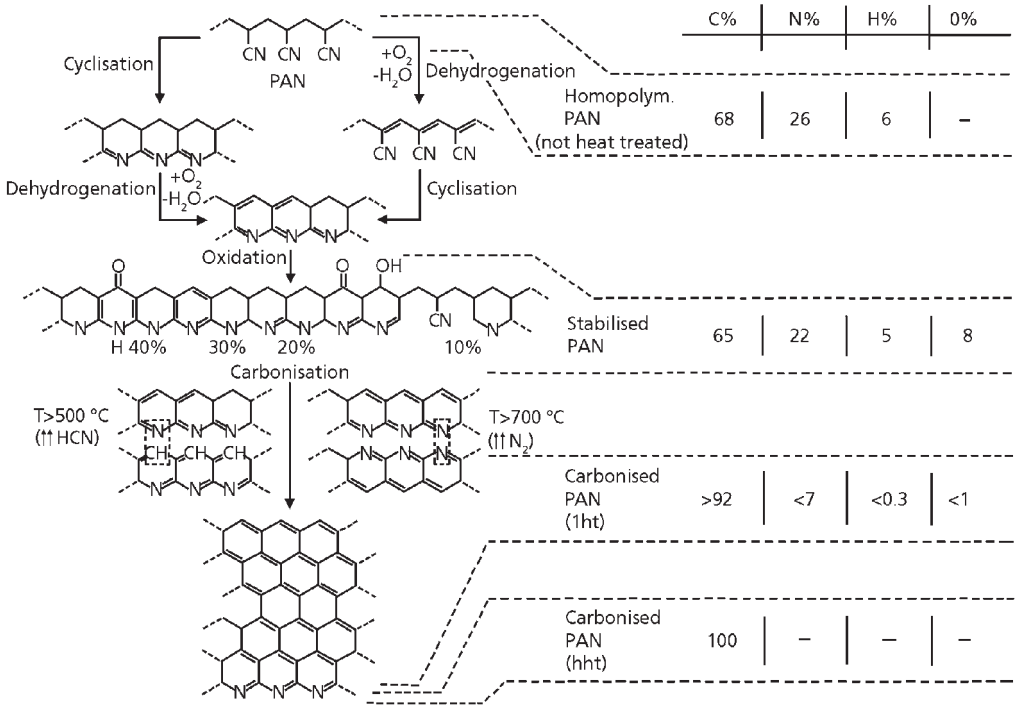

Figure 4.8 Carbon fibre from PAN. The three steps are (1) cyclisation, (2) oxidation or stabilisation, and (3) carbonisation. Most of the weight loss is in step (3), at temperatures of 500-1000 °C

The use of carbon fibres is almost exclusively in composites. Two main types are offered: a high strength type (1.9-3.9 N/tex tenacity, 140 N/tex modulus) and a high-modulus type (2.2 N/tex tenacity, 280 N/tex modulus). Carbon fibre moduli are much higher than those of aramid and gel spun polyethylene. Recently Goodyear launched the use of carbon fibre in sidewall insert application for radial passenger tyres.

4.2.6.2 Poly(ethylene naphthalate) (PEN)

Poly(ethylene naphthalate) (PEN), a new generation polymer, is a high performance member of the polyester family (**Figure 4.9**).

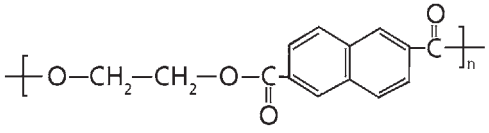

Figure 4.9 Chemical formula of poly(ethylene naphthalate)

PEN based fibres extend the performance of polyesters. PEN fibres have excellent heat resistance, modulus, and dimensional stability relative to PET. Both PEN and poly(butylene 2,6-naphthalate) (PBN) based fibres retain their mechanical properties in a hot/wet environment and offer improved chemical resistance *versus* PET or poly(butylene terephthalate) fibres. With naphthalate modification, polyester fibres can meet the application requirements, which are currently served by other high performance industrial fibres such as Rayon, Nylon 6,6, aramids, polyphenylenesulfide (PPS), and even steel. Current and potential applications of PEN and PBN based fibres are discussed next. Applications are considered from a multifilament and a monofilament perspective.

Tyre Reinforcement

PEN's superior thermal and mechanical properties make it a natural candidate for the reinforcement of radial passenger and light truck tyre carcasses.

PEN yarn has higher tenacity and improved modulus compared with PET, Nylon and Rayon. Its thermal properties, e.g., dry heat shrinkage, are also superior. This lower thermal shrinkage is a significant benefit in tyrecord manufacture because of the heat-setting treatment and pre-shrinkage relaxation required to convert yarn to twisted cord. Relative to PET, the lower thermal shrinkage of PEN enables less pre-shrinkage treatment, which results in a final cord that has improved tenacity and modulus. There are multiple opportunities for PEN fibre use in tyre construction.

Carcass Reinforcement

There are several fibres currently used in carcass reinforcement. High modulus/low shrinkage PET is typically used in most radial passenger tyres and offers a good mix of properties. Nylon is used extensively in bias ply tyres where strength is paramount. Rayon is the reinforcement cord of choice in Europe for high performance tyres, due to its ability to maintain mechanical properties at high temperature. Aramid fibre offers ultra high performance properties but at a high cost. This cost limits aramid use to high-end luxury and racing cars. The performance properties of PEN present opportunities for Rayon or polyaramide replacement in carcass construction. The use of PEN cord in these applications is currently being evaluated in both Asia and Europe. PEN has a demonstrated acceptable flexural fatigue equivalent to PET and Rayon. It has equivalent toughness to Rayon, which is important for sidewall impact resistance and curb scuffing resistance. PEN's superior mechanical properties also afford opportunities to use less fibre in carcass construction enabling production of lighter weight, more fuel-efficient tyres.

Belts and Hoses

As automotive design trends toward higher engine operating temperatures, the requirements for under the hood reinforcement fibres have changed. Today, fibres not only require good mechanical and thermal properties, but also improved chemical/hydrolytic resistance in a hot-wet environment. PEN fibre meets these more demanding requirements. Performance advantages of PEN include:

- Very low tension decay;
- High modulus (twice that of PET);
- Low shrinkage after cure;
- High adhesion and adhesion retention;
- Good fatigue resistance.

Several types of PEN or PBN reinforced belts and hoses, ranging from transmission belts to oil brake hoses have been produced. Additional applications include timing belts, conveyer belts, high pressure hydraulic, steam, fuel and coolant hoses as well as polychain belt cord.

4.2.6.3 High-Temperature Polymer (HTP) Fibres

There is quite a variety of fibres with high-temperature resistance, most of them with textile properties (low tenacity, high elongation). The fibres find application in insulation, hot gas filtration, and so on.

Large volume products are meta-aramid ('Nomex', 'Teijinconex') and polybenzimidazole, both dry spun. Smaller products are PPS, several aromatic polyketones (for example polyetheretherketone) and aromatic polysulfones; these are melt spun products.

The properties of the different sorts of polymers are listed in **Table 4.4**. These are average values.

Judging the various properties it is worthwhile to present the stress-strain characteristics of textile fibres. It is evident from **Figure 4.10** that cotton is weakest, whereas aramid has the highest strength. However, the individual fibre (or hair strength) of cotton is higher than Rayon due to the larger MW and the higher degree of orientation. However, Rayon is continuously spun and therefore is total stronger than cotton. Cotton, Rayon and aramid do not have a melting temperature.

Table 4.4. Cord properties of reinforcing material [13]						
	Cotton	Rayon	Nylon 6	Nylon 6,6	Polyester	Aramid
Density (kg/m^3)	1540	1520	1140	1140	1380	1440
Moisture content* (%)	7-8	12-14	4	4	0.4	1.2-7
Decomposition temperature (°C)	230	210	-	-	-	500
Melting temp. (°C)	-	-	255	255	285	-
T_g (°C)	-	-	50	57	69	>300
E-mod (cN/tex)	225	600-800	300	500	850	4000
Tensile strength (MPa)	230	685-850	850	850	1100	2750
* *Measured at 65% relative humidity at 20 °C*						

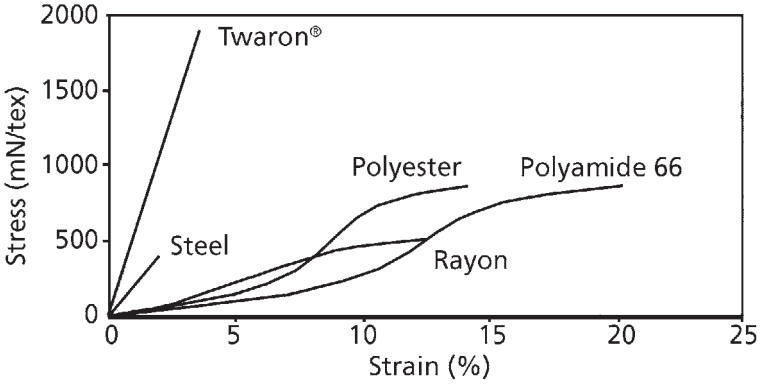

Figure 4.10 Stress-strain properties of textile fibres at 65% relative humidity at 20 °C

4.3 Yarn and Cord Processes

There are very few applications where textile fibres can be used in the form in which they are originally produced. It is usually necessary to modify the yarn form or construction, in order to obtain the optimum benefit from their incorporation as reinforcement in elastomeric components. For some applications, single-end yarns or cords (several twisted yarns twisted together, **Figure 4.11D**) are the preferred form, especially for hose and V-belts. In some cases, particularly in tyres, although the single-end cord is the right form of reinforcement, it is preferable for the cords to be assembled together into a cord fabric. This represents a halfway stage between the single cord and fully woven construction.

The most common methods of obtaining the required yarn construction are twisting and texturing (the bulking up the yarns). For some of the lighter fabrics, a chemical modification in the form of sizing is employed for the wrap yarns.

4.3.1 Twisting

The process from polymer to fabric is shown schematically in **Figure 4.12**.

The spun polymers are called filaments. These filaments form a yarn, a yarn forms a cord and the textiles consist of cords. Several possibilities of yarn and cord formation are shown in **Figure 4.12** [13].

There is no general theory on which twist gives maximum properties [14]. Many properties can be measured as a function of the number of twists per unit length. Takeyama [14] has shown results of the breaking strength and the breaking strength after dynamic load for Rayon cords as a function of the number of twists per unit length. In **Figure 4.13**, different twist levels in the plied cord (type D from **Figure 4.12**)

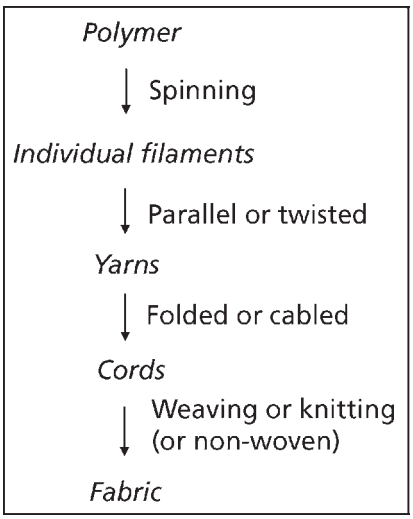

Figure 4.11 From polymer to fabric

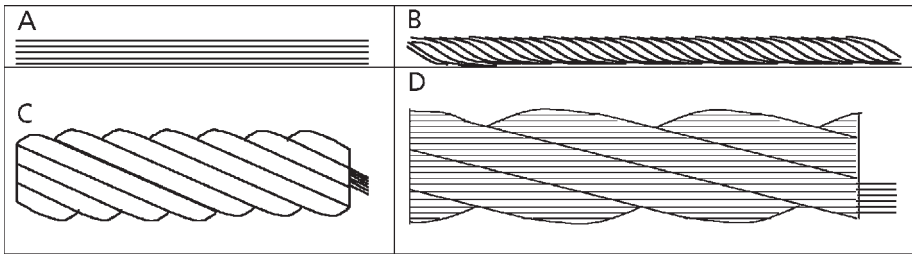

Figure 4.12 Four examples of yarn formation from individual filaments. A: the filaments are placed parallel, B: the filaments are twisted together, C: the filaments are placed parallel and folded afterwards, D: the filaments are twisted and afterwards folded

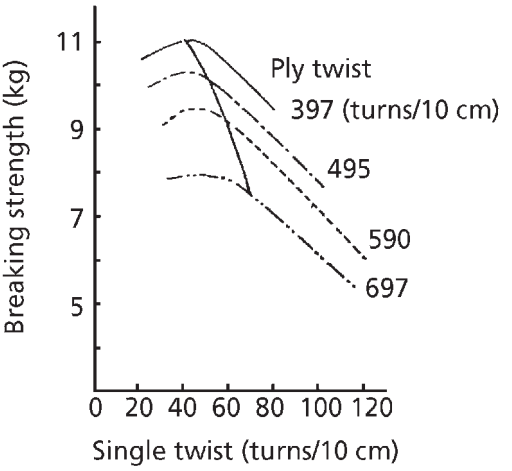

Figure 4.13 Breaking strength *versus* twist level for Rayon cord

are shown and the breaking strength is depicted. Both the single twisting and the ply twisting (cabling) are varied. It seems that for all ply twist levels a maximum breaking strength is observed at a certain amount of twist. This was also observed after dynamic loading. Probably this is related to the alignment of the single filaments. If most filaments lie in the direction of the applied stress, maximum mechanical properties are achieved. However, Takeyama stated that the ratio of ply and twist level for maximum properties was not equal to unity.

Wootton [13] has formulated a twist multiplier for cabling a twisted yarn. The cabling must occur in the opposite direction from the twisting. The resulted cable can be twisted into a larger cable and so on. After cabling, the linear density increases. The linear density is usually expressed in tex (g/1000 metre cord) or denier (g/9000 metre cord):

$$\text{Twist multiplier} = \text{twist} \times \sqrt{\text{linear density}} \tag{4.1}$$

The twist multiplier is a constant.

Wootton [13] states that a higher twist and cable level improves the fatigue resistance. Takeyama [14], however, stated that a higher twist level leads to a lower E-modulus, cord strength and fatigue resistance in cyclic tension. The fatigue resistance in cyclic compression would increase as well as the elongation at break and the rupture energy.

Pidaparti [17] has modelled the axial, torsional and bending stiffness for aramid rubber composites as a function of the number of twists per unit length using a finite element model. To calculate the Young's modulus, he used Equation 4.2.

$$E_c^i = E_f \cos^4\beta \cdot \cos^2\alpha \; 1 - 1.5\tan^2\beta \; 1 + \frac{2\log\cos\alpha}{\sin^2\alpha} \tag{4.2}$$

E^i_c is the contribution of the i^{th} twisted filament, E_f is the modulus of an untwisted filament. The total Young's modulus is obtained by summing over all filaments in the cord. The parameters α and β are defined as:

$$\tan\alpha = II \cdot d \cdot tpi_{yarn}$$

$$\tan\beta = II \cdot d^* \cdot tpi_{cord}$$

Where tpi is the number of twists per unit length. The diameters, d and d* are according to **Figure 4.14.**

4.3.2 Texturing

Texturing covers various processes whereby the continuous filament yarns are bulked up; this modifies their properties and increases the bulk of the yarn, allowing certain specific properties to be achieved in the final yarn or fabric. There are two main systems used for texturing yarns for industrial applications, air texturing and false-twist texturing. In general the texturing process modifies the properties of the yarn significantly, not just the bulk and linear density, but also reduces tensile strength, increases elongation and increases the inter-yarn frictional properties. Details of the processes will be not covered as it is outside the scope of the chapter.

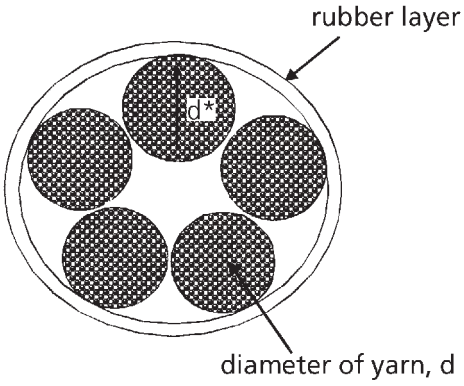

Figure 4.14 Schematic representation of cords in rubber with the diameters used in Equation 4.2

4.4 Fibre Units

4.4.1 Titer: Tex and Denier

It is difficult and inaccurate to measure the diameter of fibres or filaments. The cross-section can be unround, and even the diameter of round filaments can fluctuate along their length. It is much easier to weigh a certain length of filament or yarn. We thus determine a linear density, or titer. The word 'count' is also used: yarn count or filament count. [Dutch: titer]

The unit *tex* is officially included in the SI system, and has become the standard in Europe. The older unit *denier* stems from the silk industry and is still common in the USA and in many Asian countries. The definitions are:

tex = grams per 1000 metre (filament or yarn).

denier = grams per 9000 metre (filament or yarn).

It is fairly common practice to use decitex (dtex) instead of tex (dtex = grams per 10,000 metre). Numbers in dtex and denier differ about 10%. Conversion factors are shown in **Table 4.5**.

The weight of a filament depends on density ρ, diameter D and length L (**Figure 4.15**). For the definition of tex we use L=1,000 m, for dtex L=10,000 m and for denier L=9,000 m. If ρ is known we can easily calculate D from a tex, dtex or denier value.

Table 4.5. Conversion factors for denier, tex and dtex

Multiply	To obtain		
	denier	*tex*	*dtex*
denier	1	1/9	10/9
tex	9	1	10
dtex	0.9	0.1	1

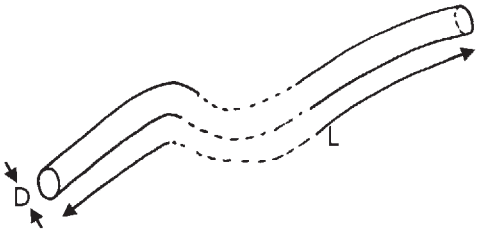

Figure 4.15 Schematic of a filament showing where measurements are taken to calculate tex or dernier

The diameter of a filament can be calculated from the filament titer if the density is known. Using the definition of dtex (g/10000 m) and expressing density in g/cm^3 we can calculate the diameter D in µm from:

$$D = 10 * \sqrt{\frac{4 * dtex}{\partial * \tilde{n}}}$$

For example, a polyester filament (ρ = 1.38 g/cm^3) of 10 dtex has a diameter of 30.4 µm, a filament of 1 dtex has a diameter of 9.6 µm.

For yarn titers it is useful to specify the number of filaments. For example, an aramid yarn type could be indicated as 1500 denier f 1000, which means that the yarn contains 1000 filaments, each of 1.5 denier. In dtex this yarn type would be 1670 dtex f 1000, a filament titer of 1.67 dtex.

Calculations

The unit tex, or dtex or denier, makes some calculations simple.

Example 1. We have a 12 kg package of yarn with a titer of 500 dtex. How much yarn length is on the package? Dtex definition: 10,000 m (10 km) has a mass of 500 g. 12 kg = 12,000 g; 12,000/500=24. There must be 10 x 24=240 km yarn on the package.

Example 2. The winding speed is 1200 m/min; what is the mass flow to the winder?

The mass of the yarn is 500/10,0000 g/m. Multiply this with the speed: (500/10,000) g/m x 1200 m/min = 60 g/min. It takes 12,000/60 = 200 min to wind the 12 kg package. Of course, 240 km length and a speed of 1.2 km/min also give 200 minutes winding time.

4.4.2 Tenacity and Modulus: g/denier, N/tex or GPa

After having introduced the denier and tex units the next logical step is to express breaking strength (tenacity) and modulus in g/denier or N/tex instead of in Pascal (Pa = N/m^2), MPa or GPa. Fibre engineers often deviate from using the basic SI units and convert N/tex to cN/tex or mN/tex, or even cN/dtex: 1 N/tex = 100 cN/tex = 1000 mN/tex = 10 cN/dtex.

g/denier (g/den, g/d, gpd) stands for gram*force* per denier. In conversion factors to Newton the gravity constant therefore appears: 1 gf = 9.806650 x 10^{-3} N. In combination with the conversion factor from denier to tex this results in:

1 g/denier = 8.826 x 10^{-2} N/tex, or 1 N/tex = 11.33 g/denier

Table 4.6. Conversion factors for g/d, N/tex and GPa (express ρ in g/cm³)			
Multiply	**To obtain**		
	g/denier	***N/tex***	***GPa***
g/denier	1	$8.826*10^{-2}$	$8.826*10^{-2}*\rho$
N/tex	11.33	1	ρ
GPa	11.33/ρ	1/ρ	1

For conversion of g/denier or N/tex to Pa or GPa one needs to know the density ρ of the yarn (**Table 4.6**).

4.5 Adhesion

4.5.1 Types of Adhesive Interactions

The properties of the composite depend greatly on the adhesion of the cords to the rubber. In the literature, the most commonly described types of interactions are:

- Mechanical
- Physical
- Chemical
- Interdiffusion

The degree of adhesion is strongly dependent on the wetting conditions of the polymer on the fibre. The two surfaces must be thermodynamically compatible. The compatibility can be calculated by the rules of thermodynamics of mixing:

$$\Delta G_m = \Delta H_m - T\Delta S_m \tag{4.3}$$

The change in the Gibbs free energy should be negative in order to have a high compatibility. Therefore the mixing enthalpy should be low, the bonding temperature should be high as well as the change in mixing entropy. The equation for the heat of mixing is [13, 18]:

$$\Delta H_m = V_m \nu_a \nu_b \left\{ \left(\frac{\Delta E_a}{V_a} \right)^{\frac{1}{2}} - \left(\frac{\Delta E_b}{V_b} \right)^{\frac{1}{2}} \right\}^2 \tag{4.4}$$

Where:

ΔE_i = energy of vaporisation of component i.

V_i = molar volume of component i.

ν_i = volume fraction of component i.

ΔH_m = heat of mixing

A solubility parameter can be defined. This concept is based on the geometric mean rule of molecular interactions. It applies strictly for systems without polar or hydrogen bonding interactions:

$$\delta_i = \left(\frac{\Delta E_i}{V_i} \right)^{\frac{1}{2}} \tag{4.5}$$

For a low enthalpy of mixing, the components should have solubility parameter values as close to each other as possible.

Walker [19] has modified the equation to correct for the interactions between the molecules. An interaction parameter φ was introduced:

$$\Delta H_m = V_m \nu_a \nu_b \left[\left(\delta_a - \delta_b \right)^2 + 2\left(1 - \varphi\right)\delta_a \delta_b \right] \tag{4.6}$$

Induction forces and dipole-dipole interactions could result in a value for $\varphi < 1$. For non-interacting systems $\varphi = 1$, and the equation becomes the one of the geometric mean rule. Hydrogen bonding leads to a value for $\varphi > 1$. This means that when hydrogen bonding plays a role, the heat of mixing can be zero even when the solubility parameters are not equal.

Four methods of determining the solubility parameters of components are [13]:

(i) Solubility experiments: An insoluble polymer is swollen in several solvents with different, known solubility parameters. The degree of swelling is plotted *versus* the solubility parameter. A peak is obtained at the solubility parameter of the polymer under investigation.

(ii) Heat of evaporation: By determining the heat of evaporation ($\Delta H_{vap,i}$), the solubility parameter can de calculated by the following equation:

$$\delta_i = \left(\Delta H_{vap,i} \frac{RT}{V_i} \right)^{\frac{1}{2}} \tag{4.7}$$

(iii) Surface tension:

$$\delta_i = 4{,}1 \cdot \left(\frac{\gamma_i}{V^{\frac{1}{3}}} \right)^{0{,}43} \tag{4.8}$$

where: γ_i is the surface free energy and V is the volume.

(iv) Calculations: Small [20] has calculated molar attraction constants for several commonly known bonds and functional groups. With these molar attraction constants, solubility parameters can be calculated with the following equation:

$$\delta_i = p \cdot \frac{\sum C}{MW} \tag{4.9}$$

where: C is the molar attraction constant; MW is the molecular weight and p is the density.

Fedor [21] has derived atomic and group contributions from the energy of vaporisation as well as their molar volumes. The energy values of the atoms or groups of a molecule simply have to be added, then divided by the total molar volume. The square root of that number is an indication of the solubility parameter.

4.5.1.1 Mechanical Bonding

When the cords are properly wetted by the rubber, in the case of cotton no further treatment is needed. Cotton fibres are not smooth; filaments stick out of the fibre (**Figure 4.16**). These filaments are anchored in the rubber matrix. The frictional forces that need to be overcome to pull or strip the fibre out of rubber are sufficient to provide adequate adhesion for most applications.

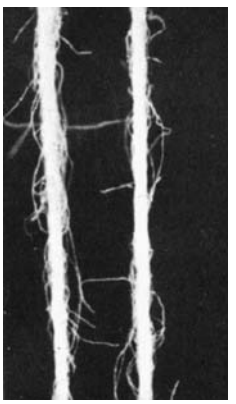

Figure 4.16 Magnification of a cotton fibre

The man made fibres also show some mechanical bonding but not that much because the fibres are smoother.

4.3.1.2 Physical Bonding (or Secondary Bonding)

Physical bonding is due to the intermolecular forces. In **Table 4.7**, several secondary bonding mechanisms are listed with the bond length they act on and the binding energy they produce.

Table 4.7. Types of physical bonding [22]		
Type of force	**Bond length (nm)**	**Bond energy (kJ/mol)**
Hydrogen bond	0.2-0.4	8-30
Dispersive force	0.3-0.5	0-20
Dipole orientation force	0.3-0.5	0-4
Dipole induction force	0.3-0.5	0-4

4.5.1.3 Chemical Bonding (or Primary Bonding)

Several types of primary bonds are listed in **Table 4.8**.

In general, the bond energies are higher for the primary bonds in comparison to the secondary bonds. In rubber-metal adhesion, the ionic bonds and the coordination bonds are most important. The primary and secondary bonding mechanisms become important if there is sufficient intermolecular contact between the surfaces.

4.5.1.4 Interdiffusion

In the case of rubber-rubber contact, interdiffusion can occur. This means that the segments of the polymer chains can diffuse through a polymer-polymer interphase, and a diffusion layer originates. This was proposed by Voyutskii [23], for interphases of the same polymer type (autohesion) and for different polymers (adhesion). In **Figure 4.17**, the adhesion strength between three sorts of polymer are plotted as a function of contact time. An increase in contact time results in an increase in adhesive strength. At longer contact times the adhesive strength reaches a maximum value. According to the Voyutskii this can only be explained by diffusion of polymer chains through the interface.

4.5.2 Promoting Adhesion

The man-made fibres hardly adhere to rubber due to their incompatibility; rubber has a lower stiffness and a lower polarity in comparison to the fibres. This makes an

Table 4.8. Types of chemical bonding [22]		
Type of bond	**Bond length (nm)**	**Bond energy (kJ/mol)**
Covalent bond	0.1-0.3	200-800
Example (C-C)	0.154	347
Ionic bond	0.3-0.6	-
Example (NaCl)	0.563	766
Metal bond	-	-
Example (Fe-Fe)	0.25	406
Coordination bond	0.2-0.3	20-48

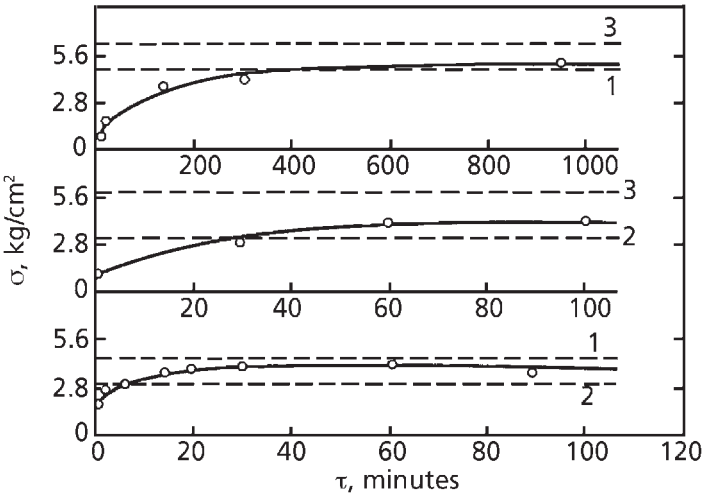

Figure 4.17 Adhesion strength between three types of polymers as a function of contact time; 1: natural rubber, 2: butyl rubber, 3: nitrile rubber

adhesive treatment necessary. Some examples of fibre treatments are dipping [24], surface roughening [25, 26] and chemical modification, for example grafting [27]. The rubber can also be treated for example by mixing ingredients in the rubber that enhance adhesion [28, 29] or by grafting functionalities to the rubber polymer [30].

4.5.2.1 Fibre Treatment

The most standard treatment used for adhering fibres to rubber is *via* a dip treatment. This dip has an affinity with the matrix material as well as the fibre. The dip that is most commonly used commercially is called resorcinol formaldehyde latex (RFL). Attempts are made to replace RFL dips by for instance coupling agents similar to the ones used for glassfibre-reinforced composites. Next to using a dip on the fibre, an increase of adhesion can be achieved by improving the mechanical interlocking of the fibre in the matrix material. A third approach is to chemically modify the surface of the fibre by adding or changing functional groups.

4.5.2.2 Dip Treatment: RFL

The most commonly used adhesive is resorcinol/formaldehyde latex, invented in 1938 by Charch and Maney [24]. RFL adhesives contain a resin part and a latex part. If latex alone is applied to the cords, good adhesion cannot be obtained because of lack of functional groups of the latex; furthermore, the adhesive dip would have weak tensile

properties. A resin is added to overcome this; resorcinol and formaldehyde act as the resin. They react in a similar way as in the formation of Bakelite [31], but instead of phenol, resorcinol is used (**Figure 4.18**).

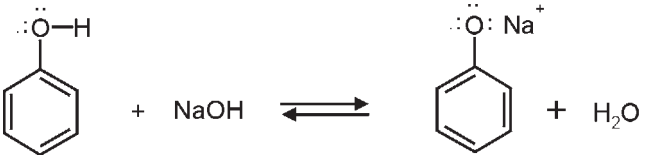

Figure 4.18 Reaction of phenol with sodium hydroxide

Phenol has acidic properties, therefore it reacts with the hydroxyl group and the oxygen gets a negative charge. This negative charge can be stabilised by the following resonance structures (**Figure 4.19**).

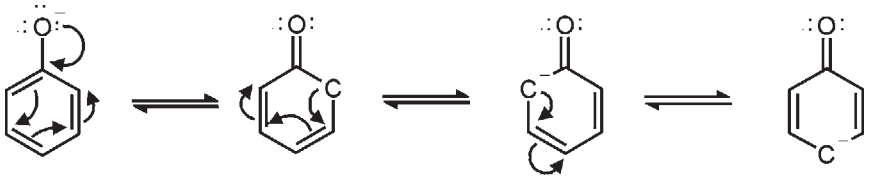

Figure 4.19 Resonance structures of phenol

The negative charge is stabilised by the carbon atoms at the *ortho* and *para* positions. Therefore, the hydroxyl group is an *ortho*, *para* director. Formaldehyde acts as a methyl donor according to the reaction scheme shown in **Figure 4.20**.

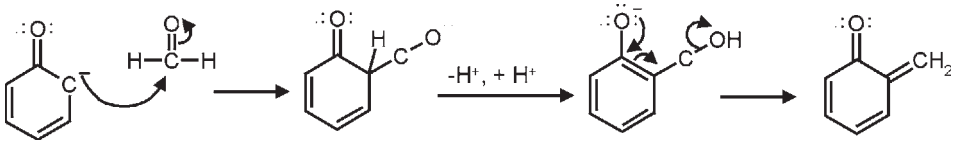

Figure 4.20 Reaction of phenol with formaldehyde

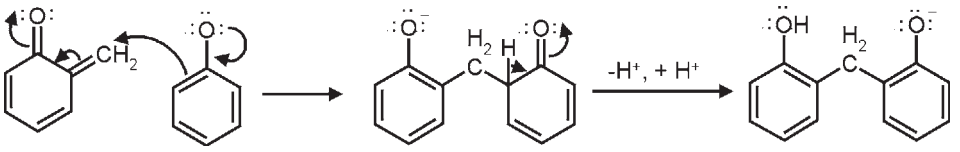

Figure 4.21 Bakelite formation

Further reaction can occur in excess of formaldehyde, eventually resulting into a thermoset polymer: Bakelite (**Figure 4.21**).

In RFL, resorcinol is used instead of phenol. The structural formula of resorcinol is given in **Figure 4.22**.

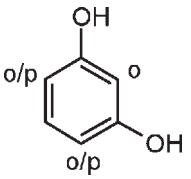

Figure 4.22 Structural formula of resorcinol

Instead of one, two hydroxyl groups are present. In **Figure 4.18**, the *ortho* and *para* positions are mentioned. On these positions, formaldehyde can donate its methyl group. On the *meta* position, it will not. Because of the two hydroxyl groups, the reaction with resorcinol proceeds faster in comparison to phenol. The structure of the resorcinol/ formaldehyde resin is given in **Figure 4.23**.

Instead of formaldehyde and resorcinol, often Penacolite is used. Penacolite is the acid catalysed prepolymerised form of the two monomers. By keeping the formaldehyde/resorcinol ratio close to 1, linear polymers are obtained. When the dip is prepared, extra formaldehyde is added to obtain the required formaldehyde/resorcinol ratio for resin formation. The acid catalysed polymerisation of resorcinol and formaldehyde can be derived from the phenol formaldehyde reaction and can be found in many organic chemistry textbooks (**Figure 4.23**) [32].

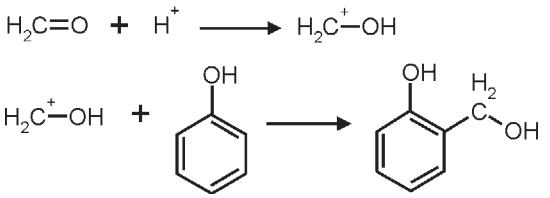

Figure 4.23 Acid catalysed reaction of formaldehyde and phenol

The electrophilic substitution to the aromatic ring shown in **Figure 4.23** can take place on the *ortho* and *para* positions [33], producing the structure shown in **Figure 4.24**.

Dip Composition for Rayon and Polyamide

From **Table 4.9** it can be concluded that for Nylon, a higher level of vinyl pyridine (VP) latex is necessary to obtain the desired level of adhesion. From **Figure 4.25** can be seen that the more VP latex, the better the adhesion. Solomon [35] gave three possible explanations. The first one is based on the high strength of vulcanised VP latex. Another explanation relates the adhesion as being due to the dipole interaction between VP and

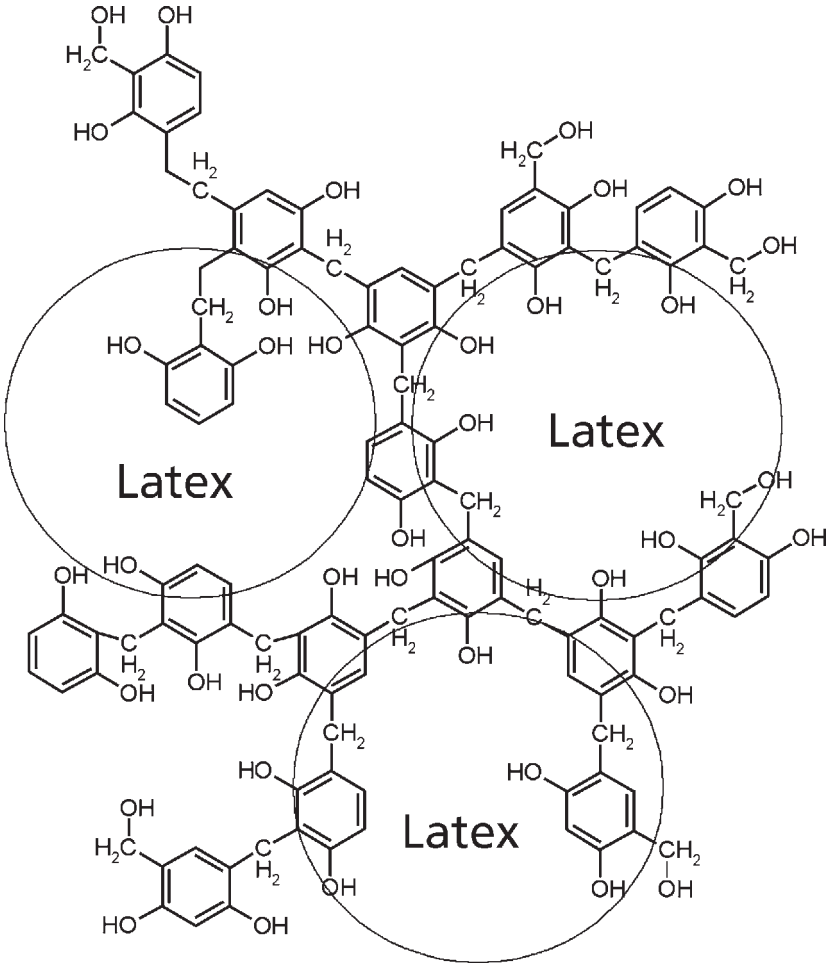

Figure 4.24 Structure of resorcinol/formaldehyde resin

Table 4.9. Dip ingredients according to Wootton [34] for Rayon and polyamide in weight parts for a styrene-butadiene-rubber (SBR) matrix		
RFL ingredients	**Rayon**	**Polyamide**
Resorcinol	8.0	9.4
Formaldehyde (37%)	14.5	13.8
Sodium hydroxide (10%)	8.0	7.0
SBR latex (35% solid)	204.3	0
VP latex (41% solid)	35.0	206.8
Water	230.2	263.0
	500 parts	**500 parts**

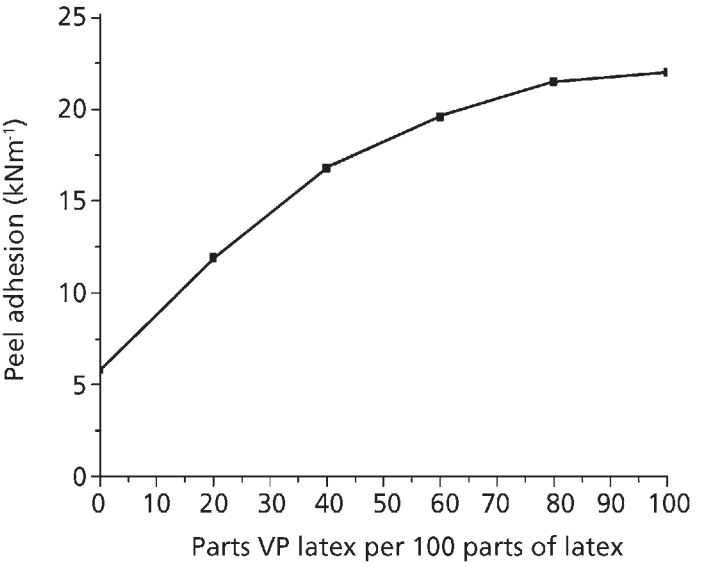

Figure 4.25 Adhesion of Nylon *versus* VP latex content, the rest of the latex is SBR

the fibre. The third view concerns the interaction between the pyridine nucleus and the resin phase in RFL.

The structural formula of VP latex is given in **Figure 4.26**.

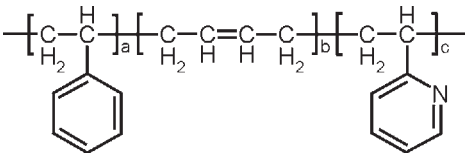

Figure 4.26 Styrene-butadiene-vinyl pyridine latex (VP latex)

When using the systems described above, the resin can be cured after addition of the latex (*in situ*). When using natural rubber (NR) as a latex however, the resin must be cured to some extent before adding the latex because the ammonia present in the latex would react with the formaldehyde.

4.5.2.3 RFL to Rubber

When the RFL dip is brought into contact with the rubber, several mechanisms can occur. The latex and the matrix rubber can form a diffusive layer, similar to the diffusion described by Voyutskii [23]. The compatibility of the latex and the rubber matrix was investigated by Basin and co-workers [36], who concluded that when the compatibility is high, diffusion occurs and the resulting bonding strength is high.

The latex and matrix rubber can also be bonded together by means of co-vulcanisation [37].

Another explanation of the adhesion between RFL and rubber is the fact that resorcinol and formaldehyde resin can react with the rubber matrix; RF resin is able to vulcanise diene rubbers. Many authors have investigated phenol-formaldehyde resin as a vulcanisation agent in diene rubbers because the resulting crosslinks are thermally stable and resistant to reversion. The mechanism of the crosslinking reaction is still under debate. There are two proposals for the mechanism of crosslinking [38], the chroman mechanism and the allylic hydrogen mechanism. The chroman mechanism was first proposed by Greth [39] (**Figure 4.27**):

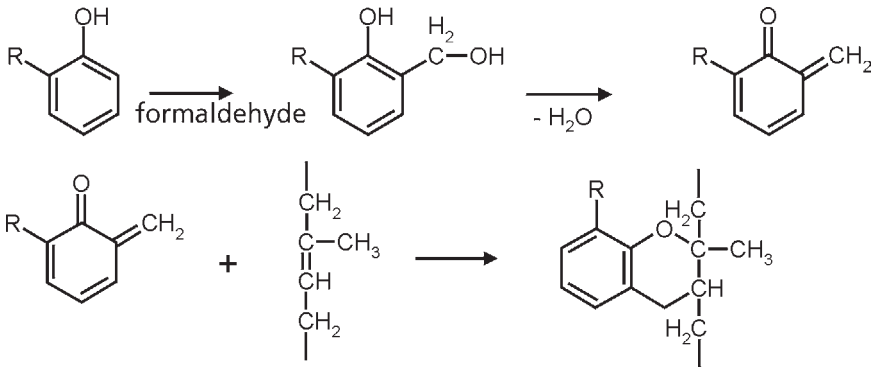

Figure 4.27 Chroman mechanism for curing a diene elastomer with a resin derivative

The allylic hydrogen mechanism was proposed by van der Meer [40]. This mechanism involves an *o*-methylene quinone intermediate. This intermediate would abstract an allylic hydrogen from the rubber (**Figure 4.28**).

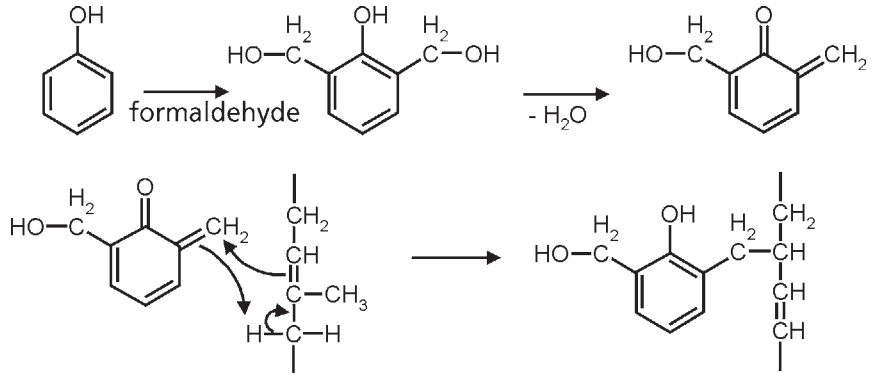

Figure 4.28 Allylic hydrogen mechanism for curing a diene elastomer with a resin derivative

In this mechanism the hydroxyl group as well as the unsaturation in the rubber is retained. The allylic mechanism received little support from other authors [38]. Their

scepticism lasted until 1995 when van Duin and Souphanthong [41] found evidence for the allylic hydrogen mechanism. They performed a model compound vulcanisation study with ethylene norbornane as a model for ethylene-propylene-diene terpolymer (EPDM). High-performance liquid chromatography was used for analysis. It was found that after vulcanisation hydroxyl groups as well as unsaturations were present in the samples [41].

4.5.2.4 RFL to Cord

It is under debate if the RFL to cord adhesion is due to chemical or physical bonding. Moult [42] suggests covalent bonding between Rayon or Nylon and the resorcinol-formaldehyde (RF) resin according to **Figures 4.29** and **4.30**.

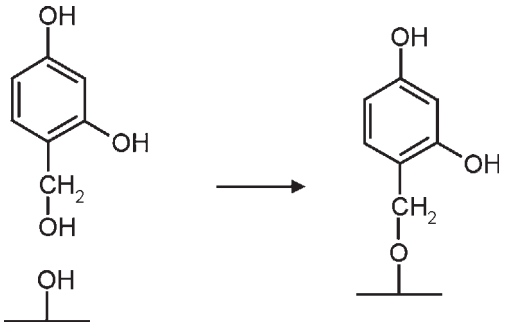

Figure 4.29 Reaction of the RF resin with the hydroxyl group of Rayon according to Moult

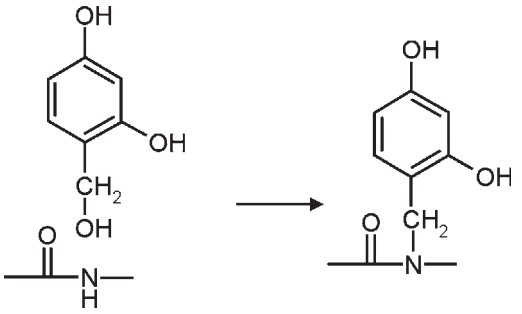

Figure 4.30 Reaction of the RF resin with the amine group of polyamide according to Skeist [31, 42]

Skeist [31, 42] however, suggests a dipole-dipole interaction between the RF and the active group on the fibres.

4.5.2.5 Dip Composition for Polyester and Aramid

Polyester does not contain as many reactive functional groups as Rayon or polyamide [34]; therefore only a standard RFL dip would not result in a sufficient adhesion. Several attempts have been made to develop a two-step dipping process in which the second step is a standard RFL dip. First highly active isocyanates in an organic solvent were used as a predipping step. In order to be able to use an aqueous solution, DuPont [43] developed a phenol blocked isocyanate system with a small amount of epoxy to improve film formation. An example of such a phenol-blocked isocyanate is Hylene (**Figure 4.31**).

These isocyanates are also used for aramid. Hepburn [29] incorporated blocked isocyanates into the rubber and used short aramid fibres for reinforcement. The two types of products between isocyanate and aramid are given in **Figure 4.32**.

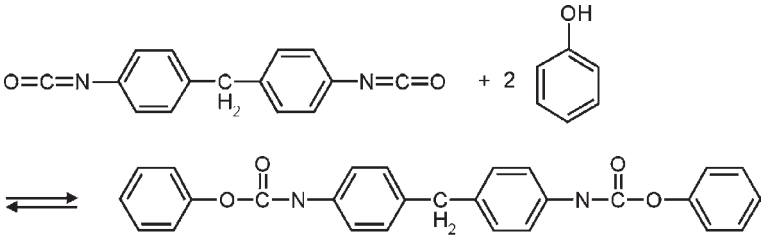

Figure 4.31 Structural formula of a phenol blocked diisocyanate (Hylene: phenol blocked methylene bis(phenylene diisocyanate))

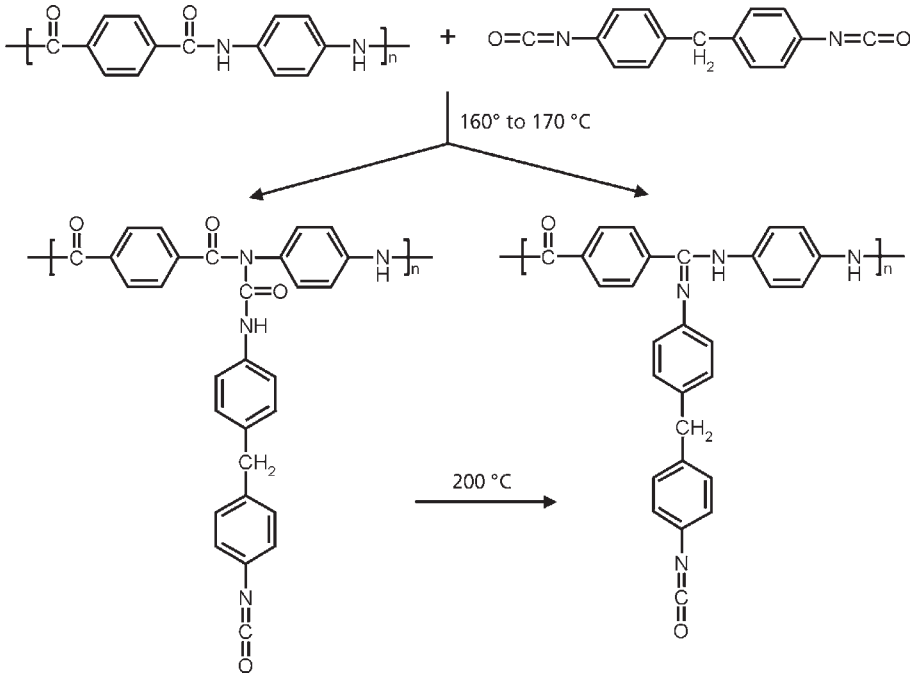

Figure 4.32 Two types of products of the reaction of isocyanate with aramid

No mechanism was given for these reactions but in standard organic chemistry textbooks (e.g., Sykes [44]) it is said that an isocyanate functionality can undergo a Schmidt rearrangement (**Figure 4.33**).

Figure 4.33 Schmidt rearrangement of an isocyanate functionality

Via this rearrangement it is most likely for the mechanisms to be as given in **Figure 4.34**.

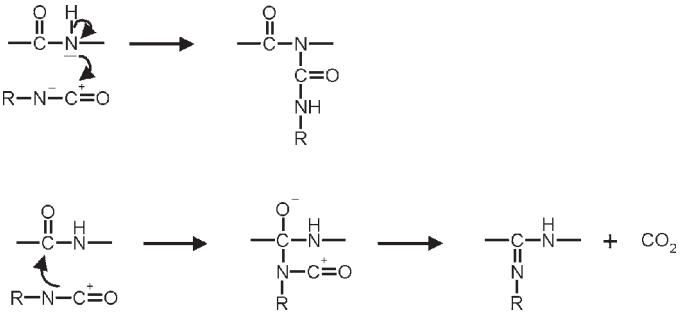

Figure 4.34 Probable mechanism for the two reactions of isocyanate with aramid

A single step system for polyester makes use of a RF resin in combination with 'Pexul'. Pexul is a trimer produced by de reaction of *p*-chlorophenol with resorcinol. This was developed by ICI [45].

Another two dip system that is frequently used for aramid is an epoxy-based dip, based on the reaction of glycerol with epichlorohydrin [13] (**Figure 4.35**).

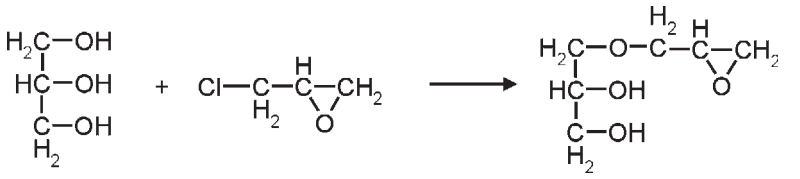

Figure 4.35 Reaction of glycerol with epichlorohydrin

Garton [46] investigated the crosslinked epoxy resin adjacent to an aramid surface by internal reflection spectroscopy (IRS). An IRS element was immersed in a 5 wt% solution of aramid in sulfuric acid and afterwards in an aqueous coagulation bath. On top of this aramid coating, a small layer (100 nm) of epoxy and hardener was applied. Cure cycles were applied in the oven and periodically samples were taken out and investigated by infra red (IR). The author found that the water present in the aramid affected the crosslinking agent (anhydride) used in epoxy. No evidence was found for participation

of the amide group of aramid in the resin crosslinking process (**Figure 4.36**), because the IR technique is too insensitive towards those highly localised surface reactions that take place at a thickness smaller than 10 nm.

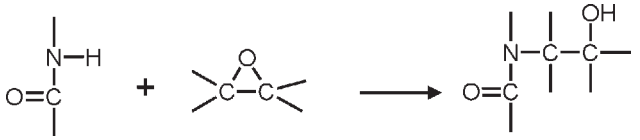

Figure 4.36 Reaction of epoxide with an aramid functionality

Mahy and co-workers [47] used an epoxy derivative in the spin finish of aramid fibres. The chemistry of the spin finish was investigated using a model for the spin finish. The model was prepared by solving glycidol and piperazine in a 50/50 mixture of water and ethanol. An aramid cord was treated with this model finish, dried at 70 °C and afterwards cured at 240 °C for 5 seconds. The aramid surface and the interface were investigated with X-ray photoelectron spectroscopy (XPS). The maturing of the spin finish was monitored by measuring the pH and nuclear magnetic resonance spectroscopy. The following reaction mechanism for maturing was proposed (**Figure 4.37**).

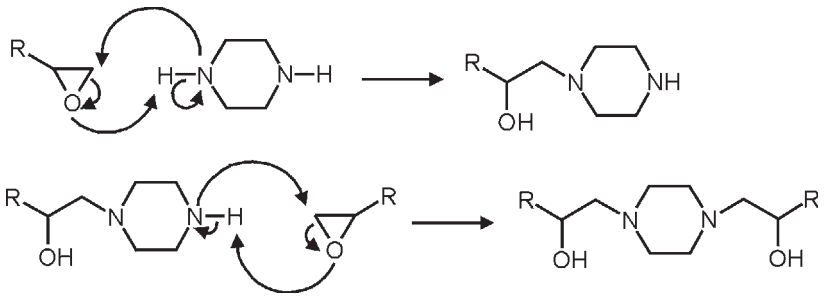

Figure 4.37 Maturing reaction of piperazine with two epoxy molecules

When epoxy has reacted to some extent, the remaining epoxy molecules can react with another epoxy molecule, with water or with the reaction product of **Figure 4.37**. These reactions are slower in comparison to the reaction in **Figure 4.37**, because in an early stage of the maturing process, the pH decreases quickly due to the amine consumption.

The matured and unmatured spin finish was applied to the fibre surface and XPS measurements were made before and after curing [47]. By XPS measurements the amount of nitrogen, oxygen and carbon was determined and the layer thickness of the spin finish on the fibre was calculated. After extraction of ethanol, it seemed that maturing the finish resulted in a larger layer thickness after extraction with ethanol. This is due to the insolubility of crosslinked epoxy. Also after curing both the matured and the unmatured spin finish, the remaining layer was thicker when the finish had been matured. There was no evidence found by microcalorimetry for epoxy diffusing into the

surface of aramid. Therefore, it is believed that a physisorption adhesion mechanism is dominant between fibre and matrix instead of a chemical reaction between the epoxy and the aramid.

Iyengar [48] has compared the solubility parameters of several predip systems, which showed acceptable adhesion levels. A solubility parameter of 23 $(J/m^3)^{1/2}$ was calculated for the epoxy predip. The solubility parameter of aramid was calculated by the method of both Hoy and Fedor and was found to be 29 $(J/m^3)^{1/2}$. The acquired level of adhesion is explained by the possibility of hydrogen bonding ($\varphi > 1$, Equation 4.6).

4.6 Dipping Process

A general scheme for a dipping unit is given in **Figure 4.38**. In this picture, the cord is moving from right to left. The entry nip picks up the cord from the feed roll; when a feed roll is empty, the entry accumulator is used to gain time to attach a new feed roll. Before entering the impregnator bath and after the oven, a series of rolls is present. These rolls have a relative velocity between each other, allowing application of stress on the cord during dipping and drying. After the cord has passed the impregnator bath, the amount of dip on the cord (dip pickup) is regulated by the so-called pickup control system. This is mostly a squeeze roll unit but can also be a vacuum unit or a beater. The second dipping proceeds similar to the first system. The exit accumulator functions in the opposite way to the entry accumulator, as a buffer for the rebatch unit.

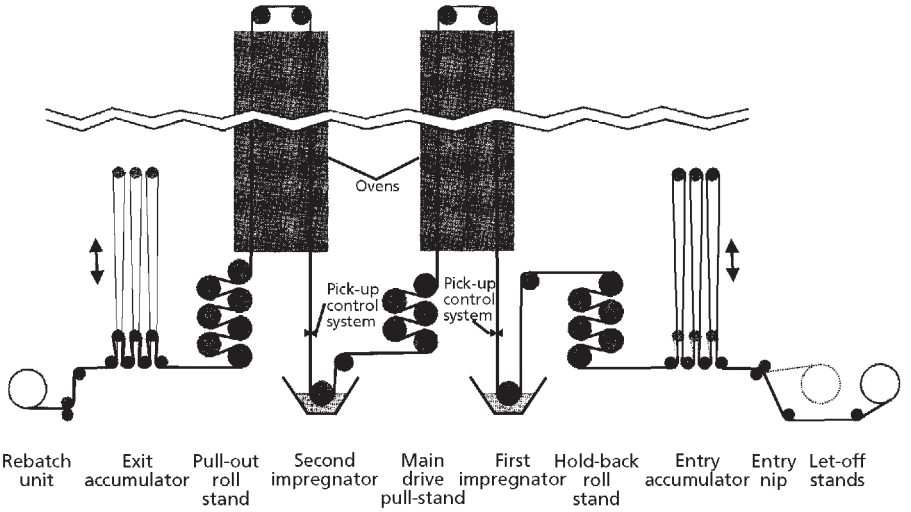

Figure 4.38 General layout for a fabric treatment unit for a two dip system [13]

Reproduced with permission from D.B. Wootton, The Application of Textiles in Rubber, Rapra Technology, Shawbury, Shrewsbury, UK, 2001. ©2001, Smithers Rapra Technology

4.6.1 Factors Influencing Adhesion in Standard Resorcinol Formaldehyde Latex (RFL) Treatment

Several aspects regarding the RFL adhesive are important:

- F/R ratio;
- RF/L ratio;
- RFL pickup;
- Acidity of the dip;
- Type of base in the RFL dip;
- Vulcanisation behaviour of the rubber matrix; and
- Environmental aspects.

F/R Ratio

In RFL, the rate of methylol formation, MW and the structure of the resin vary with the F/R ratio. Takeyama [14, 49] has investigated these aspects.

It can be concluded from **Figure 4.39** that a higher F/R ratio results in a higher reaction rate. The results were obtained by titration of the free formaldehyde from resins with several F/R ratios [14]. If formaldehyde reacts with all the available sites on resorcinol, a maximum of three moles of formaldehyde would react with one mole of resorcinol. According to **Figure 4.39**, the methylol reaction is complete at a F/R ratio of 2.2:1.

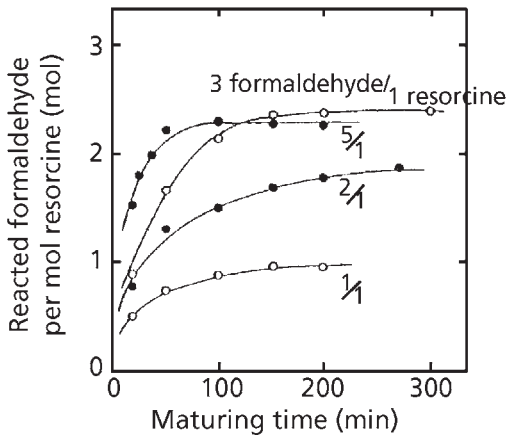

Figure 4.39 Reacted formaldehyde *versus* reaction time

The viscosity rises due to the curing of the resin. From **Figure 4.40** [14] it can be observed that at an F/R ratio of ½, no change in viscosity takes place. This means that no crosslinking takes place. When the F/R ratios in **Figure 4.40** and **Figure 4.41** are compared, it seems that the viscosity is increasing at the moment that formaldehyde stops reacting. This is at a reaction time of 200 minutes. This means that the reaction rate for the methylol reaction is higher than for the polymerisation reaction. When an excess of formaldehyde is used, 2.2 mole of formaldehyde reacts with 1 mole of resorcinol. The reason that it is 2.2 instead of 3, can be the steric hindrance of the two hydroxyl groups in resorcinol.

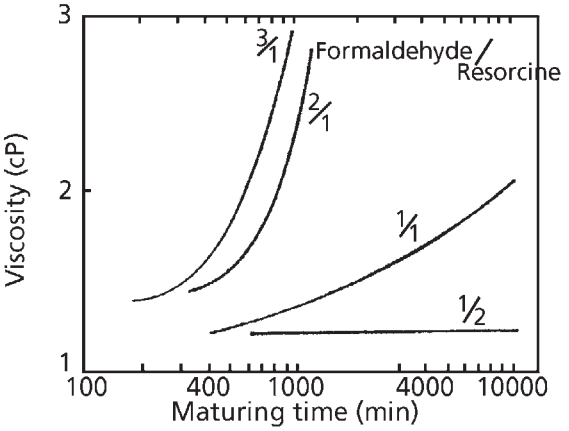

Figure 4.40 Viscosity *versus* reaction time

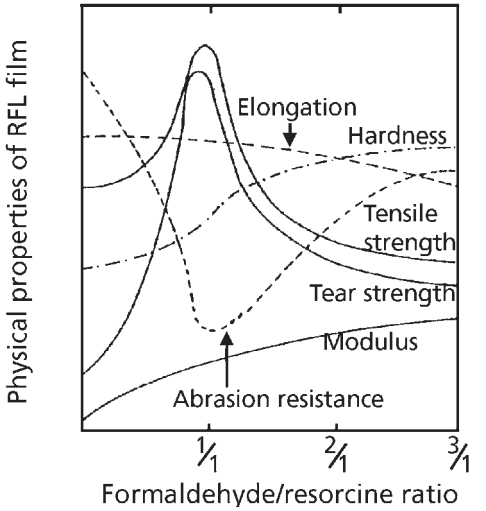

Figure 4.41 Mechanical properties of the resin *versus* F/R ratio [50]

The mechanical properties change due to the difference in network properties for the different F/R ratios. Hupje [51] stated that the ideal relative E-moduli for a rubber:dip:fibre system would be 1:80:1000 (**Figure 4.42**).

The effect of the F/R ratio on the pull through load was investigated by Miller and Robinson [52], Dietrick [37], and Uzina and co-workers [53] (**Figure 4.43**).

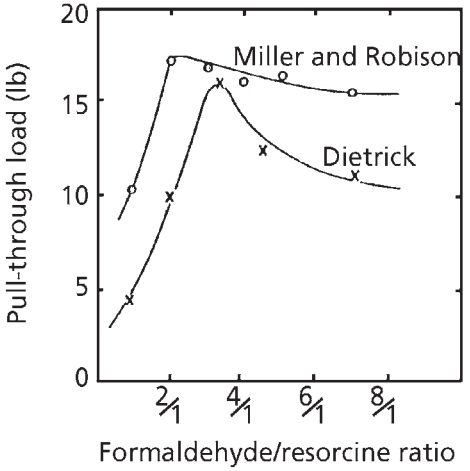

Figure 4.42 Effect of F/R ratio on the pull through load
(Note: 1 lb load ≡ 4.448N force)

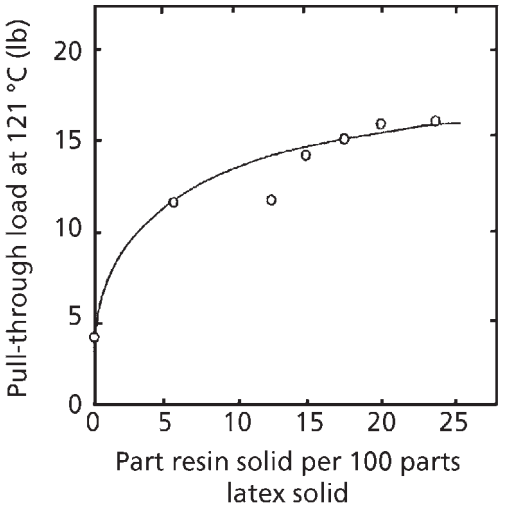

Figure 4.43 Pull through load *versus* RF/L ratio [14]
(Note: 1 lb load ≡ 4.448N force)

RF/L Ratio

Besides the R/F ratio, the level of adhesion also depends on the resin to latex ratio. If only the latex is applied, the bonding force is very low due to lack of interaction with the fibre [54]. If the resin content were too high, the dipped cord would be too stiff and the modulus of the dip itself too high.

Dietrick [37], Miller and Robinson [52] demonstrated that a higher resin content leads to better adhesion as shown in **Figure 4.44**.

Hupje [28, 51] has also investigated the influence of the amount of resin *versus* latex on the adhesion. In this study a SBR/NR mixture was used with both PET and polyamide. The latex used for the dip contained 100% vinylpiridine.

The type and number of functional groups, the mechanical properties of the total dip, the type of cords, the rubber compound and the dipping conditions influence the level of adhesion. Therefore, the position of the maximum in **Figure 4.44** has to be determined for a particular compound.

RFL Pickup

The pickup level of the dip on the cord influences the adhesion property. Takeyama [14] has reported a result of Dietrick [37], that adhesion increases as a function of pickup and reaches a saturation point. The same conclusion was drawn by Hupje [51]. The dip however, can influence the stiffness of the cords. This was pointed out by Murphy [55] and the author warned at the end of the article that good tyre cord adhesion does

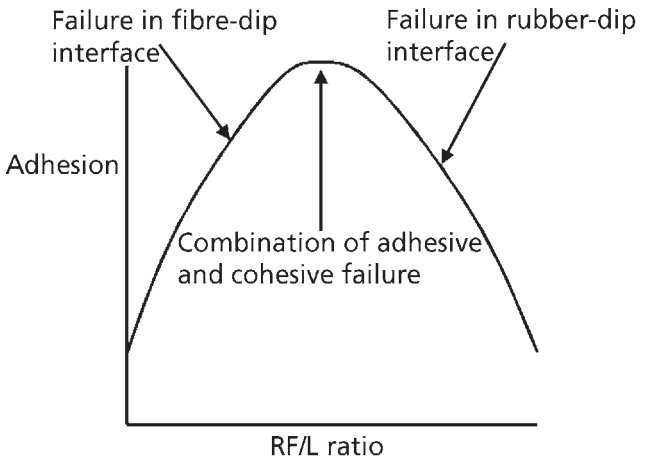

Figure 4.44 Adhesion *versus* RF/L ratio according to Hupje [51]

not guarantee good tyre performance. An optimal pickup level for every system has to be determined [14]. The dip pickup is influenced by the type of textile and finish used, concentration and viscosity of the dip and the squeezing conditions.

Takeyama [14] published results of Tsuji [56] for pickup of polyamide and Rayon under different squeezing conditions and different lattices (see **Table 4.10**).

At a constant squeezing pressure, the pickup for Rayon is generally higher than for Nylon. A higher squeeze pressure leads to lower pickup and a lower adhesion.

Acidity of the Dip

The influence of acidity on the adhesion has been described in both the (review) articles of Takeyama [14] and Solomon [54]. When NaOH is used in the dip, there is a large variation of the adhesion for different values of pH (**Figure 4.45**).

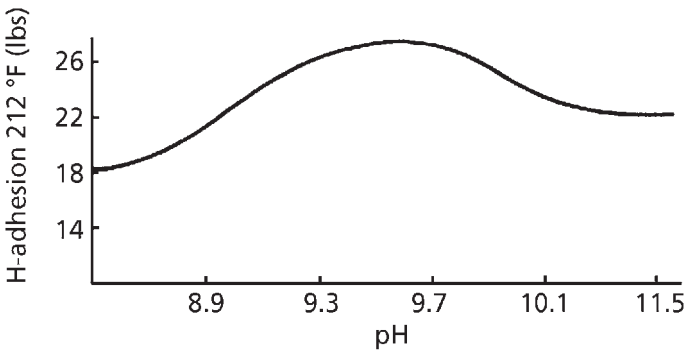

Figure 4.45 Value for the adhesion as a function of the pH when NaOH is used [54] (Note: 212 °F ≡ 100 °C; 1 lb load ≡ 4.448N force)

Table 4.10. Dip pickup for different latices and squeezing conditions for polyamide and Rayon

Latex RFL	RFL concentration	Squeeze, N	Rayon		Nylon	
			Pickup, wt%	Pull through, N	Pickup, wt%	Pull through, N
Butyl	12.5 %	0	8.5	76.5	3.3	50.7
	12.5 %	66.7	2.2	64.5	2.8	47.6
	12.5 %	155.7	3.5	55.6	2.2	47.1
SBR	-	0	7.3	117.4	3.2	78.7
	-	66.7	4.9	106.3	2.9	70.7
	-	155.7	3.7	85.4	2.5	63.2

When ammonium hydroxide is used in the dip, this large variation is not observed. Experience has pointed out that a combination of sodium hydroxide and ammonium hydroxide is favourable. Solomon [35] stated that the ammonium hydroxide takes part in the reaction between resorcinol and formaldehyde in forming a $–CH_2\text{-}NH\text{-}CH_2\text{-}$ functionality. When ammonium hydroxide has reacted, sodium hydroxide remains present to catalyse the RF cure.

Vulcanisation Behaviour of the Rubber Matrix

Hupje [28] has described the influence of vulcanisation behaviour on the adhesion.

Factors related to the vulcanisation behaviour that influence the adhesion positively are [28]: Low minimum plasticity during flow (A), a long scorch time (B), a low rate of curing (proportional to tan α), and a high modulus of the rubber after the curing (C). In **Figure 4.46** it can be seen that these factors lead to a higher marked area. Hupje [28] has plotted the adhesion as a function of this shaded area and found that there is a significant correlation.

Environmental Aspects

Environmental effects on RFL adhesion have been studied by Wenghoefer [57]. In this work, adhesion is measured as a function of exposure time to ozone, humidity, ultraviolet light and heat. The effect of heat was less severe than the effect of ozone, humidity and UV light. In **Figure 4.47**, the influence of exposure time to ozone concentration on the adhesion is shown.

The physical properties of the RFL dip were tested with RFL sheets that had been exposed to the environment and no changes were observed. This would mean that

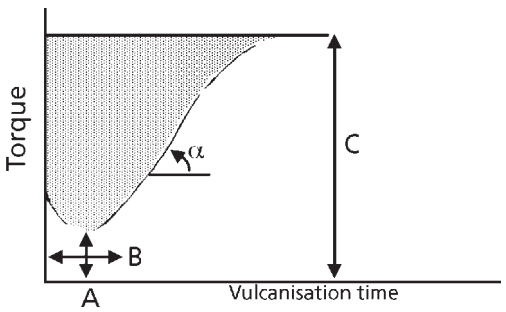

Figure 4.46 Schematic representation of a rheometer curve

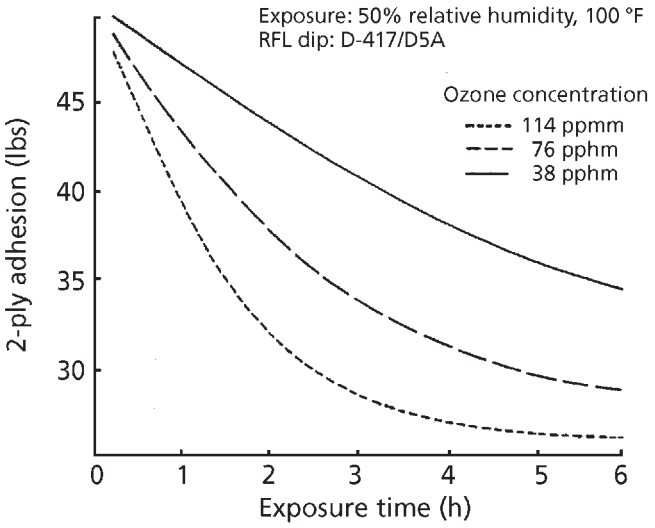

Figure 4.47 Influence of adhesion to exposure time to three ozone concentrations for polyester cords. pphm = parts per hundred million

no cohesive failure takes place in the RFL dip itself but rather at the surface and the interface between RFL and rubber.

4.7 Alternative Dip Treatments for Polyester or Aramid

Solomon [58] patented an alternative for the RFL dip for both aramid and polyester. This dip was used after the conventional epoxy predip. This was an acrylic resin dispersed in latex. In the example, styrene (A) and methyl methacrylate (B, **Figure 4.48**) in combination with vinyl pyridine latex were tested. Compared to the conventional RFL dip system, the H adhesion to a NR compound increased by 3.7%.

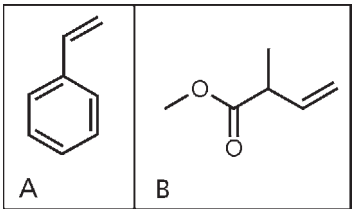

Figure 4.48 Monomers used by Solomon [58]. Styrene (A) and methyl methacrylate (B)

Van Gils [59] has added trimethylolphenol (**Figure 4.49**) in the RFL recipe for better adhesion of rubber to aramid.

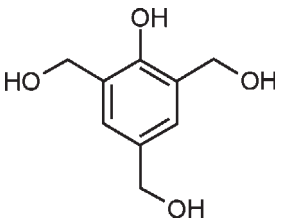

Figure 4.49 Structure of trimethylolphenol

Table 4.11. Composition of RFL with trimethylolphenol [59]	
Component	**Amount (phr)**
Latex	100
Trimethylolphenol	2-28
Resorcinol/formaldehyde resin	0.5-24
NH_3, NaOH	0-3
Water	170-1100

The trimethylolphenol is synthesised by adding an excess of formaldehyde to phenol in a basic environment. The composition of the dip is shown in **Table 4.11**.

The drying conditions of the dip were 90-260 °C for 5 to 300 seconds. The rubber to which the fibres were adhered was a blend of NR, SBR and butadiene rubber. Vulcanisation temperature was 157 °C. Adhesion was measured by an H-test according to ASTM D2138-83 [60]. Adhesion was found to increase 60% when trimethylolphenol was added. This is ascribed to the fact that when all the methylol functionalities are converted into methylene groups, the solubility parameter of this compound is 30 J/m^3. This is close to the value of 29 J/m^3 of aramid [48].

Burlett [61] in his patent from 1991 has described treating aramid with an aramid-polydiene copolymer, as a replacement for the epoxy/RFL dip. An example of the structural formula is shown in **Figure 4.50**. B and X in this structure are aromatic compounds.

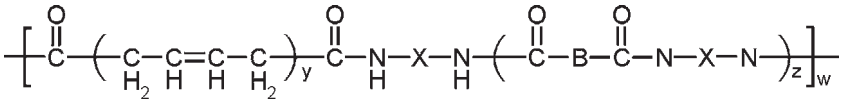

Figure 4.50 Example of an aramid-polydiene copolymer

where: W is between 1 and 25, Y is between 70 and 90, and

Z is between 4 and 100.

This copolymer can be placed on the fibre by using a solution as a dip, or by using it in the finish of the fibre. Drying occurs at a temperature between 100 °C to 300 °C for 3 to 10 seconds.

The copolymer has aramid functionalities as well as allylic hydrogens. The adhesion properties are maximal when used in a rubber that contains unsaturations, capable of sulfur vulcanisation. The adhesion increases by 10 to 15% in comparison with fibres without any treatment.

Sharma [62] first treated aramid cord with a cold plasma of air, N_2, He, Ne or Ar. After this, an aqueous dip was used that contained a vinyl pyridine latex, soluble epoxy and a polyfunctional amine. An excess of the amine was used to ensure that all epoxy was cured. The amounts are given in **Table 4.12**.

Table 4.12. Amounts in the dip of Sharma [62]

Component	Amount (phr)
Latex	100
Epoxy	10-30
Amine	2-8

The amount of water in the aqueous solution is 15 to 25 wt%.

The amount of dip in the fibre is preferably between 15 to 20 wt% on basis of the fibre weight. The drying conditions are 93 °C to 316 °C for 5 to 300 seconds.

Li [63] has used a mixture of two silane compounds. One compound contained an amine functional group, the other a radical functional group or unsaturated double bonds (**Figure 4.51**).

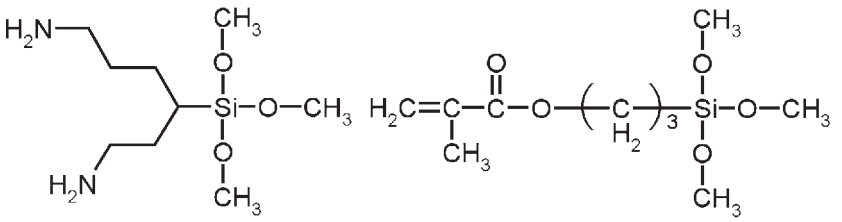

Figure 4.51 Two examples of the structures patented by Li [63]. Both types of silanes are commercially available (Dow Corning)

A dispersion of the two silane components in water was added to the fibre; this fibre can be both polyester and aramid. Although one of the two types of silane components is not soluble, no surfactant should be used because that influences the adhesion in a negative way. The amount of silanes on the textile should be between 0.5 to 2 wt% and the heating conditions are 120 °C to 250 °C for about 3 minutes. Optionally a RFL treatment can be applied after the silane treatment.

These types of coupling agents were proven successful in glass fibre reinforced epoxy compounds. In **Figure 4.52** the hydrolysis and chemisorption is given of a similar coupling agent to that used by Li. The surface of glassfibres contains hydroxyl groups and these groups bond with the coupling agent. The amine part of the coupling agent can react with epoxy. Looking at this mechanism it is most likely that the coupling agents Li used are meant to react with the amide functionality of aramid.

Surface Roughening

Breznick [25] has treated aramid with bromine to modify its surface. The bromine is adsorbed into the fibre surface and afterwards the fibre passes through an ammonia solution. The chemical reaction that takes place is:

$$3Br_2 + 8NH_4OH \rightarrow 6NH_4Br + 8H_2O + N_2$$

The nitrogen gas that is produced escapes from inside out through the surface. In this way the fibre surface is chemically etched. The aramid should be in contact with the bromine only for a short time to prevent a strong reduction in the tensile properties of the fibre. The roughened surface was studied by scanning electron microscopy (SEM).

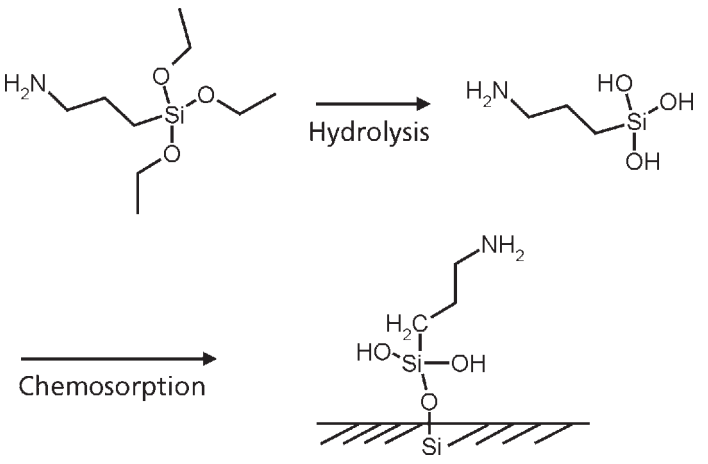

Figure 4.52 Reaction of coupling agent in glassfibre reinforcement [64]

Under optimal conditions, the adhesion was improved 20%. The fibre strength loss was 15%.

Roebroeks [26] investigated the influence of fibrillation on the adhesive strength of aramid to thermoplastic polyetherimide resin. Aramid is easily split in the transverse direction, giving structures as illustrated in **Figure 4.53**.

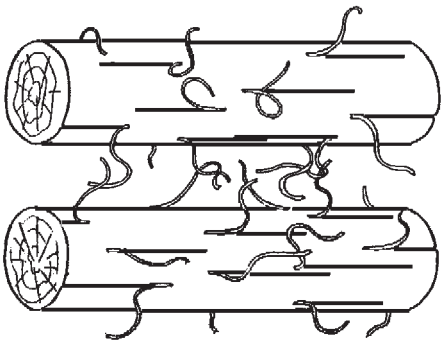

Figure 4.53 Fibrillation of aramid fibres

Controlled fibrillation is obtained by bringing the surface in contact with small oscillating particles. Only a small layer is affected and the rest of the fibre remains intact to carry the tensile load. The author states that an increase of more than 600% in adhesion is obtained without any loss in mechanical properties of the fibre. The increase in adhesion can be ascribed to an increase in mechanical anchoring of the fibrils.

4.8 Chemically Altering the Surface

Fibres surface modifications have been used in the past to either improve adhesion or enhancing yarn properties. It is well known that some of the fibres, like PET or aramid, are inert in nature as compared to cellulosic or polyamide. In this review the modifications of PET and aramid are outlined next.

4.8.1 Polyester

Gillberg-LaForce [65] has patented surface modification of polyester by an electron beam for improved adhesion. The electron beam promotes free radical formation and carboxyl and hydroxyl functionalities are formed on the surface. These functionalities can be used to form bonds with an epoxy or isocyanate sublayer. This treatment resulted in an increase in adhesion of 21.8% measured by H-tests in comparison to a standard epoxy RFL dip system.

Dixon [66] has improved the adhesion for polyester cord by fluorination. The polyester cord passed through an oxygen-free gas chamber, containing fluorine gas. The residence time should be less than 5 minutes. Fluorinated polyester cord in combination with a RFL layer, doubles the measured adhesion in comparison to RFL treated polyester. The rubber used was a NR/SBR blend.

Aramid

Penn [67] has given three options for organic chemical modification of aramid via ionic or polar reactions. These options are shown in **Figures 4.54** to **4.56**. The bromination and nitration modification of aramid was studied by Wu [68] by means of a model compound study.

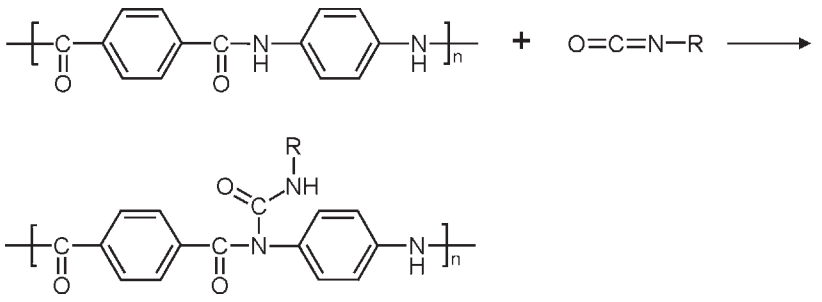

Figure 4.54 Attachment of functional group R to the amide functionality of aramid via isocyanate reagents

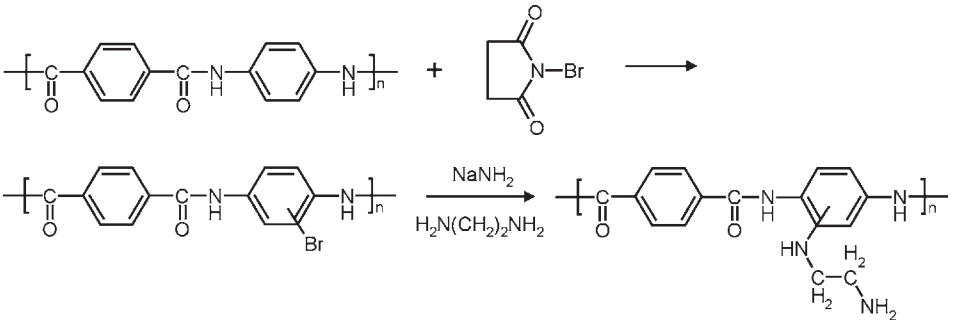

Figure 4.55 Bromination of the benzene ring of aramid

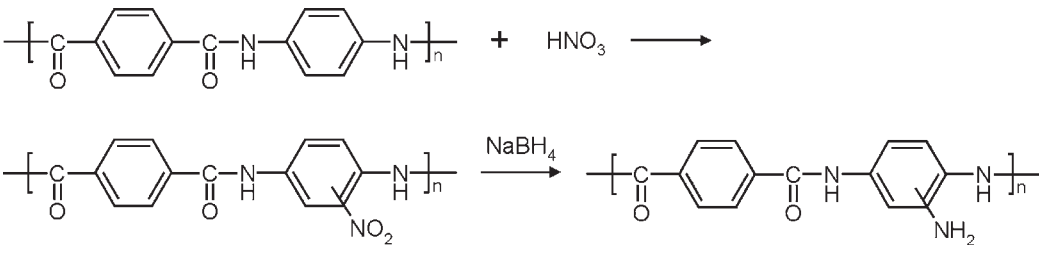

Figure 4.56 Attachment of the NH_2 functional group to the benzene ring of aramid

Takayanagi [27, 69, 70] has chemically modified the surface of aramid in order to improve the adhesion to an epoxy resin (**Figure 4.57**). Epoxy functional groups were grafted on the surface of aramid according to the following reaction schemes: 1, 2 and 3. The aramid fibre passes through a bath in which sodium hydride and dimethyl sulfoxide are present. If the reaction time is too long, the aramid will be totally consumed. Therefore it is necessary to control the reaction time. The second bath contains the halogen-functional group. The halogen forms a salt with the sodium and the functional group is positioned on the amide part of aramid.

This treatment can lead to an improvement of 50% of the peel strength. This is probably not only due to the chemical modification but also to the swelling of the surface by the chemicals, improving the mechanical anchoring. The strength of the fibre itself however, decreased to some extent.

Chatzi [71] has studied the chemical modification of aramid by means of hydrolisation. The reaction scheme is shown in **Figure 4.58**.

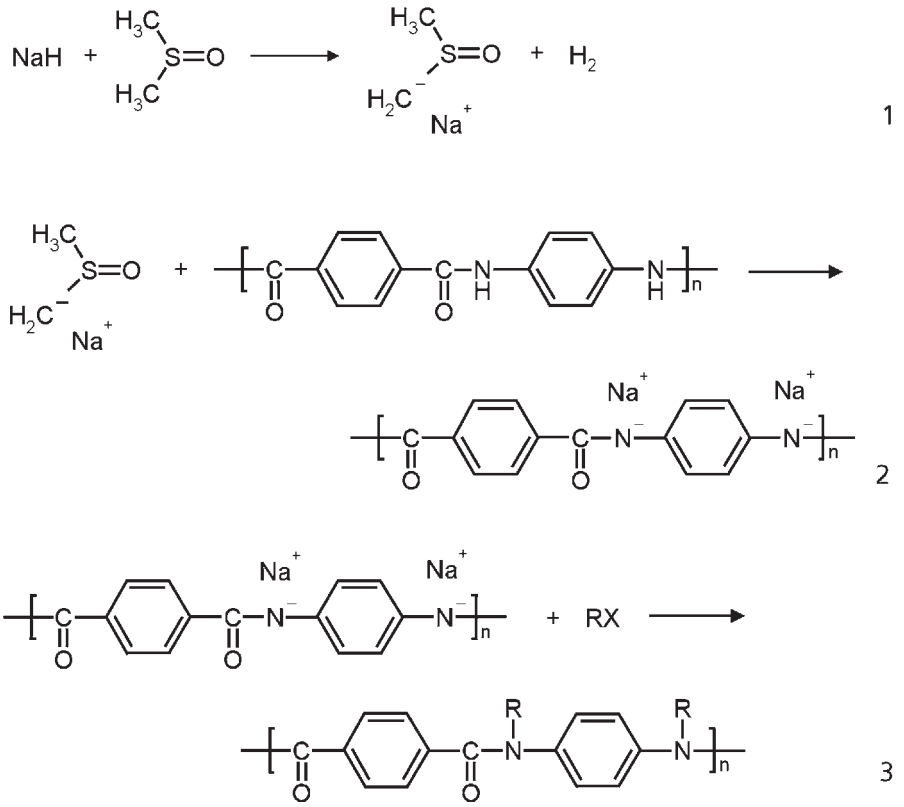

Figure 4.57 Reaction scheme for grafting functional groups to aramid, X represents a halogen functionality

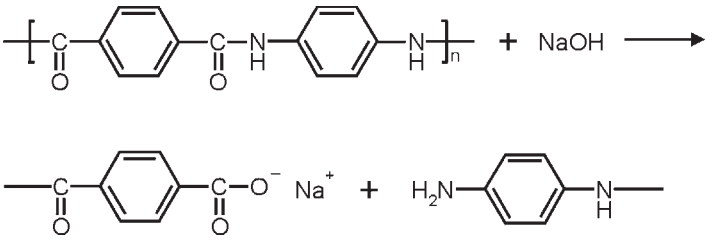

Figure 4.58 Reaction scheme of hydrolisation of aramid

This reaction results in formation of pendent amine groups and carboxylate groups. These functional groups are more reactive towards epoxy groups for example. In order to improve the adhesion without damaging the bulk properties of aramid, which can occur due to chain scission, it is important only to treat the outermost surface. This is influenced by the reaction time.

Mercx [72] has introduced specific organic groups at the surface of aramid *via* the reaction with oxalylchloride (**Figure 4.59**).

Mercx has used water, methanol, ethylenediamine and glycidol to react further with the reaction product of aramid with oxalylchloride.

The products from **Figure 4.60** were experimentally observed via model compound experiments and XPS measurements of aramid fibres.

Rebouillat [73] has grafted polyaramid fibres with nitrobenzyle, nitrostilbene and allyl functionalities. These are given in **Figure 4.61**. These functionalities are positioned on the amide of polyaramid. The rubbers mentioned are, among others, NBR, EPDM, SBR and NR. Preferably, the grafting is performed after the coagulation bath. The fibre

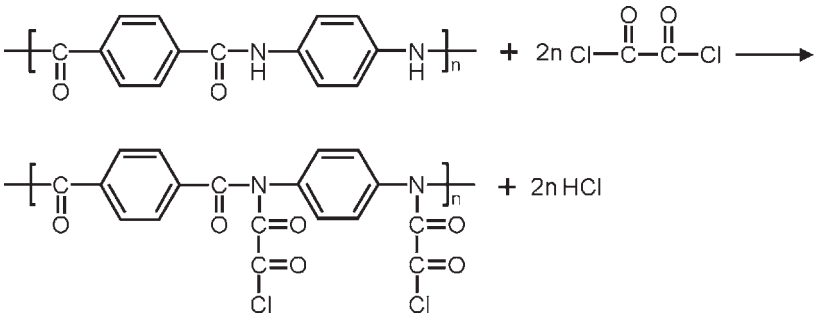

Figure 4.59 Reaction of aramid with oxalylchloride

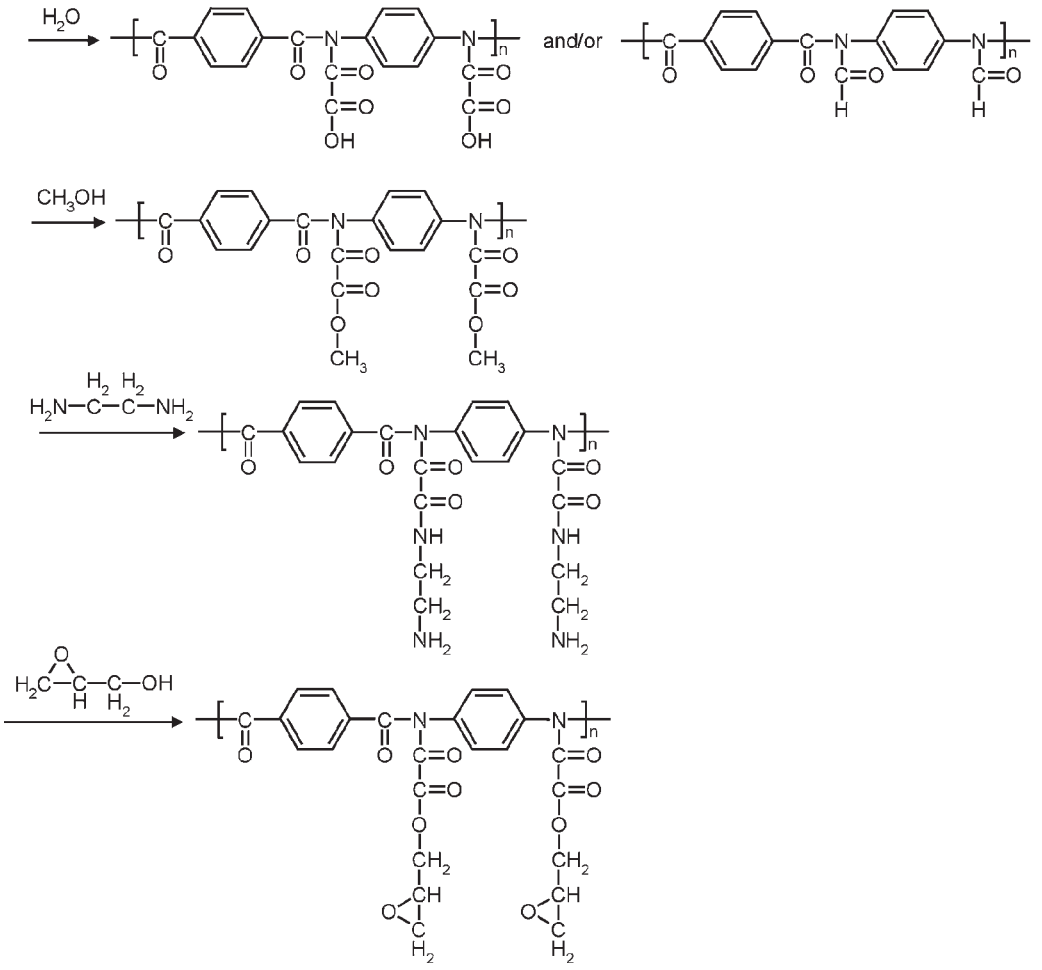

Figure 4.60 Resulting functional groups attached to the aramid repeating unit

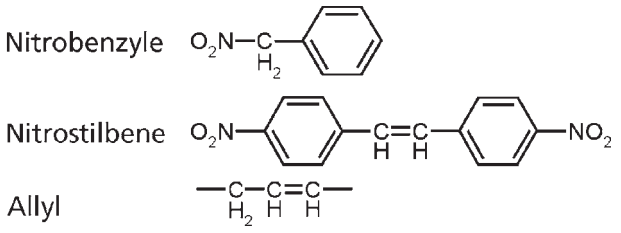

Figure 4.61 Nitrobenzyle, nitrostilbene and allyl functionalities

should still contain 30 to 100 wt% water (on basis of the weight of the fibre material), for the reason that the structure of the dried fibre is too compact, making the amine functionality less available. The grafting is performed in a base environment between 15 °C and 50 °C. On the surface of the fibre 0.25 to 75% of the amine functionalities is grafted.

4.9 Plasma Treatment

Plasma treatment has been of interest since the late 1950s. A plasma state is a complex gaseous state containing free radicals, electrons, photons, ions, etc. A fibre is treated with plasma for several reasons [67]. First, it can be used to clean or etch the surface of the fibre. Inert gases are then used like argon, nitrogen, etc. Second, the use of more reactive gases introduces functional groups on the surface. Third, the use of monomers causes a thin polymer coating. Plasma treatment can therefore be used for all three approaches mentioned before: the mechanical interlocking of the fibre (etching), changing the fibre surface chemically (reactive gases) and adding an extra component (polymer coating). The advantage of plasma treatment is elimination of the need for hazardous solvents. A disadvantage is that the nature of the plasma-modified surface is difficult to control due to the complex plasma state.

Luo [74] has investigated plasma polymerisation on cords. During a plasma treatment, the fibre passes an electrical field that contains an inert gas and gaseous monomers. The types of monomers Luo used were pyrrole and acetylene (**Figure 4.62**).

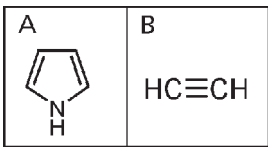

Figure 4.62 Structural formulas of A: pyrrole and B: acetylene

The monomers polymerise and form a film with a thickness between 100 and 200 nm on the fibres. Previously, the fibres were etched and cleaned by argon plasma. However, the use of argon plasma alone did not improve the adhesion of aramid to the fibre. Luo determined the influence of the pressure of the gas and the electrical power to the adhesion properties. It seemed that a high concentration of monomer and a low electrical power lead to higher adhesion. Luo explains this by the hardness of the layer. A higher concentration of monomer combined with a low electrical power would lead to a lower degree of crosslinking. This would make the structure less dense and the level of penetration of rubber polymers would increase.

4.10 Rubber Treatment

4.10.1 Mixing Ingredients

From the 1950s adhesion activators have been mixed into the rubber to enhance the adhesion to fabrics [28]. Generally three components are added extra to the rubber compound: resorcinol, a formaldehyde donor and an active white filler. The role of the filler is not fully understood; it can improve the miscibility of the resorcinol and formaldehyde donor or it can act as a catalyst. In the case of aramid fibres, isocyanate derivatives can be mixed into rubber to improve the adhesion [29], especially in the case of short fibre reinforcement.

Iyengar [48] has investigated the addition of adhesion promoters to rubber compounds. Hexamethylenetetramine/resorcinol and methoxymethylmelamine/RF resin systems were tested. These adhesion promoters seemed to improve the adhesion in peel tests also after exposure to ozone for 3-8 hours. The author explained this by assuming that the promoters diffuse into the RFL layer and bond with sites not attacked by ozone.

D'Sidocky [75] has added a certain amount of hydrated thiosulfate and bismaleimide to a diene rubber compound. The preferred types are given in **Figure 4.63**.

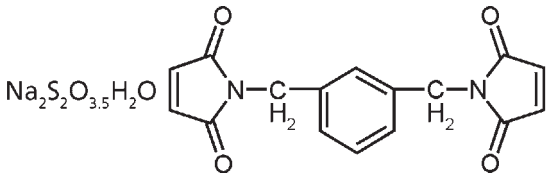

Figure 4.63 Structure of the thiosulfate and bismaleimide used

The amount of hydrated thiosulfate is between 0.1 and 1 phr and the amount of bismaleimide lies between 0.5 and 5 phr. If only one of these two compounds were used, a decrease of the adhesion of aramid to rubber was observed. The combination showed an increase of the adhesion of 24.4% compared to naked aramid to rubber measured by pullout tests.

4.10.2 Chemical Modification of Rubber

Hardly anything is published about chemical modification of rubber for adhesion purposes. The only article found is about grafting glycidyl methacrylate and *N*-vinyl pyrrolidone functionalities (**Figure 4.64**) to NR for improving the adhesion of tyre cords to rubber [30]. In this article only the preparation of NR graft copolymer has

been described; the actual adhesion testing of these rubbers to cords has never been published.

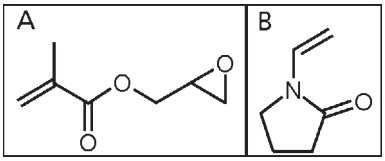

Figure 4.64 Molecules used for grafting NR by Egboh [30]. A: Glycidyl methacrylate. B: *N*-vinyl pyrrolidone

4.11 Methods for Analysis

Adhesion of fibres to rubber is very difficult to measure; the result is always influenced by the conditions under which the test proceeds. The elastic deformation causes a stress distribution and this distribution can hardly be calculated due to the complexity of the system (cord-dip-rubber). When local stress exceeds local strength, rupture takes place. Since the local stress is unknown, it is hard to draw conclusions about the local strength. Therefore it is important to use standardised tests. If all experimental conditions are the same, comparative conclusions can be drawn regarding the adhesion [35]. In the literature, efforts have been made to obtain absolute values for interfacial strength. This has been done for the single cord pullout test.

4.11.1 Pullout Tests

A standard static test is the cord pull out test. The force is measured that is needed to pull a cord out of a rubber block. Three variations are the H-test, T-test and the U-test (**Figure 4.65**). The square blocks represent the rubber and the dotted lines indicate how

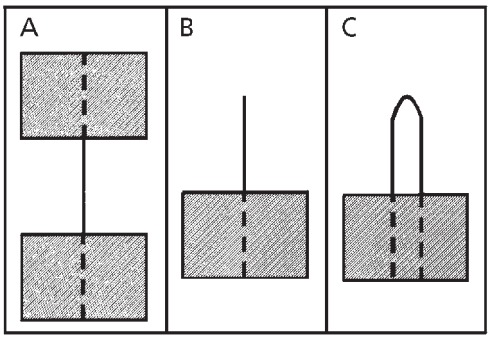

Figure 4.65 Three types of static tests, H-test (A), T-test (B), U-test (C)

the cords are positioned within the rubber. The way samples are positioned in the tensile tester differ between these three measurements. During the H-pullout test, the rubber blocks are gripped and separated; with the T-test, the cord itself is pulled out of rubber; and the same is the case for the U-test, with the difference that the loop the cord makes is gripped and two times the embedment length is separated from the rubber block in one single measurement. The length of the embedded cord, the rate of loading and the temperature of the sample influence the measured adhesion forces [13].

Some authors have performed research on the determination of the exact value for the adhesion from experimental tests. Jiang [76] has modified an existing energy balance for a single filament pull out test. The main point of interest was the influence of the embedded length. Liang created a model from the energy balance using two extra components: a matrix compression contribution and the work of friction between debonded fibre and the matrix material. He divided the system in to three regions according to **Figure 4.66**.

The first region is the fibre alone, the second is fibre and matrix debonded and the third is fibre and matrix bonded. For the overall system, the energy balance is given by Equation 4.10.

$$\frac{1}{2\pi r}\frac{\partial U}{\partial a} \geq G_C + \frac{1}{2\pi r}\frac{\partial W_f}{\partial a} \tag{4.10}$$

On the left side there is the strain energy released by the system upon pullout. In order for a crack to occur, the energy must be sufficient to propagate a crack (G_C) and to overcome the friction in region 2. U is the total elastic energy stored in the system, W_f is the work of friction in the debonded area, $2\pi r$ is the circumference of the interphase and G_C is the interfacial fracture energy. For all three regions the stored strain energy is determined as well as the work of friction. An experimental pathway for determining G_C

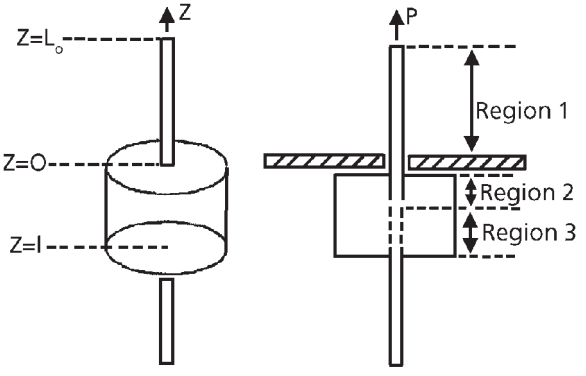

Figure 4.66 Schematic representation of the single filament pull-out test according to Jiang [76]

is to measure the load as a function of displacement. When the embedded length is large enough, this plot shows a transfer from linear to non-linear behaviour (**Figure 4.68**).

The right figure in **Figure 4.67**, shows a transfer from linear to non-linear. The load at which this occurs is P_C and can be used to calculate G_C.

Jiang suggests a method for determining G_C for different surface treated fibres in a standard matrix. If the elastic constants and the specimen dimensions remain the same over a range of measurements, relative values for G_C can be obtained. In **Figure 4.67** two theoretical load *versus* embedded length plots are shown for different G_C values.

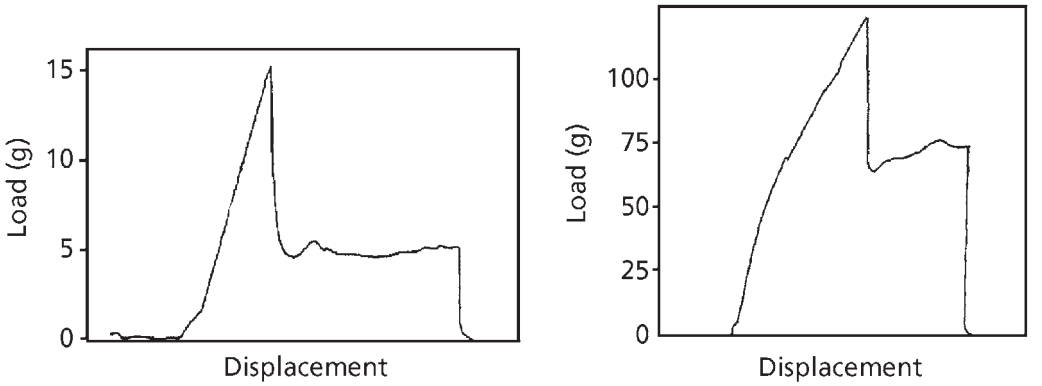

Figure 4.67 Load-displacements plots for fibre pullout tests for small embedded lengths (left) and large embedded lengths (right)

Figure adapted from Jiang [64]

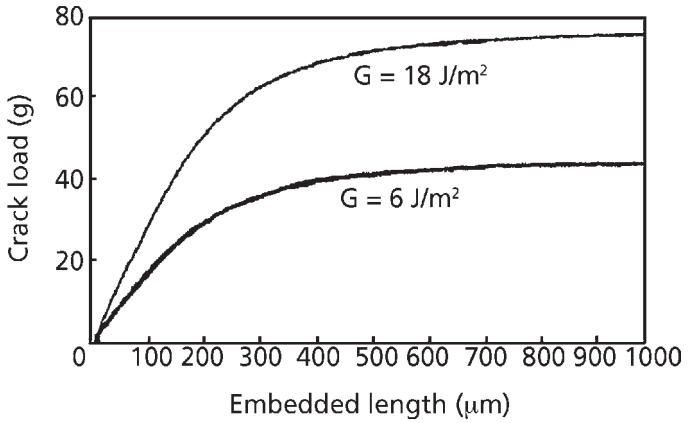

Figure 4.68 Load *versus* embedded length plots for different theoretical values for G_C

Figure adapted from Jiang [64]

The slope at the beginning of the P *versus* l plot is proportional to the square root of G_C according to Equation 4.11:

$$P_C = \sqrt{\frac{E_f \cdot A_f \cdot 2\pi r \cdot G_C}{(2+\alpha)}} \cdot \left(\frac{n}{r}\right) \cdot l \tag{4.11}$$

with:

$$\alpha = \frac{E_f A_f}{E_m A_m}$$

$$n^2 = \frac{E_m}{E_f (1+\nu_m) \ln\left(\frac{R}{r}\right)}$$

where: R is matrix radius and r is the fibre radius.

There is in this region a linear relationship between l and P_C and the slope contains the factor square root of G_C.

Takayanagi [69] has used a force balance for interpretation of the pull-out test (Equation 4.12):

$$\pi r^2 \sigma = \frac{2\pi r}{\tau_i} \tag{4.12}$$

Where r is the radius of the fibre, σ is the tensile stress and τ_i is the interfacial stress. The ultimate stress is measured and plotted as a function of the immersion length (**Figure 4.69**).

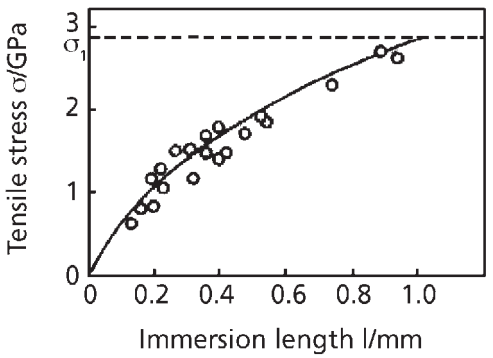

Figure 4.69 Tensile stress *versus* immersion length according to Takayanagi and co-workers [69]

Reproduced with permission from M. Takayanagi, S. Ueta, W-Y. Lei and K. Koga, Polymer Journal, 1987, ***19****, 5, 467*

The immersion length at which the pullout stress equals the breaking strength of the fibre is called the critical length. This value can be used in the following equation.

$$\sigma_f = \frac{2\tau_{if} l_c}{r} \tag{4.13}$$

The τ_{if} is assumed to be the measure of interfacial adhesion.

4.11.2 Peel Tests

Another common static test is stripping of a two ply specimen. Such a specimen consists of rubber-cord-rubber-cord-rubber. The two cord layers are peeled from each other.

In this peel test the amount of rubber between the two fabrics influences the peel strength (**Figure 4.70**). The peel force is calculated as the average force between a displacement of 40 and 140 mm. Not only the measured force but also the so-called rubber coverage is of great importance when evaluating the adhesion. When both sides are covered with rubber after peeling, the adhesive strength was higher than the tear strength of the rubber. When one side is covered with rubber and the other is not, the adhesive strength is lower than the tear strength of rubber.

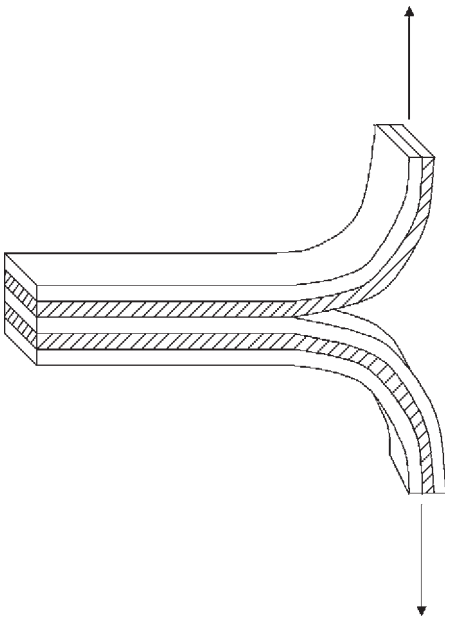

Figure 4.70 Strip test specimen

4.11.3 Surface Analysis

General information regarding techniques for surface analysis of polymers can be found in several textbooks [77, 78]. The techniques most commonly used in the literature [67] for characterisation of polymer systems are briefly explained here.

SEM-Electron Dispersive X-ray Analysis (EDX)

Begnoche [79] has used SEM in combination with EDX to analyse the aramid-epoxy-RFL-rubber system; EDX is an elemental analysis. He reported that the use of backscattered electrons provided contrast between the rubber phase and the RFL phase. To investigate the failure in the epoxy predip, he added TiO_2 in the predip. TiO_2 can easily be

detected by SEM. By the presence of TiO_2 the location of the tear can be observed.

Both Begnoche [79] and Causa [80] have reported that sulfur and zinc diffuse through the RFL-rubber interface and cure the RFL. Causa states that this diffusion takes place in the form of zinc complexes.

SEM was also used by Mahy [81] on the aramid surface after adhesion testing with an epoxy matrix. After pullout of aramid from epoxy it was observed that the surface was smooth: this indicated that the interlocking mechanism in the epoxy-aramid interface plays no significant role. Mahy referred to unpublished results that pointed out that there were also no interpenetrating networks. The remaining mechanism of adhesion in the aramid-epoxy interface would be polar interactions.

X-ray Photoelectron Spectroscopy (XPS)

When a surface is irradiated with soft x-ray photons, electrons from inner shells of the atoms can be ejected with a specific kinetic energy. An XPS spectrum is a plot of the photoelectron intensity *versus* the kinetic energy (or binding energy) of the photoelectrons. No two elements of the periodic table possess the same kinetic energy. For qualitative analysis a so-called wide scan is used, where all kinetic energy ranges are explored. This range is between 0 and 1500 eV. XPS can also be used for higher resolution scans on a shorter range. An atom has in its oxidised state a slightly different kinetic energy, therefore with a high resolution scan oxidised carbon-atoms can be distinguished. The photoelectron intensity is directly proportional to the atomic distribution of photo-emitting atoms, therefore XPS is suitable for quantitative analysis.

The lateral distribution is at best a few micrometers, and the sampling depth is dependent on the mean length of the path the electrons can travel between collisions. By tilting the sample relative to the beam, the sample depth probed can be influenced. Typically it is 3 to 10 nm.

XPS has been used to investigate the aramid-epoxy interface [47, 64, 81] because of the ability of XPS to distinguish between the carbon atoms of aramid and the carbon atoms of the epoxy phase.

Ion Scattering Spectroscopy

Primary ions of inert gasses have a high electron affinity and after collision with a solid surface, they have a high probability of being neutralised. Examples of those primary ions are He^+, Ar^+, Ne^+, Li^+, etc. By measuring the energy distribution of ions scattered by a solid surface, information can be obtained of that surface. There are three forms of ion scattering spectroscopy: low energy, medium energy and high energy. The low and high energy ion

scattering spectroscopy are surface specific techniques. Since inert gasses have such a high probability of being neutralised, only the outermost atomic layer is analysed.

Static Secondary Ion Mass Spectrometry (SSIMS)

In secondary ion mass spectrometry a surface is irradiated by an ion beam. This beam produces ions from a solid surface. These secondary ions are analysed as a function of their mass/electric charge ratio. The lateral resolution can be very high, up to 50 nm. This technique is also regarded as chemical microscopy. By SSIMS, the outermost atomic layer is analysed.

Attenuated Total Reflection Infra red Spectroscopy

For attenuated total reflection infra red (ATR-IR) spectroscopy, the infra red radiation is passed through an infra red transmitting crystal with a high refractive index, allowing the radiation to reflect within the ATR element several times (**Figure 4.71**).

The previously described surface analysis methods and the well-known contact angle technique are summarised in **Table 4.13**.

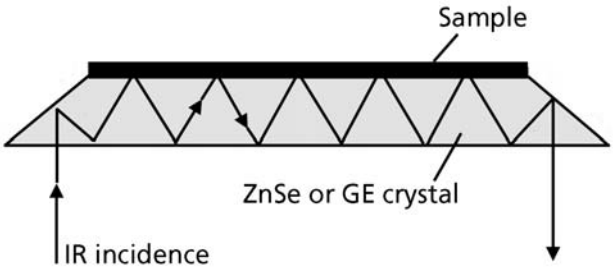

Figure 4.71 Schematic representation of an ATR-IR measurement [82]

Table 4.13. Surface analysis methods

Analytical technique	Aspect on surface	Penetration depth (approximate)
Contact angle	Surface energy and surface chemistry derived there from	0.5 nm or less
XPS	Types of atoms/bonds	0.3 to 10 nm
Low energy light scattering	Composition and chemical structure	Outermost atomic layer
SIMS	Composition and chemical structure	Outermost atomic layer
ATR-IR	Absorption of functional groups	1000-2000 nm

4.12 Fibres in Tyres

Because of the diversity of properties of fibres and their demanding requirements, it is always worthwhile to present the possibilities of the use of fibres in a tabular form (**Table 4.14**). The Table shows a matrix showing the use of fibres in various parts of a tyre.

Table 4.14. Use of fibres in tyres

Tyre type index*	Standard, S, T	Performance, H, V	Ultrahigh performance, W, Y, >300 km/h	Racing	Run flat, H, Z	Ultralight, H, V, Z
Carcass	PET, Rayon	Rayon, PET	Rayon, aramid	Rayon, aramid (rad and cr)	Rayon, Rayon and steel, PET (PAX**)	Rayon, aramid
Belt	Steel	Steel, aramid	Steel, PEN	Aramid	Steel	Aramid
Capply	No	Nylon, aramid	Aramid, Nylon	Aramid, Nylon	Aramid, Nylon	Aramid, Nylon
Chafer		Nylon, aramid	Aramid, Nylon	Aramid	Nylon	Aramid
Bead	Steel	Steel	Steel	Steel, aramid	Steel	Aramid, steel
Ring in PAX inter belt layer bead filler			Aramid pulp/DCF	Aramid pulp/DCF Aramid pulp/DCF	Aramid	

** S, T, H, V, W, Y, Z are the speed rating of tyres*
*** PAX is Michelin's innovation in a new tyre system*
DCF: dipped chopped fibre

References

1. H. Brody, *Synthetic Fibre Materials,* 1st Edition, Longman Scientific & Technical, Essex, UK, 1994.

2. C.F. Cross and E.J. Bevan, inventors; no assignee; GB9676, 1894.

3. W.H. Carothers and D. Wilmington, inventors; E.I. DuPont de Nemours and Company, assignee; US2071253, 1937.

4. P. Schlack, inventors; I.G. Farbenindustrie Aktiengesellschaft, assignee; US2142007, 1938.

5. J.R. Whinfield and J.T. Dickson, inventors; E.I. DuPont de Nemours and Company, assignee; US2465319, 1949.

6. T.I. Bair and P.W. Morgan, inventors; E.I. DuPont de Nemours and Company, assignee; CA928440, 1973.

7. S.L. Kwolek, inventor; E.I. DuPont de Nemours and Company, assignee; FR2010753, 1969.

8. H. Blades and D.E. Hockessin, inventor; E.I. DuPont de Nemours and Company, assignee; DE2219703, 1971.

9. H. Blades and D.E. Hockessin, inventor; E.I. DuPont de Nemours and Company, assignee; DE2219646, 1972.

10. L. Vollbracht, V. Arnheim, J. Teunis and N.L. Giesbeck, inventors; Akzo GmbH, assignee; DE2605531, 1976.

11. P. Smith and P.J. Lemstra, inventors; Stamicarbon B.V. Te Geleen, assignee; NL7900990, 1980.

12. J.W.S. Hearle in *Encyclopedia of Materials: Science and Technology*, Eds., K.H.J. Bushow, R. Cahn, M. Flemings, B. Ilschner, E. Kramer, S. Mahajan and P. Veyssiere, 2001, p.16.

13. D.B. Wootton, *The Application of Textiles in Rubber*, Rapra Technology, Shawbury, Shrewbsury, UK, 2001.

14. T. Takeyama and J. Matsui, *Rubber Chemistry and Technology*, 1969, **42**, 1, 159.

15. G.G. Odian, *Principles of Polymerisation*, 3rd Edition, John Wiley and Sons, Inc., New York, NY, USA, 1991.

16. Indian Rubber Institute, *Rubber Engineering*, McGraw-Hill, New York, NY, USA, 2000, p.907.

17. R.M.V. Pidaparti, *Composite Structures*, 1993, **24**, 4, 291.

18. J.H. Hildebrand in *Structure-Solubility Relationships in Polymers*, Eds., F.W. Harris and R.B. Seymour, 1977, p.1-10.

19. E.E. Walker, *Journal of Applied Chemistry*, 1952, **2**, 470.

20. P.A. Small, *Journal of Applied Chemistry*, 1953, **3**, 71.

21. R.F. Fedors, *Polymer Engineering and Science*, 1974, **14**, 2, 147.

22. K. Mori, *International Polymer Science and Technology*, 1992, **19**, 6, 14.

23. S.S. Voyutskii, *Autohesion and Adhesion of High Polymers*, John Wiley, New York, NY, USA, 1963, p.272.

24. W.H. Charch and D.B. Maney, inventors; EI DuPont de Nemours & Company, assignee; US 2128635, 1938.

25. M. Breznick, J. Banbaji, H. Guttmann and G. Marom, *Polymer Communications*, 1987, **28**, 2, 55.

26. G. Roebroeks and W.H.M. van Dreumel in *High Tech - the Way into the Nineties,* Eds., K. Brunsch, H-D. Gölden and C-M. Herkert, Elsevier, The Netherlands, 1986.

27. M. Takayanagi and T. Katayose, *Journal of Polymer Science Part A: Polymer Chemistry Edition*, 1981, **19**, 2, 1133.

28. W. Hupje in *De Nederlandse Rubber Industrie*, 1970.

29. C. Hepburn and Y.B. Aziz, *International Journal of Adhesion and Adhesives*, 1985, **5**, 3, 153.

30. S.H.O. Egboh and A.K. Mukherjee, *Journal of Applied Polymer Science*, 1992, **44**, 2, 233.

31. T.W.G. Solomons, *Organic Chemistry*, 6th Edition, John Wiley & Sons, Inc., New York, NY, USA, 1996, p.1218.

32. I.L. Finar, *Organic Chemistry, the Fundamental Principles*, 4th Edition, John Wiley, New York, NY, USA, 1963.

33. H. Zimmerman and I. Zimmerman, *Elements of Organic Chemistry*, Glencoe Press, Encino, CA, USA, 1977.

34. D.B. Wootton in *Developments in Adhesives-1*, Ed., W.C. Wake, Applied Science Publishers Ltd., London, UK, 1977, p.181.

35. T.S. Soloman in *Proceedings of the 124th ACS Rubber Division Meeting,* Fall, 1983, Houston, TX, USA, Paper No.57.

36. V.E. Basin, A.A. Berlin and R.V. Uzina, *Soviet Rubber Technology*, 1962, **21,** 9, 12.

37. M.I. Dietrick, *Rubber World*, 1957, **136**, 847.

38. R.P. Lattimer, R.A. Kinsey, R.W. Layer and C.K. Rhee, *Rubber Chemistry and Technology*, 1989, **62**, 1, 107.

39. A. Greth, *Angewandte Chemie*, 1938, **51**, 719.

40. S. van der Meer, *Rubber Chemistry and Technology*, 1945, **18,** 4, 853.

41. M. van Duin and A. Souphanthong, *Rubber Chemistry and Technology*, 1995, **68**, 5, 717.

42. *Handbook of Adhesives*, Ed., I. Skeist, 3rd Edition, Van Nostrand Reinhold, New York, NY, USA, 1990.

43. C.J. Shoaf, inventor; no assignee; US 3307966, 1967.

44. P. Sykes, *A Guidebook to Mechanism in Organic Chemistry*, Wiley, New York, NY, USA, 1965, p.397.

45. T.J. Meyrick and D.B. Wootton, inventors; no assignee; GB 1092908, 1967.

46. A. Garton and J.H. Daly, *Journal of Polymer Science Part A: Chemistry Edition*, 1985, **23**, 4, 1031-1041.

47. J. Mahy, L.W. Jenneskens, L.L.T. Vertommen, P.J. de Lange and O. Grabandt in *1st Internastioanl Congress on Adhesion Science and Technology*, Eds., W.J. van Ooij and H.R. Anderson, Jr., VSP, The Netherlands, 1998.

48. Y. Iyengar, *Journal of Applied Polymer Science*, 1978, **22,** 3, 801.

49. N.K. Porter, *Journal of Coated Fabrics*, 1992, **21**, 4, 230.

50. J.L. Bras and I. Piccini, *Industrial and Engineering Chemistry*, 1951, **43,** 2, 381.

51. W.H. Hupje, *De Tex*, 1970, **29,** 4, 267.

52. A.L. Miller and S.B. Robinson, *Rubber World*, 1957, **137**, 397.

53. R.V. Uzina, I.L. Schmurak, M.S. Dostyan and A.A. Kalinia, *Soviet Rubber Technology*, 1961, **20,** 7, 18.

54. T.S. Solomon, *Rubber Chemistry and Technology*, 1985, **58**, 3, 561.

55. R.T. Murphy, L.M. Baker and R. Reinhardt, Jr., *Industrial and Engineering Chemistry*, 1948, **40,** 12, 2292.

56. T. Tsuji, *Setchaku*, 1964, **8**, 847.

57. H.M. Wenghoefer, *Rubber Chemistry and Technology*, 1974, **47,** 5, 1066.

58. T.S. Solomon, inventor; The Uniroyal Goodrich Tire Company, assignee; CA 1249386A1, 1984.

59. G.E. van Gils and E.F. Kalafus, inventors; The General Tire & Rubber Company, assignee; US 3888805, 1975.

60. ASTM D2138-83, *Test Methods for Rubber Property-Adhesion to Textile Card*, 1983.

61. D.J. Burlett and R.G. Bauer, inventors; The Goodyear Tire & Rubber Company. assignee; EP 0445484A1, 1991.

62. S.C. Sharma, inventor; GenCorp, Inc., assignee; US4680228, 1987.

63. S. Li and D.F.M. Michiels, inventors; Milliken and Company, assignee, US 20030092340, 2003.

64. B. Chabert and G. Nemoz in *High Performance Fibres, Textiles and Composites*. Conference proceedings, 1985, Manchester, UK.

65. G.E. Gillberg-LaForce, inventor; Hoechst Celanese Corp., assignee; US 4794041, 1988.

66. D.D. Dixon and W.M. Smith, Jr., inventors; Air Products and Chemicals, Inc., US 4009304, 1977.

67. L.S. Penn and H. Wang, *Polymers for Advanced Technologies*, 1994, **5**, 12, 809.

68. Y. Wu and G.C. Tesoro, *Journal of Applied Polymer Science*, 1986, **31**, 4, 1041.

69. M. Takayanagi, S. Ueta, W-Y. Lei and K. Koga, *Polymer Journal*, 1987, **19,** 5, 467.

70. M. Takayanagi, T. Kajiyama and T. Katayose, *Journal of Applied Polymer Science*, 1982, **27**, 10, 3903.

71. E.G. Chatzi, S.L. Tidrick and J.L. Koenig, *Journal of Polymer Science Part B: Polymer Physics Edition*, 1988, **26**, 8, 1585.

72. F.P.M. Mercx, *Surface Modification of High-Performance Aramid and Polyethylene Fibres for Improved Adhesive Bonding to Epoxy Resins*, University of Eindhoven, Eindhoven, The Netherlands, 1996. [PhD Thesis]

73. S. Rebouillat, inventor; EI DuPont de Nemours and Company, assignee; US 6045907, 2000.

74. S. Luo, W.J.van Ooij, E. Mader and K. Mai, *Rubber Chemistry and Technology*, 2000, **73**, 1, 121.

75. R.M. D'Sidocky, L.J. Reiter, L.T. Lukich and L.R. Spadone, inventors; The Goodyear Tire & Rubber Company, assignee; US 5985963, 1999.

76. K.R. Jiang and L.S. Penn, *Composite Science and Technology*, 1992, **45**, 2, 89.

77. E. Desimoni and P.G. Zambonin in *Surface Characterisation of Advanced Polymers*, Eds., L. Sabbatini and P.G. Zambonin, VCH, Weinheim, Germany, 1993.

78. D.R. Clarke, S. Suresh and I.M. Ward, *Surface Analysis of Polymers by XPS and Static SIMS*, Cambridge University Press, Cambridge, UK, 1998.

79. B.C. Begnoche and R.L. Keefe, *Rubber Chemistry and Technology*, 1987, **60**, 4, 689.

80. A.G. Causa, *Tyre Reinforcement and Tyre Performance*, ASTM STP 694, ASTM, West Conshohocken, PA, USA, 1979, p.200-238.

81. J. Mahy, L.W. Jenneskens and O. Grabandt, *Composites*, 1994, **25**, 7, 653.

82. *Surface Analysis Methods in Materials Science*, Eds., D.J. O'Connor, B.A. Sexton and B.St.C. Smart, 2nd Edition, Springer Verlag, Berlin, Germany, 2003.

5 Naval and Space Applications of Rubber

C.M. Roland

5.1 Introduction

Nine months before Pearl Harbor, an article describing the use of rubber by the United States Navy stated 'Throughout the extensive network of Naval ships and bases, rubber is playing a vital part in the nation's first line of defense' [1]. Certainly over the ensuing 60-plus years, the military's utilisation of elastomers has increased substantially. Applications range from the sublime – a 900 kg rubber disk for the ejection of torpedoes [2] – to the mundane – ersatz rubber bricks for concealing sensors during Marine reconnaissance missions [3]. This chapter reviews current and potential future uses of rubber for Navy and aerospace applications. For many decades the military and the space program have both fostered development of new technologies, and that is true for elastomers. Longevity is a special concern, Navy ships having a 30 year life cycle (with aircraft carriers designed for 50 years of service life); nevertheless, the applications described herein very often were or are cutting-edge technologies. Although details of military applications are sometimes classified, a more common barrier to information is the proprietary nature of the materials. Since the US government does not manufacture, private companies provide the rubber components and are responsible for much of their development. This limits the descriptions herein to largely a qualitative nature.

5.2 Acoustic Applications

Rubber is very commonly used in various acoustic applications, especially by the Navy, taking advantage of the acoustic impedance match between rubber and water. If two materials have the same acoustic impedance, defined as the product of the mass density of a material and the sound speed, there will be no reflections at their interface [4]. For low loss materials, the sound speed is proportional to the square root of the ratio of the density and the modulus (bulk modulus for longitudinal waves, or shear modulus for shear waves). Since the bulk modulus varies weakly among elastomers, fine-tuning the acoustic impedance of rubber relies mainly on adjusting its density. The acoustic properties of a variety of rubbers of interest to the Navy are available [5], although specific formulations tend to be proprietary. The attenuation

coefficient of rubber is a measure of the loss of intensity of the transmitted wave, the sound amplitude decreasing exponentially with product of the distance travelled and the attenuation coefficient. For longitudinal waves (oscillating in the direction of the sound propagation), this attenuation coefficient is proportional to the ratio of the bulk loss modulus to the bulk storage modulus. For elastomers, the loss tangent for longitudinal strains is usually less than 10^{-3} [1, 6]. Thus, sound waves can be transmitted long distances with minimal loss.

When avoiding detection is the objective, sound waves must be attenuated. This can be accomplished by converting the longitudinal sound waves into shear waves ('mode conversion') [2, 7], since the loss tangent for sheared rubber is of the order of unity. This mode conversion can be achieved in various ways, such as constraining the rubber as a thin film between two rigid surfaces, or by incorporating inclusions such as small glass spheres or gas bubbles. The interfacial rubber in such a confined geometry deforms in a shear (or extensional) mode, which is readily attenuated.

The rubber itself can be formulated to be highly dissipative at the frequencies of interest. Maximum energy dissipation occurs when the viscoelastic response of the material falls into the rubber-glass transition zone at the applied frequency and temperature. For high frequency sound waves, the transition occurs well above the conventional glass transition temperature (T_g). As measured using scanning calorimetry at typical heating rates, T_g corresponds to a deformation time scale of approximately 100 seconds. Since the effective activation energy for local motion in polymers is very large (a 10 °C temperature change can alter the relaxation time by three orders of magnitude [3, 8]), relatively high T_g elastomers are required to obtain a room-temperature rubber-glass transition at acoustic frequencies [4, 5, 9, 10].

Conventional dynamic mechanical testing is often used to predict the material's response to acoustic frequencies, by construction of master curves *versus* reduced frequency [5]. Even filled rubber is linearily viscoelastic for deformations less than 10^{-3} strain amplitude [11]. The strain amplitude of acoustic waves propagating through rubber is typically in the range from 10^{-5} to 10^{-10}. Note that for detection, acoustic signals must be stronger than the ambient noise level. Under typical wind conditions, this corresponds to strain amplitudes equal to about 10^{-14}. The important point is that acoustic properties can be characterised from conventional, small-strain dynamic mechanical measurements.

Diverse methods are used by the Navy for quieting. One example is the rubber coating ('acoustic tiles') on submarines. The rubber's acoustic impedance is designed so that the main echo of impinging sonar is amplified (constructive interference) and directed away from the source. Diffuse echoes and internal noise are attenuated by a combination of the rubber formulation and the geometry of the coating layer. In the past these were blends of natural rubber (NR) with nitrile, polychloroprene (PCR), or (in some former Soviet submarines) 1,2-polybutadiene. Most acoustic tiles today are made from polyurethane (PU) or polyurea.

5.2.1 Sonar Rubber Domes

Although sound enables their detection, it also provides underwater 'vision' to sea vessels. The sonic transducers on Navy surface ships are covered with rubber (**Figure 5.1**), and contained in a steel-reinforced rubber dome. On large ships the dome is located on the bow (forward part of the lower hull) while on smaller vessels it is on the keel (keel refers to the bottom beam running from bow to stern). The purpose of the bow and keel domes is to provide a hydrodynamically smooth surface, to minimise noise from water flow, and to protect the transducer. The latter was exemplified in the terrorist bombing of the *USS Cole* in October 2000. The dome and its transducer survived intact, despite the damage to the ship itself (**Figure 5.2**). The sonar dome must transmit with minimal loss the sound energy, and cannot be disrupted by the flow of seawater. Initially domes were made of steel but these had poor sound transmission, were susceptible to corrosion and marine fouling (from barnacles, sea weed, slime-producing bacteria, etc.), and required internal supports, which obstructed the sound. The first rubber sonar dome was installed in 1965, with actual production beginning in 1972.

Figure 5.1 Sonar rubber bow dome

Figure 5.2 The guided missile destroyer *USS Cole* being returned to the United States after a terrorist attack in Yemen in October 2000. Despite the 150 m^2 gash in the port side of the hull (upper photograph), as well as the jostling when the ship was mounted on a salvage transport vessel, the bow dome (seen in lower photograph hanging off the edge of the transport) was still functional. After repairs that included replacement of 550 tonnes of exterior steel plating, the *Cole* returned to sea duty 18 months later

Sonar bow domes (**Figure 5.3**) are the largest moulded rubber articles in the world. They weigh 8,600 kg, are 11 m long, 6.4 m wide, and stand almost 2.5 m high. The rubber wall thickness varies up to a maximum of 20 cm. The construction involves manual lay-up of multiple steel-cord reinforced polychloroprene plies. The steel cords provide structural rigidity. To avoid interference with acoustic performance, the spacing of the cords must be less than the wavelength of sound (e.g., 1.5 m at 1 kHz). The rubber itself has minimal absorption over the sonar frequencies. The dome is fabricated on an open (one-sided) mould and vulcanised in a large autoclave. The bow dome is inflated with approximately 95,000 litres of water, to an internal pressure of 240 kPa. Its location below the baseline of the ship minimises hydrodynamic resistance.

Figure 5.3 Rubber sonar dome assembly mounted to bow of ship

Since their introduction, various improvements to the design of rubber sonar domes have been made, greatly increasing the expected lifetime. Problems with water migration and consequent wire corrosion were corrected by blocking the migration pathways in the wire. Problems with wire fatigue have been addressed by identifying cracks using X-ray radiography of the high stress regions. Such inspections have enabled targeted dome replacement, eliminating at-sea failures. Some sonar domes have been in continuous service for over twenty years.

Recently, a rubber and plastic laminate dome (**Figure 5.4**) has been developed to replace the steel-cord reinforced keel dome. A prototype composite keel dome has been in sea trials since 1997 on a destroyer surface ship and production for other ships has begun. Composite domes using fiberglass and polychloroprene have been used on submarines for over two decades.

5.2.2 Active Sonar

Another acoustic application of rubber is the use of active sonar for detection of submarines and surface ships. Advances in quieting of naval vessels and the use of inherently quiet diesel electric submarines, requires greater detection capability than

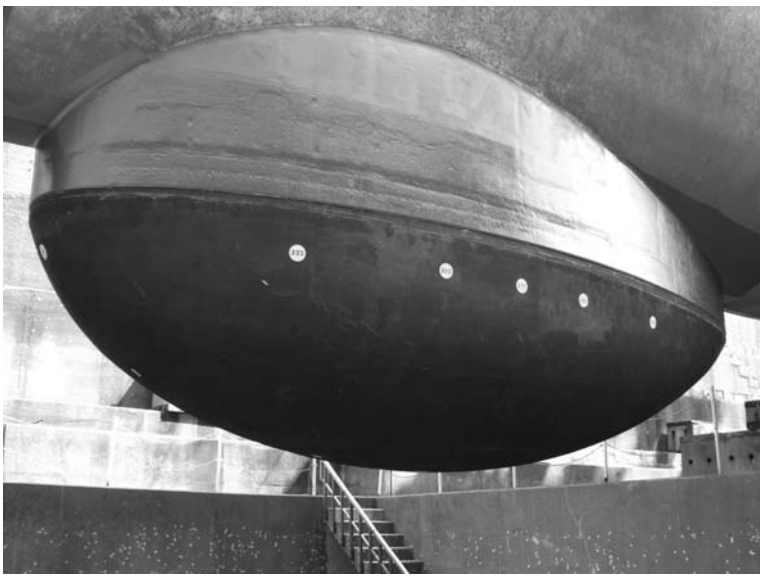

Figure 5.4 Composite keel dome composed of two resin-impregnated fibreglass outer layers and a soft rubber core. The geometry of the structure is tuned to be acoustically transparent over a limited frequency range

passive sonar. Most active sonar relies on low frequencies (100-500 Hz) because the attenuation coefficient for sound waves is inversely proportional to the wavelength, and thus, active sonar can provide detection over many kilometers. The actual range of course depends on the size of the target, as well as sea state, temperature, and depth since these influence the dispersion and absorption of sound waves by the water. Of course, the longer wavelength reduces the resolution, resulting in poorer discrimination among undersea objects. Although a ship using active sonar reveals its location, the improved detection capabilities, especially in shallow water, makes it an invaluable anti-submarine warfare development [12]. More recently, high frequency sonar (>10 kHz) has been developed, which yields greater bearing resolution than conventional medium frequency systems. This provides better discrimination among undersea targets, bottom and surface echoes, and marine life, which can be crucial in shallow water operation. The higher absorption of high frequencies also facilitates undetected operation.

On surface ships, active sonar transducers are typically operated 'off-board', towed behind the vessel, while submarines employ both active and passive arrays mounted to the bow, keel and fins. Since a high sound level yields louder return echoes, long-range active sonar uses high sound levels. The volume can exceed 200 decibels at the source (right up to the point of cavitation), raising concerns about the possibility of hearing loss in marine animals [13-15]. Elastomers are used herein as an outer casing on the transducer, functioning analogously to the sonar domes on ships. The amount of acoustic information obtained using active sonar is enormous. Detection and classification of submarines in the complex acoustic environment of shallow water requires sophisticated mathematical algorithms for processing the data. The acoustic properties of the rubber must be known to a high degree of accuracy so that the effect of the rubber on the transmitted sound can be corrected for. For low frequencies, for which the wavelengths are on the order of the test chamber, characterisation of acoustic properties of rubber can be complex [16].

5.2.3 Insulation

Sound is a form of mechanical energy and similar to acoustic applications, elastomers are used for vibration damping, such as in shock and motor mounts. Throughout the ship rubber is used for acoustic and thermal insulation. For example, PU rubber blocks are positioned around the ship reactor for insulation, while foam rubber is placed on submarine walls to avoid moisture condensation. Decoupling tiles of rubber are located behind the ship bulk head for quieting of shipboard machinery. The thrust reducer on submarines (**Figure 5.5**), which decouples the hull from propeller vibrations, uses NR sandwiched between steel and polyethylene (PE) rings. Elastomeric bearings are used in the propeller shafts of the V-22 Osprey tilt-rotor aircraft.

Figure 5.5 Thrust reducer used to decouple the submarine propeller shaft. The natural rubber is sandwiched between the steel ring and an outer layer of polyethylene

5.3 Solid Rocket Propellants

Rocket propellants fall into two groups, liquid propellants, in which the fuel and oxidiser are stored separately, then mixed to effect combustion, and solid propellants, which rely on premixed ingredients residing in a casing, which also serves as the combustion chamber when the propellant is ignited. Although liquid propellants offer several important advantages (they yield substantially greater thrust and their combustion can be throttled or even halted and restarted), the storage requirements and handling complexity largely rule out their use for military firepower. The first rockets (dating to the first millennium AD) used solid propellants - a Chinese variation on black powder (potassium nitrate, charcoal and sulfur). The rockets used in the War of 1812 (and referred to in the US national anthem) were of very similar design. The age of modern solid propellants began in the 1950s with the use of synthetic polymers as a binder and subsidiary fuel. This enabled moulding of the propellant. The other significant development at the time was the use of aluminum powder as fuel, which greatly increased the obtainable thrust.

The first solid propellant ballistic missile, which used an elastomeric binder, was the US Navy Polaris, operational in 1960. It was launched from a submarine and carried a nuclear warhead. Presently both the US and the UK deploy the Trident intercontinental ballistic missile (ICBM). Trident missiles have three-stages, each using solid propellant fuel.

The Air Force's Minuteman is a solid propellant ICBM based in underground silos. Not having the complex storage and filling requirements of liquid propellant missiles, the Minuteman could be encased in thick concrete for protection from nuclear attack. Some Minuteman ICBM remain in service today, along with the MX (or Peacekeeper) missile. The Peacekeeper uses three stages of solid propellant, along with a post-boost liquid fuel motor.

Many spacecraft launches involve both propellant types – solid propellant boosters attached to liquid-propelled rockets. The Scout rocket (**Figure 5.6**), in use from 1960 through to 1994 to launch commercial and military satellites, was the only launch vehicle fuelled entirely by solid propellant. Its replacement is the Pegasus, an air-launched solid-propellant rocket. The Delta series of rockets derived from the Thor ballistic missile began in 1960 and continue presently as a civilian and government launcher. The Delta

Figure 5.6 Launch of Scout, the only United States' launch vehicle fueled exclusively with solid propellants

II and III versions (**Figure 5.7**) can have up to nine solid rocket motors strapped onto the first stage, whose main engine is liquid fuelled as is the second stage. Two-stage Delta II rockets can launch payloads into low Earth orbit, while an optional third-stage, powered by solid propellant, is used for geosynchronous transfer orbit or deep space exploration. The newer Delta IV, which uses a liquid hydrogen/liquid oxygen fuel similar to the space shuttle, can launch substantially heavier payloads.

A generic recipe for military propellants is given in **Table 5.1**. The binder is a rubbery polymer, such as polysulfide, polyvinyl chloride (PVC), PU, plasticised cellulose, polyisobutylene, polyvinylacetate, and carboxyl- or hydroxyl-terminated polybutadiene. While also serving as fuel, the function of the binder is to cohere the propellant into a thixotropic, low-viscosity paste that can be moulded into the desired shape. This

Figure 5.7 Delta III rocket with nine solid rocket motors strapped around the first stage

Table 5.1. Representative solid rocket propellant formulation		
Function	**Examples**	**Typical mass (%)**
Oxidiser	Ammonium perchlorate, ammonium nitrate, nitronium perchlorate, potassium perchlorate, cyclotrimethylene trinitramine, cyclotetramethylene tetranitramine	70
Fuel	Aluminum, magnesium, beryllium, boron	14
Binder	Elastomer	11
Plasticiser	Dioctyl adipate, isodecyl pelargonete, dioctyl phthalate, dioctyl azelate	3
Catalyst	Ferric oxide, butyl ferrocene, dibutyl ferrocene, lithium fluoride	<1
Curing agent	Isocyanate, epoxy	1
Stabiliser	Aluminum, zirconium, zirconium carbide	<1

is followed by curing, which, for hydroxyl-terminated polybutadienes, is usually accomplished with isocyanates. The mechanical integrity of the cured propellant is important to its proper functioning. The propellant structure must withstand the pressure gradients developing within a few milliseconds of ignition. The triaxial tension exerted on the material cannot cause vacuole formation, which requires both adhesion of the polymer to the filler and good cohesive strength in the elastomer itself [17]. The shelf-life of a cured propellant must be many years, requiring resistance of the polymer to air oxidation and hydrolysis. The service life upon ignition is minutes or less, with the soot-free combustion of the polymer contributing to thrust generation.

5.4 Blast Mitigative Coatings

The rise of terrorism has led to efforts to develop methods of alleviating the effect of bomb explosions. A role for elastomers is their use as coatings to minimise the damage from the blast to the underlying structure and to personnel. Towards this end, the US military has been using polyurea spray-on elastomeric coatings on building and vehicles. The polyureas are formed from the reaction of isocyanates, based on diphenylmethane diisocyanate (MDI), with polyetheramines. The reaction is fast with gel times significantly less than one minute. This means the reaction proceeds largely independently of ambient temperature and humidity, facilitating application of the coating under diverse conditions. The modulus of polyurea coatings can be tailored to span the range from moderately soft to very hard rubbers (e.g., from Shore A ~ 60 to Shore D ~ 75) [18]. They are very tough materials due to the plethora of intermolecular hydrogen bonds. Polyurea coatings have been used commercially since the early 1990s, their processing and property advantages leading to widespread use notwithstanding the higher cost.

Applications include concrete coatings and repair of roofs and parking decks, as well as liners for storage tanks, freight ships, and truck beds. Some of the more prominent uses include the Boston tunnel project, the Inchon, Korea airport, and the San Mateo, CA, bridge [19].

The US Air Force has a programme to coat the walls of buildings, including the Pentagon, with a spray-on elastomeric coating. The coating adheres to the structure, (e.g., cinder block, concrete foundation, or wood beams) and must remain intact during an explosion. The polyurea coating mitigates the effect of the blast. For example, on a lightweight structure (similar to a mobile home), 100 kg of trinitrotoluene (TNT) (typical of a car bomb) would cause failure of the building if detonated within 40 metres [20]. This standoff distance can be reduced to 24 metres with a 3 mm thick polyurea coating on the inner walls. A second, very important function of the coating is to minimise fragmentation, that is, objects propelled by the blast pressure (see **Figure 5.8**). Such flying debris can have speeds of hundreds of metres per second and are a leading cause of injury from terrorist bombings. Although the exterior walls may be broken by an explosion, the fragments are contained by the coating, which can reduce injuries to the building occupants.

The coating material being used by the Air Force is a commercial polyurea, similar to that used for truck bed-liners. It is a high modulus (> 100 MPa) and low elongation (< 90%) material [21]. The Air Force's material selection focused on cost and ease of application.

Figure 5.8 High speed photograph of building being deformed by pressure from a bomb explosion

Air Force photograph

Subsequent to the Air Force initiative, the Navy undertook a programme to explore the use of polyurea coatings to mitigate the damage to their 'High Mobility Multipurpose Wheeled Vehicle' (HMMWV) from fragmenting explosives. These coatings are also polyureas but considerably more compliant (modulus ~ 10 MPa with elongations exceeding 600%). They are sprayed onto the outer surface of armor plate, which is used to up-armor the aluminum HMMWV structure (**Figure 5.9**). A substantial number of the US Marine Corp's HMMWV currently in Iraq have this polyurea coating.

The US Office of Naval Research has an on-going S&T effort to develop coatings for various applications, with objectives of both blast and ballistic (bullet) protection. The principal material remains polyurea. It is remarkable that a single material can afford both ballistic and blast protection, given the wide range of pressures and deformation frequencies. The origin of the blast mitigation from rubber coatings is presently unknown, but it is believed that a variety of mechanisms contribute. Although lacking the spray-on capability of polyureas, high molecular mass polymers can also function in this application. **Figure 5.10** depicts the response of an unfilled polybutadiene coating on armor plate to impingement with a 0.50 caliber (i.e., 12.7 mm diameter) slug traveling in excess of 820 m/s. Such experiments are used to simulate the fragments from the shell of an exploding bomb.

5.5 Aircraft Tyres

Aircraft tyres differ from automotive passenger tyres in several respects. About 85% of aircraft tyres are bias ply, rather than radial design [22]. While the first bias aircraft tyres were constructed about a century ago, radial tyres were not used on airplanes until

Figure 5.9 Military vehicles with polyurea-coated steel plates on sides of HHMWV and on sides and back of truck

Photograph courtesy of USMC

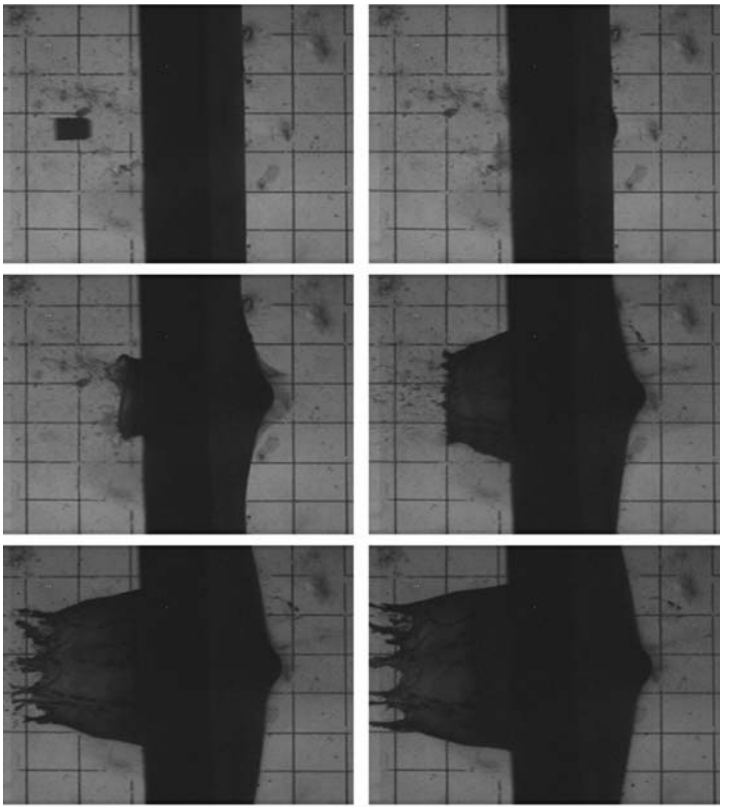

Figure 5.10 Fragment-simulating 0.50 caliber projectile striking steel armour plate coated with 1,4-polybutadiene rubber. Projectile, shot from a rifled Mann barrel and traveling at 3 km/h, makes initial contact with the rubber-coated side and dents but does not penetrate the high-hard steel plate. The grid lines are spaced 25 mm apart

1981. Because of the high temperatures attained during takeoff and landing (exceeding 100 °C), aircraft tyres are based primarily on NR. Tyres on large aircraft are frequently filled with nitrogen.

Although military aircraft tyres perform a similar function to their commercial counterparts, the demands imposed on the former can be more severe. Tyres for fighter jets such as the F-16 and F/A-18 are speed rated for over 400 km/h. The inflation pressures can be as high as 2 MPa. Fighter aircraft, of course, are smaller and faster than bombers. Jet fighters usually have two main wheels and a single- or double-wheel at the nose, the latter being steerable. The main tyres are significantly larger - on the F/A-18, for example, they are 76 x 29 cm *versus* 56 x 16.8 cm for the nose tyres (these numbers refer to the diameter and section width of the tyre, respectively). The tyre size is predicated on the

weight of the aircraft. When the gross weight of the F-16 was increased by almost a factor of two, a significantly larger tyre size had to be adopted.

In general, tyre wear is due to frictional forces, arising from sliding at the road-tread interface. In automotive tyres, cornering manoeuvers, and to a lesser extent braking, are the primary causes of tread wear [23]. A similar situation exists for aircraft using land-based runways – about 70% of tread wear is ascribed to braking. However, much of this wear does not transpire when the tyre makes contact with the runway. Wear depends very strongly on the alignment of the tyre with the direction of the airplane. Crosswinds prevent the tyres from simply rolling along the runway. Outside the contact patch, the tyre is severely distorted (on large aircraft, landing speeds can reach 425 km per hour with an acceleration of 20 G). The combination of crosswinds on rollout and the steering forces exerted during taxiing accounts for 90 to 95% of the total tread wear. Typically, the tyres on a bomber, such as the B-52, are replaced every 30 to 40 flights, depending on conditions. During present combat operations in Iraq, two or three of the tyres on a B-52 get changed each day (see **Figure 5.11**). Each tyre weighs 230 kg and stands 1.2 m high.

The situation for aircraft carrier-based fighter aircraft is worse, with the tyre treads wearing out after only two or three flights. Ironically, this reduced lifetime has little to do with the extreme acceleration of launching or the rapid deceleration of carrier

Figure 5.11 Military personnel mount a tyre on a B-52H Stratofortress. The replaced tyre is deflated after its removal. The change-over takes about 20 minutes

US Air Force photograph by Tech. Sgt. Jason Tudor

landings; for example, during launch, an F/A-18 Hornet attains a speed of 265 km/h within a space of 75 m. The acceleration relies on steam-assisted catapulting, while landings utilise arresting wires rather than relying on tyre friction. Thus, the contribution to tread wear is minimal for both cases. An additional factor is that carrier launches and landings take place with the ship turned into the wind, which adds (or subtracts) to the relative speed, putting less demand on the tyres.

The high wear rate of carrier-based aircraft tyres is due to the maneuvering on the deck required to position the plane (**Figure 5.12**). Rollout and alignment prior to launch and straightening after arrestment impose severe cornering forces on the tyres. The scuffing of the rubber on the non-skid deck governs the tread lifetime. This wear rate depends on the nature of the deck surface, which are always high in friction to minimise skidding. A worst-case example was during the first war in the Persian Gulf. Makeshift plates were used for a landing deck, with a surface so abrasive that tyre treads wore out after only four to five landing cycles.

Figure 5.12 Nimitz-class aircraft carrier, the world's largest warship. Manoeuvering required to position planes for launch is responsible for much of the tread wear

In aircraft used at high speed for extended durations, aerodynamic friction on the skin creates heat, which radiates to the tyres. The tyres themselves can be given a silver coating to reflect the heat. The heating problem manifests itself with blow-out of the tyres upon landing.

The tyres for the space shuttle are not especially large, 81 x 22 cm for the nose and 113 x 41 cm (diameter x width) for the main tyres, even though the shuttle weighs as much as 110,000 kg on landing. This means the main landing tyres support about three times the load of a tyre on a Boeing 747. The space shuttle tyres are inflated with over 2 MPa of nitrogen. The main tyres on the shuttle are used only once, while the nose tyres are used for two landings.

5.6 Airships

There are two types of airships: Blimps are non-rigid airships lacking any internal support structure. They rely on the pressure of the internal gas, enclosed in a rubber-coated fabric, for support and to provide lift. The gas is commonly helium at pressures exceeding ambient. Hydrogen, which provides about 10% more buoyancy (lifting capacity ~1.1 kg/m^3 *versus* 1.02 kg/m^3 for He), still finds limited use, notwithstanding its flammability (it has an energy content threefold higher than gasoline). Rigid airships (e.g., 'Zeppelins') have rigid internal frames and are largely obsolete. The main component of an airship is the envelope, which contains the pressurising gas. On the Goodyear blimps, which were used by the military during World War II, this envelope is a PCR-impregnated polyester fabric. Because of the large gas volume (about 7 million litres) and low pressure, gas leaks are very slow. For this reason the elastomer selection is guided by manufacturing ease and mechanical durability, as well as by the requirement of low permeability. In 1994 tests by the British Ministry of Defence determined after hundreds of bullet punctures of an airship envelope, the craft remained inflated and aloft for several hours.

The US military employed blimps during the last century (**Figure 5.13**) along the North American coasts, for enemy submarine reconnaissance and as 'radar pickets' to detect incoming aircraft. They also served as convoy escorts to watch for surfacing submarines. None of the ~89,000 ships escorted by blimps during WWII were lost to enemy fire. With the development of satellites, these blimps became obsolete and were decommissioned in 1962. Since 1980, the Air Force has used 60 m long, tethered blimps ('Tethered Aerostat Radar System') flying at 4.5 km over the US - Mexican border to watch for low-flying aircraft used by smugglers.

In 2002 the US Department of Defense began development of the 'High Altitude Airship' – an unmanned, solar-powered blimp for reconnaissance (using both cameras and radar) to detect low-flying missiles, and as a communication relay that could serve as an alternative to low Earth orbit communication satellites. Flying at an altitude of

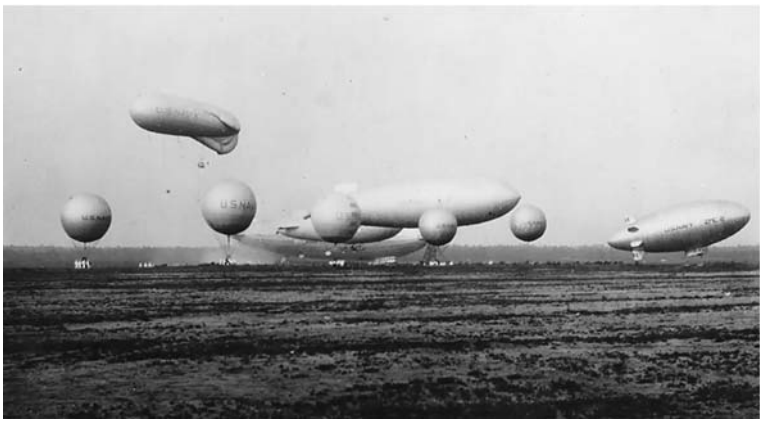

Figure 5.13 Demonstration (*circa* 1930) of several Naval airships, including five spherical balloons, a kite balloon (upper craft at left), the USS Los Angeles in the middle distance, two J-class non-rigid blimps in the center, and a ZMC-2, a rigid metal-skinned blimp, at right

Photograph courtesy of US Naval Historical Center

20 km, the blimp would be beyond the range of ground-launched antiaircraft weapons. Prototypes will be 150 m long with a volume of 150 million litres (25 times larger than the Goodyear blimp), and carry a 1800 kg payload. One technical barrier is achieving sufficient buoyancy in the stratosphere - this may require new technologies for the envelope. Since the internal gas will expand as the blimp rises, it will initially be filled with air, which is replaced by pressurised helium gas as higher altitudes are reached. Initially flight tests are contemplated in 2008.

Very recently, the US Department of Defense initiated a research programme to develop large airships ('WALRUS') for rapid strategic airlifts (**Figure 5.14**). The intention is to carry enormous payloads of transport cargo and troops over very long distances (10,000 km) without refuelling. Current plans call for construction of a 30 tonne prototype by 2008. The air-buoyant blimp would have to be weather-independent and require only minimal ground assistance in order to meet the goal of deploying troops worldwide within a couple of days.

An even more ambitious application of airship technology is the 'space blimp' (**Figure 5.15**), a mile-long airship intended to carry payloads to and from low Earth orbit (350 – 1400 km high). The space blimp would have to be very light, with a high surface to volume ratio and very thin walls. Consequently, it could not survive atmospheric pressures, so a conventional airship must be used to lift the payload up to ~35 km above the Earth's surface (this is the highest altitude achievable with conventional air buoyancy).

Figure 5.14 Artist's conception of the giant blimp WALRUS intended for rapid strategic airlifts

Figure 5.15 Prototype space blimp, 53 m in length, being float tested

Photograph courtesy of J.R. Aerospace; www.jpaerospace.com

The airship then docks at a suborbital space station, where the payload is transferred to the space blimp. The space blimp itself would originally have been constructed at this same space station. An ion engine, which accelerates a beam of charged particles for thrust, would horizontally propel the space blimp. Even in the outer periphery of the Earth's atmosphere, the helium-filled structure could 'float' upwards to about 60 km, with the ion engine then used to achieve low Earth orbit. Reaching orbital velocity would

require several days. The putative advantage of the space blimp is economic, i.e., a low cost per payload weight. It could be configured for both cargo and passengers and use a three-member crew.

5.7 Inflatable Seacraft

5.7.1 Combat Rubber Raiding Craft

An important military use of rubber is the Combat Rubber Raiding Craft (CRRC), a 4.6 m long boat made of an aramid-reinforced blend of chlorosulfonated polyethylene and polychloroprene (**Figure 5.16**). The CRRC is used by the Marines and Navy SEALs (Sea-Air-Land Team) to reach the shoreline when dropped in littoral waters. The CRRC is usually preloaded with outboard motors, fuel, weapons and other equipment, then lowered from a helicopter while fully-inflated. It is then held in place by a cargo hook, as troops descend *via* a rope. The entire operation can be accomplished in less than one minute [24]. The CRRC can also be launched from the air while bound on top of a wooden platform with an attached parachute, and be subsurface or deck-launched from submarines. Sometimes referred to as the Zodiac, in reference to the manufacturer, the CRRC is also used by law enforcement and civilian fire and rescue authorities.

Figure 5.16 Combat Rubber Raiding Craft ferrying military personnel between ship and shore

5.7.2 Hovercraft

An extension of the rubber inflatable concept is the military hovercraft, known as the Landing Craft Air Cushion (LCAC) or 'boat that flies' (**Figure 5.17**). First deployed in 1987 by the US Navy, these hovercraft are presently used by the armed services of many countries. LCAC is an amphibious vehicle which uses two 3 MW (4000 HP) gas turbine engines to drive four centrifugal fans. The fans provide lift, allowing the craft to float on an air cushion above the ground or water. No part of the hull penetrates the water. This greatly reduces friction and allows the vehicle to travel independently of terrain, enabling transport over water (independently of tides), rock, sand, and so on, and to clear obstacles up to 1.2 metres high. LCAC can access more than 80% of the world's coastlines. A second identical pair of engines propel the craft forward at speeds up to 50 knots (93 km/h). A hovercraft can carry a payload exceeding 50 tons (45,000 kg), along with 30 personnel. LCAC consume about 3,800 litres of fuel per hour and have a 19,000 litre fuel tank - this yields a range of approximately 400 km fully loaded. Their stopping distance exceeds 500 m.

Elastomers are used in two key areas of hovercraft: A NR/Nylon fabric forms a skirt, which hangs from the sides in the form of conical flaps to guide the downward airflow. In addition, a polychloroprene/Nylon fabric forms an inflated tube along the periphery. This serves to cushion the craft and as an auxiliary floatation device.

Figure 5.17 Landing Craft Air Cushion propelled by two four-bladed 3.7 m diameter, variable-pitch propellers. The polychloroprene/Nylon tube can be seen at the water interface

The primary military use of hovercraft is for ship to sea transport, shuttling troops and equipment, and for traversing beaches. They are especially effective for mine sweeping in shallow waters and have also been used for humanitarian relief. LCAC played an important role in the recent 'Iraqi Freedom' military campaign.

Presently the US Navy is collaborating in the development of an advanced hovercraft of Russian design, the EKIP (Russian acronym for Ecology and Progress). This vehicle will support a 100 ton payload, at speeds up to 700 km/h in air and 160 km/h while skimming the surface. One intended non-military application is fighting forest fires.

5.8 Rubber Sealants

The ability of an elastomer to store energy makes it an ideal material for sealing purposes. The stored energy causes retraction of the rubber after completion of the duty cycle. O-rings, gaskets, and other sealants are widely used in the military and aerospace industries. Most of these products are supplied by private companies who insist on the confidentiality of the formulations, and thus, generally, only the base polymer can be identified with the other ingredients being proprietary.

Polysulfide rubber is a common gasket material and caulk on military aircraft (for floorboards, windscreens, canopies, and so on) and rockets (e.g., at nozzle to case joints), and as grout on aircraft carrier runways. These seals require periodic replacement. However, many of the polysulfide materials release volatile organic compounds during cure. They also contain chromium, so that their disposal is treated as hazardous waste. For these reasons polysulfides are being replaced with more benign materials, for example with polytetraflouroethylene foam or adhesive tape.

More advanced sealants are based on polyphosphazene fluoroelastomers [25]. Originally developed by the Firestone Tyre & Rubber Co., for the US Army, polyphosphazene elastomers have a phosphorous-nitrogen repeat unit, [NP(OR)(OR´)], with various organic constituents yielding different properties. In polyphosphazene fluoroelastomers, the pendant moiety is OCH_2CF_3 or other fluoroalkoxy groups. These materials have a wide service range (minus 65 to 175 °C), being used in both aerospace and military applications. The good fuel and oil resistance of polyphosphazene fluoroelastomer has led to their use for O-rings and diaphragms in jet engines. They are also used in vibration isolation due to their large, broadband damping properties.

When the constituent is an aryloxy group, rather than a fluoroalkoxy, the resulting elastomer is flame-resistant and produces low smoke upon burning. Polyaryloxyphophazenes have been used for wire and cable insulation and insulating foams, although cost is a barrier to more widespread usage [25]. Work has been done to develop blends of polyaryloxyphophazenes with PU as flame-retardant materials for use on aircraft. The most infamous use of rubber in aerospace applications was the O-ring

in the *Challenger* Space Shuttle [26]. In 1986 during its tenth mission, the *Challenger* exploded 73 seconds after launch due to a leak in the right solid rocket booster (SRB), which ignited the hydrogen tank. The leak was caused by failure of an O-ring to seal the gap between the two lower steel sections of the SRB. The joint between the sections contained two 11 m O-rings (two for redundancy), each 7 mm in diameter. The O-ring material was a (proprietary) 90-durometer fluoroelastomer, coated with a zinc chromate putty to protect the rubber from the hot exhaust gases. It was known that the sealing capabilities of the O-ring were compromised by low temperatures. There was no data for performance below 12 °C and at this temperature the predicted failure rate of the seals was 33% [27]. Nevertheless, 12 °C was recommended as the lower temperature limit for launching. At the time of the shuttle's launch, the ambient temperature was 22 °C, with that at the SRB joint estimated to be -2 ± 3 °C. At this low temperature, the rubber lacked the resilience necessary to follow the opening in the gap between the tang and cleavis joint. Hot gases escaped and ultimately led to the explosion of the shuttle. For subsequent missions, the same fluoroelastomer was used, but in conjunction with heaters to provide temperature control.

5.9 Miscellaneous Applications

5.9.1 Rubber Bullets

An offbeat military application of rubber is the use of rubber bullets as non-lethal weapons. Peace-keeping missions involving crowd control, as well as military prison duty, often require the use of non-deadly force. After the September 11, 2001 terrorist attacks, the US military stock-piled large quantities of rubber bullets. In military parlance, the function of these and other non-lethal weaponry is 'to incapacitate personnel and material, while minimising fatalities, permanent injuries to personnel, and undesired damage to property and the environment' [28]. Civilian police and security services employ rubber-coated metal bullets, plastic (e.g., PVC or polymethyl methacrylate) bullets, and beanbags filled with lead pellets for riot control and personnel protection. However, rubber bullets generally cause less injury than other nonlethal rounds. The misuse of nonlethal weaponry is a paramount legal issue [29]. Rifles, grenades and a variant on the claymore mine are used by the military to spray nonlethal rubber pellets. The polymers used in various rubber bullets include ethylene-propylene-diene (EPDM), polybutadiene, natural and synthetic polyisoprene, styrene-butadiene copolymer, butyl rubber, and various blends thereof [30-32]. The elastomer is usually highly filled with carbon black, clay, calcium carbonate, or metallic fillers such as copper or iron.

5.9.2 Intrusion Barriers

Marine security zones are demarcated by barriers to prevent unauthorised entry. One method used by the US Navy against intrusion by small craft is to string a cable across the entryway. Typically the cable is steel encased in rubber connecting cables. The line is anchored to both the sea floor and the shore, with buoyancy maintained by foam-filled structures attached across its length. The latter can be brightly coloured to enhance visibility. A 90 m EPDM/steel cable assembly has been operation at a Naval base in Norfolk, VA, since 2002.

5.9.3 Elastomeric Torpedo Launcher

Rubber can function very effectively as an energy storage device (mechanical capacitor) due to its ability to store and quickly return a large energy density. This feature of rubber is exploited in commercial applications, for example the propulsion mechanism of aerosol containers [33, 34] and for intravenous drug delivery. Other ideas, such as regenerative braking systems for automobiles [35] and pressurised systems for carbonated beverage containers, were technically sound but failed due to other factors. In a propulsion device the stored energy is converted to the kinetic energy of a projectile, with the performance dependent on the amount of stored energy. Although this is proportional to the modulus of the material, even soft elastomers can yield large energy densities due to their high elongation. Moreover, this energy can be recovered very rapidly.

Although an internal propulsion mechanism takes over after launching, the torpedo must be ejected from the submarine. This requires that an exit velocity of 50 km/h be reached in one second – this is about 3 G acceleration (the Mark 48 torpedo, for example, weighs 1600 kg). Conventional torpedo launchers employ ram pumps or 1.5 MW (2000 HP) air turbine pumps, which rely on pressurised air for ejection. These systems weigh over 20,000 kg, cost millions of dollars, and take up space inside the pressure hull. The advantages of an elastomeric ejection system include a reduction in weight, cost, and complexity, as well as superior acoustic properties. Another benefit is that the elastomeric device can be situated in the seawater, between the pressure and outer hulls.

One concept for the torpedo ejection system is illustrated in **Figure 5.18**. A small (approximately 50 kw) pump inflates the two metre diameter disk, which comprises one or more rubber plies, having with a total thickness of about 20 cm. The rubber mass is about 1,400 kg. Although an optimal strain to volume ratio would be achieved using a sphere, a disk geometry avoids the potential for buckling and consequent noise. A disk geometry also provides more flexibility in design and arrangement within the submarine.

The elastomeric ejection system must function independently of the time span between inflation and launch, and survive at least 1000 cycles (which assumes a 15 year

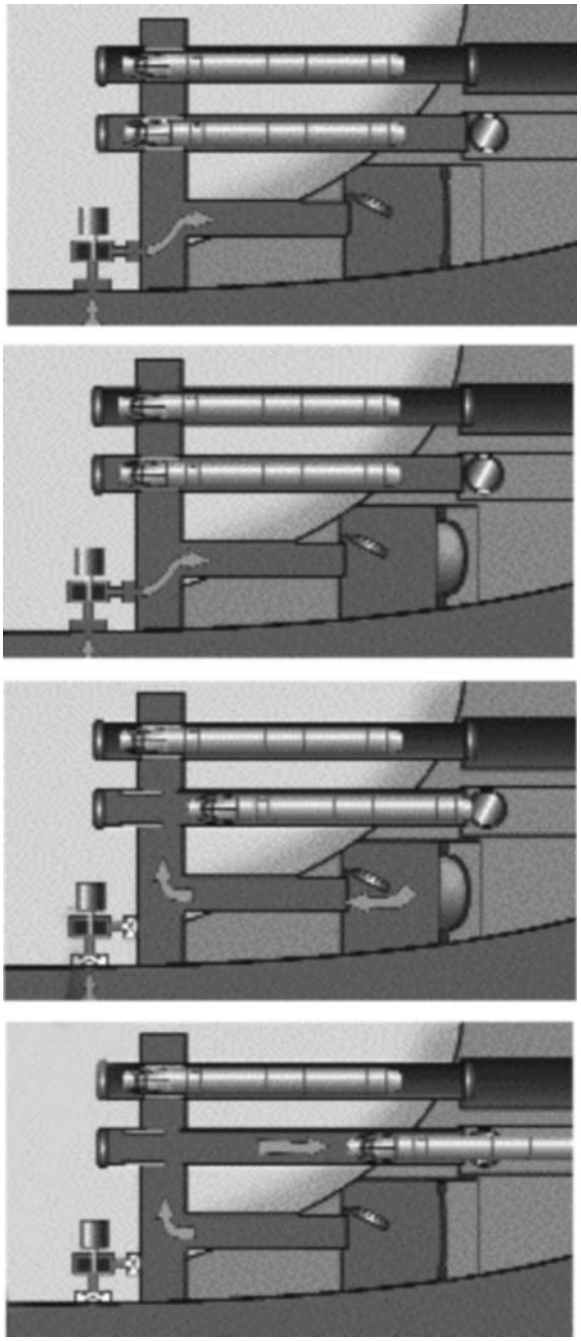

Figure 5.18 Schematic depiction of elastomeric ejection system. From top to bottom: Pump inflates rubber disk, which retracts when the slide valve is opened, accelerating torpedo from shutterway

lifetime). The criteria governing the rubber include high elastic energy, minimal creep and hysteresis, and sufficient fatigue life. Testing of full-scale prototypes indicated that the outer circumference of the disk was the locus of failure. This is due to the presence of planar extension mode of deformation at the periphery, while toward the center the rubber is in a state of biaxial extension [36].

The material for the elastomeric launcher is natural rubber, deproteinised to minimise water absorption [37, 38], with a semi-EV cure system [2, 39]. A small recharge pump inflates the disk with water drawn from the ocean. A biaxial strain of about 100% is attained in the rubber, which yields 1.8 MW (2,400 HP). Opening of a slide valve collapses the rubber disk, forcing water into the torpedo tube to effect the launching. Currently the elastomeric ejection system is under consideration for installation in future submarines [40].

5.9.4 Mobile Offshore Base

Another potential future naval use of rubber is in the Mobil Offshore Base (MOB). MOB, or 'artificial beach', would be the largest floating structure ever built – a self-powered, mile-long open-sea platform [41-43]. Intended to be deployed in international waters in proximity to areas of military interest, MOB would house 70 acres (0.3 km^2) of the enclosed storage space, while simultaneously serving as a runway for fixed-wing aircraft. The size and functions of the MOB platform make it unique compared to other floating structures (**Figure 5.19**).

The eventual design for the MOB has yet to be decided, with various concepts being investigated. The platform could be a single, continuous elastic hull, or involve as many as five individual modules, connected by hinges or elastic connectors. A critical aspect of the design is the response of the runway structure to wave-induced dynamics over its one mile length. The base must support fixed wing cargo planes operating up to sea state 6 (4.6 m waves and wind speeds of 56 km/h). The platform itself must survive all sea states, including hurricanes and typhoons (15 m waves and wind speeds exceeding 160 km/h).

The connectors between modules, and a method to control positioning, are the critical feasibility aspects of a modular approach. The assembly must be rigid enough to minimise relative motion between modules in order to provide a useable flight deck, but also be sufficiently compliant to reduce stresses generated over its length by ocean waves. Various connections methods are under consideration. One promising approach employs five metre long elastomeric conical connectors between the modules [44]. Elastomers offer the ability to tailor both the frequency response and the damping behavior of the connector. Advantage is taken of a conical geometry and the inherent damping afforded by rubber to control yaw motions, enhancing MOB maneuverability.

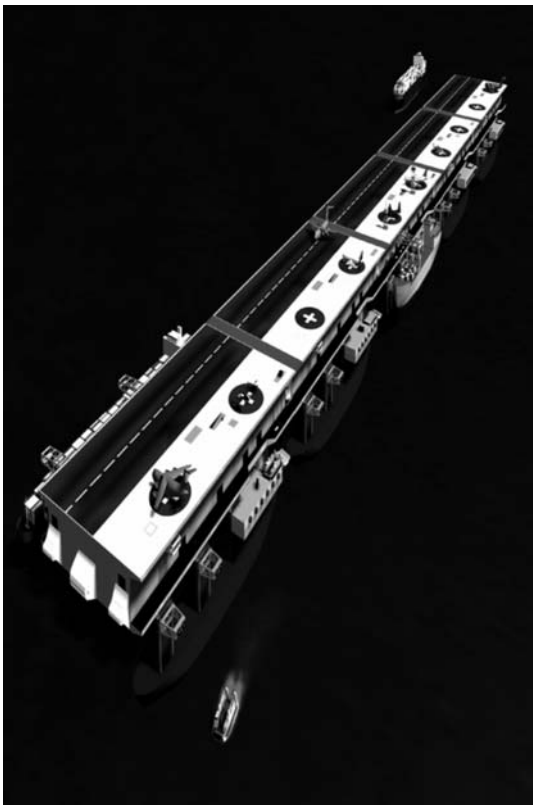

Figure 5.19 Illustration of one conception of the Mobile Offshore Base
With permission from McDermott Technology, Inc.

The technical feasibility of the MOB concept has been established and currently the program is under assessment by the Defense Department and Congress. Potential off-shoots of the floating platform technology, such off-shore airports, are also being explored.

Acknowledgements

Helpful comments from Robert Corsaro and Peter Mott of NRL are gratefully appreciated. This work was supported by the Office of Naval Research.

References

1. A.N. Wecksler, *Rubber Age*, 1941, **4**, 31.

2. I.S. Choi, C.M. Roland and L.C. Bissonnette, *Rubber Chemistry & Technology* 1994, **67**, 5, 892.

3. D. Vergun, *Sea Power*, April 2003, **46**, 4.

4. M.P. Hagelberg and R.D. Corsaro, *Journal of the Acoustic Society of America,* 1985, **77**, 1222.

5. R.N. Capps, *Elastomeric Materials for Acoustical Applications*, Naval Research Laboratory, Washington, DC, USA, 1989.

6. J-D. Ferry, *Viscoelastic Properties of Polymers*, 3rd Edition, Wiley, New York, NY, USA, 1980.

7. J. Jarzynski in *Sound and Vibration Damping with Polymers*, Eds., R.D. Corsaro and L.H. Sperling, ACS Symposium Series No.424, American Chemical Society, Washington, DC, USA, 1990.

8. C.M. Roland, K.L. Ngai, P.G. Santangelo, X.H. Qiu, M.D. Ediger and D.J. Plazek, *Macromolecules*, 2001, **34**, 18, 6159.

9. R.E. Wetton, *Applied Acoustics* 1978, **11**, 2, 77.

10. A.K. Sircar and M.I. Drake in *Sound and Vibration Damping with Polymers*, Eds., R.D. Corsaro and L.H. Sperling, ACS Symposium Series No.424, American Chemical Society, Washington, DC, USA, 1990.

11. M. Roland and G.F. Lee, *Rubber Chemistry & Technology,* 1990, **63**, 4, 554.

12. G.D. Tyler, *Johns Hopkins APL Technical Digest*, 1992, **13**, 145.

13. M.C. Hastings, A.N. Popper, J.J. Finneran and P.J. Lanford, *Journal of the Acoustical Society of America,* 1996, **99**, 3, 1759.

14. L.A. Crum and Y. Mao, *Journal of the Acoustical Society of America*, 1996, **99**, 5, 2898.

15. L.A. Crum, M.R. Bailey, J.F. Guan, P.R. Hilmo, S.G. Kargl, T.J. Matula and O.A. Sapozhnikov, *Acoustic Research Letters Online*, 2005, **6**, 214.

16. P.H. Mott, C.M. Roland, and R.D. Corsaro, *Journal of the Acoustical Society of America,* 2002, **111**, 4, 1782.

17. Y. Traissac, J. Ninous, R. Neviere and J. Pouyet, *Rubber Chemistry & Technology*, 1995, **68**, 1, 146.

18 M. Broekaert, *Huntsman Corporation Technical Bulletin*, 2002.

19. J.L. Reddinger and K.M. Hillman, *Huntsman Corporation Technical Bulletin,* 2001.

20. K.J. Knox, M.I. Hammons, T.T. Lewis, and J.R. Porter, *Polymer Materials for Structural Retrofit,* Air Force Research Laboratory Technical Report, AFRL, Tyndall AFB, FL, USA, 2001.

21. J.S. Davidson, J.R. Porter, R.J. Dinan, M.I. Hammons and J.D. Connell, *Journal of Performance of Constructed Facilities,* 2004, **18**, 2, 100.

22. P. Raleigh, *Rubber and Plastics News,* Sept. 2002, **9**, 13.

23. A.G. Veith, *Rubber Chemistry & Technology,* 1992, **65**, 3, 601.

24. J.P. Klose, *Sea Power,* July 2003, **46**, 7.

25. D.F. Lohr and H.R. Penton in *Handbook of Elastomers*, Eds., A.K. Bhowmick and H.L. Stephens, Marcel Dekker Inc., New York, NY, USA, 1988, p.535.

26. *Report of the Presidential Commission on the Space Shuttle Challenger Accident*, June 6, 1986, Washington DC; science.ksc.nasa.gov/shuttle/missions/51-l/docs/rogers-commission/table-of-contents.html.

27. L. Tappin, *Mathematics Teacher*, 1994, **87**, 423.

28. O. Kreisher, *Sea Power*, May 2002, **45**, 5.

29. S. Ijames, *Police Journal,* 2001, **25**, 7.

30. No inventor; J.P. Lefebvre, assignee; FR 2,532,742, 1982.

31. B. Dubocage and J. Mautcourt, inventors; SNPE, assignee; US 6,295,933 B1, 2002.

32. J.E. Puskas, B. Kumar, A. Ebied, B. Lamperd, G. Kaszas, J. Sandler and V. Altstadt, *Polymer Engineering Science*, 2005, **45**, 7, 966.

33. F. Venus, Jr., inventor; Container Industries, Inc., assignee; US 4,387,833, 1983.

34. H. Katz, inventor; Container Industries, Inc., assignee; US 4,423,829, 1984.

35. L.O. Hoppie, *Rubber Chemistry & Technology*, 1982, **55**, 1, 219.

36. P.H. Mott, C.M. Roland and S.E. Hassan, *Rubber Chemistry & Technology*, 2003, **76**, 2, 326.

37. A.V. Chapman and M. Porter in *Natural Rubber Science and Technology*, Ed., A.D. Roberts, Oxford University Press, Oxford, UK, 1988, p.589.

38. K.N.G. Fuller, M.J. Gregory, J.A. Harris, A.H. Muhr, A.D. Roberts, and A. Stevenson in *Natural Rubber Science and Technology*, Ed., A.D. Roberts, Oxford University Press, Oxford, UK, 1988, p.929.

39. C.M. Roland and I.S. Choi, *Rubber Technology International*, 1996, p. 12.

40. J. Little, *Undersea Warfare,* 1999, **1**, 3, 12.

41. *Popular Science*, 1998, **10**, 32.

42. R. Zueck, R. Taylor and P. Palo in *Proceedings of the* 10th *International Journal Offshore and Polar Engineering Conference*, Seattle, USA, 2000, Volume 1, p.17.

43. R. Zueck, R. Taylor and P. Palo in *Proceedings of the 11th International Journal Offshore and Polar Engineering Conference*, Stavanger, Norway, 2001, Volume 1, p.13.

44. T.R.J. Mills and L. Chen, *Logistics Spectrum* (Society of Logistics Engineers), 2001, **35**, 1.

6 Advances in Fillers for the Rubber Industry

Meng-Jiao Wang and Michael Morris

6.1 Introduction

Fillers are one of the most important components in the manufacture of rubber products, with consumption second only to rubber itself. Fillers have held this position due to their unique ability to enhance the physical properties of elastomers. In fact, the term 'filler' is somewhat misleading as one would regard a filler as a material that is cheaper than the polymer matrix and so can be added to reduce cost per unit volume. For most rubber products, the fillers should be more accurately referred to as 'reinforcing agents' since they generally increase modulus and tensile strength of the compound. In addition, fillers often improve the processability of rubber compounds, and can have a significant effect on other rubber product performances.

There is a wide range of materials, both inorganic and organic, that can be added to rubber at some level as a filler. These include natural and precipitated calcium carbonates, various clays, talc, mica and aluminum trihydrate, amongst others. A recent review provides a fairly complete list of different filler materials and their surface modifications [1]. Carbon black has historically been the predominant filler used in almost all rubber products due to its outstanding reinforcing ability and relatively low cost. Since the introduction of the 'Green Tyre' in the 1980s, precipitated silica has become a second major class of rubber fillers. These two filler types are by far the most important for the rubber industry, not only in their volume of consumption, but also in the performance they bring to rubber products. In recent years, the development of new carbon black grades with different surface areas and structures to meet changing customer needs has continued. Similarly, new grades of precipitated silica have been introduced to satisfy customer needs, particularly in the area of dispersability. Since the use of silane coupling agents is critical to the success of silica as a filler, the development of new coupling agents has also been an area of continued development. The ongoing incremental improvements in existing filler materials will not be covered here. This chapter will review significant new technologies in fillers and filler-related materials that have been introduced in recent years, both for tyres and for other rubber products.

6.2 Requirements for Fillers in Tyre Applications

The tyre sector represents by far the largest segment of rubber products. Continuous demand for increased durability, better fuel economy and improved safety requires the continuous development of new tyre compounds, particularly tread compounds. The performance requirements can be translated to the well-known 'magic triangle' of wear - resistance, rolling resistance and skid resistance, especially wet skid. In addition, heat buildup is a concern, especially in heavier vehicle tyres, as it is one of the key factors for tyre failure due to tread, shoulder and ply separations. Lower heat buildup in the compound also enhances the retreadability of the tyre, an important part of the life cycle of the tyre. In developing the optimum combination of tyre performance requirements, it has been recognised that both polymer and filler play a major role.

With respect to the filler, it has been well established that wear resistance of filled rubber is essentially determined by filler morphology and polymer-filler interaction. For fillers having similar morphologies, an increase in polymer-filler interaction, either through enhancement of physical adsorption of polymer chains on the filler surface or via creation of chemical linkages between filler and polymer, is crucial to the enhancement of wear resistance [2]. In addition, good filler dispersion is also essential to wear performance.

Hysteresis, typically characterised by the loss factor, tan δ, at high temperature, is a key parameter of tread compounds. It not only indicates the heat buildup of the compounds under dynamic strain but also shows a good correlation with the rolling resistance of tyres. Hysteresis is in turn determined by filler networking, which is governed by polymer-filler, and especially filler-filler interactions [3]. The stronger the filler-filler interaction, the more developed the filler network will be, or the poorer the micro-dispersion of filler. These conditions lead to higher rolling resistance and heat buildup.

With regard to wet skid resistance, the mechanism is more complicated. It is now understood that while dynamic hysteresis at low temperature is of importance due to the high-frequency nature of the dynamic strain involved in the skid process, elasto-hydrodynamic lubrication (EHL) and boundary lubrication (BL) are also critical [4]. It has been found that besides dynamic properties, the test conditions, such as vehicle type (passenger *versus* truck), braking system (locked wheel *versus* anti-lock brake system (ABS)), speed, temperature, road surface, and load have a great impact on micro-elasto-hydrodynamic lubrication (MEHL) and BL. The relative role of MEHL is also determined by the composition of the tread compound, such as the nature of the polymer and filler, and their interaction. Whereas silica-filled compounds are favourable for reducing MEHL, carbon black is good for boundary and dry friction [4].

In the last few years, great efforts have been made by carbon black manufacturers to develop new products in response to ever more demanding requirements from the tyre industry. The commercialised products include carbon-silica dual phase filler, chemically modified carbon black, and inverse blacks.

6.3 Advances in Carbon Black

6.3.1 Chemically-Modified Carbon Blacks

For most of its long history, the carbon black industry has concentrated on morphology as the key factor controlling product performance and grade differentiation. Recently the importance of the nature of the interface between the carbon black and the medium has been recognised. Early attempts at surface modification of carbon black include physical adsorption of chemicals on the surface, heat treatment, and frequently oxidation. During the 1980s and 1990s, some work on plasma treatment was reported. Chemical and polymer grafting modifications were also extensively studied from the 1950s onwards.

Recently, several new approaches have been published in the literature for carbon black modification [5-7]. Among others, a number of patents have been issued to Cabot [8, 9] which describe that the decomposition of a diazonium compound derived from a substituted aromatic or aliphatic amine precursor results in the attachment of a substituted aromatic ring or chain onto the surface of the carbon black. This results in a stable attachment that is not affected by moisture. Examples show attachment of amines, anionic and cationic moieties, alkyl, polyethoxyl, vinyl groups and polysulfide moieties. One of the precursors is 4-aminophenyl disulfide (APDS), which yields a modified carbon black that can be used in elastomers. With APDS-modified carbon black, the dispersive component of surface energy of the carbon black can be drastically reduced [10], reducing the driving force of carbon black agglomeration, resulting in a better microdispersion. On the other hand, the sulfide group is able to react with polymer molecules upon heating, so that the coupling reaction between polymer and filler can be achieved during vulcanisation. The effectiveness of surface modification in suppression of filler networking due to both lowering filler-filler interaction, and increasing polymer-filler interaction via chemical bridges, has been verified by dynamic rheological testing [11]. These fillers were tested in typical passenger tyre tread compounds alongside the virgin carbon black and silane modified silica. In filled rubbers, the elastic modulus decreases with strain amplitude, which has been termed the 'Payne effect' [12, 13]. This effect is generally used as a measure of filler networking, controlled mainly by filler-filler interactions. The strain dependence of elastic modulus results (**Figure 6.1**) show that the APDS-modified carbon exhibits a lower Payne effect compared to bis(3-(triethoxysilyl) propyl)tetrasulfide (TESPT)-modified silica, which is itself much lower than that found for unmodified carbon black. This is a clear indication that filler networking is substantially reduced. Accordingly, a striking similarity between the modified carbon black and coupled silica is observed in the tan δ at 70 °C measured in strain sweep (**Figure 6.2**), and the temperature sweep results. Thus, the APDS-modified carbon black provides viscoelastic properties comparable to TESPT-modified silica, which is now well known to be better in terms of hysteresis and hence rolling resistance compared to conventional

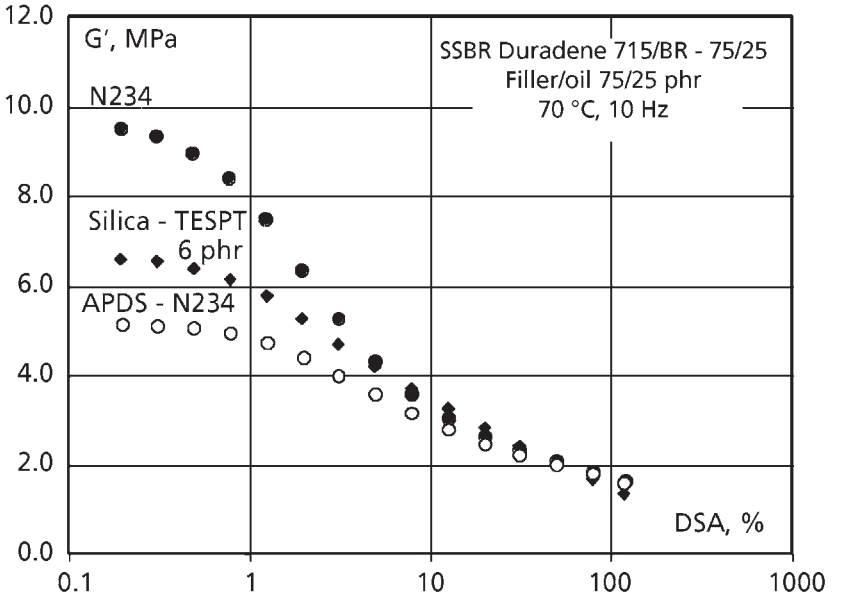

Figure 6.1 Strain dependence of G′ for vulcanisates filled with N234 carbon black, aminophenyl disulfide-modified N234, and bis(3-(triethoxysilyl)propyl)tetrasulfide treated silica. DSA = double strain amplitude

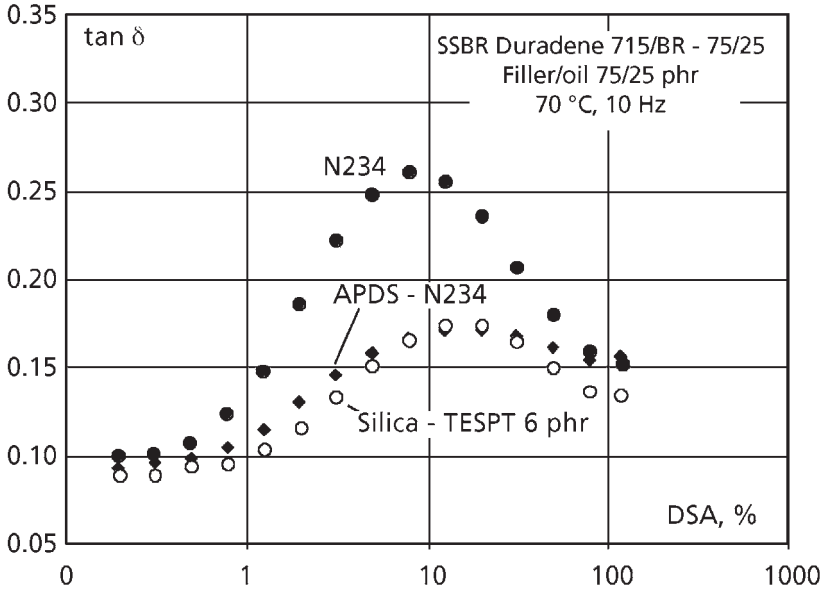

Figure 6.2 Strain dependence of tan δ at 70 °C for vulcanisates filled with N234 carbon black, aminophenyl disulfide-modified N234, and bis(3-(triethoxysilyl)propyl)tetrasulfide treated silica. DSA = double strain amplitude

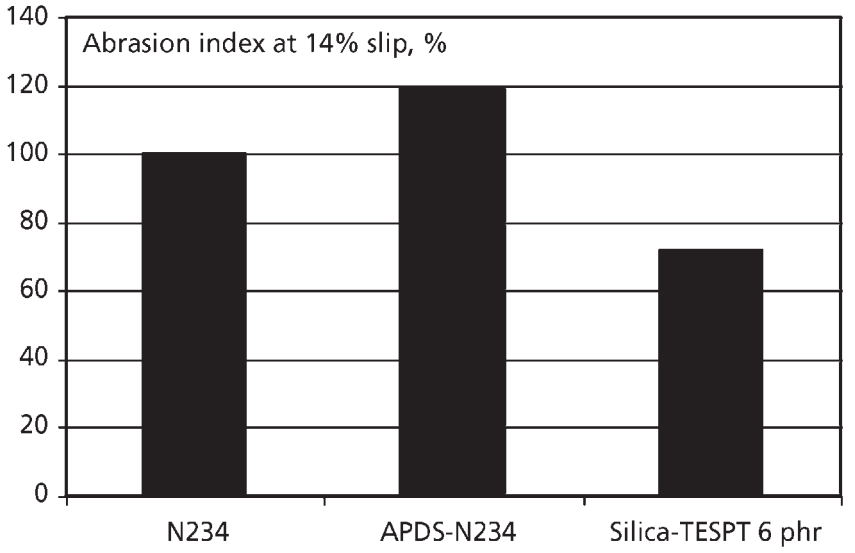

Figure 6.3 Abrasion resistance for vulcanisates filled N234 carbon black, aminophenyl disulfide-modified N234, and bis(3-(triethoxysilyl)propyl)tetrasulfide treated silica

carbon black. Additionally, the ability of the chemically-modified carbon black to form chemical bonds with the polymer through its disulfide groups provides improved polymer-filler interaction, leading to increased abrasion resistance (**Figure 6.3**).

6.3.2 Inversion Carbon Blacks

Targeting a reduction in rolling resistance, a group of carbon black fillers have been developed under name of inversion blacks [14, 15]. The term 'inversion' refers to the phenomenon that in certain rubber formulations, the change in temperature dependence of tan δ can be increased. These carbon blacks are manufactured in conventional carbon black reactors. Morphologically, they are characterised by a broad aggregate size distribution with a larger portion of large size aggregates compared to conventional carbon blacks (**Table 6.1**) [16]. According to observations by scanning tunneling microscopy (STM) [16] and atomic force microscopy (AFM) [17], the inversion blacks seem to feature smaller graphitic-crystallite sizes and rougher surfaces compared with conventional carbon blacks. The main advantage of the rubbers reinforced with these materials is their low hysteresis and high rebound at high temperature, which is expected to impart lower rolling resistance to tread compounds compared to conventional carbon black. In solution polymerized styrene-butadiene rubber (S-SBR)/butadiene rubber (BR) based tread compounds for passenger tyres, the tan δ at 60 °C was reduced by about

Table 6.1. Analytical properties and some in-rubber properties for inversion blacks					
		N220	**EB111**	**N356**	**EB145**
NSA	m^2/g	115	117	93	96
CTAB	m^2/g	111	113	90	88
Iodine number	mg/g	121	122	93	103
DBP	ml/100 g	114	113	153	147
CDBP	ml/100 g	98	98	110	106
Tint	%	115	115	105	94
Aggregate size distribution					
Mean aggregate size	nm	77	111	104	140
Width (standard deviation)	nm	26	72	31	74
Width at half height	nm	54	74	71	96
Fraction > 150 nm	%	2~4	17	7	37
OE-SSBR/BR (Passenger tyre tread)					
Ball rebound @ 0 °C	%	13.9	13.6	13.5	13.1
Ball rebound @ 60 °C	%	35.8	40.4	44.5	47.6
DIN abrasion	mm^3	84.0	79.0	54.0	58.0
MTS E´ @ 0 °C, 50 ± 25 N	MPa	43.1	36.5	41.5	34.9
MTS E´ @ 60 °C, 50 ± 25 N	MPa	9.0	8.6	11.8	10.4
MTS tan δ @ 0 °C, 50 ± 25 N		0.481	0.466	0.452	0.466
MTS tan δ @ 60 °C, 50 ± 25 N		0.262	0.231	0.230	0.202
Tyre test					
Rolling resistance index	%	100	107		
Wet traction index	%	100	100		
Tread wear index	%	100	103		
NR (truck tyre tread)					
Ball rebound @ 0 °C	%	31.9	33.8	34.0	36.1
Ball rebound @ 60 °C	%	59.8	64.8	65.9	68.9
DIN abrasion	mm^3				
MTS E´ @ 0 °C, 50 ± 25N	MPa	11.7	10.8	12.5	10.0
MTS E´ @ 60 °C, 50 ± 25 N	MPa	7.0	6.9	7.8	6.9
MTS tan δ @ 0 °C, 50 ± 25 N		0.254	0.221	0.230	0.202
MTS tan δ @ 60 °C, 50 ± 25 N		0.140	0.114	0.120	0.100

NSA: Nitrogen surface area
CTAB: Cetyl trimethyl ammonium bromide surface area
DBP: Oil absorption number (di-butyl phthalate)
CDBP: Compressed oil absorption number (di-butyl phthalate)
OE-SSBR: Oil extended solution polymerised styrene-butadiene rubber

12% compared with their conventional carbon black counterparts, and in the case of an NR-based tread compound for truck tyres, the tan δ reduction was about 18%.

In a later publication, a new group of carbon blacks of a similar type, termed 'nano-structure blacks' was introduced [18]. Compared to the inversion blacks, their aggregate size distribution (see **Table 6.1**) is narrower due to a smaller fraction of large aggregates. This resulted in improved abrasion resistance compared to the earlier inversion blacks. These new carbon blacks were recommended for use in truck tyre tread compounds.

6.4 Filler Particles Containing Both Carbon Black and Silica

6.4.1 Carbon-Silica Dual Phase Filler

During the last decade, a group of dual and multiple phase fillers in which silica or/and other metal oxides and carbon are co-formed in a carbon black-like reactor have been developed. In particular, two types of carbon-silica dual phase fillers (CSDPF) have been commercialised under the tradename ECOBLACK™ CRX™ XXXX. The two series, identified by the numbers 2XXX and 4XXX differ in the silica domain distribution within the aggregates. In the aggregates of CSDPF 2XXX, the carbon black and silica are intimately intermixed on a nanometer scale, that is in the about the same size as the carbon black crystallite. For the CSDPF 4XXX, the silica location is more on the exterior of the aggregates. In each type of material, there are several grades having different morphologies and silica contents.

6.4.1.1 Nomenclature of Carbon-Silica Dual Phase Fillers

The classification system of CSDPF is based on the type, particle size, structure and silicon content. It is composed of a prefix CSDPF (for academic publication) or CRX (for commercial uses) followed by 4 numerals. The first numeral represents the technology: 2 for the materials produced with single stage process [19, 20] and 4 for those produced with a multi-stage process [21, 22]. The second numeral represents the particle size of the filler, which corresponds to the ASTM designation for carbon blacks. For CSDPF 2XXX, the third letter indicates the structure, with 0 = low, 1 = normal and 2 = high, and the last letter represents the silicon content as shown in **Table 6.1**. In the case of CSDPF 4XXX, the silica content is expressed by the last two numbers (**Table 6.2**).

6.4.1.2 Features of CSDPF 2XXX and CSDPF 4XXX Series

Table 6.3 shows the basic properties of typical CSDPF 2XXX and 4XXX materials compared with those of conventional fillers. CSDPF 4XXX has much higher silica-surface

Table 6.2. Numbers representing silica contents in CSDPF nomenclature			
CSDPF 2XXX		CSDPF 4XXX	
Last number	Silicon content (% by weight)	Last two numbers	Silicon content (% by weight)
0	0.1 – 0.9	00	0.1 – 0.9
1	1.0 – 1.9	01	1.0 – 1.9
2	2.0 – 2.9	02	2.0 – 2.9
3	3.0 – 3.9	03	3.0 – 3.9
4	4.0 – 4.9	04	4.0 – 4.9
5	5.0 – 5.9	05	5.0 – 5.9
6	6.0 – 6.9	06	6.0 – 6.9
7	7.0 – 7.9	07	7.0 – 7.9
8	8.0 – 8.9	08	8.0 – 8.9
9	9.0 – 9.9	09	9.0 – 9.9
		10	10.0 – 10.9
		11	11.0 – 11.9
		12	12.0 – 12.9
		…	…
		19	19.0 – 19.9
		20	20.0 – 20.9
		…	…

Table 6.3. Analytical properties of some typical carbon blacks and CSDPF								
	Silica content, %		BET-surface area, m^2/g		STSA, m^2/g		CDBP[a]	
Filler	As is	HF	As is	HF	As is	HF	ml/100 g	%
N134	N/A	N/A	146	NA	134	NA	104	NA
N234	N/A	N/A	122	122	118	118	100	NA
CSDPF CRX2125	5.2	0.58	194	368	138	171	118	22
CSDPF CRX4210	10.0	0.01	154	167	123	155	108	55
Silica Z1165	46.7	N/A	168	N/A	132	N/A	NA	100

BET: Brunauer, Emmett, and Teller surface area theory
a: The silica-surface coverage of CSDPF was estimated from iodine number and surface area that was the averaged value of BET-surface area (NSA) and statistical thickness surface area (STSA)
HF – hydrofluoric acid treated

coverage relative to CSDPF 2XXX, due to the silica domain distribution and higher silicon content of the 4000 series. This is demonstrated by the changes in silica content and surface area upon hydrofluoric acid (high frequency) extraction. During high frequency extraction, the silica will be dissolved with the carbon domain remaining unchanged. The fact that significant portions of silica still remain, and surface areas drastically increase upon high frequency treatment, suggest that the silica of CSDPF 2XXX is distributed throughout the aggregates. By contrast, CSDPF 4XXX shows a small change in surface area, and the fact that there is almost no silica left after high frequency extraction indicates that the silica in the CSDPF 4XXX aggregates is located predominantly on the surface. This observation is supported by the images and the carbon- and silicon-maps obtained using scanning transmission electron microscope (STEM) equipped with an energy dispersive X-ray analyser (STEM/EDX). In the aggregates of CSDPF 4XXX, the silica is obviously concentrated at the aggregate surface, whereas in CSDPF 2XXX, the silica domains are distributed within the aggregates [4, 23]. The silica distributions can be also visualised from transmission electron microscope (TEM) images of the filler particles before and after ashing. **Figure 6.4** shows a TEM image of a CSDPF 2XXX aggregate and an image of the same aggregate that was ashed, leaving behind the silica phase. The silica domains can be seen as having been finely distributed throughout the aggregate. Ashing of the CSDPF 4XXX aggregates however, resulted in a quite different picture (**Figure 6.5**): silica is left as a shell-like structure whose shape is similar to the contour of the unashed particles. It is apparent that the silica domain was intimately attached onto the carbon black surface with a high surface coverage.

When incorporated in hydrocarbon polymers, both CSDPF 2XXX and 4XXX are characterised by higher filler-polymer interaction in relation to a physical blend of carbon black and silica, and lower filler-filler interaction compared to either traditional carbon black or silica. Evidence of the higher filler-polymer interaction of the

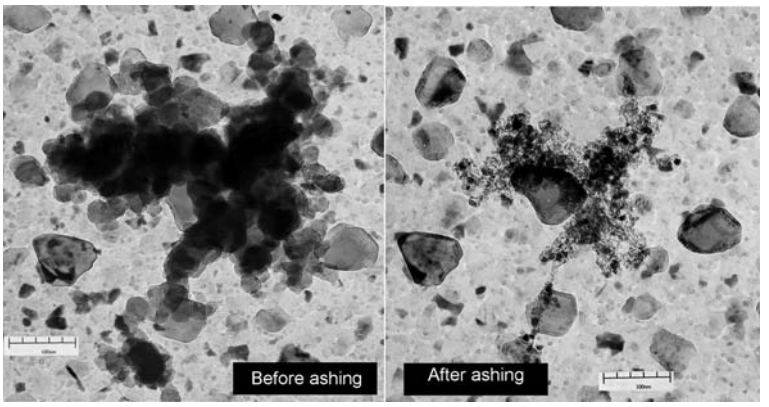

Figure 6.4 TEM images of CRX 2XXX aggregate before and after ashing

silica-containing fillers in hydrocarbon polymers can be obtained by comparing the adsorption energies of polymer analogs on the filler surfaces [24]. The adsorption free energies of heptane, a model compound for hydrocarbon polymers, were measured by inverse gas chromatography (IGC) [25]. The results for both CSDPF 2XXX and 4XXX are presented along with those of blends of carbon black N234 and silica (**Figure 6.6**). Regardless of the difference in surface areas, at the same silica contents, the silica-containing fillers give significantly higher adsorption energies than the physical blend. The high surface activity of CSDPF is attributed to the presence of heteroatoms in the

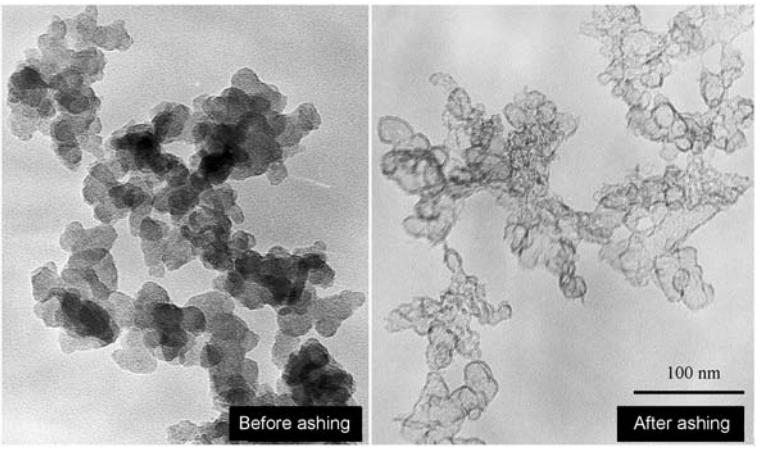

Figure 6.5 TEM images of CRX 4XXX aggregate before and after ashing

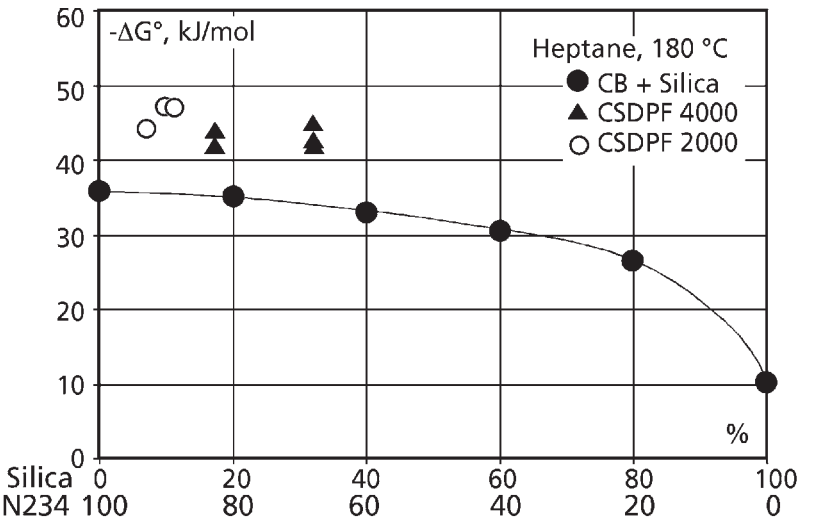

Figure 6.6 Adsorption energies of heptane on a variety of fillers. CB = carbon black

carbon domains. This leads to an increased population of crystal defects in the graphitic crystal lattice and/or smaller crystallite dimensions, leading to more edges of carbon basal planes. The edges of basal planes and crystal defects have been proposed as the active centres for rubber adsorption [26].

The weaker filler-filler interaction of CSDPF 2XXX and 4XXX is demonstrated by the strain dependence of the elastic modulus, G´ (**Figure 6.7**). Although from the chemical composition point of view, both CSDPF 2XXX and 4XXX are between carbon black and silica, what is actually observed here is that the two new fillers give a lower Payne effect than either the carbon black or the silica. This unique behaviour is readily explained by the hybrid surfaces of the new materials, which minimises the contact between like surfaces. It has been established from surface energy studies, that interaction between unlike surfaces is lower than that between the same type of surface [3]. The high polymer-filler interaction and low filler-filler interaction of CSDPF should allow a better compromise between abrasion resistance and dynamic hysteresis at high temperature (see Section 6.2). This will result in a good balance between wear resistance and rolling resistance in tyres. Furthermore, the lower surface silica content and high surface activity of the carbon domains means that these fillers will require significantly lower silane coupling agent compared to silica. Although both types of CSDPF can be used advantageously in passenger tyre tread compounds, considering the global performance requirements of different tyres, the CSDPF 4XXX is recommended for passenger tyres, and the CSDPF 2XXX for truck tyre tread formulations.

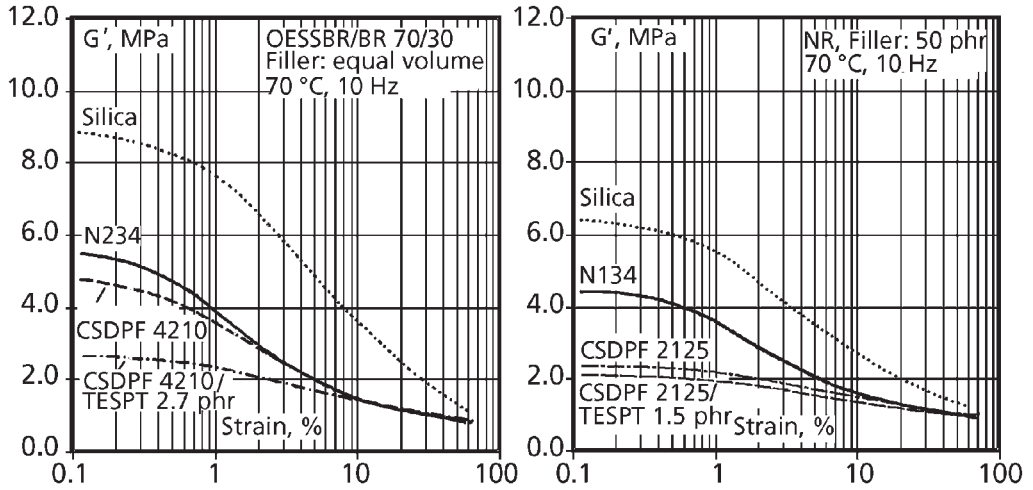

Figure 6.7 Strain dependence of G´ for vulcanisates filled with a variety of fillers. CSDPF = carbon silica dual phase filler (see **Table 6.2** for complete descriptions of 4210 and 2125)

6.4.1.3 Application of CSDPF 4XXX Series to Passenger Tread Compounds

The recommendation for use of CSDPF 4XXX for passenger tyres is based on its high silica surface coverage, which is very favourable to wet skid resistance. During service, a passenger tyre has a smaller footprint and lower load compared with a truck tyre. Therefore, according to the 3-zone model for wet traction, the water squeezing and transition zones are relatively large in comparison to the smaller traction zone [27]. In passenger car tyres, tread materials that enable faster removal of water in the squeezing and transition zones, and consequently increase the relative size of the traction zone where most of the friction is generated, provide improved performance. The use of silica as the main filler in tread compounds achieves this goal and its advantage over carbon black for wet traction in passenger car treads is well known. The high silica surface coverage in CSDPF 4XXX provides a similar advantage over carbon black. The high silica coverage of CSDPF 4XXX results in shorter water squeezing and transition zones compared to carbon black and CSDPF 2XXX, similar to the behaviour of silica. Although CSDPF 4XXX has a disadvantage over silica in the water squeezing and transition zones due to its less than 100% surface coverage, this is offset to a certain degree by its superior performance in the traction zone. In the traction zone, the boundary lubrication (BL) friction is high due to the improved dynamic properties, i.e., high hysteresis and lower modulus at low temperature. As a result, the overall wet skid resistance of the tyres filled with CSDPF 4XXX is equal to or better than silica-filled compounds. On the other hand, it has been recognised that the abrasion resistance of silica compounds is still significantly poor relative to carbon black compounds. This is explained by the relatively weak polymer-filler interaction between silica and hydrocarbon rubber, even with solution polymers and a high dosage of coupling agent. In the CSDPF 4XXX material, the weak interaction between polymer and silica is significantly compensated for by the high surface activity of the carbon domain. In **Figure 6.8**, the average performances of passenger car tyres with different fillers in tread compounds are shown. Compared with a silica tyre, CSDPF 4210 gave similar rolling resistance, close wet skid resistance for the ABS vehicle, higher dry skid resistance and significantly improved treadwear resistance. When CSDPF is used to replace carbon black, the rolling resistance and wet skid resistance will be significantly improved without significant trade-off in treadwear and dry traction [4].

6.4.1.4 Application of CSDPF 2XXX in Truck Tyres

In truck tyres, the principal requirements of higher wear resistance, lower rolling resistance and improved wet skid resistance are the same as those for passenger cars. However, unlike passenger car tyres, very little silica has been used in heavy truck tyres. The main reason for this arises from the different polymers used. In car tyres, solution styrene-butadiene rubber (SBR) is the dominant polymer in tread compounds, whilst heavy truck tyres use mainly natural rubber (NR) for its low heat build up and

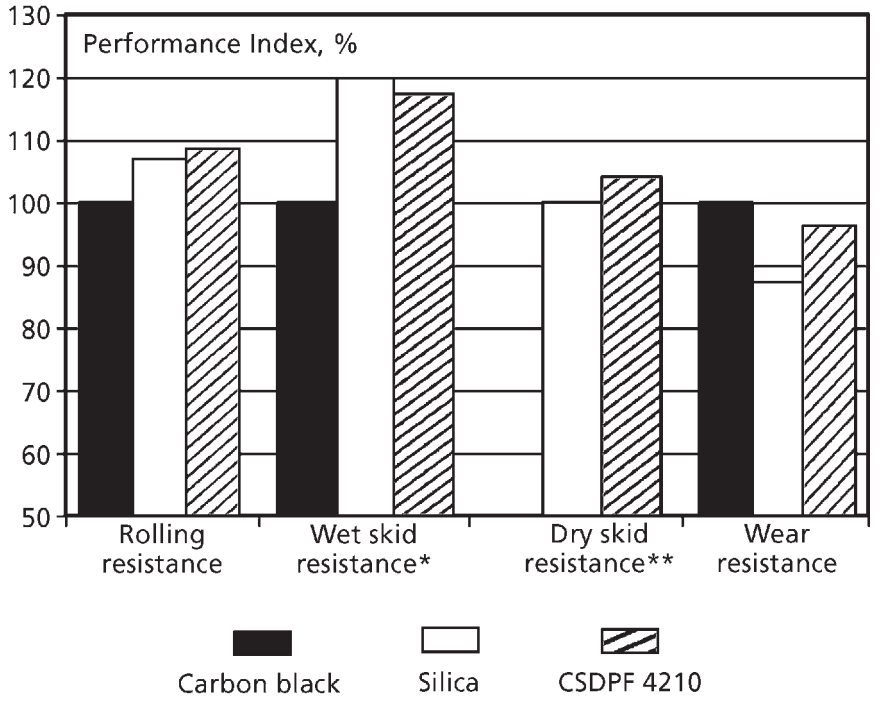

Figure 6.8 Summary of tire performance of the tread compounds filled with different fillers. *Wet skid resistance was obtained with the vehicles having ABS on asphalt road surface. **Dry skid resistance is not available for the carbon black tyre

resistance to tearing [28, 29]. Silica gives relatively poor treadwear in these compounds due to the high non-rubber content of the NR and high polarity of the silica surface. The weak polymer-filler interaction is not well compensated for by coupling agents, so that there is a significant deficiency in abrasion resistance [30]. The CSDPF 2000 series, with its lower silica surface coverage and high surface activity of carbon domains is very favourable in this system. As the silica coverage is smaller, the low polymer-filler interaction on the silica domains due to the lower efficiency of the coupling agent is largely offset by the high surface activity of the carbon domains. Therefore, treadwear is not significantly deteriorated when carbon black is replaced by CSDPF 2XXX, especially its higher surface area and high structure grades CSDPF 2124 and 2125 (**Figure 6.9**). On the other hand, the lower filler-filler interaction of CSDPF leads to an improved balance of dynamic properties at different temperatures, even at very low dosages of coupling agents. Consequently, while the low hysteresis at high temperature imparts substantially reduced rolling resistance, the wet skid resistance is significantly increased. The reason for this is that in truck tyres, the length of the traction zone is dominant over the water squeezing and transition zones due to the bigger size and high load. Under

these circumstances, the wet skid resistance of the tyre is governed by BL, which is determined by the dynamic properties of the compounds. Under BL conditions, the high hysteresis at low temperatures of CSDPF 2XXX compounds [30] results in higher energy dissipation, and low dynamic modulus leads to a larger contact area between road surface and tread. Both of these phenomena lead to higher wet skid resistance, as demonstrated by the load dependence of the friction coefficient (**Figure 6.10**). Accordingly, CSDPF 2XXX, is an excellent filler for NR-based truck tyre tread compounds to ensure the best global performance.

6.4.2 Silica-Coated Carbon Blacks

As an alternative to producing a co-fumed carbon black silica particle in carbon black-like reactors, patents have also been issued on particles produced by depositing silica on the surface of carbon black [31-33]. This was achieved using an aqueous solution of sodium silicate, and adjusting the pH with acid. When the silica coated blacks are used in tyre tread compounds, the hysteresis of the compounds at high temperature can be significantly reduced, depending on the silica content of the materials and the coupling agents used.

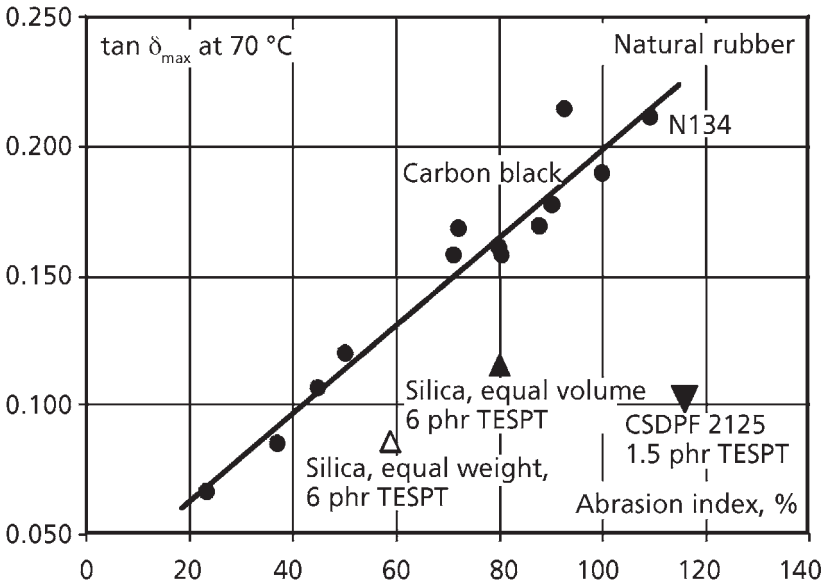

Figure 6.9 Hysteresis and abrasion resistance of NR compounds filled with a variety of fillers

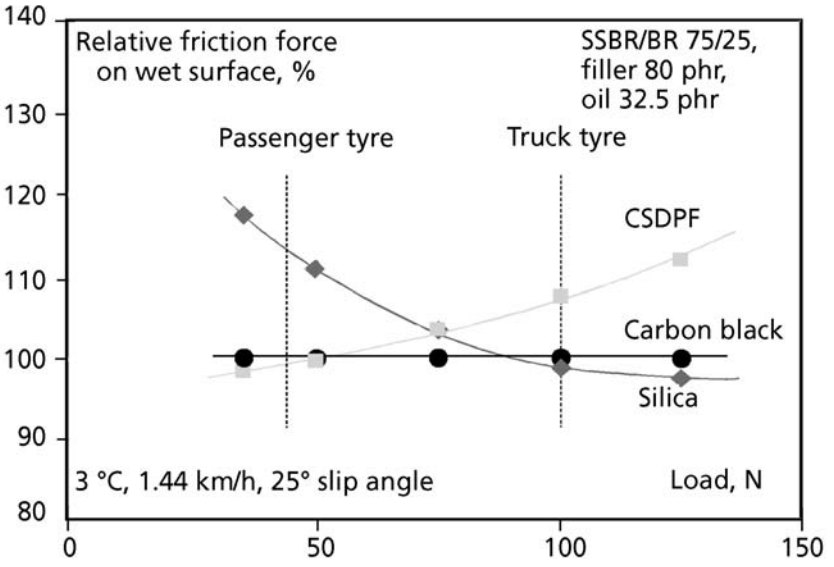

Figure 6.10 Relative friction forces as a function of normal load measured by Grosch Abrasion and Friction Tester (GAFT) for vulcanisates filled with a variety of fillers

6.5 Advances in Silica and Other Filler Materials

6.5.1 New Precipitated Silica for Silicone Rubber

Although many new grades of precipitated silica have been introduced since the introduction of the 'Green Tyre' in the 1990s, most of them seem to have been incremental improvements on the original highly dispersible silica. In addition to variations in morphology, further improvements in dispersibility and reduced need for coupling agents have been the goals. A new grade of precipitated silica introduced by Rhodia under the tradename SilOa seems to represent a significant new development, which is targeted at silicone rubber reinforcement. According to Rhodia, SilOa can give performance similar to fumed silicas, at a lower cost [34]. Conventional precipitated silicas, which are substantially lower in cost than fumed silica, have hydrophilic and irregular surface properties, making them less effective in reinforcement and leading to high water content, compared with fumed silica. This leaves a big gap between the performance and the price of the two families of silicas. The new grade of precipitated silica aims to fill the gap by reducing its affinity for water while still providing a cost advantage. Another benefit of the SilOa product is low dusting, as the particle size is larger than fumed silica particles [34].

The development of this silica is aimed at those silicone rubber applications that need better performance than ordinary precipitated silicas, but do not need the full range of benefits offered by fumed silica. One of the key markets for this material is likely to be silicone extrusions. One of the problems with precipitated silica in this application is the explosive decompression of bubbles in the silicone material, as the extrusion emerges from the die head. This is caused by the high population of silanol groups on the surface of conventional precipitated silica, attracting more moisture. The surface of the SilOa material is made up primarily of silicon-oxygen bonds and the silanol concentration is considerably reduced. In addition, the surface geometry is claimed to be stable and regular, without the disordered surface detail seen at the 0.5 nm scale on other silica particles.

6.5.2 Starch

In the late 1990s, Goodyear introduced a new line of tyres, whose tread formulation contains a certain amount of a starch-based filler material called BioTred [35]. The starch filler, in the form of a starch/plasticiser composite, is applied with a fairly high dosage of organosilane coupling agent to improve polymer-filler interaction.

Starches $(C_6H_{10}O_5)_n$, are natural products made of a mixture of two polymers: amylose, composed of long straight chains containing 200-1000 glucose units linked by α-1,4-glycoside links, and amylopectin, consisting of comparatively short chained glucose (about 20 glucose units) crosslinked by α-1,6-glycoside links. Most starch materials have about 25% linear and 75% branched/crosslinked molecules [36].

Starches exist in nature in the form of granules with a quasi-crystalline structure. The size of starch granules varies in diameter from 1 to 150 μm, depending on the sources from which the starch is produced. Cornstarch, the main commercially available starch material, which was used in the new tyres, has granules with a size from 5-26 μm with an average diameter of 15 μm.

Due to a very high softening point (200 °C or above) and a large granule size, starch by itself can not be mixed directly into rubber compounds using a conventional mixing facility, since the typical temperature for compound mixing is in the range of about 150 to 170 °C. The mixing temperature is not sufficient to cause starches to melt and to blend uniformly with the rubber composition [37]. A procedure was therefore developed to mix starch first with polymeric plasticisers and other ingredients in a separate operation to form a starch composite so that the starch filler can be incorporated with other rubber compound ingredients using conventional mixers [38]. The polymeric plasticisers used include poly(ethylene-vinyl alcohol), ethylene-glycidyl acrylate, vinyl acetate and cellulose that is compatible with the starch. It is believed that the strong chemical and/or physical interactions between the starch and the plasticiser result in the reduction of the softening point of the starch composite such that it can be well mixed with polymer and other ingredients for rubber compounding [37, 39].

Apart from the ecological advantages, tyres are claimed to exhibit remarkably low rolling resistance when part of the carbon black or silica, for example 30%, is replaced with the starch/plasticiser composite in tread compounds. These results were explained in terms of lowering compound hysteresis and reduction of tyre weight. Some enhanced wet skid resistance, without compromise in treadwear, was also claimed in comparison to conventional carbon black-based tyres [39].

6.5.3 Organo-Clays

There has been considerable recent research interest in layered silicates, particularly the Montmorillonite type, which have been cation exchanged with organic ammonium salts, including ammonium terminated liquid rubbers [40, 41]. These materials are sometimes termed nanoclays. The cation exchange reaction makes the clay organophilic, enhancing dispersion in organic polymers, and also facilitates exfoliation of the silicate layers. The result is a potentially very high aspect ratio filler. Filler networking can therefore be achieved at much lower loading levels than are required for carbon black or silica. In rubber reinforcement applications, increased tensile properties at equivalent loadings have been observed compared to conventional fillers. Another advantage of this type of filler is the low gas permeability, which could be useful for tyre inner liners, for example. On the negative side, the organo-clays tend to give high hysteresis and loss tangent, and often high permanent set. Research is continuing, particularly through the use of coupling agents, and blending with other fillers, with the aim of maintaining the advantages of the organo-clays and overcoming their disadvantages.

6.6 Advanced Rubber-Filler Masterbatches

Mixing filler with rubber is one of the most critical processes in rubber compounding. Along with physical changes of the materials, the primary functions of mixing are incorporation, dispersion and distribution of the filler and other ingredients in the polymers. Traditionally, this is achieved using batch mixing of fillers and solid rubber blocks or pellets, referred to as dry mixing. The final dispersion quality of the filler in the polymer is a critical parameter in controlling the performance of rubber products, including mechanical failure properties, dynamic properties and electrical properties. The degree of filler dispersion is determined by the filler morphology, aggregate-aggregate interactions and the shear stress applied during mixing [10]. Carbon blacks with high surface area or low structure are known to be very difficult to disperse. Blacks that have a structure that is too low and/or a surface area that is too high cannot be satisfactorily dispersed using existing mixers, so they are not considered to be usable in rubber compounds and so are not classified as rubber blacks.

For a number of years, great efforts have been made to produce carbon black-polymer masterbatches by mixing polymer latex with filler slurry and then co-coagulating the mixture. Most commercial products of this type are made in batch processes using a chemical coagulation. With such a process, the filler dispersion can be improved relative to dry mixing, however the long mixing and coagulation time reduces productivity. Another drawback of these processes is that when NR latex is used, some non-rubber substances from the latex, such as protein, can be adsorbed onto the filler surface and interfere with polymer-filler interaction. Recently, two technologies have been developed which represent significant breakthroughs in this area. One is a continuous liquid phase process for producing NR/carbon black masterbatch, and other is a batch process to produce powdered rubbers, which are masterbatches filled with carbon black or silica. These technologies enable certain grades of carbon black, which were previously thought to be unusable due to their poor dispersability, to be used in rubber compounds.

6.6.1 Cabot Elastomer Composites

Cabot Elastomer Composites, known as CEC, are NR-carbon black masterbatches produced using a unique continuous liquid phase mixing/coagulation process [42]. In this process, carbon black incorporation, dispersion and distribution are completed in a very short period of time. It has been found that this liquid phase mixing offers the following benefits over the conventional dry mixing and wet batch processing:

- Simplified mixing procedure;
- Reduced mixing costs due to reduced mixing equipment, energy and labour;
- Elimination of free carbon black handling and reduced dust emission;
- Excellent dispersion of filler independent of filler morphology;
- Improved vulcanisate properties;
- Improved capital efficiency; and
- Facilitation of continuous mixing.

6.6.1.1 Process of CEC Production

The process of CEC production, as presented in **Figure 6.11**, consists of carbon black slurry preparation, NR latex storage, mixing and coagulation of carbon black slurry and latex, dewatering of the coagulum, drying, finishing and packaging [43].

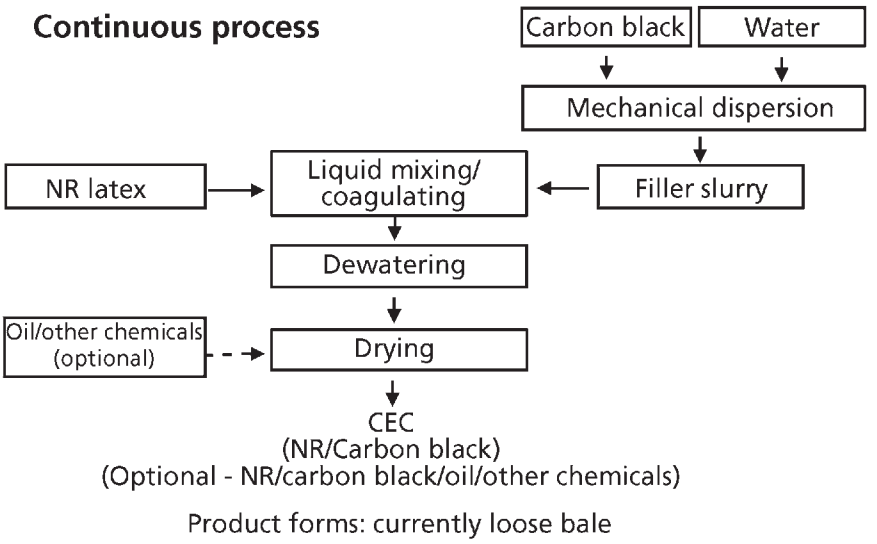

Figure 6.11 Flow diagram of the CEC process

The carbon black slurry is prepared by finely dispersing carbon black in water mechanically without any surfactant. The slurry is injected into the mixer at very high speed and mixes continuously with the latex stream. Under highly energetic and turbulent conditions, the mixing and coagulation of polymer with filler is completed mechanically at room temperature in less than 0.1 second, without the aid of chemicals.

After dewatering of the coagulum in an extruder, the material is continuously fed into a dryer to further reduce the moisture content to less than 1%. The residence time in the dryer is 30-60 seconds. Over the entire drying process, only for a very short period, typically 5-10 seconds, will the compound temperature reach 140-150 °C, so that the thermo-oxidative degradation of NR can essentially be prevented. In the dryer, small amounts of antioxidants are also introduced as a stabiliser for storage. Optionally, other ingredients in the compounds, such as zinc oxide, stearic acid, antiozonants, antioxidants, and wax can be added at this stage.

The dried material can then be slabbed, cut or pelletised. Currently, CEC is packaged into a highly friable bale form consisting of compressed small strips.

The key feature of the CEC process is the fast mixing and coagulation, and a short drying time at high temperature. This achieves excellent performance for the material because polymer-filler interaction can be better preserved and polymer degradation can be eliminated.

6.6.1.2 Further Compounding of CEC

One of the features of CEC is its superior filler dispersion. The dispersion of carbon black in the polymer is, therefore, not a concern for compounders. Mixing other ingredients, such as antioxidants, wax, oil, vulcanisation activators and curatives, requires distinct procedures to take full advantage of CEC's unique properties. The materials can be mixed with either two-stage or single-stage mixing. They can even be mixed by continuous mixing after pelletisation. The exact mixing procedures will be dependent on the type of compounds, mixing equipment, desired downstream processability, product performance requirements, and other factors [43].

CEC has a high viscosity relative to pure polymer and dry mixed masterbatch. The high viscosity of CEC is caused mainly by the hardening of the material during storage. This is especially severe for highly loaded compounds with high surface area carbon blacks, such as those used in tyre treads. Three mechanisms are responsible for the hardening effect in CEC: polymer gelation, bound rubber formation and carbon black flocculation. Equilibrium is reached in a short period, however, and compared with dry-mixed carbon black masterbatch, the Mooney viscosity of CEC drops more rapidly upon mastication. This may be associated with the high viscosity of CEC, which gives rise to high shear stress during mixing, facilitating the mechano-oxidative mastication and breakdown of agglomerates to release trapped rubber. After mixing, the compound viscosity can easily reach the same level as that for dry-mixed compounds, and the viscosity will also be stabilised, giving a Mooney viscosity of the compound that does not change with storage [43].

6.6.1.3 Dispersion Quality of Carbon Black in CEC

One of the greatest advantages of CEC is the superior dispersion of carbon black in the polymer. **Figure 6.12** shows a comparison of macrodispersion, measured by optical microscopy, for two N134-filled vulcanisates: one prepared from CEC using two-stage mixing and another by four-stage dry mixing. Clearly, the dispersion of filler in CEC is considerably better than in the dry mixed compound, even though the energy input in CEC mixing is much lower. In fact, the carbon black dispersion and distribution are fully completed at the very early stages of the CEC process. This was demonstrated by an investigation of the carbon black dispersion in CEC by TEM [43]. For N234-filled CEC, the carbon black is already well dispersed and uniformly distributed throughout the polymer matrix after dewatering of the coagulum, where only minor mechanical energy has been input. For the dry-mixed compound, the dispersion and distribution are still very poor, even though extensive mixing has been applied. This demonstrates that high quality of filler dispersion can be achieved with CEC technology without significant mechanical breakdown of the polymer molecules.

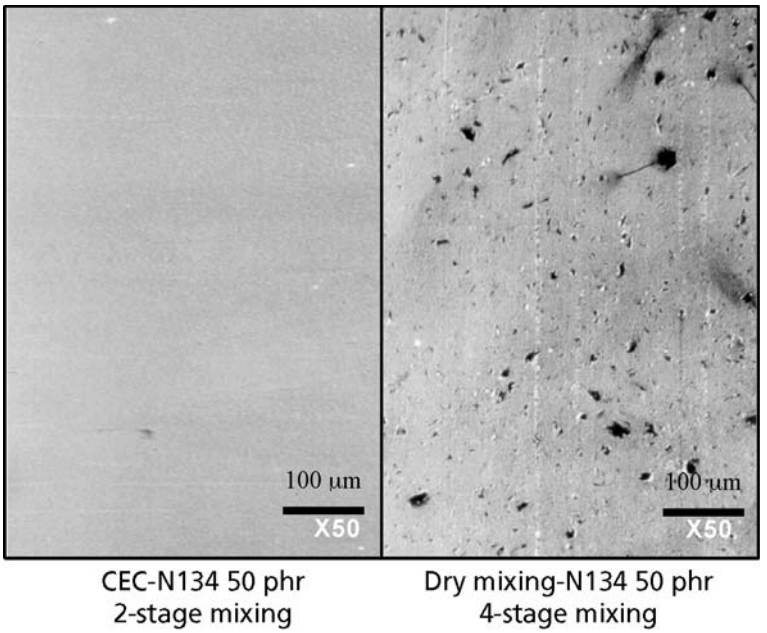

Figure 6.12 Dispersion of carbon black N134 in CEC and dry-mixed compounds

6.6.1.4 Physical Properties of CEC Vulcanisates

The physical properties of CEC vulcanisates are compared to the equivalent dry mixed compounds in **Figure 6.13**. This summary is based on the average data from a large number of studies, both in the laboratory and actual rubber product tests. It can be seen that the excellent filler dispersion compared with dry mixed compounds, leads to higher tear and tensile strengths, lower hysteresis and heat build-up, and substantially longer flex fatigue life. The unique flex fatigue resistance makes the CEC compounds very suitable for anti-vibration rubber goods. For example, the fatigue life of tank bushings made from CEC was almost twice as long as that of bushings made from the dry-mixed counterparts [44]. The lower hysteresis would be expected to result in lower heat build-up and longer service life if CEC were used in tread compounds. In a typical endurance test for truck tyres, the tyre with CEC treads gave 10 °C lower temperature and 17% longer endurance compared with dry-mixed tread compounds [45]. With regard to abrasion resistance, it is generally found that the abrasion resistance of CEC is comparable to that of dry mixed counterparts for carbon blacks that are easily dispersed. For the high surface area- and/or low structure-carbon blacks, however, CEC provides an advantage over dry mixing, especially at high filler loading. When CEC technology was applied to the off-the-road tyre tread compounds, the tread wear was improved by 14% compared with a conventionally compounded tyre [46].

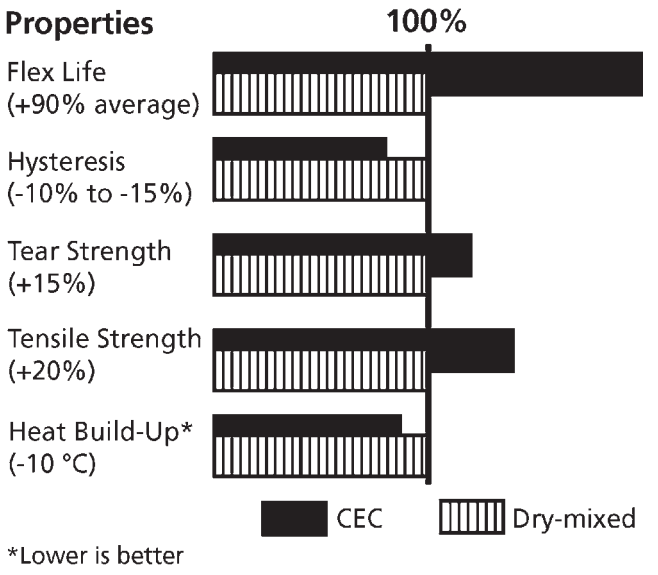

Figure 6.13 Comparison of vulcanisate properties between CEC and dry-mixed compounds

Most of the commonly used carbon black grades are shown on a plot of nitrogen surface area *versus* dibutylphthalate absorption of the compressed sample (CDBP) in **Figure 6.14**. It can be seen that there is a line of increasing structure and decreasing surface area below which carbon black is considered to be un-dispersible in rubber. Hence, those grades below the line are considered to be non-rubber grades. With CEC technology, the dispersion of carbon black in the compound is independent of its morphology. So the grades of carbon black that can be used for rubber reinforcement can be greatly expanded *via* CEC technology. In fact over the practical range of loading, carbon blacks with surface areas as high as 260 m^2/g and CDBP as low as 40 ml/100 g (BP 1100) have been successfully dispersed in the polymer matrix with excellent dispersion quality. This effectively opens up a new range of filler materials for use in rubber reinforcement. The carbon blacks that are now accessible may impart some unusual properties to the filled rubber compounds, such as superior tear strength, and high ultimate properties with much lower hardness dependence than have ever been seen with conventional vulcanisates [10].

6.6.2 Powdered Rubber

The development of filler/rubber masterbatches in a free flowing powder form was first carried out in the 1970s with the goal of simplifying the production of rubber compounds

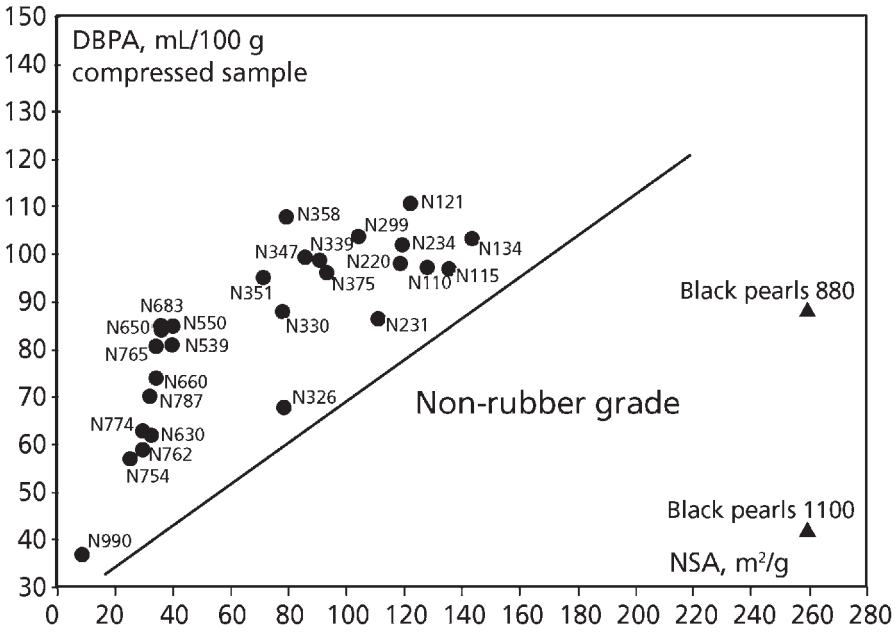

Figure 6.14 Map of structure *versus* surface area showing rubber grades of carbon black and some non-rubber grades. DBPA: dibutyl phthalate absorption number. NSA: Nitrogen surface area. The N numbers are ASTM designations

and reducing compounding cost [47]. This technology has been further developed in the last decade, and like CEC, it has enabled some new levels of performance to be achieved with conventional types of fillers. Powdered rubber technology is also well suited to continuous mixing as well as batch mixing processes.

6.6.2.1 Production of Powdered Rubber

The production process for powdered rubber, which is basically a batch process, is presented in **Figure 6.15** [48]. First, a stable polymer latex (either NR latex, emulsion polymerised polymer latexes or emulsionised solution-polymerised polymers) is prepared. A filler suspension that has previously been exactly adjusted according to the particular particle size of the filler is then added, together with various additives. The mixture of the latex and filler suspension is homogenised under intensive stirring in an agitator tank. Co-precipitation of the mixture is achieved using various chemicals that influence the pH of the suspension, causing the coagulating latex to surround each individual filler particle. A separate filler fraction is added to form an efficient separating layer around each powdered rubber particle so that after precipitation,

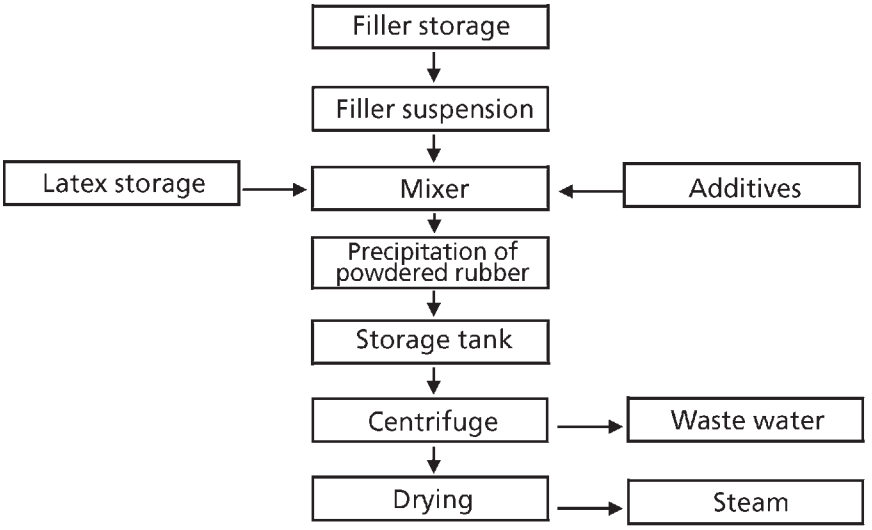

Figure 6.15 Flow diagram of powdered rubber production

the particles do not stick together. If necessary, the product in water can be subjected to a maturing process of several hours in a homogenisation tank. Then, most of the water is removed in a centrifuge, after which the finely divided batch is further dried down to a moisture content of under 1%. The products end up in a free flowing form after drying.

6.6.2.2 Mixing of Powdered Rubber

Powdered rubber can be mixed with other compounding ingredients using typical batch mixing processes (internal mixer or open mill) or by continuous mixing processes. In the internal mixer, it is suggested that the other ingredients are best added in a modified upside-down process. Because a high quality of dispersion can be obtained after a very short mixing time, it is suggested that the mixing stages and time can be reduced.

Due to the free-flowing form of the masterbatch, the powdered rubbers are especially suitable for the continuous mixing processes that have long been applied to thermoplastic materials. With powdered rubber, all compound ingredients can be fed into a continuously operating extruder mixer that can achieve enough shear force to equal to the shear condition of a mill or internal mixer over a relatively short time.

6.6.2.3 Properties of Powdered Rubber Compounds

Compared with conventionally mixed compounds, the emulsion SBR (ESBR)/carbon black powdered rubber gives better filler dispersion and higher bound rubber. The die swell at different shear rates is also lower. With regard to the physical properties of vulcanisates, slightly better or comparable ultimate properties were observed in the carbon black powdered rubber compounds, with almost equal rebound, hysteresis and hardness. The DIN abrasion was somewhat improved, which is consistent with good filler dispersion [48, 49].

In a NR formulation, comparable compound viscosity was achieved at 3 phr lower filler loading compared to the standard mixed counterpart. The powdered rubber material gave similar vulcanisate stress-strain properties, higher ball rebound and lower hysteresis, but the abrasion resistance has not been reported.

6.6.2.4 Silica-Loaded ESBR Powdered Rubber

When all-silica tread compounds were introduced to passenger car tyres, one of the disadvantages was their poor processability, especially related to mixing. Another feature of these compounds was the application of solution-polymerised polymers, i.e., S-SBR and BR [50]. ESBR has not been used much in all-silica tread compounds due the high concentration of surfactants and other polar substances remaining in the polymer from its production. These small chemicals may interfere with the coupling reactions between silane and polymer chains, resulting in a poor polymer-filler interaction, hence unsatisfactory tread wear resistance [2, 30]. By using the powdered rubber process, it is possible to complete the reaction of the silane coupling agent with the silica before it is exposed to the emulsion polymer, thus overcoming this problem. In practice, silica and silane are brought together during the production of the silica suspension in water. Since the two materials have very different polarities, a homogeneous phase that is essential for the silane attachment on the silica surface is not formed. Therefore, so-called phase mediators are also added in the suspension. After the rubber emulsion is added, the silica/silane/rubber system is coagulated at room temperature using acids. This process takes place exclusively in the aqueous phase, i.e., in a single-phase system. During coagulation, the silica treated with silane is enveloped by the polymer. After coagulation, the process water is separated mechanically and the product is dried. During the drying process, the organosilane is chemically reacted on the silica surface with ethanol being split off [51]. The silica/silane/ESBR powdered rubbers can be mixed with either conventional internal mixers or a continuous mixer. In both cases, the mixing procedures can be significantly simplified. When the materials are compared with their conventionally mixed counterparts, filler dispersion is improved, the Mooney viscosities of the compounds are higher, and die swell is smaller. For the physical properties of the vulcanisates, the powdered rubber is characterised by higher tensile strength and

stress at 300% elongation, somewhat lower hysteresis, and significantly improved DIN abrasion. However, no comparison was reported with the dry mixed S-SBR compounds, which are commonly used in silica tyres.

6.7 Concluding Remarks

A number of potentially significant breakthroughs in reinforcing fillers for the rubber industry have been achieved in recent years. Whilst carbon black has been for many years, and is likely to remain, the dominant reinforcing filler for many applications, recent work on this material has shown that in addition to traditional approaches of changing particle morphology, new approaches can significantly change the performance of carbon black in rubber reinforcement. Examples are the surface chemical modification of carbon black and control of microstructure. Silica is already established as an alternative reinforcing filler to carbon black, with certain advantages and disadvantages. Recent advances in silica materials include development of more hydrophobic and more easily dispersible grades of precipitated silica. Other non-black fillers such as starch and organo-clays have been developed to provide specific advantageous properties to certain rubber compounds.

The development of dual phase particles, containing both silica and carbon domains, was an attempt to combine the advantages of both of these materials. In fact, these new particles have been found to provide an excellent combination of rolling resistance, wear resistance and wet traction, the critical requirements for tyre applications. In some respects these 'composite' particles provide better performance than either silica or carbon black. The successful development of these dual phase particles could lead to further development of other non-homogeneous particles to provide specific performance properties in rubber compounds.

In any particulate-filler rubber compound, the degree and quality of dispersion of the particles in the compounds is often a critical aspect of performance. Achieving the dispersion of filler in rubber is also generally energy intensive and time consuming. It is therefore not surprising that considerable research effort has gone into new technologies for mixing and dispersing fillers in rubber. The development of powdered rubber and Cabot Elastomer Composite technology are two examples of novel ways in which rubber and filler can be combined. It seems likely that with increasing demands for automation, energy efficiency and quality, the trend towards these new mixing processes will continue.

References

1. R.N. Rothon, *Particulate Fillers for Polymers*, Rapra Review Report No.141, 2002, **12**, No 9.

2. M-J. Wang in *Powders and Fibers: Interfacial Science and Applications*, Eds., M. Nardin and E. Papirer, CRC Press, Boca Raton, FL, USA, 2007.

3. M-J. Wang, *Rubber Chemistry and Technology*, 1998, **71**, 3, 520.

4. M-J. Wang, Y. Kutsovsky, P. Zhang, L. J. Murphy, S. Laube and K. Mahmud, *Rubber Chemistry and Technology*, 2002, **75**, 4, 247.

5. S. Wolff and U. Görl, inventors; Degussa AG, assignee; US 5,159,009, 1992.

6. B. Keoshkerian, M.K. Georges and S.V. Drappel, inventors; Xerox Corporation, assignee; US 5,545,504, 1996.

7. G.A. Joyce and E.L. Little, inventors; Columbian Chemical Company, assignee; US 5,708,055, 1998.

8. J.A. Belmont, inventor; Cabot Corporation, assignee; US 5,554,739, 1996.

9. J.A. Belmont, R.M. Amici and C.P. Galloway, inventors; Cabot Corporation, assignee; US 5,851,280, 1998.

10. M-J. Wang, *Kautschuk und Gummi Kuntstoffe,* 2005, **58**, 12, 626.

11. N. Tokita, M-J. Wang, B. Chung and K. Mahmud, *Journal of the Society of Rubber Industry, Japan*, 1998, **72**, 522.

12. A.R. Payne, *Journal of Applied Polymer Science*, 1962, **6**, 19, 57.

13. J.A.C. Harwood, A.R. Payne and R.E. Whittaker, *Rubber Chemistry and Technology*, 1971, **44**, 3, 440.

14. C. Vögler, K. Vögel, W. Niedermeier, B. Freund and P. Messner, inventors; Degussa-Hüls AG, assignee; EP 949303B1, 2004.

15. C. Vögler, K. Vögel, W. Niedermeier, B. Freund and P. Messner, inventors; Degussa-Hüls AG, assignee; US 6,251,983, 2001.

16. W. Niedermeier and B. Freund, *Tire Technology International*, 1998, p.25.

17. B. Freund and F. Forster, *Kautschuk und Gummi Kunststoffe*, 1996, **49**, 11, 774.

18. W. Niedermeier and B. Freund, *Kautschuk und Gummi Kunststoffe*, 1999, **52**, 10, 670.

19. K. Mahmud, M-J. Wang and R.A. Francis, inventors; Cabot Corporation, assignee; US 5,830,930, 1998.

20. K. Mahmud and M-J. Wang, inventors; Cabot Corporation, assignee; US 5,869,550, 1999.

21. K. Mahmud and M-J. Wang, inventors; Cabot Corporation, assignee; US 5,904,762, 1999.

22. K. Mahmud, M-J. Wang and Y. Kutsovsky, inventors; Cabot Corporation, assignee; US 6,364,944, 2002.

23. L.J. Murphy, M-J. Wang and K. Mahmud, *Rubber Chemistry and Technology*, 2000, **73**, 1, 25.

24. M-J. Wang, Y. Kutsovsky, P. Zhang, G. Mehos, L.J. Murphy and K. Mahmud, *Kautschuk und Gummi Kunststoffe*, 2002, **55**, 1-2, 33.

25. M-J. Wang, H. Tu, L.J. Murphy and K. Muhmud, *Rubber Chemistry and Technology*, 2000, **73**, 4, 666.

26. M-J. Wang, K. Mahmud, L.J. Murphy and W.J. Patterson, *Kautschuk und Gummi Kunststoffe*, 1998, **51**, 348.

27. M-J. Wang, Internal Cabot Data, to be published.

28. R.B. Knill, D.J. Shepherd, J.P. Urbon and N.G. Endter in *Proceedings of the International Rubber Conference*, Kuala Lumpur, Malaysia, 1975, Volume V, p.212.

29. K. Mahmud, M-J. Wang, S.R. Reznek and J.A. Belmont, inventors; Cabot Corporation, assignee; US 5,916,934, 1999.

30. M-J. Wang, P. Zhang and K. Mahmud, *Rubber Chemistry and Technology*, 2001, **74**, 1, 124.

31. T. Kawazura, H. Kaido, K. Ikai, F. Yatsuyanagi and M. Kawazoe, inventors; Yokohama Rubber Co., assignee; US 5,679,728, 1997.

32. P.J. Watson in *Proceedings of the IRG Tyretech '99 Conference*, Prague, Czechoslovakia, 1999, Paper No.10.

33. K. Mahmud, M-J. Wang, S.R. Reznek and J. A. Belmont, inventors; Cabot Corporation, assignee; US 6,197,274, 2001.

34. D. Shaw, *European Rubber Journal*, 2004, **186**, 4, 22.

35. *European Rubber Journal*, 2001, **183**, 4, 34.

36. R.L. Whistler and J.R. Daniel in *Kirk-Othmer Encyclopedia of Chemical Technology*, 4th Edition, John Wiley and Sons, New York, NY, USA, 1997, Volume 22, p.699.

37. F.G. Corvasce, T.D. Linster, and G. Thielen, inventors; The Goodyear Tire and Rubber Company, assignee; EP795581B1, 2001.

38. C. Bastioli, V. Bellotti and G. Del Tredici, inventors; Butterfly Srl, C. Bastioli, V. Bellotti, G. Del Tredici, assignees; WO 91/02025, 1991.

39. H. Sandstrom, inventor; The Goodyear Tire and Rubber Company, assignee; EP1074582, 2001.

40. M. Ganter, W. Gronski, H. Semke, T. Zilg, C. Thomann and R. Muhlhaupt, *Kautschuk und Gummi Kunststoffe*, 2001, **54**, 4, 166.

41. W. Gronski and F. Schon, *Proceedings of the IRG International Rubber Conference 2003*, 2003, Nuremberg, Germany, p.297.

42. M.A. Mabry, F.H. Rumpf, J.Z. Podobnik, S.A. Westveer, A.C. Morgan, B. Chung and M.J. Andrew, inventors; Cabot Corporation, assignee; US 6,048,923, 2000.

43. M-J. Wang, T. Wang, Y.L. Wong, J. Shell and K. Mahmud, *Kautschuk und Gummi Kunststoffe*, 2002, **55**, 7-8, 388.

44. T. Wang, M-J. Wang, J. Shell, Y-L. Wong and V. Vejins in *Proceedings of the 16th ACS Rubber Division Meeting*, Cleveland, OH, USA, Fall 2003, Paper No.24.

45. M-J. Wang and T. Wang, *Cabot Internal Report, CIM-01-37*, 2001. unpublished.

46. T. Wang, M-J. Wang, J. Shell, V. Vejins, Y-L. Feng, G-Q. Feng and Z. Jin, *Rubber World*, 2003, **227**, 6, 33.

47. K-H. Nordseik and G. Berg, *Kautschuk und Gummi Kunststoffe*, 1975, **28**, 7, 397.

48. U. Görl and K-H. Nordseik, *Kautschuk und Gummi Kunststoffe*, 1998, **51**, 4, 250.

49. U. Görl and M. Schmitt, *Rubber World*, 2001, **224**, 1, 41.

50. R. Rauline, inventor; Michelin & Cie, assignee; EP 0501227B1, 1995.

51. U. Görl in *Proceedings of the ACS Rubber Division Meeting*, Pittsburgh, PA, USA, Fall 2002, Paper No.11.

7 Thermoplastic Elastomers by Dynamic Vulcanisation

Kinsuk Naskar

7.1 Introduction

This chapter introduces various aspects of dynamic vulcanisation as applied to thermoplastic elastomers. The classification of polymer blends and thermoplastic elastomers, the development of thermoplastic vulcanisates, and the application of various types of crosslinking systems with special emphasis on peroxides/co-agents, and phenolic resins as crosslinking agents for PP/EPDM blends are reviewed. The morphology and rheology of thermoplastic vulcanisates and their typical end-use applications are also discussed.

7.2 Polymer Blends

Polymer blends have played a significant role in the last few decades in revolutionising polymer technology, leading to important and useful applications. The term 'polymer blend' may be defined as a combination of two or more structurally different polymers giving rise to materials with a range of properties, not delivered by any of the constituents. Thus, the reasons for using blends include the attainment of specific article performance, by improving the technical properties of the original polymers, or by adjusting the processing characteristics and reducing the cost [1-5].

Polymer blends may be categorised in general into two broad classes: immiscible and miscible blends. Immiscible blends are those, which exist in two distinct phases, but are still very useful materials, e.g., toughened plastics. Miscible blends are those that exist in a single homogeneous phase and may exhibit synergistic properties, different from those of the pure components. Apart from these two, there exists a third category of blends, often known as technologically compatible blends or alloys. Alloys are those blends which exist in two or more different phases on the micro-scale, but exhibit macroscopic properties akin to that of a single-phase material [5, 6].

Depending on the relative proportions of the constituent polymers, rubber-thermoplastic blends can be classified broadly into three types:

- *High plastic-low rubber blend*: Impact resistant rubber toughened thermoplastics;

- *Low plastic-high rubber blends*: Vulcanisable rubbers containing various amounts of resins acting as reinforcing or stiffening agents;

- *Rubber-plastic blends* in compositions such as 70:30 showing thermoplastic elastomeric (TPE) behaviour [6-10]. A TPE is thus a rubbery material with properties and functional performance similar to those of a conventional vulcanised rubber but it can still be processed in a molten state as a thermoplastic polymer.

7.3 Classification of TPE

TPE may be divided into the following classes according to their chemistry and morphology:

1. (Soft) triblock copolymers; e.g., styrene-butadiene-styrene (S-B-S) or styrene-ethylene butylene-styrene (S-EB-S) and so on,

2. (Hard) multiblock copolymers; e.g., thermoplastic polyurethanes (TPU), thermoplastic polyamides (TPA) and so on,

3. Blends of rubbers and thermoplastics (EPDM/PP) wherein the rubber phase remains either uncrosslinked or dynamically crosslinked to different extents [6-10].

The field of TPE based on polyolefin rubber/thermoplastic compositions, has grown along two distinctly different product-lines or classes: one class consists of simple blends and is commonly designated as thermoplastic elastomeric olefins (TEO). In the other class, the rubber phase is dynamically vulcanised (by simultaneously mixing and crosslinking), giving rise to a thermoplastic vulcanisate (TPV) or dynamic vulcanisate (DV) according to ASTM D6338 [11].

7.4 Dynamic Vulcanisation

The dynamic vulcanisation process was discovered by Gessler [12] in 1962. The first TPE introduced to the market based on a crosslinked rubber-thermoplastic composition (1972), was derived from Fischer's [13] discovery of partial crosslinking of the EPDM phase of EPDM/PP with peroxide. Fischer controlled the degree of vulcanisation by limiting the amount of peroxide, to maintain the thermoplastic processability of the blend. Significant improvements in the properties of these blends were achieved in 1978 by Coran, Das and Patel [14] by fully vulcanising the rubber phase under dynamic shear, while maintaining the thermoplasticity of the blends. These blends were further improved by Abdou-Sabet and Fath [15] in 1982 by the use of phenolic resins as curatives, in order to improve the rubber-like properties and the processing characteristics.

Extensive studies on dynamically vulcanised TPE were carried out by Coran and Patel in the early 1980s [16-22]. Compositions containing all possible combinations of selected types of rubber with selected types of thermoplastics were prepared. The rubbers included butyl rubber (IIR), EPDM, natural rubber (NR), butadiene rubber (BR), styrene-butadiene-rubber (SBR), ethylene vinyl acetate, acrylate rubber, chlorinated polyethylene, polychloroprene and nitrile rubber (NBR). The thermoplastics included PP, polyethylene, polystyrene, acrylonitrile-butadiene-styrene terpolymer, styrene-acrylonitrile copolymer, polymethyl methacrylate, polybutylene terephthalate, polyamide and polycarbonate [23]. Only a few of the blends were commercialised, because most of these blends were not technologically compatible and they required one or more steps to make them compatible. The TPV represent the second largest group of soft thermoplastic elastomers, after styrenic based block copolymers. Commercialised dynamic vulcanisates are commonly based on blends of unsaturated EPDM rubber and PP, and to a lesser extent on a combination of BR [24], NR [25-27] or NBR [6, 232] with PP. For blends of dissimilar polymers, for example NBR/PP, compatibilising agents are used. These systems show the closest match in properties with regularly vulcanised rubbers within a hardness range of Shore A of 40-90. TPV have shown a consistently strong market growth (~ 12% per year) over the last two decades.

7.5 Production of TPV

Polymer blends are generally prepared by melt mixing, solution blending or latex blending. TPV are normally produced by melt mixing techniques. In general, mixing extruders and co-rotating close-intermeshing twin screw extruders with a high length:diameter (L/D) ratio are suitable for the preparation of TPV in a continuous process. For batch processes, internal mixers are generally employed.

Dynamic vulcanisation processes are not entirely satisfactory for making soft products, because as the rubber level rises, the resulting compositions become more difficult to process. For example, the compositions give poor extrudates and sometimes cannot be extruded at all. Accordingly, there is scope for research in process development for preparing soft, extrusion-fabricable thermoplastic elastomeric products. Abdou-Sabet and Shen [28] found that in a process for preparing TPV based on PP/EPDM blends by dynamic vulcanisation, improved properties could be achieved when the mixing shear rate was at least 2000/s in a co-rotating twin screw extruder, with the thermoplastic component in the molten condition, typically at about 170-230 °C. Preferably, the blend is subjected during vulcanisation to a shear rate of about 2500-7500/s. In that case, vulcanisation is complete within 20-60 seconds. The resulting TPV exhibits higher tensile strength and greater elongation, and processability of the products improves as well.

7.6 PP/EPDM TPV

Characteristics of various commercially available PP/EPDM TPV are shown in **Table 7.1** [29].

A whole range of grades of varying hardnesses is made available by changing the PP/EPDM ratio and adding an extender oil.

7.6.1 Crosslinking Agents For PP/EPDM TPV

Several crosslinking agents have been used to crosslink the EPDM phase in PP/EPDM blends: co-agent assisted peroxides, activated phenol-formaldehyde resins, commonly known as resol-resins, platinum catalysed hydrosiloxane, vinyltrialkoxysilane/moisture, catalysed quinonedioxime and bisthiols [30]. Recently, the use of a special crosslinking agent like benzene-1,3-bis(sulfonyl)azide for the preparation of TPV was investigated by Lopez Manchado and Kenny [31]. They concluded that the sulfonyl-azide group can act as an effective crosslinking agent for the elastomeric phase and as a coupling agent between the elastomeric and thermoplastic phases. The cure rate, the final crosslink density, the thermal stability of the crosslinks formed, the safety, health and environmental characteristics of the chemicals used and the cost are all relevant parameters for the final choice of the crosslinking system [30].

Sulfur vulcanisation of EPDM rubber and other elastomers is normally performed in the presence of activators (ZnO and stearic acid) and accelerators, e.g., dibenzothiazole

Table 7.1. Manufacturer, trade name, hardness range and area of applications of various commercialised TPV

Manufacturer	Trade Name	Hardness Range	Area of Application
Advanced Elastomer Systems (AES)	Santoprene	35 Shore A to 50 Shore D	Automotive, construction, consumer goods, electrical, fluid delivery, grips, medical and packaging etc.
DSM	Sarlink	35 Shore A to 50 Shore D	Automotive, building and construction, industrial and consumer products (specially, soft touch applications) etc.
Softer SpA	Forprene	35 Shore A to 65 Shore D	Automotive, construction, consumer goods, etc.
Himont	Dutralene	35 Shore A to 50 Shore D	Automotive, construction, consumer goods, etc.
Mitsui	Milastomer	50 Shore A to 40 Shore D	Automotive, construction, consumer goods, etc.

disulfide (MBTS), tetramethyl thiuram disulfide (TMTD) and so on. It is proven that the mechanism of sulfur vulcanisation of EPDM is more or less similar to the mechanism normally accepted for polydiene elastomers [32, 33]. Sulfur/accelerator combinations have been demonstrated by Coran and Patel [16] to be applicable in principle to dynamic vulcanisation of PP/EPDM blends. A typical recipe is shown in **Table 7.2**.

An increase in the amount of sulfur from 0 to 2.0 phr in the above recipe resulted in a dramatic improvement in the elasticity of a PP/EPDM 40/60 blend. The tensile strength increased from 4.9 to 24.3 MPa, the elongation at break from 190 to 530% and the tension set decreased from 66% to 16%. Particle size in the dynamically vulcanised blends had a pronounced effect on mechanical properties, as demonstrated by Coran and Patel [16]. As the particle size was reduced, the elongation at break and tensile strength increased rapidly. However, sulfur crosslinking systems are not used in commercial PP/EPDM TPV, since PP has a relatively high melting point and the crosslinks lack thermal and UV stability. Moreover, the production and processing of these TPV suffer from severe stench problems [29].

The most important crosslinking agents for PP/EPDM TPV are peroxides, phenolic resins and grafted silanes. They are discussed next.

7.6.1.1 Peroxides

Crosslinking elastomers with peroxides has been known for many years. In 1915, Ostromyslenski announced that NR could be converted to a crosslinked state by treatment with dibenzoyl peroxide [34, 35]. However, serious interest in vulcanisation with peroxides commenced only with the commercial introduction of dicumyl peroxide (DCP) in the late 1950s [36]. Because of this interest, a number of peroxide types and

Table 7.2. Typical recipe of TPV composition (sulfur cured)

Component	Amount (phr)
EPDM	100
Polyolefin resin	X
ZnO	5
Stearic acid	1
Sulfur	Y
TMTD	Y/2
MBTS	Y/4

phr: parts per hundred rubber
X: variable phr of polyolefin resin
Y: variable phr of sulfur

formulations were developed, which overcame various drawbacks related to thermal stability, crosslinking efficiency and the handling and safety aspects of the few existing peroxide types.

The mechanism of peroxide crosslinking of EPDM is less complicated than sulfur vulcanisation. In principle, the crosslinking of high polymers by organic peroxides can be divided into three successive steps [37-39]. A general scheme for the mechanism of action of a peroxide is shown in **Figure 7.1a**. The first step is the homolytic decomposition of the peroxide and the generation of free radicals. This is the rate-determining step of the overall reaction. The second step is the abstraction of hydrogen atoms from the polymer chain, resulting in stable peroxide decomposition products and polymer radicals. The final step consists of the combination of two polymer radicals to form a C-C crosslink. Sometimes, undesirable side reactions like disproportionation or β-chain scission can also take place during the crosslinking process, which is shown in **Figure 7.1b**.

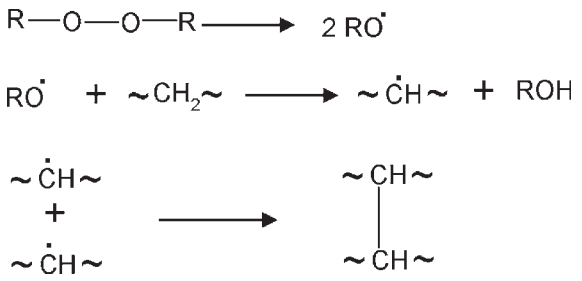

(a) *General crosslinking mechanism of a peroxide*

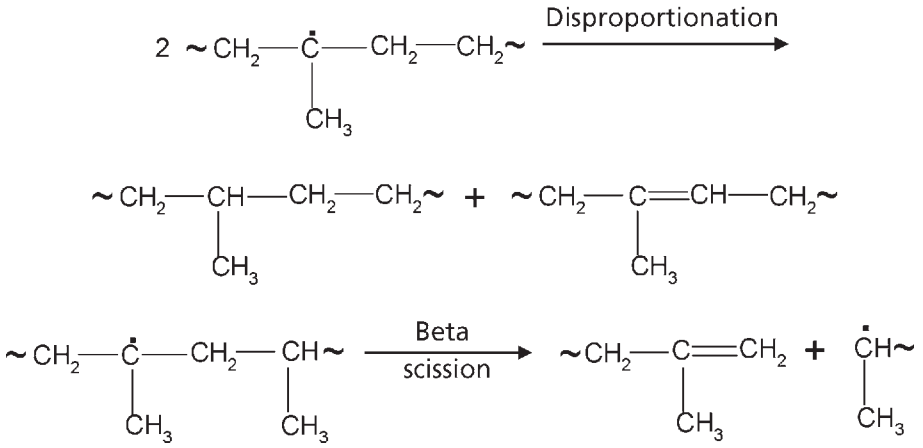

(b) *Disproportionation and beta chain scission reaction*

Figure 7.1 General crosslinking mechanism of a peroxide

The crosslinking efficiency (ε_c), of a peroxide is defined as the number of moles of chemical crosslinks formed per mole of reacted peroxide. Normally for the peroxide vulcanisation of some highly unsaturated elastomers like SBR and BR, ε_c values higher than 10 are found, whereas for saturated elastomers, values of ε_c of less than 1 are generally observed. For example, for the crosslinking of ethylene propylene rubber (EPR) without any diene, crosslinking efficiencies of 0.1 to 0.8 were reported [40, 41]. The overall crosslinking efficiency of a peroxide is the result of the efficiencies of all five reaction steps mentioned before [42]. Various types of side reactions may also interfere with the crosslinking process, either by consuming the peroxide in non-productive ways or by simply degrading the polymer [43]. The efficiency of the total crosslinking reaction depends mainly on the type of peroxide and polymer radicals formed during the process. The relationship between peroxide structure and crosslinking efficiency has been described by Endstra [42].

The main peroxide categories, depending on their chemical nature, used in the crosslinking of rubber-based compounds are [44, 45]:

- Dialkyl peroxides,
- Alkyl-aralkyl peroxides,
- Diaralkyl peroxides,
- Peroxy-ketals, and
- Peroxy-esters.

Compounds of the dialkyl peroxide class belong to the most thermally stable category, whereas the peroxy-esters possess only a limited thermal stability: for a rubber compound this greatly restricts the practical suitability of these materials for crosslinking.

The general advantages of peroxide crosslinking systems can be summarised as follows [46]:

1. Simple formulation,
2. Ability to store the peroxide containing compound over a long time without scorching,
3. Rapid vulcanisation without reversion,
4. Ability to crosslink saturated as well as unsaturated rubbers,
5. High temperature resistance of the vulcanisates,
6. Good compression set properties of the vulcanisates (elastic recovery) at elevated temperature,

7. No moisture uptake of the TPV, and

8. No staining or discoloration of the finished products.

The most important characteristic of a crosslinking peroxide is its decomposition rate, which is generally expressed by its half-life ($t_{1/2}$) at a particular temperature. The latter is also a measure of the thermal stability of the peroxide. The half-life is the time required for one-half of the molecules in a given amount of peroxide to decompose at a certain temperature. Commonly, the half-life is determined by differential scanning calorimetry - thermal activity monitoring (DSC-TAM) of a dilute solution of the peroxide in monochlorobenzene [46]. The dependence of the half-life on temperature can theoretically be described by an Arrhenius equation:

$$k_d = A.e^{-\frac{E_a}{RT}} \tag{7.1}$$

$$\text{and } t_{1/2} = \frac{\ln 2}{k_d} \tag{7.2}$$

where:

k_d = rate constant for the peroxide decomposition (s^{-1})

A = Arrhenius frequency factor (s^{-1})

E_a= activation energy for the peroxide decomposition (J/mol)

R = gas constant = 8.3142 (J/mol.K)

T = temperature (K) and

$t_{1/2}$ = half-life (s)

As a rough estimation, the cure time needed for a peroxide-containing EPDM rubber compound is about seven times the half-life value at a specific temperature [45]. Other important considerations while selecting a peroxide for crosslinking are the minimum cure time, the self accelerating decomposition temperature and the maximum storage temperature.

When peroxides are added to PP/EPDM blends, however, the PP tends to undergo degradation *via* β-scission of the polymer backbone under the action of the free radicals generated by the decomposition of the peroxide. This reaction occurs when two tertiary carbon atoms along the main polymer chain are separated by only one secondary carbon atom, as discussed earlier (**Figure 7.1b**). On the other hand, the EPDM phase of the blend can be crosslinked in the presence of the peroxide.

The main factors that influence the peroxide crosslinking efficiency of EPR and EPDM are [47-50]:

- The type and amount of termonomer,
- Ethylene/propylene ratio,
- The randomness of monomer distribution,
- Polymer molecular weight, and
- Molecular weight distribution.

For example, the higher the ethylene/propylene ratio, the better is the crosslink density of EPR or EPDM. Baldwin and co-workers [41] studied about ten different kinds of dienes and concluded that methylene-norbornene and vinylidene-norbornene (VNB) are most efficient for peroxide curing. The effects of termonomer type and content on the peroxide crosslinking efficiency of EPDM were also studied by van Duin and Dikland [51] by identifying the products formed on peroxide decomposition in low-molecular weight model substrates (alkanes and alkenes), using gas chromatography combined with mass spectroscopy detection. They reported that EPDM containing termonomers with terminal unsaturated groups are more reactive than those with internal unsaturated groups. Advances were made recently in the attempt to further increase the crosslinking density of TPV, cured with a peroxide/co-agent through the use of a reactive VNB-containing EPDM rubber [52].

The damaging effects of β-scission of propylene-rich sequences in EPDM can be partially avoided, and the crosslinking efficiency of a peroxide enhanced, by the addition of a suitable co-agent. Co-agents are basically multi-functional reactive compounds, in most cases possessing multiple allylic groups. Several mechanisms for the increase in crosslinking efficiency in the presence of co-agents with unsaturated moieties have been proposed. In most cases, a fast reaction is supposed to take place between the co-agent and the labile tertiary macroradical, thereby suppressing the unwanted side reactions like β-scission and disproportionation [38, 53-55]. According to Dikland and co-workers [56-58], polar co-agents do not dissolve in the non-polar polyolefin EPDM matrix. Upon peroxide decomposition, the co-agent domains become rapidly crosslinked *via* free radical addition and cyclo-polymerisation reactions, resulting in small, vitrified thermoset particles. Consequently, they act as multifunctional crosslinkers for EPR or EPDM. However, the solubility of the co-agent in the rubber is also an important issue. So, Dikland's model primarily depends on the solubility parameter values of actual co-agents and rubbers being used.

Some of the benefits [43, 59, 60] that co-agents afford are:

- Improved heat ageing,
- Higher modulus,

- High tensile and tear strength,
- Higher hardness,
- Improved compression set, and
- Increased abrasion resistance.

Co-agents are generally classified into two main categories, based on their effects on the rate of cure [38, 43, 61]. The first type includes acrylates, methacrylates, and bismaleimides, which increase the rate of cure. Most of them contain readily accessible unsaturation without allylic hydrogens and therefore they react only *via* addition reactions. Examples of the second category are triallyl cyanurate (TAC), triallyl isocyanurate, triallyl phosphate, divinyl benzene and a small amount of sulfur. Unlike the first category, most of the co-agents of the second type contain readily accessible vinyl unsaturation and sites for radical addition as well as an ample amount of easily abstractable allylic hydrogens. Addition is their most important mechanism, but hydrogen-abstraction can also be expected to take place to a considerable extent. 1,2-Polybutadiene resins as co-agents also improve the heat, chemical and solvent resistance of EPDM and EPR [62].

The effect of different types of peroxides as crosslinking agents in combination with TAC as a co-agent on the properties of PP/EPDM TPV at a fixed as well as at varied blend ratios was studied recently by Naskar and Noordermeer [63]. **Table 7.3** shows the TPV compositions at varied PP/EPDM blend ratios with peroxide/coagent and their corresponding properties.

The main roles of the co-agent here are twofold: first, to improve the crosslinking efficiency of the peroxide and second, to diminish the PP-degradation (*via* chain scission). The physical properties of TPV change significantly with the chemical nature of the peroxides, the extent of crosslinking of the EPDM-phase and the extent of degradation of the PP-phase. Three main parameters are identified as governing the final mechanical properties of the TPV: the solubility parameter of a peroxide relative to the polymers, PP and EPDM; the decomposition mechanism of the peroxide and the kinetic aspects of the peroxide fragmentation. Variation of the tensile strength and compression set of the TPV with the various peroxides can be related to the solubility parameter of the peroxide and the rubber. The closer the solubility parameter of the peroxide to that of the EPDM, the higher is the tensile strength and the better is the compression set property. The Young's modulus of peroxide-cured TPV only shows a slight correlation with the delta torque (maximum torque – minimum torque) values of rubber process analyser (RPA) measurements on 'equivalent' pure EPDM vulcanisates (without any PP). The values of delta torque generally correspond to the crosslinking efficiencies of the peroxides. The higher the delta torque value, the better is the crosslinking efficiency of the peroxide and consequently the higher is the modulus of TPV. Dicumyl peroxide

Table 7.3. TPV compositions (phr) at varied PP/EPDM blend ratios with peroxide/co-agent and corresponding properties

Components	A1	A2	A3	A4	A5
EPDM	200*	200	200	200	200
PP	25	50	75	100	125
Peroxide					
DCP (40%)	6.1	6.1	6.1	6.1	6.1
Co-agent					
TAC (50%)	4.0	4.0	4.0	4.0	4.0
Stabilisers					
Irganox 1076	0.4	0.4	0.4	0.4	0.4
Irganox 168	0.4	0.4	0.4	0.4	0.4
Physical Properties					
Tensile Strength (MPa)	2.4	4.7	6.5	7.4	8.9
Elongation at break (%)	419	472	428	375	401
Young's Modulus (MPa)	2.4	14.0	40.8	71.2	108.7
Modulus at 300% (MPa)	1.8	3.4	4.5	5.5	6.8
Hardness (Shore A)	39	61	79	88	93
Overall crosslink density (v+PP) x 10^5 (mol/ml)	6.6	13.5	15.6	19.3	22.4
* *Including 50 wt% paraffinic oil*					

(DCP) in combination with TAC gives the best overall balance of all properties, since it performs the best considering the most important parameters described previously.

Commonly used peroxides generally produce volatile decomposition products, which provide an unpleasant smell or can show a blooming effect. For example, the typical sickly sweet smell of acetophenone, one of the decomposition products of DCP is well known. On the other hand, blooming phenomena can take place due to the formation of dihydroxy isopropyl benzene from the decomposition of di(*tert*-butylperoxyisopropyl) benzene, because of its limited solubility in the rubber matrix. Recently multifunctional peroxides were developed to overcome the previously mentioned drawbacks of the commonly used peroxides. They contain functional unsaturated groups (having co-agent functionality) in addition to a peroxide group. In this manner, part of the decomposition products is no longer volatile, nor gives rise to smell or blooming phenomena. The multifunctional peroxides provide performance properties of TPV, which are comparable with commonly used co-agent assisted peroxides [64]. Particularly, 2,4-diallyloxy-6-*tert*-butylperoxy-1,3,5-triazine (DTBT) turns out to be a good alternative for the DCP/TAC combination. DTBT has a solubility parameter on the high side of the spectrum, which

directs this peroxide and co-agent combination preferentially to the EPDM-phase during mixing. The co-agent functionality of this compound helps to improve the crosslinking effect, and it is comparable with DCP. The half life time of DTBT is very close to that of DCP, which results in a similar rate of vulcanisation. Moreover, the multifunctional peroxides investigated, do provide by-products after their decomposition, but without an unpleasant smell, unlike DCP.

7.6.1.2 Phenolic Resins

Phenolic resins are the polycondensation products of phenols and aldehydes. Phenolic resins are generally classified into two main classes: resols and novolacs. They have different chemical structures and reactivity, because of the variations in the phenol to aldehyde molar ratio and different pH levels used during their preparation [65]. Resols are generally characterised by the presence of reactive methylol groups and dimethylene-ether units, whereas novolacs do not contain any reactive methylol functionalities and thereby cannot act as crosslinking agents. The typical structure of an uncrosslinked resol-resin, containing a substituted alkyl group at the *para* position, is shown in **Figure 7.2**.

The application of resols as crosslinking agents for TPV is gaining importance due to the excellent high temperature properties of the products. Influence of different types of crosslinking systems on properties are given in **Table 7.4**.

The reaction mechanism of resol curing of ethylidene norbornene-containing (ENB) EPDM was extensively investigated by van Duin and co-workers [39, 66, 67] by using 2-ENB as a low molecular weight model compound. A mixture of crosslink precursors, crosslinks and side products with either an unsaturated methylene bridge structure or a saturated chroman ring was found to form, as shown in **Figure 7.3**.

Resols are used extensively for the crosslinking of EPDM in the production of TPV. The EPDM phase is generally crosslinked with reactive alkylphenolic resins (e.g., Schenectady® SP 1045) and halogen containing compounds. Metal halides from Brönsted acid complexes such as hydrated stannous chloride, ferric chloride or zinc chloride have been proposed as catalysts for this crosslinking system. During the crosslinking reaction, ether bridges are first split, yielding mono-phenolic units having benzylic cations (as shown in **Figure 7.3**). These benzylic cations then react with the unsaturation of EPDM rubber to accomplish the crosslinking [39, 65-67].

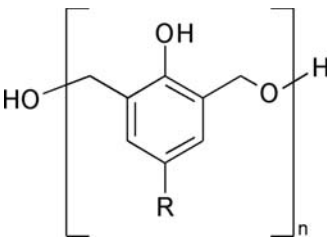

Figure 7.2 Typical structure of resol (R = iso-octyl and n = 1-3)

Table 7.4. Influence of various crosslinking agents on properties of EPDM/PP compositions

Property	Without Crosslinking Agent	Sulfur	Phenolic Resin	Peroxide
Hardness, Shore D	36	43	44	39
Tensile strength, MPa	5.0	24.3	25.6	15.9
M100, MPa	4.8	8.0	9.7	8.1
Ultimate elongation, %	190	530	350	450
ASTM No. 3 Oil swell, %	Disintegrated	194	109	225
Compression set, 22 h at 100 °C, %	91	43	24	32
** 60/40 EPDM/PP weight ratio*				

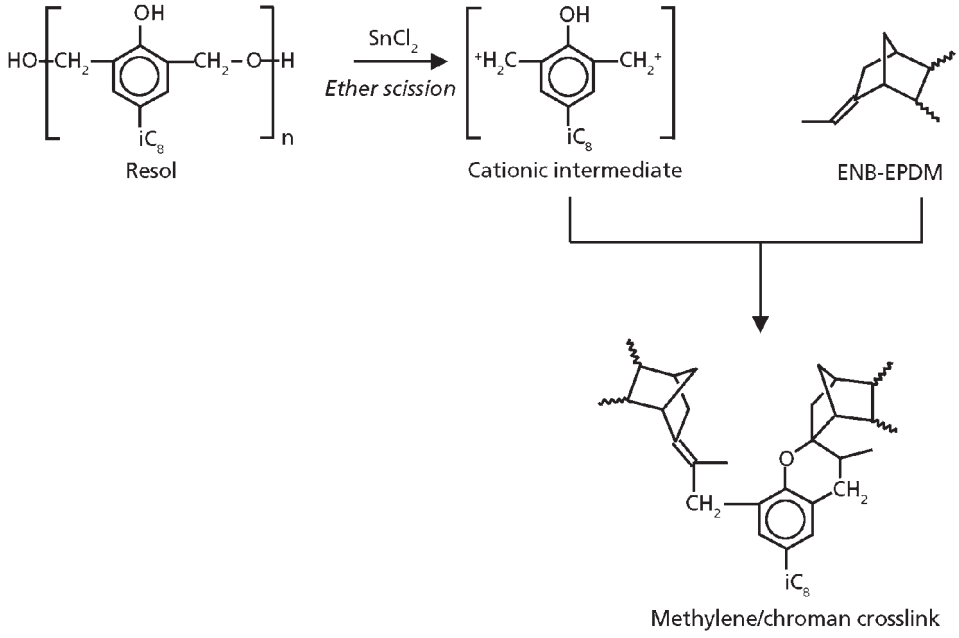

Figure 7.3 Reaction mechanism of activated resol cure of EPDM [66, 67]

Abdou-Sabet [68] demonstrated that the rubber-like properties of PP/EPDM or PP/NBR TPV could be improved by using dimethylol-octyl phenol curing resin. Improvements in compression set, oil resistance and processing characteristics of the material were achieved. These improvements were beyond those expected from the state of cure, and are probably due to *in situ* formation of a block copolymer between the rubber particles and the PP matrix [6]. The graft copolymer was assumed to be generated through the functionalisation of PP with dimethylol-octyl phenol, which then reacts with the rubber like EPDM or NBR as shown in **Figure 7.4**.

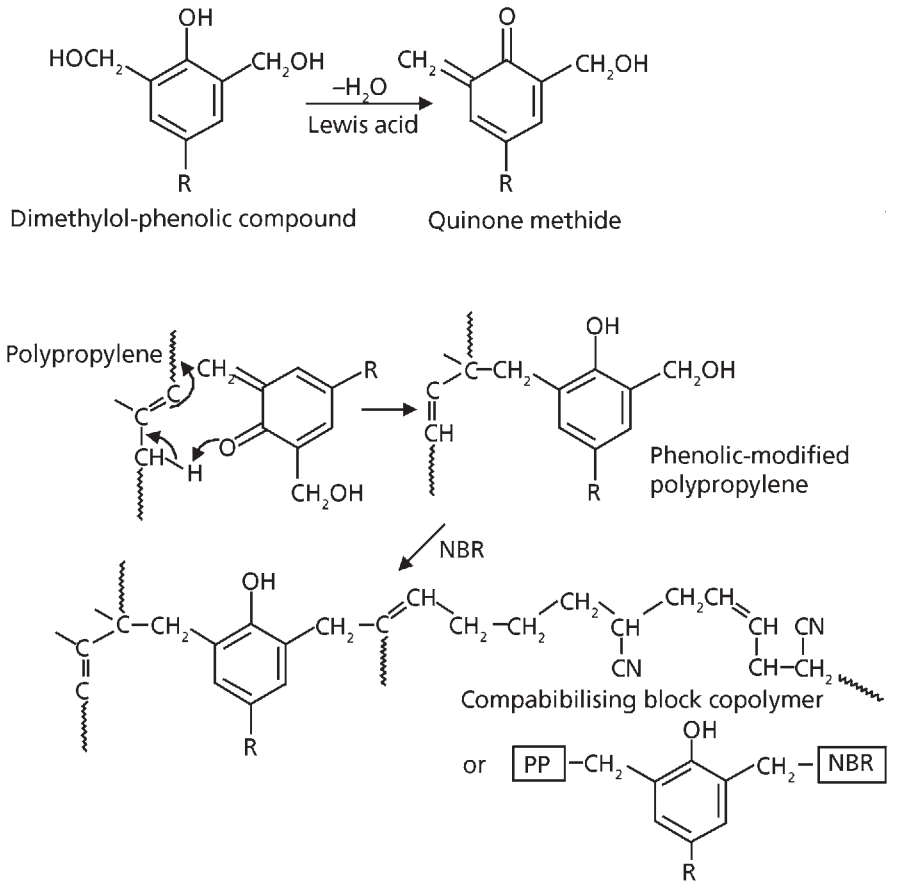

Figure 7.4 *In situ* formation of compatibilising block copolymer [6]

Phenolic resin curatives having a majority of dibenzyl-ether linkages were unexpectedly found to be effective in curing the rubber in a blend of a crystalline polyolefin and EPDM [69]. Their effectiveness exceeds that of conventional phenolic resins for many TPV compositions.

TPV cured with conventional phenolic resins often stain painted surfaces, when in contact. This has resulted in the exclusion of TPV cured with phenolic resins from many applications where the elastomer will have extended contact with a painted surface, such as the bodies of cars, structural mouldings and glass-to-metal laminates. When the phenolic resin curatives are esterified (e.g., acetylated, tosylated, silylated or phosphorylated) before use as a curative, staining is reduced or eliminated [70].

7.6.1.3 Silane Grafting

PP/EPDM blends can also be crosslinked by silane grafting in the presence of a small amount of peroxide. Fritz and co-workers [71] studied the tension set and repeated tensile-stress to characterise the elastic properties of organosilane crosslinked PP/EPDM TPV. Grafting, hydrolysis and condensation crosslinking reactions were carried out in a single stage process. The general mechanism of crosslinking of polymer in presence of silane is shown in **Figure 7.5**. There are several patents describing hydrosilane in presence of a catalyst as a curative for the preparation of TPV [72, 73].

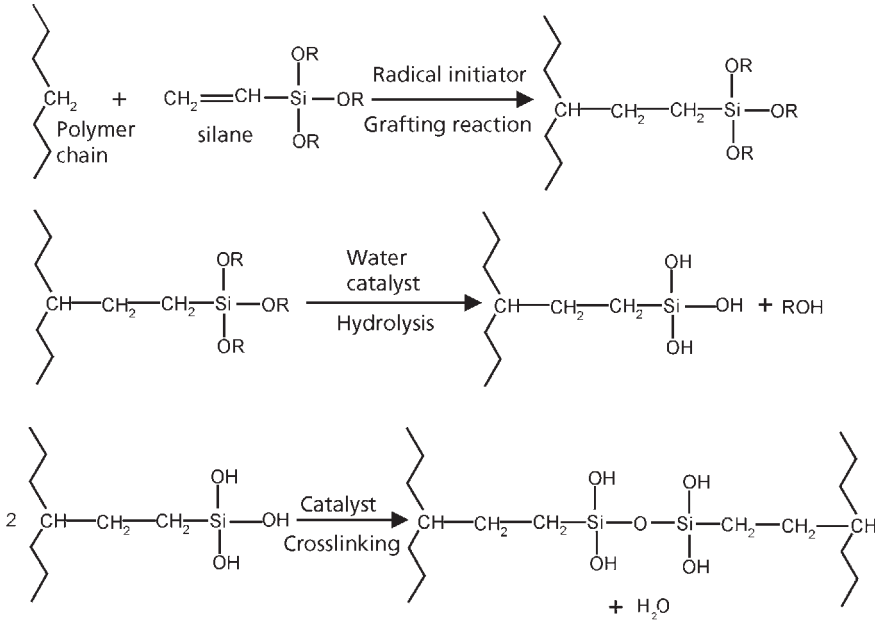

Figure 7.5 Mechanism of crosslinking of polymer by silane

7.6.2 Morphology of PP/EPDM TPV

Several studies have been carried out on the morphology of polymer blends [74-78], which depends primarily on:

1. The viscosity of individual components,
2. The ratio of the components,
3. The interfacial tension between the two polymeric components,

4. Other ingredients such as extenders, fillers, stabilisers, and lubricants, and

5. Processing conditions such as shear rate, temperature, and type of flow during processing.

The morphology of an immiscible polymer blend can be visualised as an emulsion in which one liquid is dispersed in another. When the fraction of the dispersed phase exceeds a critical value, a region of composition can exist where the blend exhibits phase co-continuity. This co-continuous morphology can be considered as the intermediate structure at which phase inversion takes place; the dispersed phase becomes the matrix phase and *vice versa*. The midpoint of the phase inversion region can be generally expressed [79] by:

$$\frac{\varphi_1}{\varphi_2}\frac{\eta_2}{\eta_1} = 1 \tag{7.3}$$

in which η_1 and η_2 represent the melt viscosities of the pure components, and φ_1 and φ_2 are the volume fractions of the components at phase inversion.

The mechanical properties depend not only on the type and content of the components, but also on the phase morphologies and the interactions between the phases. Morphology formation, thermodynamic compatibility between the polymeric components and the crosslinking parameters of the dispersed rubber phase determine the final properties of TPV [80]. Kresge [81] studied the morphology of dynamically sulfur-cured PP/EPDM blends and concluded that the net result of crosslinking and chain cleavage during mixing and blending could be the small gel particles of elastomer of around 0.5 to 5 μm found in the continuous PP phase. Abdou-Sabet and Patel [82] and later Radusch and Pham [81] studied the morphology generation during the dynamic vulcanisation of phenolic resin cured PP/EPDM TPV. According to Radusch and Pham, the main aim of the dynamic vulcanisation procedure is the generation of the TPV-typical phase morphology. Only a fine dispersion of the relatively high amount of rubber into small particles <0.5 μm surrounded by the thermoplastic matrix guarantees a typical elastomer with a high mechanical property level. Here the problem lies in the difficulty of dispersing the rubber components, representing the major component and having the highest viscosity, in the less viscous thermoplastic component, which has to form the matrix at the end of the process. In binary systems, the major component generally forms the matrix phase and the minor component forms a droplet-like dispersed phase. Normally, only low viscosity droplets in a high viscosity matrix are able to disperse effectively. In shear flow fields it is impossible to destroy a droplet effectively if the viscosity ratio of the dispersed phase *versus* the matrix phase is higher than 1. However, for dynamic vulcanisation it is necessary to realise an inverse phase morphology characterised by a matrix phase representing the minor content. Therefore, there is no shear deformation to act as the main mixing mechanism, but elongational deformations are required as a precondition for effective dispersion [83]. Grace [84] reported that non-rotational, elongational flow

appeared to produce more effective break-up and dispersion than rotational shear flow. In this connection, it was found that a co-continuous phase morphology at the beginning of the mixing process was a prerequisite to generate the dispersed phase morphology at the end. With TPV, immediately after the start of the selective crosslinking process the viscosity of the rubber became very high and as a result the stresses in the material increased very strongly, leading to the break-up of the co-continuous rubber phase into small particles. The investigation [80] showed that the period of morphology transformation from a co-continuous blend morphology to the island (rubber) – matrix (thermoplastic) morphology was very short. The crosslinking of the rubber molecules increased the viscosity of the rubber particles and prevented the coalescence of the particles. The development of the dispersed phase morphology from the co-continuous phase is depicted in **Figure 7.6**. It is generally accepted that one of the major advantages of dynamically cured blends over unvulcanised ones is that the morphology is fixed on crosslinking and is not altered by subsequent melt processing.

Dispersed phase morphology can be proven with the help of combined electron microscopy and energy-dispersive microanalysis techniques [82]. According to Kanauzova and co-workers [85], at high temperatures, PP crystallisation (γ-modification) results in the intermolecular interaction between PP and EPDM chains at a boundary layer. The formation of the latter in PP/EPDM blends was determined by radiothermoluminescence from the appearance of a new maximum in the relationship between the intensity of luminescence and the temperature. D'Orazio and co-workers [86] studied the morphology of dynamically peroxide-vulcanised isotactic polypropylene (iPP)/EPR by using DSC, optical, scanning and transmission electron microscopy (TEM), wide angle and small angle X-ray scattering. They observed that blends containing uncured EPR were characterised by the presence of iPP domains randomly distributed in the EPR rubbery matrix, whereas in blends containing cured EPR, the iPP phase became the continuous phase. The latter crystallised in a structure that resembled a cobweb, tending to surround

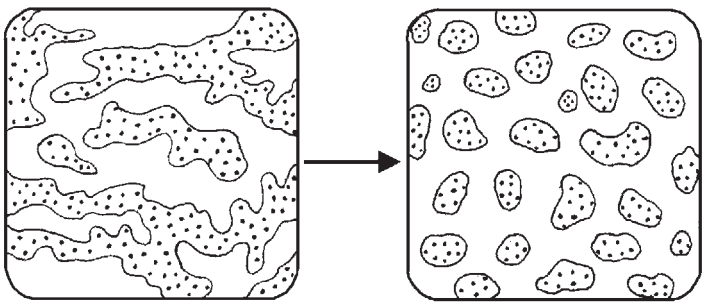

Figure 7.6 Development of morphology in a thermoplastic vulcanisate: from co-continuous to dispersed phase [80]

the EPR cured particles. Moreover, such an iPP-cobweb appeared to be constituted by a row structure of stacked lamellae. It was found that the addition of the EPR-phase interfered dramatically with the crystallisation process of the iPP, thus inducing drastic modification of its intrinsic morphology (size, neatness and regularity of spherulites, inner structure of spherulites). Such interference was more marked when the iPP phase crystallised in presence of cured EPR. The elastic behaviour of the thermoplastic elastomer was accounted for by applying the 'leaf spring model' to the morphology and structure of the iPP phase, crystallised in the presence of the cured EPR.

Radusch and co-workers [87] have reported recently that for sulfur-cured PP/EPDM TPV with increased curative concentration, the tensile strength increased but the storage modulus (E′) obtained from dynamic mechanical analysis decreased. It may be due to thinning down of the PP interstices for the finer dispersion of rubber particles in the PP-matrix. The morphology development, rheological behaviour and viscoelastic properties of carbon black filled, dynamically vulcanised, sulfur cured thermoplastic elastomers based on PP/EPDM with various blend-ratios, were studied and compared with similar but unfilled samples by Katbab and co-workers [88]. Two-phase morphology was observed at all ratios of the dynamically cured samples, in which rubber particles were dispersed in the thermoplastic matrix. Carbon black distribution in each phase and the damping behaviour were dependent on the mixing conditions and the method of carbon black feeding. However, carbon black tends to stay mainly in the rubber phase, which leads to an increase in the viscosity difference and, therefore, an increase in the rubber particle size. Tensile strength and rupture energy were found to increase with carbon black loading.

Katbab and co-workers [89] also studied the morphology of sulfur-cured PP/EPDM (40/60 *w/w*) blends. Their morphology in the molten condition was dispersed i.e., the rubber particles were dispersed throughout the PP matrix. However, the final morphology was controlled simultaneously by the rate of break-up and coalescence of the rubber droplets, i.e., by two mutually counteracting mechanisms. However, when the molten samples of those blends were cooled to room temperature, a typical co-continuous two-phase morphology was observed as the coalescence of the rubber particles predominated.

Ellul and co-workers [90] used scanning TEM to characterise dynamically vulcanised TPE. In recent years, atomic force microscopy has also been widely used for the high resolution imaging of polymer surfaces. The effects of composition and processing conditions on the morphology and final properties of saturated olefinic thermoplastic elastomer blends of PP/EPDM/oil and S-EB-S/PP/oil were compared by Sengupta and co-workers [91].

Understanding the elasticity of TPV is still a subject of debate, because the elastic recovery upon tension or compression at moderate temperatures seems to be in conflict with the low yield-strain of the thermoplastic component. Finite-element modelling studies have been recently published by Boyce and co-workers [94, 95], but could not give a

satisfactory explanation, mainly because the outcome of such calculations is strongly affected by the assumptions and by the description of the morphology and morphological changes upon deformation.

Soliman and co-workers [92] studied the deformation mechanism of phenolic resin cured PP/EPDM TPV. According to them, during the stretching of PP/EPDM TPV most of the PP acts as a glue between the EPDM particles, which are deformed. Only a small fraction of the PP is irreversibly deformed and yielded. During the recovery process this PP fraction is partially pulled back by the recovery of the EPDM. Their model for the TPV deformation mechanism is shown in **Figure 7.7**.

According to Abdou-Sabet [93], the PP-interstices between the rubber-particles are too small to allow proper PP crystallisation. So the PP-phase remains amorphous and is deformable.

The stress-strain behaviour of TPV was also studied experimentally by Boyce and co-workers [94]. A constitutive model behaviour was proposed by them and found to predict successfully the important features of the observed stress-strain behaviour. They showed that most of the PP matrix does not yield at all but undergoes rigid body motion. The micro-mechanisms of deformation and recovery in TPV were also extensively studied by Boyce and co-workers [95], using a series of micro-mechanical models. Application of a dynamic scaling model for the analysis of the process of agglomerate formation between the cured rubber particles during dynamic vulcanisation of TPV was investigated by Goharpey and co-workers [96].

7.7 Rheology and Processing of TPV

The processing of a rubber-plastic composite into a finished part is a function of the melt rheology of the composition. The melt rheology in turn is a function of temperature

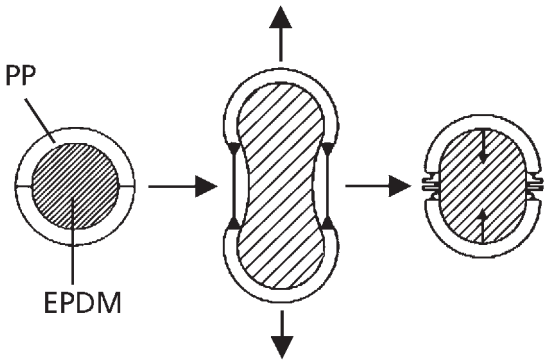

Figure 7.7 Model for TPV deformation mechanism [92]

and shear rate. The processing of a TPV is determined primarily by the properties of its thermoplastic phase, yet the properties of the same TPV are determined by the nature of the crosslinked rubber phase. Thus a PP/EPDM TPV has essentially the same melting point as rigid PP, and is processed in much the same manner as PP.

The rheological properties of TPV have been studied by several research groups [25, 97, 98]. It was shown that fully cured thermoplastic vulcanisates behave similarly to highly filled fluids in shear flow. They exhibit highly pseudoplastic behaviour, and they lack a viscosity plateau at low shear rates and they have low extrusion swell. Han and White [99] have studied the rheological behaviour by various measurement techniques, including sandwich squeeze flow, cone-plate stress build-up, dynamic analysis and capillary rheometry. They concluded that the dynamically vulcanised blends show behaviour, that is characteristic of materials with a rest state structure. From plots of the viscosity as a function of the shear stress, a critical stress or yield stress of flow was observed. Steeman and Zoetelief [100] showed that stress is the important factor, determining the rheological behaviour of TPV-melts. At low stress, the materials behave mainly elastically, which is attributed to the presence of an interacting network of rubber particles. At intermediate stresses, above the yield stress, this network is broken and the materials behave as a melt of PP, filled with stiff rubber particles; the viscosity is heavily dependent on the rubber content. At high stresses, the viscosity of the TPV increases with increasing hardness, i.e., with the PP-content.

High elasticity, as demonstrated by lower residual deformation upon release of deformation, is highly desirable in PP/EPDM TPV. Ellul [101] showed that this property could be achieved by the application of a PP-phase, having a high degree of long-chain branching. Thus, the TPV so obtained, behaves as a dual network material, one network being the chemically crosslinked rubber phase, the other being the physical network arising from extensive long-chain branching in the PP.

The effects of the degree of crosslinking on the rheological properties of PP/EPDM TPV were studied by means of a rubber process analyser (RPA 2000), by Marinovic and co-workers [102]. Their results confirmed that tighter crosslinking contributes to the formation of more rigid EPDM domains dispersed in the continuous PP-phase. The heterogeneity of such systems, affecting the molecular dynamics, was also explored by an electron spin resonance spin probe.

Processing methods and equipment for TPV are essentially the same as those of the thermoplastic in the material. The most widely used method is thermoplastic injection moulding, which differs from vulcanisable rubber injection moulding in that the final step in the fabrication process does not involve vulcanisation [69]. Extrusion is also widely used to fabricate sheeting, intricate profiles, tubing, hose, and electrical insulation and jacketing from TPV. It does not require the expensive vulcanisation equipment commonly used in the rubber industry. Recent developments have resulted in the generation of a foamed TPV [103] *via* extrusion with water as a foaming agent. Blow

moulding, thermoforming and heat welding are TPV fabrication methods, not feasible with vulcanised rubber. The generation of hollow TPV articles *via* blow moulding has been found to be more efficient than forming similar articles from vulcanised rubber by injection moulding [69].

7.8 Compounding in TPV

Compounding of TPV is even trickier than that of conventional elastomers. In fact all the TPV-manufacturers use some stabilisers such as antioxidants, fillers, process aids, pigments and so on, as compounding ingredients in their products to match the final performance requirements.

The most commonly used antioxidants in TPV are the primary antioxidants such as amines and hindered phenols (e.g., Irganox 1076). They are also called 'chain stoppers', because they stop the free-radical chain reaction of oxidation. Conversely, thio-compounds or phosphites (e.g., Irgafos 168), known as secondary antioxidants or preventive antioxidants are also used. They basically decompose hydroperoxides and thereby stop the propagation of the radicals by forming stable products. Phosphites show strong synergistic effects in combination with phenolic antioxidants and thus are used frequently in TPV compounds.

Different types of reinforcing (mostly carbon black and silica) and non-reinforcing fillers (mainly to reduce the cost) are used in TPV formulations. As already mentioned in the morphology section, carbon black tends mostly to stay in the rubber phase. Generally, tensile strength and rupture energy of TPV are found to increase with the loading of carbon black. Different types of mineral fillers are also used in TPV. Examples of some suitable halogen free mineral fillers include aluminum trihydroxide, magnesium dihydroxide, ammonium phosphate, diammonium hydrogen phosphate, polyammonium phosphate, and tribromoneopentyl esters of phosphoric acids etc. On the other hand, examples of fire-retardant fillers are halogenated fire-retardant agents such as chlorinated biphenyl and halogenated cyctopentadieno used jointly with metal oxides such as antimony oxide, halogenated polymers, mixtures of halogen and phosphorus fire-retardants. Examples of some sound dampening mineral fillers include magnesium sulfate, calcium sulfate, barium sulfate, aluminum sulfate, aluminum ammonium sulfate, aluminum potassium sulfate, aluminum sodium sulfate, magnesium carbonate, calcium carbonate, calcinated clay, calcium borate, talc, mica, zinc borates, and aluminum phosphate. Very recently different types of nano-sized mineral fillers such as nano-clays, nano-talc and so on have also been used to prepare nano-TPV.

Processing oils and plasticisers are used in large quantities in most TPV to get better processability and to control the hardness. Primarily, paraffinic (hydrocarbon) type oils are used in PP/EPDM TPV because of better compatibility. However, their presence and distribution over the two phases can affect the properties of TPV both in the solid

state and in the melt. Solid state ^{13}C-NMR spectroscopy and electron paramagnetic resonance were used by Winters and co-workers [104] to determine quantitatively the distribution of processing oil over the two phases in EPDM/PP/oil based TPV in the melt, with and without talc filler. The oil has a strong influence on both the processing and the mechanical properties of TPV. ^{13}C-NMR of the pure oil revealed that it closely resembled a low molecular weight EPR with a M_n of 800 g/mol and an ethylene content of 70 wt%. They also determined the location of the oil in the melt. The NMR and electron paramagnetic resonance results provided evidence that in the melt, about one-third of the oil is neither mixed within the EPDM nor the PP. The data also indicated that the oil might form a very thin layer around talc filler particles.

Later, Sengers and Gotsis [105] applied dielectric relaxation spectroscopy as a new technique to determine the oil distribution both in the melt and at room temperature. They studied the relaxation of molecular dipoles in terms of dielectric constants by measuring the capacitance. *N*,*N*-Dibutyl amino nitrostilbene was used as a probe molecule. Contrary to the results of Winters and co-workers, they decided that the oil is equally distributed over the PP and EPDM phases, giving rise to a distribution coefficient of one.

7.9 End Use Applications of TPV

Potential and proven applications of recently developed thermoplastic elastomers and thermoplastic vulcanisates are as follows [6, 69]:

Mechanical rubber goods applications: convoluted bellows, flexible diaphragms, gaskets, seals, extruded profiles, tubing, mounts, bumpers, housings, glazing seals, valves, shields, suction cups, torque couplings, vibration isolators, plugs, connectors, caps, rollers, oil-well injection lines, handles and grips.

Under-the-hood applications in the automotive field: air conditioning hose cover, fuel line hose cover, vacuum tubing, vacuum connectors, body plugs, seals, bushings, grommets, electrical components, convoluted bellows, steering gear boots, emission tubing, protective sleeves, shock isolators, and air ducts.

Industrial hose applications: hydraulic (wire braided), agricultural spray, paint spray, plant air-water, industrial tubing and mine hose.

Electrical application: plugs, strain relief, wire and cable insulation and jacketing, bushings, enclosures, connectors and terminal ends.

Furthermore, TPV can also be used in the manufacture of consumer goods, for example: floor and personal care, business appliances, sporting goods, portable kitchen appliances and so on. Soft touch applications of TPV are also becoming increasingly popular nowadays.

7.10 Concluding Remarks

Nowadays TPV occupy a vital position in the family of thermoplastic elastomers because of their huge potential. Currently TPV are one of the fastest growing elastomer market with an annual growth rate of about 12-15%. However, there are still some unsolved technological problems, which are associated with lack of proper understanding of the TPV. Both the process of TPV production and the structure-properties relationship of the TPV are still a mystery. For this reason, the development of TPV-based products is generally pursued somewhat by trial and error. More scientific investigation is required to get a better insight into the process of dynamic vulcanisation. For example, the development of morphology during dynamic vulcanisation in a batch process as well as in a twin-screw extruder for a continuous process is still not clear. The TEM photomicrographs of the final TPV morphology differ from a conventional 2D image to a 3D image. Sometimes, it is very difficult to distinguish between a true dispersed phase morphology and a true co-continuous morphology. Distribution of oil over the two phases during mixing and its redistribution upon cooling of TPV-melt is still a topic of controversy. As already mentioned, the deformation mechanism and elasticity of TPV are still not well understood. Hence, even better models are required to explain why TPV behave as a fully elastic compound. More fundamental studies are needed on TPV-melt rheology to explain the excellent processability of TPV even at a very high EPDM/PP blend ratio. Furthermore, development of novel crosslinking agents with simple crosslinking chemistry could be explored to enrich the field of applications of TPV in future.

References

1. J.A. Manson and L.H. Sperling, *Polymer Blends and Composites*, Plenum Press, New York, NY, USA, 1976.

2. *Polymer Blends, Volumes I and II*, Eds., D.R. Paul and S. Newman, Academic Press, New York, NY, USA, 1978.

3. M.T. Shaw, *Polymer Engineering and Science*, 1982, **22**, 2, 115.

4. L.M. Robeson, *Polymer Engineering and Science*, 1984, **24**, 8, 587.

5. L.A. Utracki, *Polymer Alloys and Blends: Thermodynamics and Rheology*, Hanser, Munich, Germany, 1990.

6. *Thermoplastic Elastomers: A Comprehensive Review*, Eds., N.R. Legge, G. Holden and H.E. Schroeder, Hanser Publishers, Munich, Germany, 1987.

7. H.L. Morris in *Handbook of Thermoplastic Elastomers*, Ed., B.M. Walker, Van Nostrand Reinhold, New York, NY, USA, 1979.

8. *Handbook of Thermoplastic Elastomers*, 2nd Edition, Eds., B.M. Walker and C.P. Rader, Van Nostrand Reinhold, New York, NY, USA, 1988.

9. *Handbook of Elastomers: New Developments and Technology*, Eds., A.K. Bhowmick and H.L. Stephens, Marcel Dekker, New York, NY, USA, 1988.

10. *Thermoplastic Elastomers from Rubber-Plastic Blends*, Eds., S.K. De and A.K. Bhowmick, Horwood Publishers, London, UK, 1990.

11. ASTM D6338, *Standard Classification System for Highly Crosslinked Thermoplastic Vulcanisates (HCTPV)*, 2003.

12. A.M. Gessler and W.H. Haslett, inventors; Esso Research and Enginering Co., US 3,037,954, 1962.

13. W.K. Fischer, inventor; Uniroyal, Inc., assignee; US 3,758,643, 1973.

14. A.Y. Coran, B. Das and R.P. Patel, inventors; Monsanto Co., assignee; US 4,130,535, 1978.

15. S. Abdou-Sabet and M.A. Fath, inventors; Monsanto Company, assignee; US 4,311,628, 1982.

16. A.Y. Coran and R. Patel, *Rubber Chemistry and Technology,* 1980, **53**, 1, 141.

17. A.Y. Coran and R. Patel, *Rubber Chemistry and Technology*, 1980, **53**, 4, 781.

18. A.Y. Coran and R. Patel, *Rubber Chemistry and Technology*, 1981, **54**, 1, 91.

19. A.Y. Coran and R. Patel, *Rubber Chemistry and Technology*, 1981, **54**, 4, 892.

20. A.Y. Coran, R. Patel and D. Williams, *Rubber Chemistry and Technology*, 1982, **55**, 1, 116.

21. A.Y. Coran and R. Patel, *Rubber Chemistry and Technology*, 1983, **56**, 1, 210.

22. A.Y. Coran and R. Patel, *Rubber Chemistry and Technology*, 1983, **56**, 5, 1045.

23. A.Y. Coran, *Rubber Chemistry and Technology*, 1995, **68**, 3, 351.

24. R.C. Puydak, D.R. Hazelton and T. Ouhadi, inventors; Advanced Elastomer Systems, assignee; US 5,073,597, 1991.

25. B. Kuriakose and S.K. De, *Polymer Engineering and Science*, 1985, **25**, 10, 630.

26. B. Kuriakose, S.K. De, S.S. Bhagawan, R. Sivaramkrishnan and S. K. Athithan, *Journal of Applied Polymer Science,* 1986, **32**, 6, 5509.

27. A.J. Tinker in *Proceedings of the 134th ACS Rubber Division Meeting*, Fall 1988, Cincinnati, OH, USA, Paper No.48.

28. S. Abdou-Sabet and K-S. Shen, inventors; Monsanto Company, assignee; US 4,594,390, 1986.

29. C. Koning, M. van Duin, C. Pagnoulle and R. Jerome, *Progress in Polymer Science,* 1998, **23**, 4, 707.

30. M. Van Duin, in *Proceedings of the International Rubber Conference*, 2001, Birmingham, UK.

31. M.A. Lopez Manchado and J.M. Kenny, *Rubber Chemistry and Technology*, 2001, **74**, 2, 198.

32. A.V. Chapman and M. Porter in *Natural Rubber Science and Technology*, Ed., A.D. Roberts, Oxford University Press, Oxford, UK, 1988.

33. M.R. Kresja and J.L. Koenig, *Rubber Chemistry and Technology*, 1993, **66**, 3, 376.

34. I.I. Ostromyslenski, *Journal of the Russian Physical-Chemical Society*, 1915, **47**, 1467.

35. I.I. Ostromyslenski, *Indian Rubber Journal*, 1916, **52**, 470.

36. J.B. Class, *Rubber and Plastics News*, 1995, **25**, 5, 91.

37. K. Hummel, W. Scheele and K.H. Hillmer, *Kautschuk und Gummi*, 1961, **14**, 6, 171.

38. W. Hofmann, *Kautschuk und Gummi Kunststoffe*, 1987, **40**, 4, 308.

39. M. van Duin, *Kautschuk und Gummi Kunststoffe*, 2002, **55**, 4, 150.

40. L.D. Loan, *Rubber Chemistry and Technology*, 1967, **40**, 1, 149.

41. F.P. Baldwin, P. Borzel, C.A. Cohen, H.S. Makowski and J.F. Van de Castle, *Rubber Chemistry and Technology*, 1970, **43**, 3, 522.

42. W.C. Endstra in *Proceedings of the 8th Scandanavian Rubber Conference (SRC '85) on Technology for Improved Design with Rubber*, Copenhagen, Denmark, 1985.

43. P.R. Dluzneski, *Rubber Chemistry and Technology*, 2001, **74**, 3, 451.

44. *Elastomer Technology Handbook*, Ed., N.P. Cheremisinoff, CRC Press, Boca Raton, FL, USA, 1993.

45. *Peroxide Crosslinking of EPDM Rubbers*, Akzo Nobel Company Brochure, XL 00.250.01/0300, Akzo Nobel, The Netherlands, 2000.

46. *Crosslinking Peroxides and Coagents*, Akzo Chemicals, Horsham, UK, 1991.

47. W. Hofman, *Progress in Rubber and Plasics Technology*, 1985, **1**, 2, 18.

48. D. Ogunniyi, *Rubber Chemistry and Technology*, 1998, **71**, 5, 821.

49. D. Ogunniyi, *Progress in Rubber and Plastics Technology*, 1999, **15**, 2, 95.

50. J.B. Class, *Rubber World*, 1999, **220**, 5, 35.

51. M. van Duin and H.G. Dikland, *Rubber Chemistry and Technology*, 2003, **76**, 1, 132.

52. M.D. Ellul and P.S. Ravishankar in *Proceedings of the American Chemical Society, PMSE Division*, Boston, MA, USA, 1988.

53. W. Hofman, *Vulkanisation und Vulkanisationschilfsmittel*, Bayer AG, Leverkusen, Germany, 1965.

54. R.C. Keller, *Rubber Chemistry and Technology*, 1988, **61**, 2, 238.

55. W.C. Endstra in *Proceedings of the International Conference on Various Aspects of Ethylene-Propylene Based Polymers*, 1991, Leuven, Belgium.

56. H.G. Dikland, S.S. Sheiko, L. van der Does, M. Möller and A. Bantjes, *Polymer*, 1993, **34**, 8, 1773.

57. H.G. Dikland, L. van der Does and A. Bantjes, *Rubber Chemistry and Technology*, 1993, **66**, 2, 196.

58. H.G. Dikland, R.J.M. Hulskotte, L. van der Does and A. Bantjes, *Kautschuk und Gummi Kunststoffe*, 1993, **46**, 8, 608.

59. *Application of Coagents for Peroxide Crosslinking*, Akzo Nobel Company Brochure, XL 00.245.01/0300, Akzo Nobel, The Netherlands, 2000.

60. A. Johansson in *Proceedings of the Scandanavian Rubber Group, Inc.*, Winter Technical Session on Peroxide Dispersions and Their Applications, 2000.

61. R.E. Drake, J.J. Holliday and M.S. Costello, *Rubber World*, 1995, **213**, 3, 22.

62. R.E. Drake, *Elastomerics*, 1982, **114**, 1, 28.

63. K. Naskar and J.W.M. Noordermeer, *Rubber Chemistry and Technology*, 2003, **76**, 4, 1001.

64. K. Naskar and J.W.M. Noordermeer, *Rubber Chemistry and Technology*, 2004, **77**, 5, 955.

65. *Phenolic Resins*, Eds., A. Gardziella, L. A. Pilato and A. Knopp, Springer Verlag, Berlin, Germany, 2000.

66. M. van Duin and A. Souphanthong, *Rubber Chemistry and Technology*, 1995, **68**, 5, 717.

67. M. van Duin, *Rubber Chemistry and Technology*, 2000, **73**, 4, 706.

68. S. Abdou-Sabet, R.C. Puydak and C.P. Rader, *Rubber Chemistry and Technology*, 1996, **69**, **3**, 476.

69. R.E. Medsker, G.W. Gilbertson, R. Patel, inventors; Advanced Elastomer Systems, assignee; EP 850991 A1, 1998.

70. R.E. Medsker, R. Patel and S. Abdou-Sabet, inventors; Advanced Elastomer Systems, assignee; US 5,750,625, 1998.

71. H.G. Fritz and R. Anderlik, *Kautschuk und Gummi Kunststoffe*, 1993, **46**, **5**, 374.

72. J.D. Umpleby, inventor; Union Carbide Corporation, assignee; US 4,803,244, 1989.

73. J.M. Quirk and B. Kanner, inventors; Union Carbide Corporation, assignee; US 4,668,812, 1987.

74. G.N. Avgeropoulos, F.C. Weissert, P. Biddison and G.G.A. Böhm, *Rubber Chemistry and Technology*, 1976, **49**, 1, 93.

75. S. Danesi and R.S. Porter, *Polymer*, 1978, **19**, 4, 448.

76. K. Min, J.L. White and J.F. Fellers, *Polymer Engineering and Science*, 1984, **24**, 17, 1327.

77. S. Wu, *Polymer Engineering and Science*, 1987, **27**, 5, 335.

78. B.D. Favis and D. Therrien, *Polymer*, 1991, **32**, 8, 1474.

79. G.M. Jordhamo, J.A. Manson and L.H. Sperling, *Polymer Engineering and Science*, 1996, **26**, 8, 517.

80. H.J. Radusch and T. Pham, *Kautschuk und Gummi Kunststoffe*, 1996, **49**, 4, 249.

81. E.N. Kresge in *Polymer Blends, Volumes I and II*, Eds., D.R. Paul and S. Newman, Academic Press, New York, NY, USA, 1978.

82. S. Abdou-Sabet and R.P. Patel, *Rubber Chemistry and Technology*, 1991, **64**, 5, 769.

83. C. van den Reijden-Stolk, *A Study on Deformation and Break-Up of Dispersed Particles in Elongational Flow*, Delft University of Technology, The Netherlands (1989). [PhD. Thesis]

84. H.P. Grace, *Chemical Engineering Communications*, 1982, **14**, 225.

85. A.A. Kanauzova, T.T. Rakhmafulin, S.V. Reznichenko and Y.L. Morozov in *Proceedings of International Rubber Conference*, 2002, Prague, Czech Republic.

86. L. D'Orazio, C. Mancarella, E. Martuscelli, G. Sticotti and R. Ghisellini, *Journal of Applied Polymer Science,* 1994, **53**, 4, 387.

87. S. Ilisch, H. Menge and H.J. Radusch, *Kautschuk und Gummi Kunststoffe*, 2000, **53**, 4, 206.

88. A.A. Katbab, H. Nazockdast and S. Bazgir, *Journal of Applied Polymer Science*, 2000, **75**, 9, 1127.

89. F. Goharpey, A.A. Katbab and H. Nazockdast, *Journal of Applied Polymer Science*, 2001, **81**, 10, 2531.

90. M.D. Ellul, J. Patel and A.D. Tinker, *Rubber Chemistry and Technology*, 1995, **68**, 4, 573.

91. P. Sengupta, J.W.M. Noordermeer, W.G.F. Sengers and A.D. Gotsis in *Proceedings of the 163rd ACS Rubber Division Meeting*, Spring 2003, San Francisco, CA, USA, Paper No.8.

92. M. Soliman, M. van Dijk, M. van Es and V. Shulmeister in *Proceedings of ANTEC '99*, New York, NY, USA, 1999, Volume 2, p.1947.

93. S. Abdou-Sabet in *the Proceedings of the 158th ACS Rubber Division Meeting*, Fall 2000, Cincinnati, OH, USA, Paper No.1.

94. M.C. Boyce, K. Kear, S. Socrate and K. Shaw, *Journal of the Mechanics and Physics of Solids,* 2001, **49**, 5, 1073.

95. M.C. Boyce, S. Socrate, K. Kear, O. Yeh and K. Shaw, *Journal of the Mechanics and Physics of Solids,* 2001, **49, 6,** 1323.

96. F. Goharpey, H. Nazockdast, A.A. Katbab and A. Mousavi in *Proceedings of thePolymer Processing Society (PPS) Congress*, 2003, Athens, Greece.

97. L.A. Goettler, J.R. Richwine and F.J. Wille, *Rubber Chemistry and Technology*, 1982, **55**, 5, 1448.

98. I. Mathew, K.E. George and D.J. Francis, *Kautschuk und Gummi Kunststoffe*, 1991, **44**, 5, 450.

99. P.K. Han and J.L. White, *Rubber Chemistry and Technology*, 1995, **68**, 5, 728.

100. P. Steeman and W. Zoetelief in *Proceedings of ANTEC 2000*, 2000, Orlando, FL, USA, Paper No.640.

101. M.D. Ellul in *Proceedings of the 160th ACS Rubber Division Meeting*, Fall 2001, Cleveland, OH, USA, Paper No.82.

102. T. Marinovic, Z. Susteric, I. Dimitrievski and Z. Veksli, *Kautschuk und Gummi Kunststoffe*, 1998, **51**, 3, 189.

103. G.L. Dumbauld, inventor; Advanced Elastomer Systems, assignee; US 5,070,111, 1991.

104. R. Winters, J. Lugtenburg, V.M. Litvinov, M. van Duin and H.J.M. de Groot, 2001, *Polymer*, **42**, 24, 9745.

105. W.G.F. Sengers and A.D. Gotsis in *Proceedings of the Polymer Processing Society Conference (PPS)*, 2003, Athens, Greece.

8 Polymers in Cable Application

Dipak Khastgir

8.1 Introduction

Polymers can be used for three major components of a cable:

1. Dielectric (insulation),
2. Semi-conducting materials presented generally in double layers for high voltage cables, and
3. Cable jacket materials (**Figure 8.1**).

Insulation provides the required dielectric or insulating properties mainly provides the physical barrier to prevent dangerous proximity between energised conductor and living object (human or animal body). Semi-conducting materials are used to minimise the partial discharge due to void formation between conductor and insulator or in the body of insulator and uniformly and radially distribute the electrical stress generated in a power cable. The jacket material protects the cable from different types of environmental hazards, like the mechanical damage during installation, damage due to chemicals and fire during use and under any adverse situations. Different polymers can be used as cable materials [1].

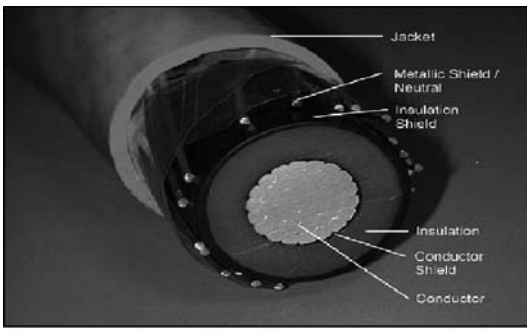

Figure 8.1 Different components of high voltage cable

In fact cables can be broadly classified into two categories namely: overhead cables and underground cables. The latter is preferred over the former mainly because of better safety and higher reliability. Compared to overhead cables which are exposed to the atmosphere, underground cables are hidden and there is always much less chance for close proximity of energised cable with a living object during a cable fault with an underground cable. The loss of life and property either due to direct contact with or fire hazards caused by broken overhead cable is nothing new. Moreover, underground cables can provide uninterrupted service during cyclonic weather, which may not be always possible using overhead cable systems. However, underground cables are substantially costlier than their overhead counterparts in the same voltage range. A rough comparison of relative prices of two types of cables is given in **Table 8.1**. The higher cost for underground cable compare to overhead ones is mainly because of complicated design and materials used in the former. But the repair of underground cable is more cumbersome process though failures are very few.

A trouble free, reliable service and long life are two key requirements for underground cables. These cables are being used more and more in recent years to supply electricity to household electrical utilities and for industrial operations. However the failure of any cables means severe economic loss coupled with revenue loss and loss due to repair. Power failure always leads to customer dissatisfaction and negative publicity. Performance of cable insulation in underground and moist conditions is critical and has been studied in detail [2-4].

In a power cable segment, the conventional oil/resin impregnated paper was a time-tested material used even up to 32 kV. A special type of oil impregnated, paper has been used for the last 80 years or more as a solid dielectric for cables with proven reliability (**Figure 8.2**). However, the paper insulation is now mostly replaced by solid dielectrics made from crosslinked polyethylene (XLPE), ethylene–propylene rubbers (EPR and EPDM), and also by polyvinylchloride (PVC) in specific areas. The paper cables though time tested has some negative points such as higher dielectric loss, higher operating loss, and lower productivity compared to cables having polymeric solid dielectrics such as

Table 8.1 Comparison of costs of underground cable and overhead lines

Voltage, kV	Ratio = Cost of underground Cable/Cost of Overhead lines
400	18 (23 for heavy duty)
275	13 (17 for heavy duty)
132	8
66	7
33	5
11	3
0.42	2 or less

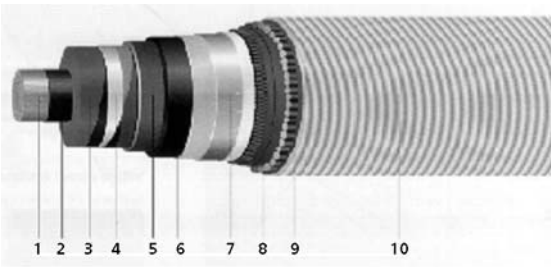

Figure 8.2 Paper insulated high voltage cable

1 - Conductor (key-stone type), 2 - Conductor shielding, 3 - Insulation (oil impregnated paper), 4 - Insulation shielding, 5 - Lead sheath, 6 - Plastic jacket, 7 - Tape armour, 8 - Optical fibre (optional), 9 - Steel wire armour, 10 - Sheath

EPR/EPDM or XLPE. Polymer-based cables can be produced at a much faster rate through extrusion process compared to the spiral lapping process used in the manufacture of paper cables.

Various types of polymeric insulating materials are in use today. The choice for polymeric material for other components of a cable is also quite large. However the proper selection of materials for different components of a cable is very crucial. The choice of the insulating material depends on the duty the cable has to perform, and also on commercial factors.

8.2 Broad Classification of Cables

8.2.1 Rigid Power Cables

This is by far the largest application type, and the field was previously dominated by paper insulation, which is gradually being replaced by solid dielectric such as XLPE and EPR/EPDM. The use of EPR/EPDM is relatively less wide spread unlike XLPE because of its poor mechanical properties, but it offers a very good blend of electrical properties and high degree of flexibility to make it attractive in the high voltage as well as high temperature range. PVC, mainly plasticised grades and sometimes rigid grades are widely used for low voltage range, especially in house hold applications and also for low to medium voltage power cables over a short distance.

For cables in the high voltage (>3 kV) and extra high voltage range (>11 kV), the design incorporates a conductor screen and an insulation screen, generally composed

of a layer of semi-conducting materials. The function of these screens is to equalise the electric field over the dielectric and make it radial and to eliminate partial discharge problem due to voids generated in the thick insulators and at the interface of conductor and insulation due to bending, flexing and difference in thermal expansion between polymeric dielectrics hot metallic conductor due to passage of current during use. For elastomer-insulated cables, the semi-conducting layers are composed of specially compounded semi-conducting elastomeric compound. This has been discussed in detail later in the text.

8.2.2 Flexible Power and Control Cables

Such cables are widely used in mines, railway locomotives and rolling stock, ships, materials handling equipment in ports, steel andcement plants, overhead cranes, and a variety of other applications (**Figure 8.3**).

Although the use of natural rubber (NR), styrene butadiene rubber (SBR) is limited as an insulant for these cables, synthetic elastomers such as, butyl rubber (IIR) EPR, ethylene-propylene-diene terpolymer (EPDM), especially the last two polymers, are more widely used.

Figure 8.3 Flexible power and control cable

8.2.3 Special Purpose Cables

With the growth of technology now the cable has to cater to the needs of various specialised applications and has to perform under unique environmental and operating conditions. As a result these cables are often tailor-made to operate under specific

conditions. Flexible polymers like polychloroprene (PCR), silicone (MQ), various fluoropolymers, ethylene vinyl acetate copolymers (EVA), acrylate elastomers (ACM), are being used because of their improved and special properties. Along with those polymers mentioned earlier, other polymeric materials such as polyesters and polyamides may be used in different parts of power cables as well as in the control and instrumentation cables.

There are quite a few special cables to cater the need of special applications such as:

a) Extra flexibility combined with strength needed for lift cables.

b) Lightness, resistance to oil and fuel, extremely low temperature, heat and fire resistance as required for aircraft and space applications.

c) Cables for high temperature applications in industrial locations near furnaces.

d) Cables for underwater and bore-hole applications such as for oil and mineral extraction, for example mining cables.

e) High-voltage flexible applications such as those required for X-ray applications.

f) Cables requiring long durability and exposure to extreme conditions encountered in defense and strategic applications.

8.3 Components of Cable

All power cables consist of three essential components:

1. A metallic conductor, which provides an electrical conducting path.

2. The insulation of a cable often called 'dielectric' or 'insulation' which is applied over the conductor and insulates it from direct contact and dangerous proximity between the energized conductor and other objects. A conductor with its insulation but without any other protective covering is known as the 'core' of a cable. A cable may consist of single core or multi-core depending on requirements (**Figures 8.4** and **8.5**).

3. The external protection preventing ingress of moisture, mechanical damage, chemical or electrochemical attack, fire or any other harmful influences which are detrimental to the cable itself.

Each of these cable components will now be considered in a greater detail.

Figure 8.4 Single core EP rubber insulated high voltage cable

Figure 8.5 Multi-core power cable

8.3.1 Conductor

Generally plain annealed copper (PAC) and aluminum conductors are used for most applications, but tinned annealed copper are also be used where additional protection from corrosion is required. Conductors are generally composed of copper or aluminum wires mainly because of their high conductivity (**Table 8.2**), good mechanical properties (**Table 8.3**) and ease of availability and processing.

Because of its exceptional plasticity, without any critical range of working temperature, copper can be rolled and or extruded over a wide range of temperature. Copper, being malleable and ductile, may readily be worked cold by any process involving rolling and wire drawing, and so on. Aluminium conductors are sometimes preferred in place of copper because of price factor and ease of availability. The properties of electrical grade copper and aluminium are shown in **Table 8.3**.

Table 8.2 Relative electrical conductivity of metals

Metal	Relative electrical conductivity (Copper = 100)
Silver	106.3
Copper	100.0
Gold	73.8
Aluminium	61.7
Sodium	35.4
Zinc	29.0
Iron	17.2
Tin	15.0
Lead	7.9

Table 8.3 Physical properties of metals used in cables			
Property	**Unit**	**Copper**	**Aluminum**
Density at 20 °C	kg/m^3	8890	2703
Thermal expansion	/°C	17×10^{-6}	23×10^{-6}
Melting point	°C	1083	659
Thermal conductivity	W/cm °C	3.8	2.4
Tensile strength, soft tempered	MN/m^2	225	70 – 90
Tensile strength, heat treated	MN/m^2	-	125-205
Elastic modulus	MN/m^2	26	14

Aluminum is widely used because of its relative cheapness, and particularly where cables will not face flexing in service. A copper conductor is preferred because of better fatigue resistance and higher durability. To provide enough flexibility and strength instead off solid thick conductor, the actual conductor is composed of a large number of thin copper or aluminum wires, stranded together.

Economy and versatility make copper and aluminium the two best choices for conductors. However, to compensate the conductivity deficiency of aluminum the cross-sectional area for aluminum conductor has to be increased by a factor of 1.6 compared to copper for the same amount of current flow. The weight due to higher size conductor is somewhat compensated by lower density of aluminum compared to copper. But aluminum conductor needs extra materials to be used in insulation, sheathing and armouring of cables.

Copper clad aluminum comprising 27% copper by weight has been used to overcome the problems in making mechanical connections to aluminium in wiring type cable accessories which are predominantly of the pinch-screw type. However, the use of copper-clad is relatively less compared to pure copper [5]. The copper-clad conductor is also protected from theft compared to conductor made from only copper, as the extraction of copper from clad is not an easy process.

In cable meant for high temperature applications tinned copper is replaced by nickel coated copper or silver coated copper.

So in cables where the strength of the conductor should be very high, copper-cadmium alloy is used in place of normal copper though it is little less conductive, but this does not pose much problem. In certain cases bronze is used to replace copper where it is necessary to withstand service conditions containing a severe corrosive atmosphere.

A copper conductor is coated with metallic tin by passing the conductor through the bath of molten tin before assembling it into a wire. Tinned copper wire is easier to solder

because a tin coating prevents copper oxide formation on the copper conductor, further the tin coating on copper is especially useful when prolonged self life of the conductor is required. Another point is also noteworthy here that copper sometimes interferes with the curing process used to produce thermosetting polymer or rubber insulation. Copper can also act a poison to some polymers; this effect can be reduced to a great extent through tin coating. However, the tin coating process requires an extra processing step and adds to cable cost. Moreover, an electrical phenomenon known as skin effect, adversely affects the performance of cable conductors in high frequency applications. Annealing is a process of heat treatment, which is used for copper conductor, to improve its mechanical properties. Aluminum conductors, on the other hand is relatively less reactive towards polymer due to presence of very thin aluminum oxide coating on its surface and does not require any tin coating. However using some thermal treatment one can improve the mechanical properties of aluminium conductor.

Water blocked conductors can also be designed for some under ground cables other special cables like telephone cables. This is achieved by incorporating water swellable tapes that contain a super absorbent polymer, between the strands of the conductor. On contact with moisture the polymer absorbs the water, swells and forms a gel. The gel fills the interstices of the conductor and acts as a water block restricting the water ingress into the conductor. Super absorbent polymers give the optimal combination of a quick swelling reaction and good blocking properties. The water penetration into the conductor is restricted to a very short length that remains constant with time, heat or loading cycles.

8.3.2 Insulation

Flexible polymer based insulants are in demand for manufacturing of various grades of power, control and instrumentation cables. As a result of developments that have taken place in recent years, these materials can be produced with various electrical, thermal and mechanical properties. The selection of materials for a particular application depends on various factors. Different thermal, electrical and fire testing techniques are applied for quality check up of various cable materials [6-9].

In the majority of cable insulants, it is important to restrict the current in the insulant and to avoid dangerous proximity between conductor and living bodies. Thus, under direct current (DC) condition, it is evident that high resistivity materials will permit the use of less thickness of insulation to achieve a given resistance path, and similar economy will result under alternating current (AC) condition by using a materials having low permittivity and loss factors. This is essential to restrict the dissipation of energy in the (insulated) power line. However, in many occasions, especially in the low voltage application (V<10 kV), the mechanical and thermal endurance properties become more important compared to electrical properties. For example, a furnace cable, which operates at about 500 V should have good and stable mechanical properties at elevated temperatures throughout its service

life. The mechanical properties and their retention at elevated temperature even after prolonged ageing are the most important considerations here. Similarly for oil resistant cables or the flame and fire retardant cables, the requirements will be quite different as they have to cater to altogether different needs.

The relatively new class of polymeric materials called thermoplastic elastomers can also be used in wire and cable applications both as insulation and as an inner-sheathing material. Because of its many favourable properties, XLPE is widely used in wire and cable insulation. In some countries low, medium and high voltage cables with XLPE and EPR/EPDM insulations have gained great importance. These cables conform to a continuous conductor temperature of 90 °C and a short circuit temperature of 250 °C. Blends of EPR and chlorosulfonated polyethylene (CSP) have been used as insulation of ship cable. Blends of EVA (28% vinyl acetate) with low-density polyethylene (LDPE) and EPDM can provide heat resistant medium voltage cable insulating materials [10-11].

The properties of an insulant, which are of interest to a cable designer, are:

a) Electrical properties

i) Dielectric constant

ii) Dielectric strength (break down voltage)

iii) Power factor (loss tangent), loss factor

iv) Resistance to corona discharges

b) Physical properties

i) Tensile strength and elongation

ii) Retention of tensile strength and elongation at break after ageing

iii) Hardness and tear strength

iv) Resistance to flexing

c) Thermal properties

i) Thermal conductivity – heat dissipation

ii) Maximum temperature for continuous operation

iii) Maximum temperature for short-term operation

iv) Withstanding low temperatures

d) **Chemical properties**

Resistance to moisture, acids, alkalis, oils, solvents, flame, sunlight, weathering, radiation and ozone.

8.3.3 Significance of Different Properties on Cable Insulation Quality and Performance

8.3.3.1 Electrical Properties

a) **Dielectric constant (permittivity).** The lower the dielectric constant and the lower the dielectric loss factor, the better is the insulation. Dielectric constant is related to the storage of electrical energy in the dielectrics or insulation. Higher the dielectric constant more will be the electrical energy loss per cycle of alternating electrical field. Dielectric constant and loss factor depends on dipole density and ability of dipoles to orient in accordance with the change in polarity of the applied electrical field. The ability of orientation of dipoles depends on physical environment of dipoles, for example temperature, plasticisation and any factor affecting the molecular mobility like degree of crosslinking. Polar polymers have higher dielectric constant and loss factor and these are lower for a non-polar polymer. Polymers show increased dielectric constant at higher temperature mainly above their glass transition temperature (T_g). Extremely low loss insulation is preferred both for very high voltage and high frequency applications.

b) **Dielectric loss (loss tangent)/power factor** represents actual electrical energy loss due to insulant/dielectrics. Polar polymers exhibit a higher loss compared to non-polar ones. Addition of polar additives such as plasticisers, filler to non-polar polymers will increase their dielectric loss. In fact dielectric loss plays a very important role in the selection of cable insulation to be used in high voltage applications.

c) **Break down voltage/dielectric strength** is the maximum voltage limit up to which the dielectric (insulation) will retain its insulating properties.

d) **High insulation resistance or DC resistivity**

e) **Resistance to corona discharge** is the property related more to the performance of the cable material under bending.

8.3.3.2 Mechanical Properties

Good mechanical properties are also required for an insulating material. High tensile, and elongation at break, good flexibility, hardness, and abrasion resistance are the

requirements for safe handling, installation, repair and satisfactory service. Retention of mechanical properties after ageing is also an important requirement. This is mainly because cables once installed are expected to give satisfactory service at least 5-15 years. The frequent change of a cable system is not desired and the changing process also needs to be done by experts especially for high voltage application. So some satisfactory service life is always expected from any cable. Other important mechanical properties include, fatigue resistance, low temperature flexibility for low temperature application.

8.3.3.3 Thermal Properties

Thermal expansion coefficient: differential thermal expansion of conductor metal and polymeric insulation may lead to corona problems, thermal conductivity: energised conductor gets heated so the heat dissipation characteristic of insulation is important, melting and decomposition temperature: gives an idea about thermal endurance for normal use and in the event of fire. Some important thermal endurance characteristics of cable polymer is given next.

a) Maximum conductor temperature for continuous operation

Due to the passage of current through the conductor, the conductor temperature may rise. Insulation, which will be in direct contact with the conductor, must withstand this elevated temperature and render its service satisfactorily for a long time (service life). The actual conductor temperature during operation is different from the ambient temperature. There will always be some rise in temperature in excess of ambient temperature due to passage of current. Sometimes the cable has to function at an elevated temperature compared to the normal environmental temperature. In that case, insulation should also have a higher temperature rating. Electrical properties of cable insulation also change with temperature, which makes selection of the material more complicated, especially as the dielectric constant and loss factor of the cable insulant change with temperature (**Figures 8.6** and **8.7**). Generally the loss factor of insulation increases with the rise in temperature. This increase in loss factor will increase the electrical energy loss during power transmission through the cable; moreover the dielectric placed over the conductor will be over heated when operating under high voltage [10-11]. That is why for very high voltage application non-polar polymeric insulation with low dielectric loss factor and higher thermo-mechanical stability is preferred.

b) Maximum temperature for short time operation

This includes two conditions:

- Maximum conductor temperature for overload in the distribution line. During over load condition the conductor carries about 20–25% more current than the normal current rating as a result the temperature rise may be 1.5 to 2 times more than the normal

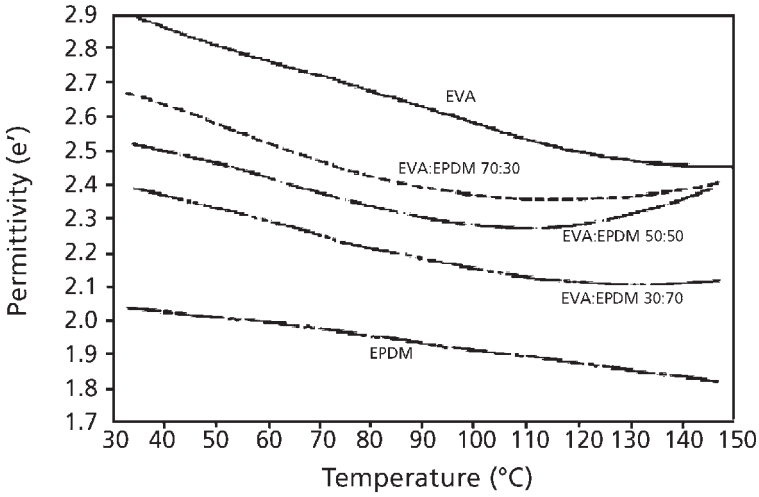

Figure 8.6 Variation of dielectric constant (permittivity) against temperature for different EVA-EPDM blend insulations

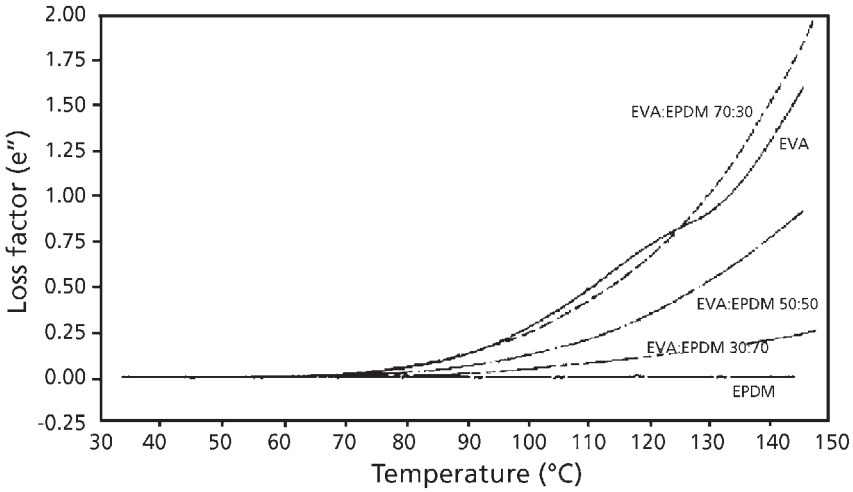

Figure 8.7 Variation of dielectric loss against temperature for different EVA-EPDM blend insulations

temperature rise at a normal current rating. The duration of this over voltage may vary from a few minutes to a few hours. Generally a total of 100 hours over voltage situation (intermittently) is specified for a cable life of 5 years. The insulation must have enough heat resistant characteristics so that it will perform well at this elevated temperature.

- Maximum conductor temperature during short-circuiting [12]. In the event of short circuit momentarily heavy rush of current flows through the conductor. This leads to a high rise in temperature in the conductor. Insulation in close contact with the conductor must withstand this high temperature, duration of which may range from a fraction of a second to a few seconds.

8.3.4 Chemical Resistance

Resistance to weather, heat, fire oil, solvent, chemicals sunlight and any other high-energy rays are the requirements of a cable for satisfaction performance depending upon the environment in which it will be used. However, these properties are more important for cable jacket material.

8.3.5 Selection Criteria for Insulation

While selecting a cable dielectric for specific applications mentioned previously, properties have to be considered. The polymeric dielectric can be classified depending on their suitability to cater different voltage gradients as well as the temperature range for application. These gradations are known as voltage grading and temperature rating and shown in **Table 8.4a** and **8.4b**, respectively.

Table 8.4a Voltage grading of different polymers used as cable insulation

Working Voltage	Polymers Used				
≤ 3.3 kV	NR	IIR	EPR/EPDM	XLPE	MQ
= 6.6 kV to 11kV	Not Suitable	Applicable	Suitable	Suitable	Not Suitable
>11kV	Not Suitable	Not Suitable	Suitable	Suitable	Not Suitable
33kV	Not Suitable	Not Suitable	Suitable	Suitable	Not Suitable

Table 8.4b Temperature rating of different polymers used as cable insulation

Temperature Limit	Type of Polymers Used			
	NR	IIR	EPR	MQ
Maximum conductor temperature for continuous use (°C)	70	85	90	150
Maximum conductor temperature for emergency overload (°C)	--	--	130	200
Maximum conductor temperature for short circuit (°C)	200	220	250	250

The maximum conductor temperature is a combination of the ambient temperature and the temperature rise in conductor due to current flowing in it.

Once the insulating material has been selected, the other parameters for cable can be quickly established from data available in specifications for various types of cables. The conductor size is chosen to suit the required current carrying capacity, the insulation thickness for a particular insulating material is given for each voltage grade, and armour wire dimensions and sheath thickness are available from standard specifications.

8.4 Cable Jacket (Sheath)

The polymeric jacket (sheath) material in cable basically protects the cable from mechanical and environmental damages. Depending upon the specific application, it may have properties such as different degree of flexibility coupled with other mechanical properties like tear and tensile strength, abrasion resistance, ageing resistance under different conditions, high heat resistance for performance at elevated temperature, environment stress cracking resistance, oil resistance, flame resistance, low smoke and toxic gas generation in the event of fire, and so on. Polymers used for sheathing generally include NR, PCR, CSP, IIR, PVC, NBR and PU. Apart from conventional elastomeric materials, thermoplastic elastomers are also used as sheathing materials. Filled compounds based on PVC, PVC-NBR blend and rubbers like CSP, PCR, NR, NBR, and PU are being widely used in sheathing (protective layer) applications.

Carboxylated nitrile rubber (XNBR) gives higher modulus, tensile and abrasion than normal nitrile but is more prone to scorch and thereby makes processing difficult. Its applications include sheathing of oil-rig cables. To meet the different properties required for the cable jacket, the choice of the polymer or polymer blend is an important criterion. To improve upon mechanical properties and also to impart flame resistance, stiffness and so on, and the normal practice is to use a blend of NBR and PVC for heavy-duty cable sheathings.

Like base polymer selection of filler is also crucial for cable application especially for cable insulation. Generally non-conducting moisture and ionic impurity free white fillers are preferred for cable insulation selection becomes more stringent when operating voltage is high. Some special filler need to be incorporated to meet specific requirements for example, if the cable is to be used for a heat resistant application, EPDM filled with inorganic fillers like calcined clay, silicates, carbonates need to be used. Selection of filler in jacket is also important apart from imparting good mechanical properties the filler may also modify certain required properties. For example in an oil field application, carbon black filled nitrile rubber, and its blends with other polymers like PVC can be used as cable jacket materials whereas if the cable is intended to possess fire retardant properties - it is wise to use halogenated polymers such as PVC, PCR, CSP, CM etc.,

filled with antimony trioxide, borax and so on. Low smoke and non-toxic gas generating cable jacket may contain EVA filled with trihydrated alumina, and other fire retarding chemicals.

Cable sheath compounds from blends of EVA (45%) and hydrogenated nitrile rubber (HNBR) are suitable for application requiring both flame and oil resistance. A blend of functionalised polyolefin and PVC can be useful as a low halogen, fire resistant and low smoke sheath compound. The modern and latest trend in cable manufacturing is the development of fire retardant and low smoke generating cable-sheathing compound. Fire retardant and low smoke generation, along with reduced or no toxic and corrosive gas generation are highly desirable properties for a cable which is to be used in closed and confined areas such as underground metros, theatres, movie halls, or research laboratories. Low smoke and low toxic gas generation are must for prevention of casualties by suffocation and to protect sophisticated electronic systems, equipment, computers, and so on. The restriction of gas emission during cable fire is also essential to safeguard human life and to make fire fighting easier, as dense smoke not only hides the fire source but also impairs human vision to find an escape route. As a result for applications in railways, ships, community centres, auditoriums, movie halls, research laboratories, completely non-halogenated, low smoke, fire resistant cables are often in demand.

The combustion of organic polymers involves chemical and physical processes, which occur both within the polymers and in the surrounding gas phase.

A number of polymers and polymer blends have been tried for use as fire and flame retardant, low smoke generating, cable sheath compounds. EVA copolymer is an excellent material for this purpose. A large number of patents have been granted on flame retardant, low-smoke generating, sheath compounds, which reflects the importance of the topic in modern technology. The effect of different fillers on flammability and suppression of smoke generation of different polymers is an interesting topic of research. As will be evident, electrical property requirements are much less important for sheathing materials, although in some applications the surface resistivity or resistance to tracking is required to withstand the operating and environmental conditions for that particular application, and its compatibility with the other components of the cable.

It is needless to say the importance of cable jacket material which will not only have fire resistant coupled with low smoke properties, combined with good mechanical properties, weather resistance. In fact along with set of good performance properties an easy processability to form into cable are also mandatory requirement for any cable component. Depending on the demands of application areas different requirements like high temperature, oil, flame, fire resistance low or no smoke or toxic gas generation are also very specific [13-17].

8.4.1 Property Requirements of Cable Jacketing Materials

Materials used in cable jackets (sheaths) should have good combination of mechanical and environmental properties to withstand the service conditions and mechanical handling and service hazards. Electrical properties are relatively less important, for jacket material it should be generally insulating in nature to prevent electrical shock to live object. Property requirements of cable jacket are:

1. Good mechanical properties
2. Good environment resistance
3. Resistance to different chemicals, solvent and oil, depending on the field of application.
4. Flame and fire resistance
5. Satisfactory electrical resistance minimum resistivity ≥ 10^8 Ω.cm.
6. Low emission of smoke, non-toxic and-corrosive gas in the event of fire hazard.

The wire and cable industry has an enviable record for designing safer products for end users. The present day cable systems have been improved over the years, and have a long history of scientific research and investigation, which is reflected in their very satisfactory and reliable performance over a long period. The widespread use of electric cables in a large number of areas often causes outbreaks of fires either by accidental short circuit condition or burning of some extraneous matter, which ignites the cables. So, more attention is being focused on the fire performance of the cables with particular emphasis on reduced combustion emission. It is also essential to maintain the integrity of power circuit during the fire for fire alarm and rescue operation.

Protective coverings are applied over the insulated cores. They are generally applied by extrusion and are called 'sheaths' or 'jackets'. Some cable designs may incorporate two sheaths, designated as 'inner sheath' and 'outer sheath'. In such cases, the inner sheath is of a softer material designed to hold the cores together and fill the interstices, while the outer sheath is stronger and harder material, designed to withstand abrasion, weathering and action of other harmful influences.

8.4.2 Criteria for Selection of Sheaths (Cable Jacket)

a) Temperature rating

The temperature rating of the sheathing material must be compatible with that of the insulating material. The common sheathing polymers suitable for the temperatures are shown in **Table 8.5**.

Table 8.5 Temperature rating of polymers used as cable sheathing				
Type of polymer	NR	**IIR, CR, PVC, and NBR-PVC blend**	**HNBR**	**CSP**
Maximum temperature for continuous use (°C)	70	85	90-120	110

b) Environmental resistance

The selection of sheathing polymer is dependent on its ability to withstand the harmful environmental influences and requires detailed study of the environmental conditions and the properties of the compounds. PVC, polyethylene (PE), XLPE, polyamide and polyurethanes (PU) are popular thermoplastic sheathing materials. PCR, CSP, CPE, NBR, NBR-PVC blend are popular elastomeric sheathing materials for cables. NR and NR –SBR blend has some limited use as jacket material for general purpose cable.

8.5 Semi Conductive Components for High Voltage Cable

Semi conductive compounds are essential components for high voltage cables (voltage ≥ 3 kV). According to most of the specifications, all cables operating at the voltage gradient equal to 3 kV or more should have two different semi-conducting screens:

1. Semi-conducting screen between conductor and insulator

2. Semiconductor screen over insulator

The semi-conducting screen radially distributes the electric field, prevents partial discharge and takes care of fault current. Generally, the conductivity of the semi-conductive component is kept at around 10^4 Ω cm (maximum) and strength of the compound at 10 MPa (minimum).

Polymers in general are well known for their high electrical resistivity (volume resistivity $10^{12} – 10^{20}$ Ω cm). But the electrical resistivity of the insulating polymer matrix can be reduced appreciably through incorporation of sufficient amount (>percolation limit) of, suitable conductive filler when the resistivity of the filled system drops down to $10^4 – 10^3$ Ω-cm to become semi-conducting/conducting in nature. In order to obtain such drop in resistivity, the normal practice is to incorporate sufficient amount of conductive carbon black or carbon fibre in the polymer matrix. In such carbon filled composites the conducting carbon particles forms a continuous conductive network for flow of electric current through insulating polymer matrix. When conductive fillers like carbon black/ carbon fibre/carbon nanotube CNT) is added to an insulating polymer suddenly an abrupt drop in resistivity occurs at certain critical concentration of filler known as percolation limit (**Figure 8.8**). A semi conductive composite having resistivity ~10^3 –

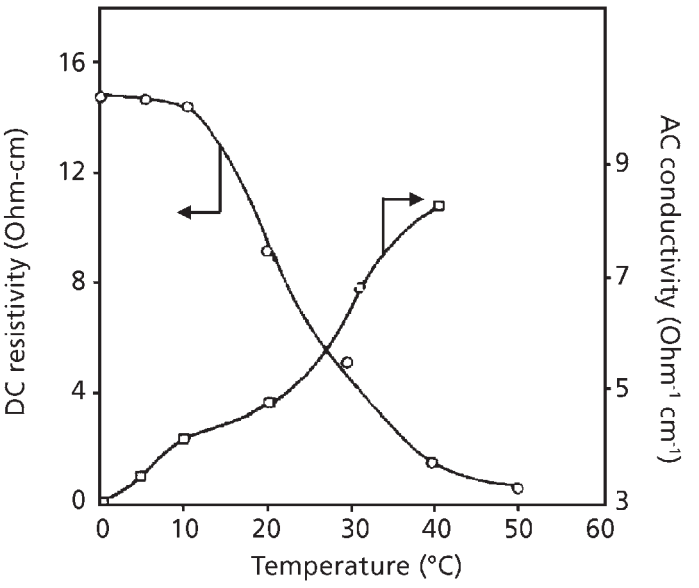

Figure 8.8 Change in DC resistivity and AC conductivity with addition of conducting black in 50/50 EVA-EPDM blends

10^4 Ω cm, along with other desired properties has an important application in the field of high voltage and extra high voltage power cables. In high voltage cables, generally two layers semi-conducting materials are used as mentioned earlier. The first semi-conducting layer is placed between conductor and insulator and other between insulation and sheath. The first semi-conducting layer is known as conductor shield (screen) and the second one is known as insulation shield (screen). The conductor shield generally firmly bonded with polymeric insulation is non-strippable type but the insulation shield is not so firmly bonded and is strippable type. This strippable and non-strippable characteristic is important from view point of cable repairing and cable joining. The conductor shield is generally applied through extrusion whereas polymeric shield may be provided in a cable either through extrusion or in the form of semi conducting tapes lapped over the insulation depending on type of cables. Generally the conductor shield takes care of partial discharge and corona discharge and the insulator shield takes care of fault current.

8.5.1 Property Requirements of Semi-conductive Compounds

Semi-conducting layers used in the high voltage cable should have following properties:

1. Low resistivity = $10^3 - 10^4$ Ω cm
2. High level of bonding with insulator surface
3. Cure compatibility between semiconductor and insulator
4. Similar temperature rating as that insulator and protective covering
5. Good processability

EVA, EPDM and blends of EVA-PE and EVA-EPDM filled with appropriate type and amount of conducting carbon black will give rise to a semi-conducting component. These compounds will have cure compatibility with XLPE and EPDM cable insulants so that these compounds can be a semi-conducting component for high voltage XLPE and EPDM/EPR insulated cables. Semi-conducting materials used in high voltage application generally derived from suitable polymer or polymer blends filled with the appropriate quantity of carbon black.

8.6 Different Cable Materials

8.6.1 Polymers used in Cables as Insulation, Sheathing and Semi-conducting Materials

In the present day, synthetic polymers have replaced natural materials such as paper, mineral oil and even NR for distribution and wiring type cable insulation and for cable jacket in general. The range of polymers available today is extensive and variations in chemical composition enable cable designer to achieve specific mechanical, electrical and thermal properties required for specific applications. With the advance of compounding ingredients and the availability of many new materials, the required properties of the base polymers can be extensively modified to achieve different goals through addition of specific fillers, plasticizers, softeners, extender, antioxidants and many other ingredients.

Along with the established polymers such as PVC, PE, NR SBR, IIR, EPR EPDM, PCR, NBR, CSP, MQ and so on, new polymeric materials are also used for cables. One can also find the application of many newly developed polymers in different parts of the cable.

8.6.2 Common Elastomers for Cables

8.6.2.1 Natural Rubber (NR)

Cable specifications for insulations and sheathing based on NR invariably require the best grade of smoked sheets like RMA 1 to 5 (graded by the Rubber Manufacturers' Association, USA), ribbed smoke sheet grade ribbed smoke sheet (RSS1X 1 to 5) these gradings are generally based on visible dirt content , standard NR grades like standard Malaysian rubber (SMR), Indian standard natural rubber (ISNR) grades. Similar standard grades are now also available for other natural rubber producing countries.

NR for cable components has to meet many stringent tests as specified in different standard specifications; especially for insulation it must be free from wooden splinters, grit or other such foreign matter. Various types of superior processing rubber and technically specified grades of NR are preferred over old conventional grades. De-proteinised NR has better electrical properties. NR is mainly chosen for low voltage cables requiring good flexibility. At present its use in the cable industry is very limited.

8.6.2.2 SBR

The grade of SBR used in the cable industry should preferably be a cold polymerised and non-staining one with a medium Mooney viscosity range, say in between 46 and 58 at 100 °C. This rubber may find use in coloured, and low voltage insulation, or in general purpose jacket material. However, its use is very limited at present.

8.6.2.3 Isobutene – Isoprene Rubber – IIR (Butyl Rubber)

Among the distinctive properties of butyl rubbers are:

- Excellent electrical properties
- Excellent ozone and weather resistance
- Good resistance to wet and dry heat
- Excellent chemical resistance
- Low permeability to gases
- Low to medium voltage cable insulation and for heat resistant jacket compound.

A range with isoprene contents between 0.5 and 3.0 mole% is commercially available.

The electrical properties of bromobutyl are very similar to regular butyl, only there is a slight increase in dielectric constant and loss factor may be encountered here in comparison to regular butyl because of introduction of small polarity (1-2% IIR) in the system. Because of good mechanical and environmental properties it may be good candidate for jacket material.

8.6.2.4 Ethylene-Propylene Co-polymer/Terpolymer – (EPR and EPDM)

These polyolefin rubbers are produced in two main types, the saturated copolymers (EPR) and the unsaturated terpolymers (EPDM). EPR is copolymer of ethylene and propylene and EPDM is a terpolymer of ethylene, propylene and small amount of non-conjugated diene monomer. Both EPR and EPDM are non-polar in nature.

By varying the ethylene ratio, products ranging from elastomeric to plastomeric are possible. The type of diene and its concentration regulate cure and ultimate crosslink density with sulfur-based accelerator systems. The effect of molecular weight and structure are reflected in polymer viscosity, processibility and physical properties of vulcanised compounds.

EPR and EPDM elastomers are very good candidates for different cable components especially for cable insulation [18-30]. They are characterised by the following combination of properties:

- Excellent electrical properties.
- Excellent resistance to dry and wet heat and steam.
- Excellent resistance to degradation by oxygen and weather.
- Excellent resistance to corona discharge.
- Good to excellent tensile strength, hot stress-strain properties.

EPR is completely saturated rubber whereas EPDM has unsaturation not in the main chain but in pendent group.

Because of a lack of unsaturation EPR is very slow curing, but has better heat and ageing resistance compared to EPDM. So EPR is preferred over EPDM when age and heat resistances are primary requirements for cable insulation, otherwise EPDM is preferred because of its easier processing and better curing ability coupled with overall good properties. Different grades of EPDM and EPR rubber are available on the market.

EPR has a little edge over EPDM in the very high voltage cable insulation but EPDM of selective type and with proper compounding may be used as a good substitute for EPR. EPR/EPDM insulation can retain their electrical characteristic within specified limit for long time as shown in **Table 8.6**.

Table 8.6 Changes in electrical properties during water immersion testing for a typical EPDM insulation compound [24]

Aged	Dielectric Constant	Power Factor (%)
1 Day	2.60	0.76
1 Week	2.60	0.70
1 Month	2.63	0.62
1 Year	2.84	0.50
3 Years	3.16	0.46
7 Years	3.87	0.68
10 Years	4.17	0.99
Condition – Immersion 90 °C, Water, 600 V/60 Hz Continuously Applied, Electric field 80 V/mil (=3200 V/mm) 1 mil = 0.001 inch = 0.0254 mm		

8.6.2.5 Polychloroprene Rubbers (PCR)

It is used mainly as a cable sheathing material where protection against flame, fire and oil is demanded. It is occasionally used as heat resistant low voltage insulation. Though PCR is now getting replaced by cheaper polymers such as CSP, CM or blends of NBR-PVC. However, in certain applications PCR is still being used as cable jacket mainly because of its good mechanical properties coupled with oil and fire resistance properties.

8.6.2.6 Chlorosulfonated Polyethylene – CSP/CSP

The most striking service characteristics of nitrile rubbers are:

- Their resistance to non-polar oils, fuels and solvents
- Their ability to maintain good service performance at elevated temperature for extended periods
- Their excellent resistance to permeation by gases

- Their poor electrical properties because of high polarity

The noted technical advantages of CSP are:

- High resistance to oil, flame and weathering
- Excellent resistance to wet and dry heat
- Excellent resistance to ozone and corona
- Excellent resistance to abrasion and flexing

The electrical properties of CSP make it adequate for use as an integral insulation jacket for low voltage applications. However, the main use of CSP is as heavy-duty cable jacket material for high voltage as well as flame resistant applications.

8.6.2.7 Nitrile Rubber and Hydrogenated Nitrile Rubber (HNBR)

Nitrile rubbers are copolymers of acrylonitrile and butadiene and are polar in nature. The composition of the polymer affects its mechanical properties and oil resistance, and low temperature flexibility. These rubbers are mainly used as cable jacket material as such or in blends with other polymers like PVC.

HNBR was developed as a high heat and oil resistant, special purpose rubber based on saturated hydrocarbon chains with polar nitrile group. Different grades of this rubber have various degree of unsaturation, for example HNBR grades can range from low unsaturation to completely saturated one. Because of the very low or no unsaturation being present in the back bone hydrocarbon chain the conventional vulcanisation is rather avoided. Generally the radical forming agents such as peroxides or high energy radiation are often used for crosslinking of HNBR. The presence of nitrile groups ensures good resistance of the rubber to swelling in oil and fuels.

HNBR barring the ease of sulfur vulcanisation has almost all the properties of nitrile rubber (NBR) along with several advantages over regular NBR as a cable jacket material, and they are as follows:

- Resistance to oil
- Heat resistant to 150 °C
- Good low temperature performance (brittleness temperature below –50 °C)
- Good mechanical properties
- Excellent ozone resistance

- Flame resistance

The additional advantages of carboxylated nitrile rubber (XNBR) over the NBR are:

- Higher resistance to abrasion
- Higher modulus and tensile strength

In the cable industry nitrile rubbers are extensively used for oil and fuel resistant cable jacket materials. To improve upon the mechanical properties, weather resistance and flame resistance of NBR it is the normal practice to use a blend of NBR–PVC for the heavy-duty cable sheathing material.

There are two other types of modified nitrile rubbers, which are available, namely XNBR and HNBR.

HNBR is recommended for outer sheath (cable jacket) of cables for use in a wide temperature range requiring oil, abrasion and ozone resistance but with moderate mechanical properties.

8.6.2.8 Silicone Rubber

Silicone elastomers are widely used for high temperature wire and cable insulation where no other organic elastomers can withstand the temperatures, for example in furnace cable. But silicone is generally preferred for low voltage applications (<3 kV). However, silicone is not good for wet heat conditions [31].

The general types of silicone rubber used in the cable industry are dimethyl polysiloxane, and diphenyl polysiloxane, methyl-phenyl polysiloxane and so on.

8.6.3 Specialty Elastomers for Cables

8.6.3.1 Polyacrylate Rubbers (ACM)

As per ASTM the polyacrylate rubber is designated as ACM and Vamac is a special type of compounded polyacrylic rubber produced and marketed by Dupont.

The salient properties of acrylic elastomers are:

- Very high resistance to heat, second only to acrylic elastomers,
- Excellent ozone resistance, and

- Excellent resistant to hot oils.

These are suitable for high temperature insulation and jacketing but in low voltage applications.

VAMAC grade of polyacrylate rubber provides effective insulation for low voltage high temperature equipment wires; appliance and motor lead wires operating at a maximum 110 to 120 °C and has the ozone and environmental resistance required of a jacketing material in high voltage construction. Its low emission of smoke and toxic by-products is another advantageous characteristic for a modern cable application.

8.6.3.2 Ethylenevinylacrylate Copolymers (EVA)

By varying the level of vinyl acetate in an EVA copolymer, significantly different materials can be produced. EVA with a low vinyl acetate content (up to 18%) are useful thermoplastics and those with a vinyl acetate content (of about 40%) have much less crystallinity and are graded as a rubber and can be compounded and vulcanised. EVA exhibits outstanding resistance to ozone, oxygen, light, oil and weather and has very high heat stability up to approximately 110 to 120 °C. It is a versatile polymer and is used widely in the cable industry for high performance wiring for ships, aircraft, oil rigs, military vehicles and control panels. EVA is again recommended as a semi-conducting layer used over an insulated core, which needs to be a strippable type. It also helps in formulating compounds for smokeless, halogen free flame retardant cables.

8.6.3.3 Chlorinated Polyethylene (CPE/CM)

This elastomer is made from high-density polyethylene chlorination using the suspension process. The properties of the resulting CPE/CM are influenced by the part PE structure, degree of chlorination and chlorine distribution in the polymer molecules. It is the chlorine content, and the saturated linear backbone that give CPE/CM advantages over many other synthetic polymers providing enhanced properties such as:

1. Excellent heat ageing characteristics
2. Excellent weather and ozone resistance
3. Outstanding oil and chemical resistance
4. Inherent resistance to ignition
5. Performance over broad temperature range
6. Good processability on equipment common to wire and cable industries

The present trend in the cable industry is to use chlorinated polyethylene replacing established elastomer like PCR, CSP, NBR-PVC and so on in different types of cable sheaths and low voltage cable insulation.

8.6.3.4 Fluorocarbon Rubbers - FPM

The outstanding properties of the fluorocarbon elastomers are

- Flame resistance
- High resistance to oxygen and ozone attack
- High resistance to chemical, oils and solvents

8.6.4 Thermoplastic Elastomers for Cables

This is a new class of polymers combining high elasticity, which is typical for rubber vulcunisates, and the processing properties of thermoplastics. These polymers are based on polyurethanes (PU), block co-polyesters (Hytrel) having hard and soft blocks and block copolymers of butadiene and styrene (SBS), block copolymer styrene-isoprene-styrene (SIS). Some of these thermoplastic-elastomers are specifically tailored to the needs of the cable industry. Applications range from general wiring and flexible cords to power cables, which are combined with attractive savings in volume cost. It is claimed that a reduction of insulation thickness is possible for its superior electrical properties. Some of the harder grades may even meet the hot test requirement for crosslinked PE at 150 °C as per the International Electrotechnical Commission (IEC). These thermoplastic elastomers find wide application as inner sheathing materials in single as well as multi-core cables.

8.6.4.1 Thermoplastics for Cables

Different thermoplastic materials are being used in different parts of the cable. Non-polar thermoplastic like polyethylene and polypropylene are used as mainly as insulation and sometimes as jacket. Polar thermoplastics like Nylon and polyester are used as barrier tape.

8.6.4.2 Polypropylene (PP)

Interest in polypropylene arises because the commercial grades of this homopolymer are freely available and extrusion is quite easy as all machinery available for PE can

be used. Polypropylene melts at 160 °C in comparison with the melting temperature for LDPE of approximately 100-115 °C. Polypropylene is used for the insulation of geophysical cable where its toughness, tensile along with excellent electrical properties are appropriate for this typical application.

8.6.4.3 Polyamides (Nylons)

Thermoplastic polymers like polyamides are often used in the form of film or coat in different cables. The toughness, good abrasion resistance, good chemical inertness and biological inertness of this polymer justify its use as an overcoat. The moisture absorption and poorer electrical characteristics limit its general use as an insulating material. But they are used as a barrier tape in rubber insulated and other cables where compound used in insulation may adversely interact with. conductors.

Nylon can also be used as an additional sheath over an existing PVC or PE sheath where additional physical or chemical protection is required (e.g., termite or geothermal) [32].

8.6.4.4 Thermoplastic Polyester (PET)

In cable construction some materials are used for insulation bedding and sheathing or as tapes, string, and polypropylene being an example of the latter. Polyethylene terephthalate (PET), Melinex or Mylar, is widely used as a binder tape for multi-core cables and as a barrier layer to retard migration of any detrimental chemical to and from the insulation, also to separate insulation from a stranded conductor.

8.6.5 High Temperature Thermoplastics and Thermosets

8.6.5.1 Fluorinated Polymers PTFE

It is by far the most important member of this group and is manufactured by the polymerisation of tetrafluoroethylene. The polymer is non-polar and has outstanding electrical properties. It cannot really be considered to be a thermoplastic because the melt viscosity is so high that extrusion is not possible. The insulation has to be applied to conductors by a cold shaping operation or by taping followed by a sintering process to cause the polymer particles to fuse and coalesce. Service operation up to 260 °C is possible with this material and it is highly resistant to chemicals.

This polymer has been modified through copolymerisation with ethylene and propylene to produce new polymers having different composition to give products like ethylene-

tetrafluoroethylene (ETFE) polymer and fluorinated ethylene propylene (FEP) polymer. These fluorine-containing copolymers are now increasingly used because of their good extrudability and physical properties. This group of polymer is widely used as insulation for instrumentation cables and is characterised by good mechanical, electrical, thermal and environmental resistance properties.

8.6.5.2 Fluoropolymer Resin (Tefzel)

Partial replacement of fluorine in fluorocarbon polymers by hydrogen or hydrogen and chlorine leads to new type of polymers having modified mechanical and chemical properties. In fact, the resulting polymers have significantly different properties from those of fully fluorinated resins. When this substitution occurs by regular alternation, polarity and mechanical properties are maximised. The polarity of polymer increases because of the substitution of hydrogen and chlorine having different electro- negativities compared to fluorine. Moreover the bond lengths of C-F, C-Cl, and C-H are different. So there is charge imbalance in polymer chain and polymer become polar in nature leading to increase in intermolecular force of attraction. The increased interpolymer chain attraction results in higher mechanical properties. In addition, the increased polarity/ interpolymer attraction influences the solvent resistance and permeation characteristic behaviour of the resin. Tefzel grade of fluoropolymer resin are partially fluorinated resin, have improved chemical and electrical properties, coupled with enhanced mechanical properties and good processability.

8.6.5.3 Crosslinked Polyethylene (XLPE)

The starting material for XLPE is LDPE, a plastic material which has long been used as a cable dielectric (insulation) because of its excellent electrical properties, light weight, good low temperature flexibility and good resistance to moisture and chemicals. The use of LDPE was restricted because of its two major drawbacks – its softening temperature is as low as 105 –115 °C and secondly its tendency to undergo stress-cracking failure when comes in contact with certain surface-active agents.

By the use of special additives and post extrusion treatment reminiscent of the vulcanisation of rubber, the properties of LDPE are greatly improved because it becomes crosslinked giving XLPE.

Presently there are three different methods of crosslinking methods for LDPE – curing through use of organic peroxide, curing through high energy irradiation like electron beam and lastly Sioplas technology where a silane coupling agent is added and curing is subsequently done in water. The process is simple but suitable only for low voltage applications [33].

Extrusion technique of XLPE is similar to that of LDPE. With vulcanisation, the good attributes of PE are still retained in XLPE along with the retention of physical properties at elevated temperature is considerably enhanced. Unlike PE which melts at around 100 °C, XLPE physically remains over the conductor even at150 °C. The high resistance to hot deformation and resistance to hot air ageing obtained for XLPE provide an important advantage in cable ratings and are of specific significance in locations where the ambient temperature is high. The performance characteristics of typical XLPE and other insulations are summarised in **Table 8.5**.

The crosslinked structure of PE that is XLPE is:

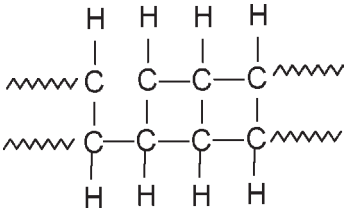

The most striking physical and electrical properties of XLPE are:

1. Little deformation at high temperature
2. Higher operation temperature
3. Excellent electrical properties – lower transmission losses
4. Superior mechanical properties
5. Lighter weight

Different grades of PE after crosslinking that is converting them to XLPE can also be used as cable sheath material. Rubber and PVC based cable compounds contain several ingredients apart from base polymers whereas almost virgin polymer PE or XLPE is suitable for cable application. In polyethylene based insulation fillers, plasticiser and other ingredients except antioxidants are avoided to retain good electrical properties. A comparative study of properties of different cable materials with that of XLPE is given in **Table 8.7**. It can be seen that XLPE has better electrical properties like lower dielectric loss and higher resistivity compared to other insulants (except PE). Moreover XLPE has better mechanical, thermo-mechanical properties and higher temperature rating compared to other insulating materials. Other hydrocarbon based cable materials which have comparable electrical properties of XLPE is EPR and EPDM as given in **Table 8.8**.

Table 8.7 Comparison of XLPE and other insulating materials					
Property	**XLPE**	**EPR/ EPDM**	**PVC**	**Impregnated paper**	**PE**
A **Electrical properties**					
Dielectric constant at 50 Hz and at 200 °C	2.3	3	5	3.5	2.3
Loss factor, tanδ at 50 Hz and at 200 °C	0.0005	0.003	0.07	0.003	0.0003
3. Volume resistivity at 50 Hz and at 200 °C (Ω-cm)	10^{17}	10^{15}	10^{14}	10^{15}	10^{17}
B **Thermal properties**					
Maximum conductor temperature for continues operation (0 °C)	90	90	70	70	70
2. Maximum conductor temperature during short circuit (0 °C)	250	250	160	160	150
3. Hot deformation resistance at 1500 °C	Good	Excellent	Poor	---	Melt
Mechanical properties					
Tensile strength (MN/m^2)	15	5	15	NA	14
Elongation at rupture (%)	500	700	250	NA	400
Abrasion resistance	Good	Poor	Good	---	Good
NA: Not applicable					

Table 8.8 Typical properties of XLPE *versus* EPR [4, 26, 28, 29]		
Physical properties	**XLPE**	**EPR**
Density (g/cm^3)	0.92	1.2-1.4
Tensile strength (MPa)	19	9-12
Elongation (%)	500	250-350
Modulus of elasticity, (MPa)	121	5-14
Heat distortion (%)	20	5-8
Thermal conductivity (w/m °C at 90 °C)	0.27	0.27-0.35
Electrical properties		
Dielectric constant	2.3	2.5-3.0
Dissipation factor (%) at 23 °C at 90 °C	<0.03 <0.03	0.16-0.30 0.30-1.0
Volume resistivity (Ω-cm) at 23 °C	10^{16}	10^{13}
Short-term AC breakdown on miniature cable (kV/mm)	48	30-40

Table 8.8 shows a comparison of electrical and mechanical properties of XLPE and EPR used as cable insulations.

It is clearly seen that XLPE insulation has better electrical and mechanical properties than EPR/EPDM insulation. However EPR and EPDM are better than XLPE if a high degree of flexibility is wanted.

8.7 Different Methods of PE to XLPE Conversion

There are three different methods of crosslinking LDPE to produce XLPE namely using high energy irradiation technique mostly without using any chemicals at room temperature or slightly above, using chemicals such as an organic peroxide with or without co-agent at elevated temperature in dry heating in presence of nitrogen or wet heating in presence of steam. The third method uses completely different technique known as Sioplas, where polyethylene chains are crosslinked through a siloxane bridge in the presence of moisture and catalyst. This method does not need pressure or high temperature and is suitable for medium to low voltage application. General chemical reactions involved in peroxide curing of polyethylene are given in **Figure 8.9**.

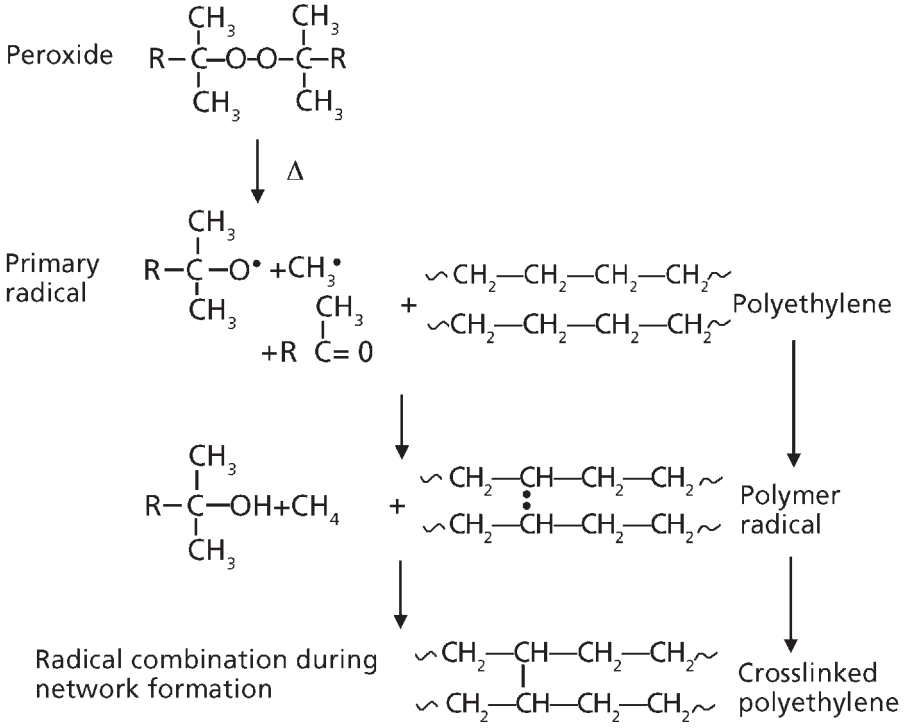

Figure 8.9 Peroxide curing of polyurethane

8.7.1 Crosslinking by High-Energy Irradiation (Electron Beam)

If PE is subjected to a high-energy irradiation, then the ionic bombardment causes chain scission and bonding to occur simultaneously (**Figure 8.10**). The latter is beneficial but the former is a form of degradation process. Thin wall dielectrics or material in the form of tape can be quite successfully crosslinked in this way using electron radiation, but for thick insulations the complications and expense of capital plant involved is high, and preferential absorption of the radiation in the outer layer of cable leads to excessive deterioration before the inner layers are adequately crosslinked. The use of suitable crosslinking promoters may overcome these problems to a great extent. However high energy radiator is required for curing of cables having higher insulation thickness.

8.7.2 Crosslinking by the Sioplas Technique

The basic component of the Sioplas system is a PE, which has been grafted with a suitable silane compound to form a graft co-polymer. A smaller quantity of PE is mixed with a suitable catalyst to form a masterbatch. The co-polymer and masterbatch are then premixed just prior to their introduction to the extrusion hopper, and the extrusion process is carried out using normal thermoplastic extrusion techniques. The extruded silane grafted LDPE will cure naturally by the gradual absorption of moisture from the environment at ambient temperature without the evolution of gaseous products or the formation of micro-voids. The general temperature of curing varies from 30-100 °C. The reaction scheme of crosslinking polyethylene *via* Sioplas is given in **Figure 8.11**.

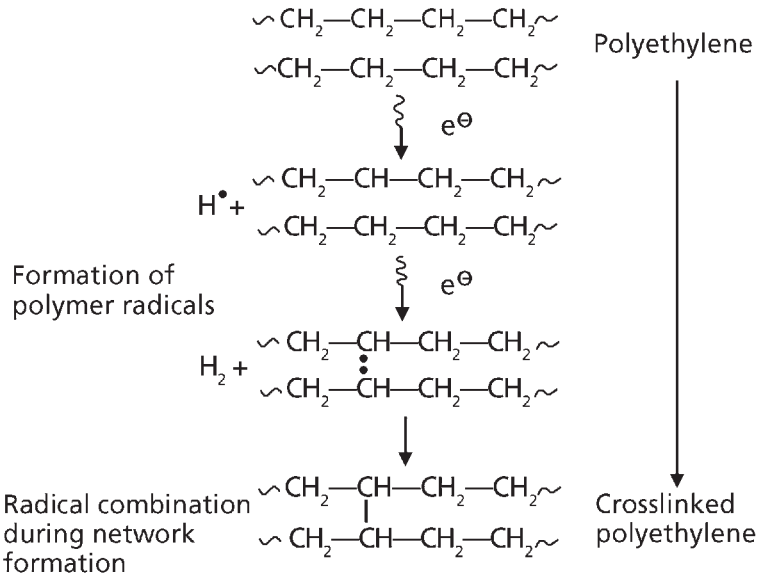

Figure 8.10 Electron beam radiation curing of polyethylene

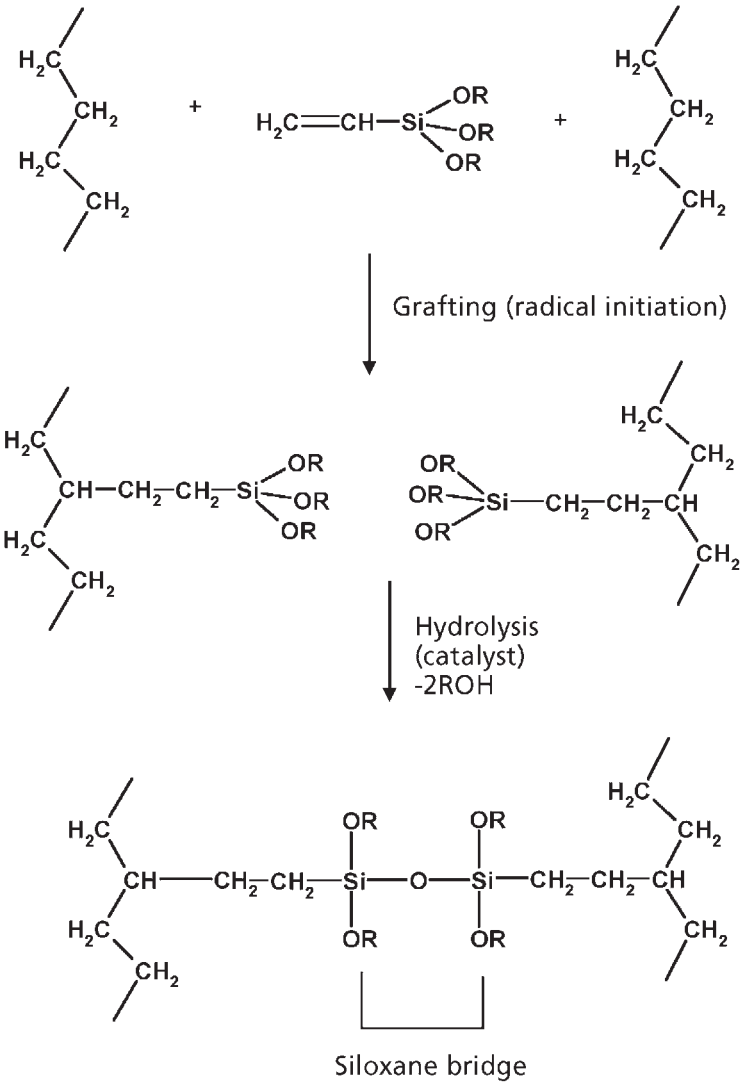

Figure 8.11 Crosslinking of polyethylene by Sioplas technique

8.8 Different Compounding Ingredients

Rubber as well as PVC cable compounds contain many ingredients other than the base polymer, which helps to make them suitable for specific applications.

8.8.1 Crosslinking Agents

For unsaturated elastomers such as NR, NBR and SBR, sulfur still remains the main vulcanising or crosslinking agent.

However, at times to achieve better heat resistance characteristics, use of elemental sulfur is either minimised or avoided and organic compounds such as tetramethyl thiuram disulfide and polysulfides, which liberate sulfur at the vulcanising temperature. Though sulfur curing can be accomplished relatively easily and provides better mechanical properties than other types of curing for example organic peroxides but it introduce polar groups into the polymer matrix thus impairing electrical properties important for high voltage application, and wet electrical properties of EPR based insulation is also a disadvantage for sulfur curing. Again for high temperature applications sulfur-based crosslinks are less suitable compared to peroxide-based ones as the latter introduces carbon-carbon crosslinks in the polymer matrix, which is thermally more stable and non-polar in nature.

8.8.2 Metal Oxides

A zinc oxide and magnesium oxide combination with or without suitable organic accelerators are used for PCR-based cable compounds. Litharge and/or magnesia are chosen for CSP. Litharge and other lead oxides are found to improve water ageing properties of the cable compound.

8.8.3 Organic Peroxides and Other Curing Agents

Dicumyl peroxide is a common curing agent for silicone rubber, EPR, EPDM and XLPE.

Benzoyl peroxide is more suitable for SMQ. However, selection of peroxide is crucial for cable manufacturing especially where a higher temperature is needed during processing (for example extrusion) prior to the final curing. During extrusion at high temperature for example of XLPE cable, the peroxide used in the formulation should not get activated at the extrusion temperature otherwise it can cause scorching and jamming of the extruder. An organic peroxide like dicumel peroxide with a higher decomposition temperature is preferred. Apart from organic peroxide other curing agents which are used are difunctional compounds like quinoxime, PF resins mainly for butyl rubber.

P-Quinone dioxime is used for curing of butyl rubber to produce high heat resistant vulcanisate. However use of this chemical is now limited because of its carcinogenic tendency. Halogenated PF resin can also be used for butyl rubber curing to produce heat resistant applications.

8.8.4 Accelerators

The main functions of accelerators are to speed up the crosslinking reaction and to provide vulcanisates with greatly improved properties through achievement of higher state of cure.

While selecting the accelerators for cable insulation and sheathing, time of cure, scorch safety and good ageing properties must be taken into consideration. They should also not cause excessive discoloration and should not impair electrical parameters. The accelerator or combination of accelerators must provide flat 'plateau' cure to avoid over curing and thereby lowering the properties on long-term service.

8.8.5 Antioxidants

Antioxidants are essential ingredients for cable compounds to protect them from ageing and thereby prolong the life of a cable generally two decades.

Due to detrimental effects of heat, light, oxidation, weathering and metal poisoning, there is some changes occur in polymeric systems, these are mainly chain scission, unwanted cross linkages and introduction of new chemical groups in the matrix polymer.

No single antioxidant is really ideal for all purposes - it may be necessary to go in for more than one type of antioxidant. The antioxidants available are mainly aromatic amines and phenols.

While selecting antioxidants for insulation and sheathing these points are considered:

a) It should not stain or migrate to such an extent that the identifying colours of cores get spoilt.

b) It should not accelerate, retard or bloom unnecessarily.

c) It should not hamper electrical properties.

8.8.6 Antiozonants

Ozone formation in cable may occur during partial discharge under high voltage. This discharge converts oxygen to ozone and very small concentration (even in ppm level) of ozone may be detrimental to cable polymers under static or dynamic strain.

Furthermore in places like the in the sea, or on the sea-shore, the cable is surrounded by a higher ozone concentration. To fight against the deteriorating effect of ozone

unsaturated polymer compound should contain adequate amount of chemicals known as antiozonant.

There are two ways of inducing protection against ozone. The first one is to use chemical antiozonant and second one is to use physical antiozonants like special waxes, e.g., microcrystalline wax which when bloomed to the surface acts as an ozone barrier. Cables which may encounter a high degree of fatigue may contain both types of antiozonants. Many potent chemical antiozonants have staining effect so they are not suitable for light coloured product where non staining antiozonants are preferred. The staining antiozonants are more effective and used in black coloured insulation and especially in sheathing compounds. The antiozonants also help to get superior flex-cracking resistance.

8.8.7 Fillers

Fillers are needed mainly:

a) To facilitate processing

b) To reinforce the vulcanisate

c) To reduce the cost of the formulations

When added to polymer insulation, the filler must maintain a high level of electrical resistance. It should not adversely affect the electrical properties of the polymeric insulation when dipped in water. The fillers must be of fine powder having a maximum residue of 0.1% on a 300 mesh sieve and 85% of the particles should have fineness of 2 μm size and below. They must be free from copper, manganese and so on and shall be almost free from moisture. Filler treatment prior to addition to polymer compounds improves both electrical and mechanical properties. In elastomer-based cables fillers are required for improvement of mechanical properties processability and cost factor. Filler often impairs electrical properties such as electrical loss breakdown voltage especially wet electrical properties so their selection for high voltage application is more critical than that in low voltage. Fillers such as calcined clay, calcium carbonate, magnesium hydroxide, barytes (barium sulfate), trihydrated alumina are used as fillers in cable compounds. Dry filler shows better electrical properties than normal filler as shown in (**Figure 8.12**). How the filler can affect mechanical and electric properties of polymeric insulation based on EPDM rubber is shown in **Table 8.9**.

For use in sheathing, carbon black with its high reinforcing properties is the obvious choice. Silica and silicates are also used especially when a coloured sheath is required. For cheapening and also for facilitating processing non-reinforcing fillers such as soft and hard clays, other mineral fillers like calcium silicate, calcium carbonate, are used.

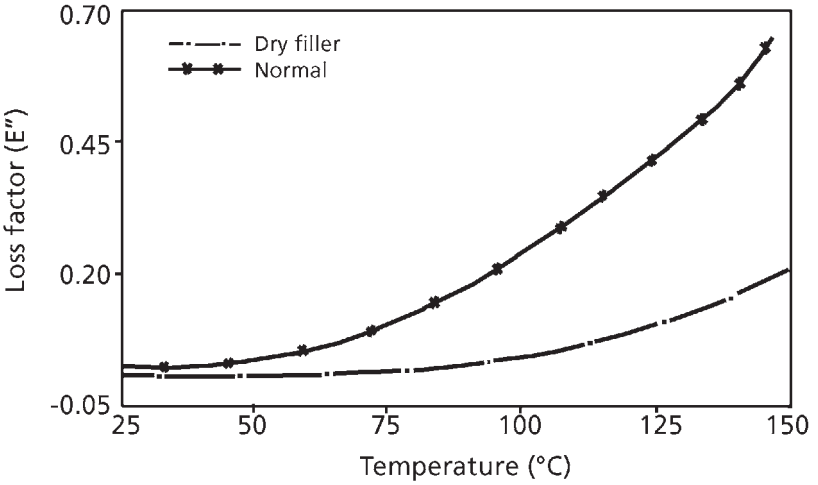

Figure 8.12 Variation of loss factor against temperature for 50:50 EVA: EPDM blend insulation containing dry and normal calcined clay filler

Table 8.9 Effect of clay filler level in semi crystalline EPDM insulation [24]

Compound	A	B	C	D
Parts filler/100 parts EPDM	0	30	60	90
Density (g/cm^3)	0.90	1.04	1.20	1.31
Tensile strength (MPa)	5.2	8.3	10.3	11.7
Elongation (%)	450	400	320	260
Dielectric constant	2.4	2.4	2.5	3.0
Power factor (%)	0.06	0.20	0.25	0.60
AC breakdown (Volts/mil) 1mil = 0.001 inch = 0.0254 mm	850-1000	750-850	700-800	550-650
After 26 Weeks in 90 °C Water				
Dielectric constant	2.4	2.5	2.75	3.1
Power factor (%)	0.40	0.65	0.80	1.5

Talc, activated calcium carbonate, natural and precipitated calcium carbonates, china clay and so on are found to be good fillers for insulation. For high voltage insulation, calcined clay is the preferred choice because of its high electrical stability properties. Thermal blacks up to a certain dosage can be used in the low voltage insulation. Carbon blacks are used mainly in semiconducting and cable jacket compounds some times as coloring material in the level 5-10 phr to protect against detrimental effect of ultra-violet rays.

8.8.8 Auxiliary Additives

These are added to compounds only when needed. In the cable industry, these may include:

a) A peptiser like pentachlorothiophenol is used for quick mastication and decreasing viscosity.

b) Promoters such as polyparadinitrosobenzene are used in butyl stocks for heat treatment purposes for providing stiffness to vulcanised stock. These additives promote strong polymer-filler interaction, perhaps creates some linkages, between rubber chains and active centres on the surfaces of filler particles. However better improvement from heat treatment is realized from mineral filler like clay, silica etc rather than in carbon black. The use of promoter leads to better dispersion of filler, better mechanical and electrical properties and better extrusion behaviour.

c) Retarders such as salicylic acid, benzoic acid are used for greater scorch safety.

d) High styrene resins (styrene butadiene copolymers) may be used with a base elastomer to maintain the dimensional stability of the extrudate. Because of their plastic nature high styrene grade of SBR in an extruder at temperature around 90-100 ^{0}C the resin becomes soft and easily flowable and helps in extrusion. But when it comes out of extruder solidifies quickly at atmospheric temperature and controls the die-swell.

e) Flame-retardants such as chlorinated wax, naphthalenes, some organic bromo compounds, antimony trioxide, different phosphates are used for imparting fire resistance properties to a cable.

f) Colours – the use of inorganic colours, like different metal oxides iron oxide, chromium oxide are to be used with proper care because, their use in high dosages may impair crucial electrical properties but metal oxide like titanium dioxide, zinc oxide are frequently used as white pigments. Organic pigments contains different chromophor groups, these are mainly amines and azo-compounds such as phthalocyanines. Phthalo blue, Phthalo green, Red Lake C and so on are mostly used for coloring purpose because they give bright colour but need a lower dosage. Though coloring materials are polar in nature but their loading is small consequently their presence has minor effect on electrical properties of the insulation compound.

8.8.9 Plasticiser, Softeners, Processing Aids

To counteract the hardening effect of fillers, and to improve dispersion and incorporation of fillers, softeners are added. These also help with the extrusion and calendaring process. Softeners may be classified by considering their usage in cable compounds:

a) Processing aid

b) Lubricant

c) Plasticiser

Processing aids are those, which help dispersion and incorporation of fillers. Mineral oil, petroleum jelly and salts of fatty acids are all examples of different types of processing aids.

Addition of lubricants like paraffin wax, stearic acid, and zinc stearate in compound facilitate extrusion and calendaring and also provide non-sticking to rolls during mixing. Plasticisers like aromatic and paraffinic type of mineral oil, phthalate and phosphate do enhance the plasticity of compounds to aid in processing.

The following points should be kept in mind while selecting softeners/plasticisers-proper grades and their dosages in cable compounds are also equally important:

a) These must not impair electrical properties when used in insulation

b) These must not sweat-out or migrate, and should have adequate compatibility

c) These must not impair mechanical and ageing properties

Polar plasticisers are not preferred where electrical property requirements are stringent.

8.8.10 Coupling-agents

Different types of coupling agents in broad categories of silane and titanates are available. However, silane types, (e.g., Si-69, Vinyl-172) are more often used to improve polymer-filler interaction and the mechanical properties of filler-polymer composites. Silane coupling agents also improve wet electrical properties of filled polymer compounds.

A typical cable compound formulation based on EPDM rubber along with functions of different added ingredients is given in **Table 8.10**.

8.9 Cable Manufacturing Process

The main steps of cable manufacture generally include: cable compounding, application of covering, and quality checks and tests. A schematic flow chart for rubber cable manufacturing is given in **Figure 8.13**.

Table 8.10 Formulation for flexible high voltage cable insulation compound		
Ingredient	**Rubber/polymer (phr)**	**Function**
EPDM rubber	85.0	Base elastomer, selected for 90 °C continuous operation with excellent electrical and ozone, corona resistance properties.
PE	15.0	For further betterment of electrical properties, shape retention and so on.
Zinc oxide	5.0	Activator and enhances heat resistance.
Calcined clay (moisture free)	120.0	Main filler which does not impair electrical properties and gives reasonably good mechanical properties.
Carbon black (FEF)	5.0	Secondary filler - used for better extrusion and as a UV protector.
Vinyl silane A-172	1.0	Improves bond between filler and polymer and thereby improves long term wet electrical stability of the compound.
Sunpar 2280	10.0	Saturated paraffinic process oil, because unsaturated oils will impair peroxide curing.
Paraffin wax	5.0	Lubricant - aids extrusion process.
Polymerised dihydroquinolines	1.5	Heat resistant antioxidant.
Litharge	5.0	Improves water resistance considerably.
Dicumyl peroxide	2.5	Crosslinking agent.
Triallyl cyanourate (TAC)	0.5	Co-agent, increases degree of crosslinking.

This section emphasises the basic principles of rubber compounding and processing technique for the manufacture of general and special purpose plastomeric and elastomeric cables.

The first step of the approach of the cycle is the compounding of elastomer with the appropriate chemicals. The compounding procedures followed for general purpose and special purpose elastomers are more or less the same only there are some modifications in processing conditions and special care has to be taken depending on the nature of the elastomers. For example, silicone rubber compounding has to be done under very

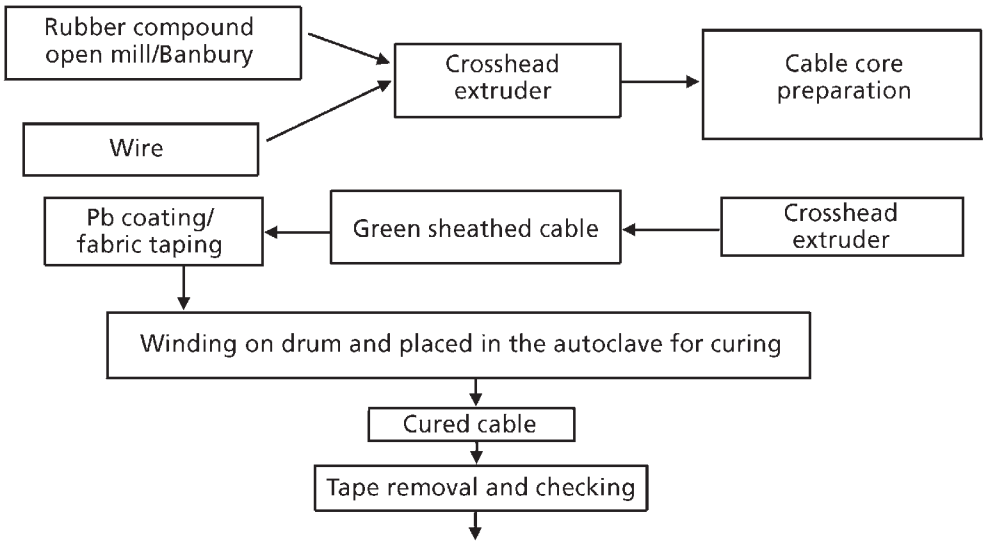

Figure 8.13 Schematic diagram of cable manufacturing steps

neat and clean conditions, and during butyl and EPDM compounding contamination from unsaturated materials are to be avoided. PVC cable compound generally contains plasticizer, stabilizer, filler, colour. PE and XLPE-based cable insulation generally do not contain any filler. Mostly these are neat polymers with antioxidant and some time curing system.

8.9.1 Basic Principles of Compounding

Compounding is done by mixing in an internal mixer or an open mill.

The choice of the mixing method depends on the compound recipe and on the condition of the available mixing equipment. However, which method is chosen, the following parameters should be taken into account:

a) As a rule the batch weights to be applied in the mixer must be kept within its optimum capacity.

b) Mixing time and temperature.

c) Cooling of compound after mixing.

8.9.2 Internal Mixing

Conventional method – in this method order of mixing is:

Elastomer,

Reinforcing filler and half of the oil loading,

Other ingredients,

Non-reinforcing filler and rest half of the oil,

This method is adopted when:

i) Rubber content is high,

ii) Reinforcing filler with a small particle size is to be incorporated.

Using the upside down method, the order of mixing is:

Dry compounding ingredients and half oil and elastomer,

Full ram pressure immediately, and

Balance oil after one minute.

This method is to be adopted when:

i) Large quantities of highly or moderately high reinforcing filler need to be incorporated, and

ii) The internal mixer is capable of coping with high peak load at the beginning.

Semi-conventional method – this is in between conventional and upside down method.

8.9.3 Open Mixing

Cable compound of small batches can be mixed in open mixing mill. Big size batches can be mixed in internal mixer like a Banbury.

8.9.4 Application of Cable Insulation Covering

Insulated conductors are covered with the requisite rubber compound following three techniques: longitudinal, lapping and extrusion.

There are two basic curing processes namely: batch curing, and continuous curing.

8.9.4.1 Longitudinal and Lapping Method

These techniques have now been superseded by extrusion technique because of their economical and technical deficiencies.

Both involve the application of calendared tapes of uncured compound. Longitudinal covering consists of passing the wire, sandwiched between two rubber tapes, between grooved rollers so that a seam is formed on each side. A longitudinal machine has three or four sets of rolls in tandem. The requisite thickness of covering is built up by applying the appropriate number of tapes of suitable thickness.

8.9.4.2 Lapping Method

The lapping method consists of wrapping tapes spirally on to the wire with an overlap. Again, the appropriate thickness is obtained by using several tapes from lapping heads in tandem.

These two methods require compounds capable of being handled in roll form with the conflicting properties of good building tack, good green strength and low stretch.

Cores made by these two methods are curing by batch curing process.

8.9.4.3 Extrusion Method

Extrusion of insulation and sheath is carried out using conventional extruders fitted with crossheads. The conductor to be covered, or the core or laid up cores to be sheathes, as the case may be, pass through a core tube supported coaxially within the head and located concentrically with the die by a tapered extension to the core tube, i.e.,'core point'.

The cores/cable after extrusion can be cured either by a batch process or by a continuous process.

8.9.5 Curing of Cable

XLPE and elastomer-based cables at final stage of forming need curing to develop mechanical and thermal resistance properties. There are different methods of curing. It may be continuous process or a batch process.

8.9.5.1 Batch Curing Process

Curing by batch process is easy to accomplish in autoclave where certain length of cable can be cured depending on the size of the autoclave curing can be done by hot air or steam. The curing conditions maintained in autoclave are as follows:

Temperature - 140 °C to 160 °C

Time cycle - Varies between 15 minutes to 90 minutes overall depending on cable compound and cross-sectional thickness of the polymeric materials used in the cable. Only cable core (conductor covered with insulation) or preformed cables (conductor + insulator + jacket + other components) are placed in a French chalk bed or drums and then placed in an autoclave for curing using hot air or steam. Small cross-section cable can be cured as such but if higher cross section cable has to be cured more precautions have to be taken to avoid dimensional deformation during cure. To maintain circular dimension of the cable and to avoid any eccentricity, flattening and formation of blisters, cores or cables of higher diameter cables are normally wrapped with proofed cotton tape or even covered with lead jacket by lead extruder or lead press. After curing the lead jacket is stripped off from the cable.

8.9.5.2 Continuous Vulcanisation (CV) Process

The continuous vulcanisation is accomplished in pressurised steam heated metallic tube known as CV tube. In this process the CV tube may be attached with the crosshead of the extruder. Earlier CV tubes were arranged horizontally but later vertical and catenenary (inclined) arrangements are used for the curing of larger diameter cables. This eliminates sagging and dragging problem of heavy weight cables.

A continuous curing (CV) plant consists of:

Extruder – L/D ratio varies from 4:1 to 20:1

Pressurised steam tube – 50 to 80 Mt

Pressurized cooling water tube – 30 to 60 Mt

Ratio of steam to water depends on size of cable and thickness of covering

Curing temperature – 170 °C to 200 °C

8.9.6 Dual Extrusion System

Simultaneous application of two components of composite insulation or insulation/sheath, e.g., EPDM-CSP, NR-PCR over a conductor is now done by a dual extrusion system where two extruders may be placed side-by-side at an angle or face-to-face opposite one to the other with a common die head or head extruders placed on after another in tandem.

8.9.7 Triple Extrusion System

There are three extruders in this system, which use three layers of rubber compound.

For high voltage cable insulation, the smallest of the three extruders applied the semi-conducting layer over conductor followed in tandem by two larger extruders, which simultaneously apply the main insulation, and semi-conducting layers through a common dual die head.

8.9.8 Improvement in CV Curing Techniques

Many ideas have been generated and some modifications of the heating system of the CV tube have been introduced, replacing steam with dry nitrogen at a lower pressure.

Such modified installations are:

i) Dry cure system – Electrical heating with nitrogen atmosphere inside the CV tube. The curing temperature used is very high around 300-350 °C.

ii) Microwave dry curing (MDC) process, where the curing is done by means of microwave, fully or partly followed by conventional curing.

iii) Pressurised liquid continuous vulcanisation (PLCV) system, which uses a hot liquid like water at high temperature.

Electron beam curing is a relatively recent technique commercially used for low voltage cables having a lower thickness because of a restriction in penetration depth. Wide range polymers can be efficiently cured by the electron beam technique. In fact it gives low loss insulation compared to peroxide cured ones (**Figure 8.14**).

8.10 Quality Checks and Tests

Strict control of quality starting from raw material used to processing steps and conditions followed and final inspection and laboratory tests on finished product are

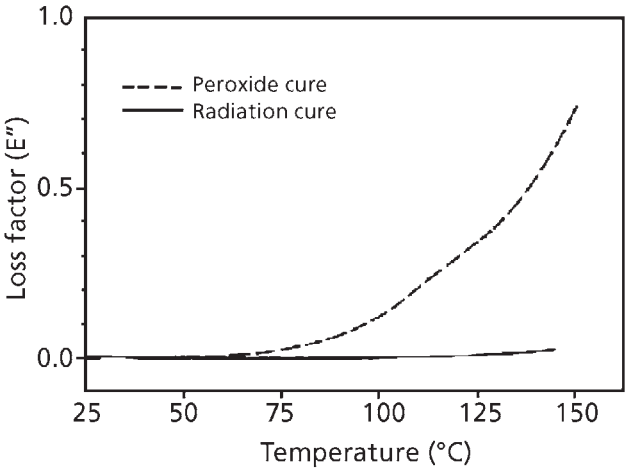

Figure 8.14 Dielectric loss of peroxide and radiation cured XLPE against temperature

very important. Why and how such quality checks are made are depicted below:

- To ensure that the correct product is produced and for it to provide a safe and satisfactory service performance of cables it is absolutely important to introduce quality checks at every stage of the entire production chain.
- Raw materials checks: The incoming raw materials required for the manufacture of cables must be tested to their respective standards before acceptance. The idea is to check purity, genuinity and usefulness of the materials for the intended purpose.
- Sieving, weighing and mixing: Bulk fillers are sieved to separate out grits, foreign matter and so on and also heated at times to drive out moisture.
- Strict vigilance is necessary during weighing, and mixing, as the compound properties are entirely dependent on these two stages.
- Checks of batch weight and specific gravity of the mixed compound are helpful as a countercheck.
- Straining and testing of compound: straining in an extruder type strainer is done to eliminate agglomerates, grits or any contaminants and also to ensure better dispersion.

At this stage extensive tests are done to obtain the right compound, namely:

- Plasticity and scorch,

- Rheometric analysis,
- Physical properties like TS, EB, and so on, and
- Electrical properties, e.g., volume resistivity

The results of all batches are compared with standards for final approval from the process and material control departments.

Checks during application of covering – thickness of insulation or sheath and concentricity of extrudates are mainly checked when the covering is applied by any process.

The vulcanization of cable core or final cables may be done either in curing trays or drums in case of batch process or from take-up in case of CV process are subjected to the stipulated QC checks against the standards. These checks include:

- Mechanical properties
- Final wall thickness
- Insulation resistance
- High voltage tests

8.11 Polymers in some Specialty Cables

8.11.1 Mining Cable

There is a wide range of industrial mining cables, which is required for oil platforms, electrical submersible pumps and armoured cables for the oil industry. Different range of mining cable are available having variety of construction and insulating materials, making them suitable for different industrial and mining applications, where a high degree of mechanical stresses and environment resistance are expected [34-39].

Characteristics of cable used in open hearth and underground mines are:

- Must be flexible
- Covered with insulating material
- Protected efficiently from mechanical damage
- Must be fire resistant

- Must be heat resistant
- Must be oil resistant
- Efficiently protected against corrosion
- Should be high voltage conductor with minimum loss
- Should be electrically and mechanically continuous throughout

Depending on voltage gradient mining cables may be graded as follows,

- Low voltage: voltage does not exceed 250 V
- Medium voltage: voltage does not exceed 650 V
- High voltage: voltage does not exceed 33,000 V
- Extra high voltage: voltage does exceed 33,000 V

Properties of a typical XLPE based cable insulation is given in **Table 8.11**.

Table 8.11 Properties XLPE used for insulation in cables used in mining

Property	For low voltage	For medium and high voltage
Density (g/cm^3)	0.925	–
Tensile strength (MPa)	18	16
Elongation at break (%)	550	375
Dielectric strength (kV/mm)	25	24.7
Volume resistivity (ohm.cm)	22.4×10^{16}	1.4×10^{17}
Power factor at 50 Hz at 23 °C	0.0004	0.0004

Other polymers are also used for different types of mining cables to meet different requirements they are as follows:

- PVC is used for low voltage insulation and fire retardant jacket materials.
- EPR/EPDM is used for high and extra high voltage cable insulation.
- Silicone rubber: is used for low to medium voltage and high temperature fire resistant insulation especially for equipment and instrument cables used in mines.
- CPE is suitable for jacket material with oil and flame resistance cables.

- CSP is suitable for heavy duty jacket materials having oil resistance, flame resistance, coupled with good mechanical properties in mining cable.
- PCR is used as cable jacket material for mining cable.
- XLPE is used as cable insulation for mining cable.
- Some underground mining cables need stringent requirement against fire and toxic gas generation. In such cases olefinic polymers such as XLPE or EPR are used as an insulator and inner and outer sheaths are developed from EVA.

8.11.2 Aircraft and Spacecraft Cable

The stringent weight and space requirement of advanced space and aerospace systems have lead to a need for stronger, lighter, smaller and more flexible cable and wiring components to be used in aircraft. There are several different types of cables used in aircraft:

i) Air frame cables are intended to be sufficiently robust to satisfy the requirement of open air frame wiring and general wiring of power plant. Very thin insulation which is harder and stiffer than common insulation such as PVC is preferred in some applications. XLPE and PVC are also used in airframe cables.

ii) Inter connect cables, are used in protected areas of wiring such as interconnection of equipment. These cables are generally stationery and will not be subjected to much handling stress.

iii) Equipment wires, these are intended to be used within equipment and therefore need to be very flexible and suitable for soldering.

iv) Fireproof and fire resistant cables, these cables are fireproof and supposed to perform their service for at least 15 minutes under designated fire conditions at much elevated temperatures.

v) Data bus cables, used to transmit data and operate under relatively low voltage and high frequency [40].

Aero cables have to satisfy certain stringent quality requirements. These cables generally have a high temperature rating. The temperature rating of an airframe cable is determined by its construction and materials used in these cables need a temperature rating of 105 °C, 135 °C, 150 °C, 210 °C and 2600 °C. So, there are mainly high heat resistant polymers such as silicone. Fluoropolymers are often used for high temperature cables and XLPE and PVC are sometimes used in airframe cables.

Another consideration is voltage rating. All cables used in aircraft have a rated voltage. Some cables such as equipment wire may have a very specific voltage rating. An example of cables which perform at voltage higher than normal ones are cables used in discharge lamp circuit and windscreen heating.

Flammability and toxicity are two important criteria for selection of such cables. These cables should have a defined level of resistance to burning when exposed to a standard flame test. It is also important that in the event of fire the release of toxic gas and smoke from burning cables should be within the specified limits.

These cables should have a minimum mechanical strength to withstand the pressure of sharp edge (cut through) and should have the ability to withstand scrapping with a defined blade. These cables are required to withstand a defined level of resistance to commonly used aircraft fluids. Though it is not common that these cables in service will come in contact with these hydraulic fluids.

The size and weight are two important criteria for selection of these cables. The space available for accommodating cables in aircraft is relatively much less than other applications and weight reduction is always preferred. These cables generally have very thin insulation may be as low as 0.15 mm.

8.11.2.1 Some Polymeric Cable Materials for Aircraft Applications

XLPE and ethylene-chlorotrifluoroethylene co-polymer (XETFE) are used as cable materials in aircraft cables. Some typical electrical insulation used in aircraft comprises of two layers of polymeric materials, an inner layer of a crosslinked polymer, e.g., XLPE, and ethylene/tetrafluoroethylene copolymer, an ethylene/chlorotrifluoroethylene polymer or a vinylidene fluoride polymer, and an outer layer of an aromatic polymer having a glass transition temperature of at least 100 °C., e.g., a PEEK, a polyether ketone or a polyether sulfone. Such insulation combines excellent properties under normal service conditions with low smoke evolution on burning, and is therefore particularly useful for aircraft wire and cable. Lightweight high performance insulation for aerocables is developed from crosslinked modified ethylene tetrafluoroethylene copolymer.

Different heat resistant polymers such as MQ, fluoropolymers like ethylene-tetrafluoroethylene polymer (ETFE), polyvinylidene fluoride (PVDF), fluorinated ethylene propylene polymer (FEP) and polytetrafluroethylene (PTFE) are used in aero cables along with common materials like XLPE and PVC. The wrapped insulation based on a highly heat resistant aromatic polyamide: Kapton (Dupont) is also used as cable material. Polyether ketones such as polyether ether ketone (PEEK) or sulfones are also used [41-43]. Perfluoroalkoxy (PFA) copolymer resin is available in pellet or powder form. PFA combines the processing ease of conventional thermoplastic resins with the excellent properties of polytetrafluoroethylene (PTFE). PFA has continuous service

temperatures up to 260 °C coupled with superior creep resistance at high temperatures, excellent low-temperature toughness, and exceptional flame resistance.

Table 8.12 depicts mechanical and electrical properties of typical silicone rubber based insulations used in aircraft/aerospace applications.

Electrical properties of a typical fluoroelastomer based cable insulation used in aerospace application is shown in **Table 8.13**.

Table 8.12 Properties of silicone elastomer based extruded aircraft/ aerospace cables

Property	Typical values
Hardness, Shore A (± 5)	55
Tensile strength (MPa)	7.5
Elongation (%)	350
Tear strength, die B (kN/m)	18
Volume resistivity at 29 °C (Ohm-cm)	~ 10^{16}
Dielectric constant at 50 Hz	3

Table 8.13 Electrical properties of typical aero cable insulation based on FEP

Properties	Magnitude
Flame resistance	Excellent
Dielectric constant, 60-10 Hz	2.1
Dissipation factor, 60-10 Hz	<0.0007
Volume resistivity (Ohm-cm)	<10^{18}
Surface resistivity (Ohm/Sq)	<10^{16}

8.11.2.2 Transducer Cable

This cable is used for strain gage testing on airframes during flight testing. It is also used by the automotive industry for crash dummy sensors. This cable uses four conductors insulated with Teflon for reduced size, braided shield for electromagnetic interference (EMI) and a silicone rubber jacket for flexibility.

8.11.2.3 Spacecraft Cable

Performance of spacecraft is heavily dependent on successful performance of individual components used in it. Most of these components are made from noncommercial and tailor-made materials. Requirement of polymeric materials for spacecraft in cables or other applications are much more stringent than any other applications. Spacecraft cables have to perform under temperatures ranging from –110 ºC-200 ºC, pressure range from 0.1 MPa to13.3 MPa. The material should have adequate radiation resistance up to 200 MRad. As often-ambient pressure in outer space is often too low, the problem of out-gassing is encountered. The volatile content in polymer matrix used in different parts of the cable should have very low mass loss. It is measured as total mass loss and it should be less than 1% (typical 0.1%). The collected volatile condensate should also be very low less than 0.1%. These cables should have low electrical loss and should be light in weight. These cables should have good mechanical properties and low temperature flexibility. Some of theses cables have layers of air spaced PTFE taping (an air gap is kept in between the tape layers) over stranded copper wire with diamond braid or helically wrapped copper as outer conductor to provide flexibility and EMI shielding with extruded polymers like PFA, FEP, Tefzal, PU or PVC as jacket. Polymers used in space and aircraft cables. Different polymeric materials in spacecraft and aircraft cables are given in **Table 8.14** and development of cable material for aerospace application is given in **Table 8.15**.

8.11.3 Nuclear Power Cables

Nuclear power plants require high quality cables, which meet stringent nuclear regulatory Commission (NRC) standard of their respective countries [44-45]. These cables are used for different purposes and major types of nuclear cables are as follows**:**

- Switchboard wire
- Instrumentation and thermocouple cable
- Power and control cable
- Coaxial and tri-axial cable
- Specialty cable

Nuclear power cables need good long term thermal stability ,good mechanical properties coupled with good environmental properties. Properties and application area of different polymers used in nuclear power cables are given in **Tables 8.16** and **8.17**.

Table 8.14 Polymeric materials selection for space craft and aircraft applications		
Applications	**Construction Considerations**	**Materials Used**
Spacecraft	Radiation resistant, flexibility, low outgassing	Tefzel, Aracon, silicone rubber and silicone which can meet the TMI requirement of space agencies.
Aircraft	Fire retardancy, flexibility, low smoke, low halogen	FEP, PFA, Tefzel, flame retardant PU, Tefzel insulations, fire retardant jackets

Table 8.15 Development of cables materials for aerospace applications		
Year	**Materials**	**Features**
1950	Glass braid and rubber	Introduction of extruded insulation technology
	Silicon rubber and PET glass braid	
	Silicon rubber and glass braid + FEP	
1960	Glass braid and PTFE	
	PVC, glass and Nylon	
	Alkene amide polymer	
1970	Polyether ketone	
	PVC, glass, Nylon	
	XETFE	
1980	Polyimide tape	Introduction of tape wrap insulations
	Polyimide tape (Boeing)	
	PTFE and polyimide tape (Airbus) Teflon/Kapton tape wrapped ('TK') wire	
	Polyimide tape + PTFE/FEP topcoat (Airbus)	
1990	PTFE and polyimide tape (Airbus)	
	PTFE/Polyimide/PTFE sandwich tape (Boeing)	Teflon/Kapton/Teflon 'TKT' hybrid or composite wires
	PTFE/Polyimide/PTFE sandwich tape	
	PTFE/Polyimide/PTFE sandwich tape (Boeing)	
2000	Enhanced PTFE and polyimide tape (Airbus)	
	PTFE and polyimide tape + Aluminium alloy conductor (Airbus)	

Table 8.16 Polymer used in Nuclear Power Cables		
Insulator	**Features**	**Applications**
Fire resistant XLPE based **(Fire resistant XLPE)** **Light coloured** **No additional jacket**	• Long-term thermal endurance and superior electrical properties. • Excellent mechanical cut through properties. • Long-term moisture and radiation stability. • Radiation resistant (up to 200 MRad)	Low voltage applications 600 V, 90 °C. Flame and fire retardancy is critical.
Fire resistant crosslinked polyethylene **(FR-XLPE) -** **Black** **No additional jacket**	• Radiation resistant (up to 200 MRad) • Long-term thermal endurance and superior electrical properties. • Excellent mechanical cut through properties. • Long-term moisture and radiation stability.	Low voltage 600 V, 90 °C. Insulated heavy wall, single conductor used in nuclear generating stations without additional jacketing protection. Flame retardancy is critical. Used in trays, conduit and ducts.
Crosslinked polyethylene **(FR-XLPE) - Black** **Jacket: heavy duty chlorosulfonated polyethylene** **(CSM) – Black, as mentioned above**	• Long-term thermal endurance and superior electrical properties. • Excellent mechanical cut through properties. • Long-term moisture and radiation stability • Radiation resistant (up to 200 (MRad)	Low voltage 600 V, 90 °C. Insulated dual wall, single conductor used in nuclear generating stations where additional jacketing protection is required. Flame retardancy is critical. Used in trays, conduit and ducts.
FR-XLPE - **Black** **Jacket: heavy duty CSM - Black**	• Radiation resistant (up to 200 MRad) • Long-term thermal endurance and superior electrical properties. • Excellent mechanical cut through properties. • Long-term moisture and radiation stability	Multi-conductor used in flame retardancy applications. Used in monitoring data, recording and transmitting information on low energy circuits where shielding from external electrostatic interference is not required.

Table 8.17 Polymers used in nuclear instrumentation, power and fibre optic communications cables		
Insulator and Jacket	**Features**	**Applications**
Fluorinated ethylene propylene (FEP) - coloured **Jacket: FEP - coloured conductor jacket - high strength Nylon**	FEP insulation/jacket system with a 200 °C temperature rating.	For high-speed data transmission.
Low smoke zero halogen (LSZH) Polyolefin (PO) **Jacket: UV resistant** **LSZH (PO)**	Low smoke, zero halogen cable that maintains circuit integrity in the event of fire and results in minimum smoke, acid and toxic gas generation.	For high speed data transmission. Suitable for use in tunnels, trays and ducts.

8.11.4 Ship Board and Marine Cables

The marine cables have been of interest due to their wide range of applications in above and deep-ocean engineering. Normally, marine cables may be deployed under the sea. But there are applications above sea for example on board ship. The type of applications of these cables is [46-48]:

- In power or lighting networks.
- For connection to movable or portable equipment used on board ships.
- Especially designed for shipbuilding and electric systems such as control panels, signal systems, sensor leads, solenoid valves, electromagnets.
- In power or lighting networks; for connection to movable or portable utilising equipment.
- Flexible marine cables are suitable for use as signal, measurement and control cables used in data processing equipment, office machines and machine tools, telephone.

These cables have to function in dry, moist and wet environments. Environments in which these cables are performing their service are important. Some of theses cables are have to function under deep water and are particularly susceptible to vibration since their shapes attract fluctuating forces when situated in a current field. For this reason, most of the marine cable systems are operating in a three-dimensional space. So it is important to know both static and dynamic behavior of these cables under different

environmental conditions. The service property requirements and other technological aspects of these cables are:

- Oil resistance and resistance to sea water are also important requirements.
- The service temperature of these cables may vary from –5 °C to +80 °C.
- Windy, salty environment can easily corrode metals used in different parts of the cables and cable system. Protective coatings are used on metallic structures in coastal areas to prevent surface degradation by corrosion.
- As marine application demands resistance against dynamic stress a metallic conductor is usually composed of a large number of finer strands compared to normal cable. As a result these cables are much more flexible and much less prone to fatigue failure.
- The individual conductor strands are tin coated copper for protecting them from corrosion.
- The insulation used in some of the marine cable should be able to withstand much higher temperatures, making them suitable for use in immediate proximity to engines.
- Usually marine cables should have flame and fire resistance characteristics.
- Shipboard grades of cables may be power cables or control cables or telephone cables.

The polymers generally used for insulation in marine cables are, PVC, XLPE, MQ, EPR/EPDM, PCR, IIR and for sheaths, CSP, PCR, PVC, NBR-PVC blend. Because of their superior electrical properties of XLPE compared to other polymers the required minimum average thickness of XLPE insulation is 0.7 mm whereas it is 0.8 mm for the other insulating polymers.

References

1. L. Heinhold, *Power Cables and their Applications*, Part 1, 3rd Edition, John Wiley Sons, Hoboken, NJ, USA, 1990, p.15-27.
2. R.B. Blodgett and co-workers in *Proceedings of IEEE Underground Transmission and Distribution. Conference*, Atlantic City, NJ, USA, 1976.
3. P. Metra and A. Lombardi in *Proceedings of IEEE Underground Transmission and Distribution Conference*, Atlantic City, NJ, USA, 1976.

4. R.M. Eichhorn, *IEEE Transactions on Electrical Insulation*, 1981, **16**, 6, 469.

5. A. Givson, *Wire and Cable Technology,* 2005, **33**, 4, 82.

6. S. Yasufuku, *IEEE Electrical Insulation Magazine,* 1990, **6**, 1, 24.

7. J.M. Braun, *IEEE Electrical Insulation Magazine*, 1992, **8**, 5, 27.

8. A. Tewarson, *IEEE Electrical Insulation Magazine* 1990, **6**, 3, 20.

9. A. Pal, *Kautschuk und Gummi Kunststoffe*, 1991, **44**, 10, 958.

10. I. Ray and D. Khastgir, *Plastics, Rubber and Composites Processing and Applications,* 1994, **22**, 1, 37.

11. I. Ray and D Khastgir, *Journal of Applied Polymer Science*, 1994, **53**, 3, 297.

12. *Guide to short circuit temperature limit of electrical cables with a rated voltage not exceeding 0.6/1.0 kV*, IEC publication No.724, Geneva, Switzerland, 1984.

13. L.K. Djiauw and M.O. Westbrook, *Wire Journal International*, 1987, **20**, 51.

14. S. Bhaumik and N.K. Datta, *Plastics Rubber and Composites Processing and Applications*, 1991, **15**, 1, 39.

15. M.M. Sain, J. Lacok, J. Beniska and J. Bina, *Kautschuk und Gummi Kunststoffe*, 1989, **42**, 8, 672.

16. E. Leonelli and F.T. Ferrera, *Kautschuk und Gummi Kunststoffe*, 1991, **44**, 960.

17. H.G. Dageforde, W. Berchem and H.A. Mayer in *Proceedings of the 31st International Wire and Cable Symposium*, Cherry Hill, NJ, USA, 1982, p.401.

18. R.J. Arhart in *Proceedings of the 1990 Minnesota Power Systems Conference*, Minnesota, USA, 1990, p.53-62.

19. R.J. Arhart in *Proceedings of the IEEE, Power Engineering Society, Insulated Conductors Committee Meeting*, St. Petersburg, FL, USA, 1992.

20. R.J. Arhart in *Proceedings of the IEEE, Power Engineering Society, Insulated Conductors Committee Meeting*, Birmingham, AL, USA, 1993.

21. A. Pack in *Proceedings of the IEEE, Power Engineering Society, Insulated Conductors Committee Meeting*, Birmingham, AL, USA, April, 4-7, 1993.

22. M.D. Walton, B.C. Bernstein, J.T. Smith, III, W.A. Thue and J.H. Groeger in *Proceedings of the IEEE, Power Engineering Society, Insulated Conductors Committee Meeting*, Birmingham, AL, USA, 1993.

23. R.J. Arhart, IEEE, *Electrical Insulation Magazine*, 1991, **7**, 31.

24. R.J. Arhart, *IEEE, Electrical Insulation Magazine*, 1993, **9**, 11.

25. M. Brown, *IEEE, Electrical Insulation Magazine*, 1994, **10**, 16.

26. M. Brown in *Proceedings of the IEEE/ICC, PES Summer Meeting*, San Francisco, CA, USA, 1982.

27. E. Occhini, P. Metra, G. Poritinari and B. Vecellio in *Proceedings of the IEEE Transaction /Power Apparatus and System,* Winter Meeting, New York, NY, USA, 1983, Volume PAS-102, No.7.

28. J.C. Chan and L.J. Hiivala, *Revue General de L'Electricite*, 1988, No. 3.

29. J.C. Chan, M.D. Hartley and L.J. Hiivala, *IEEE Electrical Insulation Magazine*, 1993, **9**, 8.

30. M.D. Hartley and F.W. Hintze in *Proceedings of the IEEE/PES, ICC Fall 1992 Meeting*, St. Petersburg, FL, USA, 1992

31. S. Kole, D. Khastgir, D.K. Tripathy and A.K. Bhowmick, *Die Angewandte, Makromolekulare Chemie,* 1995, **225**, 21.

32. *General Cable Australia Pty Ltd*, website www.generalcable.com.au

33. L.M. Sloman and A.E. Williamson, *Electrical Review*, 1979, 7th September.

34. www.amercable.com/www.olex.com.au/Products/Mining.html

35. www.philatron.com/NewPDFCatalog/TAB5-MiningCables.pdf

36. http://gemscab.exportersindia.com/mining-cable.html

37. http://www.mining-technology.com/contractors/cables/pirelli/

38. http://www.generalcable.com/GeneralCable/en-US/Products/MiningCables/Catalog/

39. Airworthiness Information Leafland co-workers/0140, Issue 2 UK Civil Aviation Authority

40. www.mrs.org/s_mrs/bin.asp?CID=2723andDID=62689andDOC=FILE.PDF

41. www.netmotion.com/htm_files/advisory/advisor_peek**aero**2.htm

42. www.engineeringtalk.com/news/vic/vic112.html

43. General Cables, Nuclear Cable Catalogue, www.generalcable.com/GeneralCable/en-US/Products/NuclearCables/Catalog

44. www.nrc.gov, Nuclear power plant Electrical Cable Fundamentals, United States Nuclear Regulatory Commission, Review Report.

45. http://www.jaycor.co.za/products/cables/marine.htm

46. http://www.rscc-exane-oil.com/MarineCableTechNewsletter.pdf

47. http://www.jaycor.co.za/products/cables/

9 Durability of Rubber Compounds

N.M. Huntink and R.N. Datta

9.1 Introduction

Rubber compounds can be degraded by reactions with oxygen, ozone, light, metal ions and heat. Antidegradants protect rubber against aerobic ageing (oxygen) and ozone attack. They are of prime importance and play a vital role in rubber products to maintain the properties at service conditions. Protection of rubbers or stabilisation of crosslinked networks against anaerobic ageing can be achieved *via* other approaches: using an efficient vulcanisation-curing system, application of 1,3-bis(citraconimidomethyl) benzene, hexamethylene-1,6-bis(thiosulfate) disodium salt dihydrate, hexamethylene-1,6-bis(dibenzylthiuram disulfide), zinc-soaps, and so on [1, 2].

Degradation by oxygen and ozone proceeds *via* different chemical mechanisms and results in different effects on physical properties of rubber [3-14]. Ozone degradation results in discoloration and eventual cracking of samples. Ozone degradation is primarily a surface phenomenon. Oxygen degradation results in hardening or softening (depending on the base polymer) throughout the rubber article. For example, vulcanisates that are based on natural rubber (NR), synthetic polyisoprene rubber (IR) and butyl rubber (IIR) preferably undergo cleavage reactions during the oxidation process - they generally become softer. During progressive ageing, a crosslinking mechanism starts to dominate again: completely oxidised NR is usually hard and brittle. On the other hand, vulcanisates obtained from styrene-butadiene rubber (SBR), nitrile-butadiene rubber (NBR), chloroprene rubber (CR), ethylene propylene diene rubber (EPDM), and so on, undergo cyclisation and crosslinking reactions that lead to hardening of the aged part. When completely oxidised, these vulcanisates are turned into hard and brittle products. Rubbers that do not contain C=C unsaturation, such as acrylic rubber (ACM), chlorinated polyethylene, chlorosulfonated polyethylene, polychloromethyloxiran, ethylene-ethyl acrylate copolymer (EAM), epichlorohydrin rubber (ECO), ethylene propylene rubber (EPR), ethylene-vinylacetate copolymer, rubbers with fluoro and fluoralkyl or fluoralkoxy substituent groups on the polymer chain (FKM), silicone rubber (Q), and others are much less sensitive to oxidation than diene rubbers.

Although conventional antidegradants such as 6PPD and IPPD provide protection against oxidation and ozonation, the protection lasts only short-term. Longer-term

protection requires a different class of antidegradants. Long-lasting antioxidants must be polymer bound or must have a lower volatility and leachability than conventional antioxidants, whereas long-lasting antiozonants must have a lower migration rate than the conventional antiozonants.

The purpose of this chapter is to review the developments on long-term protection of rubbers against aerobic ageing, especially on long-term (more than five years, depending on service conditions) protection against ozone. Although numerous reviews of antioxidants and antiozonant aspects have been published [3-14], in most cases they only cover one element, i.e., fracture and fatigue in SBR and butadiene rubber (BR) vulcanisates [6]; the black sidewall surface discoloration and non-staining technology [7]; ozonolysis of natural rubber [12] and so on, bound antioxidants, migration of the total field. In this chapter attempts will be made to summarise most developments with the emphasis on long-term antioxidant as well as antiozonant protection.

9.2 Oxidation and Antioxidant Chemistry

9.2.1 Introduction

The changes in properties observed on ageing of different elastomers and their vulcanisates, and of many other polymeric materials, are well known. Antiozonants and antioxidants are used to limit these changes. However, the most effective antioxidant for one material may be ineffective, or even harmful in another material or under different conditions. A rubber compounder must be aware of the effect of oxygen attack on rubber and should know how to compound for oxygen resistance.

9.2.2 Mechanism of Rubber Oxidation

The oxidation of polymers is most commonly depicted in terms of the kinetic scheme developed by Bolland [15]. The scheme is summarised in **Figure 9.1**. The key to the process is the initial formation of a free-radical species. At high temperatures and at large shear forces, it is likely that free radical formation takes place by cleavage of carbon-carbon and carbon-hydrogen bonds.

Many elastomers are already observed to oxidise at moderate temperatures (below 60 °C), where the energetics would not favour cleavage of carbon-carbon and carbon-hydrogen bonds. Thus, several studies have been conducted to determine whether trace impurities present in the polymer systems could account for the relative ease of oxidation. Two separate studies concluded that traces of peroxide were present in the polymer and that initiation occurred at low temperatures due to the relatively easy homolysis of these

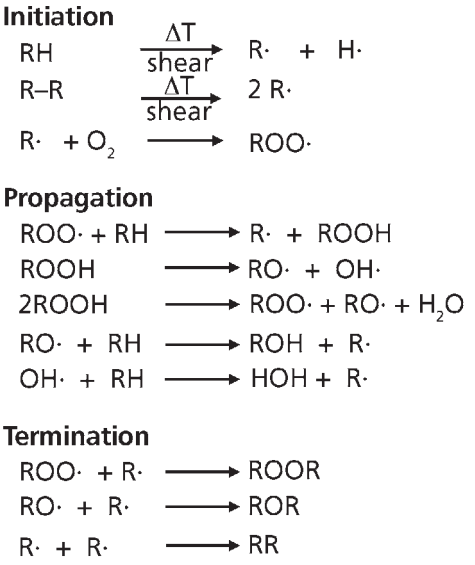

Figure 9.1 Bolland oxidation mechanism (RH = rubber hydrocarbon)[14]

peroxides into free radicals [16-17]. Due to the high reactivity of free radicals, only trace amounts of these peroxides need to be present to provide initiation of the oxidative chain process. On the other hand, mechanical shear during processing and bale compaction and localised heat during the drying and packaging of the raw polymer are the most important causes of carbon-carbon and carbon-hydrogen bond cleavage. The resultant free radicals react with oxygen to form the peroxides responsible for degradation.

The oxidation of hydrocarbon polymers resembles the oxidation of low MW hydrocarbons, with the polymer having its own internal source of peroxide initiators present. By making the assumption that peroxides are present in even the most carefully prepared raw rubber, the ease of oxidation of rubber at low to moderate temperatures can be understood. Therefore, it is extremely important to compound rubber for extended oxidation resistance through the use of protective additives and to be aware of pro-oxidant impurities present in the rubber or the rubber compound.

Probably an important pro-oxidant for all rubbers is ultraviolet (UV) light. Blake and Bruce performed a study of the oxygen absorption rates of unvulcanised NR rubbers under exposure to UV light [18]. It was observed that exposure to light caused dramatic increases in the oxygen absorption rate of NR. They studied the oxygen absorption rates of NR with various compounding additives. A summary of their results is given in **Table 9.1**. This table shows that phenyl-β-naphthylamine, an additive previously used for prevention of rubber oxidation (hardly used anymore because of toxicity reasons)

Table 9.1 Oxidation of NR Pale Crepe at 46 °C, accelerated by UV light [18]	
Additive	**Absorption of O_2 (cm^3/h)**
None	0.067
2% Sulfur	0.028
2% Benzidine	0.014
2% Hydroquinone	0.014
2% Phenyl-β-naphthylamine	0.076
5% Zinc oxide	0.010
1% P-33 Carbon black*	0.018
**: P-33 is a fine thermal black, ASTM nomenclature N880*	

can operate as a pro-oxidant under exposure to UV light. Fillers like zinc oxide, titanium dioxide, whiting and especially carbon black, lowered the rate of oxygen absorption of NR with exposure to UV light. This was attributed to the ability to make the compound opaque, thus limiting the penetration of UV light into the test films of NR. In the case of benzidine and hydroquinone, the effects were attributed to the ability of these materials to preferentially absorb the harmful UV light. Thus, it is very important to consider the pro-oxidant behaviour of UV light when compounding rubbers for extended life.

The rate of peroxide decomposition and the resultant rate of oxidation is markedly increased by the presence of ions of metals such as iron, copper, manganese, and cobalt [14]. This catalytic decomposition is based on a redox mechanism, as in **Figure 9.2**. Consequently, it is important to control and limit the amount of metal impurities in raw rubber. The influence of antioxidants against these rubber poisons depends at least partially on a complex formation (chelation) of the damaging ion. In favour of this theory is the fact that simple chelating agents that have no ageing protective activity, like ethylene diamine tetraacetic acid (EDTA), act as copper protectors.

The rather simple sequence of reactions described in **Figure 9.1** is complicated by other reactions, when oxidisable impurities or compounding ingredients are present. There are also the secondary processes whereby peroxides and free radicals undergo reactions leading to chain scission as well as crosslinking reactions. These reactions are closely related to the primary oxidation process, so that for a given type of polymer or vulcanisate the degree of deterioration of physical properties is generally proportional to the extent of oxidation.

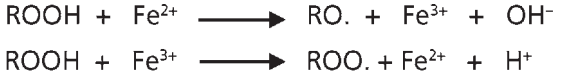

Figure 9.2 Decomposition of peroxides by ions of metals (Redox mechanism)

9.2.3 Stabilisation Mechanism of Antioxidants

Complete inhibition of oxidation is seldom obtained in elastomers by addition of antioxidants or stabilisers. What is usually observed is an extended period of retarded oxidation in the presence of the antioxidant. It has been demonstrated that during this period the rate of oxidation decreases with increase in inhibitor concentration until the optimum concentration is reached and then increases again. The rate of the retarded reaction is affected by changes in oxygen concentration [19], in contrast to the uninhibited reaction, which proceeds at the same rate in oxygen or in air. These and other differences observed in the presence of oxidation inhibitors reflect significant changes in initiation and propagation, as well as in termination reactions.

It is important to recognise that different types of inhibitors often function by different mechanisms, and that a given antioxidant may react in more than one way. Thus a material that acts as an antioxidant under one set of conditions may become a pro-oxidant in another situation. The search for possible synergistic combinations of antioxidants can be conducted more logically and efficiently if we seek to combine the effects of different modes of action. Five general modes of oxidation inhibition are commonly recognised:

Metal deactivators – Organic compounds capable of forming coordination complexes with metals are known to be useful in inhibiting metal-activated oxidation. These compounds have multiple-coordination sites and are capable of forming cyclic structures, which 'cage' the pro-oxidant metal ions. Ethylenediamine tetraacetic acid (EDTA) and its various salts are examples of this type of metal chelating compounds.

Light absorbers – These chemicals protect from photo-oxidation by absorbing the UV light energy, which would otherwise initiate oxidation, either by decomposing a peroxide or by sensitising the oxidisable material to oxygen attack. The absorbed energy must be disposed of by processes which do not produce activated sites or free radicals. Fillers which impart opacity to the compound (e.g., carbon black, zinc oxide) tend to stabilise rubbers against UV catalysed oxidation.

Peroxide decomposers – These function by reacting with the initiating peroxides to form nonradical products. Presumably mercaptans, thiophenols, and other organic sulfur compounds function in this way [20]. It has been suggested that zinc dialkyldithiocarbamates function as peroxide decomposers, thus giving rubber compounds good initial oxidative stability.

Free radical chain stoppers – These chemicals interact with chain propagating $RO_2\cdot$ radicals to form inactive products.

Inhibitor regenerators – These react with intermediates or products formed in the chain-stopping reaction so as to regenerate the original inhibitor or form another product capable of functioning as an antioxidant.

Termination of propagating radicals during the oxidative chain reaction is believed to be the dominant mechanism by which amine and phenolic antioxidants operate. The mechanism proposed to account for this behaviour is given in **Figure 9.3** and **Figure 9.4**. The deactivation of R· *via* chain braking electron acceptors (CBA) is demonstrated for a hindered amine light stabiliser (HALS). The mechanism involves reaction of the HALS with an hydroperoxide, resulting in the formation of a stable nitroxyl radical, that traps a hydrocarbon radical or abstracts a labile hydrogen from a hydrocarbon radical under formation of stable products. The hydroxylamine (CB-AH) formed *via* this mechanism can be used for the stabilisation of peroxide radicals.

R· that is not fully deactivated *via* the mechanism described in **Figure 9.3** reacts with oxygen resulting in a peroxide radical. These peroxy radicals abstract a labile hydrogen from primary stabilisers like hindered phenols or secondary amines, resulting in less

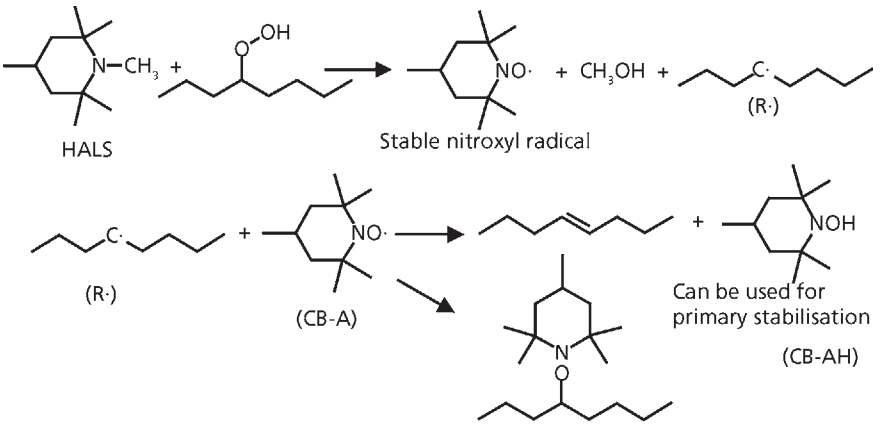

Figure 9.3 Deactivation of |R· *via* chain braking electron acceptors (CB-A)

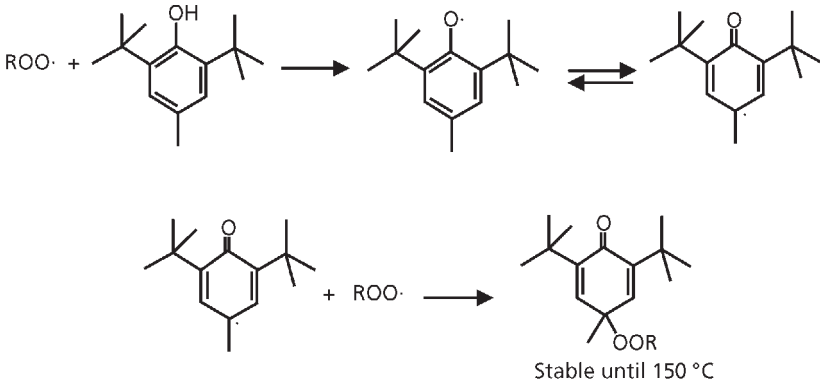

Figure 9.4 Primary stabilisation *via* radical scavenging by hindered phenolics

active hydroperoxides and preventing hydrogen abstraction from the polymer chain. The resulting antioxidant radical is more stable than the initial peroxy radical and terminates by reaction with another radical in the system. This mechanism was proposed by Shelton [21], who demonstrated that replacement of the reactive hydrogen in aromatic amine antioxidants by deuterium results in a slower abstraction of deuterium by peroxy radicals and therefore in a less effective antioxidant. It has also been proposed that aromatic compounds such as phenols and aromatic amines can form π-electron complexes with peroxy radicals, which terminate to form stable products [16]. It appears that direct hydrogen absorption, π-electron complex formation or both, describe the antioxidant action of most amine and phenolic antioxidants. It is important that the level of antioxidant be kept at the optimum, since excess antioxidant can result in a pro-oxidant effect (A-H + O_2 → AOOH).

The mechanism of secondary stabilisation by antioxidants is demonstrated in **Figure 9.5**. Tris-nonylphenyl phosphites, derived from PCl_3 and various alcohols, and thio-compounds are active as a secondary stabiliser [22]. They are used to decompose peroxides into non-free-radical products, presumably by a polar mechanism. The secondary antioxidant is reacting with the hydroperoxide resulting in an oxidised antioxidant and an alcohol. The thio-compounds can react with two hydroperoxide molecules.

9.2.4 Methods of Studying the Oxidation Resistance of Rubber

The most common test used to study the oxidation resistance of rubber compounds involves the accelerated ageing of tensile dumbbell samples in an oxygen-containing atmosphere. Brown, Forrest and Soulagnet recently reviewed long-term and accelerated ageing test procedures [23]. The ASTM practices (D454 [24]; D865 [25]; D2000 [26]; D3137 [27]; D572 [28]; D3676 [29]; D380 [30]) for these tests clearly state that these are accelerated tests and should be used for relative comparisons of various compounds and that these tests may not correlate to actual long-term ageing behaviour. However,

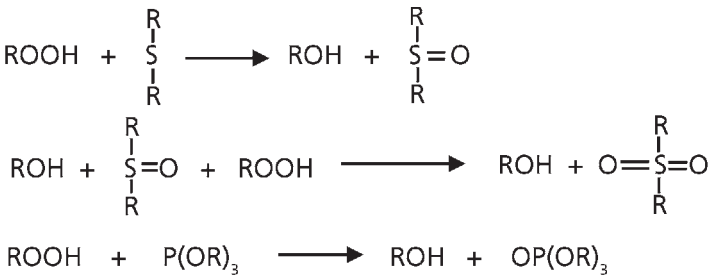

Figure 9.5 Secondary stabilisation by phosphites and thio-compounds

these tests are useful in evaluating ageing-resistant compounds and various antioxidant packages. The resistance of a compound to oxidation is generally measured by the percentage change in the various physical properties (e.g., tensile strength, elongation at break, hardness, modulus). For an elastomer which reacts with oxygen, resulting in crosslinking (generally butadiene-based elastomers such as BR, SBR, NBR), the accelerated tests result in increases in tensile modulus and hardness with a corresponding decrease in ultimate elongation. For an elastomer which reacts with oxygen resulting in chain scission (generally isoprene-based elastomers such as NR and IR), the accelerated ageing tests result in decreases in tensile modulus and hardness with either increasing or decreasing ultimate elongation, depending on the extent of degradation [31]. The most effective antioxidant package for a given elastomer compound gives the smallest changes in physical properties during an accelerated ageing test.

Thermoanalytical techniques such as differential scanning colorimetry (DSC) and thermogravimetric analysis (TGA) have also been widely used to study rubber oxidation [32-35]. The oxidative stability of rubbers and the effectiveness of various antioxidants can be evaluated with DSC based on the heat change (oxidation exotherm) during oxidation, the activation energy of oxidation, the isothermal induction time, the onset temperature of oxidation, and the oxidation peak temperature.

Spectroscopic techniques as ^{13}C-nuclear magnetic resonance [36], electron spin resonance [37], pyrolysis gas chromatography – mass spectrometry and pyrolysis-Fourier transform infrared spectroscopy [38], X-ray diffraction [39] and scanning electron microscopy [40] techniques are also used to study rubber oxidation.

9.3 Ozone and Antiozonant Chemistry

9.3.1 Introduction

Layer and Lattimer [8] and Bailey [41] gave the historical background regarding protection of rubber against ozone.

As early as 1885 Thomson observed that stretched rubber cracked on ageing [42]. In the early 1920s, a number of investigators studied this phenomenon in more detail. They found that cracks occurred only in stretched rubber, formed in a direction perpendicular to the elongation, and grew most rapidly at an elongation of about 10% [43, 44]. Fabry and Buisson observed crack formation in the presence of ozone, but questioned the influence of this ozone. Ozone was believed to be present only in the upper atmosphere and not in those places where rubber is commonly used [45]. By 1935, analytical techniques had developed sufficiently to be able to measure that trace amounts of ozone, parts per hundred million (pphm), were present in the troposphere

[46]. Even so, these trace amounts were felt to be too insignificant to be the cause of severe damage. Therefore, other factors responsible for cracking were sought. Sunlight seemed to be an indispensable factor; hence names like 'suncracking' and 'sunchecking' were frequently used to describe this phenomenon. Direct sunlight, however, was not necessary, since cracking occurred equally well on the shady side as well as on the sunny side of the rubber [47]. Also, dust was thought to be responsible for cracking. Dust, once settled on the rubber and activated by sunlight, would give off oxidising moieties and crack the rubber [47, 48]. Today, we know that only a few pphm of ozone in our atmosphere can cause severe cracking of rubber and that sunlight is responsible for its formation.

Ozone in the atmosphere is formed by the chemical reaction of atomic and molecular oxygen:

$$O + O_2 \rightarrow O_3$$

At high altitudes, the oxygen atoms are generated by the photolysis of molecular oxygen by the far UV light of the sun. In the troposphere, where only longer wavelength UV light exists, photolysis of nitrogen dioxide is the major source of oxygen atoms [49]:

$$NO_2 + h\nu \rightarrow NO + O$$

The nitric oxide produced in this reaction reacts with ozone to regenerate oxygen and nitrogen dioxide:

$$NO + O_3 \rightarrow NO_2 + O_2$$

An equilibrium is established which gives rise to a so-called photostationary-state relationship, which depends on the relative rates of the above reactions:

$$[O_3] = j[NO_2] / k[NO]$$

where:

j = reaction rate of the formation of O_3, and

k = reaction rate of the decomposition of O_3

Based solely on this relationship, it has been predicted that the ozone concentration should be about 2 pphm at solar noon in the USA. Indeed, in unpolluted environments, ozone concentrations are usually in the range of 2 to 5 pphm [8]. However, in polluted urban areas, ozone concentrations can be as high as 50 pphm. Peroxy radicals formed from hydrocarbon emissions cause this enhanced ozone concentration. These radicals oxidise nitric oxide to nitrogen dioxide, thereby shifting the above steady state relationship to higher ozone levels.

Since ozone is generated by photolytic reactions, anything which affects available sunlight will affect the ozone concentration. Consequently, ozone levels are the highest

in the summer months, when the days are longer and the sun is more intense [50]. Similarly, ozone levels are highest near midday and decrease almost to zero at night [51]. Temperature has little effect on ozone formation.

The ozone-cracking problem was first taken seriously by the United States Government in the early 1950s. On reactivating military vehicles, moth-balled since World War II, it was found that tyres were severely cracked and useless. Government-sponsored research projects rapidly led to the discovery of *p*-phenylenediamine antiozonants. Since then, these original antiozonants have been displaced by longer lasting *p*-phenylenediamine derivatives.

9.3.2 Mechanism of Ozone Attack on Elastomers

Ozone cracking is an electrophilic reaction and starts with the attack of ozone at a location where the electron density is high [52]. In this respect unsaturated organic compounds are highly reactive with ozone. The reaction of ozone is a bimolecular reaction where one molecule of ozone reacts with one double bond of the rubber, as can be seen in **Figure 9.6**. The first step is a direct 1,3-dipolar addition of the ozone to the double bond to form a primary ozonide (I), or molozinide, which is only detectable at very low temperatures. At room temperature, these ozonides cleave as soon as they are formed to give an aldehyde or

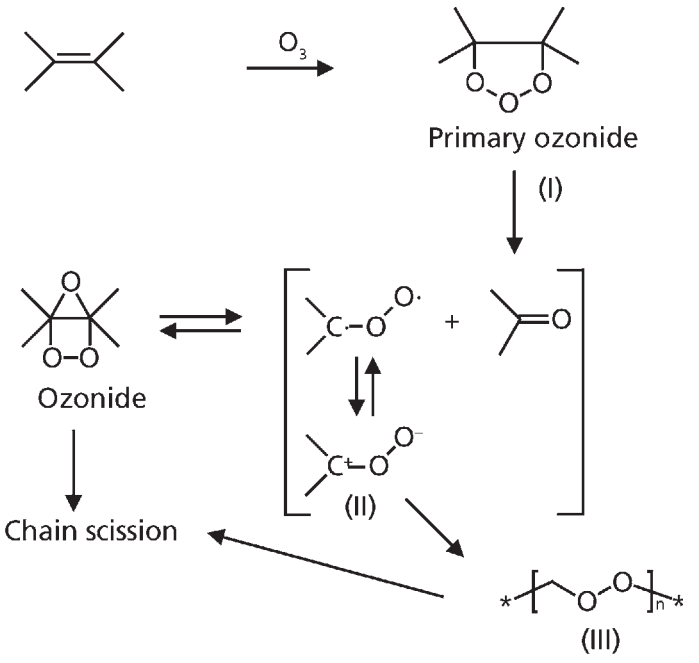

Figure 9.6 Ozone attack on double bonds

ketone and a zwitterion (carbonyl oxide). Cleavage occurs in the direction, which favours the formation of the most stable zwitterion (II). Thus, electron-donating groups, such as the methyl group in NR, are predominately attached to the zwitterion, while electron-withdrawing groups, such as the chlorine in chloroprene rubber, are found on the aldehyde [53]. Normally, in solution, the aldehyde and zwitterion fragments recombine to form an ozonide, but higher MW polymeric peroxides (III) can also be formed by combination of zwitterions. The presence of water increases the rate of chain cleavage, which is probably related to the formation of hydroperoxides. The same chemistry occurs on ozonation of rubber, in solution and in the solid state [54].

Due to the retractive forces in stretched rubber, the aldehyde and zwitterion fragments are separated at the molecular-relaxation rate. Therefore, the ozonides and peroxides form at sites remote from the initial cleavage, and underlying rubber chains are exposed to ozone. These unstable ozonides and polymeric peroxides cleave to a variety of oxygenated products, such as acids, esters, ketones, and aldehydes, and also expose new rubber chains to the effects of ozone. The net result is that when rubber chains are cleaved, they retract in the direction of the stress and expose underlying unsaturation. Continuation of this process results in the formation of the characteristic ozone cracks. It should be noted that in the case of butadiene rubbers a small amount of crosslinking occurs during ozonation. This is considered to be due to the reaction between the biradical of the carbonyl oxide and the double bonds of the BR [55].

The reaction of ozone with olefinic compounds is very rapid. Substituents on the double bond, which donate electrons, increase the rate of reaction, while electron-withdrawing substituents slow the reaction down. Thus the rate of reaction with ozone decreases as follows: polyisoprene > polybutadiene > polychloroprene [56]. The effect of substituents on the double bond is clearly demonstrated in **Tables 9.2** and **9.3**. Rubbers that contain only pendant double bonds such as EPDM, do not cleave since the double bond is not in the polymer backbone.

Although the cracking of rubbers is related to the reaction of ozone on the double bond, it must be mentioned that ozone also reacts with sulfur crosslinks. However, these reactions are much slower. The reaction of ozone with di- and polysulfides is at least 50 times slower than the corresponding reaction with olefins [57]:

$$RSSSR + O_3 \rightarrow SO_2 + RSO_2\text{-}O\text{-}SO_2R \; (+ H_2O) \rightarrow 2\ RSO_2H$$

Unstretched rubber reacts with ozone until all of the surface double bonds are consumed, and then the reaction stops [58]. The reaction is fast in the beginning, the rate progressively decreases while the available unsaturation is depleted and ultimately the reaction stops. During this reaction, a gray film, or frosting, forms on the surface of the rubber, but no cracks are noticed. The thickness of this film of ozonised rubber is estimated to be 10 to 40 molecular layers (6 to 24 nm) thick, based on the measurements of the ozone absorbed by unstretched rubber [59, 60] Disrupting this film by stretching brings new unsaturation to the surface and allows more ozone to be absorbed.

Table 9.2. Relative second-order rate constants for ozonations of selected olefins in CCl_4 at room temperature [52]	
Olefins	**Reaction rate, K_{rel} (l/mol/s)**
$Cl_2C=CCl_2$	1.0
$ClH=CCl_2$	3.6
$H_2C=CCl_2$	22.1
cis-ClCH=CHCl	35.7
trans-ClCH=CHCl	591
$H_2C=CHCl$	1180
$H_2C=CH_2$	25000
$H_2C=CHPr$	81000
$H_2C=CMe_2$	97000
cis-MeCH=CHMe	163000
$Me_2C=CHMe$	167000
$Me_2C=CMe_2$	200000
1,3-Butadiene	74000
Styrene	103000

Table 9.3. Relative second-order rate constants for ozonation of different unsaturated rubbers in CCl_4 at room temperature [8, 41, 56]	
Rubbers	**Reaction rate, K_{rel} (l/mol/s)**
CR	1.0
BR	1.5
SBR	1.5
IR	3.5

Cracks are only observed when the rubber is stretched above a critical elongation. Two factors determine cracking under static conditions: the critical stress necessary for cracks to form and the rate of crack growth. It was established that all rubbers require the same critical stored energy for cracking to occur [61]. This energy is thought to be the energy necessary to separate the two surfaces of a growing crack. Thus depending on the stiffness of the polymer, cracks are formed above a certain elongation. Cracks will only form and grow if the ozonised surface products are moved aside to expose underlying unsaturation. Energy of some form is required to accomplish this. Under static conditions, this is equal to the critical stored energy. Under dynamic conditions, flexing by itself supplies the energy to disturb the surface and no critical energy is required.

The rate of crack growth depends on the polymer and is directly proportional to the ozone concentration. The rate of crack growth is independent of the applied stress as long as it exceeds the critical value. The rate of crack growth also depends on the mobility of the underlying chain segments of rubber, which is necessary to untangle and position double bonds for further attack by ozone. Consequently, anything that will increase the mobility of the rubber chains will increase the rate of crack growth. For example, the slow crack growth rate in IIR becomes equal to that of NR and SBR when sufficient plasticiser is added or when the temperature is raised [62]. Conversely, decreasing chain mobility diminishes the crack growth rate. For this reason, increasing the crosslinking density in some cases decreases mobility and reduces the rate of crack growth.

9.3.3 Mechanism of Antiozonants

Rubbers can be protected against ozone by use of chemical antiozonants and *via* several physical methods. The chemical antiozonants protect rubber under both static and dynamic conditions, whereas the physical methods are more related towards protection under static conditions.

9.3.3.1 Protection Against Ozone Under Static Conditions

There are several physical methods that can be used to protect rubber against ozone. They are wrapping, covering, or coating the rubber surface [63]. This can be accomplished by adding waxes to the rubber and/or adding an ozone resistant polymer, which increases the critical stress. Waxes are the most important in this respect. Two types of waxes are used to protect rubber against ozone, paraffinic and microcrystalline. Paraffinic waxes are predominantly straight chain hydrocarbons of relatively low molecular weight of about 350 to 420. They are highly crystalline due to their linear structure and form large crystals having a melting range from 38 to 74 °C. Microcrystalline waxes are obtained from higher molecular petroleum residuals and have higher MW than the paraffinic waxes, ranging from 490 to 800. In contrast to the paraffinic waxes, microcrystalline waxes are predominantly branched, and therefore form smaller, more irregular crystals which melt from about 57 to 100 °C. Waxes exert their protection by blooming to the surface to form a film of hydrocarbons which is impermeable to ozone. Protection is only obtained when the film is thick enough to provide a barrier to the ozone. Thus the thicker the film, the better the protection. The thickness of the bloom layer obtained depends both on the solubility and the diffusion rate of the wax, which depend on the temperature. Bloom occurs whenever the solubility of the wax in the rubber is exceeded. Therefore, at temperatures lower than 40 °C, the smaller and more soluble paraffinic waxes provide the best protection. Lowering the temperature reduces the solubility of the paraffinic waxes and increases the thickness of their bloom. Yet, their small size allows

them to migrate rapidly to the surface, in spite of lower temperatures. Conversely, as the temperature increases, the high solubility of the paraffinic waxes becomes a disadvantage. They become too soluble in the rubber and do not form a thick enough protective bloom. Microcrystalline waxes perform better at higher temperatures, since higher temperatures increase their rate of migration to the surface and this allows more wax to be incorporated into the rubber. Therefore, blends of paraffinic and microcrystalline waxes are commonly used to guarantee protection over the widest possible temperature range [64]. Combinations of waxes and chemical antiozonants show synergistic improvement in ozone resistance [65]. Presence of the antiozonant results in a thicker bloom layer.

Another way to protect rubber against ozone is to add an ozone-resistant polymer (i.e., EPR, EPDM, halobutyl, polyethylene, polyvinyl acetate, and so on) to the rubber. Microscopic studies of these mixtures show that the added polymer exists as a separate, dispersed phase [66]. Consequently, as a crack grows in the rubber, it encounters a domain of the added polymer, which reduces the stress at the crack tip. This raises the critical stress required for cracking to occur, and crack growth ceases. Under dynamic conditions, where almost no critical stress is required, these polymer blends do not completely prevent cracking. In this case they function by reducing the segmental mobility of the rubber chains and this slows the rate of crack growth. This method is effective when the polymer is added at a level between 20 and 50%. Higher levels do not result in further improvement of the ozone resistance [67]. At lower levels, propagation cracks circumvent the stress-relieving domains or will not reduce segmental mobility sufficiently. This method of protecting rubber against ozone is used on a limited basis, since vulcanisates of these blended rubbers frequently exhibit poorer properties. However, it is the only effective nondiscoloring method of protecting rubber under dynamic conditions.

9.3.3.2 Protection Against Ozone Under Dynamic Conditions

Under dynamic conditions, i.e., under cyclic deformations (stretching and compression) the physical methods to protect against ozone are no longer valid.

Chemical antiozonants have been developed to protect rubber against ozone under such dynamic conditions. Several mechanisms have been proposed to explain how chemical antiozonants protect rubber. The scavenging mechanism, the protective film mechanism or a combination of both are nowadays the most accepted mechanisms.

The scavenging mechanism states that antiozonants function by migrating towards the surface of the rubber and, due to their exceptional reactivity towards ozone, scavenge the ozone before it can react with the rubber [68]. The scavenging mechanism is based on the facts that all antiozonants react much more rapidly with ozone than do the double bonds of the rubber molecules. This fact distinguishes antiozonants from antioxidants.

Studies of the reaction rates of various substituted paraphenylene diamines (PPD) towards ozone show that their reactivities are directly related to the electron density on the nitrogens due to the different substituents. Reactivity decreases in the following order: *N*,*N*,*N*´,*N*´-tetraalkyl- > *N*,*N*,*N*´-trialkyl- > *N*,*N*´-dialkyl- > *N*-alkyl-*N*´-aryl- > *N*,*N*´-diaryl [69]. It should be noted, that their ease of oxidation decreases in the same order. As expected, PPD substituted by normal, secondary, and tertiary alkyl groups all exhibit essentially the same reaction rates. Only the initial reaction of the antiozonant with the ozone is rapid - the resulting ozonised products always react much more slowly. Thus the number of moles of ozone absorbed by a compound is not necessarily an indication of its effectiveness. It is only the rate of reaction which is important.

By itself, the scavenging mechanism suffers from a number of shortcomings. According to this mechanism, the antiozonant must rapidly migrate to the surface of the rubber in order to scavenge the ozone. However, calculations show that the rate of diffusion of antiozonants to the rubber surface is too slow to scavenge all the available ozone [70]. Many compounds, which react very rapidly with ozone and therefore should be excellent scavengers, are not effective. A good example is the poor activity of *N*,*N*´-di-*n*-octyl-PPD (D*n*OPPD) compared to the excellent activity of its *sec*-octyl isomer, DOPPD [14]. Since these isomers have the same reactivity towards ozone, the same solubility in rubber, the same molecular weight (and diffusion rates) and melting points (both are liquids), the difference in their antiozonant activities must reside in the nature of their ozonised products.

The protective film mechanism states that the rapid reaction of ozone with the antiozonant produces a film on the surface of the rubber, which prevents attack on the rubber, like waxes do [71]. This mechanism is based on the fact that the ozone uptake of elongated rubber containing a substituted *p*-phenylene diamine type of antiozonant is very fast initially and then decreases rather rapidly with time and eventually stops almost completely. The film has been studied spectroscopically and shown to consist of unreacted antiozonant and its ozonised products, but no ozonised rubber is involved [72]. Since these ozonised products are polar, they have poor solubility in the rubber and accumulate on the surface.

Currently, the most accepted mechanism of antiozonant action is a combination of the scavenging and the protective film formation. Based on this mechanism, one concludes that the higher critical elongation exhibited by DOPPD is due to the nature of the protective film which forms while scavenging ozone. The only way a film or coating can increase critical stress is, if it completely prevents ozone from reaching the surface. Only a continuous flexible film can do this. For example, wax forms such a protective but non-flexible film and increases the critical elongation [73]. A continuous flexible film also explains why DOPPD does not increase the critical elongation under dynamic conditions. In this case, flexing would disrupt the continuity of the film and destroy its ability to completely coat the rubber surface, just as flexing destroys the effectiveness of waxes. It also explains why DOPPD does not increase the critical elongation in NBR [74]. In NBR very little DOPPD

is found on the surface. Consequently, any film, which forms on the surface, is too thin to be effective. The difference in the amount of DOPPD on the surface of NBR compared to SBR is attributed to the higher solubility of DOPPD in NBR.

The effect of ozone and DOPPD concentrations on critical stress can be explained by considering the factors involved in film formation and destruction. At a fixed ozone concentration, increasing the concentration of DOPPD will increase the critical elongation because the equilibrium concentration of DOPPD on the surface of the rubber increases with loading. This results in the formation of a thicker, more durable and flexible film. The higher equilibrium surface concentration of DOPPD, lying just below the film, also guarantees that any of the film destroyed by ozone will be efficiently repaired before cracks can form. On the other hand, increasing the ozone concentration at a fixed DOPPD level decreases the critical stress because the film reacts and is too rapidly destroyed by ozone, to be repaired. Thus, the critical elongation will be that point, where the ozone concentration destroys the film more quickly than that it can be repaired. At very high ozone levels, this barrier is so quickly destroyed that the critical stress is the same as the value for an unprotected stock. Since IPPD does not increase critical elongation, its reaction products with ozone must form a barrier which contains many flaws. Indeed, IPPD is known to give a powdery bloom. However, combining IPPD with waxes results in a dramatic increase in the critical stress. This has been attributed to the ability of IPPD to facilitate wax migration and increase the thickness and continuity of the wax bloom [75].

9.3.3.3 Protection Against Ozone by Substituted PPD

The most effective antiozonants are the substituted PPD. Their mechanism of protection against ozone is based on the 'scavenger-protective film' mechanism [76-78]. The reaction of ozone with the antiozonant is much faster than the reaction with the carbon-carbon double bonds of the rubber on the rubber surface [64]. The rubber is protected from the ozone attack until the surface antiozonant is depleted. As the antiozonant is continuously consumed through its reaction with ozone at the rubber surface, diffusion of the antiozonant from the inner parts to the surface replenishes the surface concentration to provide the continuous protection against ozone. A thin flexible film developed from the antiozonant/ozone reaction products on the rubber surface also offers protection.

In a PPD molecule, the aryl alkyl-substituted NH group is more reactive towards ozone than the bisaryl-substituted NH group owing to the higher charge density on the N-atom of the aryl alkyl-substitute [79]. This correlates very well with the literature report that aryl alkyl-PPD (e.g., 6PPD) produced nitrone, while the bisalkyl-PPD such as *N*,*N*′-bis(1,4-dimethylpentyl)-*p*-phenylenediamine (77PD) produced dinitrone instead [76, 77]. Apparently, the stabilising effect of the *N*-aryl group on the nitrone retards further reaction of the nitrone with ozone. A simplified reaction mechanism for the aryl-alkyl PPD such as 6PPD is depicted in **Figure 9.7**.

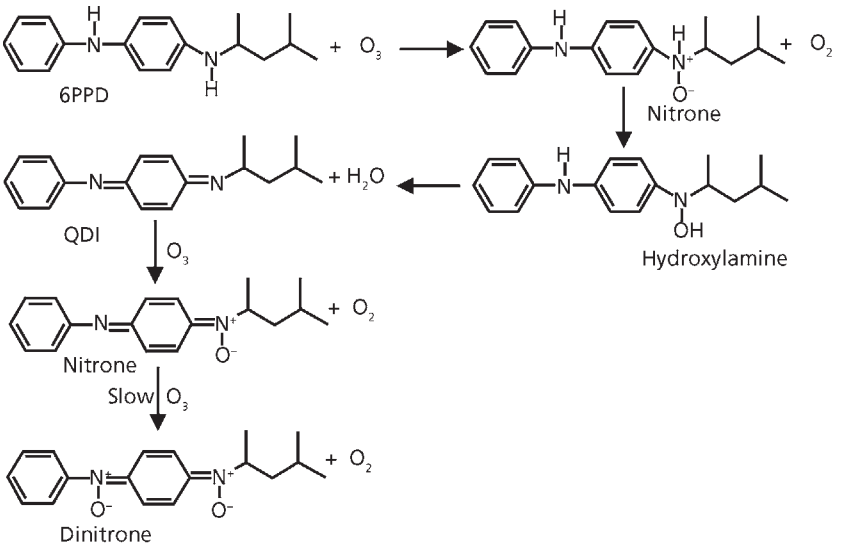

Figure 9.7 Ozonation mechanism for aryl-alkyl-PPD

9.3.3.4 Methods of Studying the Ozone Resistance of Rubber

Since ozone attack on rubber is essentially a surface phenomenon, the test methods involve exposure of the rubber samples under static and/or dynamic strain, in a closed chamber at a constant temperature, to an atmosphere containing a given concentration of ozone. Cured test pieces are examined periodically for cracking.

The length and amount of cracks is assessed according to the Bayer method [80].

The ISO standard ozone test conditions involve a test temperature of 40 ± 1 °C and an ozone level of 50 ± 5 pphm (parts per hundred million), with a test duration of 72 hours. Testing is done under static [80] and/or dynamic strain [80]. These are accelerated tests and should be used for the relative comparison of compounds, rather than for the prediction of long-term service life. The method is rather complicated and demands a long duration of ozone exposure. Therefore, in some cases the rate constants of the antiozonant's reaction with ozone in solution are used instead to evaluate the efficiency of different antiozonants [81].

The loss of antiozonants, either in a chemical or physical manner, appears to be the limiting factor in providing long-term protection of rubber products. That is why for new antiozonants not only the efficiency of the antiozonants must be evaluated, but one also has to watch other properties which influence their protective functions in an indifferent

manner, e.g., the molecule's mobility, their ability to migrate, is one of the parameters determining the efficiency of antiozonant action. Determination of the mobility kinetics of antiozonants can be done with a gravimetric method elaborated by Kavun [82]. This method was used to determine the diffusion coefficient of several substituted PPD, in different rubbers and at different temperatures [83]. The diffusion coefficients were calculated using the classical diffusion theory, see **Table 9.4**. The diffusion coefficients increase with increasing temperature and with decreased compatibility with the rubber. The lower diffusion coefficient observed for *N*-(1-phenylethyl)-*N´*-phenyl-*p*-phenylenediamine (SPPD) compared to that of IPPD and 6PPD was explained by an increased MW and/or increased compatibility with the rubbers.

9.4 Mechanism of Protection Against Flex Cracking

Flex cracking, the occurrence and growth of cracks in the surface of rubber when repeatedly submitted to a deformation cycle, is determined by fatigue testing. Fatiguing of rubbers at room temperature is a degradation process caused by repeated mechanical stress under limited access of oxygen. The mechanical deformation stress is believed to generate macroalkyl radicals (R·). A small fraction of the macroalkyl radicals reacts with oxygen to form alkylperoxy radicals, still leaving a high concentration of the

Table 9.4. Diffusion coefficients for IPPD, 6PPD and SPPD (see Figure 9.14), in different rubbers and at different temperatures [83]

Rubber	Temperature, °C	D, (cm^2/s) x 10^{-8}		
		IPDD	6PPD	SPDD
NR/BR	10	1.16	78.2	65.6
	25	2.99	1.92	1.54
	38	6.89	4.55	3.58
	62	18.8	14.7	12.0
	85	35.1	27.9	21.7
NR	10	0.34	0.17	13.0
	38	2.56	1.39	1.11
	62	11.9	7.05	6.05
	85	31.1	23.4	16.6
SBR 1500	38	1.03	0.613	0.462
	62	4.28	3.05	2.47
	85	13.6	9.72	6.02
BR	38	13.2	8.56	6.79
	62	27.1	19.9	16.4

macroalkyl radicals. Consequently, removal of the macroalkyl radicals in a catalytic process constitutes a prevailing anti-fatigue process [10]. On the other hand, the macroalkyl radicals are rapidly converted to the alkylperoxy radicals under air-oven heat ageing. The auto-oxidation propagated by the alkylperoxy radicals thus dominates the degradation process. Therefore, removal of the alkylperoxy radicals becomes the primary function of an antioxidant.

It has been shown that diarylamines are good anti-fatigue agents and that diarylamine nitroxyl radicals are even more effective than the parent amines. The anti-fatigue mechanism of the amine anti-degradants, shown in **Figure 9.8**, has been proposed where the formation of the intermediate nitroxyl radicals plays an active role [84]. Generation of nitroxyl radicals from the free amines is depicted in **Figure 9.8**. In the fatigue process, macroalkyl radicals are generated and subsequently removed by reaction with these nitroxyl radicals. The resulting hydroxylamine can be re-oxidised by alkylperoxy radicals to re-generate the nitroxyl radicals in an auto-oxidation chain-breaking process.

The nitroxyl radicals can be partially converted back to the free diarylamine during vulcanisation through the reductive action of thiyl radicals of thiols. The free diarylamine thus regenerated, would repeat the reaction described in **Figure 9.8** to form more nitroxyl radicals.

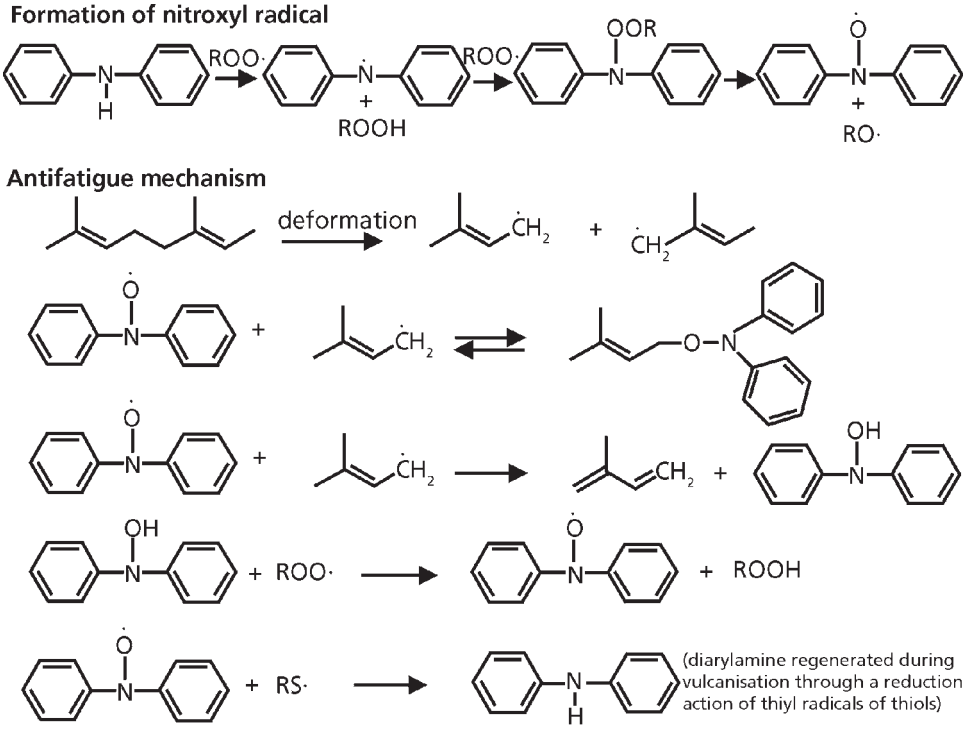

Figure 9.8 Anti-fatigue mechanism of diaryl amines

9.5 Trends Towards Long-Lasting Antidegradants

9.5.1 Introduction

Antidegradants are very important compounding additives in their role to economically maintain rubber properties at service conditions. Although conventional antidegradants such as 6PPD and IPPD provide protection against oxygen and ozone, this protection is of short duration (1-5 years, depending on the service conditions). Producers of rubber chemicals are focussing on new developments, addressing longer and better protection of rubber products [85]. Therefore, several new types of long-lasting antioxidants and long-lasting antiozonants (5-15 years, depending on the service conditions) have been developed over the last two decades.

9.5.2 Long-Lasting Antioxidants

To limit the thermal oxidative deterioration of elastomers and their vulcanisates during storage, processing, and use, different systems of antioxidants are used. The activity of the antioxidants depends on their ability to trap peroxy and hydroperoxy radicals and their catalytic action in hydroperoxide decomposition. Their compatibility with the polymers also plays a major role. Moreover, it is very important to limit antioxidant loss by extraction (leaching) or by volatilisation. Food packaging and medical devices are areas in which additive migration or extraction is of major concern. Contact with oils or fats could conceivably lead to ingestion of mobile polymer stabilisers. In an effort to address this concern, the US Food and Drug Administration (FDA) has set a code of regulations governing the use of additives in food contact applications [86]. These regulations contain a list of acceptable polymer additives and dose limits for polymers, which may be used for specific food contact. Inclusion of a particular compound in this list depends both on specific extractability and toxicological factors. Obviously, polymer bound stabilisers cannot be extracted and would therefore prevent inadvertent food contamination. An additional consideration is the effect of additive migration on surface properties. As additives migrate or bloom to the polymer surface, the ability to seal or coat the surface may deteriorate. This affects coating adhesion and lamination peel strength.

The previously described issues are the reasons for an increased interest in the synthesis of new antioxidants with the possibility of grafting to the polymer backbone or forming polymeric or oligomeric antidegradants. In the last two decades, several approaches have been evaluated in order to develop such new antioxidants:

- Attachment of hydrocarbon chains to conventional antioxidants in order to increase the MW and compatibility with polymers [87];

- Polymeric or oligomeric antioxidants [88];
- Polymer bound or covulcanisable antioxidants [89-91];
- Binding of several functional groups onto a single platform [92].

Examination of the history of antioxidants such as hindered phenols and amines shows a move from low MW products to higher MW products. Specifically, polymer industries have abandoned the use of butylated hydroxy toluene (BHT) in favour of tetrakismethylene (3,5-di-*t*-butyl-4-hydroxydrocinnamate)methane (see **Figure 9.9**). Likewise, polymeric hindered amine light stabilisers (HALS), such as polymethylpropyl-3-oxy-[4(2,2,6,6-tetramethyl)piperidinyl] siloxane, replaced the low MW hindered amine Lowilite 77 (see **Figure 9.10**). The next obvious step was to produce a new class of stabilisers, which are chemically bound to the polymer chain. This approach has had varying degrees of success. While the extraction resistance of the bound stabilisers was

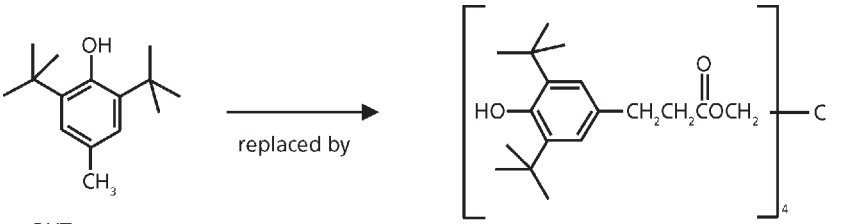

Figure 9.9. Replacement of low MW phenolic Anox by high MW product

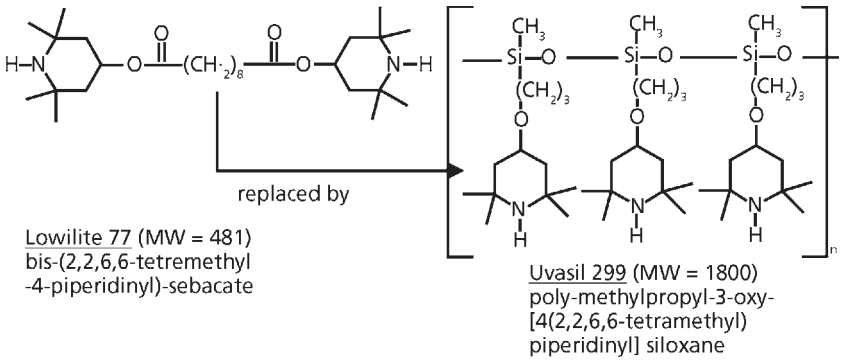

Figure 9.10 Replacement of low MW HALS by high MW product

significantly improved, performance suffered greatly. Because degradation processes may occur in localised portions of the bulk of the polymer, mobility of the stabiliser plays a key role in antioxidant activity.

The antioxidative activities of polymeric antioxidants prepared from Verona oil and the conventional phenolic antioxidant 3-(3,5-di-*tert*-butyl-4-hydroxyphenyl)propionic acid (DTBH), chemically grafted to polystyrene and polyurethanes, is similar and in some cases even better than that of the corresponding low MW phenolic antioxidants [88].

Several ways of obtaining polymer-bound antioxidants have been described. Roos and D'Amico reported polymerisable *p*-phenylene diamine antioxidants [93, 94]. Cain and co-workers reported the 'ene' addition of nitrosophenols or aniline derivatives to produce polymer-bound stabilisers [95]. The most versatile method of preparation of bound antioxidant is by the direct reaction of a conventional antioxidant with a polymer. Scott and co-workers have demonstrated that simple hindered phenols, which contain a methyl group in the *o*- or *p*-position, can react with NR in presence of oxidising free radicals to yield polymer bound antioxidants [96]. The antioxidants like styrenated phenol, diphenylamine and so on bound to hydroxyl terminated liquid NR by a modified Friedel-Crafts reaction were found to be effective in improving the ageing resistance [97]. PPD bound to NR showed improved ageing resistance compared to conventional PPD, but, as expected, a worse ozone resistance because the bound antidegradants cannot migrate to the surface [89]. Quinone diimines (QDI) have been reported as bound antioxidant and diffusable antiozonant. During vulcanisation, part of the QDI is grafted to the polymer backbone and acts as bound antioxidant, whereas the other part is reduced to PPD and is active as diffusable antiozonant [90].

The protection efficiency of antioxidant couples consisting of a classical compound (disubstituted *p*-phenylenediamines and dihydroquinoline derivatives) and compounds with a disulfide bridge, resulting from diamine and phenolic structures, was reported by Meghea and Giurginca [91]. Antioxidants containing a disulfide bridge are able to graft onto the elastomer chain during processing and curing, leading to a level of protection superior to the classical antidegradants.

One of the latest developments in stabilisers are the polysiloxanes, which provide flexible, versatile backbones for a variety of classes of polymer stabilisers. The siloxanes appear to be good backbones, because they are rather inexpensive, easily functionalised, have a high level of functionalisable sites, good compatibility with many polymers and excellent thermo and photolytic stability [92]. Hindered amines, hindered phenolics and metal deactivators have been grafted onto the polysiloxanes. The low extractability of siloxane-based additives was further enhanced by the inclusion of graftable pendant groups onto the polysiloxane backbone [98]. The grafted stabilisers maintain their activity due to the flexible siloxane platform. This was seen as a limitation of monomeric stabilisers, which have been grafted onto the polymer matrix and thus are not mobile at all.

9.5.3 Long-Lasting Antiozonants

There is a clear demand for long-lasting antiozonants (two or three times longer-lasting than conventional antiozonants such as IPPD and 6PPD), and for non-staining and non-discolouring antiozonants for better appearance products such as tyre sidewalls. The functional classes of antiozonants include substituted monophenols, hindered bisphenols and thiobisphenols, substituted hydroquinones, organic phosphites, and thioesters [3]. Triphenyl phosphine, substituted thioureas and isothioureas, thiosemicarbazides, esters of dithiocarbamates, lactams, and olefinic and enamine compounds are reported as being non-staining antiozonants [99, 100]. Approaches to completely replace the PPD with a non-discolouring antiozonant have had only limited success, leading to the development of new classes of non-staining antiozonants.

Warrach and Tsou [101] reported that bis-(1,2,3,6-tetrahydrobenzaldehyde)-pentaerythrityl acetal provides superior ozone protection for polychloroprene, butyl rubber, chlorobutyl and bromobutyl rubbers relative to *p*-phenylenediamine antiozonants, without discolouring the rubber or staining white-painted steel test panels. However, the ozone resistance of diene elastomers (NR, polyisoprene, SBR, polybutadiene, nitrile rubber) or inherently ozone-resistant elastomers (ethylene-propylene copolymers, EPDM, chlorosulfonated polyethylene, ethylene vinyl acetate) is not improved by this compound.

Rollick, Gillick and Kuczkowski [99, 102] reported a new class of antiozonants for rubber that do not discolour upon exposure to oxygen, ozone or UV light, namely triazinethiones. Only changes in substitution on the nitrogen adjacent to the thiocarbonyl group affected their antiozonant efficiency. Accelerated weatherometer ageing of a titanium dioxide/treated-clay filled SBR compound showed their non-discolouring nature. Use of 4 phr tetrahydro-1,3,5-(*n*)-butyl(*S*)-triazinethione (see **Figure 9.11**) resulted essentially in no change in colour, whereas use of only 1 phr of *N*-(1,3-dimethylbutyl)-*N´*-phenyl-*para*-phenylenediamine significantly discoloured the rubber compared to the control, see **Table 9.5**. The triazinethiones provided a significant degree of ozone protection to a NR/butadiene rubber black sidewall compound. They are reported as particularly valuable for use in light-coloured stocks.

Ivan, Giurginca and Herdan [103] reported that 3,5-di-*tert*-butyl-4-hydroxybenzylcyanoacetate is a non-staining antiozonant that affords similar protection to natural rubber and to *cis*-polyisoprene compounds as IPPD does (see **Figure 9.12**). This product lasts longer than conventional non-staining antiozonants, like the styrenated phenols.

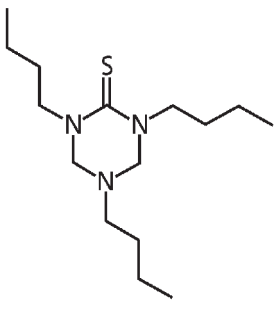

Figure 9.11 Tetrahydro-1,3,5,-tri-*n*-butyl-(S)-triazinethione

Table 9.5. Weatherometer Induced Discoloration of 6PPD and TBTT containing SBR [99]

Antiozonant[A]	Hours	L	a	b	ΔE[B]
None	24	89.89	0	7.78	
	48	89.61	-0.10	10.19	
	96	89.72	-0.10	11.90	
1 phr 6PPD	2	34.21	3.69	8.21	55.80
	48	40.25	2.47	7.93	49.48
	96	45.93	1.86	8.40	43.97
4 phr TBTT[D]	24	86.66	0.80	10.28	4.09
	48	87.81	0.81	10.99	2.17
	96	87.52	1.01	11.49	2.50

[A] Formulation: 100 phr SBR 1502, 30 phr titanium dioxide, 30 phr mercaptosilinated clay, 10 phr ZnO, 5 phr naphthenic oil, 2 phr stearic acid, 2 phr sulfur, 0.25 phr tetramethyl thiuram disulfide (TMTD)
[B] $\Delta E = \sqrt{((\Delta L)^2+(\Delta a)^2+(\Delta b)^2)}$ = change in whiteness (ΔL), hue (Δa) and chroma (Δb) upon ageing
TBTT: Tetrahydro-1,3,5-tri-(n)-butyl-(S)-triazinethione

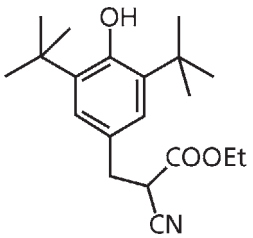

Figure 9.12 3,5-di-*tert*-butyl-4-hydroxybenzyl cyanoacetate

Wheeler [104] described a new class of non-staining antiozonants, namely the tris-*N*-substituted-triazines. 2,4,6-Tris-(*N*-1,4-dimethylpentyl-*para*-phenylenediamino)-1,3,5-triazine (see **Figure 9.13**), gave excellent ozone resistance in a NR/butadiene rubber compound when compared to *N*-(1,3-dimethylbutyl)-*N´*-phenyl-*para*-phenylenediamine, but without contact, migration or diffusion staining (see **Table 9.6**). Hong [107] reported equal dynamic ozone performance of this triazine antiozonant to the PPD in both NR and butadiene rubber compounds. Birdsall, Hong and Hajdasz [106] described that the triazine antiozonant formed a discolouring bloom on a NR/butadiene rubber compound, but that the bloom was minimal when compounded at 2 phr or lower levels. When used in combination with a PPD, better ozone protection is obtained compared to using the triazine antiozonant alone, at the same total level of antiozonant. The combination of PPD and triazine antiozonant provides longer-term protection [98].

Lehocky [83] reported the migration rates of IPPD, 6PPD and SPPD (see **Figure 9.14**), determined in different polymers and at different temperatures. SPPD showed the

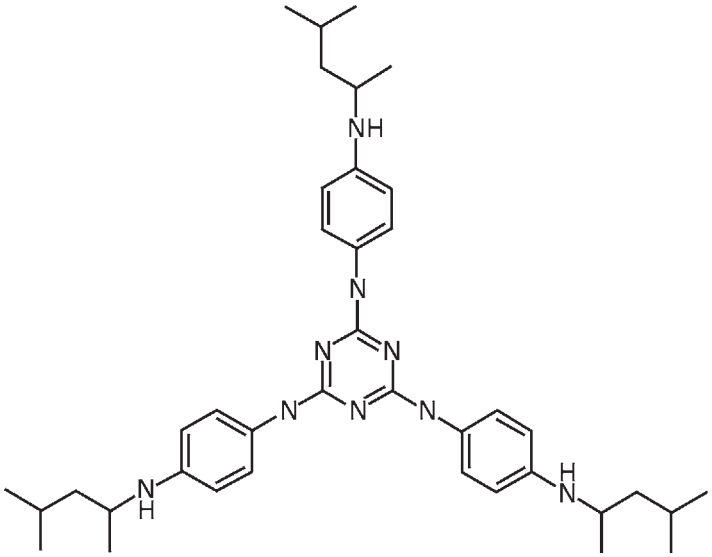

Figure 9.13 2,4,6,-Tris-(*N*-1,4-dimethylpentyl-*para*-phenylenediamino)-1,3,5-triazine (TAPTD)

Table 9.6. Staining experiments[a] of the triazine antiozonant [104] method

Antiozonant	Antiozonant	L-scale*
A. Contact stain After 96 hours	Blank	87.10
	TAPDT	83.77
	HPPD	65.59
B. Migration stain After 96 hours	Blank	86.89
	TAPDT	87.53
	HPPD	77.79
C. Diffusion stain, exposed to sunlamp for 4 hours at 55 °C	Blank	88.10
	TAPDT	82.42
	HPPD	32.65

[a] *Tests were carried out as designated in ASTM Method D925-83 [108] related to staining of surfaces by contact, migration, or by diffusion*
**Hunter colour values were measured on the L-scale. On this scale 100 is white and 0 is black*
TAPDT: Tris-(N-1,4-dimethylpentyl-para-phenylenediamino)-1,3,5-triazine
HPPD: N-(1,3-Dimethylbutyl)-N´-phenyl-para-phenylenediamine

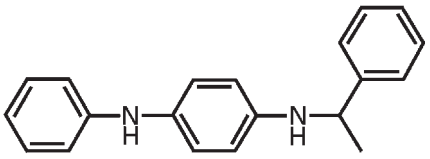

Figure 9.14 Structure of SPPD (*N*-(1-phenylethyl)-*N*′-phenyl-*p*-phenylenediamine)

lowest migration rate and is therefore expected to last longest in rubber compounds, see **Table 9.4**. However, the importance of the migration rate should not be overestimated, as the value is not sufficient to determine the effect and the efficiency of the antiozonant.

The most prevalent approach to achieve long-lasting and non-staining ozone protection of rubber compounds is to use an inherently ozone-resistant, saturated-backbone polymer in blends with a diene rubber. The ozone-resistant polymer must be used in sufficient concentration (minimum 25 phr) and must also be sufficiently dispersed to form domains that effectively block the continuous propagation of an ozone-initiated crack through the diene rubber phase within the compound. Elastomers such as EPDM, halogenated butyl rubbers, or brominated isobutylene-*co*-*para*-methylstyrene elastomers have been proposed in combination with NR and/or butadiene rubber.

Ogawa, Shiomura and Takisawa [109, 110] reported the use of various EPDM polymers in blends with NR in black sidewall formulations. Laboratory testing showed improved resistance to crack growth and thermal ageing.

Hong [111] reported that a polymer blend of 60 phr of natural rubber and 40 phr of EPDM rubber afforded the best protection of a black sidewall compound to ozone attack. Use of a higher molecular weight EPDM rubber gave good flex fatigue-to-failure and adhesion to both carcass and tread compounds. TAPDT mixed with the NR to form a masterbatch followed by blending with the EPDM rubber and other ingredients, afforded the most effective processing in order to protect the NR phase. Compounds containing this NR/EPDM rubber blend (60/40) with 2.4 phr of the triazine antiozonant passed all requirements for the tyre black sidewall.

Sumner and Fries [112] reported that ozone resistance depended on the level of the EPDM rubber. When using 40 phr of EPDM rubber in the compound there is no cracking throughout the life of the black sidewall. Ozone resistance also depends on proper mixing of the EPDM rubber with NR in order to achieve a polymer domain size of less than one micron. Otherwise cracking can be severe. The combination of high MW and high ethylidene norbornene (ENB) content afforded good adhesion to highly unsaturated polymers. The adhesion mechanism involves the creation of radicals when long chains of EPDM rubber and NR are broken down by shearing and mechanical work. Grafting between the two elastomers is believed to occur. The graft polymer is thought to act as compatibiliser. The NR/EPDM rubber compound does not rely on migration of antidegradants to achieve ozone resistance and therefore does not stain the sidewall. Appearance is excellent throughout the service life of the tyre. However, at

the current stage of development, NR/EPDM rubber sidewall compounds are difficult to mix, too expensive, result in an increased rolling resistance and have a reduced tack compared to NR/butadiene rubber sidewall compounds. Related work carried out by Polysar in this field is described in detail elsewhere [113-123].

As a general view on antidegradant activity with respect to type, structures and so on, the reader is referred to the references in the next section. Antidegradants are divided into staining and non-staining products, with or without fatigue, ozone and oxygen protection. The most commonly used antidegradants for general-purpose rubbers were reported by Huntink, Datta and Noordermeer [124]. Examples of all classes of antidegradants are given, including chemical structures and comments regarding their application and activity.

References

1. R.N. Datta and N.M. Huntink in *Proceedings of a Rapra Conference RubberChem '01*, Brussels, Belgium, 2001, Paper No.11.

2. R.N. Datta, *Progress in Rubber, Plastics and Recycling Technology*, 2003, **19**, 3, 143.

3. .R. Davies, *Plastics and Rubber International*, 1986, **11**, 1, 16.

4. R.W. Keller, *Rubber Chemistry and Technology*, 1985, **58**, 3, 637.

5. B.L. Stuck, *The Chemistry and Practical Use of Antidegradants*, Technical Report No.SC111, Sovereign Chemical Company, Akron, OH, USA, 1995.

6. J. Zhao and G.N. Ghebremeskel, *Rubber Chemistry and Technology*, 2001, **74**, 3, 409.

7. W.H. Waddell, *Rubber Chemistry and Technology*, 1998, **71**, 3, 590.

8. R.W. Layer and R.P. Lattimer, *Rubber Chemistry and Technology*, 1990, **63**, 3, 426.

9. D. Erhardt, *International Polymer Science and Technology*, 1998, **25**, 7, T/11.

10. S.K. Rakovski, D.R. Cherneva and G.E. Zaikov, *International Journal of Polymer Materials*, 1990, **14**, 1-2, 21.

11. G. Scott, *Rubber Chemistry and Technology*, 1985, **58**, 2, 269.

12. S.S. Solanky and R.P. Singh, *Progress in Rubber Plastics Technology*, 2001, **17**, 1, 13.

13. R.L. Gray and R.E. Lee in *Chemistry and Technology of Polymer Additives*, Eds., S.A. Al-Malaika, A. Golvoy and C.A. Wilkie, Blackwell Science, Oxford, UK, 1999, p.21.

14. J.C. Ambelang, R.H. Kline, O.M. Lorenz, C.R. Parks, C. Wadelin and J.R. Shelton, *Rubber Chemistry and Technology*, 1963, **36**, 5, 1497.

15. J.L. Bolland, *Quarterly Reviews of the Chemical Society*, 1949, **3**, 1.

16. J.R. Shelton and D.N. Vincent, *Journal of the American Chemical Society*, 1963, **85**, 16, 2433.

17. L. Bateman, M. Cain, T. Colclough and J.I. Cunneen, *Journal of the Chemical Society*, 1962, 3570.

18. J.T. Blake and P.L. Bruce, *Industrial and Engineering Chemistry*, 1941, **33**, 9, 1198.

19. J.R. Shelton, *Rubber Chemistry and Technology*, 1957, **30**, 5, 1251.

20. W.L. Hawkins and M.A. Worthington, *Journal of Polymer Science, Part A: General Papers*, 1963, **1**, 3489.

21. J.R. Shelton, *Journal of Applied Polymer Science*, 1959, **2**, 6, 345.

22. J.S. Dick, *Rubber Technology: Compounding and Testing for Performance*, Hanser Publishers, Munich, Germany, 2001, p.453.

23. R.P. Brown, M.J. Forrest and G. Soulagnet, *Long-term and Accelerated Ageing Tests on Rubber*, Rapra Review Reports No.110, 2000, **10**, 2.

24. ASTM D454, *Standard Test Method for Rubber Deterioration by Heat and Air Pressure,* 2004.

25. ASTM D865-9, *Standard Test Method for Rubber-Deterioration by Heating in Air (Test Tube Enclosure)*, 2005.

26. ASTM D2000, *Standard Classification System for Rubber Products in Automotive Applications*, 2005.

27. ASTM D3137-81, *Standard Test Method for Rubber Property—Hydrolytic Stability*, 2001.

28. ASTM D572, Standard Test Method for Rubber—Deterioration by Heat and Oxygen, 2004.

29. ASTM D3676, *Standard Specification for Rubber Cellular Cushion Used for Carpet or Rug Underlay*, 2001.

30. ASTM D380-94, *Standard Test Methods for Rubber Hose*, 2000.

31. A.N. Gent, *Journal of Applied Polymer Science*, 1962, **6**, 23, 497.

32. D.J. Burlett, *Rubber Chemistry and Technology*, 1999, **72**, 1, 165.

33. N.C. Billingham, D.C. Bott and A.S. Manke in *Developments in Polymer Degradation - 7*, Ed., N. Grassie, Applied Science Publishers, London, UK, 1987, Chapter 3.

34. D.I. Marshall, E.J. George, J.M. Turnipseed and J.L. Glenn, *Polymer Engineering and Science*, 1973, **13**, 6, 415.

35. H.E. Bair, *Polymer Engineering and Science*, 1973, **13**, 6, 435.

36. D.D. Parker and J.L. Koenig, *ACS Polymeric Materials Science and Engineering*, 1997, **76**, 193.

37. G. Kämpf, *Characterization of Plastics by Physical Methods: Experimental Techniques and Practical Application*, Hanser Publishers, Munich, Germany, 1986.

38. G.N. Ghebremeskel, J.K. Sekinger, J.L. Hoffpauir and C. Hendrix, *Rubber Chemistry and Technology*, 1996, **69**, 5, 874.

39. H. Lavbratt, E. Ostman, S. Persson and B. Stenberg, *Journal of Applied Polymer Science*, 1992, **44**, 1, 83.

40. D.K. Setua, *Polymer Degradation and Stability*, 1985, **12**, 2, 169.

41. P.S. Bailey, *Ozonation in Organic Chemistry*, Academic Press, New York, NY, USA, 1978, Volume I, p.3.

42. T. Thomson, *Journal of the Society of the Chemical Industry*, 1885, **4**, 710.

43. N.A. Shepard, S. Krall and H.L. Morris, *Industrial and Engineering Chemistry*, 1926, **18**, 6, 615.

44. I. Williams, *Industrial and Engineering Chemistry*, 1926, **18**, 4, 367.

45. C. Fabry and H. Buisson, *Journal of Physics and Radiation, Serie 6*, 1921, **2**, 197.

46. C. Fabry and H. Buisson, *Comptes Rendus*, 1931, **192**, 457.

47. A. van Rossem and H.W. Talen, *Kautschuk und Gummi Kunststoffe*, 1931, **7**, 6, 115.

48. C. Dufraisse, *Rubber Chemistry and Technology*, 1933, **6**, 2, 157.

49. J.H. Seinfeld, *Science*, 1989, **243**, 745.

50. D. Brück, *Kautschuk und Gummi Kunststoffe*, 1989, **42**, 9, 760.

51. A.J. Haagen-Smit, M.F. Brunelle, and J.W. Haagen-Smit, *Rubber Chemistry and Technology*, 1959, **32**, 4, 1134.

52. Y. Saito, *Nippon Gomu Kyokaishi*, 1995, **68**, 5, 284.

53. D. Brück, H. Konigshofen, and L. Ruetz, *Rubber Chemistry and Technology*, 1985, **58**, 4, 728.

54. P.S. Bailey, *Ozonation in Organic Chemistry*, Academic Press, New York, NY, USA, 1978, Volume I, p.25.

55. K.W. Ho, *Journal of Polymer Science: Polymer Chemistry Edition*, 1986, **24**, 10, 2467.

56. S.D. Razumovskii, V.V. Podmasteriev and G.E. Zaikov, *Polymer Degradation and Stability*, 1988, **20**, 1, 37.

57. D. Barnard, *Journal of the Chemical Society*, 1957, **79**, 4547.

58. F.R. Erickson, R.A. Berntsen, E.L. Hill and P. Kusy, *Rubber Chemistry and Technology*, 1959, **32**, 4, 1062.

59. E.H. Andrews and M. Braden, *Journal of Polymer Science*, 1961, **55**, 162, 787.

60. J.H. Gilbert in *Proceedings of the Rubber Technology*, 4th Conference, Ed., T.H. Messenger, Institute of the Rubber Industry, London, UK, 1962, p.696.

61. M. Braden and A.N. Gent, *Journal of Applied Polymer Science*, 1960, **3**, 7, 90.

62. M. Braden and A.N. Gent, *Rubber Chemistry and Technology*, 1962, **35**, 1, 200.

63. A. Cottin and G. Peyron, inventors; Michelin, assignee, WO 194453, 2001.

64. F. Cataldo, *Polymer Degradation and Stability*, 2001, **72**, 2, 287.

65. D.A. Lederer and M. Fath, *Rubber Chemistry and Technology*, 1981, **54**, 2, 415.

66. E.H. Andrews, *Journal of Applied Polymer Science*, 1966, **10**, 1, 47.

67. E.Z. Levit, T.E. Ognevskaya, V.N. Dedusenko and D.B. Boguslovskii, *Kauchuk i Rezina*, 1979, **5**, 14.

68. S.D. Razumovskii and L.S. Batashova, *Rubber Chemistry and Technology*, 1970, **43**, 6, 1340.

69. M. Braden, *Journal of Applied Polymer Science*, 1962, **6**, 19, S6.

70. H-W. Engels, H. Hammer, D. Brück and W. Redetzky, *Rubber Chemistry and Technology*, 1989, **62**, 4, 609.

71. W. Hofmann, *Rubber Technology Handbook*, Hanser Publishers, Munich, Germany, 1989, p.273.

72. J.C. Andries, C.K. Rhee, R.W. Smith, D.B. Ross and H.E. Diem, *Rubber Chemistry and Technology*, 1979, **52**, 4, 823.

73. P.M. Lewis, *Polymer Degradation and Stability*, 1986, **15**, 1, 33.

74. E.H. Andrews and M. Braden, *Journal of Applied Polymer Science*, 1963, **7**, 3, 1003.

75. P.M. Mavrina, L.G. Angert, I.G. Anisimov and A.V. Melikova, *Soviet Rubber Technology*, 1972, **31**, 12, 18.

76. R.P. Lattimer, E.R. Hooser, H.E. Diem, R.W. Layer and C.K. Rhee, *Rubber Chemistry and Technology*, 1980, **53**, 5, 1170.

77. R.P. Lattimer, E.R. Hooser, R.W. Layer and C.K. Rhee, *Rubber Chemistry and Technology*, 1983, **56**, 2, 431.

78. S.W. Hong and C-Y. Lin, *Rubber World*, 2000, **222**, 5, 36.

79. S.W. Hong, P.K. Greene and C-Y. Lin in *Proceedings of the 155th ACS Rubber Division Conference*, Chicago, IL, USA, Fall 1999, Paper No.65.

80. ISO 1431-1, *Rubber, Vulcanised or Thermoplastic - Resistance to ozone cracking – Part 1: Static or Dynamic Strain Testing*, 2004.

81. M.P. Anachkov, S.K. Rakovsky and S.D. Razumovskii, *Journal of International Polymeric Materials*, 1990, **14**, 1-2, 79.

82. S.M. Kavun, Y.M. Genkina and V.S. Filippov, *Kauchuk i Rezina*, 1995, **6**, 10.

83. P. Lehocký in *Proceedings of a Rapra Conference RubberChem '01*, Brussels, Belgium, 2001, Paper No.18.

84. H.S. Dweik and G. Scott, *Rubber Chemistry and Technology*, 1984, **57**, 4, 735.

85. S.W. Hong, *Elastomer*, 1999, **34**, 2, 156.

86. *Code of Federal Regulations 21*, US Food and Drug Administration, Rockville, MD, USA, 1995.

87. G. Scott in *Polymer Stabililisation and Degradation*, Ed., P. Klemschuk, ACS Symposium Series No.280, ACS, Washington, DC, USA, 1985, p.173.

88. R.R.K. Kimwomi, G. Kossmehl, E.B. Zeinalov, P.M. Gitu and B.P. Bhatt, *Macromolecular Chemistry and Physics*, 2001, **202**, 13, 2790.

89. S. Avirah, M.I. Geetha and R. Joseph, *Kautschuk und Gummi Kunststoffe*, 1996, **49**, 12, 831.

90. F. Ignatz-Hoover, O. Maender and R. Lohr, *Rubber World*, 1998, **218**, 2, 38.

91. A. Meghea and M. Giurginca, *Polymer Degradation and Stability*, 2001, **73**, **3**, 481.

92. R.L. Gray, R.E. Lee and C. Neri in *Proceedings of the Polyolefins X International Conference*, Houston, TX, USA, 1997, p.599.

93. E. Roos, inventor; Bayer AG, assignee; US 3, 211,793, 1965.

94. J.J. D'Amico and S.T. Webster, inventors; Monsanto Co., assignee; US 3,668,254, 1972.

95. M.E. Cain, G.T. Knight, P.M. Lewis and B. Saville, *Journal of the Rubber Research Institute of Malaysia*, 1969, **22**, 289.

96. K.W. Sirimevan-Kularatne and G. Scott, *European Polymer Journal*, 1978, **14**, 10, 835.

97. S. Avirah and R. Joseph, *Angewandte Makromolekulare Chemie*, 1991, **193**, 1.

98. F. Gratani, *New Achievements in the UV Stabilisation of PP for Car Applications*, MBS conference, Zurich, Switzerland, 1993, p.14.

99. K.L. Rollick, J.G. Gillick, J.L. Bush and J.A. Kuczkowski in *Proceedings of the 134th ACS Rubber Division Conference*, Cincinnati, OH, USA, Fall 1988, Paper No.52.

100. K. Fujiwara and T. Ueno, *International Polymer Science and Technology*, 1991, **18**, 7, T/36.

101. W. Warrach and D. Tsou, *Rubber and Plastics News*, 1984, 13, 24, 18.

102. K.L. Rollick, J.G. Gillick and J.A. Kuczkowski, inventors; The Goodyear Tire & Rubber Co., assignee; US 5,019,611, 1991.

103. G. Ivan, M. Giurginca and J.M. Herdan, *International Journal of Polymeric Materials*, 1992, **18**, 1, 87.

104. E.L. Wheeler in *Proceedings of the 136th ACS Rubber Division Conference*, Detroit, MI, USA, Fall 1989, Paper No.73.

105. S.W. Hong, *Proceedings of the 136th ACS Rubber Division Conference*, Detroit, MI, USA, Fall 1989, Paper No.72.

106. D.A. Birdsall, S.W. Hong and D.J. Hajdasz in *Proceedings of the Tyretech '91 Conference*, Berlin, Germany, 1991, p.108.

107. M.P. Ferrandio and S.W. Hong, *Proceedings of the 152nd ACS Rubber Division Conference*, Cleveland OH, USA, Fall 1997, Paper No.64.

108. ASTM D925, *Standard Test Methods for Rubber Property-Staining of Surfaces (Contact, Migration, and Diffusion)*, 2006.

109. M. Ogawa, Y. Shiomura and T. Takisawa, inventors; Bridgestone Corporation, assignee; US 4,801,641, 1989.

110. M. Ogawa, Y. Shiomura and T. Takisawa, inventors; Bridgestone Corporation, assignee; US 4,886,850, 1989.

111. S.W. Hong, *Rubber and Plastics News*, 1989, **19**, 11, 14.

112. A.J.M. Sumner and H. Fries, *Kautschuk und Gummi Kunststoffe*, 1992, **45**, 7, 558.

113. G.W. Marwede, B. Stollfuss and A.J.M. Sumner, *Kautschuk und Gummi Kunststoffe*, 1993, **46**, 5, 380.

114. G.W. Marwede, B. Stollfuss and A.J.M. Sumner, *Plastics and Rubber Weekly*, 1993, **1471**, 10.

115. W. Von Hellens, *Proceedings of the 142nd ACS Rubber Division Conference*, Nashville, TN, Fall 1992, Paper No.23.

116. A.J.M. Sumner and H. Fries, *Proceedings of Tyretech '91*, Berlin, Germany, 1991, p.102.

117. A.J.M. Sumner in *Proceedings of the 136th ACS Rubber Division Meeting*, Detroit, MI, USA, Fall, 1989, Paper No.37.

118. W. Von Hellens, *Proceedings of the 136th ACS Rubber Division Conference*, Detroit, MI, USA, Fall 1989, Paper No.40.

119. W. Von Hellens, D.C. Edwards and Z.J. Lobos, *Rubber and Plastics News*, 1990, **20**, 5, 61.

120. J.R. Dunn and D.C. Edwards, *Industria della Gomma*, 1986, **30**, 1, 18.

121. W. Von Hellens, S.A.H. Mohammed and R. Hallman, inventors; Polysar Ltd., assignee; US 4,645,793, 1987.

122. D.C. Edwards and J.A. Crossman, inventors; Polysar Ltd., assignee; US 4,588,780, 1986.

123. G.C. Blackshaw and I.M. Kristensen, *Journal of Elastomers and Plastics*, 1975, **7**, 3, 215.

124. N.M. Huntink, R.N. Datta and J.W.M. Noordermeer, *Rubber Chemistry and Technology*, 2004, **77**, 3, 476.

10 Radiochemical Ageing of Ethylene-Propylene-Diene Monomer Elastomers

A. Rivaton and J-L. Gardette

Introduction

It has been approximately 50 years since researchers first began exposing polymeric materials to ionising radiation. The main radiation-induced changes in polymers consist of scissions and/or crosslinking of the macromolecular chains, the formation of gaseous products (e.g., hydrogen or low molecular weight hydrocarbons), the accumulation of oxidation products and the loss and/or formation of unsaturations depending on the irradiation conditions [1-4].

Ethylene-propylene-diene rubbers (EPDM), which are composed of polyethylene (PE), polypropylene (PP) and the diene monomer - 5-ethylidene 2-norbornene (ENB), have had numerous applications and are often used as wire insulators or joints in nuclear plants:

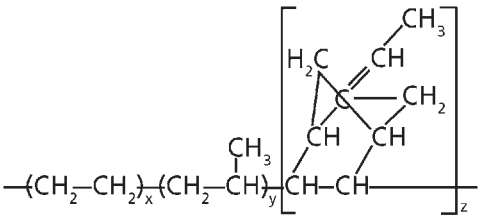

The present chapter concerns the radiative ageing of EPDM terpolymers exposed to electron beams and γ radiation. The aim is the elucidation of the mechanisms accounting for the main routes of EPDM degradation. Irradiations carried out in the presence and in absence of oxygen, and comparison with ethylene-propylene rubber (EPR) containing the same molar ratio ethylene/propylene as EPDM, allowed assessing the importance of the dienic moiety and the involvement of oxygen. Chemical structure modifications and mechanisms are firstly proposed to account for the main degradation routes of EPDM irradiated under electron beams under an argon atmosphere [5]. Secondly, chemical changes and mechanisms involved in EPDM γ-irradiated under pure oxygen are presented [6-7]. Lastly, some attempts at EPDM stabilisation to radiochemical ageing are reported [8].

Radiochemical Degradation

Units

The first unit used to measure the intensity of a radiative source was the curie (Ci), which is defined exactly as 3.7 x 10^{10} atomic disintegration's per second. The SI unit now used is becquerel (Bq), this being the best estimate of the activity of a gram of radium. One becquerel is the radiation caused by one disintegration per second. The SI unit of radiation dose is the Gray (Gy). Radiation carries energy, and when it is absorbed by matter, the matter receives this energy. The dose is the amount of energy deposited per unit of mass. One Gray is defined as the dose of one joule of energy absorbed per kilogram of matter, or 100 rad.

The metric unit measuring radiation dose is rad. 'Rad' is an acronym for 'radiation absorbed dose.' One rad is equal to a dose of 0.01 joule of energy per kilogram of mass (J/kg), or 100 ergs of energy per gram of mass. One rad equals 0.01 Gray or 1 centigray.

The units are connected by the following equation:

$$1\ Gy = 100\ rad = 1\ J/kg = 6.24 \times 10^{15}\ eV/g = 10^{4}\ erg/g$$

The dose rate is the quantity of radiation per unit time. The SI unit of radiation dose is the Gray/second (Gy/s^{-1}).

The radiochemical yield G is the number of chemical events (crosslinking, chain scissions, formation of oxidation product ...) induced by 100 electron volts (eV) of energy absorbed.

Radiation Sources

High energy ionising radiations used to initiate radiation-chemical reactions include radiations from natural and artificial radioisotopes (α, β, and γ radiation), X-rays, neutrons beam, and beams of charged particles, the latter including both electrons beams and beams of positively charged particles. Of these, gamma radiation and electrons beams are employed most frequently in radiation processing applications.

High-energy radiation sources can be divided into three groups: those employing natural or artificial radioactive isotopes, those that employ some form of particle accelerator, and nuclear reactor. The first group consists of the classical radiation sources, radium and radon, and such artificial radioisotopes as cobalt-60, cesium-137, and strontium-90/yttrium-90. The second group includes X-ray generators, electron accelerators of various

types, and accelerators such as the Van de Graaff accelerator and cyclotron used to generate beams of positive ions. Nuclear reactors have also been used as radiation sources, generally of neutrons beams, although they can also acts as sources of mixed radiation (α, β, γ, and neutrons) and, using loops that carry a liquid metal of alloy through the reactor core and external irradiation cell, as sources of beta-gamma radiation. Cobalt-60 γ-ray sources and electron accelerators (i.e., electron-beam generators) are currently the most widely used radiation sources for commercial applications.

Commercial Processes and Applications

Radiations (0.15 kGy) are used to inhibit sprouting of vegetables during storage, while doses of the order of 0.5-1.0 kGy delay the ripening of fruits and are used to control insect infestation in food. Doses in the region of 2-5 kGy bring about reduction in the microbial load of foods. Higher doses, of the order of 10-15 kGy, may be necessary to bring about complete sterilization and to eliminate viruses. Exposing food to either cobalt-60 or caesium-137 gamma radiation, or to the electron beams (10 MeV maximum energy) employed commercially, does not induce significant radioactivity, even at doses far in excess of those contemplated for food processing.

There are many other areas where irradiation may give rise to commercial processes in the future: irradiation of materials absorbed on solid surfaces or solid catalysts where the interaction of radiation and surface may bring about distinctive changes and, at very low temperature, where irradiation may be the best way of initiating ionic and radical reactions. The radiation technologies being applied to polymers comprise a diverse set, with many application objectives being addressed: crosslinking of polymers, degradation (chain-scissioning) to improve some of the properties (melt flow …), sterilisation, surface modifications, lithography for microelectronic circuit production…

Experimental

Materials

The molar content of EPDM determined by solid-state ^{13}C-NMR was 77.9% ethylene, 21.4% propylene and 0.7% diene. Processing antioxidants were removed by extraction with methanol in a Soxhlet extractor for 24 hours. The molar content of EPR determined by ^{13}C NMR was 76.6% ethylene and 23.4% propylene. It was purified by dissolution in *n*-heptane followed by precipitation in a methanol/chloroform (1:1) mixture and was then vacuum dried.

Irradiation

Gamma irradiation was delivered by ^{60}Co gamma sources. Samples were irradiated in a watertight container, at doses between 5 and 455 kGy with a dose rate of 1 kGy/h. The oxygen flow rate was 0.5 l/min and the temperature was 20 °C. Electron beam irradiation (2 MeV) was delivered by a Van de Graaff type accelerator. Samples were irradiated at doses between 50 and 1000 kGy with a dose rate of 500 kGy/h. The argon flow rate was 0.5 l/min and the temperature was 25 °C.

10.1 Degradation Under Inert Atmosphere

10.1.1 Infra Red (IR) Analysis

Figure 10.1 shows the modifications in the IR spectra in the region corresponding to the out-of-plane vibration of the C-H bond linked to unsaturations of EPDM and EPR as a function of radiation dose. One observes a progressive decrease in the γ(C-H) absorbance at 808 cm^{-1}, which indicates the disappearance of the double bond of the termonomer ENB; the remaining absorption at 808 cm^{-1} can be attributed to methylene deformation of PP moieties. One also observes the increase of three absorption bands at 965 (which overlaps with the initial C-C skeletal stretch at 971 cm^{-1}), 909 and 888 cm^{-1}. These absorption bands, which are initially present in non-irradiated EPDM, resulted from structural defects of ethylene moieties. They can be attributed to *trans*-vinylene unsaturation (-CH=CH-) at 965 cm^{-1}, 1-2 vinyl (R-CH=CH_2) at 909 cm^{-1} and vinylidene ($R_1R_2C=CH_2$) at 888 cm^{-1}.

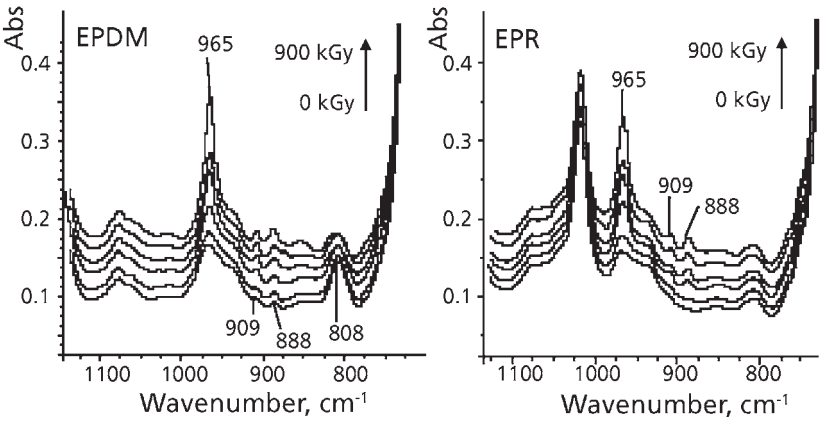

Figure 10.1 IR spectra changes of EPDM and EPR films during irradiation under electron beam in an argon atmosphere

Modifications of the spectra were also observed in the ν(C=C) region showing an increase of the absorption band centred at 1640 cm^{-1}, which is attributed to unsaturation formed under irradiation. The progressive decrease in the absorbance of the 1688 cm^{-1} band corresponds to the consumption of the double bond of the termonomer ENB.

Anaerobic radiolysis of EPDM led to dramatic modifications in the IR spectra, which were similar to those observed for EPDM, that is, the development of three bands at 965, 909 and 888 cm^{-1} and of an absorption centred at 1640 cm^{-1}.

From the spectra presented in **Figure 10.1**, it is possible to plot the concentration of unsaturations in EPDM and EPR as a function of the dose (**Figure 10.2**).

Figure 10.2 shows that the accumulation of unsaturations occurred roughly at the same rate in EPDM and EPR. In parallel, the ENB double bond was consumed in EPDM.

The *G* (radiochemical yields) of formation of *trans*-vinylene (G_{965}), vinyl (G_{909}) and vinylidene (G_{888}) in EPDM and EPR and the consumption of the ENB unsaturation (G_{ENB}) in EPDM can be calculated from the curves of **Figure 10.2**. The results are given in **Table 10.1**.

Table 10.1 *G* values for the radiolysis of EPDM and EPR

G	EPDM	EPR
G_{965}	1.1	1.0
G_{909}	0.1	0.1
G_{888}	0.1	0.1
G_{ENB}	4.5	-

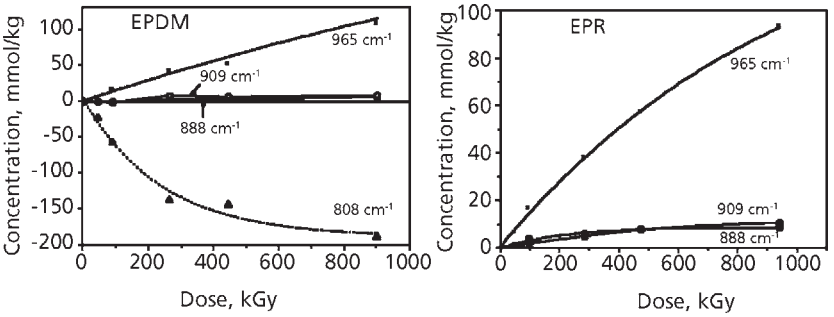

Figure 10.2 Changes of unsaturations concentrations in EPDM and EPR films during irradiation under electron beam in argon atmosphere

The value of 4.5 found for the consumption of ENB in EPDM (0.7% molar content in ENB) is in the range of values (3-10) reported in the literature for EPDM, with an ENB molar content in the range of 1.75–3.75 %, γ-irradiated *in vacuo* [9].

The *G* of formation of unsaturations are observed to be roughly the same in EPDM and EPR. The values found are 1.0 for the formation of *trans*-vinylene and 0.1 for the formation of vinyl and vinylidene. These data are in the same range as those reported for EPR (72% molar content in ethylene) under γ-irradiation [10, 11]: G_{965} = 0.7, G_{909} = 0.1 and G_{808} = 0.2.

10.1.2 UV-vis Analysis

The analysis of the UV-vis spectra of EPDM and EPR showed the development of an absorption band with a maximum centred at 240 nm that may be attributed to the formation of dienic structures. The rates of formation of the dienic structures were observed to be roughly the same in both polymers.

10.1.3 Evaluation of Crosslinking

The crosslinking of irradiated EPDM and EPR films was characterised through the increase of the gel fraction in *n*-heptane. The gel fractions (g) of irradiated samples were determined by weighing polymer samples before and after a Soxhlet extraction in *n*-heptane: $g = W_{insoluble}/W_{initial}$. The soluble fraction $s = 1 - g$.

On the basis of the curves reported in **Figure 10.3a** using the Flory-Rehner equation [12], the evolution of M_c parameter (molecular weight between crosslinks) with the irradiation dose (**Figure 10.3b**) was determined.

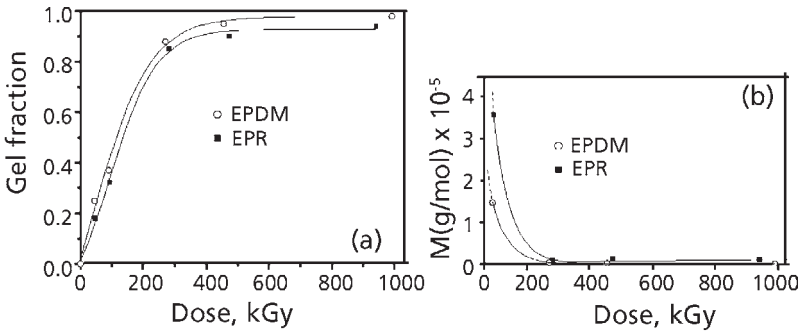

Figure 10.3 Evolution of gel fraction (A) and M_c parameter (B) in EPDM and EPR films during irradiation under electron beam in an argon atmosphere

For both polymers, a crosslinking density higher than 90% is reached for a radiation dose exceeding 300 kGy. The decrease in the M_c value accounts for an increase of the network density. The curves also show that the rate and the density of crosslinking are increased by the presence of diene. As described previously, IR analysis showed that the double bond of ENB at 808 cm^{-1} disappears with irradiation.

The evolution in soluble fraction(s) allowed plotting $s + s^{0.5}$ *versus* 1/D (where D represents the absorbed dose) (**Figure 10.4**). Using the Charlesby-Pinner theory [13], the extrapolation of the curve for 1/D to 0 allows the determination of the ratio p_0/q_0 where p_0 and q_0 are the density of chain scissions and reticulation per dose and monomer unit, respectively. The ratio p_0/q_0 was determined to be 0.01 for EPDM and 0.14 for EPR. These values indicate that the crosslinking rate exceeds the scission rate and, of course, both polymers are radiation-crosslinkable polymers [14].

Therefore, reticulation largely exceeds chain scission, which agrees with the increase in gel fraction and the decrease in M_c. Geissler and co-workers [9] demonstrated that the incorporation of ENB in EPR increases both the *G* of reticulation and chain scission. It was proposed that ENB site could be the site of reticulation through radical addition, but ENB would also present a weak site for scissions.

10.1.4 Mass Spectrometry Analysis

Mass spectrometry analysis of the volatile low molecular weight products formed was performed. An EPDM film was introduced into a Pyrex tube sealed *in vacuo*. The cell seal was maintained during irradiation. After irradiation, the cell was connected to the mass spectrometer. The analysis of the gas phase indicated that the volatile product formed by EPDM γ-radiolysis is H_2.

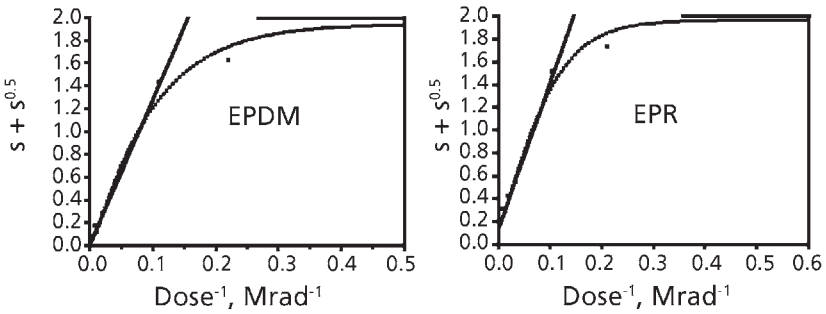

Figure 10.4 Evolution of $s + s^{0.5}$ as a function of 1/D for EPDM and EPR films during irradiation under electron beam in an argon atmosphere

10.1.5 Mechanism of Degradation Under an Inert Atmosphere

Interaction of high-energy radiation with matter is unselective: the most significant effects produced by high-energy radiations on matter result from random interactions with orbital electrons. An alternative to the energy migration theory of Partridge is that extensive C-C scission could be followed by recombination of the carbon-centred radicals, which cannot migrate apart quickly.

Radiolysis of polyolefins leads to the scission of the strongest chemical bonds C-H, whereas C-C bonds are less affected. This has been attributed by Partridge to the transfer of excitation energy along the macromolecular chains preventing main-chain scissions, whereas C-H scissions are favoured by the localisation of the excitation [3]. Consequently, irradiation under argon of EPDM (77.9% ethylene) and EPR (76.6% ethylene) mainly involves the ethylene units. The following effects are observed:

- The formation of C-C bonds between the molecular chains. The density of chain scissions/reticulation was found to be very low: the values 0.01 and 0.14 were for EPDM and EPR, respectively. PE is indeed known to undergo mainly crosslinking under high-energy radiation in an inert atmosphere [13-15].

- The increase in *trans*-vinylene, vinyl and vinylidene unsaturations. The formation of *trans*-vinylene unsaturation has been reported in the literature for the γ-irradiation under inert atmosphere of EPR [10, 11] and EPDM [9].

- The formation of dienic structures. The formation of conjugated dienes in PE has been reported under irradiation in inert atmosphere [15, 16].

- The formation of H_2.

- The depletion of the ENB double bond in EPDM.

- The influence of the double bond. The comparison between EPDM and EPR showed that the ENB double bond, which is consumed by radiolysis, increases the rate and the density of reticulation.

On the basis of these experimental results, one can propose a mechanism accounting for the effects of radiation on EPDM: Firstly, the initial radiolysis reaction involves the ejection of $H^{\bullet}$ accompanied by the formation of a macroradical [1, 3, 17]. The kinetic energy of the free-radical $H^{\bullet}$ released in the first radiolysis reaction is high enough to provoke an abstraction of other $H^{\bullet}$, producing H_2. The recombination of the macroradicals that are obtained leads to crosslinking, which appears as the major change at the molecular level. These reactions are summarised in **Scheme 10.1**.

Secondly, the formation of *trans*-vinylene unsaturation observed by IR spectroscopy as well as H_2 detection in the gas phase by mass spectrometry indicates that the initial

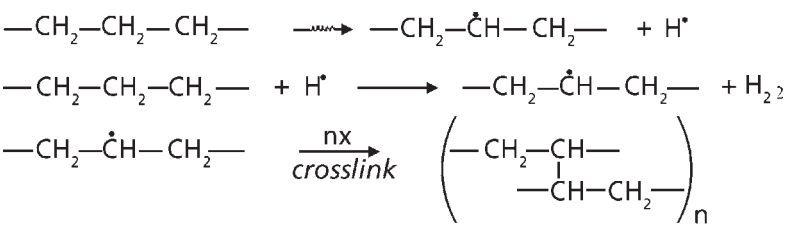

Scheme 10.1

reaction also involves C-H scissions on two neighbouring atoms of ethylene units [18] according to **Scheme 10.2**:

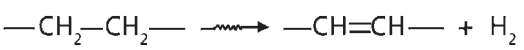

Scheme 10.2

The formation of *trans*-vinylene unsaturations in PP units would lead to the formation of methane according to **Scheme 10.3**:

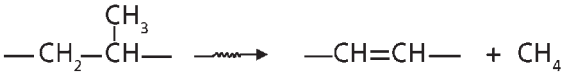

Scheme 10.3

No methane was detected by mass spectrometry, probably because it is formed at concentrations well below the sensitivity of the apparatus. It has been reported [19] that $G(H_2)$ is 2.59, whereas $G(CH_4)$ is only 0.077. The *G* values for the formation of *trans*-vinylene unsaturations are 1.1 in EPDM and 1.0 in EPR. Therefore, the formation of *trans*-vinylene unsaturations in PP and ENB units occurs at a fairly low extent compared with the ethylene units.

Thirdly, the formation of vinyl unsaturations could involve end chains according to **Scheme 10.4**:

Scheme 10.4

The *G* value for the formation of vinyl unsaturations is equal to 0.1 either in EPDM or EPR. Therefore, ENB units did not participate in the formation of vinyl unsaturations.

Fourthly, two mechanisms involving the PP units could account for the formation of vinylidene unsaturations:

- As proposed by Black and Lyons [20] disproportionation of radicals formed in the main-chain scission could occur according to **Scheme 10.5**:

Scheme 10.5

The elimination of H2 could also be proposed to occur according to **Scheme 10.6**:

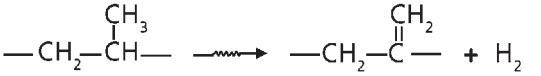

Scheme 10.6

The *G* value for the formation of vinylidene unsaturations is equal to 0.1 in EPDM and EPR. As for the vinyl unsaturations, the ENB units did not have any contribution in the formation of vinylidene unsaturations.

Fifthly, IR analysis showed that the double bond of the diene is consumed in the first steps of radiolysis. As the interaction of radiation/matter is statistical, the consummation of the double bond (0.7% ENB in EPDM), at which the intensity at 808 cm^{-1} decreased rapidly with a high yield (G_{ENB} = 4.5), cannot result from direct radiolysis. The mechanism of destruction of unsaturations probably involves radical addition by macroradicals formed in the radiolysis of EPDM according to **Scheme 10.7**:

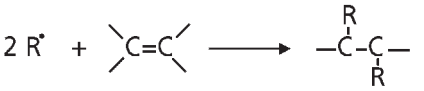

Scheme 10.7

These reactions account for the higher reticulation rate and density of EPDM as compared with EPR.

As a conclusion, the comparative study of EPDM and EPR under electron beams in an inert atmosphere allowed us to propose a general mechanism, which is reported in **Scheme 10.8**.

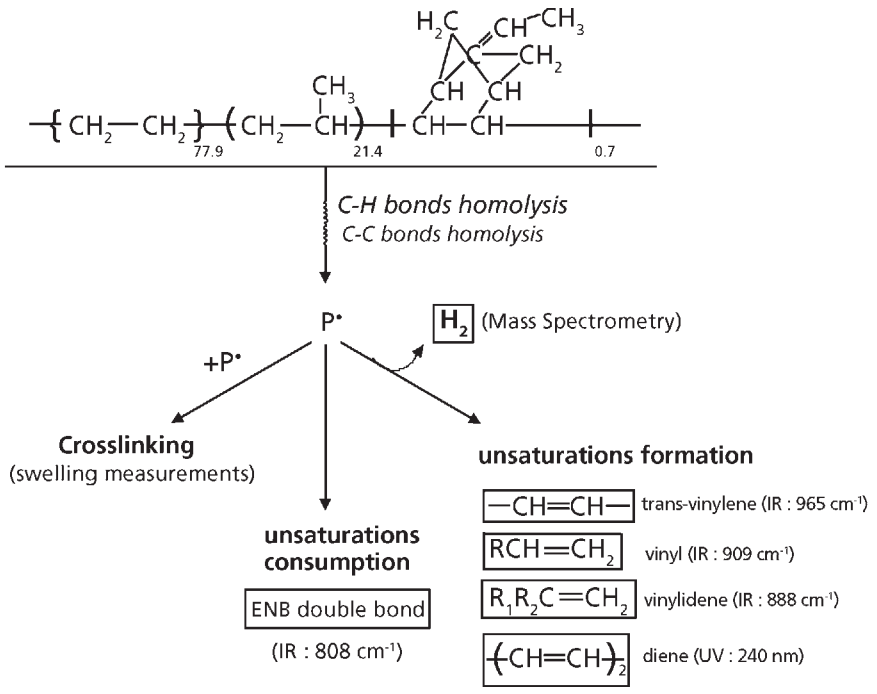

Scheme 10.8 Mechanism of radiochemical degradation of EPDM in an inert atmosphere

10.2 Identification and Quantification of Chemical Changes in EPDM and EPR Films γ-Irradiated Under Oxygen Atmosphere

10.2.1 IR Analysis

Radiooxidation of EPDM and EPR leads to notable modifications in the IR spectra of the samples. In order to facilitate the characterisation of these modifications, the spectra obtained by subtraction of the initial spectrum from the spectra recorded after each irradiation dose are presented in **Figure 10.5**.

In the case of EPDM, an increase in the absorbance in the hydroxyl absorption region is observed. The maximum around 3400 cm^{-1} is attributed to an hydrogen bonded -OH stretch of oxidation groups (alcohols around 3430 cm^{-1}, hydroperoxides around 3420 cm^{-1} and carboxylic acids around 3210 cm^{-1}). The maxima at 3600 and 3553 cm^{-1} are attributed to isolated OH stretch of alcohols and hydroperoxides respectively. In parallel, one can observe a progressive decrease in the ν(C=H) absorption intensity at 3040 cm^{-1}, which indicates the disappearance of the ENB termonomer double bond.

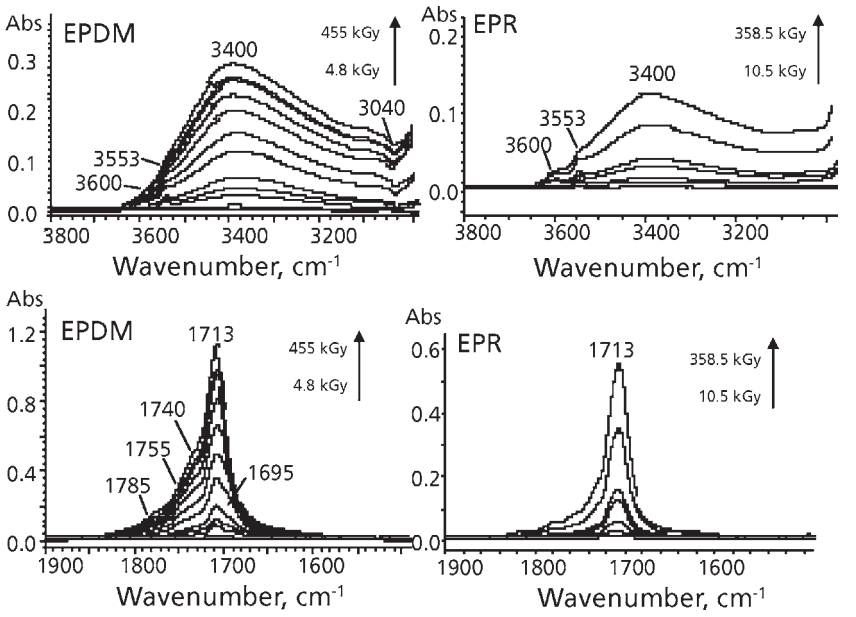

Figure 10.5 IR spectra changes during γ-irradiation under oxygen atmosphere of EPDM and EPR films

Except of course for this latter decrease, changes in the IR spectra of EPR are similar to those shown for EPDM.

In the carbonyl region, the formation of a band with an absorption maximum at 1713 cm^{-1} and several shoulders around 1785, 1755, 1740 and 1695 cm^{-1} is observed. Usually absorptions around 1785 cm^{-1} and 1740 cm^{-1} are ascribed to γ-lactones and esters, respectively. The absorbance increase in the range 1725-1718 cm^{-1} indicates saturated ketones formation whilst unsaturated ketones are observed around 1685 cm^{-1}; saturated carboxylic acids are ordinarily observed at 1755 and 1718-1710 cm^{-1} whilst unsaturated acids absorb around 1700 cm^{-1}. The comparison of the carbonyl absorption shape of the two polymers indicates that the contribution of absorptions around 1755 cm^{-1} and 1740 cm^{-1} to the whole absorption is higher in EPDM than in EPR. No shoulder around 1695 cm^{-1} attributed to unsaturated species is observed in the IR spectra of EPR.

Modifications in the EPDM spectra were also observed in the region corresponding to the out of plane vibration of the C-H bond linked to unsaturations. One observed a progressive decrease in the γ(C-H) absorbance at 808 cm^{-1}, which confirms that the dienic double bond disappears throughout radiooxidation. On the other hand, one observed no intensity variation in the absorption bands initially present in EPDM and

EPR before irradiation and attributed to structural defects of ethylene moieties [21], i.e., at 965 (*trans*-vinylene unsaturation: -CH=CH-), 909 (1-2 vinyl: R-CH=CH_2) and 888 cm^{-1} (vinylidene: $R_1R_2C=CH_2$).

The rates of formation of hydroxyl (measured at 3400 cm^{-1}) and carbonyl products (measured at 1714 cm^{-1}) during γ-irradiation of EPDM and EPR are given in **Figure 10.6a**. **Figure 10.6b** shows the curve corresponding to the decrease of the ENB double bond concentration as a function of the dose.

These results indicate that the oxidation products accumulate throughout the exposure whilst the total consumption of the diene double bond occurs within a dose of 200 kGy. **Figure 10.6a** also shows that the absorbance in the hydroxyl and carbonyl regions increases linearly with the dose for EPR films. For EPDM films, a decrease of the rate of formation of the products occurs for doses higher than 200 kGy, which corresponds to the disappearance of the ENB double bonds.

From **Figure 10.6b**, the radiochemical yield (G) of the ENB unsaturation consumption (G_{ENB}) in EPDM can be calculated. A value of 32.1 is found in radiooxidative conditions, which is significantly higher than the value 4.5 obtained under an inert atmosphere. Such a difference indicates that the disappearance of dienic double bonds is largely enhanced by the presence of oxygen during irradiation.

The distributions of the oxidation products were determined by IR-microspectroscopy following the usual cross-sectional procedure [22]. Oxidised films of about 200 μm thickness were sliced with a cryogenic microtome and the spectra were then recorded every 11 μm from the irradiated surface towards the bulk of the sample. Analysis of the oxidation products distribution within the oxidised matrix was made for EPDM and EPR thick films irradiated with various doses ranging from 100 to 450 kGy (**Figure 10.7**).

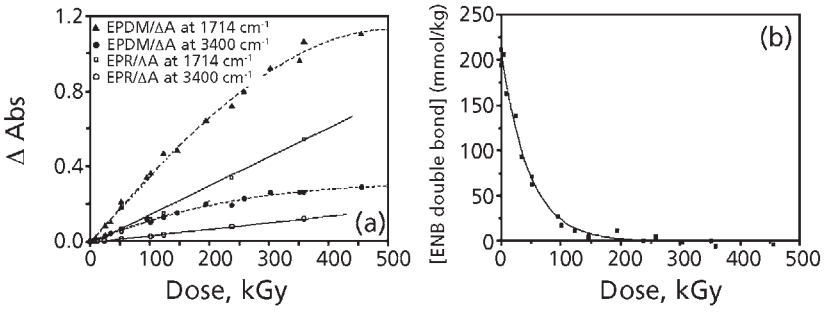

Figure 10.6 (a) Increase in the absorbance at 1714 and 3400 cm^{-1} as a function of the dose for EPDM and EPR films during γ-irradiation under an oxygen atmosphere. (b) Decay of the ENB double bonds concentration in an EPDM film during γ-irradiation under oxygen atmosphere

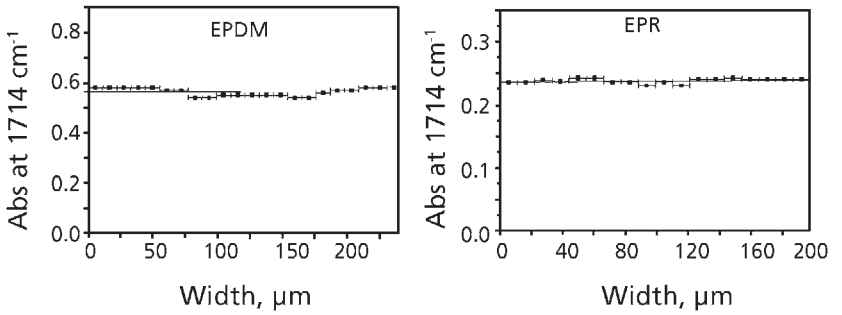

Figure 10.7 Oxidation profile measured by micro-Fourier Transform IR spectroscopy (FT-IR) in EPDM and EPR films γ-irradiated under oxygen atmosphere at 455 and 358.5 kGy, respectively

No variation in oxidation with depth was found at any dose, which indicates that in the present conditions of irradiation, the oxidation processes were homogeneously distributed within the polymeric films.

10.2.2 UV-vis Analysis

Radiooxidation leads also to dramatic modifications in the UV spectra of EPDM and EPR. The development of an absorption band with a maximum centred at 235 nm was observed accompanied by a shoulder placed around 285 nm. These absorptions could result from the overlap of the absorption bands of α,β-unsaturated carbonyl groups with the absorption bands of dienic structures (240 nm), the formation of which is observed in radiolytic conditions.

The increase in absorbance at 235 nm during γ-oxidation of EPDM and EPR is shown in **Figure 10.8**. The formation of unsaturated species increases linearly with the dose for EPDM and for EPR and is significantly higher for EPDM than for EPR.

10.2.3 Analysis of the Oxidation Products

No precise assignment for hydroxyl (broad absorption around 3400 cm^{-1}) and carbonyl regions (envelope observed in the range 1780-1680 cm^{-1}) was possible as distinct absorption bands overlap; furthermore hydrogen-bonds may provoke spectral shifts. Derivatisation methods and iodometric titration had then to be used in order to identify and quantify the various absorbing species composing the IR spectra of the oxidised materials. Derivatisation treatments selectively convert oxidation products into groups with a different IR absorption [23-26].

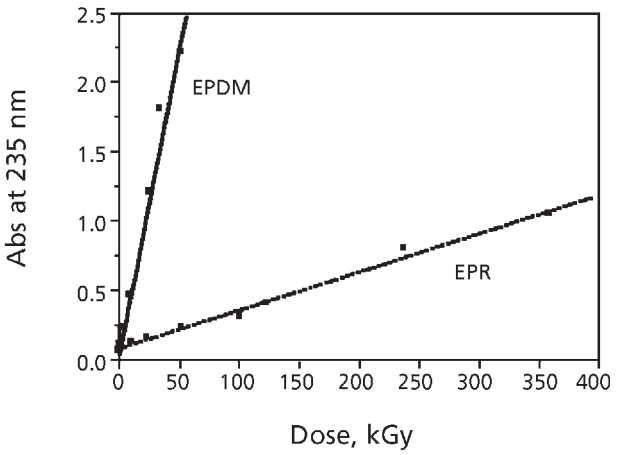

Figure 10.8 Increase in the absorbance at 235 nm as a function of the dose for EPDM (■) and EPR (□) films during γ-irradiation under oxygen atmosphere

10.2.3.1 Peroxidic Species: Hydroperoxides and Peroxides

Iodometric Titration

Iodometric titration allowed evaluation of the concentration of peroxide species (hydroperoxides and peroxides) for EPDM and EPR films. Peroxide species accumulate at concentrations up to 300 mmol/kg in EPDM and 180 mmol/kg in EPR. Selective destruction of hydroperoxides (POOH) by thermolysis (vacuum thermal treatment) at 100 °C of the irradiated samples followed by iodometric titration allowed the evaluation of the peroxides contribution (POOP). Peroxides accumulate at fairly low concentrations up to 8 mmol/kg in EPDM and 6 mmol/kg in EPR.

NO Treatment

Treatment with NO is useful to detect the formation of alcohols and hydroperoxides and permits discriminating between primary, secondary and tertiary products. NO treatments of EPDM and EPR resulted in a decrease in the absorption of the radiooxidised films in the hydroxyl region. The hydroperoxides and alcohols formation was shown by the nitrate and nitrite absorptions, respectively. Results of NO treatment are reported in **Tables 10.2** and **10.3**.

It is concluded that secondary and tertiary hydroperoxides on the one hand, secondary and tertiary alcohols on the other hand accumulate at fairly equivalent concentrations.

Table 10.2 Concentrations (mmol/kg) of POOH in EPDM and in EPR						
Dose (kGy)	EPDM			EPR		
	POOH secondary	POOH tertiary	POOH total	POOH secondary	POOH tertiary	POOH total
52	-	-	-	11	13	24
123	60	68	128	20	17	37
237.5	78	100	178	-	-	-
358.5	81	81	162	50	39	89
455	85	91	176	-	-	-

Table 10.3 Concentrations (mmol/kg) of POH in EPDM and in EPR						
Dose (kGy)	EPDM			EPR		
	POH secondary	POH tertiary	POH total	POH secondary	POH tertiary	POH total
52	12	14	26	4	6	10
123	26	24	50	12	16	28
237.5	33	34	67	-	-	-
358.5	41	46	87	31	43	74
455	46	52	98	-	-	-

10.2.3.2 Carbonyl Groups

Treatment with sulfur tetrafluoride (SF_4) was used to identify carboxylic acids, which are transformed into acid fluorides. Reaction with SF_4 enables the discrimination between saturated and α,β-unsaturated structures. Gaseous ammonia (NH_3) reacts with carboxylic acid and ester groups to give carboxylate and amide groups, respectively. 2,4-Dinitrophenylhydrazine (DNPH) reacts with aldehydes and ketone groups to give dinitrophenylhydrazone

SF_4 treatment was observed to provoke the conversion of carboxylic acids, in the range 1705-1710 cm^{-1} (non-conjugated), into non-conjugated acids fluorides (1841-1846 cm^{-1}) and the formation of traces of conjugated acids fluorides (1801 cm^{-1}). The removal of the carboxylic acid absorption band from the carbonyl envelope allowed the residual peak at 1717-1719 cm^{-1} to be assigned to ketones. Confirmation of this attribution was obtained by DNPH treatment.

From SF_4 treatments, it was possible to evaluate the concentration of carboxylic acids that accumulate in radiooxidised films. However, the concentration of conjugated and non-conjugated carboxylic acids cannot be determined separately as saturation reactions may be involved by SF_4. The ketone concentration can be evaluated by measuring the residual absorbance at 1718 cm^{-1}.

NH_3 reaction led to a decrease in the carbonyl absorption around 1710 cm^{-1} and to the formation of a 1560 cm^{-1} absorption band. This absorption corresponds to the carboxylate ions band obtained by the neutralisation of carboxylic acids (1710 cm^{-1}), confirming therefore the results of SF_4 treatments. No absorption band around 1670 cm^{-1}, that could be attributed to amide resulting from the reaction of esters with NH_3, was seen to be formed. It can then be concluded that the esters concentration in irradiated EPDM and EPR films remains fairly low throughout the exposure.

As a conclusion, from data obtained by derivatisation methods, it has been possible to plot in **Figure 10.9** the concentration of the major oxidation products in both polymers.

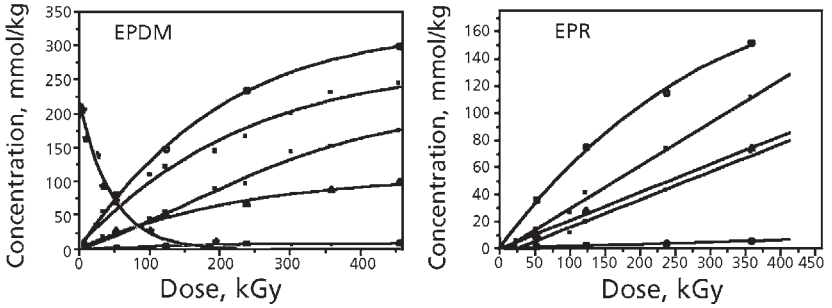

Figure 10.9 Products accumulation in radiooxidised EPDM and EPR films and ENB double bond consumption in EPDM : (●) hydroperoxides; (■) ketones; (□) carboxylic acids; (▲) alcohols; (○) peroxides; (✶) ENB double bonds

10.2.4 Gamma Irradiation in vacuo *of Hydroperoxides Formed in EPDM Films*

EPDM films pre-oxidised under γ-irradiation in the presence of oxygen at various doses were then sealed *in vacuo* in Pyrex tubes and submitted to γ-irradiation. The changes provoked by this treatment were then determined by FTIR spectroscopy combined with NO derivatisation and peroxidic titration.

Figure 10.10 shows the results of the chemical titration of peroxide species (hydroperoxides and peroxides) for EPDM films after vacuum radiolysis. This figure shows that the peroxide species (that mainly involve hydroperoxides) are rapidly destroyed under exposure to γ radiation.

In the IR domain, γ-exposure *in vacuo* of pre-oxidised EPDM samples was observed to provoke the intensity decrease of the narrow band at 3553 cm^{-1} of free hydroperoxides

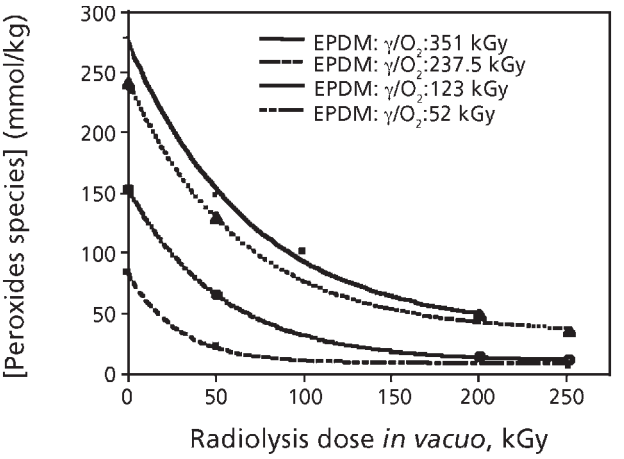

Figure 10.10 Peroxidic species decay during γ-irradiation *in vacuo* of EPDM samples pre-radiooxidised at different doses. Pre-irradiation dose: (■): 52 kGy; (○): 123 kGy; (▲): 237.5 kGy; (□): 351 kGy

and of the broad absorption around 3400 cm^{-1} of hydrogen bonded –OH species (alcohol, hydroperoxide). The remaining absorption observed after radiolysis results from alcohols and carboxylic acids. Carbonyl species are formed during *in vacuo* exposure: increase of a band with an absorption maximum at 1711 cm^{-1} (carboxylic acids and ketones) together with esters (1740 cm^{-1}) and a small increase of γ-lactones/peresters (1780 cm^{-1}). The formation of the carbonyl groups at 1711 cm^{-1} was directly correlated with the decomposition of the hydroperoxides.

In parallel, the concentration of *trans*-vinylene groups (965 cm^{-1}) increases linearly with the dose during radiolysis whereas the concentration of ENB double bonds (808 cm^{-1}) decreases rapidly and reaches a value close to zero. These changes in the absorbance of unsaturated groups are the result from direct γ-irradiation reactions in the polymer and are independent of pre-irradiation.

With the help of NO treatments it was shown that radiolysis induced a loss of the hydroperoxides and led to the formation of alcohols. Results of NO treatments of an EPDM film radio-oxidised at 52 kGy, and of an EPDM film radiooxidised at 52 kGy and then submitted to a post-radiolysis at 244.5 kGy are reported in **Table 10.4**.

The results given in **Table 10.4** show that the decomposition of hydroperoxides (*sec*- and *tert*-structures present in close concentration in the pre-oxidised film) leads to the formation of alcohols and mainly favours the formation of secondary structures. It can be concluded that the decomposition of tertiary hydroperoxides leads preferentially to the formation of carbonyl groups.

Table 10.4 Concentration of POH in EPDM films radiooxidised at 52 kGy before and after post-radiolysis under vacuum at 244.5 kGy			
EPDM radio-oxidised at 52 kGy	POH_{sec} (mmol/kg)	POH_{tert} (mmol/kg)	POH_{total} (mmol/kg)
Not post-irradiated	12	14	26
Post-irradiated *in vacuo* at 244.5 kGy	29	17	46

10.2.5 Mass Spectrometry Analysis

The analysis by mass spectroscopy of the gas phase, obtained by radio-oxidation of EPDM gave the following information. When the cell was maintained at the temperature of liquid nitrogen, oxygen and hydrogen gases were detected. Warming up the cell to the room temperature allowed the progressive detection of carbon dioxide and water. Then the cell was heated at 100 °C so that the thermal decomposition of hydroperoxides could occur, and acetic acid was identified. It is important to note that the hydroperoxides thermal decomposition in γ-irradiated EPDM gives acetic acid and no acetone.

10.2.6 Evaluation of Crosslinking

The crosslinking of EPDM and EPR, characterised through the increase of the gel fraction in *n*-heptane, as a function of the irradiation dose is shown in **Figure 10.11**. In

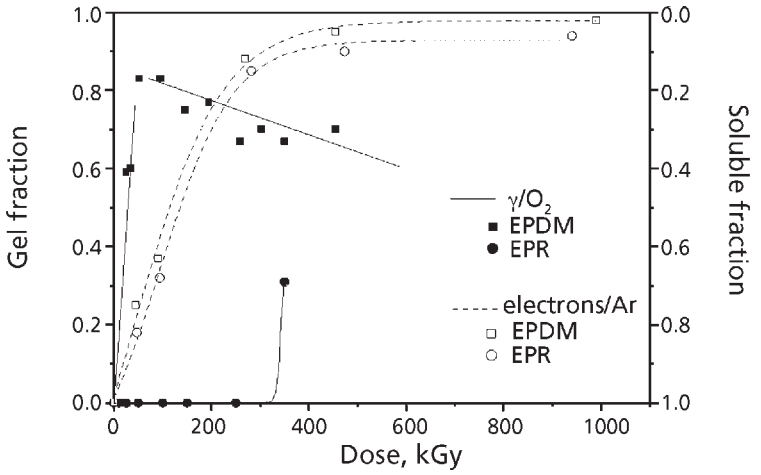

Figure 10.11 Evolution of the gel fraction with the dose. EPDM (■) and EPR (●) films γ-irradiated under oxygen atmosphere. EPDM (□) and EPR (○) films irradiated under electron beam in argon atmosphere

addition, this figure shows the results of gel fractions measured with EPDM and EPR films irradiated under electron beam under an argon atmosphere.

The curves obtained for EPDM show that crosslinking density increases very rapidly for doses up to 95 kGy. Then a weak decrease is observed, in relation to chain scissions resulting from oxidation reactions. The second conclusion is that the acceleration of the crosslinking reaction by oxygen for the lowest doses. It is worth recalling that at this dose, almost all the ENB double bonds have disappeared.

The curves obtained for EPR show that after an 'induction' period up to 250 kGy, crosslinking occurs at a very high rate. In contrast, under argon, crosslinking was observed as soon as irradiation began. These results indicate that radio-oxidative processes may be responsible for inhibiting chain scissions and therefore reticulation.

10.2.7 Post-Irradiation Analysis

Reactions that occur during the post-irradiation period are classically ascribed to the free-radicals that persist after irradiation in the crystalline region of irradiated films [27] (which represents here 12% of EPDM and 7% EPR [28]). Radicals can migrate to the interface of the crystalline/amorphous regions and initiate oxidation reactions. Another explanation for post-irradiation phenomenon is a slow decomposition of hydroperoxides [29].

Oxidation, that may occur when EPDM irradiation has stopped, has been monitored under two types of storage conditions: in the dark at – 20 °C in one case, or at room temperature in the presence of light in the other case. The increase in absorbance, which is then observed in the carbonyl region of EPDM and EPR films pre-radio-oxidised at 358.5 kGy, clearly indicates the formation of oxidative species resulting from post-irradiation effects.

Results showed that if post-irradiation reactions can be considered as negligible at – 20 °C, these oxidative reactions contribute to a certain extent to the polymer degradation at room temperature: after five months storage, the increase of absorbance 20% and 40% are observed in EPDM and in EPR, respectively.

Note: The behaviour of samples irradiated under 300 kGy in argon atmosphere was also monitored during post-irradiation period under the two same types of storage. The results showed that oxidative reactions occur at a fairly low extent only during post-irradiation at room temperature in the presence of oxygen and light.

10.2.8 Conclusion

On the basis of the curves shown in **Figure 10.9**, the radiochemical yields (*G*) of the main oxidation products formed in EPDM and in EPR and the radiochemical yield of the ENB double bond consumption have been determined. *G* values that were obtained are summarised in **Table 10.5**.

Several major conclusions can be given:

First, the accumulation of the major oxidation products in both polymers occurs in decreasing concentrations: hydroperoxides, ketones, carboxylic acids and alcohols, and peroxides (**Figure 10.9**). The oxidation products concentration is about two times higher in EPDM than in EPR. It can be also noted that for the lowest doses, which correspond to the degradation of the ENB moieties, the relative increase in ketones is favoured in EPDM at the expense of carboxylic acids.

For EPR, the concentration of all species except hydroperoxides increases linearly with the dose. For EPDM, the accumulation rate of all oxidation species decreases with the dose, once the ENB double bonds have totally disappeared. These results suggest two comments: firstly, hydroperoxides may decompose under exposure and second, the ENB plays a key role in the radicalar reactions as the oxidation of ENB moieties increases the formation rate of the major oxidation products, especially the ketones.

Besides these major oxidation species, esters and γ-lactones/peresters are formed in a higher concentration in EPDM compared to EPR.

Secondly, the presence of oxygen during irradiation accelerates the disappearance of the ENB double bonds. The radiochemical yield (*G*) of consumption of the ENB unsaturations was found to be 32.1 under oxygen but only 4.5 under an inert atmosphere.

Thirdly, secondary and tertiary hydroperoxides on one side, secondary and tertiary alcohols on the other side accumulate simultaneously with a ratio approximately equal to 50:50.

Table 10.5 Radiochemical yields (*G*) of oxidation products formation and ENB disappearance

Product	***G* (EPDM)**	***G* (EPR)**
Hydroperoxides	15.0	6.0
Ketones	13.9	3.0
Acids	4.4	2.0
Alcohols	4.1	2.0
Peroxides	0.3	0.2
ENB	32.1	-

Fourthly, as long as ENB double bonds are not totally destroyed by radio-oxidative reactions, oxygen accelerates the crosslinking reactions in EPDM. When total saturation is achieved, the reticulation rate is decreased by oxidative chain scissions reactions. In EPR, for doses lower than 250 kGy, radio-oxidative reactions prevent crosslinking.

Fifthly, the volatile product resulting from the thermolysis of hydroperoxides is acetic acid.

Sixthly, post-irradiation oxidation at room temperature in the presence of light contributes to the ageing of radio-oxidised EPR films at a higher extent than in EPDM films.

Seventhly, hydroperoxides are unstable under irradiation: the decomposition of *sec*-structures leads preferentially to the formation of alcohols and that of *tertiary* to the formation of carbonyl groups.

10.3 Mechanism of Radiooxidation

On the basis of the experimental results reported previously, the mechanisms accounting for the main routes of EPDM radiooxidation can be proposed.

As recalled previously, the interaction of high-energy radiation with matter is unselective: the most significant effects produced by high-energy radiations on matter result from random interactions with the orbital electrons. Consequently, the irradiation of EPDM (77.9% ethylene) and EPR (76.6% ethylene) mainly involves the ethylene units.

Radiolysis of polyolefins (PO) leads to the scission of the C-H chemical bonds, whereas C-C bonds are less affected. When exposure of polyolefins to high energy radiations is carried out under an oxygen atmosphere, some of the alkyl radicals ($P^{\bullet}$) resulting from the direct effects of radiation (C-H and C-C bonds scission, reaction (10.1) in **Scheme 10.9**) may combine with oxygen (reaction (10.2) in **Scheme 10.9**) dissolved in the polymer. Peroxy radicals ($PO_2^{\bullet}$) thus formed may react following two ways [30, 31]:

- Abstraction of hydrogen atoms on the polymeric backbone leads to hydroperoxides that are the primary products formed (reaction 10.3). This reaction propagates a chain-oxidation process as the macroalkyl radical ($P^{\bullet}$) thus formed restarts the chain-oxidation reactions.

- Recombination of peroxy radicals terminates the chain oxidation of the polymer (reaction 10.4), giving ketones and alcohols as final products.

Reactions (10.3) and (10.4) compete. Reaction (10.3) is one that requires a significant activation energy and is favoured at elevated temperature. Reaction (10.4) can take place at a moderate temperature and at a high concentration of $PO_2^{\bullet}$. γ-irradiation, carried

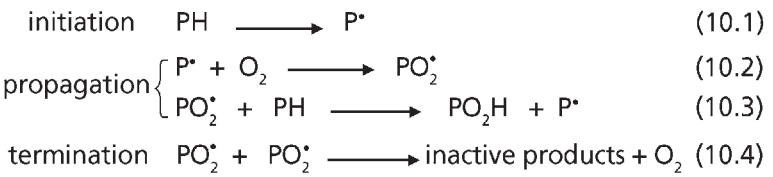

Scheme 10.9

out at 20 °C, provides a constant source of alkyl radicals which are further oxidised into peroxy radicals. It could be *a priori* presumed that the recombination of $PO_2^{\bullet}$ is favoured at the expense of hydrogen abstraction under the experimental conditions of exposure of this work. These two routes of evolution are discussed next.

10.3.1 Formation of Hydroperoxides

Hydroperoxide formation involves the abstraction of the most labile hydrogen atoms. Consequently, conversely to the statistical γ-initiation, this reaction is selective. It accounts for the fact that *sec*- and *tert*-hydroperoxides accumulate in an approximate ratio of 50:50. In a complementary experiment, hydroperoxides formed in a polypropylene film γ-irradiated under an oxygen atmosphere at 123 kGy have been titrated. The value of the molar ratio $[ROOH]_{tert}/[ROOH]_{sec}$ = 72/28, which is evidence that selective propagation reactions parallel random γ-initiation.

Two types of labile hydrogen atoms are present in EPDM:

- Hydrogen on the tert-carbon atoms of propylene units (reactivity 1/20/200 for primary, secondary and tertiary C-H attack, respectively [32]).

- Hydrogen on C atom in position α to double bonds of ENB. The high sensitivity to oxidation of CH groups α to unsaturations is well documented [33, 34]. According to Faucinato and co-workers [35], only two types of radicals (A) and (B) drawn on **Scheme 10.10** can be formed:

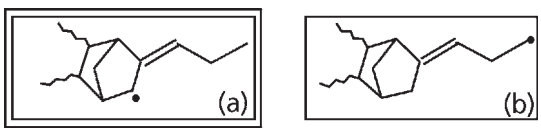

Scheme 10.10

Macroradicals resulting from hydrogen abstraction propagate the oxidation to give in particular hydroperoxides. As no primary hydroperoxides were detected by NO treatments, it is suggested that only secondary radicals (A) are formed on ENB units.

It can be then concluded that random initiation gives mainly secondary hydroperoxides (PE_{OOH}) on ethylene units whereas selective propagation gives tertiary hydroperoxides (PP_{OOH}) on propylene units and secondary hydroperoxides (ENB_{OOH}) on ENB units (**Scheme 10.11**):

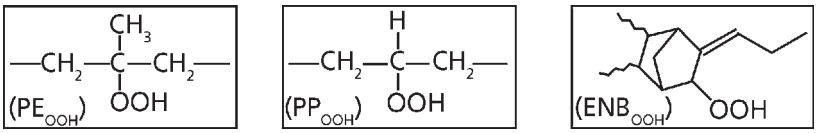

Scheme 10.11

The formation rate of the oxidation products is higher in EPDM compared to EPR. In addition, the concentrations increase linearly with the dose in EPR but decrease in EPDM, once the ENB double bonds have totally disappeared. These two quantitative results can be explained by an abstraction that is facilitated at the ENB site compared to the propylene site. Such a difference was confirmed in a complementary photodegradation experiment. In contrast to high-energy radiative oxidation, photooxidation is extremely selective. The comparison of the photooxidation rate of EPDM with that of a PP sample, exposed in the same conditions, showed that EPDM oxidised much faster than PP. The facility of hydrogen abstraction in α-position to double bonds accounts for the high radiochemical yield of disappearance of ENB unsaturations (G = 32.1).

In conditions of photo-oxidation, tertiary hydroperoxides associated in sequences deriving from a back-biting process according to **Scheme 10.12** are formed [36]:

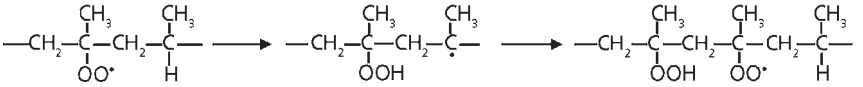

Scheme 10.12

The decomposition of these associated hydroperoxides formed in pre-photo-oxidised PP film was shown to give acetone [36]. In conditions of radio-oxidation, the volatile product resulting from the thermolysis of hydroperoxides formed in a pre-radio-oxidised film was identified as acetic acid (mass spectrometry) according to **Scheme 10.13**:

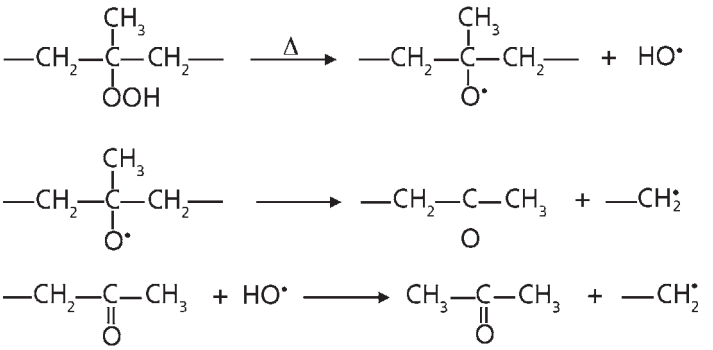

Scheme 10.13

This result clearly indicates that the *tert*-hydroperoxides formed on PP units of γ-irradiated EPDM are relatively isolated.

Exposure to γ-radiation under vacuum provokes the decomposition of *sec*- and *tert*-hydroperoxides, giving carbonyl and hydroxyl groups. Macro-alkyl radicals ($P^{\bullet}$) generated in the radiolysis of the polymer can react with oxidation products by abstracting the labile hydrogen atoms these groups possess. It has been shown that hydrogen atoms on tertiary carbons carrying oxygen groups were about a hundred times more reactive towards hydrogen abstraction [37]. Consequently, attack of the hydrogen atom in γ-position to *sec*-hydroperoxides is proposed, giving carboxylic acids and generating primary radicals (reaction **10.5**). Hydrogen abstraction on hydroperoxides sites (*sec*- and *tert*-) could also occur, generating $PO_2^{\bullet}$ radicals (reaction **10.6**).

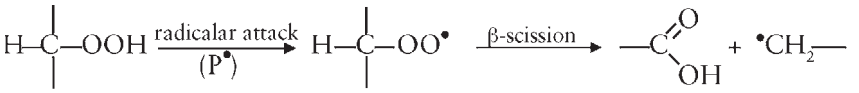

(10.5)

(10.6)

Primary radicals formed in reaction (**10.5**) propagate the chain oxidation reactions. The decomposition of hydroperoxides according to reaction (**10.6**) is a source of $PO_2^{\bullet}$ radicals, which through recombination can terminate the chain oxidation process.

10.3.2 Recombination of Peroxy Radicals

A Russel-type mechanism [37] for self-reaction of *sec*-peroxyl radicals would lead to the formation of equimolar quantities of *sec*-alcohols and ketones according to reaction (**10.7**):

(10.7)

However, the radio-oxidation of EPDM produces *sec*-alcohols in lower concentrations than ketones (ratio 1/5 at 450 kGy). Two explanations can be proposed to account for this discrepancy:

Besides the Russel-type mechanism, another possibility for $PO_2^{\bullet}$ radicals is recombination via instable tetroxide intermediate formation, as recently shown in the case of the photo-oxidation of polypropylene [38, 39], according to reaction **10.8**:

(10.8)

It can be noted that, whilst the Russel-type mechanism is limited to *sec*-peroxy radicals, the tetroxide routes involve both *sec*- and *tert*-peroxy radicals.

The major route of evolution of alkoxy radicals is diffusion out of the cage, followed by a β-scission which gives ketones (reaction **10.9**):

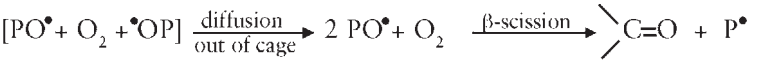

(10.9)

Additional pathways involve alkoxyl radical attack on the polymer matrix to give alcohols (reaction **10.10**), and also in-cage crosslinking by peroxide bridges that are detected in fairly low concentration (reaction **10.11**):

(10.10)

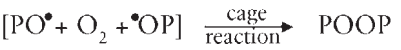

(10.11)

Sec-alcohols accumulate only in low concentrations, which could indicate that these products are not stable. It has been proposed [40] that a rapid oxidative attack on the activated *tert*-CH site of the alcohol groups could occur (reaction **10.12**) to produce ketones and H_2O (reaction **10.13**):

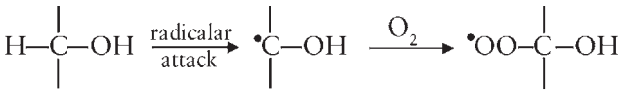

(10.12)

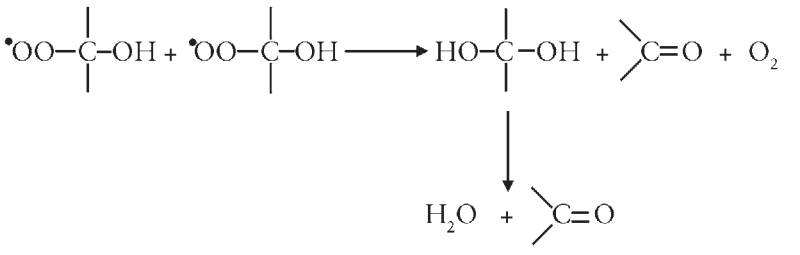

(10.13)

However, our results indicate that *sec*-alcohols groups are formed in the γ-radiolysis of pre-oxidised film. This suggests that the main route of evolution of $PO_2^{\bullet}$ radicals is the formation of a tetroxide intermediate (**10.8**) followed by β-scission (**10.9**). Russel type mechanism (**10.7**), hydrogen abstraction (reactions **10.10** and **10.12**) occurs to a lesser extent.

Besides the formation of these major oxidation products, mechanisms can be proposed to account for the formation of esters and γ-lactones/peresters:

The formation of esters has been tentatively explained [41, 42] by a radical attack of ketones by alkoxy radicals (reaction **10.14**):

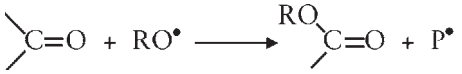

(10.14)

The formation of γ-lactone could involve a mechanism similar to the one proposed for PE, with the formation and the decomposition of 1,4-dihydroperoxides [43] (**Scheme 10.14**):

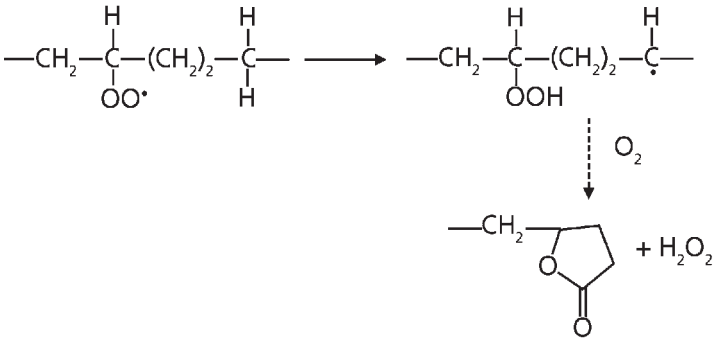

Scheme 10.14

In the case of PP [44], the formation of γ-lactones involves the γ-CH_3 group as shown in **Scheme 10.15**:

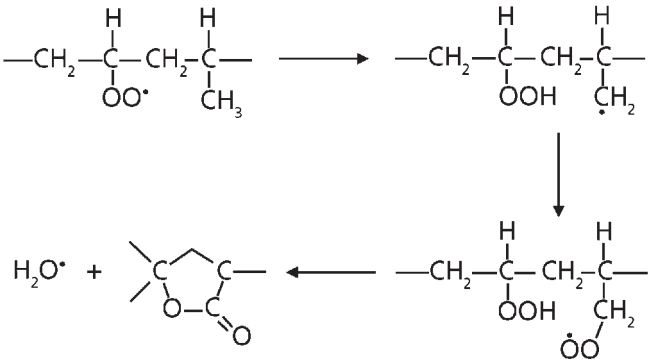

Scheme 10.15

As proposed by Geuskens and co-workers [41, 42], the radical attack of ketones by peroxy radicals would lead to the formation of perester (reaction **10.15**):

(10.15)

One important point concerning the mechanism is the orientation of the reactions (recombination or hydrogen abstraction) of peroxy radicals formed at the ENB site. During the first period of exposure (below 100 kGy), the ratio of ketones:acids is observed to be higher in EPDM compared to EPR. In addition, oxidative attack on *sec*-CH groups α to unsaturations of the ENB moieties leads to α,β-unsaturated oxidative species. Unsaturated carboxylic acids can be detected after SF_4 treatment as the corresponding acid fluoride at 1803 cm^{-1} (the relative proportion of saturated and unsaturated acids cannot be evaluated as SF_4 treatment provokes the saturation of double bonds). The results show that the oxidation in α-position to the double bonds occurs prior to the saturation reactions by radical species, which provokes reticulation as observed in EPDM, but not in EPR. These results suggest that the main route of oxidation in α-position to double bonds involves recombination (reaction **10.16**) of peroxy radicals (tetroxide or Russel route) to give ketones that are further saturated by radical species. This route is more probable than the route that involves hydroperoxides that gives carboxylic acids with chain scissions (reaction **10.17**).

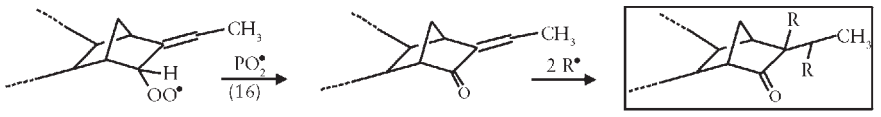

(10.16)

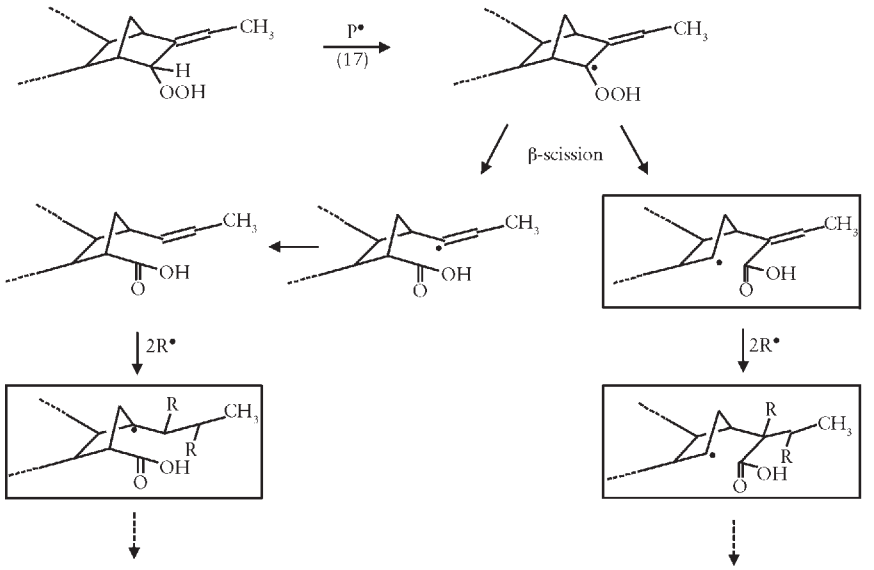

(10.17)

Comparison of EPR and EPDM irradiated at the same dose shows that the formation of oxidation species is two times higher in EPDM, but the extent of post-irradiation oxidation was monitored to be higher in EPR.

The post-irradiation effects result from a free-radical oxidation that could be related either to 'stable' radicals present after irradiation or to the decomposition of unstable tertiary hydroperoxides. Hydroperoxide decomposition at 20 °C has been reported for the post-irradiation oxidation of *tert*-hydroperoxides formed in PP (reaction **10.18**) [29]. In contrast, *sec*-hydroperoxides are considered as relatively stable at room temperature [27]. Assink showed that only 20% of *sec*-hydroperoxides formed in PE are decomposed after six months at 20 °C (reaction **10.19**) [45].

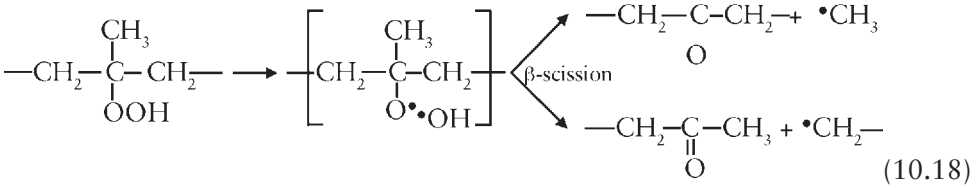

(10.18)

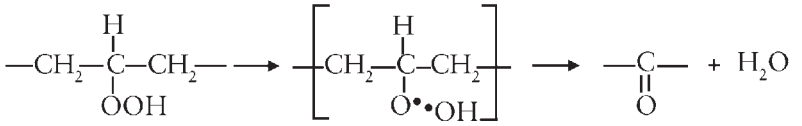

(10.19)

The concentration of hydroperoxides is however twice as high after irradiation of EPDM, which indicates that their decomposition cannot be proposed to explain the post-irradiation effects.

It is the reason why the migration of the radicals which are trapped in the crystalline phase can be considered as being responsible for the post-irradiation effects of EPDM (reaction 10.20) [43].

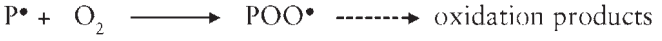

(10.20)

Before irradiation the crystallinities of EPDM and EPR were found to be 12% and 7%, respectively, crosslinking and oxidation reactions could modify these initial data, thus giving an explanation for the observed behaviour.

10.3.3 Conclusion

As a conclusion, the comparative study of EPDM and EPR γ-irradiated under an oxygen atmosphere permits the proposal of a general mechanism of EPDM radio-oxidation. This mechanism is reported in **Scheme 10.16**. The methylene groups in α-position to the double bonds of the ENB are the more oxidisable sites and saturation reactions of the ENB moieties provokes the crosslinking of EPDM films.

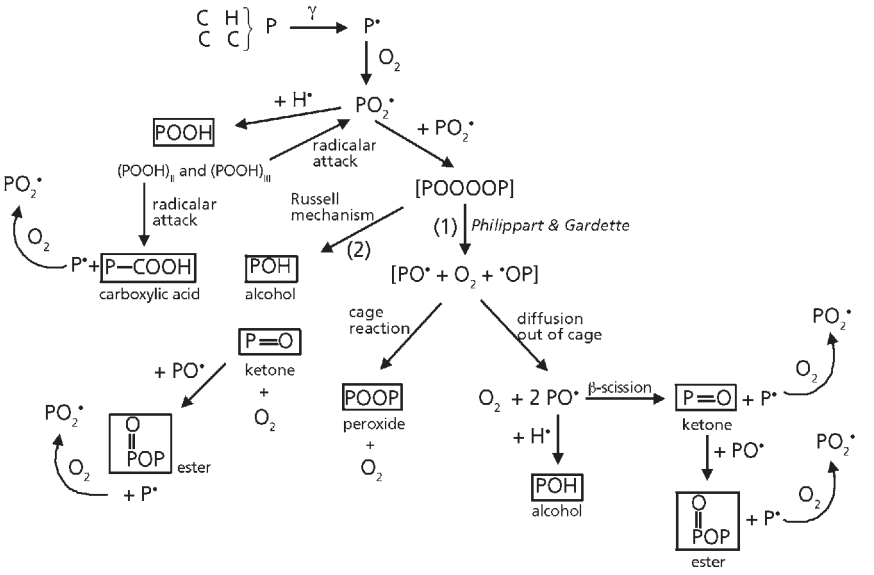

Scheme 10.16 Mechanism of γ-ageing of EPDM under an oxygen atmosphere

10.4 Evaluation of Some Antioxidants

Some recent results obtained in the field of the stabilisation of EPDM to radiochemical ageing are reported in this section. The EPDM samples were vulcanised with dicumyl peroxide and/or stabilised with hindered phenol or amine-type antioxidant. In order to verify the efficiency of the stabilisers against the chain oxidation process, the impact of the various formulations on the oxidation rate of EPDM induced by UV light or by temperature was also studied.

Thermo-, photo- and γ-initiated ageing of polymers involve a chain-oxidation process for which common points which can be described according to [29]:

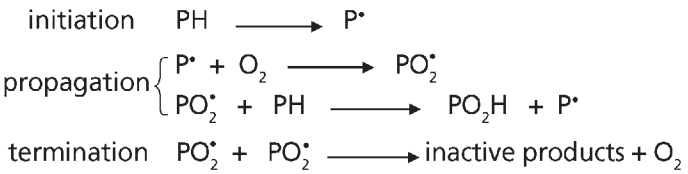

The main differences between three types of ageing lie in the initiation step and in the way the hydroperoxides decompose. It is generally admitted that photo- and thermo-oxidation starts on the ENB moiety before reaching the ethylene-propylene units [34,

46]. The thermal and photochemical degradation of hydroperoxides involves the scission of the O-O bonds [47].

It is briefly recalled that antioxidants (AH) prevent the propagation reactions [47] in any oxidation process (UV, thermal or radiation initiated), according to chain transfer (i) or termination (ii):

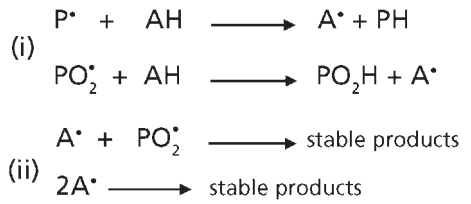

The behaviour of various formulations under conditions of oxidation initiated by UV light, temperature or γ-radiations is described in this section. The objective is to compare the efficiency of the antioxidant in stabilising EPDM against these various conditions of degradation.

10.4.1 Experimental

Various formulations of EPDM were processed: a pure gum (EPDM), an elastomer cross-linked agent with dicumyl peroxide (Aldrich) and an elastomer stabilised with two types of antioxidants: an hindered phenol (Irganox 1035, Ciba-Geigy) and an amine-type antioxidant (Vulkanox 4010 NA, Bayer). A detailed description of the samples is given in **Table 10.6**.

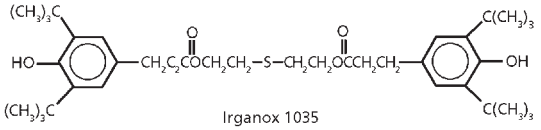

Irganox 1035

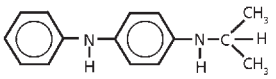

Vulkanox 4010 NA

All the EPDM samples contained processing antioxidants, which can be characterised by a UV absorption band at 280 nm with a shoulder around 230 nm. The remaining processing antioxidants were removed from the pure gum (EPDM 9) by Soxhlet extraction with methanol for 24 hours. The sample was then vacuum dried for 24 hours. This sample, which contains no residual processing antioxidants, is referred as 'additive-free EPDM 9' in **Table 10.6** (concentrations are expressed in wt%).

Thermo-oxidations were performed at 100 °C in an oven ventilated by natural convection. Photo-oxidations were performed in a polychromatic set-up based on the conventional accelerating device SEPAP equipment [48] but modified in such a way

Table 10. 6 Composition of the EPDM compounds			
Sample code	**Crosslinking agent**	**Irganox 1035 (Phenolic antioxidant)**	**Vulkanox4010 NA (Amine-type antioxidant)**
Additive-free EPDM 9	-	-	-
EPDM 9	-	-	-
EPDM 10	3	-	-
EPDM 11	3	0.1	-
EPDM 12	3	-	1
EPDM 13	-	0.1	

that photo-oxidation can be performed at 35 °C. The instrument already described [49] elsewhere contains only one medium pressure mercury lamp filtered with a borosilicate envelope (Mazda MA 400).

10.4.2 Experimental Results

10.4.2.1 Radio-Oxidation

The γ-irradiation of stabilised EPDM provoked the same modification in the IR spectra as those observed for additive-free EPDM 9 but with a different rate. The formation rates of carbonyl products measured at 1714 cm^{-1} is shown in **Figure 10.12a**. The curves corresponding to the consumption of the double bond (808 cm^{-1}) of the ENB as a function of the dose are plotted in **Figure 10.12b**.

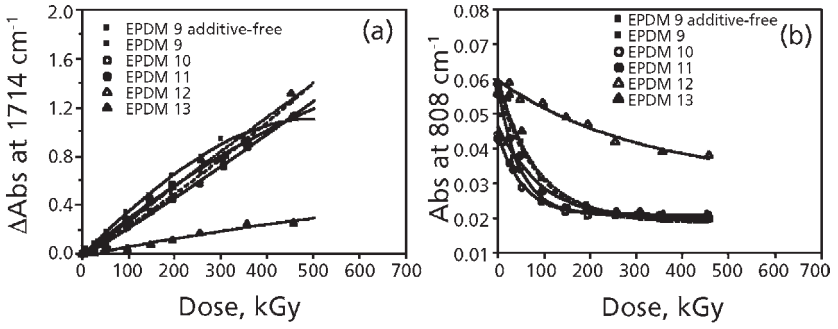

Figure 10.12 Increase in the absorbance at 1714 cm^{-1} (a) and decay in the absorbance at 808 cm^{-1} (b) as a function of the dose for various formulations of EPDM films γ-irradiated under an oxygen atmosphere

The kinetics curves given in **Figure 10.12** show that the curing process has no effect on the oxidation and that the antioxidants do not prevent the oxidation of EPDM. It is only in the case of EPDM 12, cured and stabilised with Vulkanox at 1%, that a stabilising effect can be observed: as well the rate of accumulation of the final oxidation products as the rate of consumption of the double bonds are reduced. A short induction period, before the oxidation starts is observed, below 25 kGy.

The EPDM 12 formulation has been studied in more detail because the high concentration of antioxidant used (1%) permits the evaluation, by IR spectroscopy, of the stability of the additive. After an irradiation limited to a dose of 52 kGy, it was noted that the decrease in the double bond content occurred at a lower rate in the case of EPDM 12 and that the formation of the oxidation products is accompanied by the consumption of the antioxidant as shown by the progressive disappearance of the antioxidant absorption bands.

In addition, when comparing the rates of formation of the peroxide species (hydroperoxides and peroxides) for additive-free EPDM 9 and EPDM 12 films it was observed that the antioxidant was efficient in reducing the accumulation rate of peroxidic species: a ratio about 10 was measured.

10.4.2.2 Thermo-Oxidation and Photo-Oxidation

There are many similarities between the modifications of the IR spectra provoked by radio-, photo- and thermo-oxidation: The shapes of the hydroxyl absorption bands are the same in the three oxidative conditions. The carbonyl absorption bands that appear reveal the presence of the same maxima or shoulders as reported above at 1788, 1732 and 1714 cm^{-1}. Ketones and carboxylic acids, responsible for the absorption maximum at 1714 cm^{-1}, are the main oxidation products in the three conditions of ageing. In addition, the progressive decrease of the absorbance at 808 cm^{-1} indicates that the dienic double bonds are saturated throughout oxidation.

However, a detailed analysis shows that differences exist. First, the accumulation of esters (1740 cm^{-1}) is favoured in thermo-oxidation, and photo-oxidation shows that high amounts of α,β-unsaturated carbonyl groups (ketones and acids at 1685 cm^{-1}) are formed. Second, when EPDM is stabilised by antioxidant or crosslinked, thermo-oxidation involves two steps: At low conversion degree one observes the development of a carbonyl absorption band centred at 1732 cm^{-1}, whereas no hydroxyl groups and no maximum at 1714 cm^{-1}, characteristic of the oxidation of the ethylene and propylene unit are formed and no consumption of the ENB double bonds is observed. This indicates that within the first period, it is the oxidation of the norbornene sites that occurs without attack of the double bonds (reticulation).

Then saturated ketones and carboxylic acids, responsible for the absorption at 1714 cm^{-1}, rapidly become the main oxidation products. The formation of these products indicates

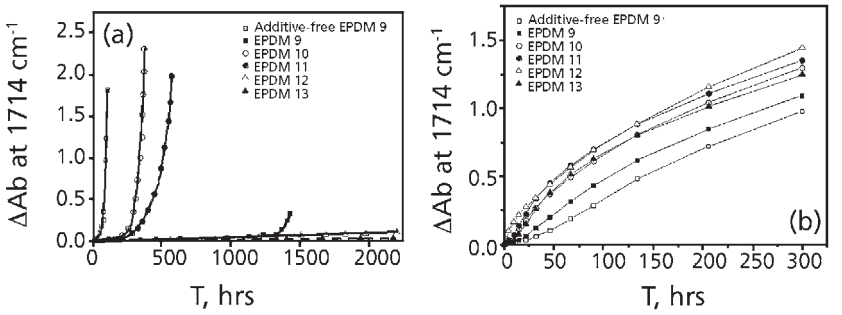

Figure 10.13 Increase in the absorbance at 1714 cm^{-1} as a function of thermooxidation duration at 100 °C (a) and as a function of photooxidation duration (b) for various formulations of EPDM films

the oxidation of ethylene and propylene units. During this second period, the double bonds disappear and hydroxyl groups are formed.

The rates of formation of carbonyl products measured at 1714 cm^{-1} throughout thermo-oxidation and photo-oxidation of the various formulations (see **Figure 10.13**).

From **Figure 10.13a**, it clearly appears that EPDM thermo-oxidation can be efficiently inhibited by antioxidants, with a notable induction period. Irganox and Vulkanox provides high stability. Crosslinking of EPDM slightly decreases the efficiency of Irganox.

From the curves drawn on **Figure 10.13b**, it is apparent that none of the additive systems causes a reduction in the formation rate of oxidation products. Some of the stabiliser systems even increase the initial rate of oxidation. If one gives particular attention to the EPDM12 formulation, it can be checked that the first five hours of exposure provoked the elimination of this antioxidant. This strongly suggests that the antioxidant photodegradation is likely to induce the polymer photooxidation.

10.4.3 Conclusion

Oxidation of polymers induced by UV light, temperature or γ-radiation results in chain scissions, crosslinking and formation of oxygen-containing functional groups. The stabiliser's role is to retard these oxidation processes. Oxidation prevention involves the scavenging of free-radical intermediates ($P^{\bullet}$ and $PO_2^{\bullet}$ radicals) and can also in some cases involve the reduction of radical formation.

The oxidation rate of EPDM can be efficiently reduced by antioxidants in thermo-oxidative conditions. In photo-oxidative conditions, antioxidants can induce the

EPDM degradation because they are not protected by UV absorbers. In γ-irradiation conditions, antioxidants are rapidly consumed and only the amine-type formulation at 1% is observed to display a limited stability, with a very short induction period (25 kGy) before the oxidation starts. Results obtained with EPDM are in agreement with previous results obtained with PP showing that the presence of residual 'conventional' antioxidants induced the γ-degradation of the matrix [50].

A more effective stabilisation system should involve the incorporation of two types of stabilisers in the polymer. For this purpose a parallel could be made between photo-oxidation and radio-oxidation. In photodegradation, a strong synergistic effect can be observed in the case of mixtures of UV absorber and antioxidant. By analogy, a synergistic effect is expected between an 'anti-rad' and antioxidant. For EPDM, fused-ring aromatics of anthracene-type (also called 'anti-rad') could be added to the amine-type formulation. Whilst antioxidants are active on the propagation of the chain oxidation reactions, 'anti-rad' stabilisers are efficient against the initiation step [51, 52]. The effect of these stabilisers is thought to be an energy transfer of radiation from polymer to the aromatic compound, producing a delocalisation of the energy, which is then changed to thermal energy. Meanwhile the introduction of antioxidant and 'anti-rad' could cause complex chemical reactions: the mixture of stabilisers could have synergistic effects or, in contrast, antagonism between the components could occur. Therefore complementary studies have to be carried out.

References

1. F.A. Makhlis, *Radiation Physics and Chemistry of Polymers*, Wiley-Interscience, New York, NY, USA, 1975.

2. A. Chapiro, *Nuclear Instruments and Methods in Physics Research B*, 1988, **32**, 1-4, 111.

3. R. H. Partridge, *Journal of Chemical Physics*, 1970, **52**, 5, 2501.

4. A. Chapiro, *Radiation Chemistry of Polymeric Systems*, J. Wiley & Sons, London, UK, 1961, pp 355.

5. A. Rivaton, S. Cambon and J-L. Gardette, *Journal of Polymer Science Part A: Polymer Chemistry*, 2004, **42**, 5, 1239.

6. A. Rivaton, S. Cambon and J-L. Gardette, *Nuclear Instruments and Methods in Physical Research B*, 2004, **227**, 3, 343.

7. A. Rivaton, S. Cambon and J-L. Gardette, *Nuclear Instruments and Methods in Physical Research B*, 2004, **227**, 3, 357.

8. A. Rivaton, S. Cambon and J-L. Gardette, *Polymer Degradation and Stability,* 2006, **91**, 1, 136.

9. W. Geissler, H. Zott and H. Heusinger, *Makromoleculare Chemie*, 1978, **179**, 3, 697.

10. D.O. Geymer in *The Radiation Chemistry of Macromolecules, Volume II,* Ed., M. Dole, Academic Press: New York, NY, USA, 1973, Chapter 1, p.5-9.

11. G.G.A. Böhm and J.O. Tveekrem, *Rubber Chemistry and Technology*, 1982, **55**, 3, 575.

12. P.J. Flory, *Journal of Chemical Physics*, 1950, **18**, 1, 108.

13. J. Olejniczak, J. Rosiak and A. Charlesby, *International Journal of Radiation Applications and Instrumentation, Part C: Radiation Physics and Chemistry*, 1991, **37**, 3, 499.

14. A. Charlesby, *Atomic Radiation and Polymers*, Pergamon Press, Oxford, UK, 1960, p.228.

15. M. Dole in *Advances in Radiation Chemistry*, *Volume 4,* Eds., M. Burton and J.L. Magee, Wiley-Interscience, New York, NY, USA, 1974, 307.

16. D.C. Waterman and M. Dole, *The Journal of Physical Chemistry*, 1970, **74**, 9, 1906.

17. E.J. Henley and E.R. Johnson, *The Chemistry and Physics of High Energy Reactions*, University Press, Washington, DC, USA, 1969.

18. M. Dole, D.C. Milner and T.F. Williams, *Journal of the American Chemical Society*, 1958, **80**, 1580.

19. J. O'Donnell and A.K. Whittaker, *Journal of Macromolecular Science - Pure and Applied Chemistry*, 1992, **A29**, 1, 1.

20. R.M. Black and B.J. Lyons, *Proceedings of the Royal Society of London Series A,* 1959, **A253**, 322.

21. F.A. Bovey, *The Effects of Ionizing Radiation on Natural and Synthetic High Polymers*, Interscience Publishers, Inc., New York, NY, USA, 1958, p.99.

22. X. Jouan and J-L. Gardette, *Polymer Communications*, 1987, **28**, 12, 329.

23. D.J. Carlsson, R. Brousseau, C. Zhang and D.M. Wiles in *Chemical Reactions on Polymers*, Eds., J.L. Benham and J.F. Kristle, ACS Symposium Series No.364, ACS, Washington, DC, USA, 1988, p.376.

24. C. Wilhelm and J-L. Gardette, *Applied Polymer Science*, 1994, **51**, 8, 1411.

25. D.J. Carlsson, R. Brousseau, C. Zhang and D.M. Wiles, *Polymer Degradation and Stability*, 1987, **17**, 4, 303.

26. J-L. Gardette and J. Lemaire, *Polymer Photochemistry*, 1986, **7**, 5, 409.

27. J. Mallegol, D.J. Carlsson and L. Deschenes, *Nuclear Instruments and Methods in Physical Research B*, 2001, **185**, 1-4, 283.

28. J. Davenas, I. Stevenson, N. Celette, S. Cambon, J-L. Gardette, A. Rivaton, L. Vignoud, *Nuclear Instruments and Methods in Physics Research B*, 2002, **191**, 1-4, 653.

29. D.J. Carlsson, C.J.B. Dobbin, J.P.T. Jensen and D.M. Wiles in *Polymer Stabilisation and Degradation*, Ed., P.P. Klemchuk, ACS Symposium Series No.280, ACS, Washington, DC, USA, 1985, p.359.

30. V. Gueguen, L. Audouin, B. Pinel and J. Verdu, *Journal of Polymer Degradation and Stability*, 1994, **46**, 1, 113.

31. D.J. Carlsson, C.J.B. Dobbin and D.M. Wiles, *Macromolecules*, 1985, **18**, 10, 2092.

32. J.A. Howard, J.C. Scaiano and H. Fisher in *Radical Reaction Rates in Liquids*, Landolt-Bornstein New Series II Volume 13, Part D, Ed., K.H. Hellwege, Springer Verlag, Berlin, Germany, 1984.

33. M. Scoponi, F. Pradella, V. Carassiti and D. Tartari, *Makromolekulare Chemie*, 1994, **195**, 3, 985.

34. F. Coiffier, R. Arnaud and J. Lemaire, *Makromoleculare Chemie*, 1984, **185**, 6, 1095.

35. A. Faucinato, F. Faucinato Martinotti, A. Buttafava and S. Cesca, *European Polymer Journal*, 1976, **12**, 7, 421.

36. J-L. Philippart, F. Posada and J-L. Gardette, *Polymer Degradation and Stability*, 1995, **49**, 2, 285.

37. M. Celina and G.A. George, *Polymer Degradation and Stability*, 1993, **40**, 3, 323.

38. J-L. Philippart and J-L. Gardette, *Polymer Degradation and Stability*, 2001, **71**, 1, 189.

39. J-L. Philippart and J-L. Gardette, *Polymer Degradation and Stability*, 2001, **73**, 1, 185.

40. D.J. Carlsson, S. Chmela and D.M. Wiles, *Polymer Degradation and Stability*, 1991, **31**, 3, 255.

41. G. Geuskens and M.S. Kabamba, *Polymer Degradation and Stability*, 1982, **4**, 1, 69.

42. G. Geuskens and M.S. Kabamba, *Polymer Degradation and Stability*, 1983, **5**, 5, 399.

43. J. Lacoste and D.J. Carlsson, *Journal of Polymer Science, Part A: Polymer Chemistry*, 1992, **30**, 3, 493.

44. J. Lacoste, R. Arnaud, R.P. Singh and J. Lemaire, *Makromoleculare Chemie*, 1988, **189**, 3, 651.

45. R.A. Assink, M. Celina, T.D. Dunbar, T.L. Alam, R.L. Clough and K.T. Gillen, *Macromolecules*, 2000, **33**, 11, 4023.

46. F. Delor, G. Teissedre, M. Baba and J. Lacoste, *Polymer Degradation and Stability*, 1999, **60**, 2-3, 321.

47. B. Ranby and J.F. Rabek, *Photodegradation, Photo-oxidation and Photostabilization of Polymers – Principles and Applications*, Wiley-Interscience, New York, NY, USA, 1975.

48. A. Rivaton, *Polymer Degradation and Stability*, 1995, **49**, 1, 163.

49. M. Piton and A. Rivaton, *Polymer Degradation and Stability*, 1996, **53**, 3, 343.

50. A. Rivaton, D. Lalande and J-L. Gardette, *Nuclear Instruments and Methods in Physical Research B*, 2004, **222**, 1-2, 187.

51. Y.S. Soebianto, Y. Katsumura, K. Ishigure, J. Kubo, H. Koizumi, H. Shigekuni and K. Azami, *Polymer Degradation and Stability*, 1993, **42**, 1, 29.

52. K. Arakawa, T. Seguchi, N. Hayakawa and S. Machi, *Journal of Polymer Science: Polymer Chemistry Edition*, 1983, **21**, 4, 1173.

11 Silicone Rubber

Amalendu Sarkar

11.1 Introduction

There has been an interest in silicone elastomers since Kipping developed a convenient method of producing organosilanes in 1904 [1]. The industrial production of silicone became possible when Rochow of General Electric first successfully synthesised alkylchlorosilane [2]. Since then, the material improved physically, chemically and economically to the point that it can now compete in the traditional organic rubber markets and helps impart a longer life to today's more demanding applications. The worldwide demand for silicone rubber at present is approximately 170,000 metric tones per year and it is growing at about 4-5% per year. The unique balance of mechanical and chemical properties of silicone rubber have already given it a good position in the market place due to its:

- High temperature resistance,
- Low temperature flexibility,
- Excellent electrical and thermal insulation properties,
- Excellent mechanical properties over a wide range of temperatures, and
- Excellent bio-compatibility and chemical inertness.

Compared to many organic elastomers, silicone rubber offers superior ease of fabrication resulting in high productivity and cost effectiveness for extended service reliability. It is used in several industrial, automotive, aerospace, electrical-electronics, household and healthcare applications [3].

This chapter summarises various aspects of silicone rubber technology including chemistry, manufacturing, properties, compounding, vulcanisation, processing, troubleshooting and applications which may inspire one to change an existing application or to create a new one using this versatile elastomer.

11.2 Chemistry

In the speciality elastomer field, silicone rubber has the distinction of having evolved originally from sand. Silicon (Si) is the second most abundant element making up 26% of the earth's crust, existing as inorganic silicate and as silicon dioxide. Elementary silicon as such does not exist in nature.

The term 'silicone' generally describes polyorganosiloxanes with a main backbone of inorganic siloxane bonds (Si-O-Si) and lateral chains of organic groups. The most common silicones are the polydimethylsiloxanes with the structure shown in **Figure 11.1**.

The shorthand skeletal structure of typical silicone polymers is formed of four units as shown in **Figure 11.2**. The mono-functional group, which has three organic groups, is designated as the 'M' unit. The di-functional group with two organic groups, the tri-functional group with one organic group and the tetra-functional group with no organic group are designated as 'D', 'T', and 'Q' units, respectively.

Polymers formed on 'M' units and 'D' units are in oil or gum form, while polymers with 'T' units and 'Q' units are in resin form. Using these structural combinations, it is possible to design a wide variety of silicone polymer molecules. This relatively simple chemistry at low molecular weights leads to fluids or oils and, at high molecular weights, leads to gums which may be crosslinked to form elastomeric products and are shown in **Figures 11.3a** and **11.3b**.

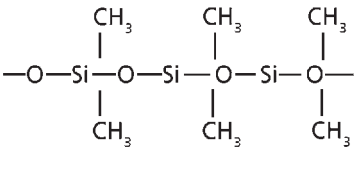

Figure 11.1 Structure of polydimethylsiloxane

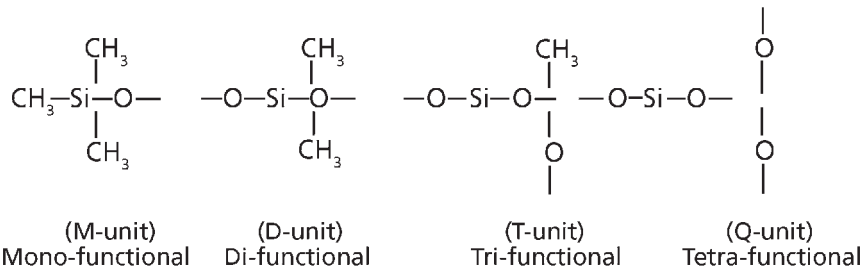

Figure 11.2 Skeletal designation of basic units of silicone

This Si-O linkage is identical to the chemical bond found in highly stable materials such as quartz, glass and sand. Compared to the rotational energy of carbon-carbon bonds (15.10 kJ/mol) or carbon-oxygen bonds (11.31 kJ/mol) in common organic rubbers, the extremely low rotational energy of silicon-oxygen bonds (less than 0.8 kJ/mol) in the silicone polymer backbone is responsible for its extended service temperature capability. Extraordinary resistance to deterioration factors such as oxidation, ozone, corona, weathering and radiation are also greatly influenced by the low rotational energy factor. The Si-O bond (444 kJ/mol) is stronger than the C-C bond (356 kJ/mol) and longer (0.164 nm *versus* 0.153 nm) than a typical carbon-carbon bond [4, 5], which is also responsible for its outstanding high temperature performance. Many organic polymers contain unsaturation in their main chain backbones, which are particularly susceptible to oxidation and ozone attack. The absence of any unsaturation in the silicone backbone makes silicone rubber extremely resistant to these environmental factors.

The polysiloxane molecules can be tailor-made by the chemist to optimise certain properties required by the particular application. In general, methyl, vinyl (Vi), phenyl and trifluoropropyl are the most common side groups used in commercially available polysiloxanes (see **Table 11.1**).

The incorporation of vinyl groups (less than 1 mol%) in the lateral chain of polysiloxane molecule (VMQ) significantly increases the crosslinking efficiency with organic peroxides resulting in elastomers with low compression set and improved hot oil

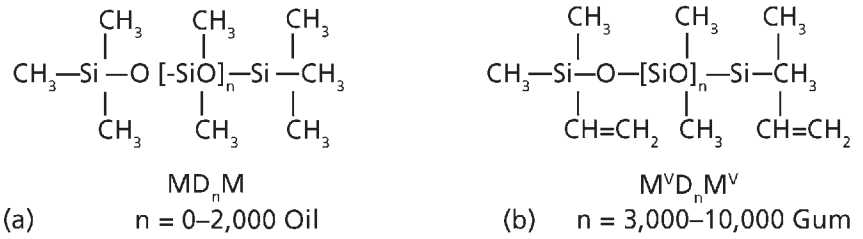

Figure 11.3 (a) Polydimethylsiloxane (MQ); (b) Polyvinylmethylsiloxane (VMQ)

Table 11.1 Substituent effects on siloxanes

Substituent groups	Imparted Quality
CH_3 (Methyl)	General purpose
$CH{=}CH_2$ (Vinyl)	Network control, strength, high hardness
C_6H_5 (Phenyl)	Extreme low and high temperature resistance, radiation resistance
$CH{-}CH_2{-}CF_3$ (Fluoro)	Oil and solvent resistance

resistance as compared to polydimethylsiloxanes (MQ). The 'vinyl' sites can be placed at predetermined selected positions within the polymer molecules so that the chemical crosslinks of the network can be controlled. This in turn influences the mechanical behaviour in beneficial ways such as allowing tougher products to be made. The use of vinyl groups in silicone rubber opened the door for new applications requiring improved performance and long-term reliability. Today, almost all commercially available silicone rubbers contain some degree of vinyl.

Similarly, partial substitution (5 to 10%) of the methyl groups by a phenyl groups extends the low temperature performance from –60 °C to –93 °C due to the steric hindrance effect of the polymer chains. This type of silicone rubber is widely used in aerospace applications where low temperature performance is important [6, 7].

In fluorosilicone rubber, introduction of trifluoropropyl side groups in the polydimethylsiloxane chain imparts polarity to the silicone molecule resulting in fuel and solvent resistance. Thus, fluorosilicone rubber combines both high and low temperature properties of regular silicone rubber along with resistance to many harsh chemicals. Commercially, a combination of organic side groups in the same polysiloxane molecule is used to get the advantage of both. Depending on the chemical side groups in polysiloxane, silicone rubbers as classified by ASTM D1418 [8] are shown in **Table 11.2**.

Table 11.2 Type and structure of silicones

Type	Structure	ASTM D1418 Classification [8]
Dimethyls	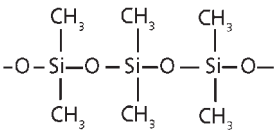	MQ
Methyl vinyls	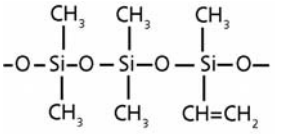	VMQ
Methyl phenyl vinyls	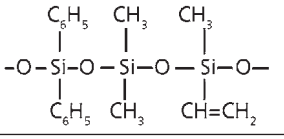	PVMQ
Methyl fluoroalkyls (Fluorosilicone)	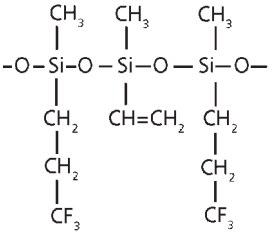	FVMQ

11.3 Manufacturing

Most silicone products including fluids, room temperature vulcanisates (RTV), heat cured rubber or high consistency rubber (HCR) and liquid silicone rubber (LSR) are derived from the same starting materials and are later differentiated by molecular weight range or degree of polymerisation and viscosity. The commercial silicones are obtained from chlorosilanes, following the direct process of Rochow [2]. The process begins with the reduction of silica (sand) to elemental silicon metal by heating with carbon in an electric furnace at high temperature as shown in **Figure 11.4**.

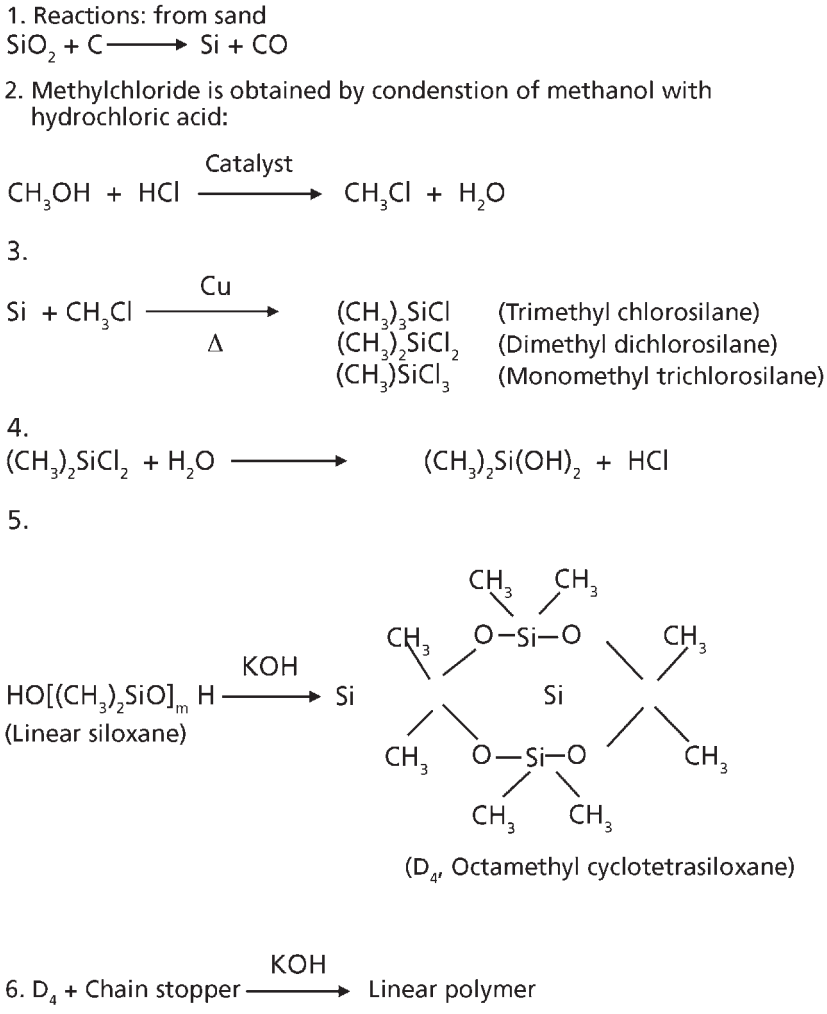

Figure 11.4 Silicone polymer manufacturing process

Octamethyl cyclosiloxane (dimethyl tetramer, D_4) is the primary input for all dimethyl silicone rubber which is a clear, low viscosity liquid. The ring opening polymerisation of the cyclic D_4 is accomplished in presence of strong base (potassium hydroxide), which produces a linear polymer. The molecular weight of polysiloxane molecules is controlled by the addition of monofunctional siloxane chain stoppers. The resulting polymer, used in the commercially available silicone rubber stocks, is a very high viscosity fluid or gum, which is composed mainly of linear polydimethylsiloxane chains. The commercial gums usually contain between 3,000 and 10,000 dimethylsiloxy units in the average chain. However, the molecular weight distribution of silicone polymer varies with the purity of the monomers.

11.4 Three Major Classifications of Silicone Rubber

Silicone elastomers can be classified into three distinct categories based on processing: pourable (RTV), pumpable (LSR) and millable (HCR). The end use application will determine the type of elastomer needed by taking into account the material requirements and the processing parameters. The comparative characteristic features of these three types of silicone rubbers are summarised in **Table 11.3.**

Table 11.3 Characteristic features of RTV, HCR and LSR

Pourable RTV	**Millable HCR**	**Pumpable LSR**
Room temperature vulcanising (RTV)	High consistency rubber or heat cured rubber (HCR)	Liquid injection moulding (LIM)/liquid silicone rubber (LSR)
Kinematic viscosity = 1-1000 cm^2/s	Kinematic viscosity = 20,000 cm^2/s	Kinematic viscosity = 300-2,000 cm^2/s
MW = 10,000-100,000 g/mol	MW = 300,000-800,000 g/mol	MW = 10,000-100,000 g/mol
Cure system = condensation or addition (Platinum)	Cure system = peroxide or platinum	Cure system = platinum
Typical applications: potting compounds, caulk, fabric, coating	Typical applications: o-rings, seals, boots, high voltage insulators, wire and cables	Typical applications: baby care products, connector seals, health care products
Typical processing: roll coat, spray on,	Typical processing: moulding, extrusion, calendering	Typical processing: injection moulding
MW: Molecular weight		

11.5 Properties

The inherent characteristics of silicone rubber such as highly stable 'Si-O-Si' chain bonds, ease of rotation of the lateral organic side groups, backbone chain flexibility, low inter- and intra-molecular forces due to the strongly polarised Si – O bond result in the retention of many desirable properties over a wide temperature range [9, 10]. It should be noted that certain specific properties of silicone rubber are generic to all silicones and a few additional performance characteristics can be imparted through material design expertise. Consultation with the material supplier is recommended.

11.5.1 Heat Resistance Property

The heat resistance and life expectancy of common silicone rubbers are dependent on the temperature to which they are exposed. The higher the exposure temperature, the shorter the performance life-expectancy. For example, at 120 °C usage temperature, the service life will be up to ~20 years; at 150 °C, the useful life expectancy is ~5 years; at 205 °C, the usage time is approximately 2 years; at 260 °C, the useful life is about 3 months; and at 315 °C, the life expectancy is ~22 to 100 hours. These are rough estimates. In general, the usage time of a rubber is measured as the period of time during which it retains an elongation of at least 50%. Certain additives improve the thermal stability of silicone rubber (discussed in the compounding section). Silicone rubber exhibits longer and better performance properties at elevated temperatures compared to most organic rubbers.

11.5.2 Low Temperature Flexibility

Cold resistance of silicone rubber is highly dependent on its structural characteristics. At room temperature, silicone rubber compounds are flexible and under repeated flexing, exhibit excellent flex crack resistance properties. The cold resistance of MQ and VMQ type silicone rubber is about –55 °C, while phenyl group containing silicone rubbers, PMQ and PVMQ, can withstand a temperature of ~ -90 °C. Phenyl groups are introduced as diphenylsiloxane [$(-C_6H_5)_2SiO$] units.

11.5.3 Mechanical Properties

The tensile strength of silicone rubber is dependent on the type of reinforcing silica filler and the way it is used. It is still difficult to raise the tensile strength of silicone rubber above 15 MPa. But, in the higher temperature applications, the retention of tensile strength of silicone rubber is much better than that of other synthetic and natural rubbers.

The shortcomings of silicone rubbers lie in their tear strength and dynamic fatigue life, though there has been considerable progress made to improve these properties. Tear strength can be improved significantly by altering the crosslink distribution within the network structure, silica surface and molecular design of the silicone polymer. There is also a significant improvement in tear propagation resistance and bend fatigue resistance. Silicone rubbers can now be made that have high strength, which are used in dynamic applications to make complex moulded products.

11.5.4 Compression Set

Silicone rubbers exhibit low compression set over a wide range of temperatures. There are many factors that determine compression set properties, but increasing crosslink density is especially effective.

11.5.5 Oil and Solvent Resistance

General-purpose silicone rubbers have moderate oil resistance. There is no deterioration or dissolution of the rubber in hot oils, a fact that distinguishes silicone rubber from organic rubbers. However, there are some chemicals added to oils that break silicone bonds, so care is required in selection of oil and polymer. In general, silicone rubber with a high crosslink density and high filler loading exhibits less swelling. Effective measures can be taken in selection of silicone rubber if the type of chemical is known beforehand. Fluorosilicone rubber, where 3,3,3-trifluoropropyl groups are incorporated as an organic group, has a much higher solubility parameter (solubility parameter = 9.6) compared to polydimethylsiloxane (solubility parameter = 7.5) and as a result, swelling due to non-polar solvents is significantly reduced [11].

11.5.6 Steam Resistance

Silicone rubber does not show any major affects from exposure to moisture in free steam form under no pressure to moderate pressure. However, at higher steam pressures, the mechanical properties are greatly affected. Generally, use of silicone rubber is not recommended for long-term service where steam pressure exceeds 0.345 MPa.

11.5.7 Water Resistance

Silicone rubbers have virtually no affinity or an extremely low degree of moisture absorption and there is very little influence on their mechanical properties. However, if silicone rubber is kept in superheated water for an extended period of time, breakdown of rubber may occur.

11.5.8 Electrical Properties

There is no elastomeric material having better electrical insulation (retention of dielectric strength, power factor and insulation resistance) than silicone rubber over a wide temperature range. Simple exposure to heat, cold, oil, steam, ozone and corona does not influence the electrical insulation properties of silicone rubber. When it is exposed to direct flame or severe fire, the surface rubber burns to non-conducting ash and if it does not undergo vibration, will continue to operate for an extended period of time. This inherent, unique feature of silicone rubber makes it extremely suitable for many marine and aerospace applications, where lower weight and higher safety are desirable. Silicone rubbers can be designed to be electrically conductive for manufacturing non-metallic conductors, shielding and similar purposes. **Table 11.4** lists the range of electrical insulating properties typical for silicone rubber.

Table 11.4 Typical electrical property ranges of silicone rubber

Tests	Results
Dielectric strength, kV/mm	20-25
Dielectric constant	2.8-3.5
Dissipation factor	0.001-0.2
Volume resistivity, Ohm-cm	$1 \times 10^{11} - 1 \times 10^{16}$
Insulation resistance, Ohm	$1\text{-}10 \times 10^{12}$

11.5.9 Bio-compatibility

Suitably designed silicone rubber processed in a clean room environment [12] can be made bio-compatible so that it has no significant influence on body tissue.

11.5.10 Permeability

Silicone rubber is highly permeable to gases due to a high degree of chain mobility. The permeability shows a downward trend with increased polymer crosslink density, filler levels, orientation or crystallinity. A higher level of crosslinking or decreased level of plasticisers (softeners) also results in lower permeability. In general, a silicone rubber based on polydimethylsiloxane is 25 times more permeable to oxygen than natural rubber and 429 times more permeable than butyl rubber [11].

11.5.11 Damping Characteristics

Low modulus of elasticity combined with a high mechanical dissipation factor over a wide range of frequency and temperatures renders silicone rubber an excellent choice for absorbing shock (impact/vibration) and sound. Its rebound resilience remains almost same from room temperature to 200 °C.

11.5.12 Surface Energy or Release Property

Silicone rubbers have lower surface energy values than most organic rubbers. Consequently, silicone exhibits an excellent release property, which helps to allow their use in many food processing operations and also in the manufacture of thermoplastic polymeric films. Their high temperature resistance properties combined with excellent release and physiological inert characteristics make silicone elastomers a great choice for bakeware and household applications.

11.5.13 Weathering Resistance

Weathering is not a problem for silicone rubber. If properly cured, it exhibits excellent resistance to sunlight, ozone, corona discharge, oxygen, bacteria, fungus, soil chemicals, and so on.

11.5.14 Radiation Resistance

Radiation (generally gamma radiation) introduces more crosslinking. So, as the total radiation dose increases, hardness increases, tensile strength may increase initially, then decreases sharply and elongation drops. Incorporation of phenyl groups improves the radiation resistance and this increases with the increase in phenyl concentration [13].

11.5.15 Thermal Ablative

Silicone rubber can withstand temperatures up to 5000 °C for a very short period of time (minutes). During such high temperature exposure, a hard charred tenacious surface is formed which acts as barrier to protect the underneath elastomeric surface. Thermal insulation properties are thus maintained.

11.6 Compounding

Typical linear organo substituted polysiloxane gums used in commercial silicone elastomers are amorphous, rubbery, flowable at room temperature (T_g is ~ –123 °C and crystallisation temperature (T_c) about –40 °C). Silicone elastomers by themselves are relatively weak and have a tensile strength of approximately 0.35 MPa when crosslinked. So, to achieve suitable green strength and practical engineering properties, it is necessary to reinforce the polymer by adding very fine particle size, high surface area, silica fillers. A typical silicone compound is a multi-component blend of silicone polymers (gums or bases), reinforcing and/or extending fillers, process aids, various additives (e.g., heat stabilisers and blowing agents for sponge), colours/pigments, curing agents and so on. A typical silicone HCR compound formulation is shown in **Table 11.5**. Other examples may have 3 to 12 ingredients depending on the specified requirements.

Compounding of silicone rubber is identical to any organic rubbers. Selection of the right silicone gum or base is crucial as the polymer itself varies in terms of mole percentage of vinyl, phenyl and methyl contents, molecular weight and viscosity, type of polymer structure, and volatile content. Fumed silica is the main reinforcing filler used for strength, precipitated silica is used for reinforcement as well as economy. Quartz silica, calcium carbonate and aluminium silicates (clays) are used as extending fillers. Proprietary stabilisers (as manufactured by various silicone and additive manufacturers) are added to improve heat stability at different temperature ranges. Acid scavengers are used to neutralise the acidity, to improve compression set and to stabilise the material with no post curing. Internal mould release additives are added to the recipe especially to moulded rubber compounds for easy removal of parts. Peroxides are used to vulcanise the rubber (described in the vulcanisation section). Special additives like a desiccant are used to improve the consistency in processing, tensile modifiers are used to improve the tensile properties of rubber, blowing agents for sponge rubber, flame retardant for flame resistance and so on.

Table 11.5 A typical silicone rubber formulation

Ingredients	**phr**
Silicone base(s)	100
Process aids	0.25 to 2.0
Fumed or precipitated silica	2 to 50
Quartz silica	10 to 100
Stabilisers	0.5 to 2.0
Peroxide (50% active)	0.75 to 1.5
Colours/pigments (preferably pre-dispersed)	0.5 to 3.0
Acid scavenger	1.0 to 6.0

11.6.1 Silicone Gums

Silicone gum is a pure polymeric form of polysiloxane whose molecular weight ranges from 300,000 to 800,000 (viscosity range – 2,000 to 20,000 Pa) on average [14]. Each manufacturer makes their own different types of polysiloxanes, which differ from one another in molecular structure, vinyl level, molecular weight, viscosity and organic groups in lateral chains. As far as polyvinyl methyl siloxane (VMQ) gum polymer molecules are concerned, they are characterised by the position of the vinyl groups in the polymer chain. For example, some VMQ contain vinyl groups only at the ends of the chain. Some contain vinyl groups both at the end of the chain as well as in between and some contain vinyl groups only along the chains, not at the chain ends. The selection of vinyl containing gums (vinyl content and end-stopper type) depends entirely on the target properties to be achieved through compound formulation.

11.6.2 Reinforced Gums (Bases)

Although pure silicone polymer (gums) may be used, it is generally easier for the rubber fabricator to compound from silicone bases. Mixing pure gums with process aids and reinforcing silica fillers mainly produces the reinforced silicone gums (bases). In some cases, either treated filler or *in situ* treatment of fillers is used to manufacture the reinforced gums. Sometimes, they contain certain additives for special functional effects, such as improved heat resistance, flame resistance or bonding properties. There are several different types of reinforced gums (bases) produced by each major manufacturer, which are available commercially. These bases are designed to cover a multitude of physical property requirements. Blending bases within a product family allows fabricators to obtain intermediate properties that meet and/or exceed a particular specification and optimise cost efficiency and effectiveness. Economic blends at appropriate ratios of fluorosilicone (FVMQ) and VMQ can also be used for fuel, solvent or oil resistance. To demonstrate the difference in mechanical properties, examples of a few classification areas are highlighted in **Table 11.6**. Similar types of product guidelines are available from each major silicone rubber manufacturers for different applications.

11.6.3 Filler

At the beginning of development of silicone rubber compound, metal oxide fillers were used. But, with the invention of fumed silica and its utilisation in silicone polymer, the whole scenario of reinforcement changed. Approximately three times higher tensile strength was achieved by switching over from metal oxide to fumed silica in polydimethyl siloxane (MQ). Now, along with fumed silica, precipitated silica is also used, although the precipitated silica does not reinforce the silicone polymer as well as fumed silica. Until now, fumed silica is the primary reinforcing filler used in silicone rubber. Fumed silica

Table 11.6 Mechanical Property overview of different types of silicone rubbers

Type	ASTM D1418 [8] Classification	Duro Shore A	Tensile, MPa	Elongation, %	Tear, kN/m	Compression Set, %
General purpose	VMQ	30-70	6.00-8.00	400-600	12-14	22 h @ 177 °C 20-25
Extreme low temperature	PVMQ	40-50	7.00-9.00	500-750	30-36	70 h @ 100 °C 15-20
High strength	VMQ	30-75	8.00-10.00	500-1100	30-40	22 h @177 °C 30-50
Low compression set	VMQ	40-70	3.50-6.50	150-350	6-14	22 h @177 °C 10-15
Fuel, solvent resistant	FVMQ	50-70	7.00-8.00	150-300	8-13	22 h @150 °C 20-25

having a surface area ranging from 150 to 400 m^2/g provides the best reinforcing effect. The extent of reinforcement is generally improved by an increase in the filler surface area, an increase in the filler structure and an increase in interaction of the polymer molecule to the filler surface [15]. In general, most commercially available fumed silica filled silicone rubbers have tensile strength values ranging from 5.0 to about 10.0 MPa. In many cases, a combination of different types of fillers can be used to achieve a specified combination of properties for a particular type of application.

The development of wet-process-hydrophobic (WPH) silica is revolutionary in silicone elastomers. The WPH silica process provides a technology, which allows control of surface area, structure and surface treatment. These are the primary controlling factors that determine the extent to which silica fillers can reinforce silicone elastomers [15-17]. Thus, it is possible to tailor a silica surface to achieve a specific desirable elastomeric property profile. The reinforcing capability of WPH silica is greater than that of pyrogenic silica (an exceptionally pure form of fumed silica).

Filler surface energy and the chemistry, play a paramount role in polymer-filler interaction. When silica and polysiloxanes are mixed, strong physico-chemical interactions occur. These interactions may be covalent chemical bonds resulting from condensation of silanols in siloxanes with silonols on the silica surface, hydrogen bonds between the silanols in the siloxane and on the silica-surface, polar and/or Van der Waals forces through dipole-dipole interactions between the silica silanols and the polar Si—O—Si of the siloxane. But, these interactions produce

crepe hardening of the silica-polymer mixed compound, which can progress to the extent that the mixed stock becomes unprocessable with common rubber processing equipment. So, it needs to be passivated or controlled. It is now a well known practice to surface treat the silica with various organosilanes and organosiloxanes, which interact with the silanol groups (Si-OH) on the silica surface, and thus reduce the amount of available hydroxyl groups. This is in turn reduces creep hardening. These organosilanes or organosiloxanes are commonly referred to as hydrophobe agents or surface treating agents [18-20]. Some of the common organosilanes are dimethyldichlorosilane (DDS), hexamethylcyclotrisiloxane, octamethyl cyclosiloxanes and hexamethyldisiloxane (HMDS), which can be either pretreated with silica filler in a pre-treatment process, or can be introduced during the compounding/mixing phase to effect *in situ* treatment. In many cases, both techniques are employed. Schematic diagrams of the hydrophilic silica surface (before organosilane treatment) and the hydrophobic silica suface (after organosilane treatment) are shown in **Figures 11.5a** and **11.5b**.

Fumed silicas have proved to be excellent reinforcing fillers for silicone rubbers resulting in good mechanical properties, high transparency and acceptable electrical properties, but they contain traces of hydrochloric acid originating from their production process. It is assumed that the presence of hydrochloric acid reduces the resistance to hot air. To improve the hot air resistance, metal oxide is added to the compound or ground quartz silica is used as filler, which neutralises the acidic nature of the fumed silica (pH ~4.5). There are applications for silicone elastomers that require high strength or high transparency - fumed silica is always preferable. Fumed silica, in general, is a higher priced product.

Apart from fumed silica, alternative precipitated silica fillers are also widely used, which are manufactured in aqueous suspension. These comparatively less expensive silica fillers have established their potential use as secondary reinforcing fillers that achieve slightly less reinforcing effect than fumed silica. The precipitated silica-based silicone compounds, however, exhibit less crepe hardening, have better compression set, high resilience and are more cost effective than their fumed silica counterparts [21, 22].

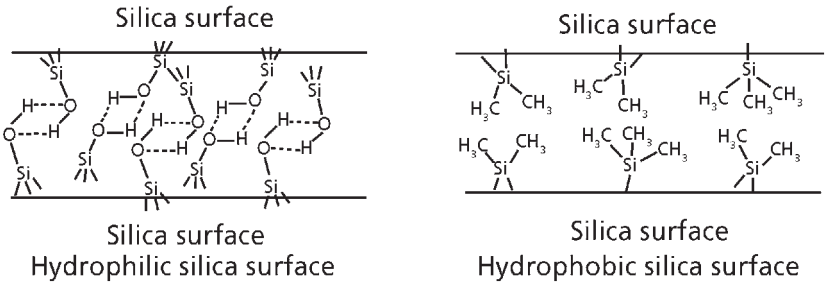

Figure 11.5 (a, b) Schematic diagram of hydrophilic and hydrophobic silica surface

The purity of reinforcing silica fillers has a significant influence on the heat resistance. So, the purity of silica fillers must be raised, in particular, ionic impurities need to be removed or minimised. Normal antioxidants/anti-ozonants as used for organic rubbers are not suitable for silicone elastomers. In order to withstand high temperatures over a long period of time, rare earth oxides/hydroxides (for example, cerium), metal oxides of titanium, zircon, manganese, iron, cobalt or nickel are commonly used in silicone rubber. Silicone rubbers with the optimum combination of these ingredients have far greater impact on heat resistance.

Other fillers like semi-reinforcing diatomaceous earth are added to improve oil resistance; ground quartz to reduce cost, shrinkage and improve thermal conductivity; iron oxide and titanium dioxide for heat stability; aluminium trihydrate for tracking resistance in insulators; and carbon blacks for conductivity. Though carbon black is an important reinforcing filler for organic polymers, it does not reinforce silicone polymer as well as silica. In fact, equal loading of carbon black has a detrimental effect on the thermal stability in a silicone polymer.

The reinforcing power of a filler in silicone rubber can be measured by its influence on the incremental effect on hardness. It is also directly correlated to the surface area and surface chemistry of the filler as shown in **Table 11.7**.

11.6.4 Softener

Process aids, also known as plasticisers or softeners, are usually low molecular weight reactive silicone hydroxyl fluids containing silanol functional groups (e.g., $OH[(CH_3)_xSiO]H$, x = 6-20). If the reinforcing filler surface is not modified by a pretreatment process (as mentioned in the section on fillers) to reduce the polymer-filler interaction, the silicone compound containing polysiloxane and untreated silica will undergo crepe-hardening over time. This adversely affects the flowability of the material

Table 11.7 Fillers used in silicone rubber

Type	Reinforcing character	Specific gravity	Surface area, m^2/g	Particle diameter, nm	1 Duro point loading, parts per 100
Fumed silica	High	2.20	200-380	10-16	0.5-1.5
Precipitated silica	High	2.00	140-200	14-22	1-1.5
Diatomaceous earth	Semi	2.15-2.30	5	3000	2.0
Ground quartz	Low	2.65	----	5,000-30,000	3.0-5.0
Red iron oxide	Low	4.95	----	1,000	----
Titanium dioxide	Semi	3.90	9	300	----

during processing. For that reason, the low molecular weight hydroxyl functional silanol fluids are used to reduce or passivate the polymer-filler interaction by forming a chemical bond with the pendant hydroxyl groups of the silica filler surface [19]. It is generally recommended that softeners are added during mixing prior to the addition of filler. Process aids also enhance the filler dispersion in the polymer matrix during mixing. Sometimes, vinyl group containing hydroxyl fluids are commercially used to balance the hardness and flowability (viscosity) characteristics of a silicone mixed stock.

11.6.5 Vulcanisation

Three different types of vulcanisation systems are commonly employed in silicone processing. In RTV both condensation cure and addition cures are used. In LSR, addition cure is mostly used and in HCR, both organic peroxide cure and addition cures are used. Up until now, organic peroxide curing is the most commonly used vulcanisation method in the majority of HCR silicone elastomers.

11.6.5.1 HCR Vulcanisation by Organic Peroxides

Silicone rubbers are traditionally cured with various commercially available organic peroxides. **Table 11.8** lists the organic peroxides commonly used with recommended cure temperatures and general application areas. However, the performance and level of each peroxide in a particular compound will depend on its decomposition temperature, level of peroxide used in composition, percentage of active oxygen, half-life and so on. Generally, the higher the active oxygen in the peroxide, the lower the amount required to be added in the compound formulation and *vice versa*.

Generally, organic peroxides for silicone rubbers fall into two broad classifications according to their ability to crosslink just vinyl groups (called 'vinyl' specific peroxides) or both methyl and vinyl groups (called 'general purpose' peroxides). The dialkyl peroxides, e.g., dicumyl peroxide, fall into the former category, while the diacyl peroxides such as benzoyl peroxide fall in the latter category. The general-purpose type peroxides can be used in all kinds of silicone rubber compounds and are active at relatively low curing temperatures (90-120 °C). However, these general-purpose peroxides are not recommended for use in combination with carbon black fillers. These peroxides generate acidic decomposition products, and a relatively long post-cure treatment is required for thick-sectioned articles. The 'vinyl specific' peroxides are not acidic, and as a result, post-cure treatment is relatively short or even not done at all. Thus, for the vinyl specific peroxides, satisfactory cure density is obtained in vinyl containing silicone rubber (150-180 °C), and can be used in formulations containing carbon black. For vinyl containing polymers, the free radical adds to the vinyl group, while in the case of the methyl group, a hydrogen atom is abstracted, leaving a methyl free radical attached to silicone. The

Table 11.8 Peroxides used in vulcanisation of silicone rubbers

Chemical name	Physical form	Temperature at $t_{1/2}$ = 6 min, °C	Typical cure temperature, °C	Recommended dosage level, phr	Classification	Recommended area of use
2,4-Dichloro benzoyl peroxide (DCBP-50)	50% Active paste	80	90	1.1-2.2	General purpose	Hot air (HAV), LCM (molten salt), ballotine (fluidised bed)
Dibenzoyl peroxide (BP-50)	50% Active paste	95	105	0.7-1.5	General purpose	Moulding, steam, LCM, HAV, ballotine
Di(4-methylbenzoyl) peroxide	50% Active paste	108	105	0.75-1.5	General purpose	Low temperature cure, steam, HAV
Tert-butyl peroxybenzoate	Liquid (100%) Powder (40%)	136	140	0.25-0.6 0.8-1.7	General purpose	HAV, Steam
Dicumyl peroxide (DCP)	Crystalline Paste Powder	162	150	0.5-1.0 1.0-2.2 1.0-2.2	Vinyl specific	Moulding thick section, LCM, HAV, ballotine
Di(*tert*-butylperoxyisopropyl) benzene	Flakes Powder	169	160	0.15-0.4 0.4-0.9	Vinyl specific	Moulding, steam
2,5-*bis*(*tert*-butylperoxy)2,5-dimethyl-hexane (DBPH)	Powder (50%) Paste (50%) Liquid (100%)	171	155	1.0-2.0 0.8-1.6 0.4-0.8	Vinyl specific	Moulding, steam
Di-*tert*-butyl peroxide	Liquid	176	160-180	0.2-0.4	Vinyl specific	Moulding

incorporation of 0.05-1.0 mol% vinyl groups into the polymer produces more selective crosslinking and hence better vulcanisates. Also, a lower concentration of peroxide is required for a good cure and less peroxide decomposition products will be formed to effect hydrolysis and siloxane rearrangement reactions. The inclusion of small amounts of vinyl groups also provides elastomers with better compression properties.

The peroxides, when heated, undergo homolytic cleavage to form free radicals that react with the pendant organic groups on the silicone polymer. This results in crosslinks between the polymer chains, which are separated from each other by a few hundred chain segments, normally in the range of 100 to 400 repeating units. The number of such crosslinks and their distribution greatly influence the ultimate physical property profile of the silicone rubber. In general, cure time is a function of the temperature of the particular peroxide type and also the thickness of the part.

11.6.5.2 Addition Cure of LSR

Since its introduction in the late 1970s, the LSR materials have never been in greater demand than it is today. Over time, LSR have become stronger, easier to produce, and has been developed to achieve unique properties dependent on the target applications. Due to its low viscosity, high flow, fast cure cycle time, clean operation and automated manufacturing process, LSR has enjoyed increasing popularity especially in countries with high labour costs. LSR are mostly commercially available as two component systems: A and B and are a mixture of low viscosity vinyl and hydrogen functional polysiloxanes with silica filler and a catalyst as well as inhibitor (controls pot-life) which react according to the principle of addition crosslinkage. The hydrogen function crosslinker component links to the vinyl functional polysiloxane under the influence of the platinum catalyst. Contrary to peroxide catalytic crosslinkage as used for HCR and generally activated only after heating, the platinum catalytic LSR system crosslinks at room temperature. For this reason, the 'A' component containing the catalyst and the crosslinking 'B' component are kept separated (see **Table 11.9**).

The vulcanisation properties are therefore dependent on the ratio of components A:B in the mixer and the quality of mixing. Most LSR are mixed in the ratio of 1:1 and

Table 11.9. Typical platinum catalytic two component LSR system

Component A	Component B
Methyl vinyl polymer	Methyl vinyl polymer
Platinum catalyst	Hydride crosslinker (SiH)
Silica filler	Silica filler
Additives	Additives
	Inhibitor

tolerate variation in the mixture ratio of +/- 10%. The structure of the SiH crosslinker and the ratio of SiH crosslinker (hydride) to SiVi are also important in determining the final properties of the vulcanisate. For different SiH to SiVi ratios, there is a trend that more hydride leads to higher network density, which gives a slightly higher hardness, lower elongation and tear. The rheological properties of LSR are characterised by free flowing to pasty consistencies.

In general, the processing ability (pot-life) of common commercial LSR products is at least three days at room temperature. An increase in temperature causes a rapid shortening of pot life of LSR, while cooling the mixture to –20 °C preserves it for months. Unlike conventional silicone rubber cured with vinyl specific peroxides, press cured LSR parts will continue to cure after removal from the mould when subjected to high temperatures due to the stoichiometric excess of methylhydrogensiloxane crosslinker in the presence of active platinum catalyst.

In the presence of a precious platinum catalyst such as chloroplatinic acid, a true addition reaction occurs resulting in a uniformly vulcanised rubber without reaction by-products. This reaction is accelerated by heat, but also occurs quite actively at room temperature. Inhibitors play a crucial role to retard or control the rate of hydrosilation to assure adequate mixed shelf life at fabrication temperatures. The main approach is to coordinate platinum ligands that block the hydrosilation mechanism, which decompose or dissociate at cure temperatures to release active catalyst. Some examples of retarding agents (inhibitors) for the hydrosilation cure mechanism are: 2,2´-bipyridine, thioacetamide, quinoline, triphenylphosphide and phosphites, bis(triphenylphosphine) dichloroplatinum, phenyl and methyl hydrazine, 2-ethynylbutane-2-ol, perchloroethylene and ethylcyclohexanol (ECH) [20].

11.6.5.3 Curing of RTV

RTV silicone rubber is also a two-component system that when fully cured yields a highly flexible, elastomeric product. The vulcanisation takes place at room temperature, hence the name room temperature vulcanisation. It is cured by addition or condensation mechanisms. The addition cure involves a platinum catalyst and generates no by-product. The condensation mechanism utilises an organo-tin catalyst and generates alcohol as a by-product. **Figures 11.6a** and **11.6b** show the schematic diagram of reaction mechanism.

11.7 Processing

Processing of silicone rubber is very similar to processing of standard organic rubbers.

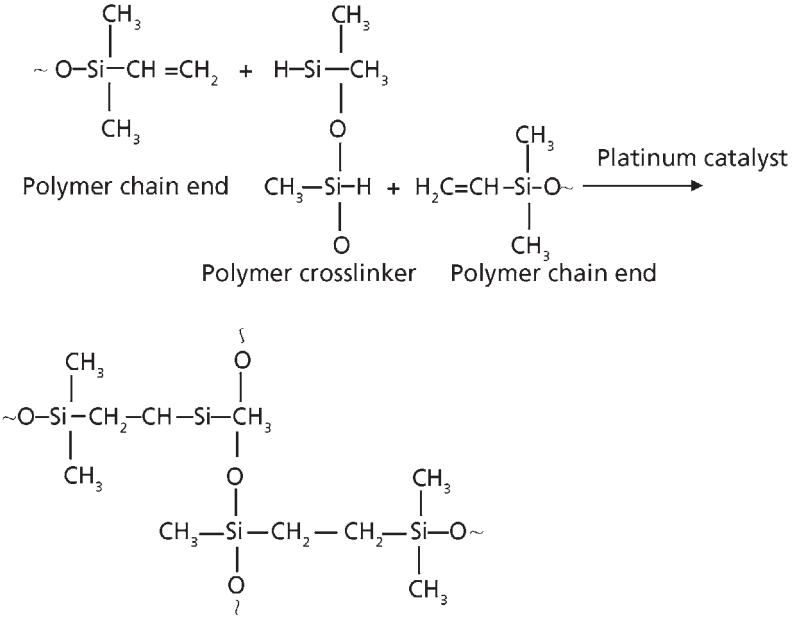

Figure 11.6 (a) Addition cure mechanism of RTV

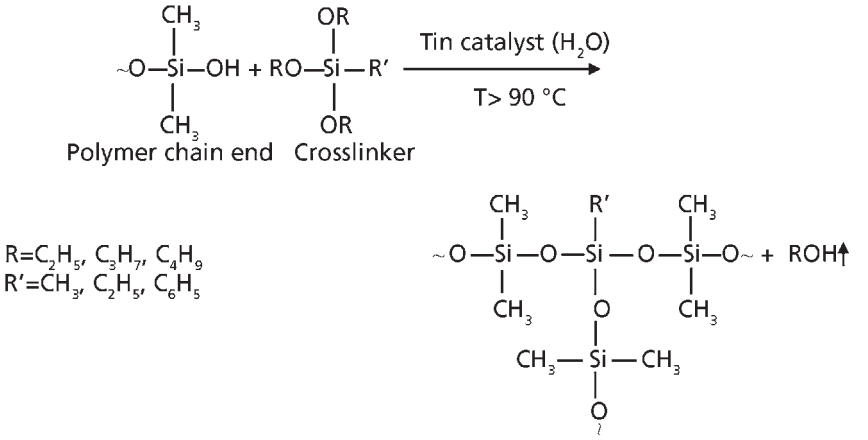

Figure 11.6 (b) Condensation cure mechanism of RTV

11.7.1 Mixing

The most common type of mixing equipment suitable for formulating HCR rubber include two roll mills, Banbury mixers, tilt internal mixers and dough mixers. For open roll mill mixing, the rolls should be water-cooled and be drawn with a friction ratio of 1.2:1 to 1.4:1. Silicone rubber will usually transfer to the faster roll during milling due to having a lower cohesive strength than most of the organic rubber compounds. Internal mixers are most commonly used commercially for the production of large size, more uniform batches to save labour, power and manufacturing costs. During mixing in an internal mixer, the rotor's speed, temperature/heat build-up, energy consumed and time of mixing should be carefully monitored. The maximum desirable temperature of mixing will vary depending on the type of the peroxide and the decomposition temperature if they are added in single-stage mixing. Care should always be taken about the batch temperature during mixing and post mixing storage for effective and efficient use of vulcanising agents. Typically, the polymer is loaded first, followed by the liquid components, reinforcing fillers and additives, although this order can be modified to provide more initial shear by partial incorporation of the filler early on. Incorporation of the high surface area reinforcing filler is usually the rate-controlling step in achieving a satisfactory mix. *In situ* filler treatment usually requires a heating cycle. Normally, it is recommended that at least 24 hours is allowed for maturation prior to use, since during this maturation period, the filler surface is getting 'wetted' with polymer which gives a better batch-to-batch consistency.

11.7.2 Moulding

Compression and transfer moulding techniques are the most widely employed fabrication methods. Generally, moulding temperature varies from 115 to 180 °C. Depending on the part size, design of the mould, flow and cure characteristics – the temperature, pressure and time is varied to get the best quality output from the moulding process. It is a good practice to freshen a silicone rubber mixed stock prior to fabrication to improve the rheological properties or flowability by reducing the structuring or crepe hardening phenomenon. However, there are many stocks which are designed not to require freshening prior to fabrication. Normally, freshening is done by remilling the compounded stock on a two-roll mill. Silicone rubber has good flow properties under pressure, even at ambient temperature. This property is responsible for its success in many fabrication methods which include compression moulding, transfer moulding, injection moulding, blow moulding, extrusion, calendering, dispersion coating on fabric, and mandrel wrapping.

Each moulding technique has its particular advantage. Compression moulding is the simplest and most flexible, but is labour intensive. Transfer moulding is suitable for complicated parts in multi-cavity, high volume moulding. With the sophisticated design

of flashless mould and cold pot technology, high productivity of more complicated parts are achievable in transfer moulding technology. Injection moulding requires short cycles and offers uniformity, excellent properties and adaptability to high production volume.

Standard rubber industry methods may be used for finishing the parts (to trim the flash). The use of liquid nitrogen in a cryogenic deflashing/tumbling operation is also used due to the extreme low temperature capability of silicone.

11.7.3 Extrusion

The equipment used to process silicone rubber is much the same as that used for organic rubbers. Typically, a screw with length/diameter (L/D) ratio of 10:1 to 16:1. Generally, extrusion screws with compression ratios ranging from 2:1 to 4:1 (single or double flight design) have been successfully used for silicone rubber. A ratio of approximately 4:1 will provide adequate delivery without causing excessive heat build-up. An 80 to 90 durometer compound will generally require a higher compression ratio than a 50 to 60 durometer stock to obtain an equal output at comparable screw speed. A higher compression ratio, if used in conjunction with adequate cooling, will also permit greater extrusion capacity. The incorporation of a positive pressure feeding roller in the extruder feeding zone will give a more steady throughput and help to maintain uniform output dimensions. Stainless steel screen packs generally consist of a backup screen of the 20 to 40 mesh variety, with a finer screen in the 60 to 100 mesh range, and are desirable to produce optimum back-pressure and remove contaminated particles. Some fabricators prefer to run without screens because of higher extrusion speeds and to eliminate the possibility of heat build-up and scorching at the breaker plate area. The use of screens, however, should not be ignored because they serve a definite purpose in screening out contamination and undispersed filler particles, if any. They also force out included air from the compound, which is a result of milling and freshening operations, especially in the softer compounds.

When long continuous runs are made at relatively high production speeds, cooling is required. The frictional working of the screw and pressure build-up at the breaker plate and in the extruder head will all contribute to heat build-up in the equipment. High green strength material, high viscosity stocks, long barrel extruders, excessive screw compression ratios, fine mesh screens (when used), all contribute to heat generation. So, it is desirable to cool the barrel, screw and head zones. It may not be necessary to cool all three on all occasions, however, the flexibility is needed. After leaving the die, the rubber extrudate is normally cured via a short exposure to saturated steam, hot air, heated fluidised beds or a molten salt system to maintain its shape and to acquire the desired physical properties necessary for the application.

11.7.4 Oven Curing

To attain the desired properties, most silicone rubber parts made by moulding or extrusion may need to be oven cured after vulcanisation especially when cured using 2,4-dichlorobenzoyl peroxide or benzoyl peroxide. Oven curing or post baking helps to remove peroxide decomposition by-products as well as volatiles. Under normal circumstances, post curing is done in a standard air-circulating oven for 2 to 4 hours at 200 °C.

11.7.5 Sponge

Cellular silicone rubber in sheet, moulded or extruded forms can be manufactured using similar processes as for other cellular rubbers. A post-cured period in a hot air oven is usually used to ensure complete vulcanisation. Also, dimensions can undergo some change during this post-cure, so wider dimensional tolerance must be allowed for particularly for moulded items. Cellular silicone rubber is almost always produced with a closed cell structure by using 'blowing agents' in which each gas cell is completely surrounded by rubber, and thus isolated from all other cells. The cure and the blow must be carefully synchronised in order to achieve the desired density, blown material properties and surface appearance.

In the extrusion process, the rubber extrudate passes through the successive heating zones in the cure media, reaches a threshold temperature at which the blowing agent decomposes and gas bubbles form, creating individual cell structures in the rubber. This is followed by a continuous cure until vulcanisation is complete. On emerging from the vulcanisation chamber, or salt bath or hot air vulcanisation (HAV) or infrared heating tunnel, the extrudate is cooled to allow it to stabilise dimensionally. The adjustment or fine-tuning of the vulcanisation process preserves the cell structure formed by the gas in the interior of the extrudate part which makes the surface of the extrudate part smooth, without exposed cells, and is referred to as a skin. Careful balance of the curing and blowing generates a smooth skin during the vulcanisation process. Sponge silicones may also have an 'open-cell' structure in which each cell is interconnected to other cells, providing a continuous gas pathway throughout the part.

The selection of peroxide systems and blowing agent(s) for a continuously extruded sponge are critical to the reproducibility of a sponge. Special precautions need to be taken to ensure that the correct percentages are placed into each batch. Use of masterbatches is preferred for better control. Dual peroxides are sometimes recommended in order to obtain the necessary initial state of cure and final cure once expansion is optimised.

Table 11.10 indicates the typical types of blowing agents most commonly used in silicone rubber.

Table 11.10 List of typical types of blowing agents		
Type	**Decomposition temperature, °C**	**Gases formed**
Nitrosan (obsolete)	80 – 100	N_2, CO_2
Hydrazides (OBSH, TSH, RA)	110 - 235	N_2 ,CO_2
Dinitrosopentamethylene tetramine	190 -195	N_2, NH_3
Azodicarbonamides	205 - 212	N_2, CO_2, NH_3, CO
Activated forms of azodicarbonamides	140 - 180	N_2, CO_2, NH_3, CO

11.7.6 Calendering

A standard three or four roll calender with linear speed range of 1 to 3 m/min is typical for silicone rubber. In most cases, the three-roll calender is a vertical stack design. A four-roll calender can also be a vertical stack type, but inverted 'L' or inclined 'Z' configurations are also used. A variable speed main drive is normally recommended, and the ratio of the take-off rolls should preferably be 1:1. In extremely stiff or hard compounds, a slight ratio change between the rolls at the take-off nip may bring an improvement by making use of friction at the nip. Silicone rubber compounds are generally calendered at room temperature. In some cases, however, some heating may be beneficial in specific compounds due to improvement of tack and adhesion to fabric, if supported. Most silicone compounds will benefit from mill freshening before the calendering operation.

11.7.7 Co-moulding and Over-moulding

Hard and flexible composites produced by co-injection moulding and over-moulding have gained a large market share. Silicone rubbers are increasingly the materials of choice for the flexible component of multi-component composites because of their ease of fabrication and their outstanding properties.

In co-moulding and over-moulding processes, the principal target is to integrate rubber and plastics or rubber and metal components. These articles are prepared either by semi-automatic or automatic steps providing significant reduction in production time and cost. The characteristics of co-moulding and over-moulding articles are significantly different from the equivalent assembled ones, i.e., mechanical fixing points are replaced by chemical bonds. This is a tremendous advantage in all those applications in which the article works in dynamic conditions or when it undergoes temperature and pressure fluctuations. Because of the high initial mould and machine costs, production will not

be economic unless production volume and the part geometry permit it to be fully automated. Moreover, as silicone rubber has a relatively high vulcanisation temperature, the materials used for composites must be high-quality thermoplastics or metals.

In general, LSR do not bond to the substrate without priming and/or post baking due to low surface energy. Presently, due to developments of siloxane chemistry, adhesion promoters and improved formulation of polysiloxanes, they bond readily to engineering thermoplastics, glass and metals. The ability of self-bonding or primerless adhesion enables a design engineer or fabricator to take full advantage of the productivity of liquid injection moulding (LIM) technology by eliminating the priming step of the process. Additionally, a self-bonding LSR enables certain design flexibility in the part itself, as the need to mechanically interlock the elastomer in place no longer exists. Self-adhesive or self-bonding LIM silicone has already been shown to work well with many engineering thermoplastics (ETP) such as polyphenylene oxide, polyamide, polybutylene terephthalate, polyphthalamide, acrylonitrile-butadiene-styrene, polyphenylene sulfide, polycarbonate and metals like aluminium, carbon steel, stainless steel, galvanised steel and so on. So, during the co-moulding and over-moulding processes, several considerations must be taken into account, including the plastic/metal used, the cycle time of the process, the injection pressures, the siloxane material used and the mould design. The process conditions must be conducive to the ETP substrate over which moulding will be done and the T_g and T_m of the material must be compatible with the mould temperature, and the injection pressures must not deform the part during the moulding cycle. In order to achieve the best design flexibility and ultimate process efficiency during production, two component or two shot moulding processes are generally adopted, in which an ETP part is first moulded followed by LIM silicone elastomer.

11.8 Troubleshooting

Silicone compound formulations, in general, consist of polymer, filler, curing agent, process aid, colorant and other special additives such as other organic rubber compounds. Processing of silicone rubber is an art backed by scientific logic coupled with material and process characteristics. The compound design and selection of catalyst will depend entirely on geometry, thickness and functional aspects of the parts. Design of the compound also depends on the type of processing and process conditions to produce good quality parts in the shortest possible time with lowest cost. Nowadays, with advanced computational power, flow of material in the mould can be simulated and analysed by finite element analysis (FEA). For transfer and injection moulding, it is especially useful for determining the location of the sprue points, sprue dimensions, and the number of sprues required to overcome process and mould filling related problems in the design stage without investing money in expensive tooling. It is also a common practice to run some parts through design of experiments where the amount of rubber is less than that required to fill the part cavity. By adding material slowly, one can get

an idea of what is happening inside the cavity of the mould as far as flow of rubber is concerned. This method also helps to predict where the possibility of knit-line formation is likely to occur. If trapped air is a major issue, sometimes this method will give the operator an initial idea where to put vents in the mould to allow the air to escape from the mould cavity.

Mould temperature of different platens also has a significant influence during the demoulding operation. The parts generally stick/transfer to the cold mould surface. In general, it is easier to take out the parts from the bottom than from the top of the mould (although, it depends on the shape of the part). The temperature of cure also has an influence on the shrinkage factor. The major shrinkage factor is influenced by the volatile content and specific gravity of the silicone compound. The higher the volatile content, the higher the shrinkage in the part after post baking or heat ageing. Normal silicone compounds contain 0.5% to as high as 6% volatile content.

If the parts are tearing during the de-moulding operation, turning down the temperature by few degrees may sometimes help to overcome the problem.

A few tips are generally followed in the silicone processing industry to overcome various material and process related issues during moulding and extrusion processes – these are highlighted in **Tables 11.11** and **11.12**.

11.9 Applications

The outstanding characteristics of silicone rubber coupled with their prolonged service life have ked to a wide range of practical applications. A number of examples are given next, and many more are anticipated as engineers and designers become more familiar and confident with this class of material.

11.9.1 Automotive Applications

The automotive industry has experienced the largest growth in the use of silicone rubbers in last two decades both from original equipment manufacturers (OEM) and from the after market/replacement markets especially in under hood and exposed applications. The following list gives some of the products used in the automotive market segment - transmission shaft seals, ignition cables/wires and protective sheaths, moulded gaskets, 'O' rings and protective caps, switch covers, spark plug boots and caps, turbo charger hoses, vibration dampers, weather packs (wiper blade rubber, sunroof seals), central locking membranes, exhaust mufflers, and connector seals.

Table 11.11 Moulding Problems		
Problem	**Probable causes**	**Recommended action for remedy**
Trapped air, brown spots or blisters	• Entrapped air or under cure • Excess mould release • Undercure	• Close mould completely and apply bump or proper level of vacuum (in vacuum press) • Avoid spraying excessive mould spray • Check uniform mould temperature • Check venting in mould cavities • Lower shot size • Use freshened rubber for uniform flow • Increase mould temperature
Excess flash or poor tear trim	• Excessive rubber charge	• Reduce to appropriate weight of charge • Increase mould pressure • Change bump or remove
Flow lines or knit lines	• Flow of rubber • Premature curing • Excessive spray of mould release	• Plasticity may be high—reduce it by milling • Load mould faster • Reduce mould temperature • Reduce mould release concentration and regulate control of mould spray
Parts sticking to mould	• Mould dirty • Temperature too hot	• Clean mould • Apply mould release • Reduce temperature
Non-fill or scorch part	• Flow of rubber • Mould closing too slowly • Preform too small	• Check rubber plasticity • Control mould temperature • Increase weight of prep • Increase material in pot
Colour variation	• Poor mix or dispersion	• Freshen higher plasticity stock before adding colour and catalyst • Check stiffness of pigment • Check consistency of colour from lot to lot • Check by using colorimeter or spectrophotometer
Back rind	• Mostly occurred in flash-type moulds due to high shrinkage, high thermal expansion and compressibility	• Lower mould temperature • Bump press as charge heats • Optimise the shot size • Reduce mould pressure • Increase hold time

Table 11.12 Extrusion Problems		
Problem	**Probable causes**	**Recommended action for remedy**
Rough surface	• Scorched compound • Die land too long • Structured compound • Surface imperfections	• Check extruder barrel and screw temperatures • Check extruded output temperature • Maintain correct land to orifice ratio • Freshen the compound • Polish the die surface
Blisters	• Moisture in rubber stock • Low volatile contamination • Temperature of vulcanisation chamber too high • Entrapped air • High humidity	• Care needs to be taken during mixing and storage • Keep it in clean area • Reduce cure temperature • Increase pressure in extruder head (through screen pack and die design) • Use vacuum extruder • Minimise moisture condensation as much as possible
Porosity	• Wrong catalyst • Low viscosity • Entrapped air or moisture	• Replace compound • Add finer mesh screen or additional screen • Check the input and output plasticity
Material misfeeding	• Incorrect extruder throat design • Poor screw design • Soft and sticky material • Carelessness of operator • Improper preform size	• Redesign the throat of extruder • Single flight screw is preferable with deeper flight screw • Dust very lightly with talc • Careful constant feeding • Use the right preform size
Inadequate or inconsistent extruded output	• Scorched material • Blocked screen pack	• Reduce back pressure and frictional heat build-up • Regulate extruder speed and temperature • Change screen pack • Check Mooney scorch test
Undercure	• Vulcanisation temperature too high • Low catalyst level • Too much air circulation in hot air vulcanisation	• Increase vulcanisation temperature • Adjust air circulation

11.9.2 Aerospace Applications

In aerospace applications silicone rubbers are mostly used in fuel tank seals, seals for fuel lines, petroleum pumps and hydraulic systems, air frame opening seals, cable insulation, dust and ice boots, gaskets, cushions, and blankets and anti-icing hoses (due to its resistance to extreme temperatures). O-rings, connectors, seals and gaskets made from silicone rubbers are also used in aircraft engines due to their low compression set property at elevated temperatures. Resistance to oxidation has led to their use in oxygen masks, control diaphragms, and tubing. Ablative and protective coatings have been used on aerospace missiles, rockets, rocket fuel supply cables and space vehicles.

11.9.3 Electrical and Electronics

A large volume of silicone rubber is consumed by the electrical industry in wire and cables for its heat resistance and flexibility. It is used in power cables, motor and transformer insulation, outdoor insulators/high voltage insulators for transmission lines and cables, and encapsulation of electrical components. Conductive silicone rubber sealant is used to provide radio frequency and microwave shielding for electronic systems. Conductive silicone rubber is also used for rolls and gaskets to dissipate electrostatic charges. It is widely used in heat shrinkable sheathing material for cable terminals, self-adhesive silicone rubber tapes for insulation of large cables, and irregular shaped conductors. A large volume of it also goes into keypads for computers, telephones and remote controls. A combination of fibreglass reinforced plastics (FRP) and silicone rubber is being used as a substitute for conventional ceramics as a high voltage insulating material.

11.9.4 Coatings

Silicone rubber coatings are used for protection against weathering, solvents, chemicals and aerospace environments and to provide release and wear resistance. Textile coatings are used to impart wrinkle resistance and give the appearance of leather.

11.9.5 Appliances

In the appliance industries, silicone rubbers are widely used in anode caps due to their resistance to moisture, corona, ozone and flame. In the television industry, RTV are used to encapsulate high voltage transformers. ‘O’ rings and seals, and conventional and semi-conducting type oven door gaskets are used in small appliances. Silicone rubber is widely used for tubes in coffee pots, steam irons and so on. Due to its good resistance to hot detergent solutions, it is used in dishwashers and washing machines.

11.9.6 Foams

Silicone rubber foams have been used to prepare watertight fire resistant seal in a nuclear power plants.

11.9.7 Medical Products

Silicone rubber is gaining popularity in many medical applications due to its chemical inertness and bio-compatibility. The areas where it has already established its usefulness are in catheters, insulated wires, breast prostheses, 'O' rings, seals, diaphragms, needless valves and check valves, seals for syringe plungers, stoppers for injection vials, bag caps, transfer sets and seals. It is also used in drug delivery tubes and dosage control devices, blood culture devices, hernia corrective devices, joint replacement, and dental impression materials based on RTV technology.

11.9.8 Baby Care

Silicone rubber is used for baby bottle nipples, baby pacifiers, bottle valves, breast pumps, and drinking straws.

11.9.9 Consumer Products

In the consumer market segment, silicone rubbers are now replacing many metallic devices because of their non-stick property, flexibility and high temperature resistance. They are becoming increasingly popular in bakeware, spatulas and handles, baking pans, baking trays, and pastry scrapers. They are also commonly used in soft touch pens and handles, silly putty, jewellery moulding, wristbands. Silicone rubber is now well accepted in leisure manufacturing items such as bathing caps, scuba masks, swimming goggles, snorkel mouthpieces, grommets and diaphragms for beverage vending machines.

Acknowledgements

The author would like to thank his wife Dr. Sujata Sarkar for her useful comments and assistance in preparation of the manuscript.

References

1. F.S. Kipping, *Proceedings of the Chemical Society*, *London*, 1904, **20**, 274, 15.

2. E.G. Rochow, *Silicon and Silicones*, Springer-Verlag, Berlin, Germany, 1987.

3. W. Lynch, *Handbook of Silicone Rubber Fabrication*, Van Nostrand Reinhold Company, New York, NY, USA, 1978.

4. J. March, *Advanced Organic Chemistry: Reactions, Mechanisms and Structure*, Wiley-Interscience, New York, NY, USA, 1985.

5. F.S. Burkus and J. Amarasekera, *Rubber World*, 2000, **222**, 3, 26.

6. W.J. Bobear in *Rubber Technology*, 2nd Edition, Ed., M. Morton, Van Nostrand Rheinhold Company, New York, NY, USA, 1973, p.368.

7. K.E. Polmanteer and M.J. Hunter, *Journal of Applied Polymer Science*, 1959, **1**, 1, 3.

8. ASTM D1418, *Standard Practice for Rubber and Rubber Latices – Nomenclature*, 2006.

9. F.O. Stark, J.R. Falander and A.P. Wright in *Comprehensive Organometallic Chemistry*, Volume 2, Eds., G. Wilkinson, F.G.A. Stone and E.W. Abel, Pergamon Press, Oxford, UK, 1982, p.305, Silicones.

10. M.J. Owen, *Chemtech*, 1981, **11**, 288.

11. K.E. Polmanteer, *Rubber Chemistry and Technology*, 1988, **61**, 3, 470.

12. ISO 14644-1, *Cleanrooms and Associated Controlled Environments – Part 1: Classification of Air Cleanliness*, 1999.

13. D.J. Fisher, R.G. Chaffee and V. Flegel, *Rubber Age*, 1960, **87**, 59.

14. M. Toub and D.L. Finney in *Basic Elastomer Technology*, Ed., K.C. Baranwal and H.L. Stephens, American Chemical Society, Rubber Division, Akron, OH, USA, 2001, p.498.

15. K.E. Polmanteer, *Rubber Chemistry and Technology*, 1981, **54**, 5, 1051.

16. R.K. Iler, *The Chemistry of Silica: Solubility, Polymerisation, Colloid and Surface Properties, and Biochemistry*, John Wiley and Sons, New York, NY, USA, 1979, p.554.

17. M.A. Lutz, K.E. Polmanteer and H.L. Chapman, *Rubber Chemistry and Technology*, 1985, **58**, 5, 939.

18. H.L. Chapman, M.A. Lutz and K.E. Polmanteer, *Rubber Chemistry and Technology*, 1985, **58**, 5, 953.

19. E.L. Warrick, O.R. Pierce, K.E. Polmanteer and J.C. Saam, *Rubber Chemistry and Technology*, 1979, **52**, 3, 437.

20. U. Schachtely in *Proceedings of the International Silicone Conference*, 2004, Cleveland, OH, USA, Paper No.12.

21. T.A. Okel and W.H. Waddell in *Proceedings of the 145th ACS Rubber Division Meeting*, Chicago, IL, USA, Spring 1994, Paper No.44.

22. W. Wolff in the *Proceedings of the 132nd ACS Rubber Division Meeting*, Cleveland, OH, USA, Fall 1987, Paper No.29.

Abbreviations

6PPD	*N*-(1,3-Dimethylbutyl)-*N′ N′ N′ N′ N′*-phenyl-*p*-phenylenediamine
77PD	*N*,*N′*-Bis(1,4-dimethylpentyl)-*p*-phenylenediamine
A/P	Area to perimeter ratio
ABS	Anti-lock brake system
AC	Alternating current
ACM	Polyacrylate rubbers
ACN	Polymerised acrylonitrile
AES	Advanced elastomer systems
AFM	Atomic force microscopy
AIAG	Automotive industry action group
AO	Anti-oxidants
AOI	Area of Interest
APDS	4-Aminophenyl disulfide
ASIC	Application specific integrated circuit(s)
ASTM	American Society for Testing and Materials
ATR-IR	Attenuated total reflection infrared spectrosopy
BDV	Dielectric strength
BET	Brunauer, Emmett, and Teller surface area theory
BHT	Butylated hydroxy toluene
BL	Boundary lubrication
BP	Dibenzoyl peroxide
BR	Butadiene rubber

CB	Carbon black
CBA	Chain braking electron acceptors
CBS	*N*-Cyclohexyl benzthiazol sulfenamide
CCD	Charge-coupled-devices
CDBP	Compressed oil absorption number (di-butyl phthalate)
CEC	Cabot elastomer composites
CPE	Chlorinated polyethylene
CR	Chloroprene rubber
CRRC	Combat rubber raiding craft
CSDPF	Carbon-silica dual phase filler(s)
CSP	Chlorosulfonated polyethylene
CTAB	Cetyl trimethylammonium bromide surface area
CV	Continuous vulcanisation
DARPA	Defense advanced research project agency
DBP	Dibutylphthalate
DBP	Oil absorption number (di-butyl phthlate)
DBPA	Dibutyl phthalate absorption number.
DBPH	2,5-B*is*(*tert*-butylperoxy)2,5-dimethyl-hexane
DC	Direct current
DCBP	2,4-Dichloro benzoyl peroxide
DCF	Dipped chopped fibre
DCP	Dicumyl peroxide
DDS	Dimethyl dichlorosilane
DIN	Deutsches Institut für Normung
DIPDIS	Bis(diisopropyl)thiophosphoryl disulfide
DMESPT	Bis-(dimethylethoxysilylpropyl) tetrasulfide
DnOPDD	*N*,*N*´-Di-*n*-octyl-PPDA
DNPH	2,4-dinitrophenylhydrazine
DOPPD	N,N´-dioctyl-*p*-phenylene diamine

DOT	Department of Transport
DPG	Diphenyl guanidine
DPPD	Paraphenylenediamine
DSA	Double strain amplitude
DSC	Dynamic scanning colorimetry
DSC-TAM	Differential scanning calorimetry-thermal activity monitoring
DTBH	3-(3,5-Di-*tert*-butyl-4-hydroxyphenyl)propionic acid
DTBT	2,4-Diallyloxy-6-*tert*-butylperoxy-1,3,5-triazine
DV	Dynamic vulcanisate
EAM	Ethylene-ethyl acrylate copolymer
EB	Elongation to break
ECH	Ethylcyclohexanol
ECO	Epichlorohydrin rubber
ECU	Electronic control unit
EDTA	Ethylene diamine tetracetic acid
EDX	Electron dispersive x ray analysis
EHL	Elasto-hydrodynamic lubrication
EKIP	Ekologiya i Progres (Ecology and Progress; Russian)
ENB	Ethylidene norbornene
EPDM	Ethylene-propylene-diene terpolymer(s)
EPR	Ethylene-propylene rubber
ESBR	Emulsion styrene butadiene rubber
ETFE	Ethylene tetrafluoroethylene
ETP	Engineering thermoplastics
EV	Efficient vulcanisation
EVA	Ethylene-vinyl acetate copolymers
FCC	Federal communications commission
FDA	US Food and Drug Administration
FEA	Finite element analysis

FEF	Fast extrusion furnace (carbon black)
FEP	Fluorinated Ethylene propylene
FKM	Rubbers with fluoro and fluoralkyl or fluoralkoxy substituent groups on the polymer chain
FPM	Fluorocarbon rubbers
FRP	Fibreglass reinforced plastics
FT-IR	Fourier transform-infra red spectroscopy
FVMQ	Silicone rubber with methyl, vinyl and fluoropropyl substituents
GAFT	Grosch abrasion and friction tester
GC-MS	Gas chromatography – mass spectrometry
HALS	Hindered amine light stabiliser
HAV	Hot air vulcanisation
HCR	Heat cured rubber(s)
HF	Hydrofluoric acid extraction
HMDS	Hexamethyldisilaxane
HMMMV	High mobility multipurpose wheeled vehicle
HNBR	Hydrogenated nitrile rubbers
HPPD	*N*-(1,3-Dimethylbutyl)-*N´*-phenyl-*p*-phenylenediamine
HR	Heat resistant
HTP	High-temperature polymer
IC	Integrated circuit(s)
ICBM	Intercontinental ballistic missile
ID	Identification
IEC	International electrotechnical commission
IGC	Inverse gas chromatography
IIR	Butyl rubber
iPP	Isotactic polypropylene
IPPD	Paraphenylenediamine
IR	Infra red

IR	Isoprene rubber
IR	Polyisoprene rubber
IRS	Internal reflection spectroscopy
ISO	International Organisation for Standardisation
L/D	Length to diameter ratio
LCAC	Landing craft air cushion
LDPE	Low-density polyethylene
LF	Low frequency
LIM	Liquid injection moulding
LSR	Liquid silicone rubber(s)
LSZH	Low smoke zero halogen
MBTS	Dibenzothiazole disulfide
MDI	Diphenylmethane diisocyanate
MEHL	Micro-elasto-hydrodynamic lubrication
MEMS	Micro-electrical mechanical system
M_n	Number average molecular weight
MOB	Mobil offshore base
mph	Miles per hour
MQ	Silicone rubber with methyl substituent
MW	Molecular weight(s)
NBR	Nitrile butadiene rubber
NMR	Nuclear magnetic resonance
NR	Natural rubber(s)
NRC	Nuclear regulatory commission
NSA	Nitrogen surface area
OEM	Original equipment manufacturer(s)
OE-SSBR	Oil extended solution polymerised styrene-butadiene rubber
PA	Polyamide
PAC	Plain annealed copper

PAN	Polyacrylonitrile
PBN	Polybutylene 2,6-naphthalate
PCR	Polychloroprene rubber
PE	Polyethylene
PEEK	Polyether ether ketone
PEN	Polyethylene naphthalate
PET	Polyethylene terephthalate
PFA	Perfluoroalkoxy
phr	Parts per hundred rubber
PMQ	Silicone rubber with methyl and phenyl substituents
PO	Polyolefin
PP	Polypropylene
PPD	*N*′-Phenyl-*p*-phenylenediamine(s)
pphm	Parts per hundred million
ppi	Pixels per inch
PPS	Polyphenylenesulfide
PPTA	Poly-*p*-phenylene terephthalamide
PTFE	Polytrifluoroethylene
PU(s)	Polyurethane(s)
PVC	Polyvinyl chloride
PVDF	Polyvinylidene fluoride
PVMQ	Silicone rubber with methyl, vinyl and phenyl substituents
Q	Silicone rubber
QDI	Quinone diimines
QTM	Quantimet image analyzing computer
RF	Resorcinol formaldehyde
RFID	Radio frequency identification
RFL	Resorcinol formaldehyde latex
RKE	Remote keyless entry

RMA	Rubber manufacturer's association
RPA	Rubber process analyser
rpm	Revolutions per minute
RSS	Ribbed smoke sheet grade
RTV	Room temperature vulcanisation(s)
S&T	Science and Technology
SANS	Small angle neutron scattering
SAW	Surface acoustic wave
SAXS	Small angle x-ray scattering
SBR	Styrene-butadiene rubber
S-B-S	Styrene – butadiene - styrene
SEAL	Sea-air-land team
S-EB-S	Styrene-ethylene butylene - styrene
SEM	Scanning electron microscopy
Semi-EV	Semi-efficient vulcanisation
SPPD	*N*-(1-Phenylethyl)-*N´*-phenyl-*p*-phenylenediamine
SRB	Solid rocket booster
S-SBR	Solution polymerised styrene-butadiene rubber
SSIMS	Static secondary ion mass spectrometry
STEM	Scanning transmission electron microscope
STM	Scanning tunneling microscopy
STSA	Statistic thickness surface area
SWT	Side wall torsion
TAC	Triallyl cyanurate
TAPDT	Tris-(*N*-1,4-dimethylpentyl-*para*-phenylenediamino)-1,3,5-triazine
TBTT	Tetrahydro-1,3,5-tri-(*n*)-butyl-(S)-triazinethione
T_c	Crystallisation temperature
TCPTS	3-Thiocyanatopropyl-triethoxysilane
TEM	Transmission electron microscope/microscopy

TEO	Thermoplastic elastomeric olefins
TESPD	Bis(triethoxysilylpropyl) disulfide
TESPT	Bis(3-(triethoxysilyl)propyl)tetrasulfide
TESPT	*Bis*-triethoxysilylpropyl tetrasulfane
T_g	Glass transition temperature
T_M	Melting temperture
TMAFM	Tapping mode atomic force microscopy
TML	Total mass loss
TMT	Thiuram
TMTD	Tetramethyl thiuram disulfide
TNT	Trinitrotoluene
TPA	Thermoplastic polyamide(s)
TPE	Thermoplastic elastomer(s)
TPMS	Tyre pressure monitoring system(s)
TPU	Thermoplastic polyurethane(s)
TPV	Thermoplastic vulcanisate(s)
TS	Tensile strength
UHF	Ultra high frequency
UV	Ultraviolet
VA	Vinyl acetate
Vi	Vinyl
VMQ	Silicone rubber with methyl and vinyl substituents
VNB	Vinylidene-norbornene
VP	Vinyl pyridine
WPH	Wet process hydrophobic
XETFE	Ethylene-chlorotrifluoroethylene co-polymer
XLPE	Crosslinked polyethylene
XNBR	Carboxylated nitrile rubber
XPS	X-ray photoelectron spectroscopy

Index

C

D

E

F

N

O

P

Q

R

S

T

U

V

W

X

Y

ISBN 978-1-84735-099-2
90000
9 781847 350992

Published by Smithers Rapra, 2009

This book is a companion volume to Rubber Technologist's Handbook published in 2001. Written by experts in their respective fields, this handbook discusses the most recent developments in the subject.

The ten chapters cover Microscopic Imaging of Rubber Compounds, Intelligent Tyres, Silica-Filled Rubber Compounds, Fibres in the Rubber Industry, Naval and Space Applications of Rubber, Advances in Fillers for the Rubber Industry, Thermoplastic Elastomers by Dynamic Vulcanisation, Polymers in Cable Applications, Durability of Rubber Compounds, and Radiochemical Ageing of Ethylene-Propylene-Diene Monomer.

This book will serve the needs of those who are already in the rubber industry and new entrants to the field who aspire to build a career in rubber and allied areas. Materials Science students and researchers, designers and engineers should all find this handbook helpful.

SMITHERS iSmithers

Shawbury, Shrewsbury, Shropshire, SY4 4NR, UK
Telephone: +44 (0)1939 250383
Fax: +44 (0)1939 251118
Web: www.ismithers.net